N71-33286

NASA CR-111947

MISSILES AND SPACE DIVISION
LTV Aerospace Corporation
P. O. Box 6267
Dallas, Texas 75222

TITLE

STUDY OF EFFECTS OF INCORPORATING A LARGER HEATSHIELD ON THE SCOUT VEHICLE

FINAL REPORT

SUBMITTED UNDER TASK ORDER 24	
REPORT NO. 23.411	DATED 24 July 1969
PROJECT SCOUT	CONTRACT NO. NAS1-6935

Scout Engineering
PREPARED

J.A. Brassard
REVIEWED
J.A. Brassard

M.D. Brinson
APPROVED
M.D. Brinson

ABSTRACT
AST-52821 R2

TITLE OF REPORT
Study of Effects of Incorporating a Larger Heatshield on the Scout Vehicle

ORIGINATING AGENCY AND LOCATION	CLASSIFICATION		
	REPORT	ABSTRACT	TITLE
Missiles and Space Division - Texas LTV Aerospace Corporation P.O. Box 6267, Dallas, Texas	U	U	U

AUTHORS	ISSUE DATE	LIMITATIONS ON DISTRIBUTION (IF ANY)
Scout Engineering	24 July 1969	NONE

ORIGINATING AGENCY'S REPORT NO.	DOD REFERENCES			OTHER IDENTIFYING REPORT NOS.
	CONTRACT NO.	PROJECT NO.	TASK NO.	
23.411	NAS1-6935		Task Order 24	

INDEXING

A. SUMMARY SENTENCE(S): Larger volume heatshield for the Scout launch vehicle

B. KEY WORDS:
Scout
Larger Volume Heatshield

WEAPON SYSTEMS NUMBERS, MODEL NUMBERS, ETC.

NASA Scout Launch Vehicle

ABSTRACT

The study was performed to determine the effects of putting larger heatshields on the Scout vehicle. Four heatshield diameters were evaluated, 40, 42, 44 and 46 inches. External shapes were defined and the effects of each size heatshield on vehicle stability and control, structure and ground support equipment was determined. The first phase of this study is based on the Scout D configuration **(Algol III motor installed).** Increased fin area, control surface area, and control gains are required for all configurations. The impact on vehicle structure varies from virtually none with the 40 inch heatshield to almost complete vehicle redesign with the 46 inch heatshield.

The 42-inch diameter heatshield was selected for the second phase of the study, to determine the effects of putting the larger heatshield on the Scout B configuration (Algol IIB motor installed). Increased fin tip control area and guidance system gains are required for this configuration. Structural changes are required on the heatshield attachment clamp.

A

TABLE OF CONTENTS

TABLE OF CONTENTS (Continued)

A

TABLE OF CONTENTS (Continued)

A

TABLE OF CONTENTS (Concluded)

LIST OF FIGURES

LIST OF FIGURES (Continued)

LIST OF FIGURES (Continued)

LIST OF FIGURES (Continued)

LIST OF FIGURES (Continued)

LIST OF FIGURES (Continued)

LIST OF FIGURES (Continued)

LIST OF FIGURES (Continued)

LIST OF FIGURES (Continued)

A

LIST OF FIGURES (Concluded)

LIST OF TABLES

LIST OF TABLES (Continued)

LIST OF TABLES (CONCLUDED)

A

LIST OF SYMBOLS

C_{N_α} - normal force derivative, $deg.^{-1}$ or $rad.^{-1}$

C_{D_o} - drag coefficient at zero angle of attack

r - sphere radius

R - Cone radius at base of cone (heatshield cylinder radius)

M_∞ - freestream Mach number

θ_c - cone semi-vertex angle, deg.

S_{ref} S_π - reference area, 5.25 ft^2

l_π - reference length, 2.58 ft.

C_{m_α} - pitching moment derivative, $deg.^{-1}$ or $rad.^{-1}$

C_{N_δ} - normal force derivative for control deflection

C_{m_δ} - pitching moment derivative for control deflection

1.0 SUMMARY

The effort under Task Order 24 of contract NAS1-6935 was to conduct a study to determine the effects of putting larger heatshields on the Scout vehicle. Four heatshield diameters were evaluated, 40, 42, 44, and 46 inches, with the resultant heatshield shapes defined and their effects on vehicle stability and control, structure and ground support equipment (GSE) determined. The study is divided into two phases with the first phase based on the Scout D configuration (Algol III motor installed). This configuration is critical from both stability and structural considerations. As specified in the contract, the NASA will select the larger heatshield configuration based upon the data presented herein. After selection of the heatshield configuration the resulting vehicle will be evaluated in the second phase of the study with the Algol II motor installed.

The results of this phase of the study, with the Scout D vehicle configuration, show the need for increased fin area, control surface area, and control gains for all heatshield configurations. The increased fin area is achieved on the 40 inch diameter heatshield configuration by increasing the control tip size. The other heatshield configurations require, in addition, increasing the basic fin planform area. The results of the evaluation of each heatshield configuration are summarized below:

40 Inch Diameter Heatshield

- No vehicle structural changes required except the control surfaces.
- Fin control tip area shall be increased from 45 sq. in to 78 sq. in. This increases the fin area from 4.5 to 4.735 sq. ft.
- Jet vane control surface area shall be increased from 35 sq. in. to 41 sq. in.

- Guidance system first stage nominal displacement gain shall be increased from 5.0 to 6.75 deg/deg and the rate to displacement ratio shall be 0.4, the same as for the basic Scout.
- The following ground support equipment requires redesign: payload umbilical retract arm, heatshield cradle, dummy heatshield, payload and heatshield hoist, heatshield storage bracket, the upper cradle assembly, proofloading fixture assembly, and the fin protractor kit. A

42 Inch Diameter Heatshield

- The following vehicle structural changes are required: redesign the base A fins to increase the area from 4.5 to 5.75 sq. ft. per fin; redesign several components of the heatshield attachment clamp; add cork insulation to the lower D section skins.
- Fin control tip areas shall be increased from 45 sq. in. to 78 sq. in. (Same as 40 inch heatshield requirement).
- Jet vane control surface area shall be increased from 35 sq. in. to 41 sq. in. (Same as 40 inch heatshield requirement).
- Guidance system first stage nominal displacement gain shall be increased from 5.0 to 6.75 deg/deg and the rate to displacement gain ratio shall be 0.4, the same as for the basic Scout.
- The following ground support equipment requires redesign: payload umbilical retract arm, heatshield cradle dummy heatshield, payload and heatshield hoist, heatshield storage bracket, the upper cradle assembly, proofloading fixture assembly, and the fin protractor kit. A

44 Inch Diameter Heatshield

- The following vehicle structural changes are required: redesign the base A fins to increase the area from 4.5 to 8.6 sq. ft. per fin; redesign base A for fin loads; test lower C transition section for increased loads; redesign upper C transition

section; test X-259 motor case for increased loads; add insulation to lower D transition section and test the section for increased loads; redesign heatshield attachment clamp.

- Fin tip control area shall be increased from 45 sq. in. to 78 sq. in. (Same as 40 and 42 inch heatshield requirements).
- Jet vane control surface area shall be increased from 35 sq. in. to 41 sq. in. (Same as 40 and 42 inch heatshield requirements).
- Guidance system first stage nominal displacement gain shall be increased from 5.0 to 6.75 deg/deg and the rate to displacement gain ratio shall be 0.4, the same as for the basic Scout.
- The following ground support equipment requires redesign: payload umbilical retract arm, heatshield cradle, dummy heatshield, payload and heatshield hoist, heatshield storage bracket, the upper cradle assembly, strap wrench, transporter aft restraint assembly, proof loading fixture assembly, and the fin protractor kit.

46 Inch Diameter Heatshield

- The following vehicle structural changes are required: redesign the base A fins to increase the area from 4.5 to 16.0 sq. ft. per fin; redesign base A for increased fin size and loads; redesign lower C transition section; redesign upper C transition section; redesign X-259 motor case; redesign lower D transition section; redesign heatshield attachment clamp.
- Fin control tip area shall be increased from 45 sq. in. to 78 sq. in. (Same as 40, 42 and 44 inch heatshield requirements).
- Jet vane control surface area shall be increased from 45 sq. in. to 78 sq. in. (Same as 40, 42 and 44 inch heatshield requirements).
- Guidance system first stage nominal displacement gain shall be increased from 5.0 to 6.75 deg/deg and the rate to displacement

gain ratio shall be 0.4, the same as for the basic Scout.

- The following ground support equipment requires redesign: payload umbilical retract arm, heatshield cradle, dummy heatshield, payload and heatshield hoist, heatshield storage bracket, the upper cradle assembly, strap wrench, vehicle transporter (complete redesign required), the launcher (significant redesign required), proof loading fixture assembly, and the fin protractor kit.

The 42 inch diameter heatshield was selected for the second phase of the study, to determine the effects of putting the larger heatshield on the Scout B configuration (Algol IIB motor installed). The results of the evaluation of this configuration are summarized below:

Scout B - 42 Inch Diameter Heatshield

- The following structural changes are required: redesign several components of the heatshield attachment clamp; add cork insulation to the lower D section skins.
- Fin tip control area shall be increased from 45 sq. in. to 78 sq. in. This increases the fin area from 4.5 to 4.73 sq. ft.
- Guidance system first stage nominal displacement gain shall be increased from 5.0 to 6.75 deg/deg and the rate to displacement gain ratio shall be 0.4, the same as for the basic Scout.
- The following ground support equipment requires redesign: payload umbilical retract arm, heatshield cradle, dummy heatshield, payload and heatshield hoist, heatshield storage bracket, the upper cradle assembly, proof loading fixture assembly, and the fin protractor kit.

A

2.0 PROGRAM DESCRIPTION

2.1 INTRODUCTION

The initial phase of the study was a parametric analysis to define the optimum shape of the heatshield considering buffet and aerodynamic characteristics. As it turned out the heatshield shape was defined primarily to satisfy the buffet criteria.

As specified by the contract the 42 inch diameter heatshield configuration was the focal point of the investigation. For those parameters that could be calculated one time and used for all configurations, i.e. the design trajectory and vehicle modal characteristics, the 42 inch configuration data was used.

The impact on the major pieces of ground support equipment was evaluated. Miscellaneous other GSE items may require redesign depending upon the detailed vehicle redesign requirements.

The analysis associated with determining the general vehicle characteristics are presented in the remainder of Section 2.0. The effects of the individual heatshield diameters on the Scout D vehicle configuration and ground support equipment are presented in Sections 3.0 and 4.0. The effects of putting a 42 inch diameter heatshield on the Scout B vehicle configuration are presented in Section 5.0.

A

2.2 PARAMETRIC ANALYSES

2.2.1 Buffet Analyses

2.2.1.1 Buffet Criteria

Unfavorable shapes and abrupt changes in the vehicle lines, especially at the forward end are the primary factors for the occurrence of buffeting during launch. Buffeting is a repeated loading of the structure by an unsteady aerodynamic flow. Vibration of structure and vehicle bending oscillations are possible effects of buffeting both of which can cause failure of the vehicle in flight. Therefore, it is advisable to avoid or minimize buffeting by using favorable configurations.

Reference 2-1 states that no general analytical method has been developed to predict buffet. However, this reference presents some criteria for avoiding buffet based on wind-tunnel tests on scale models. The basic requirements defined by these criteria are that the minimum static pressure coefficients and maximum adverse pressure gradients along the body should not exceed -0.14 and 0.20, respectively, as calculated by the equation presented in paragraph 1.3.2.2 of Reference 2-1. Using these criteria several heatshield configurations having diameters of 40, 42, 44, and 46 inches were investigated.

These configurations included shapes similar to the current Scout heat shield with nose cone angles ranging from 7.5° to 30°. Other investigated shapes included double angle nose cones and ogive noses.

2.2.1.2 Results

Results of this study showed that the heatshield nose cone angle is the primary factor effecting the static pressure coefficient and the boat tail angle controlled the pressure gradient. Therefore, the heat shield nose cone angles and boat tail angles were varied to define the configurations which fell within the criteria stated above. It was necessary to decrease the limit of the pressure coefficient to -0.16 to enable a realistic nose length to be

obtained. This relaxing of the criteria was considered reasonable because the current Scout heatshields fall close to this value.

The results indicated the need to reduce the nose cone angle from the current 22 degrees to 15 degrees for the 40 inch heatshield, 12.5 degrees for the 42 inch heatshield, 10 degrees for the 44 inch heatshield, and 7.5 degrees for the 46 inch heatshield. Bluntness ratios were varied and caused enough change in pressure coefficient to be a factor in defining the heatshield shape. A bluntness ratio was selected consistant with observing the -0.16 pressure coefficient limit (see Figure 2-1). Double angle and ogive noses were not satisfactory solutions to the problem of reducing lift on the nose while still satisfying the buffet criteria (Figure 2-1).

The majority of the shapes investigated (66 out of 84) did not include the effect of lower D Section. Initially it was assumed that lower D would not significantly influence the shape of the heatshield. This was found to be untrue and that lower D does influence the boat tail angle required to satisfy the buffet criteria for the heatshield. Therefore, the remaining 18 shapes investigated did include the effects of lower D behind the heatshield. The pressure gradient was the parameter most effected and it was found to decrease to acceptable limits by increasing the heatshield aft diameter. Figure 2-2 shows how the pressure coefficient and gradient varies with aft heatshield radius for the 40 inch diameter heatshield. This figure also shows how the aft diameter was defined. Similar parametric analyses were performed on the other heatshields. Table 2-1 is a catalog of all of the shapes investigated and gives the minimum pressure coefficient and maximum pressure gradient for each shape. Figure 2-3 presents a typical pressure coefficient and gradient as a function of body length. Although the data in Figure 2-3 is not precisely correct for the final 40 inch diameter heatshield shape, it does show the trend of these parameters. The final configurations are presented in Section 2.2.3.

FIGURE 2-1

40 IN. DIAMETER HEATSHIELD PRESSURE COEFFICIENT AND GRADIENT VS CYLINDER LENGTH AND BLUNTNESS RATIO

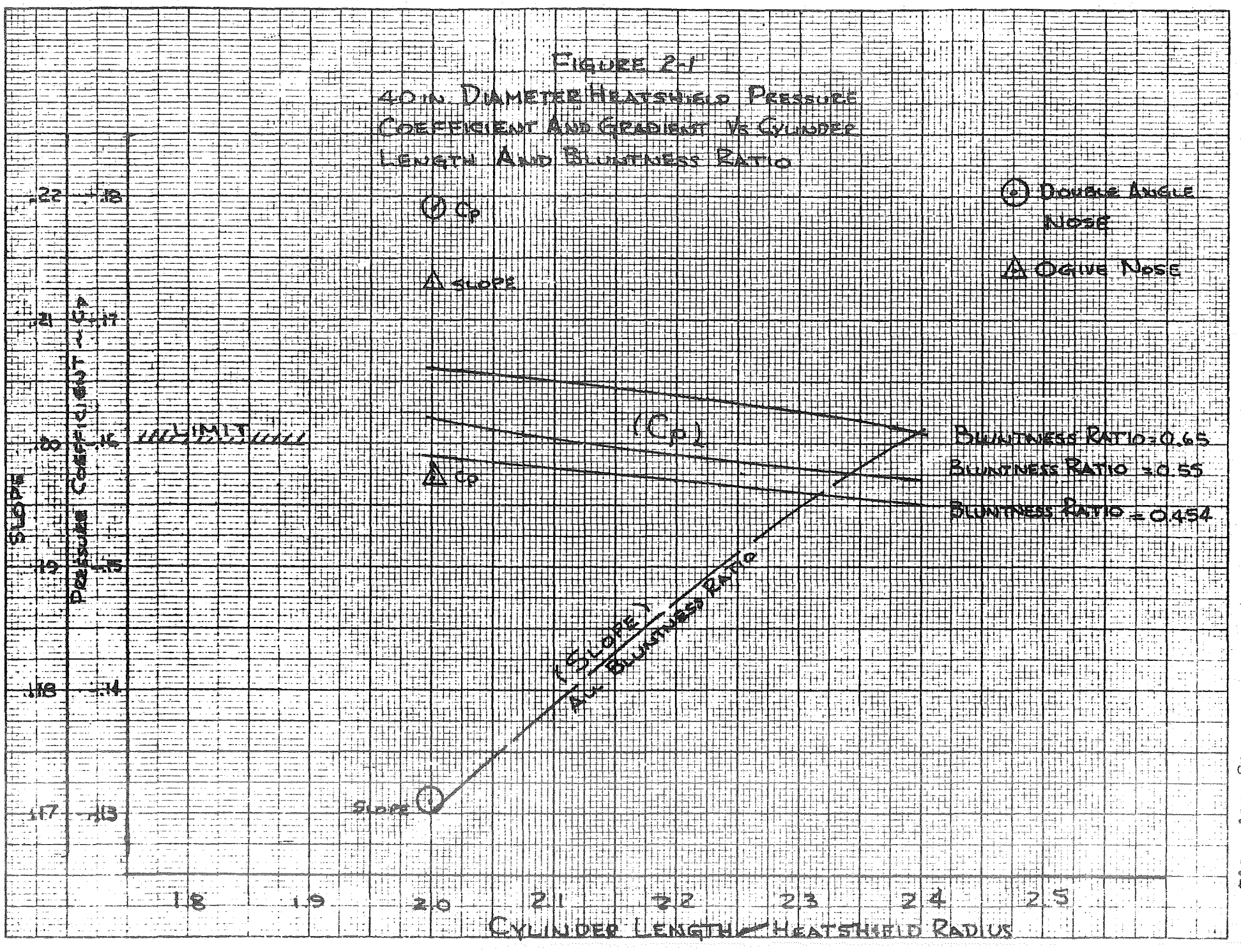

FIGURE 2-2
40 IN. DIAMETER HEAT SHIELD
PRESSURE COEFFICIENT AND GRADIENT
VS AFT HEAT SHIELD RADIUS

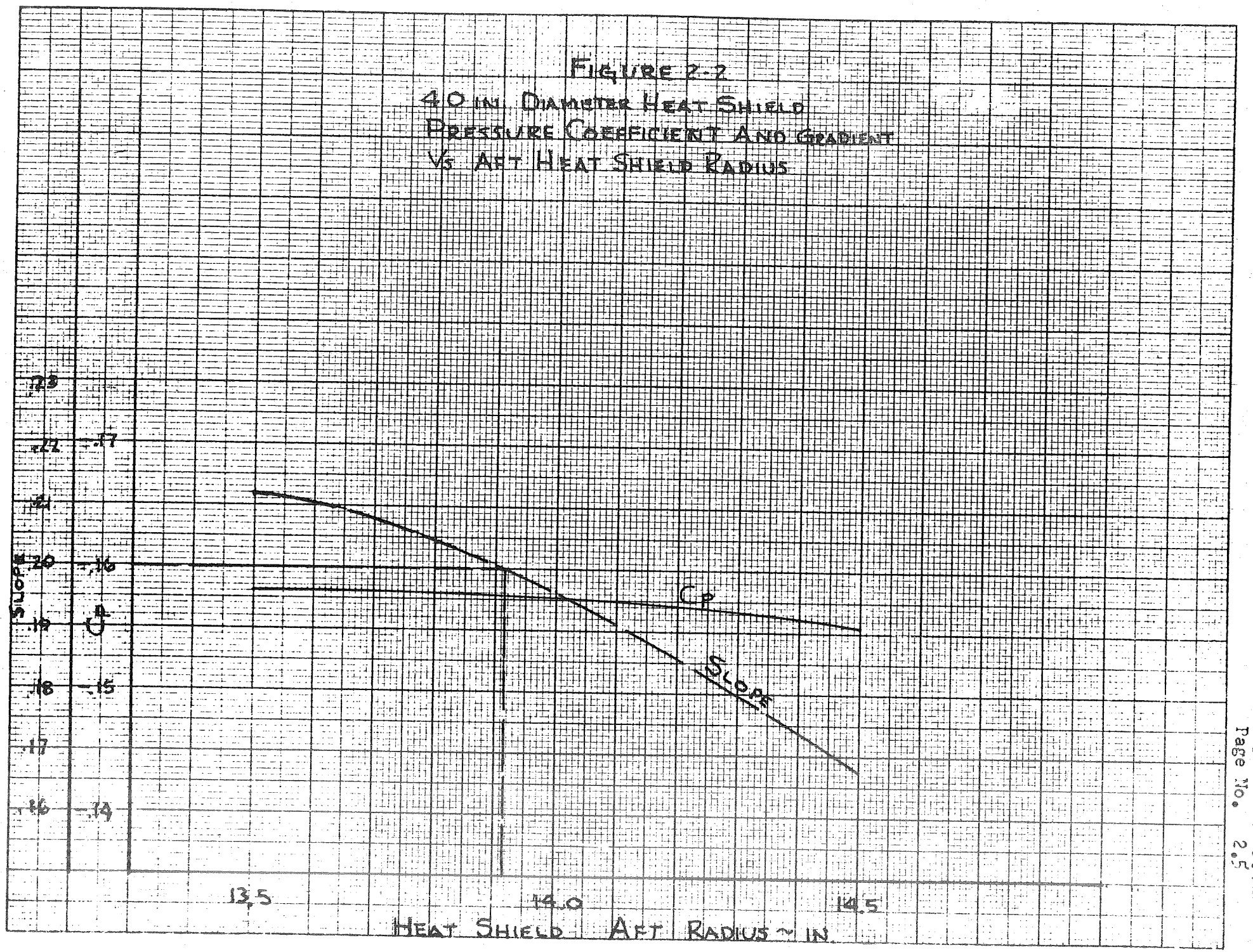

FIGURE 2-3
STATIC PRESSURE COFFICIENT AND
GRADIENT VS. HEAT SHIELD LENGTH
FOR VARIOUS CYLINDER LENGTHS
40 IN. DIAMETER HEAT SHIELD
BLUNTNESS RATIO = 0.45

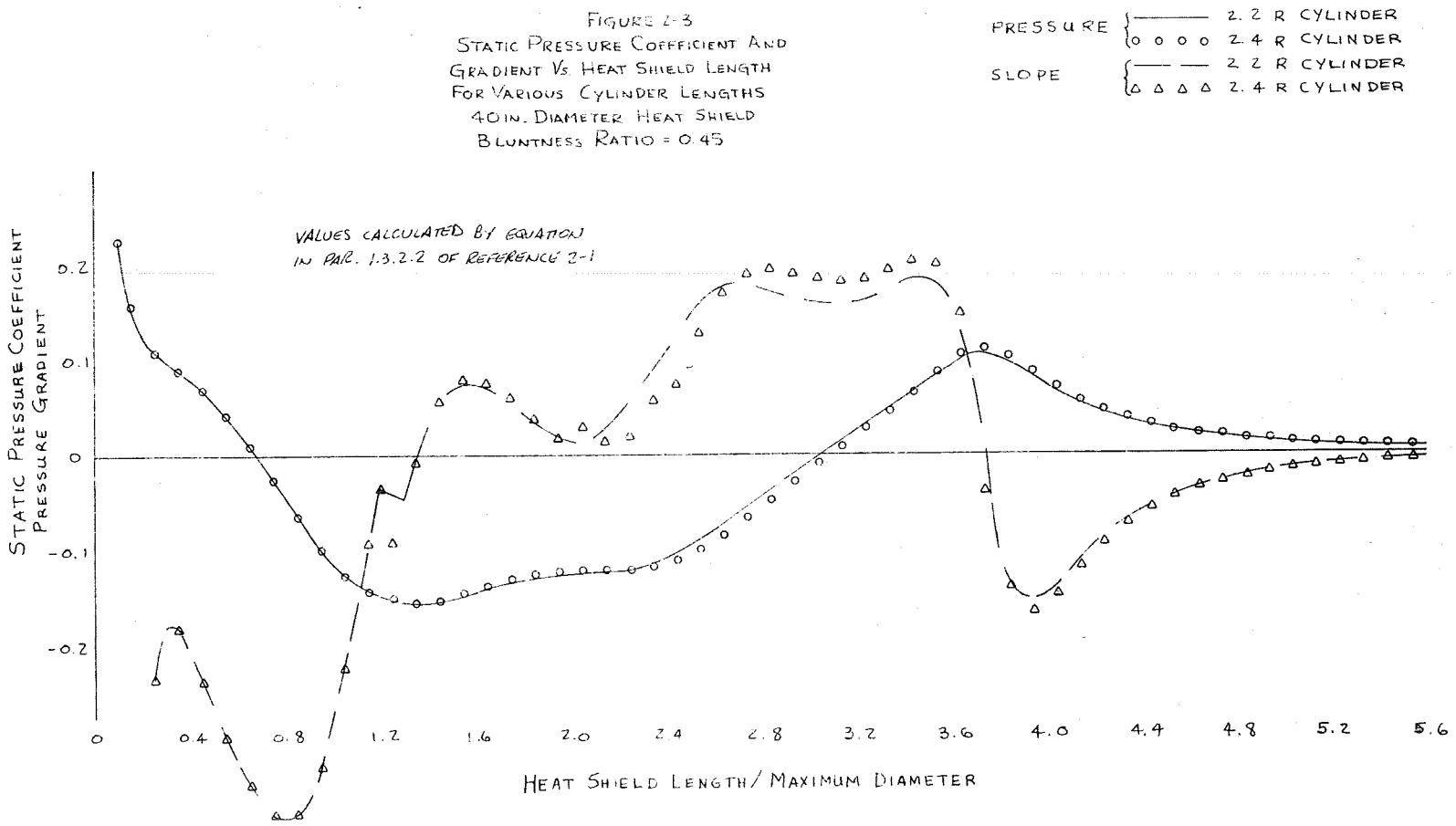

TABLE 2-1

CATALOG OF RUNS

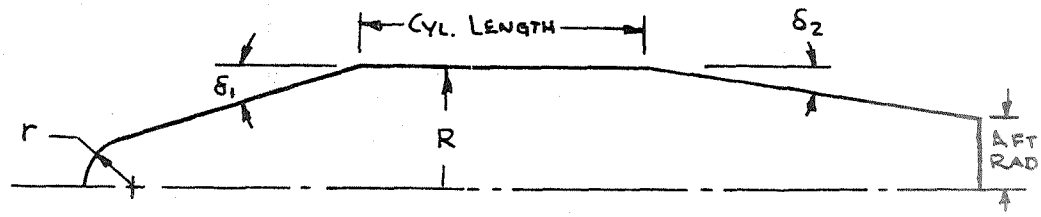

Run No.	Nose Sta.	r/R	H.S. Dia.-IN.	δ_1-Deg.	Cyld. Length	δ_2 *	Min. Pres. Coef.	Max. Slope
1		.454	40	24°	40"	A.R.	-.188	.177
2		.454	40	27°	40"	A.R.	-.197	.178
3		.454	40	30°	40"	A.R.	-.199	.180
4		.454	42	24°	42"	A.R.	-.192	.215
5		.454	42	27°	42"	A.R.	-.198	.215
6		.454	42	30°	42"	A.R.	-.204	.216
7		.454	44	24°	44"	A.R.	-.196	.266
8		.454	44	27°	44"	A.R.	-.202	.266
9		.454	44	30°	44"	A.R.	-.208	.268
10		.454	46	24°	46"	A.R.	-.200	.328
11		.454	46	27°	46"	A.R.	-.204	.328
12		.454	46	30°	46"	A.R.	-.209	.335
13		.35	40	24°	40"	A.R.	-.187	.177
14		.35	46	24°	46"	A.R.	-.195	.329
15		.55	40	24°	40"	A.R.	-.194	.177
16		.55	46	24°	46"	A.R.	-.203	.329
17		.454	40	15°	40"	A.R.	-.159	.170
18		.454	40	20°	40"	A.R.	-.178	.173
19		.454	46	15°	46"	A.R.	-.170	.325
20		.454	46	20°	46"	A.R.	-.181	.326
21		.454	46	7.5°	62"	15°	-.138	.860
22		.454	46	7.5°	1"	A.R.	-.153	.184
23		.454	46	7.5°	30"	A.R.	-.143	.224
24		.75	46	7.5°	23"	A.R.	-.157	.197
25		.75	46	7.5°	1"	A.R.	-.163	.190
26		.75	46	7.5°	46"	A.R.	-.136	.324
27	-47.45	.45	40	15°	2.2R	A.R.	-.157	.186
28	-47.45	.45	40	15°	2.4R	A.R.	-.155	.205
29	-39.1	.55	40	15°	2.0R	A.R.	-.162	.170
30	-39.1	.55	40	15°	2.2R	A.R.	-.159	.187
31	-39.1	.55	40	15°	2.4R	A.R.	-.157	.208
32	-33.13	.65	40	15°	2.0R	A.R.	-.166	.170
33	-33.13	.65	40	15°	2.2R	A.R.	-.164	.187
34	-33.13	.65	40	15°	2.4R	A.R.	-.161	.308
35	-53.86	.454	42	12.5°	1.8R	A.R.	-.155	.193
36	-53.86	.454	42	12.5°	2.0R	A.R.	-.152	.212
37	-53.86	.454	42	12.5°	2.2R	A.R.	-.149	.236
38	-46.25	.55	42	12.5°	1.8R	A.R.	-.157	.190
39	-46.25	.55	42	12.5°	2.0R	A.R.	-.154	.209
40	-46.25	.55	42	12.5°	2.2R	A.R.	-.152	.233

* A.R. - As required to get radius of 12.85 in. at base of heatshield.

TABLE 2-1 (Continued)

Run No.	Nose Sta.	r/R	H.S. Dia. -IN.	δ_1 -Deg.	Cyld. Length	δ_2 *	Min. Pres. Coef.	Max. Slope
41	-38.2	.65	42"	12.5°	1.8R	A.R.	-.163	.193
42	-38.2	.65	42"	12.5°	2.0R	A.R.	-.160	.212
43	-38.2	.65	42"	12.5°	2.2R	A.R.	-.158	.236
44	-73.06	.454	44"	10°	1.4R	A.R.	-.153	.195
45	-73.06	.454	44"	10°	1.6R	A.R.	-.148	.213
46	-73.06	.454	44"	10°	1.8R	A.R.	-.144	.231
47	-62.97	.55	44"	10°	1.4R	A.R.	-.154	.195
48	-62.97	.55	44"	10°	1.6R	A.R.	-.150	.213
49	-62.97	.55	44"	10°	1.8R	A.R.	-.146	.234
50	-52.49	.65	44"	10°	1.4R	A.R.	-.158	.195
51	-52.49	.65	44"	10°	1.6R	A.R.	-.154	.213
52	-52.49	.65	44"	10°	1.8R	A.R.	-.150	.234
53	-52.49	.454	46"	7.5°	1.0R	A.R.	-.151	.194
54	-52.49	.454	46"	7.5°	1.2R	A.R.	-.146	.210
55	-52.49	.454	46"	7.5°	1.4R	A.R.	-.141	.229
56	-52.49	.55	46"	7.5°	1.0R	A.R.	-.152	.195
57	-52.49	.55	46"	7.5°	1.2R	A.R.	-.147	.211
58	-52.49	.55	46"	7.5°	1.4R	A.R.	-.142	.230
59	-52.49	.65	46"	7.5°	1.0R	A.R.	-.155	.195
60	-52.49	.65	46"	7.5°	1.2R	A.R.	-.150	.210
61	-52.49	.65	46"	7.5°	1.4R	A.R.	-.145	.230
62	-28	Ogive	46"	-	1.0R	A.R.	-.17	.230
63	-39	Ogive	46"	-	1.0R	A.R.	-.156	.212
64	-42	Ogive	46"	-	1.0R	A.R.	-.152	.202
65	-25	.454	34	22	48.3"	A.R.	-.163	.169
66	-38.2	.65	42	12.5	7.8R	A.R.	-.157	.279

* A. R. - As required to get radius of 12.85 in. at base of heatshield.

TABLE 2-1 (Concluded)

Run No.	Dia.	r/R	δ_1 -Deg.	Cyld. Length	Aft Rad.-In.	Min. Pressure Coef.	Max. Slope
67	42	.6	12.5	33.2"	13.72	-.1575	.2155
68	40	.55	15	33.2"	12.85	-.1647	.2224
69	40	.55	15	33.2"	14.0	-.1606	.1760
70	40	.55	15	33.2"	15.0	-.1577	.1346
71	44	.65	10	32.12"	14.0	-.1511	.2337
72	44	.65	10	32.12"	15.0	-.1476	.18788
73	44	.65	10	32.12"	16.0	-.14388	.1366
74	46	.70	7.5	24.2"	14.0	-.1503	.274197
75	46	.70	7.5	24.2"	15.0	-.1445	.1960
76	46	.70	7.5	24.2"	16.0	-.1400	.1480
77	42	.6	12.5	33.2"	14.0	-.1566	.2028
78	42	.6	12.5	33.2"	14.5	-.1555	.1878
79	42	.6	12.5	40"	14	-.1516	.223
80	42	.6	12.5	40"	15	-.1489	.1770
81	42	.6	12.5	40"	16	-.1462	.1253
82	40	.55	15.0	40"	13.5	-.158	.2115
83	40	.55	15.0	40"	14.0	-.1576	.1965
84	40	.55	15.0	40"	14.5	-.1553	.1676

2.2.2 Aerodynamic Characteristics

The variations of heatshield configuration consisted of perturbations of the sphere, cone, cylinder and reverse frustrum components. For a given heatshield diameter and Mach number, the primary contributions to C_{N_α} and C_{D_o} will come from the sphere-cone components. Thus, for the parametric study, the sphere radius and cone angle were varied as the primary criteria to define a heatshield configuration. Variations of drag, payload weight penalties, and nose cone C_{N_α} with heatshield configuration were calculated. First stage aerodynamic characteristics of each heatshield diameter configuration were estimated using the Algol III wind tunnel data.

2.2.2.1 Nose Cone Lift and Drag

As cone angle decreases with a constant conical blunting ratio, the cone length increases, providing increased C_{N_α}. This effect is relieved by increasing the blunting ratio from the current Scout value r/R = .454, to shorten the blunted cone. Increasing the blunting ratio increases the drag, with a resulting performance penalty. The sphere-cone C_{N_α} were obtained from Reference 2-2 for high supersonic Mach numbers and are presented in Figure 2.2.2.1-1 for the configurations initially considered in the parametric study. Sphere-cone pressure drag coefficients were evaluated for selected configurations at M_∞ = 3.00 and 4.06 from Reference 2-3. These data are presented in Figures 2.2.2.1-2 and -3.

FIGURE 2.2.2.1-1

SPHERE-CONE NORMAL FORCE DERIVATIVE

$S_m = 5.25\ FT^2$

SUPERSONIC

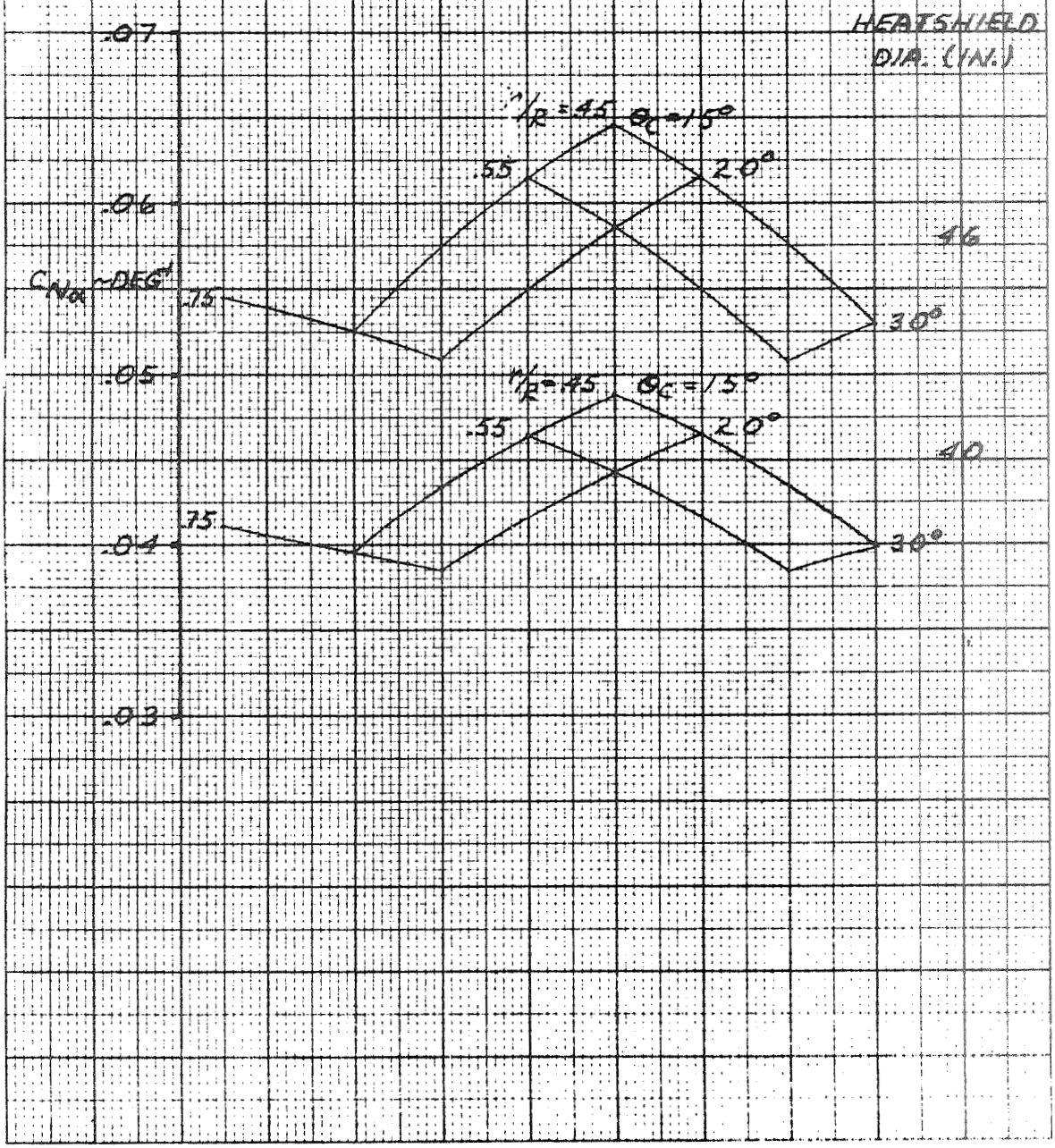

FIGURE 2.2.2.1-2
SPHERE-CONE PRESSURE DRAG COEFFICIENT

$M_\infty = 3.00$

$S_T = 5.25\ FT^2$

$r/R = .454$

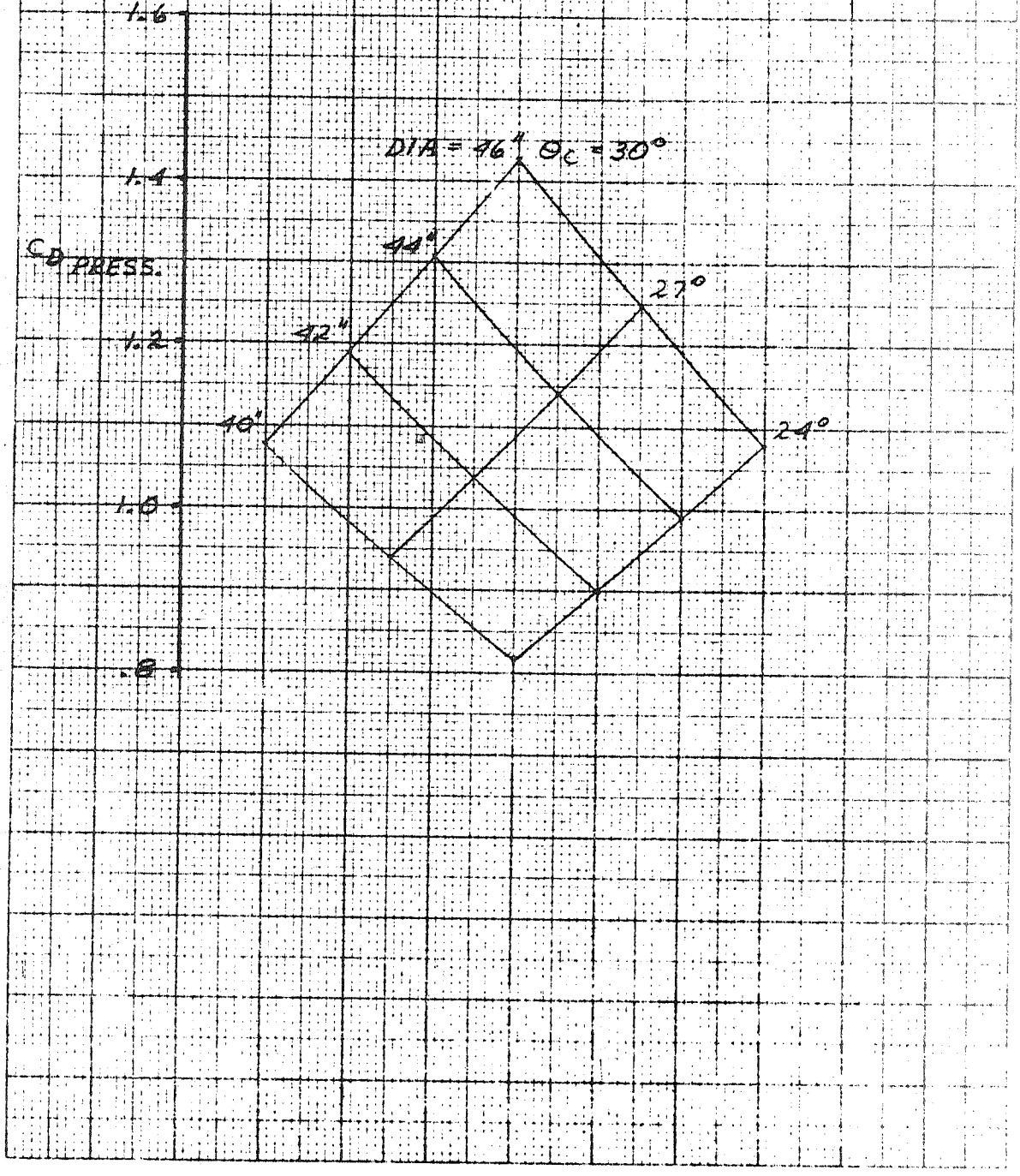

FIGURE 2.2.2.1-3
SPHERE-CONE PRESSURE DRAG COEFFICIENT

$M_\infty = 4.06$

$S_R = 5.25\ FT^2$

$r/R = .454$

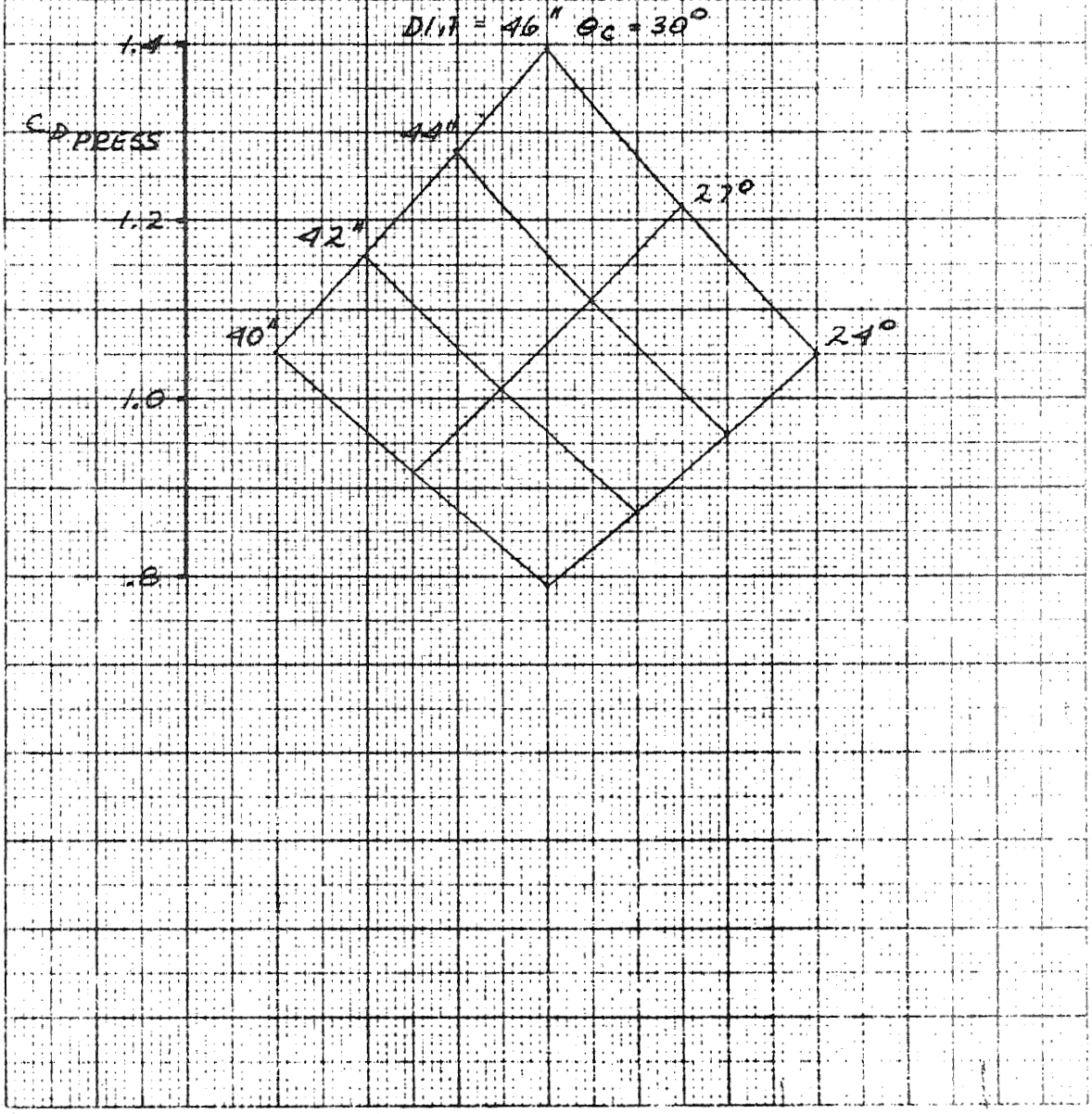

A perturbation analysis was conducted to evaluate the first stage velocity losses for the various configurations as a function of C_{D_α}. Existing Algol III drag data, Reference 2-4, was modified by the incremental drag due to the differences in the sphere-cone configurations at $M_\infty = 3.00$ and 4.03. The referenced drag data are presented in Figure 2.2.2.1-4, and the first stage drag data for the other heatshield configurations are presented in Figures 2.2.2.1-5 through -16. Velocity loss data derived from the latter C_{D_o} data are presented in Figures 2.2.2.1-17 and -18. These curves present the first stage velocity loss due to aerodynamic drag and may be compared to a velocity loss of 675 ft./sec. for the current 34 inch heatshield.

In a 600 nautical mile circular orbit, a loss of 100 ft./sec. in second stage ignition velocity requires a decrease of about 7.25 pounds of payload weight to achieve the desired orbit. Therefore, the velocity losses shown in Figures 2.2.2.1-17 and -18 can be related to decrease in payload weight. Variation of payload weight penalty and nose cone C_{N_α} with blunting ratio is shown in Figure 2.2.2.1-19 for 40 and 46 inch heatshields.

FIGURE 2.2.2.1-4
ZERO LIFT DRAG COEFFICIENT
44 IN. DIA. ALGOL III
34 IN. DIA. HEATSHIELD
NOSE @ STA -25.

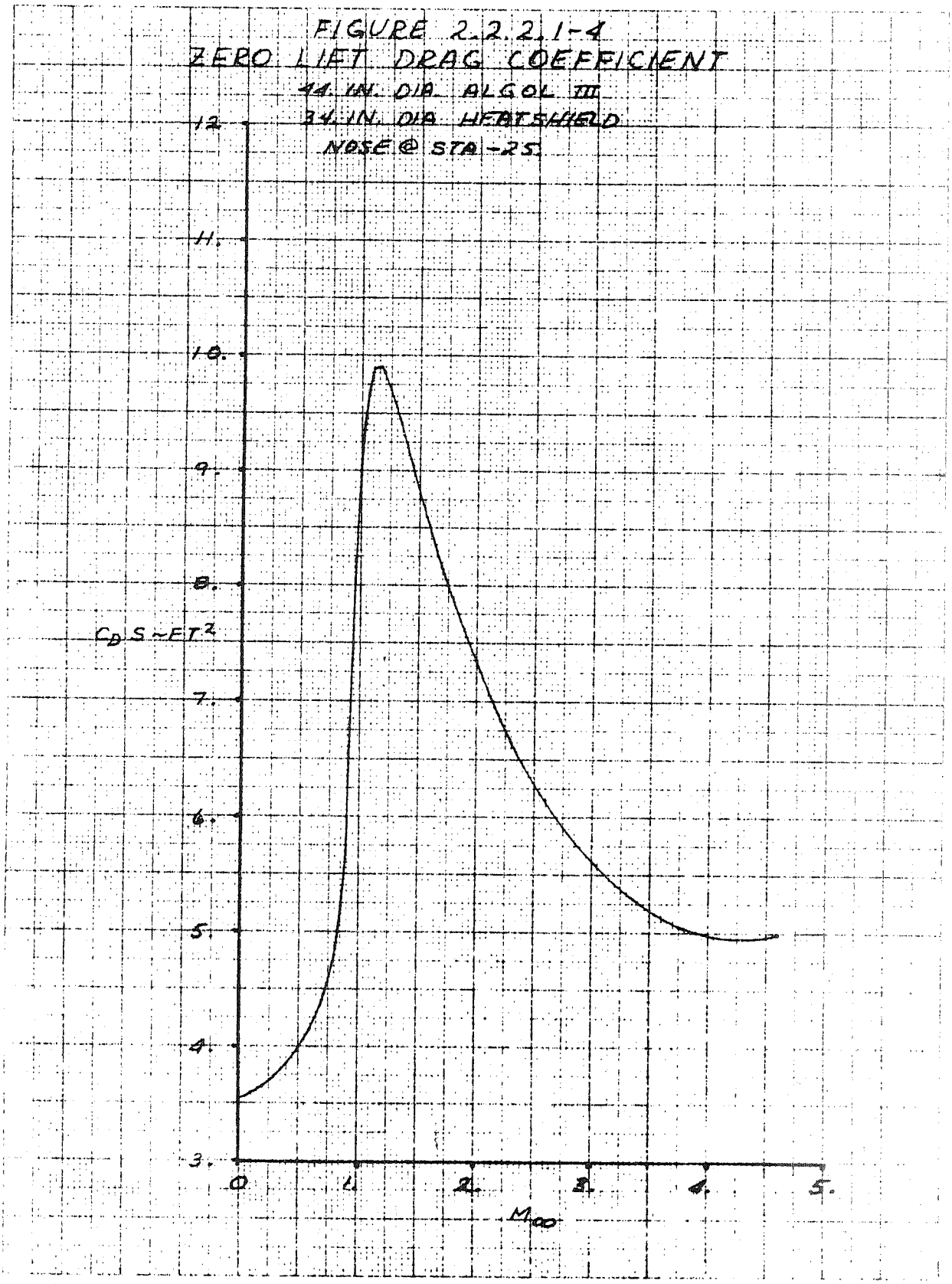

FIGURE 2.2.21-5
ZERO LIFT DRAG COEFFICIENT
$r/R = .454$ $\theta_c = 30°$

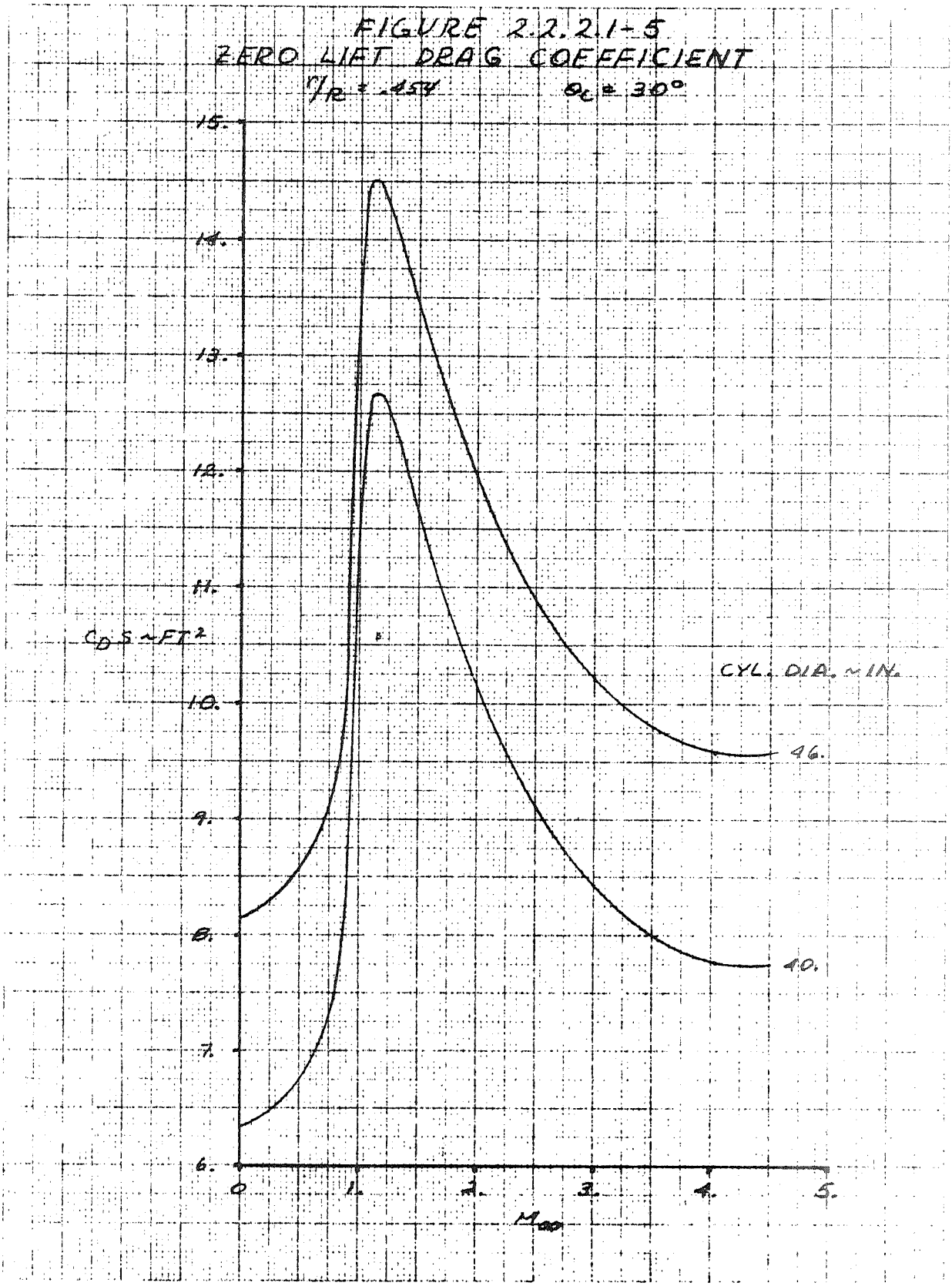

FIGURE 2.2.2.1-6
ZERO LIFT DRAG COEFFICIENT
$R_N/R_e = .454$ $\alpha_c = 2\alpha$

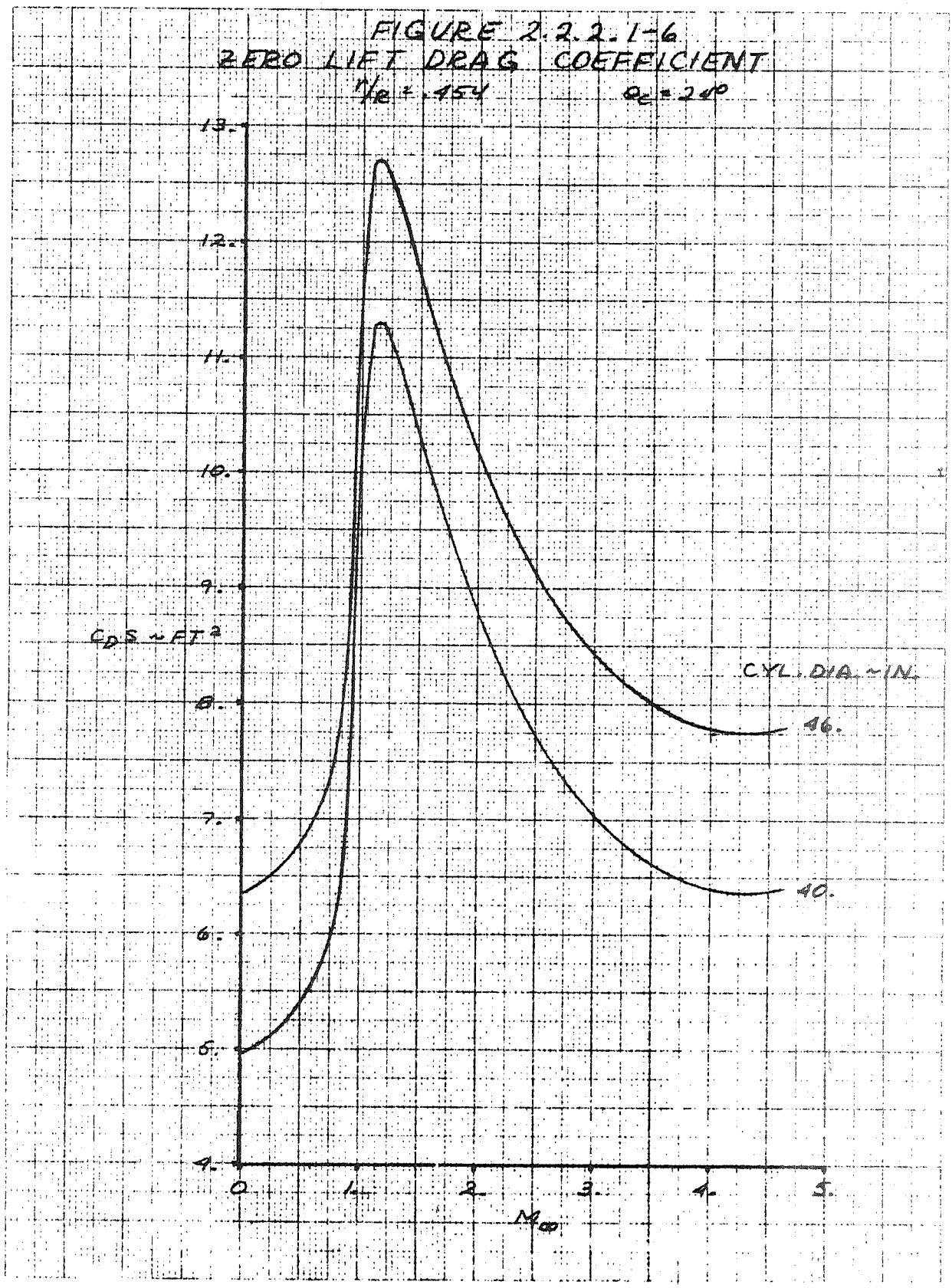

FIGURE 2.2.2.1-7
ZERO LIFT DRAG COEFFICIENT
$R/L = .454$ $\theta_c = 20°$

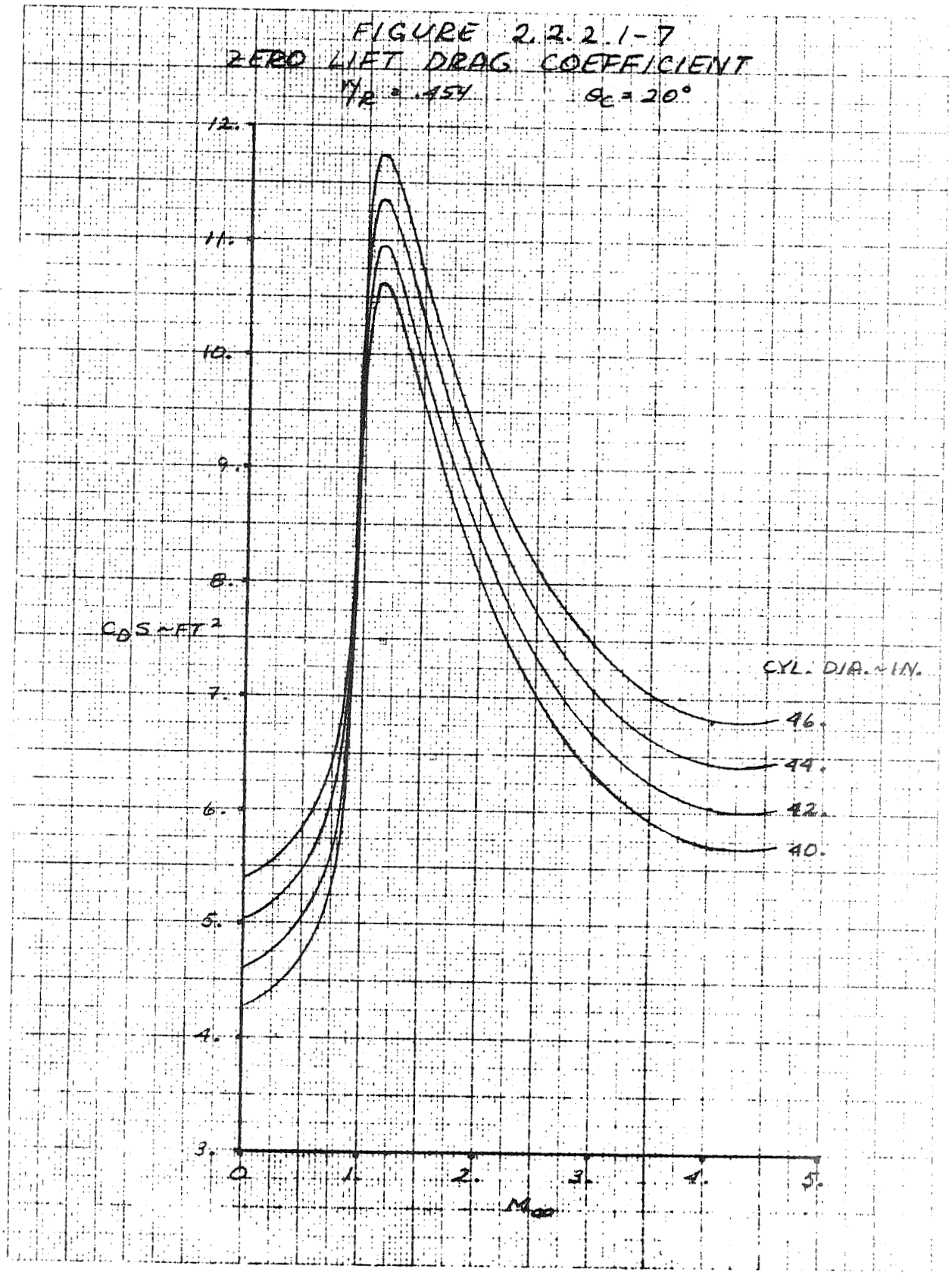

FIGURE 2.2.2.1-8
ZERO LIFT DRAG COEFFICIENT
$r/_R = .454$ $\alpha_c = 15°$

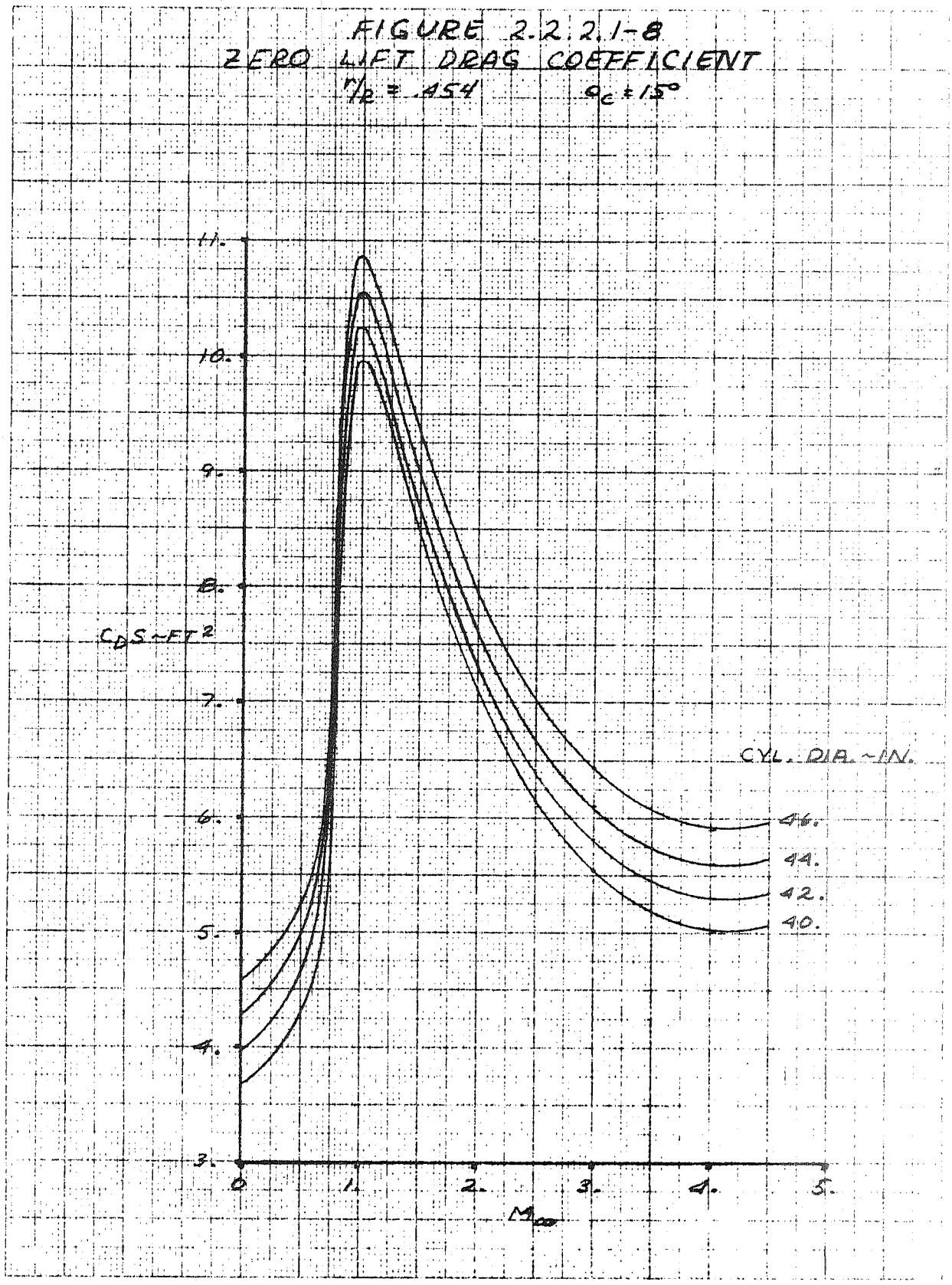

FIGURE 2.2.2.1-9
ZERO LIFT DRAG COEFFICIENT
$t/c = .454$ $\theta_c = 2.5°$

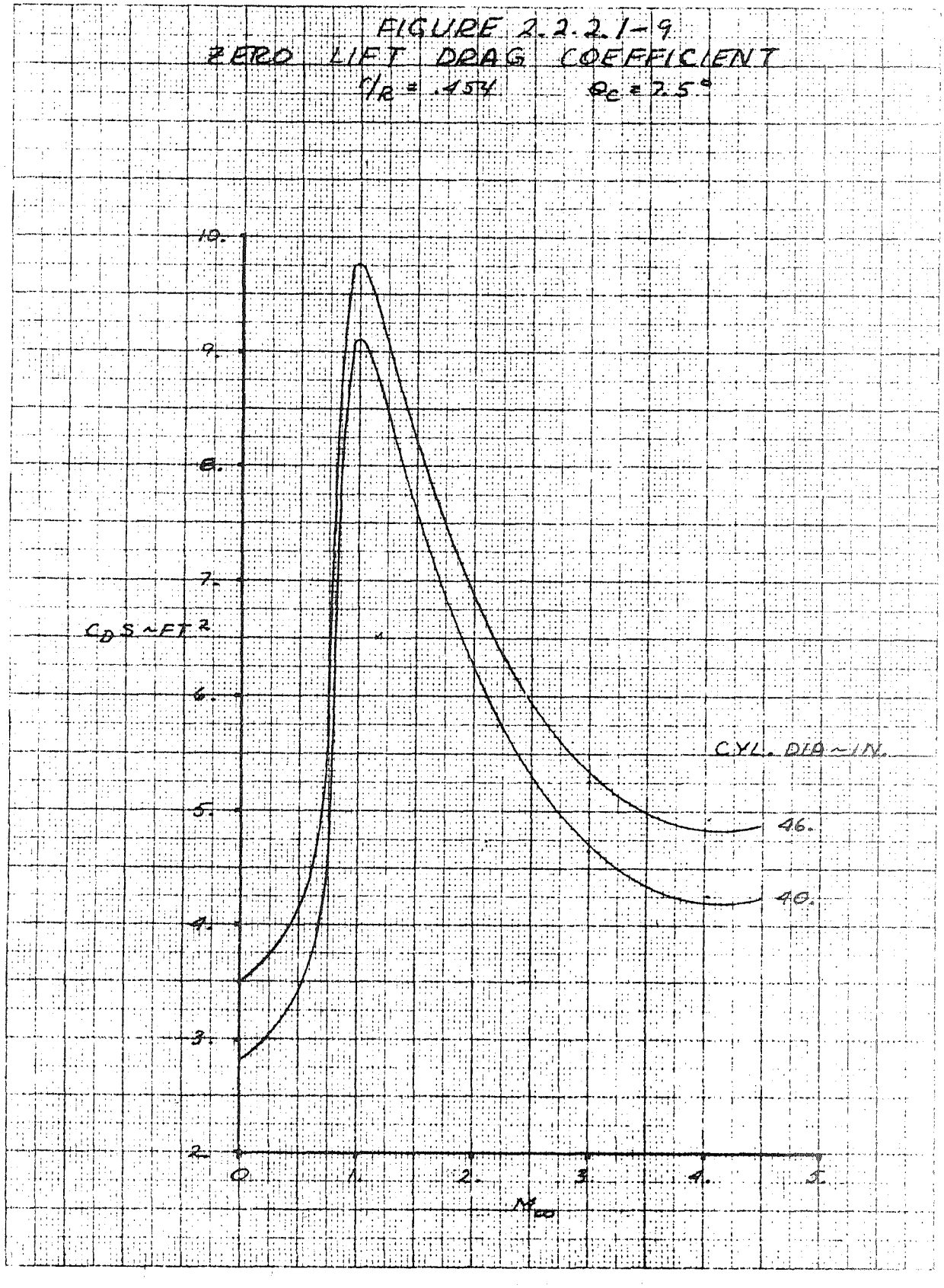

FIGURE 2.2.2.1-10
ZERO LIFT DRAG COEFFICIENT
$r/R = .55$ $\Phi_c = 30°$

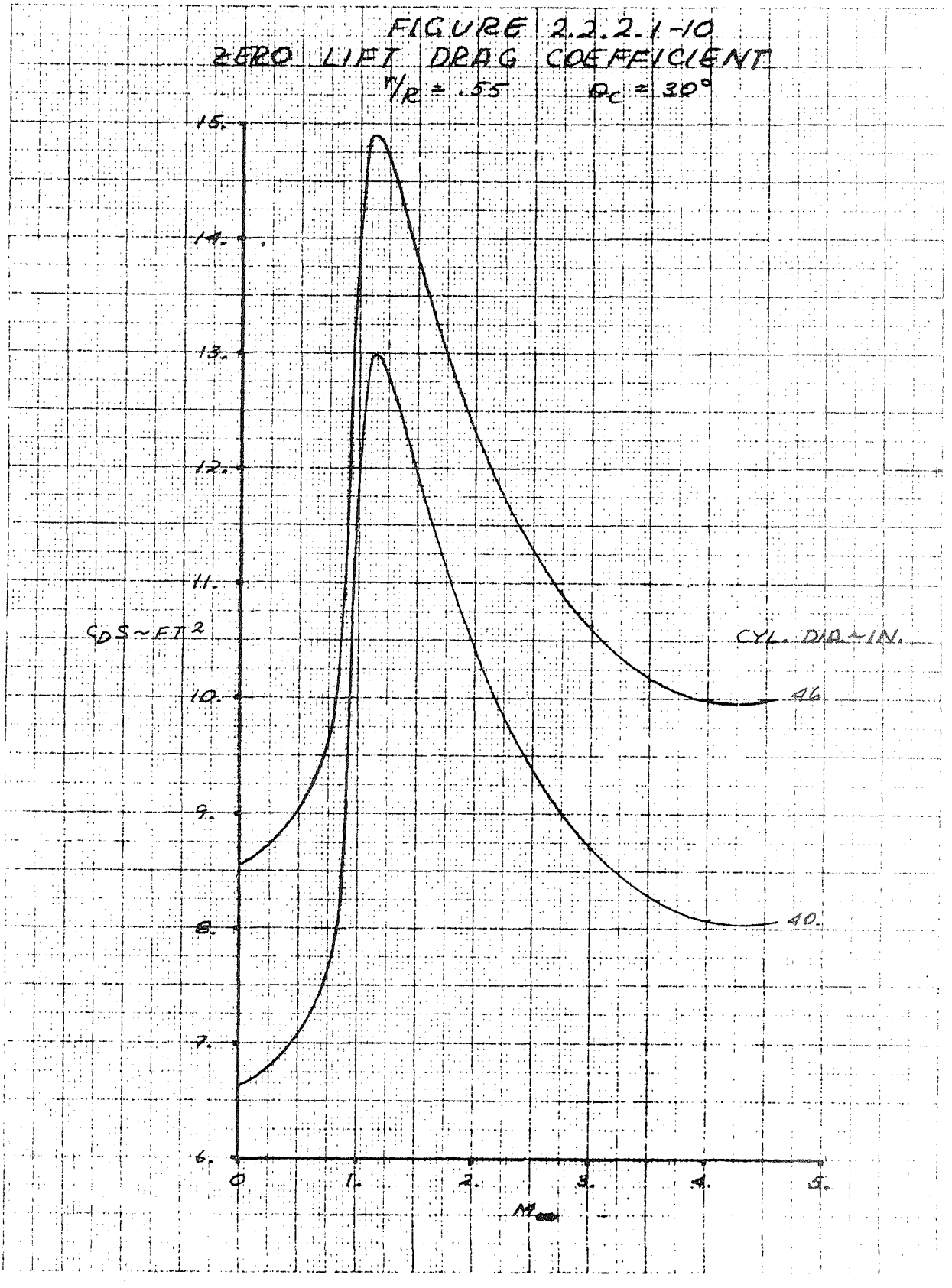

FIGURE 2.2.2.1-11
ZERO LIFT DRAG COEFFICIENT
$r/R = .55$ $\alpha_L = 2.1°$

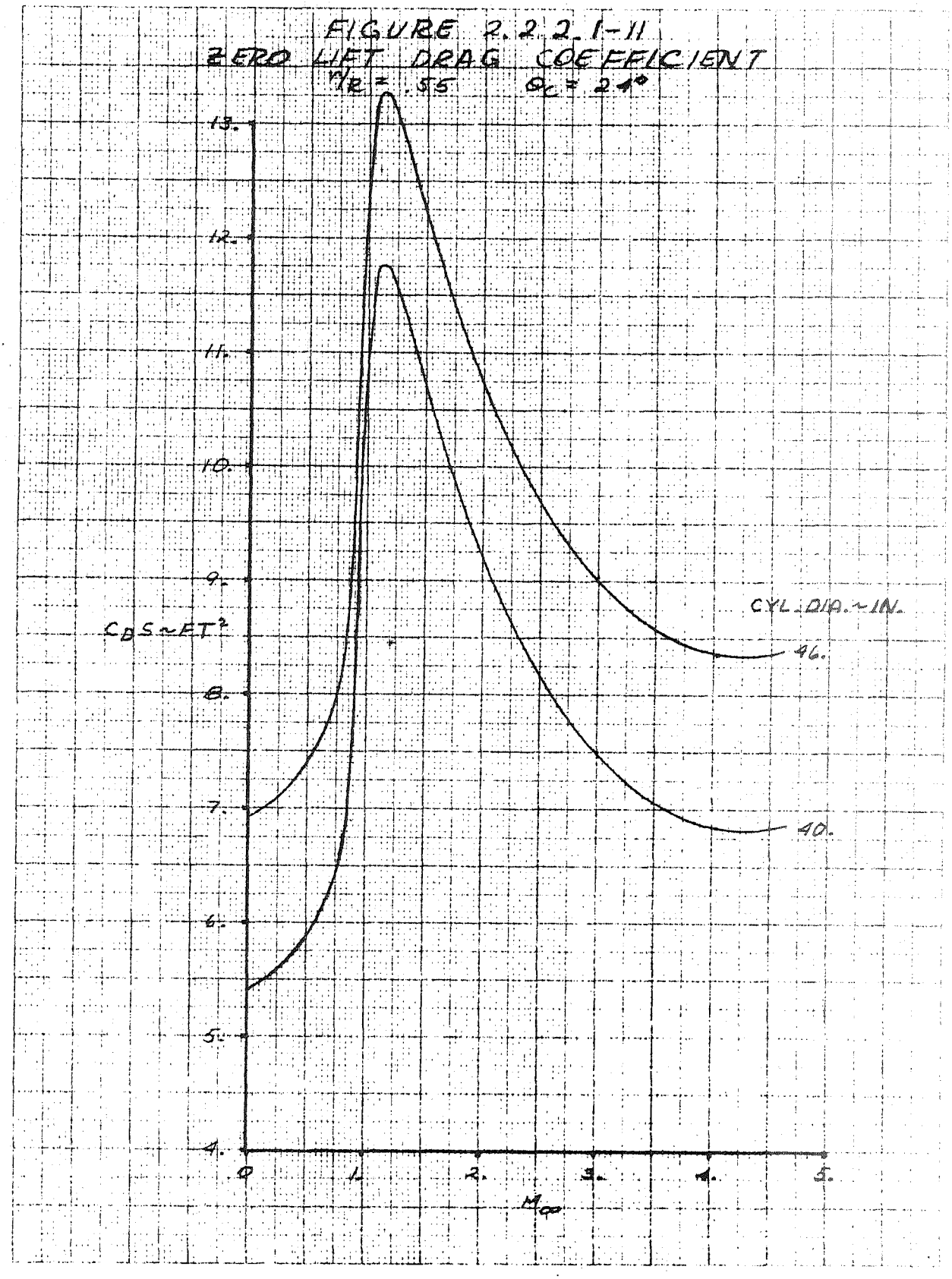

FIGURE 2.2.2.1-12
ZERO LIFT DRAG COEFFICIENT
$r/R = .55 \quad \theta_c = 20°$

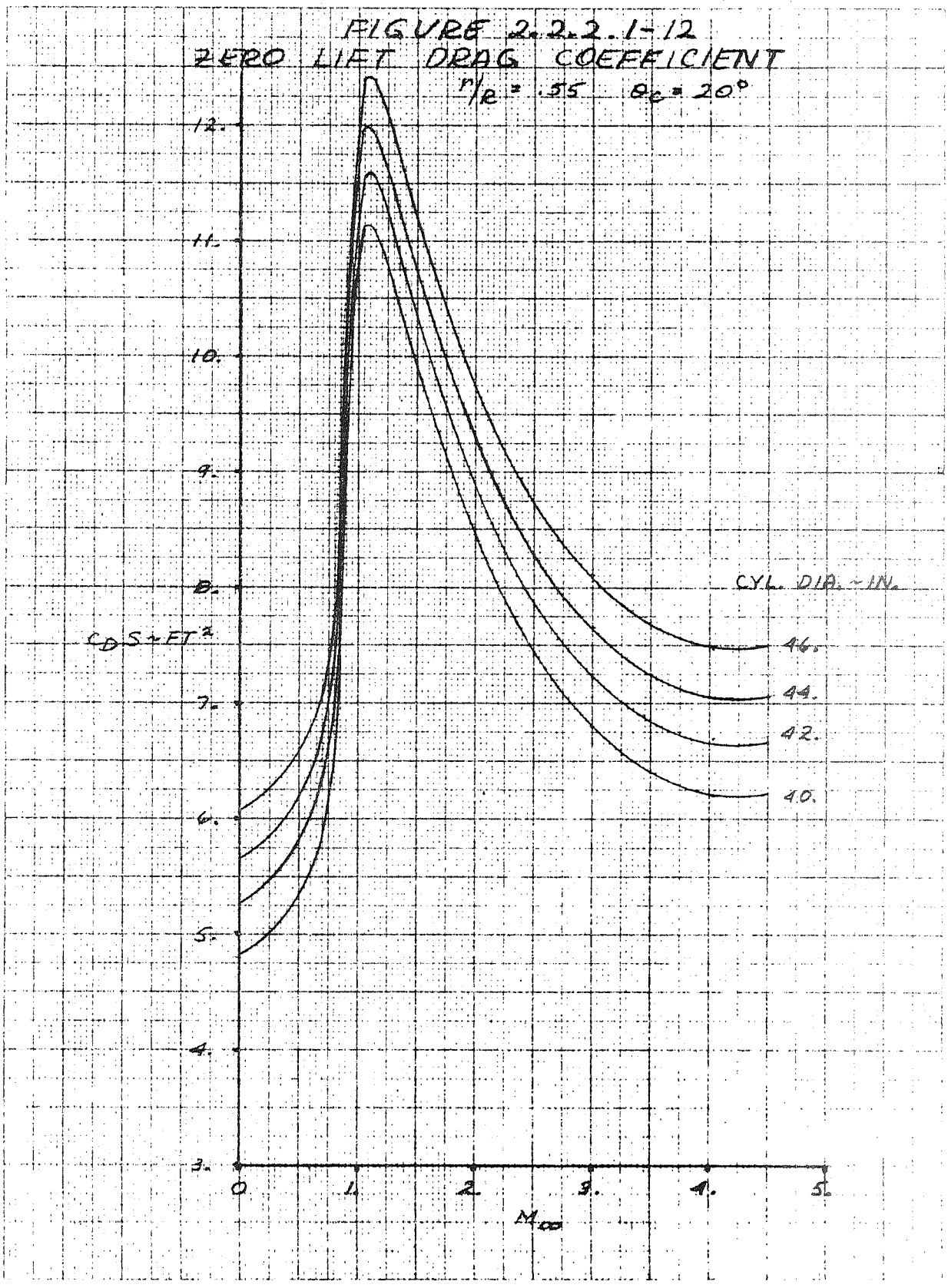

FIGURE 2.2.2.1-13
ZERO LIFT DRAG COEFFICIENT
$r/\ell = .55$ $\theta_c = 15^\circ$

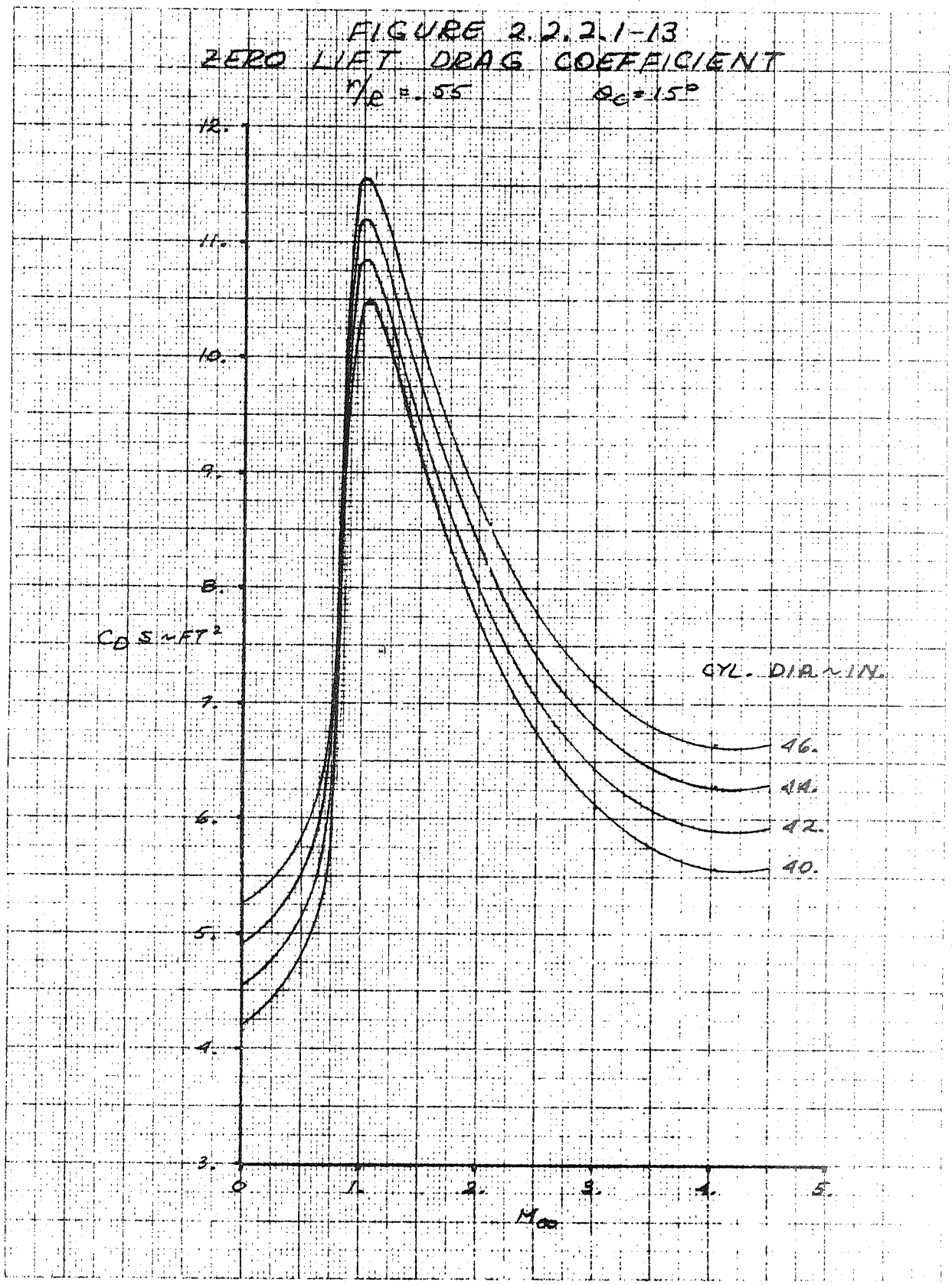

FIGURE 2.2.2.1-14
ZERO LIFT DRAG COEFFICIENT
$r/R = .55$ $\theta_c = 2.5°$

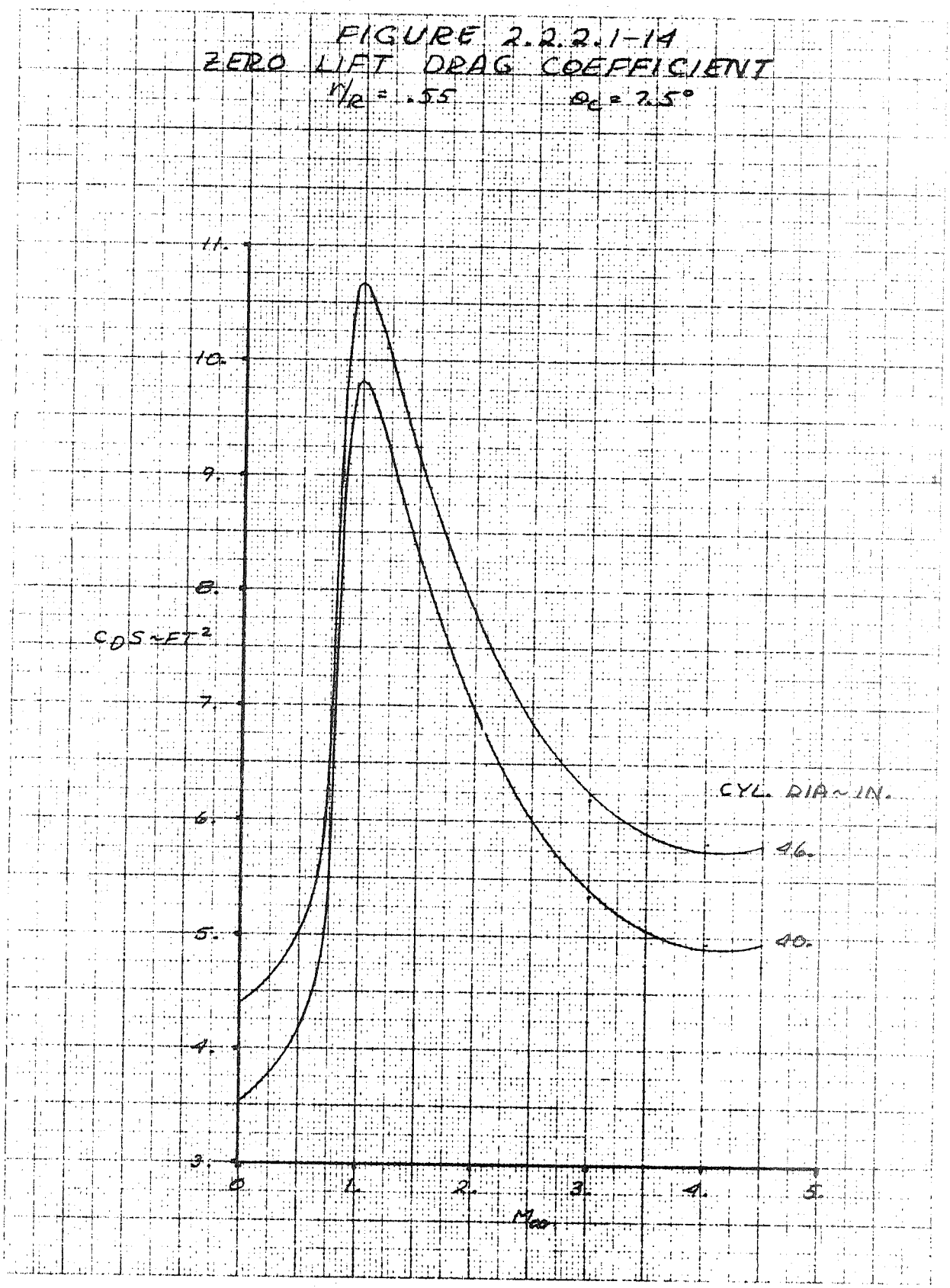

FIGURE 2.2.2.1-15
ZERO LIFT DRAG COEFFICIENT
$W_R = .75$ $\Theta_c = 15°$

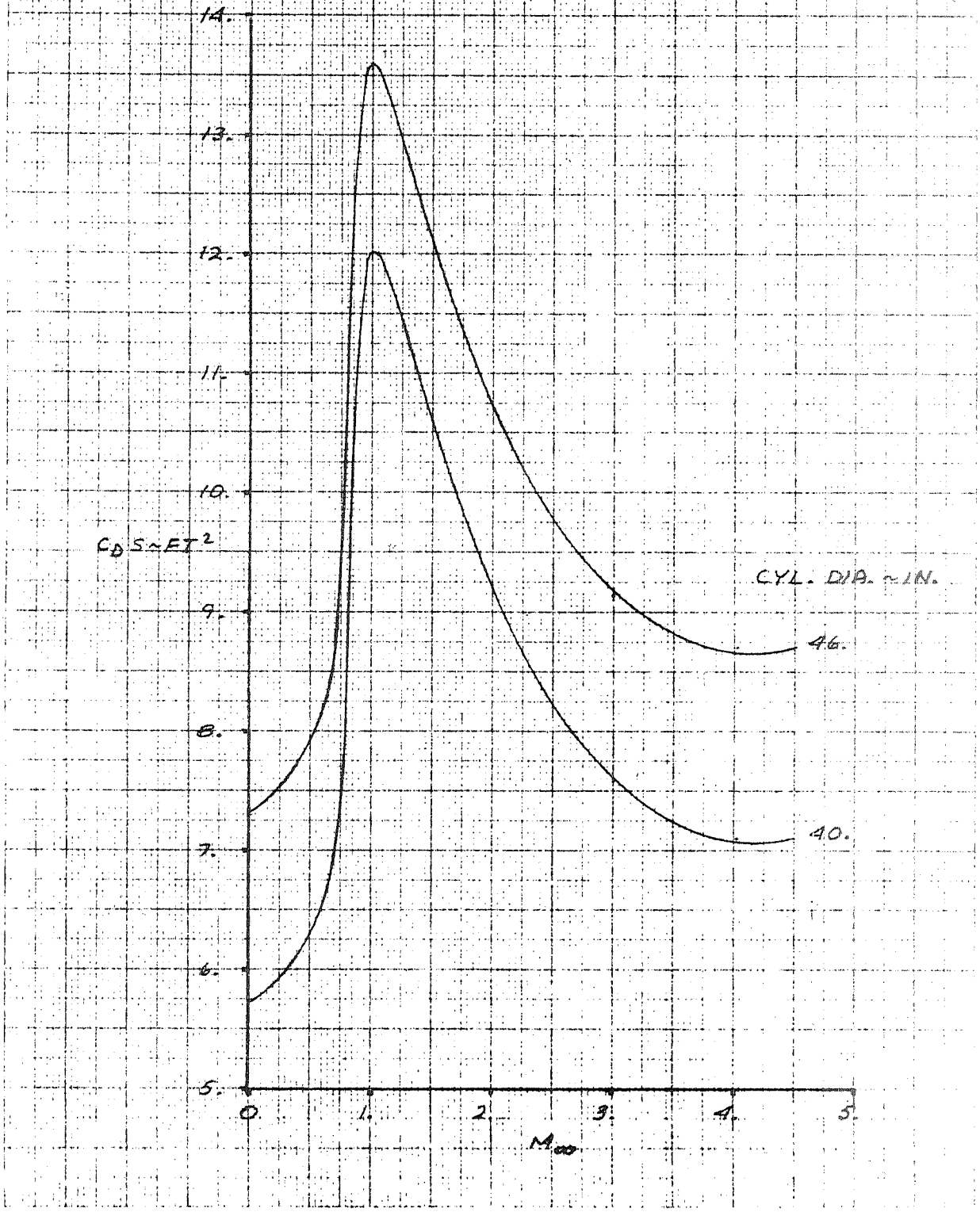

FIGURE 2.2.2.1-16
ZERO LIFT DRAG COEFFICIENT
$r/_R = .75$ $\Phi_C = 2.5°$

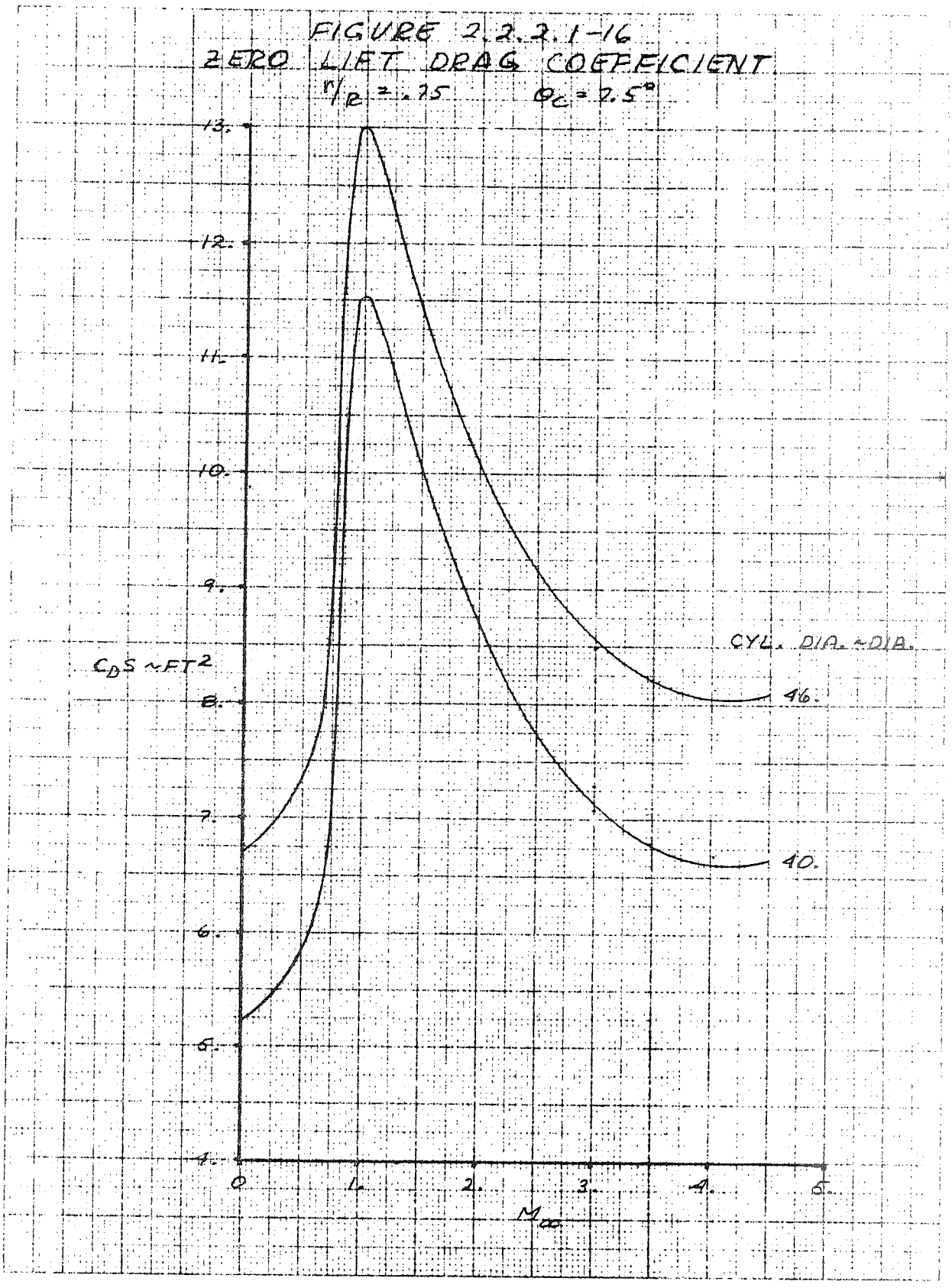

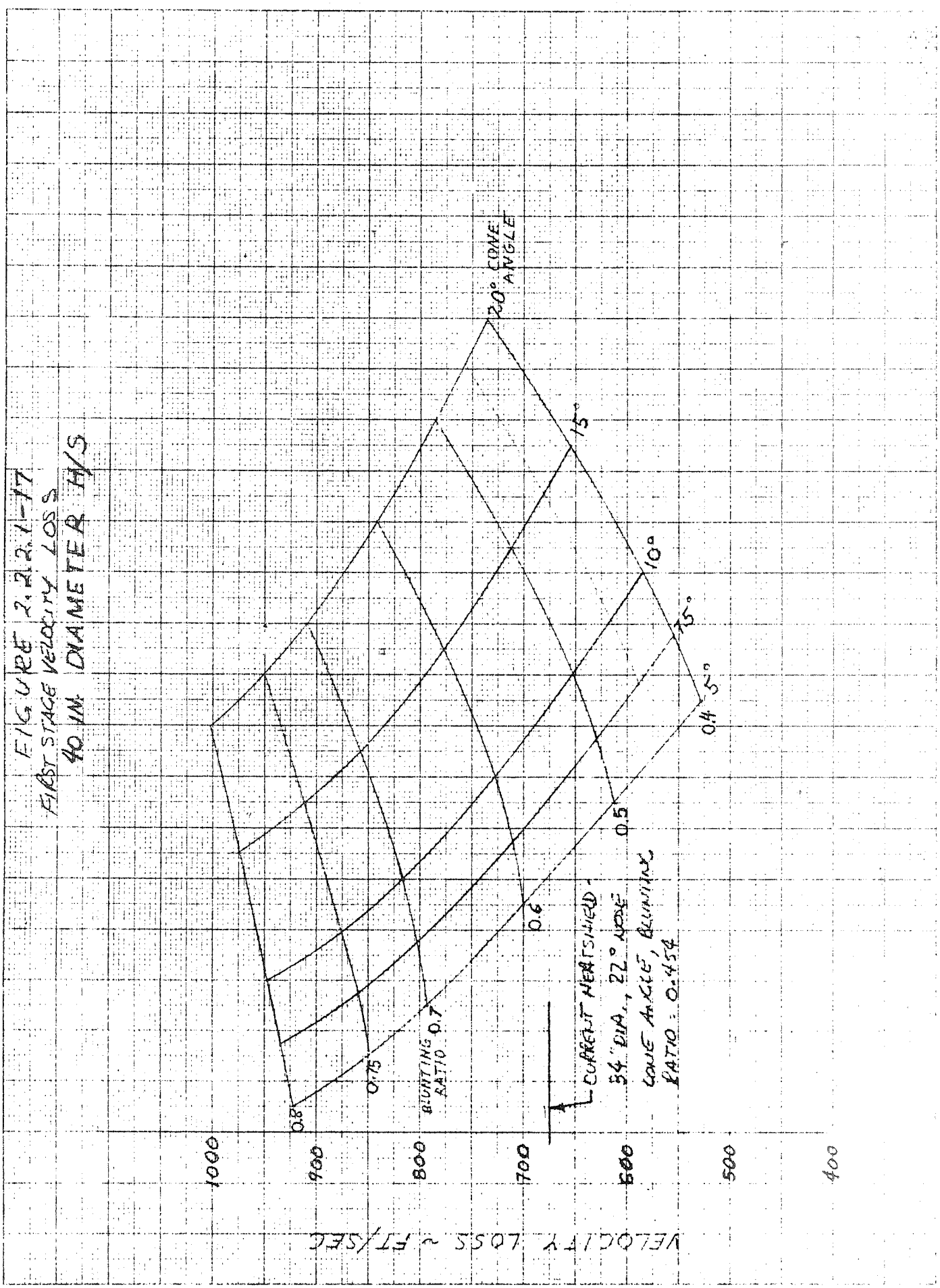

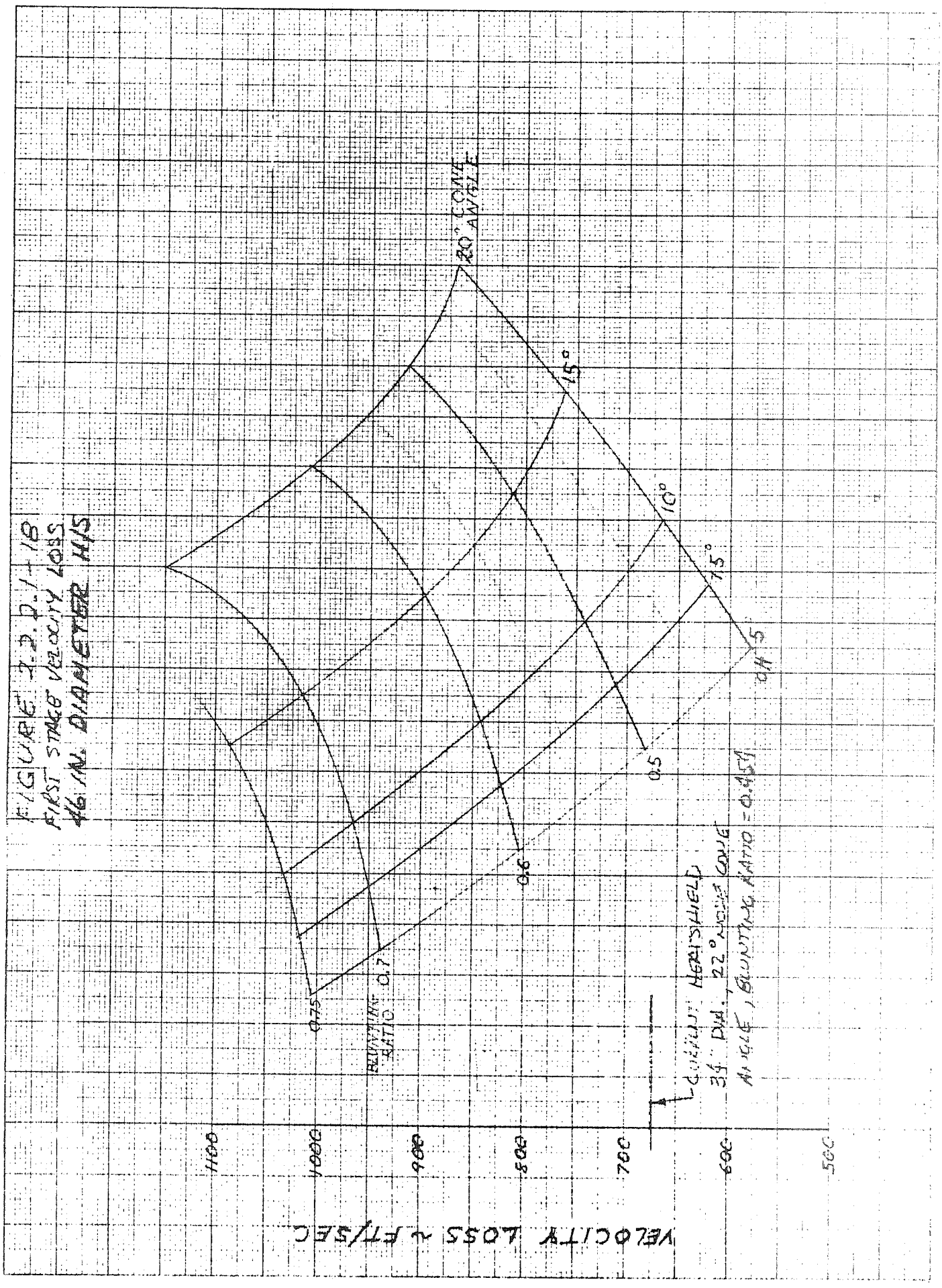
F.I.G. INLET T.P.D. + I.B.
FIRST STAGE VELOCITY LOSS
46 IN. DIAMETER H/S
VELOCITY LOSS + FT/SEC
1100
1000
900
800
700
600
500
20° CONE ANGLE
15°
10°
7.5°
5°
0.5
0.6
0.7
0.75
RUNNING RATIO
Centerline Horizontal
34° Dia. 22° Incidence Curve
Angle of Blunting Ratio = 0.45M

FIGURE 2.2.2.1-19
EFFECT OF BLUNTING RATIO

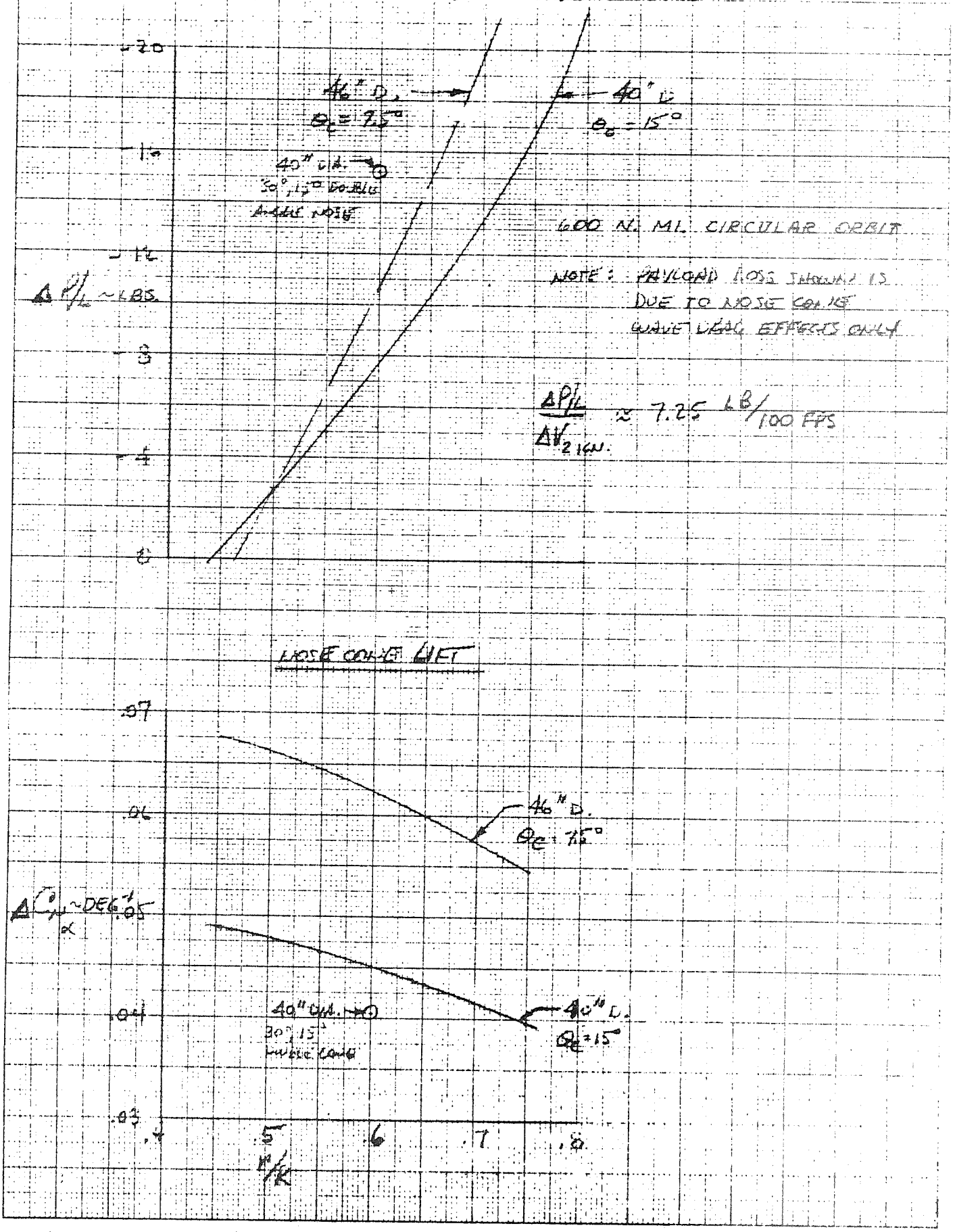

2.2.2.2 Wind Tunnel Data

A limited analysis of the NASA LRC wind tunnel data from the subsonic test, test 467, the supersonic test, project 811, and the fin effectiveness test, project 831, was performed using the configuration component buildup technique. Mechanically plotted data supplied by LRC was used with data plotted manually by MSD-T. Considering the limitations of the heatshield study, only pitch plane wind tunnel data were analyzed.

The basic wind tunnel model configurations, without protuberances, are presented in Figure 2.2.2.2-1.

Figure 2.2.2.2-2 presents complete configuration C_{N_α} wind tunnel data for two heatshield diameters, with estimates for the current and 44" diameter Algol motors. The estimated and wind tunnel data for the 34" diameter heatshield with the 44" diameter Algol show excellent agreement. Estimates for the current Scout configuration are included for comparison.

Estimated C_{m_α} and wind tunnel data are presented in Figure 2.2.2.2-3 for the same configurations. Good agreement exists for the supersonic Mach numbers, but subsonically, the estimated centers of pressure apparently were too far aft. This is shown in Figure 2.2.2.2-4, which presents estimated and experimental centers of pressure. The estimate for the current Scout configuration is included for comparison.

The incremental effect of the fins is presented in Figure 2.2.2.2-5, and C_{N_α} shows good agreement, except at $M_\infty = 1.0$. The apparent large discrepancies in center of pressure at the higher supersonic Mach numbers is probably due to data inaccuracies and the technique used to evaluate this quantity.

FIGURE 2.2.2.2-1
WIND TUNNEL MODEL CONFIGURATIONS
ALGOL III

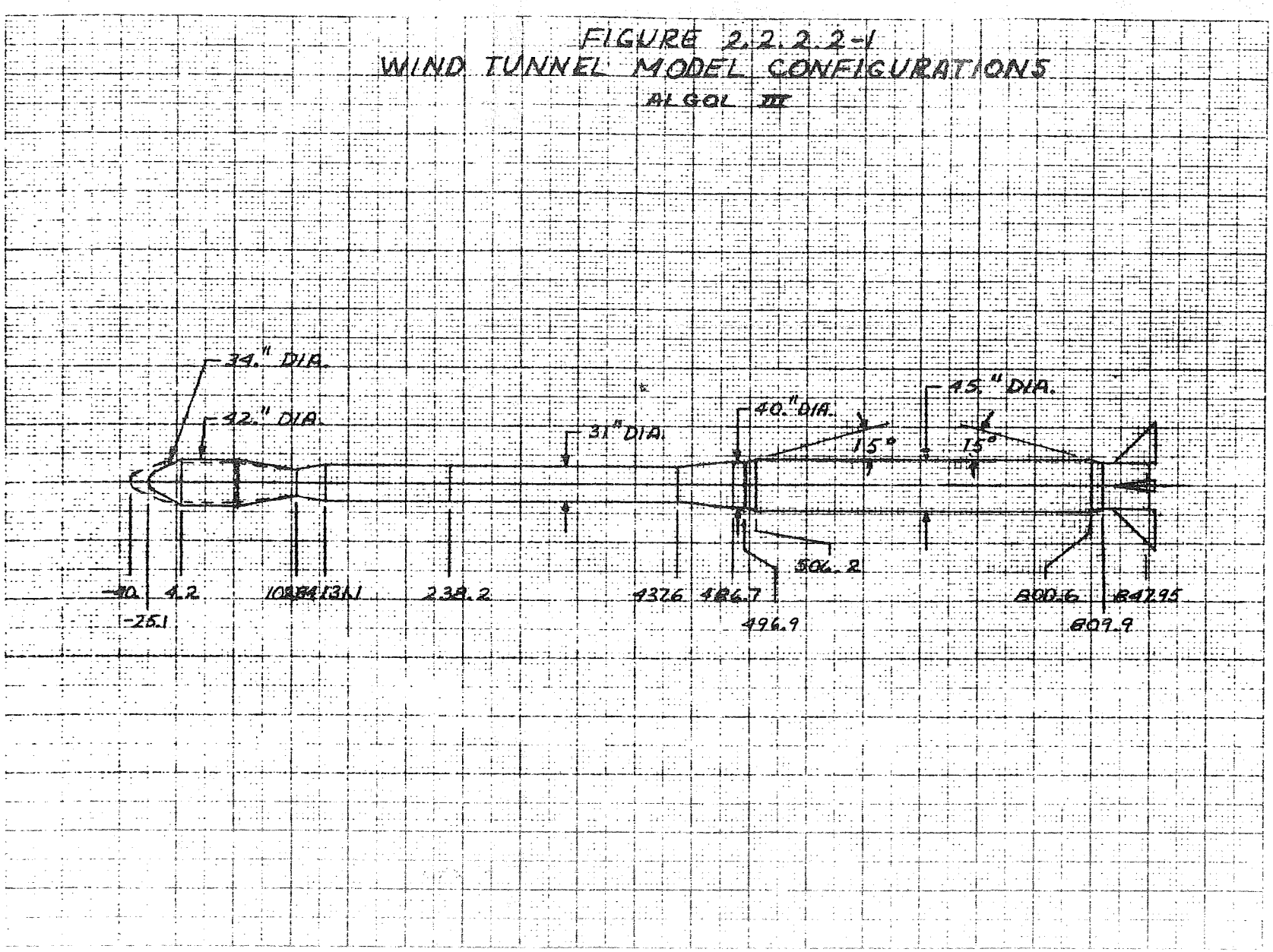

FIGURE 2.2.2.2.2-2
NORMAL FORCE COEFFICIENT DERIVATIVE

COMPLETE W.T. MODEL

$\phi = 0$ $\delta = 0$

$S_M = 5.25$ FT.^{2}

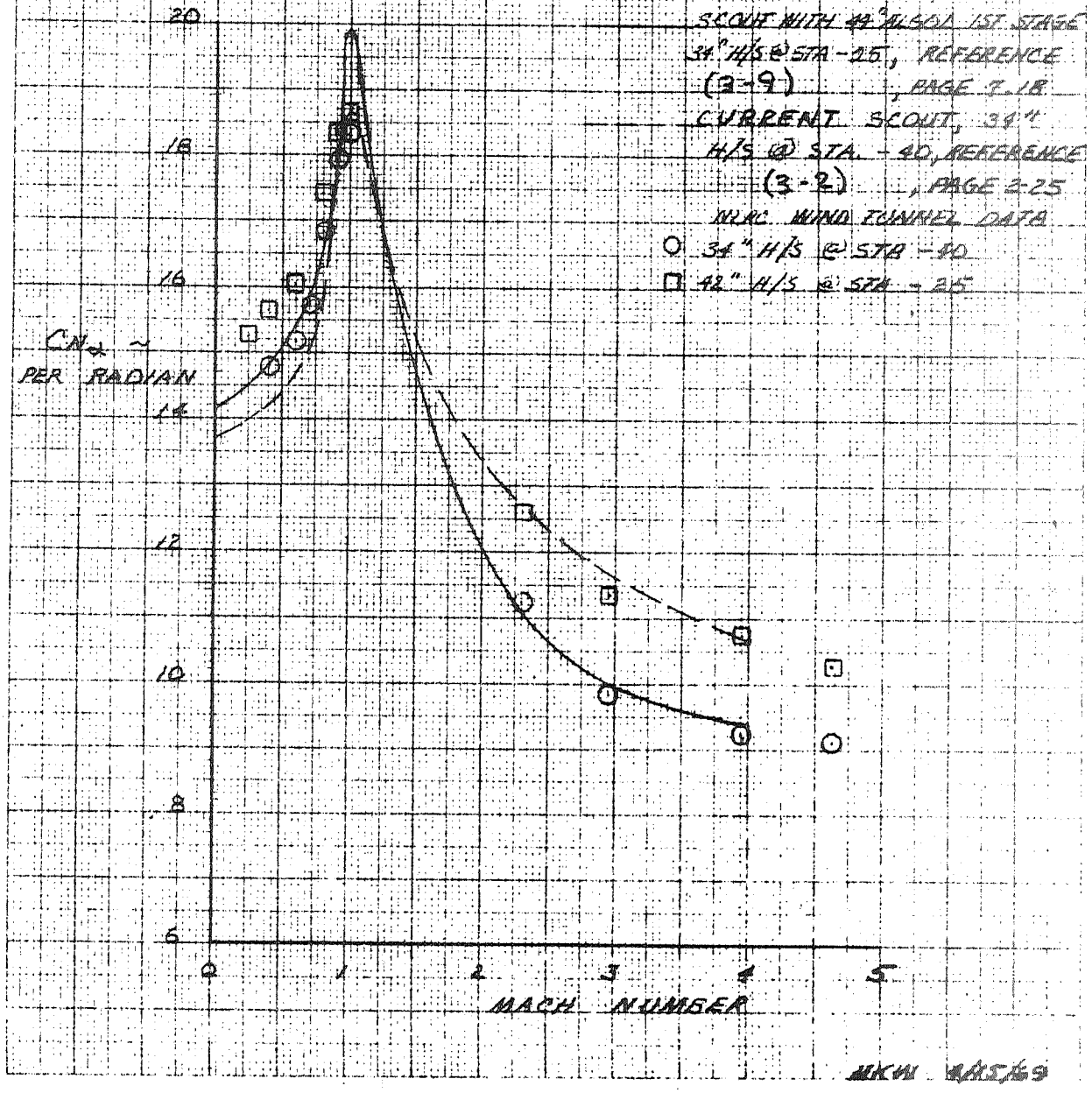

MKW MAS/69

FIGURE 2.2.2.2-3
PITCHING MOMENT COEFFICIENT DERIVATIVE
COMPLETE W.T. MODEL
$\phi = 0$ $\delta = 0$
$S_\pi = 5.25\ FT^2$ $l_B = 2.58\ FT$
CG @ STA 534.4

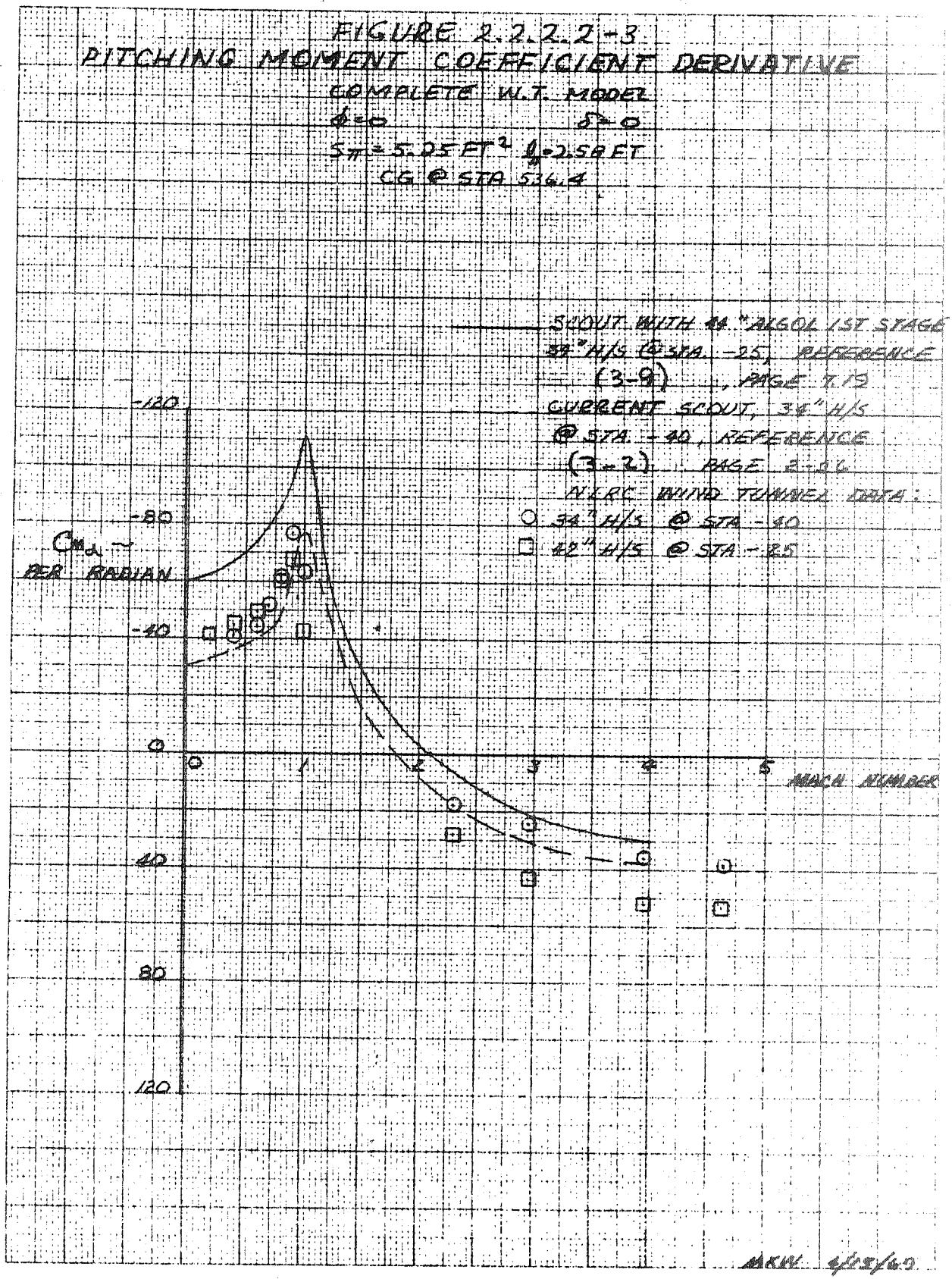

MKW 4/25/69

FIGURE 2.2.2.2-4
CENTER OF PRESSURE
COMPLETE W.T. MODEL
$\phi = 0$ $\delta = 0$

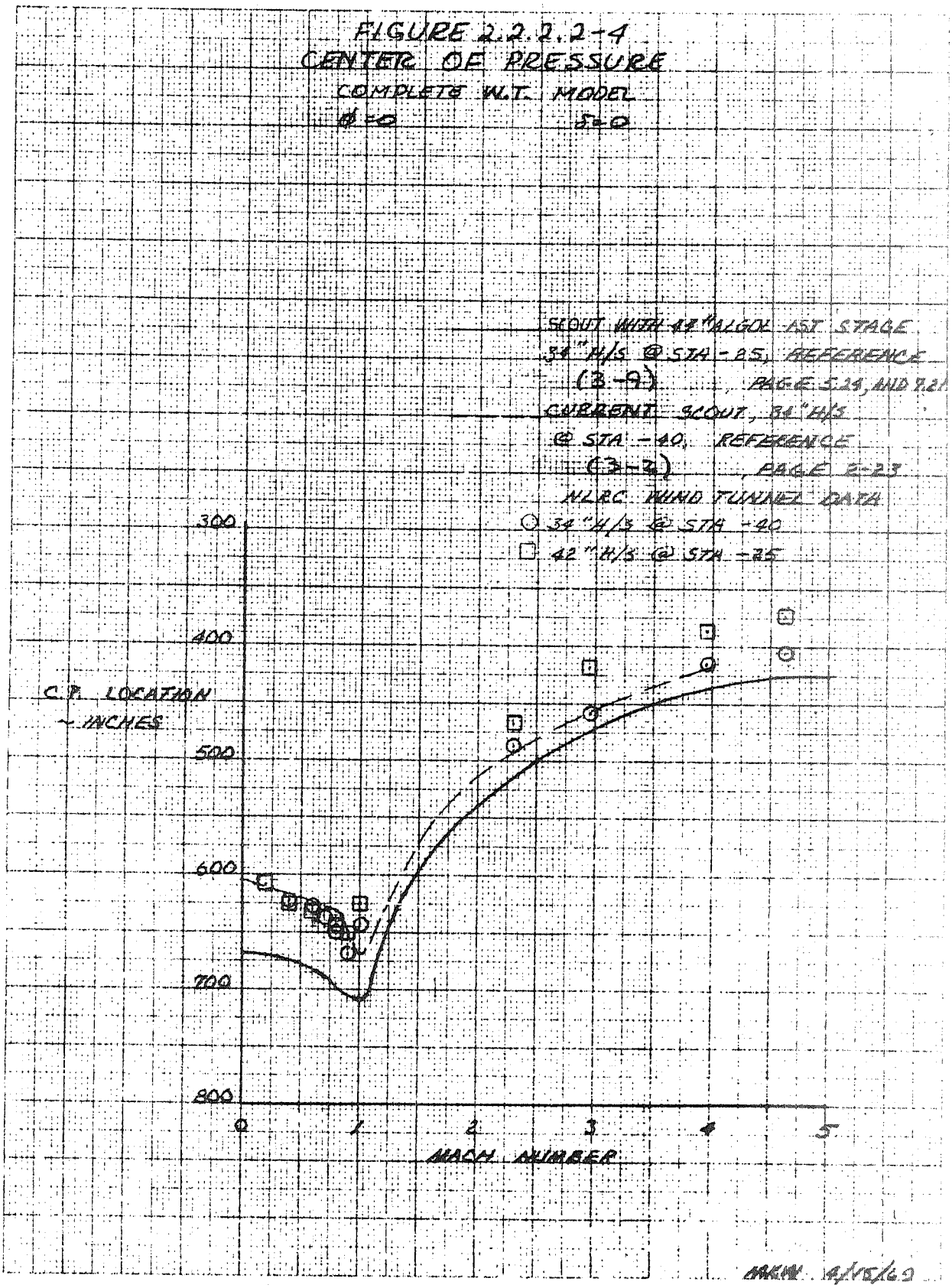

MKW 4/15/69

FIGURE 2.2.2.2-5
FIN NORMAL FORCE DERIVATIVE
AND CENTER OF PRESSURE
COMPLETE W.T. MODEL
$\phi = 0$ $\delta = 0$
$S_M = 5.25$ FT^2

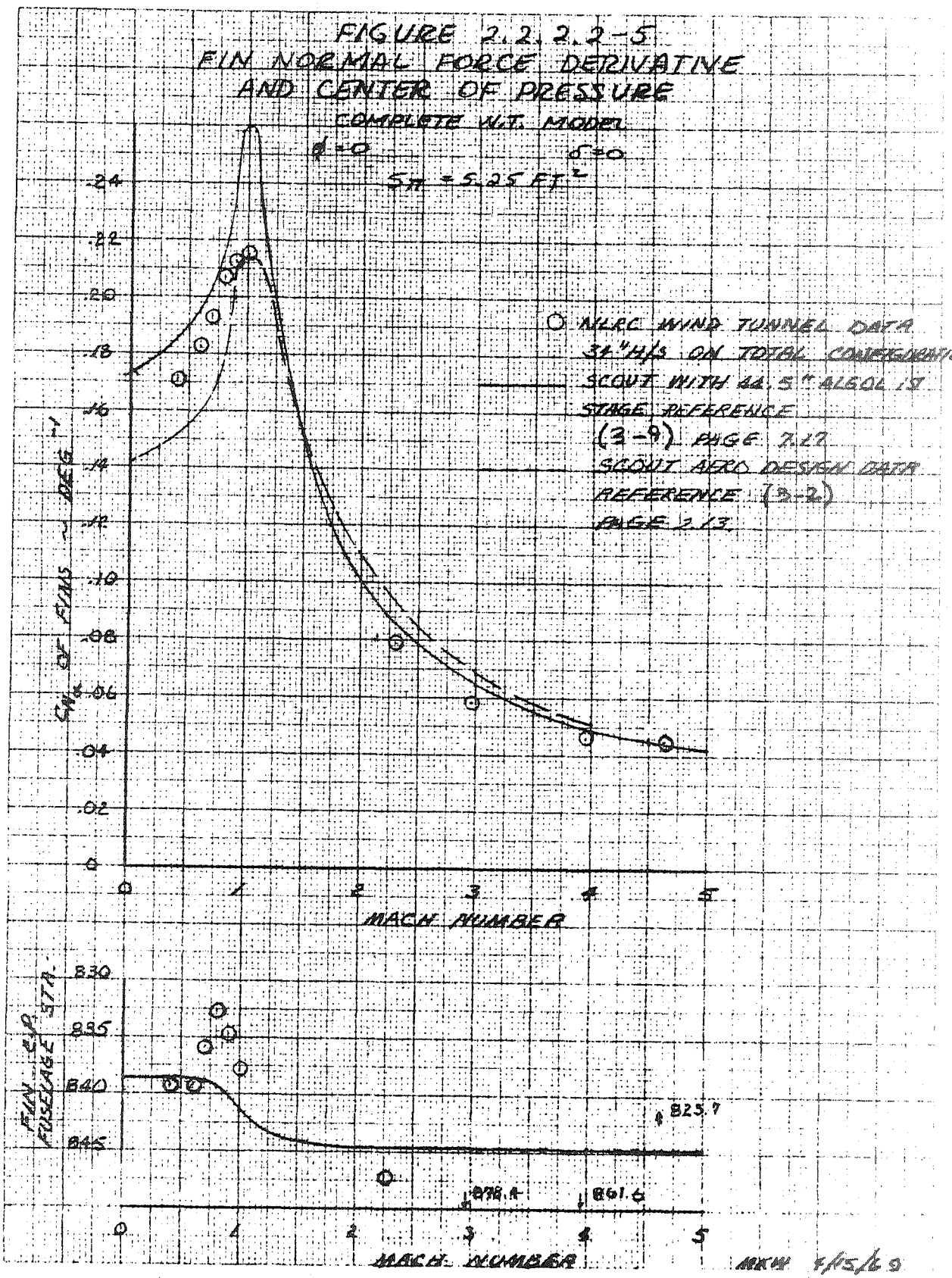

MKW 4/15/69

Estimated control effectiveness and supersonic experimental data are presented in Figure 2.2.2.2-6, and indicate good agreement. Data for control deflections of -10^{o} and -18^{o}, for the extreme test Mach numbers, were used to evaluate the experimental control effectiveness, and indicate good linearity.

FIGURE 2.2.2.2.-6
FIN TIP CONTROL EFFECTIVENESS
$\phi = 0$ $\alpha = 0$
$S_{ref} = 5.25\ FT^2$

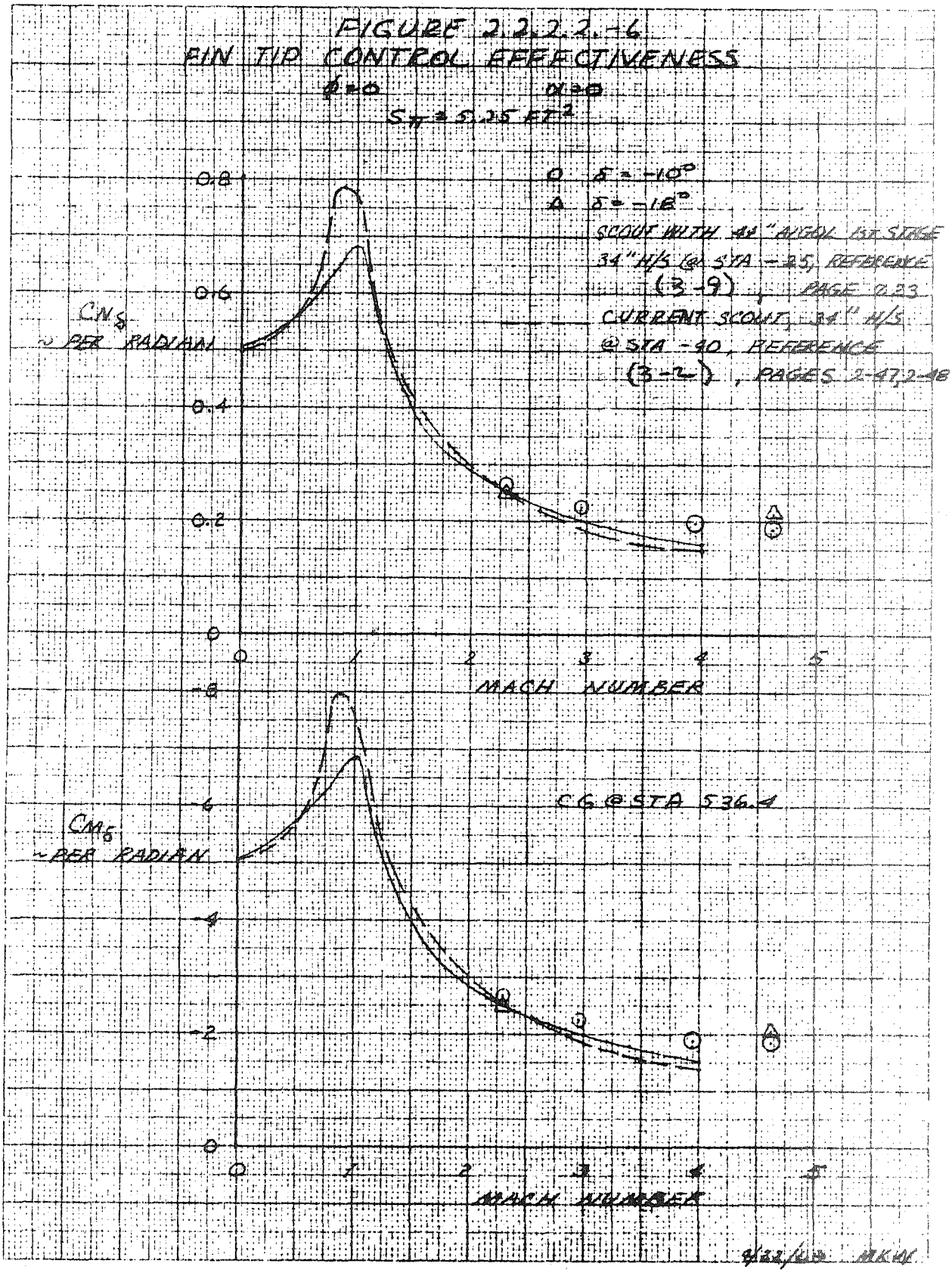

2.2.3 Heatshield Configurations

The heatshields were basically configured to satisfy the buffet criteria. The maximum allowable nose bluntness ratio was used to minimize the nose lift and subsequent destabilizing effects on the vehicle, with a resulting performance penalty. Figure 2.2.3-1 (Sheet 1) presents the shapes of the first four heatshields investigated. These configurations were used in determining the aerodynamic data and in developing the design trajectories. The final selected heatshield configurations based on buffet criteria are presented in Figure 2.2.3-1 (Sheet 2).

Certain limitations in the heatshield shape parameters were defined by the contract as follows: (a) forward cone-cylinder juncture shall be retained at Station 4.2; (b) minimum cylinder length shall be twice the heatshield radius; (c) afterbody angle shall be less than 15 degrees; (d) base diameter shall be 25.7 inches. Items (a) and (c) could be satisfied for all heatshields but items (b) and (d) could not. The afterbody angle dictated the pressure gradient which required keeping the afterbody slope to about 6 degrees to satisfy the 0.20 maximum pressure gradient criteria. A cylinder length of 40 inches (2 x R) was retained for the 40 inches diameter heatshield but lesser lengths were used for the larger diameters in conjunction with larger base diameters to provide the most usable payload volume while minimizing the discontinuity between the heatshield and D section. The differences between these shapes and the ones used in the stability and loads analyses with regard to aerodynamic lift and drag are assumed to be insignificant.

The heatshield and D section structures analyses are based on the aft diameter of the heatshields being the same as the 34 inch diameter configuration to retain compatibility with the D section. The reduction in afterbody slope angle can be achieved by external fairing.

The final configurations are summarized as follows:

Heatshield Diameter-In.	Nose Cone Bluntness Ratio r/R	Nose Cone Angle-Deg.	Cylinder Length-Inches	Base Diameter-Inches
40	0.55	15	40	27.8
42	0.60	12.5	33.07	28.2
44	0.65	10.0	32.12	29.4
46	0.70	7.5	24.38	29.8

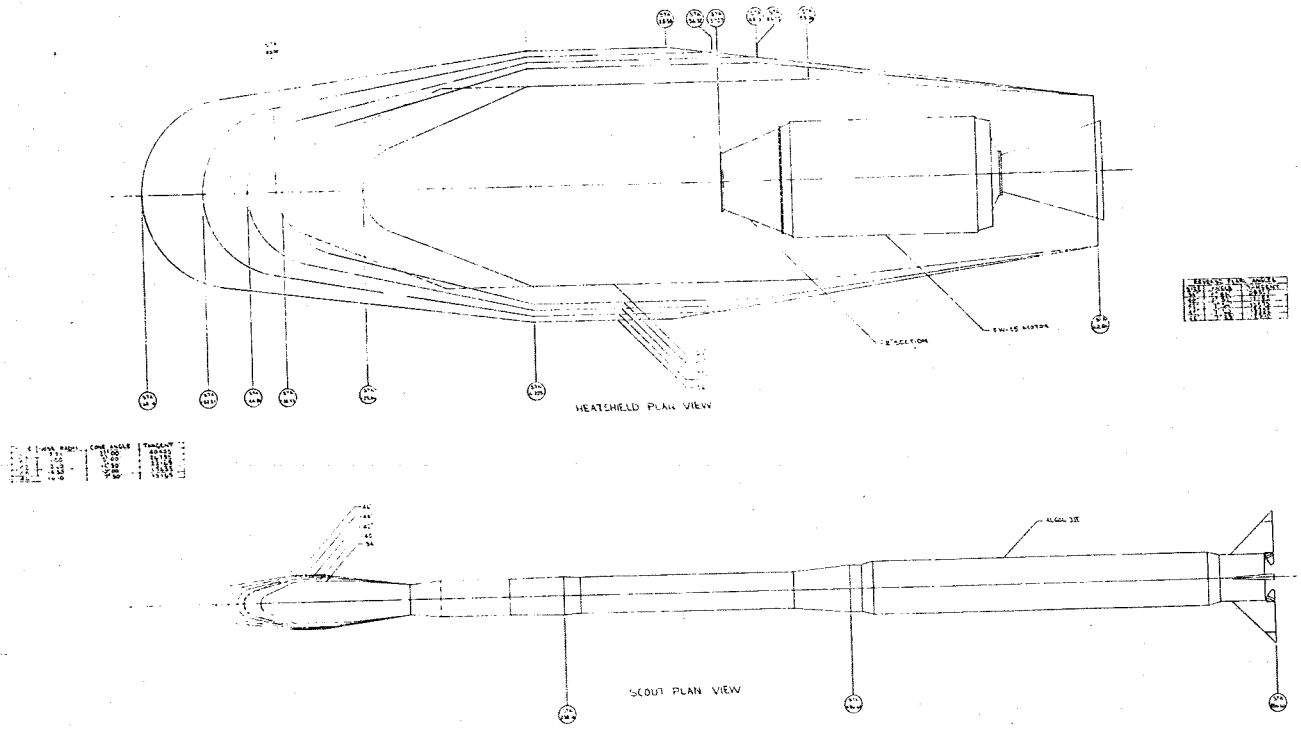

FIGURE 2.2.3-1 (Sheet 1 of 2)

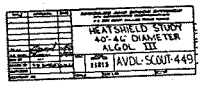

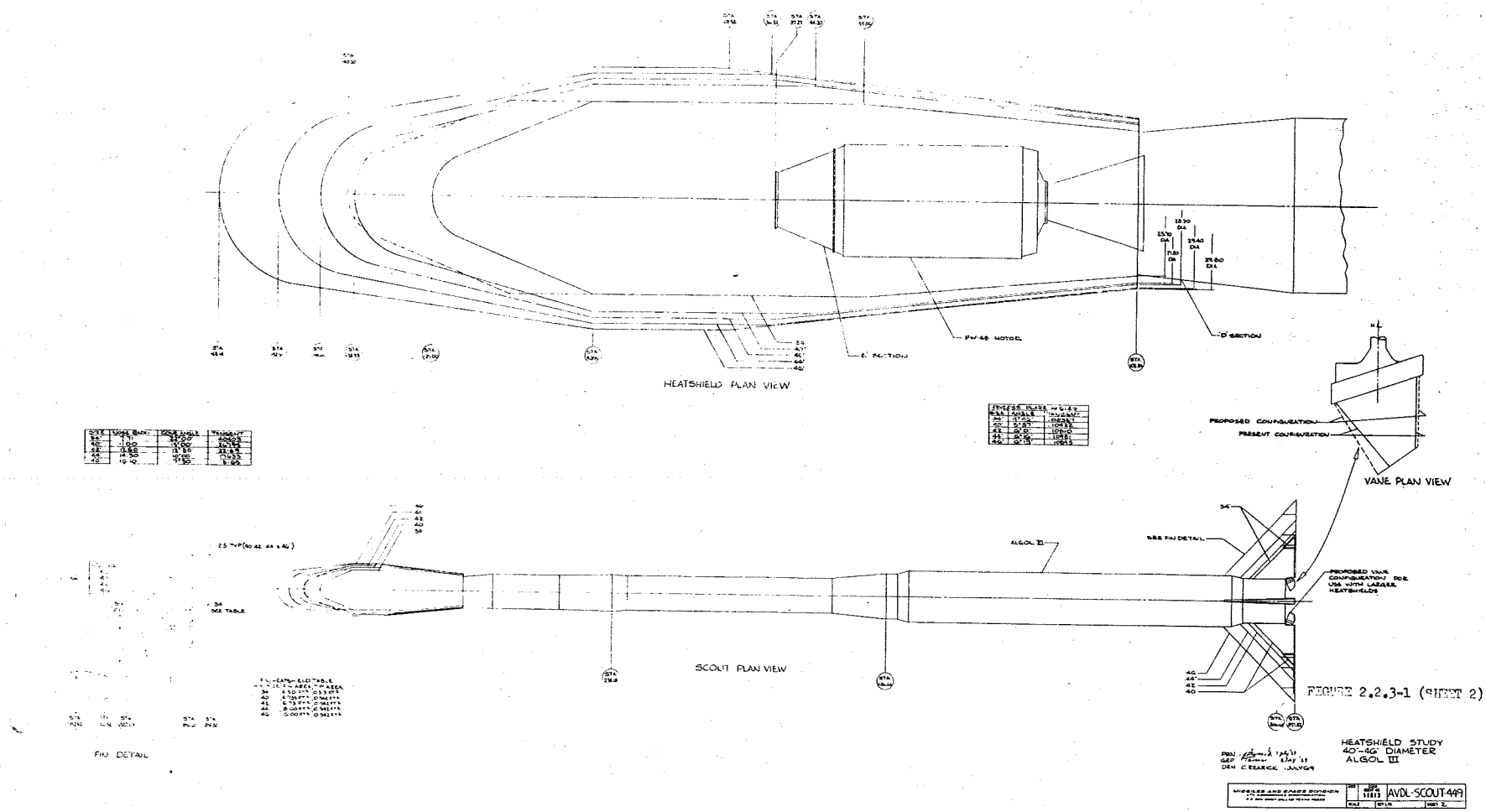

FIGURE 2.2.3-1 (SHEET 2)

2.3 ALGOL III PERFORMANCE

The Aerojet-General proposal No. 2 Algol III Motor was selected to be used in the larger heatshield study. This motor was selected because of its heavier weight and higher thrust levels at ignition; which subjected the Scout Vehicle to greater flight loads and was a less stable configuration than other motors proposed.

The weights, predicted performance and plus and minus 3 sigma range safety limits are given in Tables 2.3-1, 2.3-2 and 2.3-3, respectively. A plot of these data is presented in Figure 2.3-1.

TABLE 2.3-1

AEROJET-GENERAL PROPOSAL NO. 2 ALGOL III
(PREDICTED PERFORMANCE)

Total Weight - 31116.00 lb
Cons Weight - 27932.00 lb
Burnout Weight - 3184.00 lb
Exit Area - 5.634 Sq. ft.

Prop Weight - 27700.00 lb
Spec Impulse - 260.289 Sec.
Web (or action) Time - 52.500 Sec.
Total Impulse - 7210000.0 lb-Sec.

Step	Time-Sec	Thrust Vacuum -lb	Total Impulse (Accumulating) lb-Sec.	Weight Remaining-lb
1	0.00	0.0	0.0	27932.00
2	0.10	138391.6	6919.6	27880.00
3	5.00	132988.0	671799.4	25344.00
4	10.00	121480.4	1307970.3	22902.00
5	15.00	110172.9	1887103.5	20659.00
6	20.00	102467.8	2418705.2	18603.00
7	25.00	103368.4	2933295.6	16609.00
8	30.00	109372.4	3465147.5	14548.00
9	35.00	117477.7	4032272.7	12364.00
10	40.00	124682.5	4637673.2	10019.00
11	45.00	130586.4	5275845.4	7547 00
12	47.50	131687.1	5603687.3	6283.00
13	50.00	131487.0	5932654.9	5003.00
14	52.50	129085.4	6258370.4	3781.00
15	55.00	119479.0	6569075.9	2559.00
16	60.00	56037.1	7007866.2	816.00
17	65.00	12408.2	7178979.4	120.00
18	70.00	0.0	7210000.0	0.00

TABLE 2.3-2

AEROJET-GENERAL PROPOSAL NO. 2 ALGOL III
(PLUS THREE SIGMA-RANGE SAFETY)

Total Weight - 31274.69 lb
Cons Weight - 28098.20 lb
Burn out Weight - 3176.49 lb
Exit Area - 5.634 Sq. ft.

Prop Weight - 27866.20 lb
Spec Impulse - 262.038 Sec.
Web (or action) Time - 49.100 Sec.
Total Impulse - 7302003.3 lb-Sec.

Step	Time - Sec.	Thrust Vacuum -lb.	Total Impulse (Accumulating) lb-Sec.	Weight Remaining -lb
1	0.00	0.0	0.0	28098.20
2	0.09	149862.9	7007.9	28045.69
3	4.68	144011.4	680372.0	25494.80
4	9.35	131549.9	1324660.7	23038.27
5	14.03	119305.2	1911183.9	20781.92
6	18.70	110961.4	2449569.1	18713.69
7	23.38	111936.7	2970726.0	16707.83
8	28.06	118438.3	3509364.5	14634.56
9	32.73	127215.5	4083726.5	12437.57
10	37.41	135017.5	4696852.3	10078.61
11	42.09	141410.8	5343167.9	7591.91
12	44.42	142602.7	5675193.2	6320.38
13	46.76	142386.0	6008358.7	5032.77
14	49.10	139785.4	6338320.4	3803.50
15	51.44	129382.7	6652900.8	2574.23
16	56.11	60682.0	7097290.2	820.86
17	60.79	13436.7	7270586.9	120.71
18	65.47	0.0	7302003.3	0.00

TABLE 2.3-3

AEROJET-GENERAL PROPOSAL NO. 2 ALGOL III
(MINUS THREE SIGMA-RANGE SAFETY)

Total Weight - 30957.31 lb
Cons Weight - 27765.80 lb
Burn out Weight - 3191.51 lb
Exit Area - 5.634 Sq. ft.

Prop Weight - 27533.80 lb
Spec Impulse - 258.540 Sec.
Web (or action) Time - 55.900 Sec.
Total Impulse - 7118588.6 lb-Sec.

Step	Time - Sec.	Thrust Vacuum - lb.	Total Impulse (Accumulating) lb-Sec.	Weight Remaining - lb
1	0.00	0.0	0.0	27765.80
2	0.11	128326.3	6831.8	27714.11
3	5.32	123315.7	663282.1	25193.20
4	10.65	112645.1	1291387.3	22765.73
5	15.97	102160.0	1863178.0	20536.08
6	21.30	95015.3	2388039.8	18492.31
7	26.62	95850.4	2896106.1	16510.17
8	31.94	101417.7	3421214.9	14461.44
9	37.27	108933.5	3981149.9	12290.43
10	42.59	115614.3	4578874.9	9959.39
11	47.91	121088.8	5208956.1	7502.09
12	50.58	122109.5	5532641.4	6245.62
13	53.24	121923.9	5857438.3	4973.23
14	55.90	119697.0	6179024.2	3758.50
15	58.56	110789.3	6485790.5	2543.77
16	63.89	51961.5	6919017.7	811.14
17	69.21	11505.8	7087961.4	119.29
18	74.53	0.0	7118588.6	0.00

FIGURE 2.3-1

AEROJET-GENERAL PROPOSED ALGOL III
(Motor No. 2)

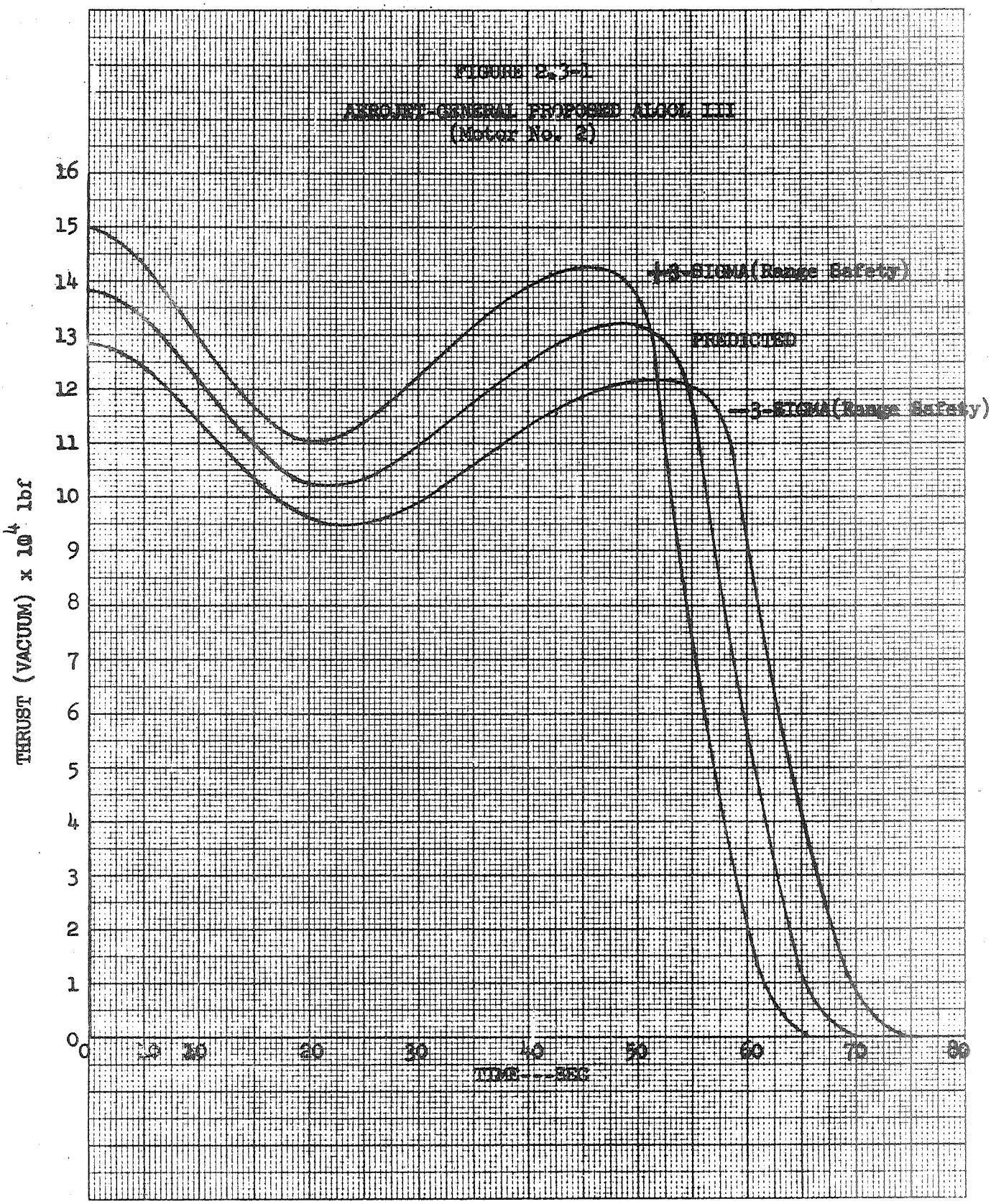

2.4 JET VANE EFFECTIVENESS

In order to determine jet vane effectiveness the characteristics of the exhaust gas at the nozzle exit plane of the Algol IIB and Algol III motors were required. The data required (Mach number, pressure ratio and ratio of specific heats) were generated by using two LTV-MSD-T computer programs, LVVM07, "Thermochemical Problem," and LVTM85, "Nozzle Analysis."

LVVM07 generated required thermochemical data for input to the LVTM85 program. These data were determined from the propellant formulation of the respective motors. Nozzle exit plane conditions (real gas properties) were then calculated (LVTM85) from the thermochemical data and given nozzle geometry. The nozzle exit conditions near the jet vane leading edge are:

Nozzle Exit Conditions

Parameter	Algol IIB	Algol III
Mach Number	2.84	2.84
Ratio of Specific Heats	1.13	1.18
Pressure Ratio P_e/P_c	0.0238	0.0227

The lift and drag characteristics for the jet vane immersed in the Algol III exhaust were estimated based on adjustments to the existing Algol IIB jet vane data. The Mach number at the nozzle exit plane of the proposed Algol III motor used in this study is the same as that of the Algol IIB. However, the ratio of exit dynamic pressure to vacuum thrust level for the Algol III configuration is different than that of the Algol IIB. The jet vane area was increased from 35 square inches to 41 square

inches for the Algol III configuration to help reduce control surface deflections in response to the first pitch program step. The ratio of jet vane lift and drag to vacuum thrust is shown in Figure 2.4-1 for both the Algol IIB and Algol III configurations. A proposed planform for the Algol III jet vane is presented in Figure 2.2.3-1.

FIGURE 2.4-1
SCOUT LARGER HEATSHIELD STUDY
JET VANE LIFT AND DRAG
PARAMETERS

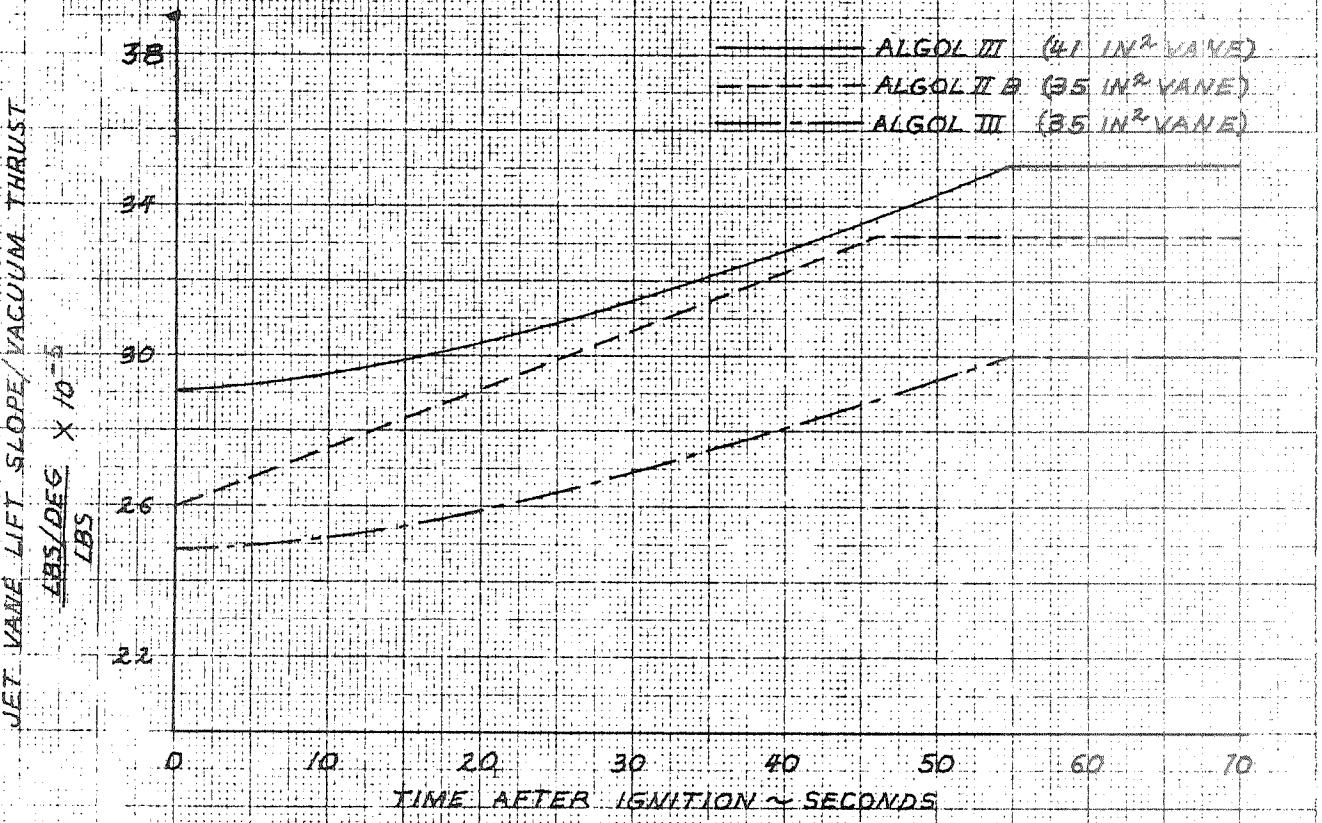

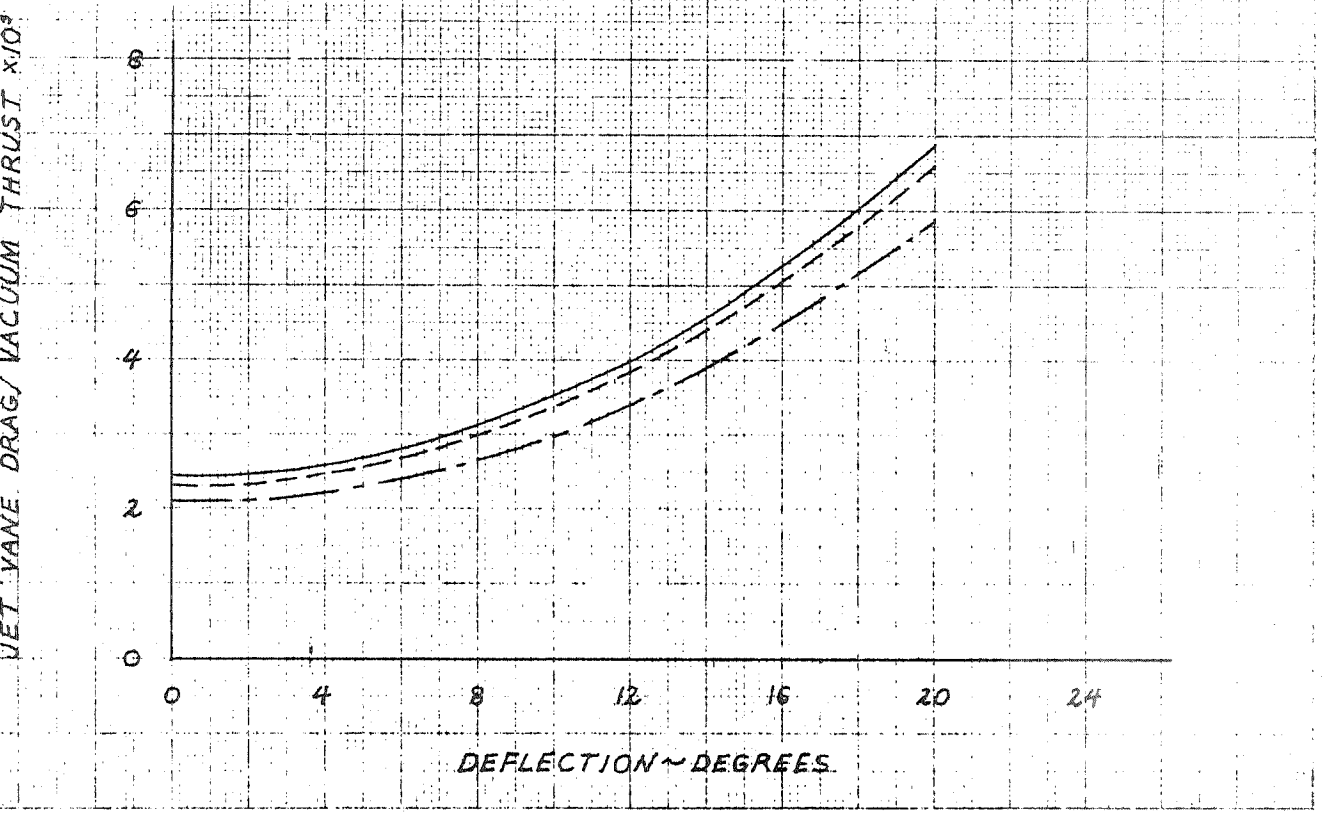

2.5 VIBRATIONAL BENDING MODES

The first through fourth bending modes of vibration for the Scout vehicle with an Algol III first stage motor and a 42 inch diameter heatshield were calculated and are presented in Figures 2.5-1 and 2.5-2. Also second stage bending modes were calculated and are presented in Figures 2.5-3 to 2.5-8. Payload weights of 50 and 400 lbs were used in these calculations.

Classical methods were used in determining these modes. The data, such as stiffness and weight distributions used, are shown in Table 3.2.2.2-1 and 3.2.2.2-2. The stiffness data for the heatshield were obtained by ratioing the new and old radii. The weight of the Algol III motor used was the weight for the + 3 sigma Aerojet configuration No. 2 model. These modal shapes were used for all heatshield configuration analyses because the variation between the range of heatshield sizes was assumed to be negligible. The heatshields are so stiff that no significant local deflections occur which would change the mode shapes between one heatshield configuration and another.

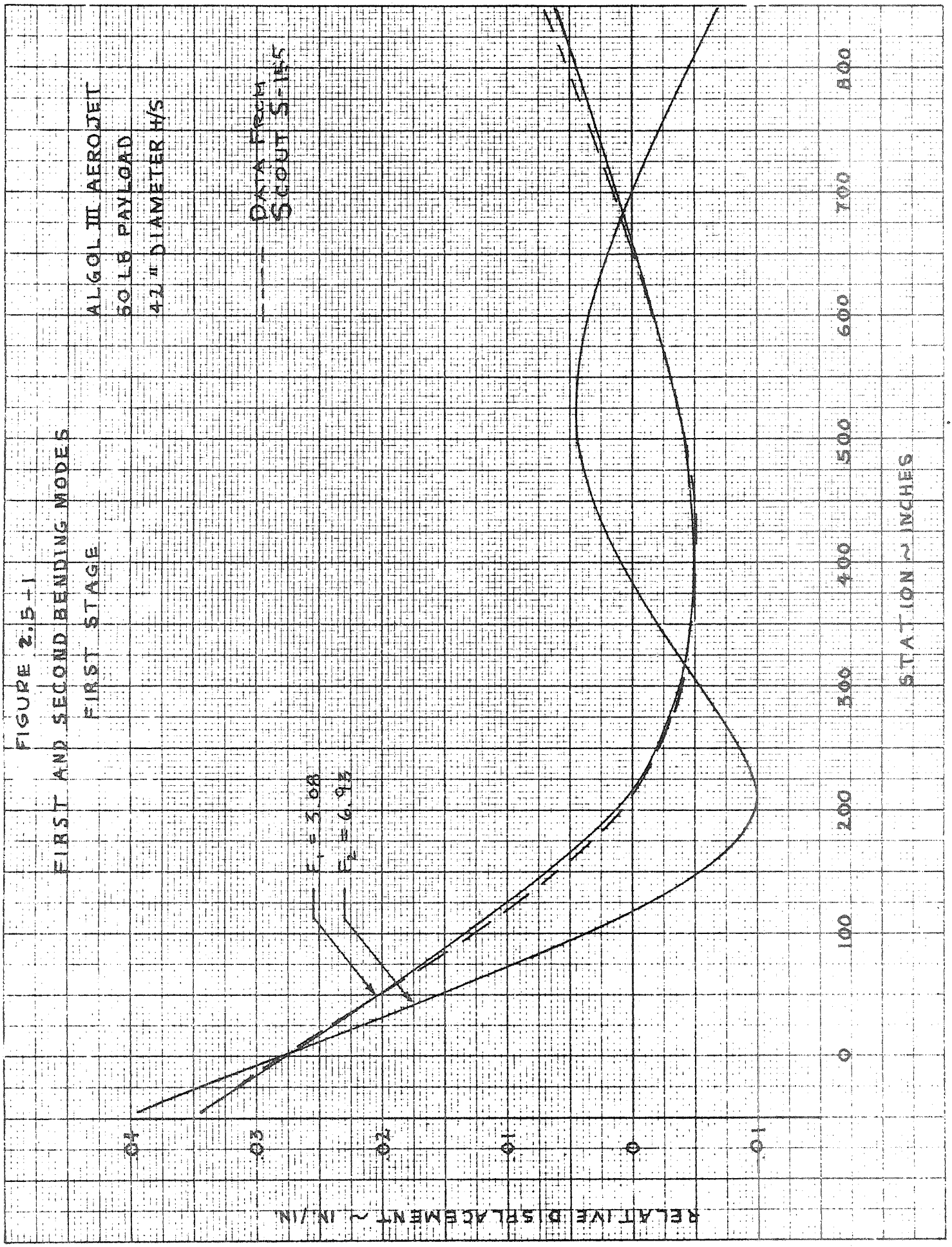
FIGURE 2.5-1
FIRST AND SECOND BENDING MODES
FIRST STAGE
ALGOL III AEROJET
50 LB PAYLOAD
42" DIAMETER H/S
DATA FROM SCOUT S-1E5
f_1 = 3.08
f_2 = 6.93
RELATIVE DISPLACEMENT ~ IN/IN
STATION ~ INCHES
.4
.3
.2
.1
0
.1
0
100
200
300
400
500
600
700
800

FIGURE 2.5-2
THIRD AND FOURTH BENDING MODES
FIRST STAGE

ALGOL III AEROJET
50 LB PAYLOAD
42" DIAMETER H/S

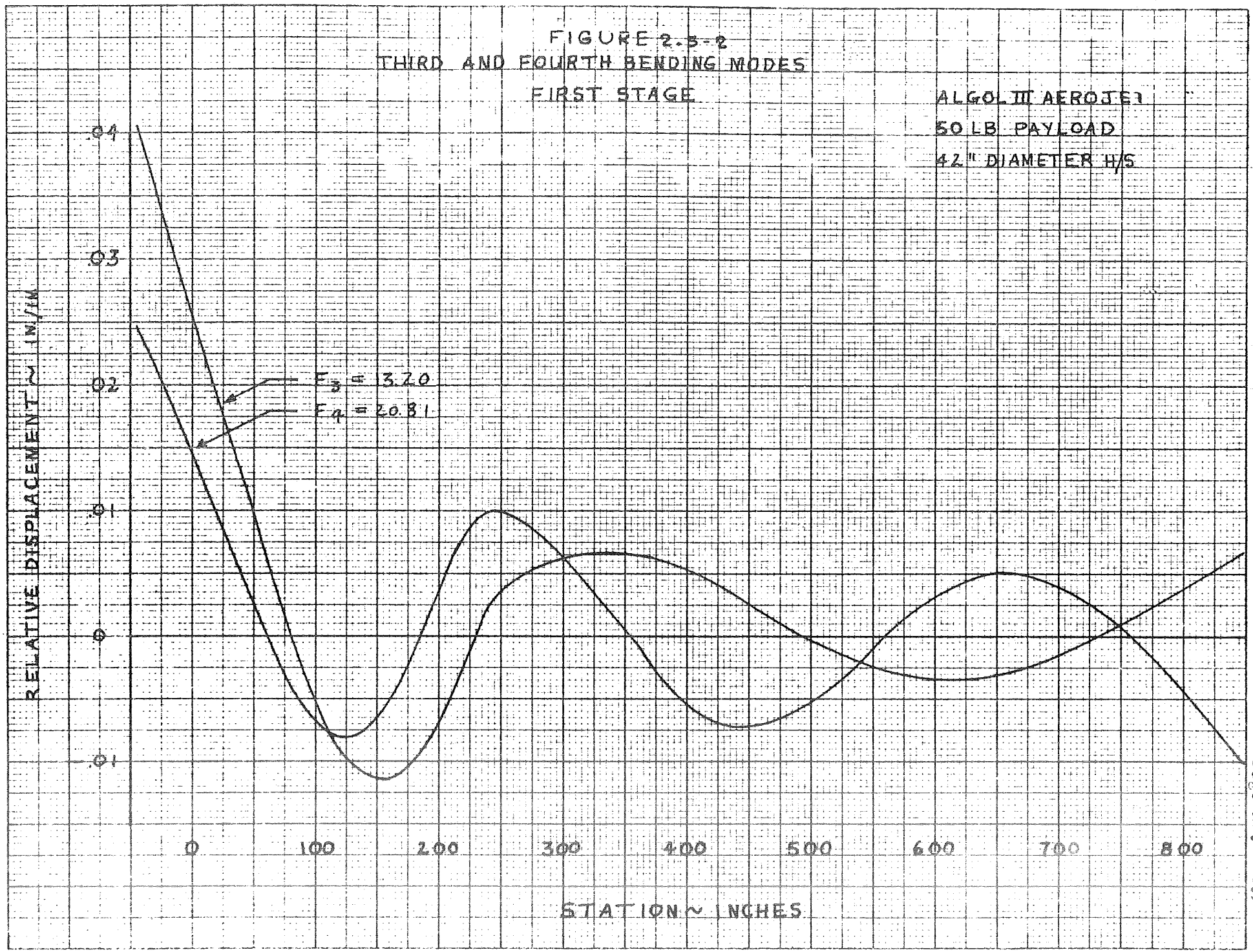

FIGURE 2.5-3

FIRST AND SECOND BENDING MODES

FIRST STAGE

ALGOL III AEROJET

400 LB PAYLOAD

42" DIAMETER H/S

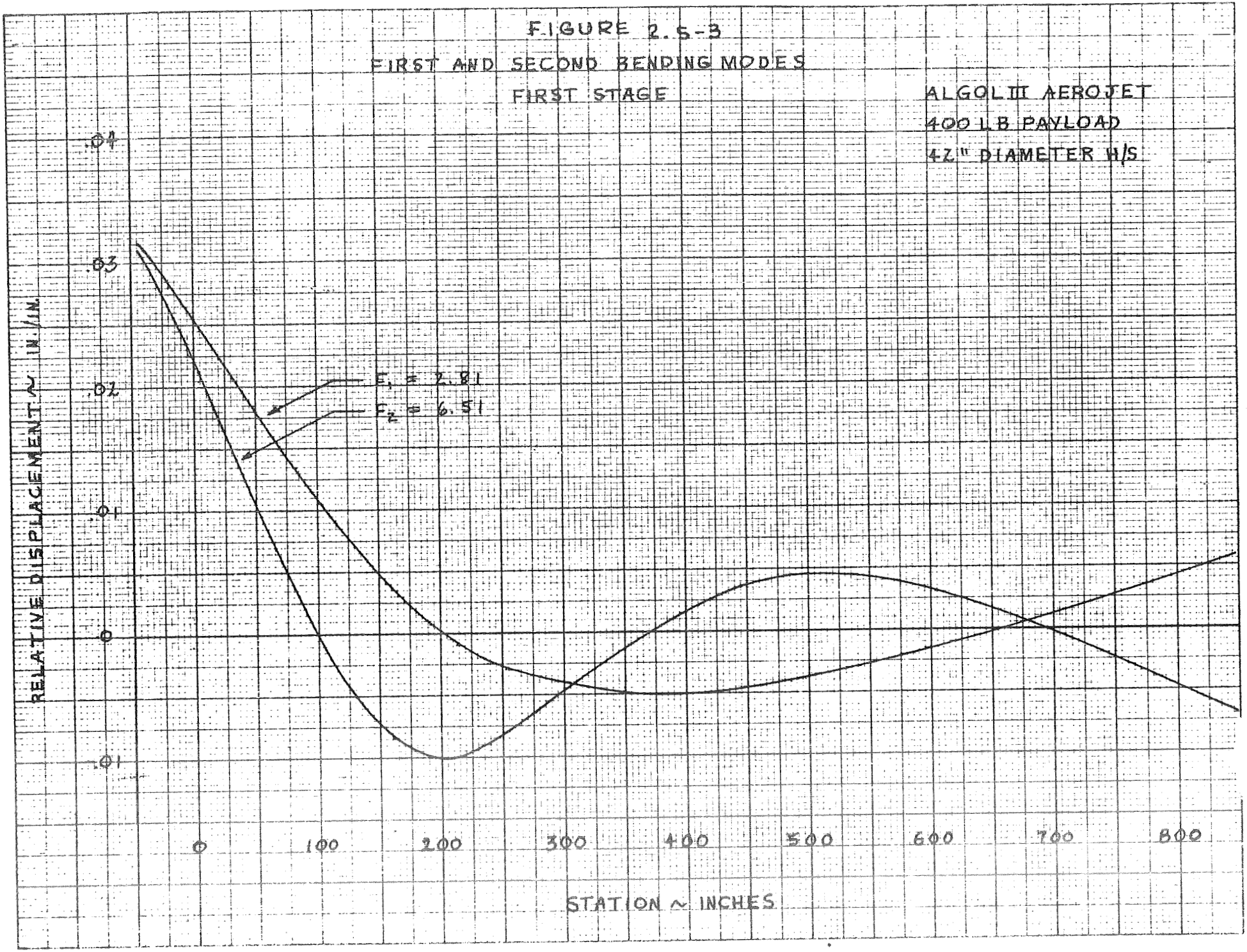

FIGURE 2.5-4

THIRD AND FOURTH BENDING MODES

FIRST STAGE

ALGOL III AEROJET

400 LB PAYLOAD

42" DIAMETER H/S

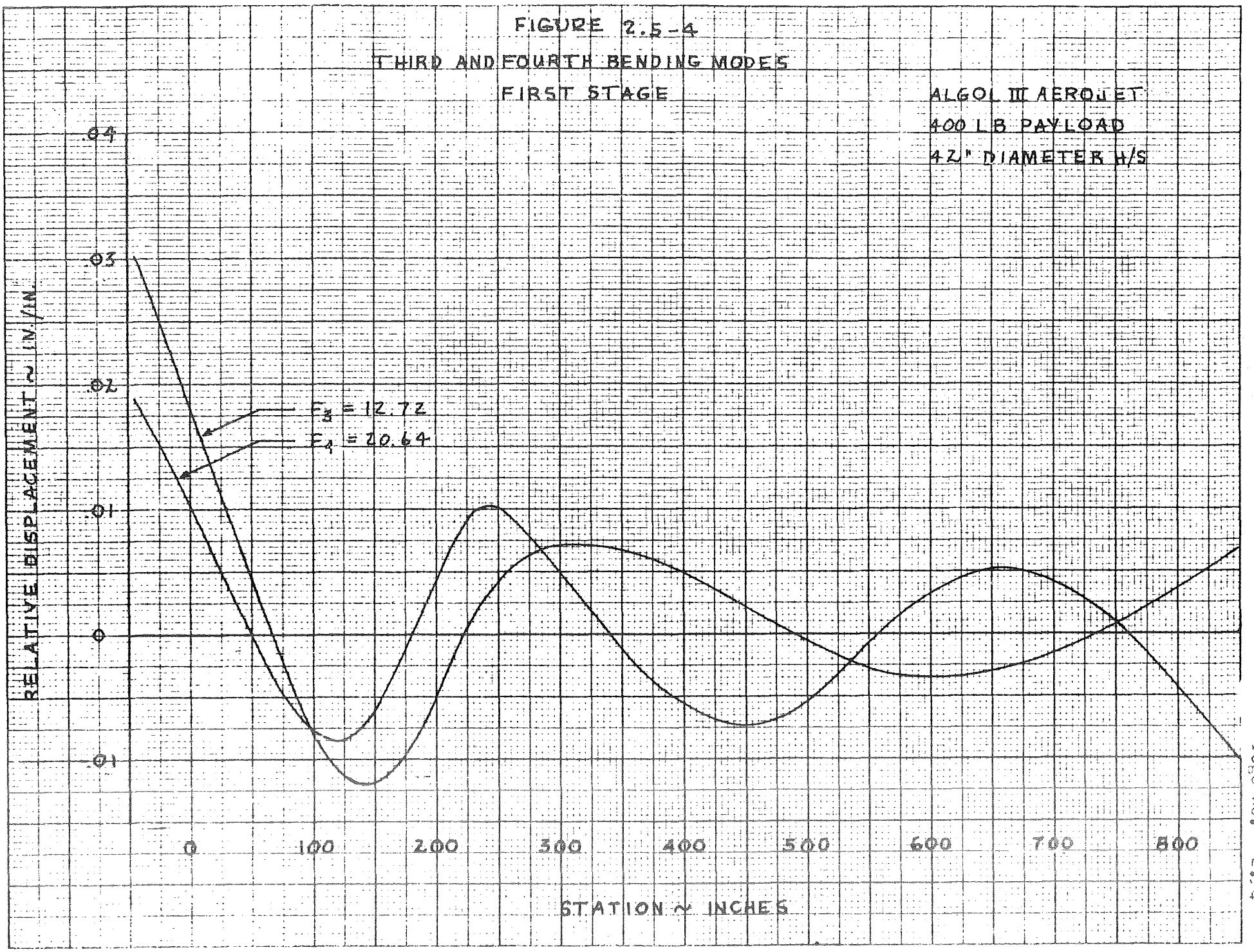

FIGURE 2.5-5

FIRST AND SECOND BENDING MODES

SECOND STAGE

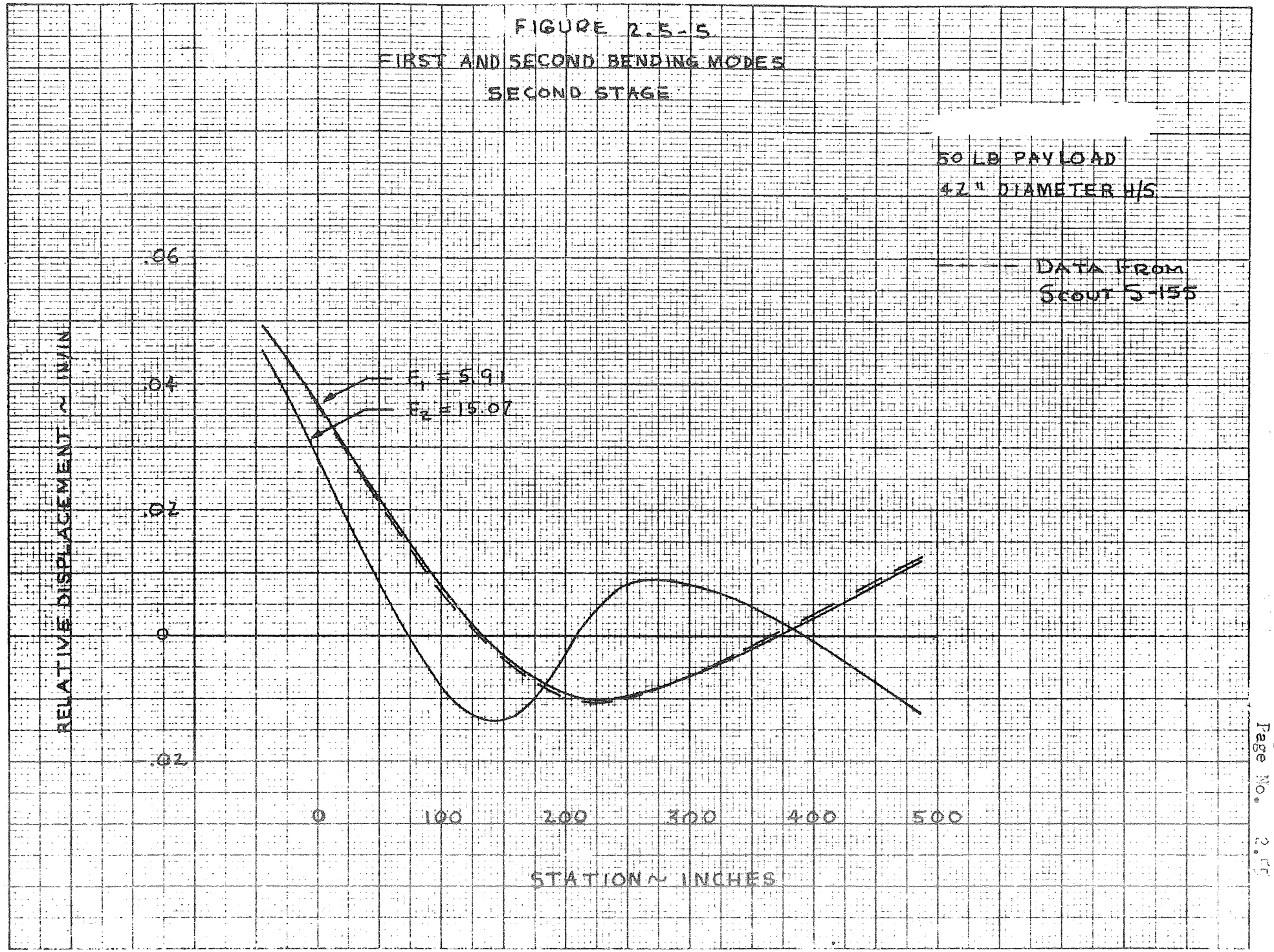

FIGURE 2.5-6
THIRD AND FOURTH BENDING MODES
SECOND STAGE

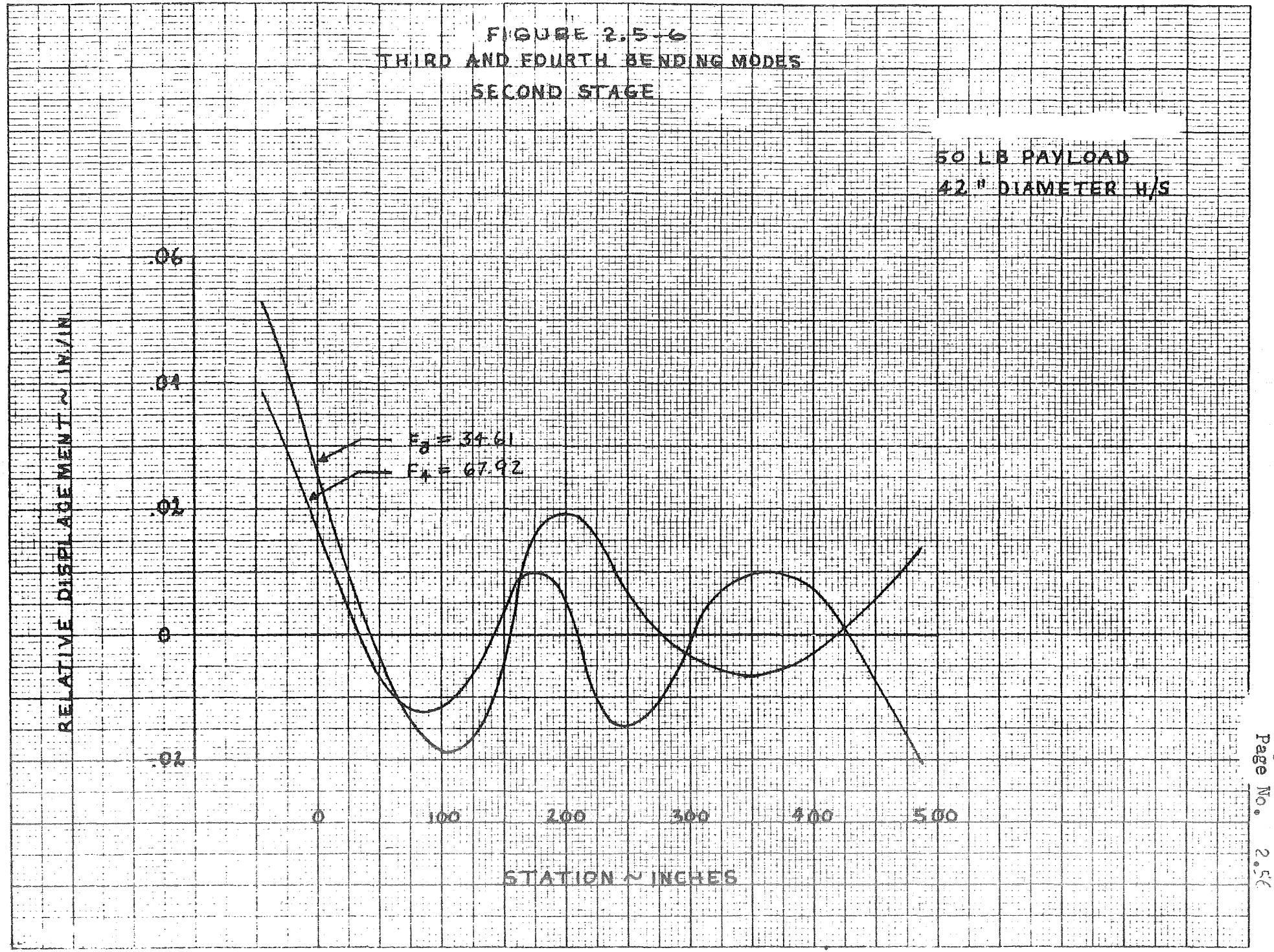

FIGURE 2.5-7

FIRST AND SECOND BENDING MODES

SECOND STAGE

400 LB PAYLOAD

42" DIAMETER H/S

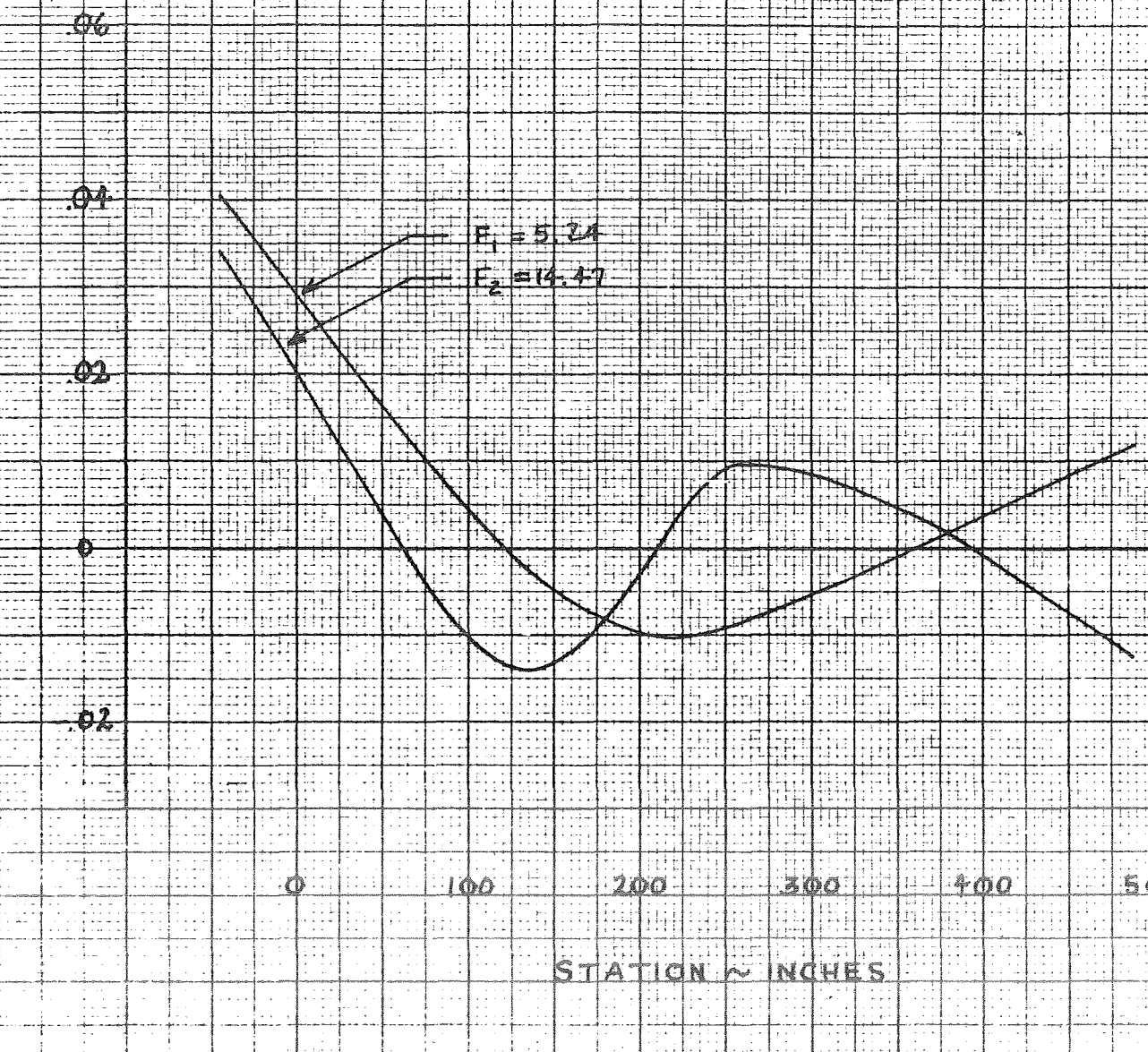

FIGURE 2.5-8

THIRD AND FOURTH BENDING MODES

SECOND STAGE

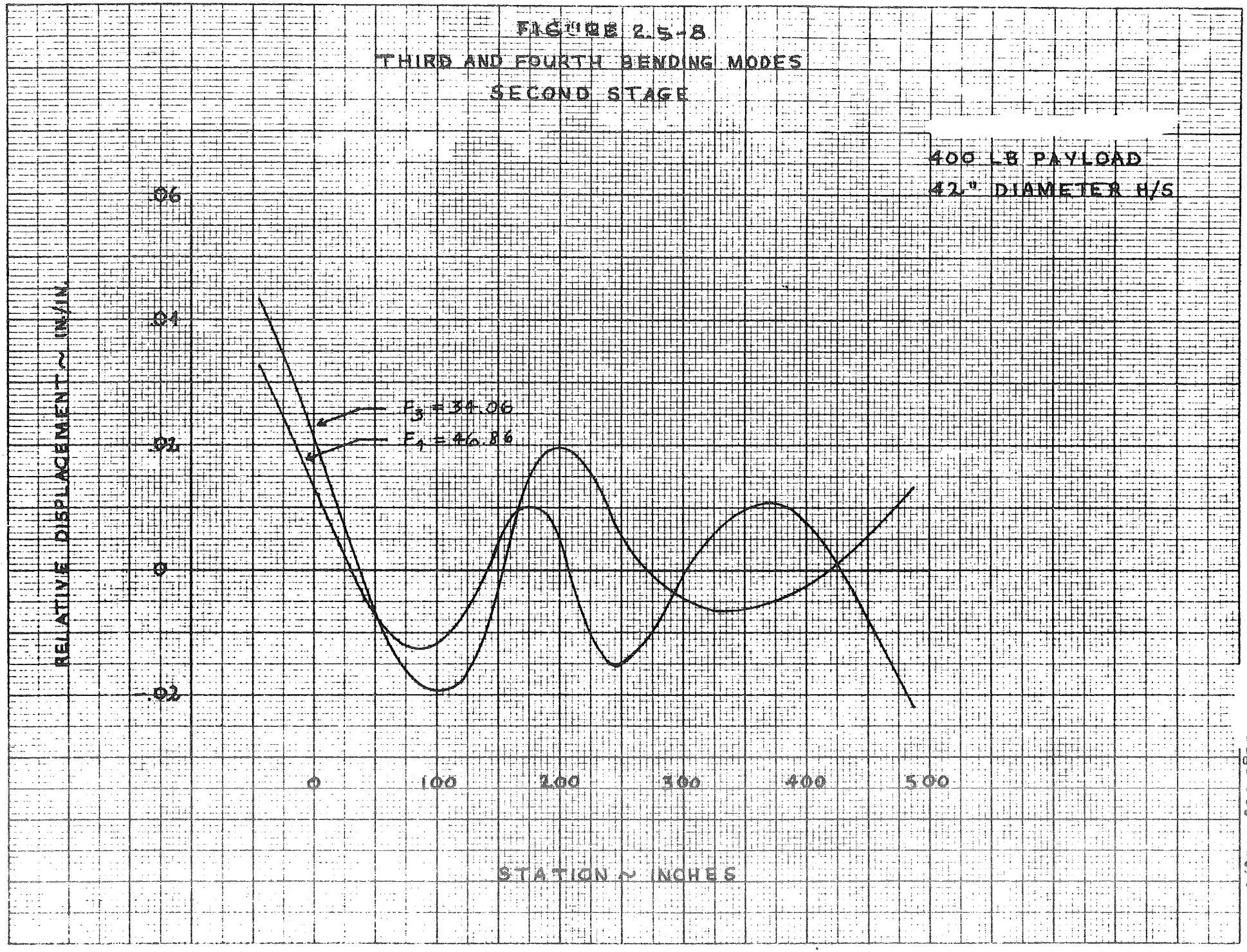

2.6 DESIGN TRAJECTORIES

A design trajectory represents the most severe environment expected to be encountered in a normal flight and provides information for the thermal, stability and control, and structural loads analyses. The selected trajectories are based on a due east launch from Wallops Island to an injection (fourth stage burnout) altitude of 100 n. mi. with 50 and 400 pound payloads.

Three design trajectories are presented in this report. The first design trajectory with a 50 pound payload was used in the stability and control and the thermal analyses. The second trajectory with a 400 pound payload was developed to show the effect of payload weight on trajectory parameters and on the pitch program. The variations from the 50 pound payload data were not significant. The third trajectory, developed with a 50 pound payload, incorporated the final aerodynamic and control characteristics and was used to generate a pitch program for the structural loads analysis.

2.6.1 Configuration

The Scout D configuration (Algol III/Castor II/X-259/FW-4) with the 42 inch diameter heatshield was used for all design trajectories. For design purposes it was directed that the +3 sigma high deviation from nominal motor performance of the Aerojet General No. 2 Algol III first stage motor be used. The Algol III motor characteristics are presented in Section 2.3. The upper stage motor characteristics are presented in Reference 2-5 . The weight data presented in Section 3.2.3 is based on the nominal Aerojet General No. 2 motor. The first stage weight was adjusted to reflect the +3 sigma motor weight.

2.6.2 Aerodynamics

The design trajectory used for thermal analysis and stability and control analysis used aerodynamics based on the Scout D configuration with the 42 inch diameter heatshield and the standard Scout first stage fins, control surfaces, and guidance system gains. As a result of the stability and control analysis, larger first stage fins and control surfaces and higher guidance system gains were used in the design trajectory for defining the pitch program for the structural loads analysis. Both sets of aerodynamic characteristics are presented in Section 3.2.2. Rigid body aerodynamics were used for all design trajectories.

2.6.3 Pitch Programs

Table 2.6-1 presents the three pitch programs developed for the design trajectories. These pitch programs differ from previous ones designed for Scout A, B, and C configurations due to the larger first stage motor. The difference occurs during the first eight seconds of flight; there are now three commanded pitch rates rather than the usual one during this same time period. The primary reason the design is different is the thrust-time trace of the Algol III motor. The Aerojet General No. 2 motor initially has a very high thrust compared to the Algol IIB motor and the thrust level decreases until approximately 20 seconds burn time. This high thrust level accelerates the Scout to approximately 600 fps velocity at 10 seconds flight time compared to 360 fps velocity for a Scout B configuration. A higher energy flight is more difficult to "turn" and thus requires larger control deflections and/or control surfaces. In other words, the higher the velocity the more difficult it becomes to change the direction of the velocity vector.

A roll and yaw compensation unit has been designed and tested for the Scout vehicle. The pitch program requirements for a low altitude orbit injection with the Algol III first stage motor exceed the design limitations of the roll and yaw compensation unit. Since the roll and yaw compensation unit provides correction to the roll gyro for only the first five pitch program steps, no roll correction will be made during the last thirty seconds or so of first stage burn using the proposed pitch programs. Each of the three pitch programs also use pitch rates which exceed the roll and yaw compensation unit design limitation of four degrees per second pitch rate. The effects on the roll and yaw compensation unit performance have not yet been defined.

TABLE 2.6-1

DESIGN TRAJECTORY PITCH PROGRAMS
100 N. MI. INJECTION ALTITUDE

NO. 1 50 LB. PAYLOAD
(ORIGINAL DESIGN TRAJECTORY)

Time after liftoff, sec.	Pitch Rate, deg/sec	Pitch Rate No.
0	0	
1.00	-5.50000	1
1.80	-5.76591	2
5.00	-1.60000	3
7.50	-0.79111	4
30.00	-0.68000	5
35.00	-0.54286	6
42.00	-0.43333	7
48.00	-0.34559	8
116.00	-0.13558	9
350.16	0	10

NO. 2 400 LB. PAYLOAD

Time after liftoff, sec.	Pitch Rate, deg/sec	Pitch Rate No.
0	0	
1.00	-5.50000	1
1.80	-5.46053	2
5.00	-1.60000	3
7.50	-0.79111	4
30.00	-0.68000	5
35.00	-0.54286	6
42.00	-0.43333	7
48.00	-0.34559	8
116.00	-0.13558	9
311.51	0	10

NO. 3 50 LB. PAYLOAD
(FINAL DESIGN TRAJECTORY)

Time after liftoff, sec.	Pitch Rate, deg/sec	Pitch Rate No.
0	0	
1.00	-4.47560	1
2.60	-6.13324	2
5.00	-1.66667	3
8.00	-0.80000	4
30.00	-0.68000	5
35.00	-0.54286	6
42.00	-0.43333	7
48.00	-0.34559	8
116.00	-0.13558	9
350.46	0	10

Therefore, large commanded pitch rates are needed early in flight before the velocity builds up, but large differences between sequenced command pitch rates will cause fin deflection to increase. As a result two pitch program design changes were made from the Scout B configuration procedure: (1) the start time of the first rate is one second after lift-off rather than three seconds, and (2) intermediate rates before and after the maximum rate are used to ease the effect on control deflections when changing rates.

2.6.4 Results

The results of the three design trajectories are presented graphically in Figures 2.6.4-1 through 2.6.4-10. These figures present time histories of vehicle and trajectory parameters important for design purposes. Because the flight profiles of the three trajectories are nearly identical, only the fin deflection and product of dynamic pressure and angle of attack ($q\alpha$) time histories are shown separately for each trajectory. The other figures are applicable for all trajectories. Also presented are time histories of weight remaining and net thrust in Figures 2.6.4-11 and 2.6.4-12 respectively.

The pitch programs for each trajectory were designed to minimize the values of fin deflection and $q\alpha$. These final values shown are at a balance; maximum $q\alpha$ can be reduced but only at the expense of increasing maximum fin deflection and vice versa.

Appendix A presents a computer listing of the three design trajectories. A glossary is provided to define the output parameters of the LVVC-27 routine.

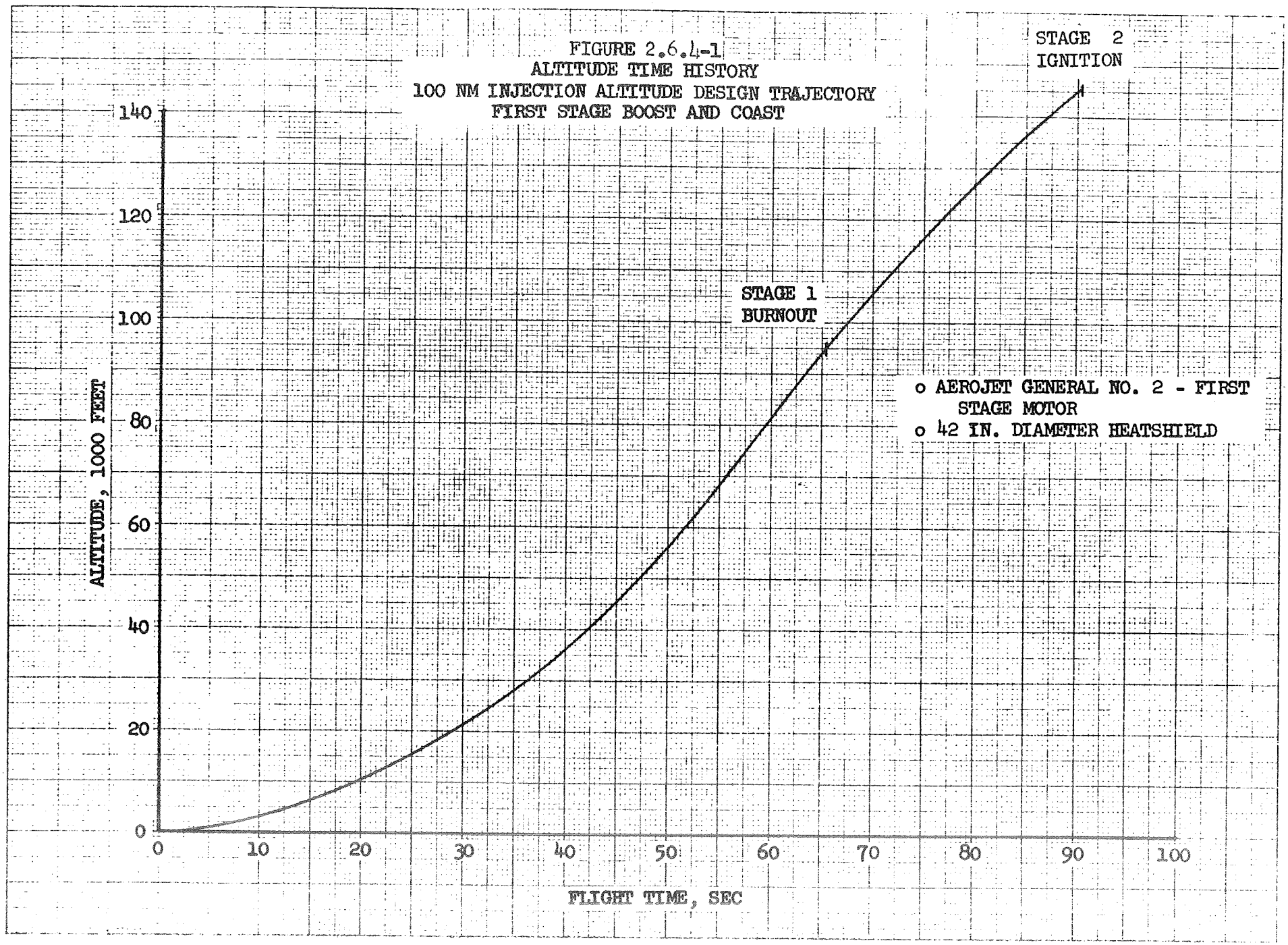
FIGURE 2.6.4-1
ALTITUDE TIME HISTORY
100 NM INJECTION ALTITUDE DESIGN TRAJECTORY
FIRST STAGE BOOST AND COAST
STAGE 2
IGNITION
STAGE 1
BURNOUT
o AEROJET GENERAL NO. 2 - FIRST
STAGE MOTOR
o 42 IN. DIAMETER HEATSHIELD
ALTITUDE, 1000 FEET
0
20
40
60
80
100
120
140
0
10
20
30
40
50
60
70
80
90
100
FLIGHT TIME, SEC

FIGURE 2.6.4-2
RELATIVE VELOCITY TIME HISTORY
100 NM INJECTION ALTITUDE DESIGN TRAJECTORY
FIRST STAGE BOOST AND COAST

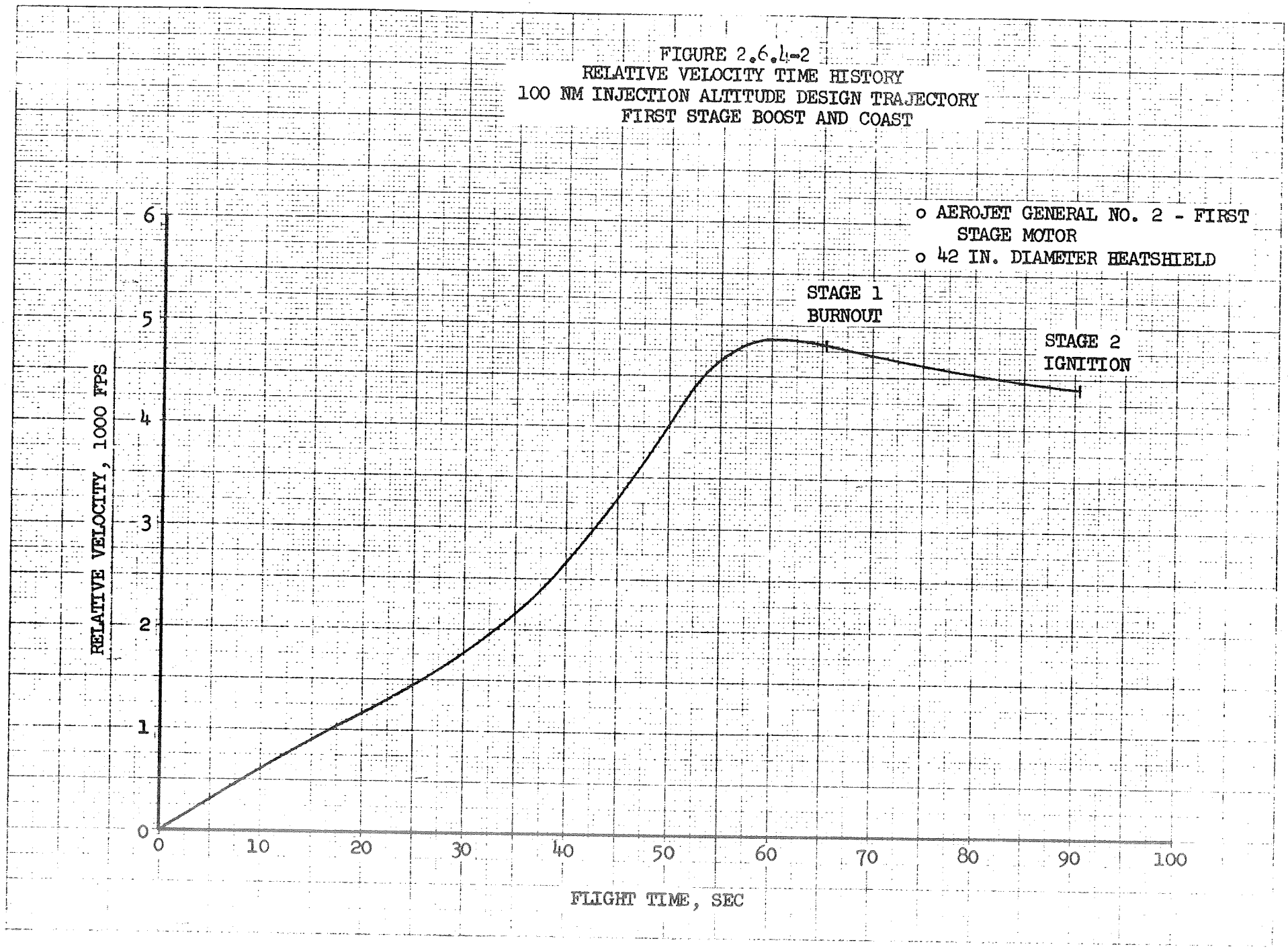

FIGURE 2.6.4-3
MACH NUMBER TIME HISTORY
100 NM INJECTION ALTITUDE DESIGN TRAJECTORY
FIRST STAGE BOOST AND COAST

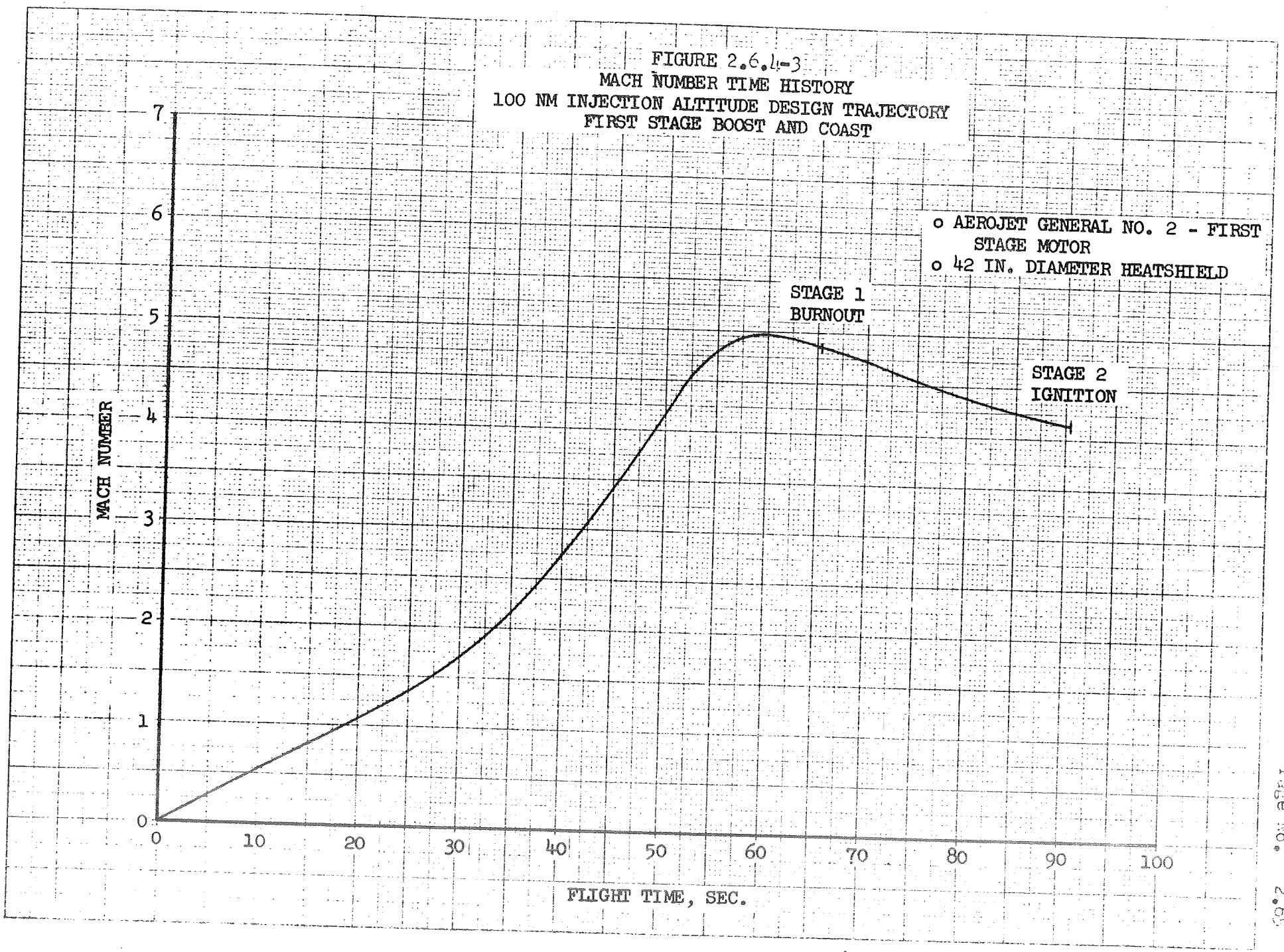

FIGURE 2.6.4-4
DYNAMIC PRESSURE TIME HISTORY
100 NM INJECTION ALTITUDE DESIGN TRAJECTORY
FIRST STAGE BOOST AND COAST

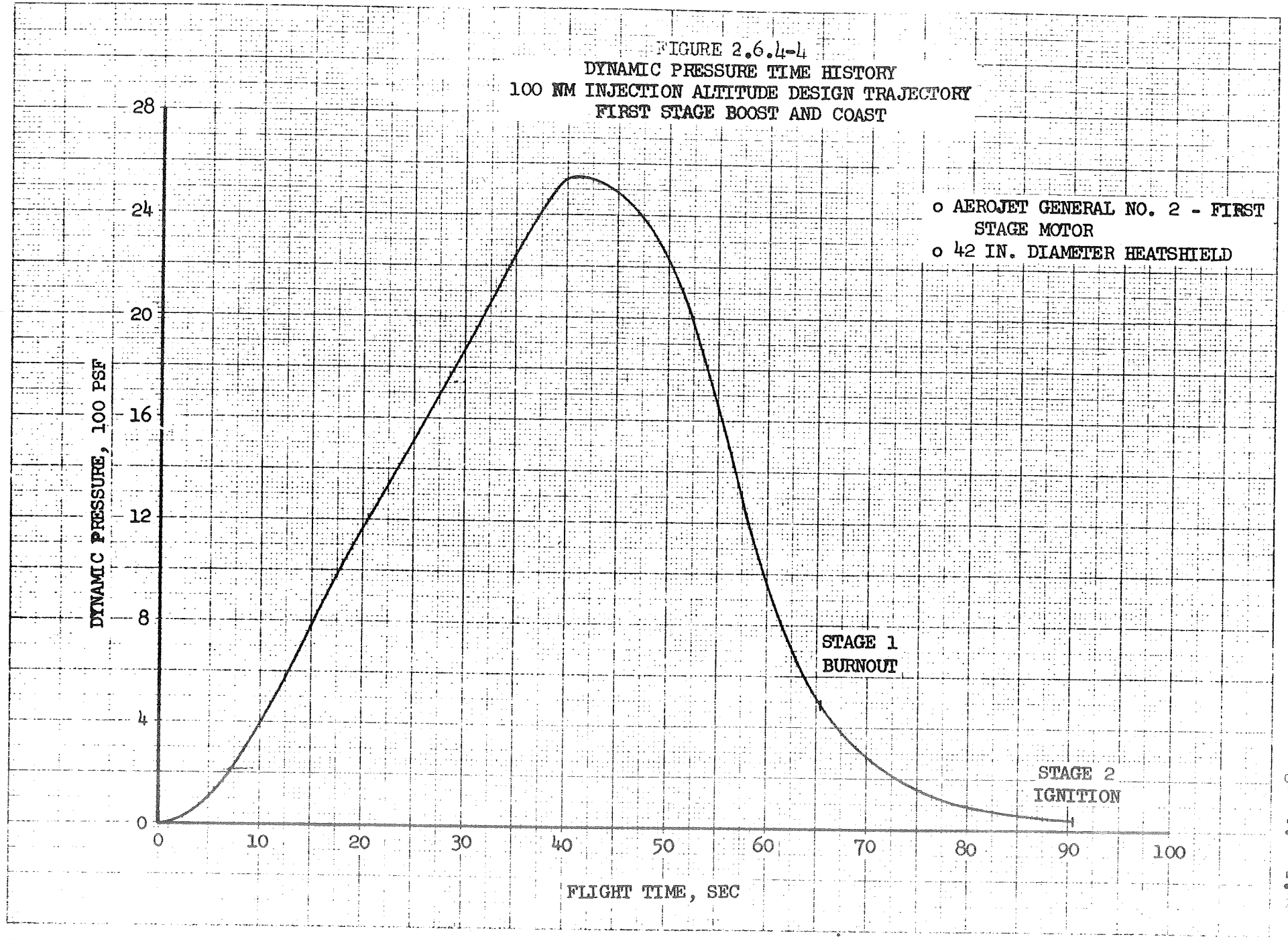

FIGURE 2.6.4-5
PRODUCT OF DYNAMIC PRESSURE AND
ANGLE OF ATTACK TIME HISTORY
100 NM INJECTION ALTITUDE DESIGN TRAJECTORY
50 LB PAYLOAD

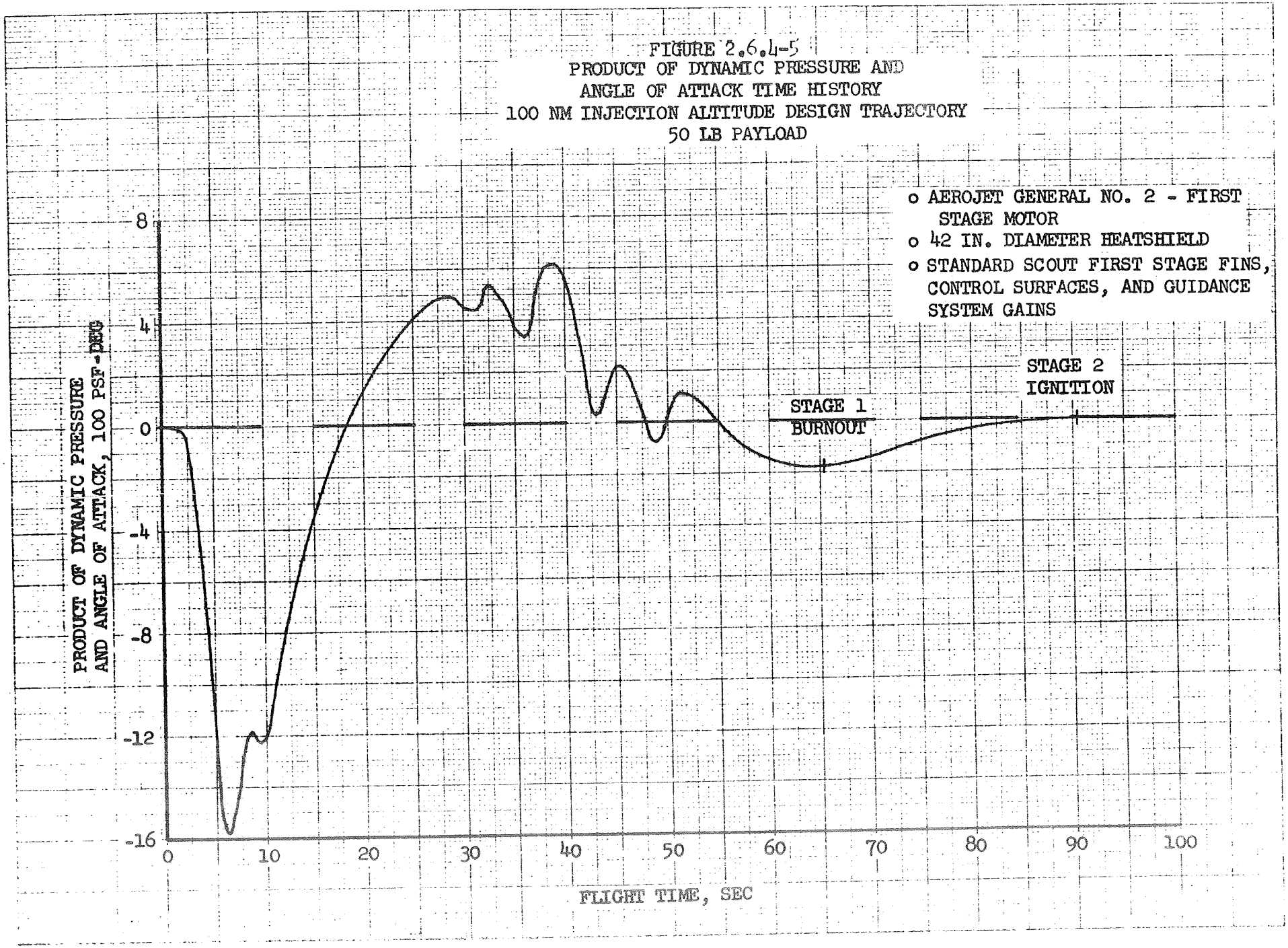

FIGURE 2.6.4-6
PITCH FIN DEFLECTION TIME HISTORY
100 NM INJECTION ALTITUDE DESIGN TRAJECTORY
50 LB PAYLOAD

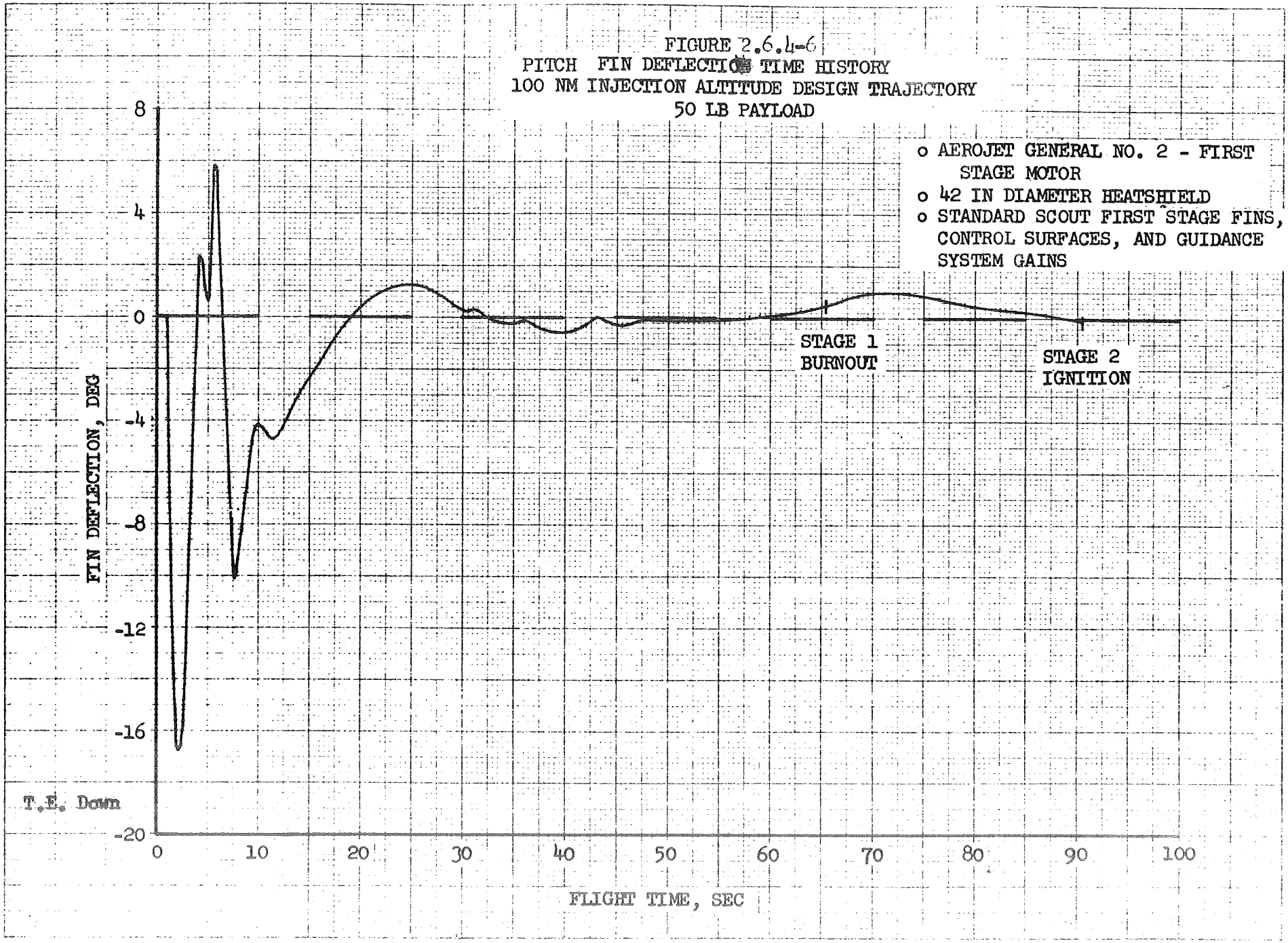

FIGURE 2.6.4-7
PRODUCT OF DYNAMIC PRESSURE AND
ANGLE OF ATTACK TIME HISTORY
100 NM INJECTION ALTITUDE DESIGN TRAJECTORY
400 LB PAYLOAD

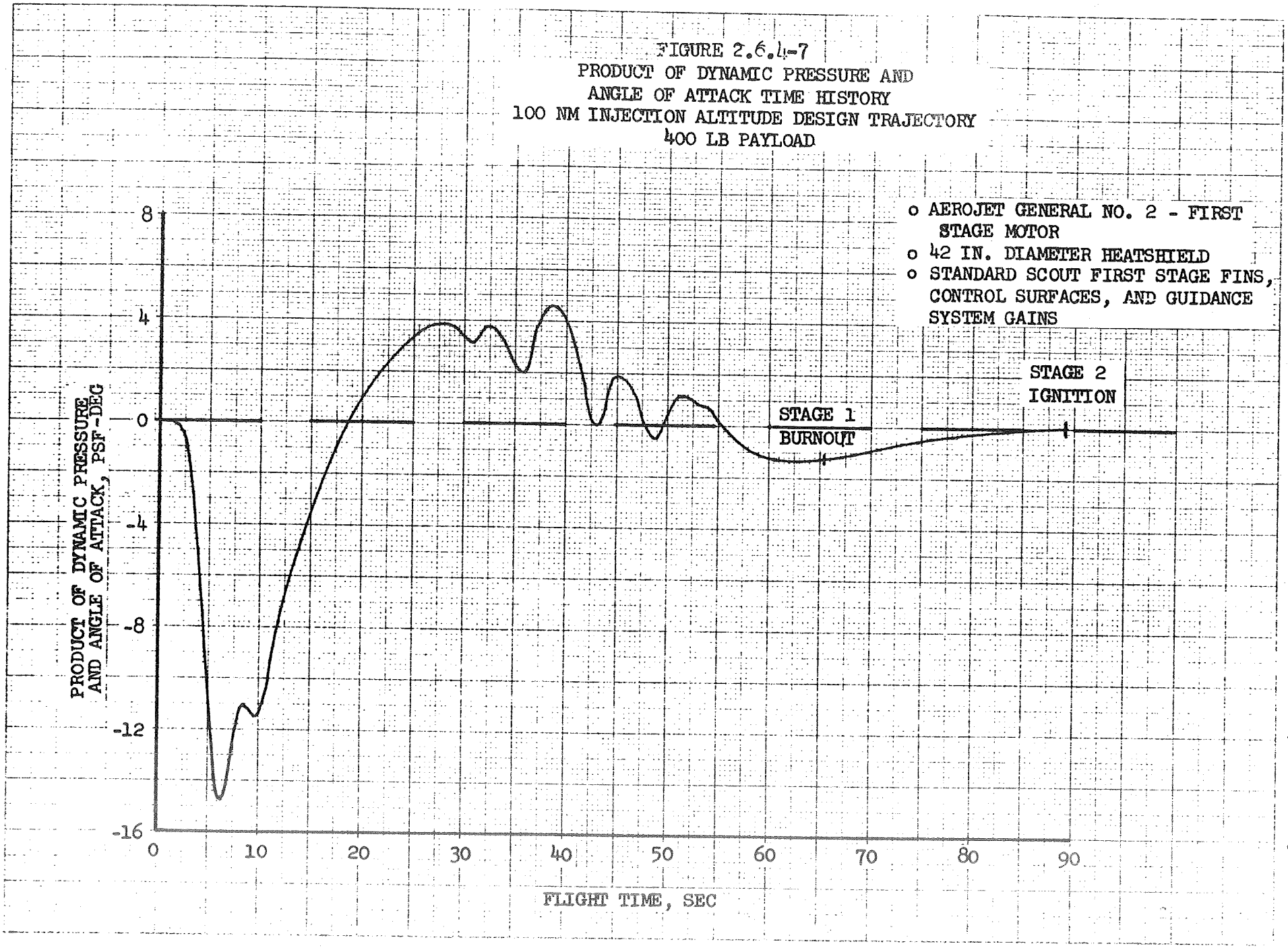

FIGURE 2.6.4-8
PITCH FIN DEFLECTION TIME HISTORY
100 NM INJECTION ALTITUDE DESIGN TRAJECTORY
400 LB PAYLOAD

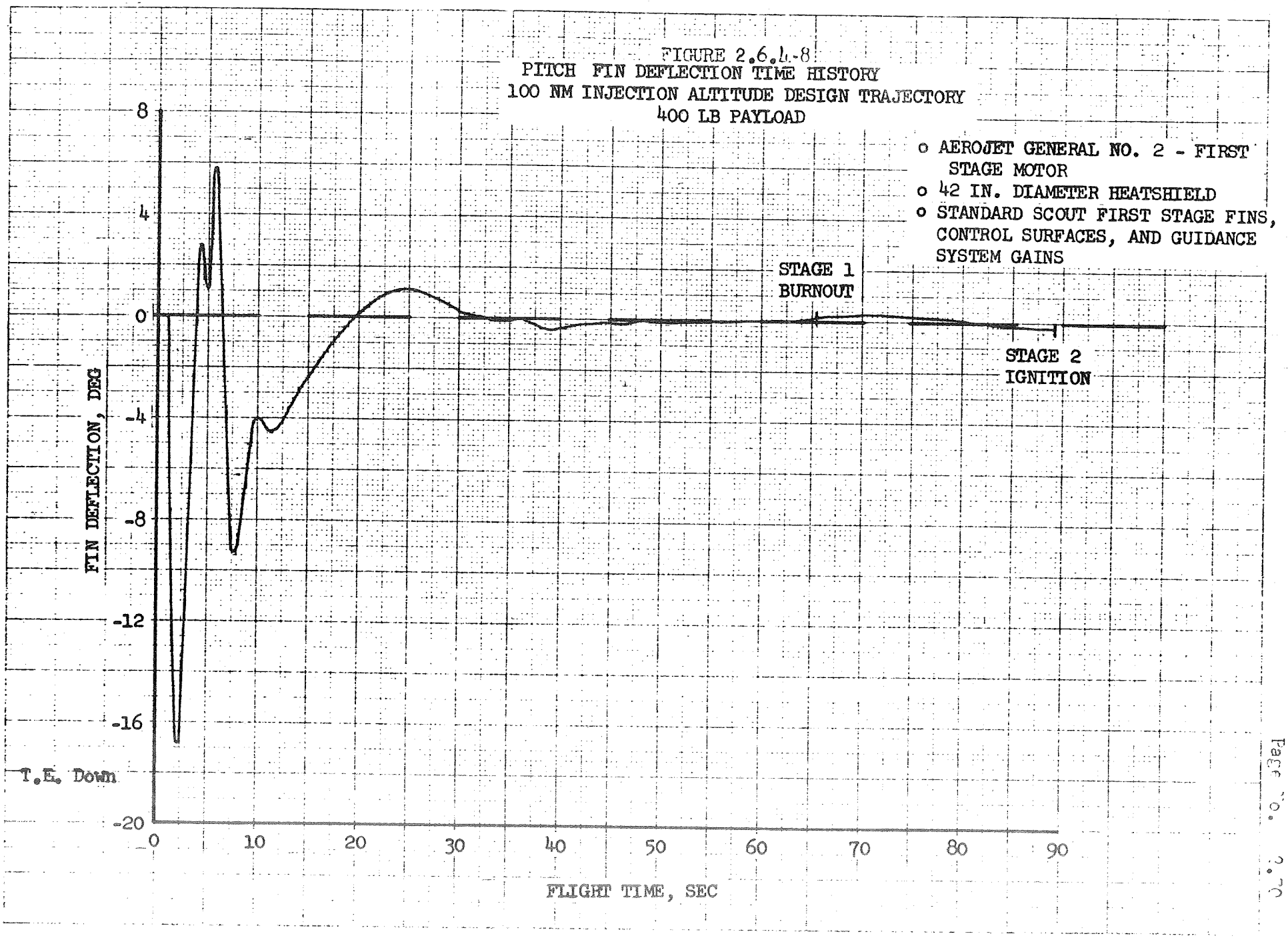

FIGURE 2.6.1-9

PRODUCT OF DYNAMIC PRESSURE AND ANGLE OF ATTACK TIME HISTORY
100 NM INJECTION ALTITUDE DESIGN TRAJECTORY
50 LB PAYLOAD

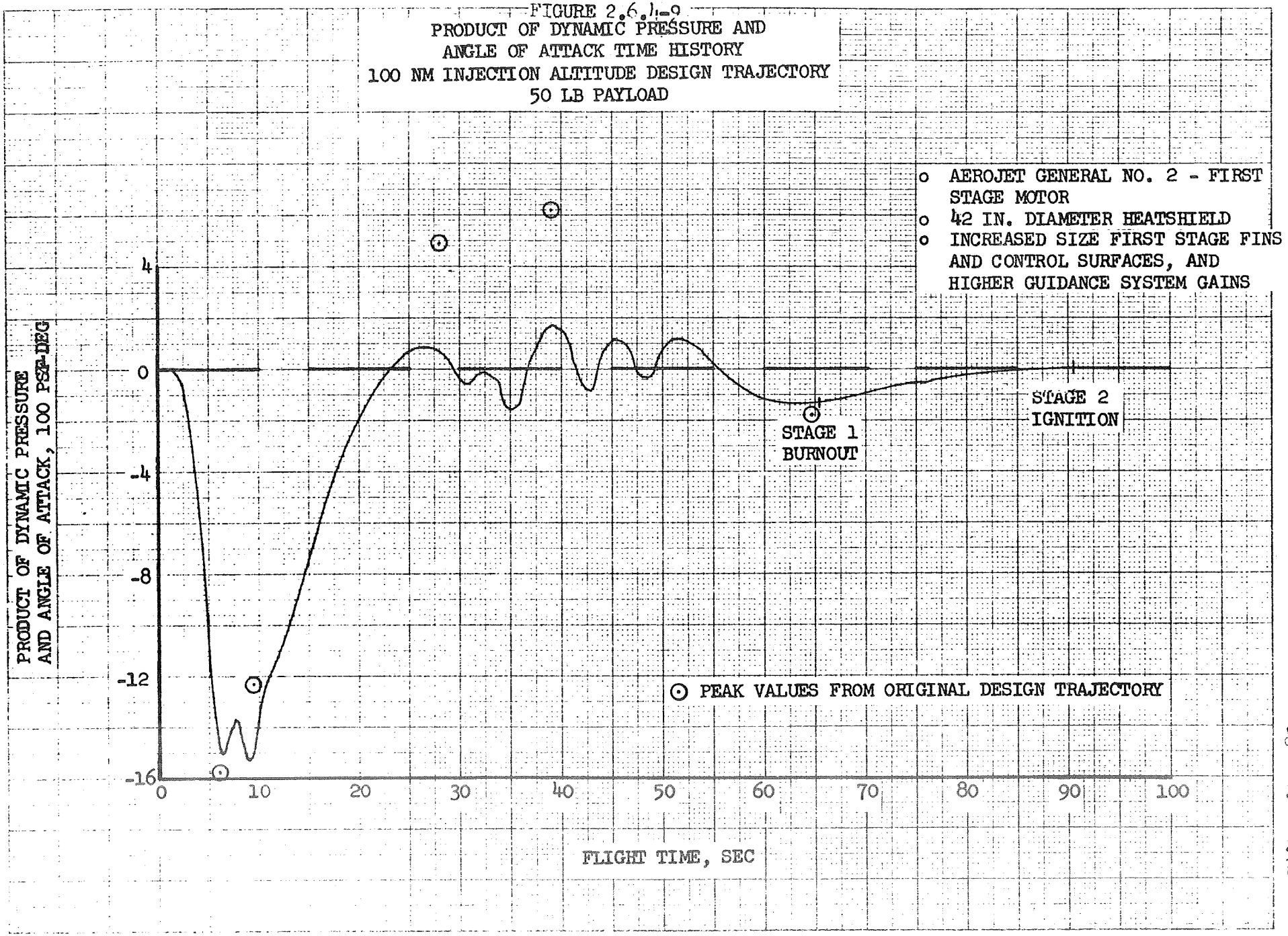

FIGURE 2.6.4-10

PITCH FIN DEFLECTION TIME HISTORY
100 NM INJECTION ALTITUDE DESIGN TRAJECTORY
50 LB PAYLOAD

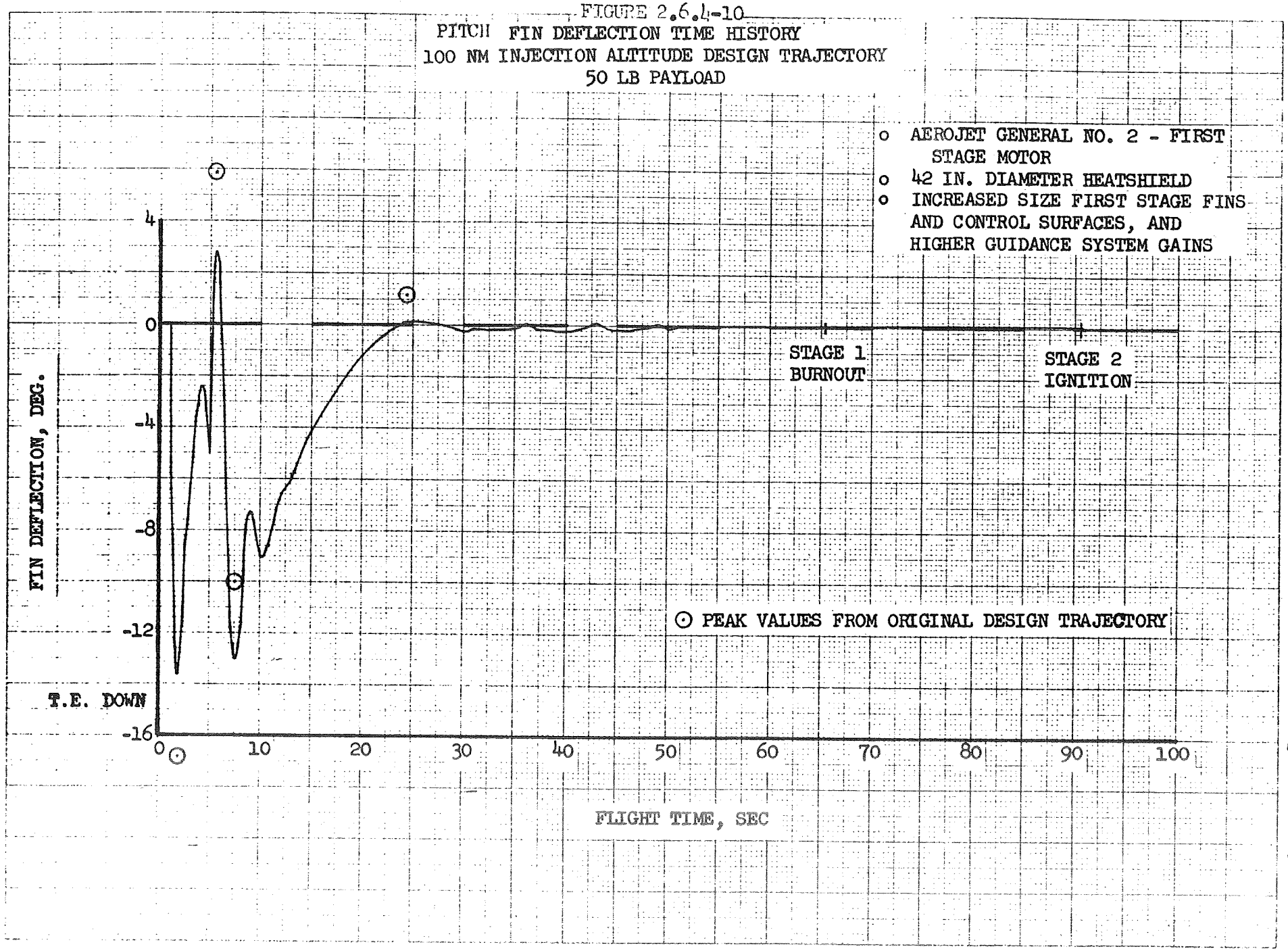

FIGURE 2.6.4-11
VEHICLE WEIGHT TIME HISTORY
100 NM INJECTION ALTITUDE DESIGN TRAJECTORY
50 LB. PAYLOAD

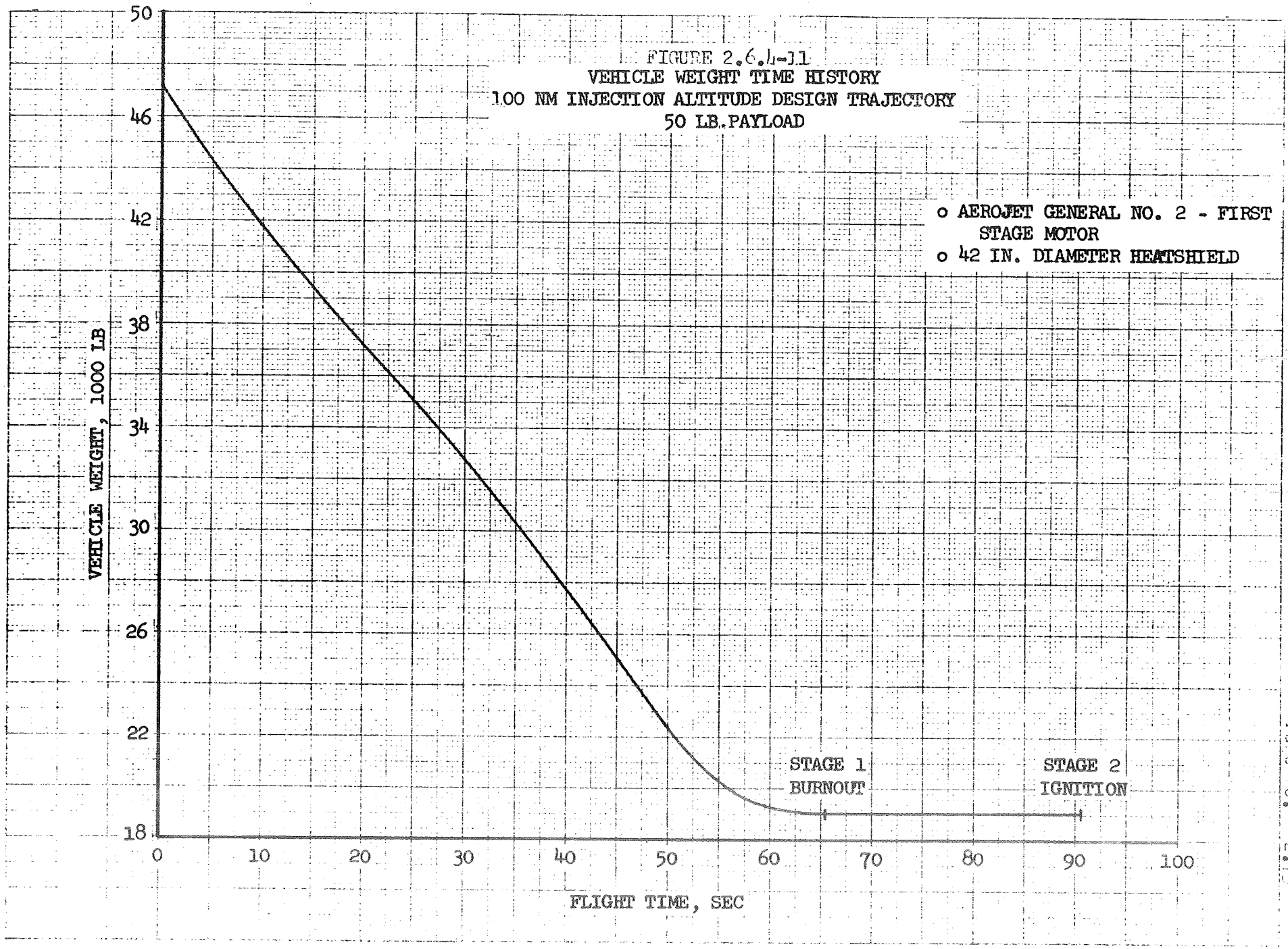

FIGURE 2.6.4-12
ACTUAL THRUST TIME HISTORY
100 NM INJECTION ALTITUDE DESIGN TRAJECTORY

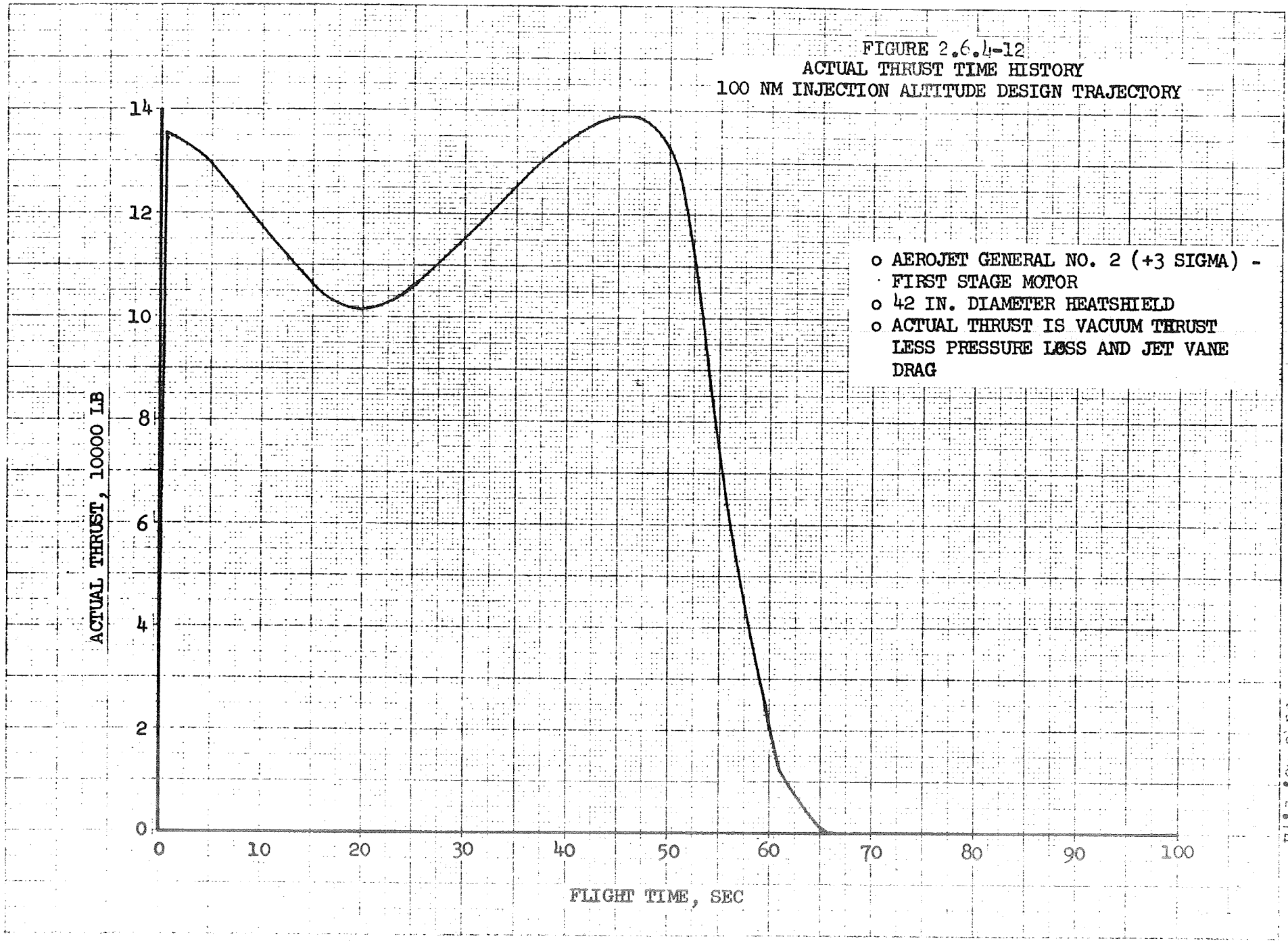

2.7 THERMAL ANALYSIS

Aerodynamic heating analyses was performed for larger Scout heatshields with heatshield diameters from 40 to 46 inches with the shapes defined in Figure 2.2.3-1. The design trajectory used was based upon an Algol III first stage rocket motor. Results showed temperatures equal to or higher than those for the current operational Scout, but lower than those for Scout with an Algol III booster and current 34 inch diameter heatshield. It was concluded that no additional thermal protection was required for the heatshields considered.

2.7.1 Method of Analysis

Figures 2.7.1-1 and 2.7.1-2 present the altitude and free stream Mach number time histories which were employed. This trajectory was based upon the Aerojet No. 2 version of the Algol III first stage motor, a 50 pound payload and a 100 nautical mile injection altitude. Trajectory data from Reference 3-9 for the current operational Scout and for Scout with the 44 inch version of Algol III are shown for comparison. The design trajectory is quite similar to the 44 inch Algol trajectory, but hotter than the current Algol II trajectories.

The temperature-time response was computed for the nose cone stagnation point and for one point each on the conical and cylindrical sections of the heatshield. Thermal Analyzer routine LVV622, which incorporates the aerodynamic heating methods of Reference 2-6 , was used in these analyses. Results were compared with previous predictions for current operational Scout.

2.7.2 Results

Figure 2.7.2-1 shows the variation of heatshield temperature with shield cylindrical section diameter. New temperature data was generated for 42 and 46 inch diameters only. To assist in establishing curves for interpolation and extrapolation to 40 and 44 inch diameters, previous results from

Reference 3-9 for a 34 inch shield were included. The Reference 3-9 temperatures were based upon use of the 44 inch version of the Algol III booster.

It is seen that heatshield temperatures decrease with increasing heatshield diameter due to reduced heating rates associated with increasing nose radius and decreasing cone angle. Temperatures are still equal to or higher than those on current operational Scout due to the hotter trajectory with Algol III compared to Algol II. However, for heatshields in the 40 to 46 inch diameter range, computed temperatures are not high enough to require additional thermal protection. It should be noted that Reference 3-9 concluded that a 34 inch heatshield on Scout with Algol III would require thicker cork (0.10 inch) on the conical section to avoid overheating the cork bond. Computed heating rates on the heatshield are shown in Figures 2.7.2-2 through 2.7.2-4.

2.7.3 Conclusions

No additional thermal protection is required for Scout heatshields in the 40 to 46 inch diameter range with the Algol III booster. Smaller heatshields may require additional cork on the conical section to avoid overheating the cork bond.

FIGURE 2.7.1-1
TRAJECTORY - ALTITUDE vs. TIME
(Comparison of Various Vehicle Configurations)

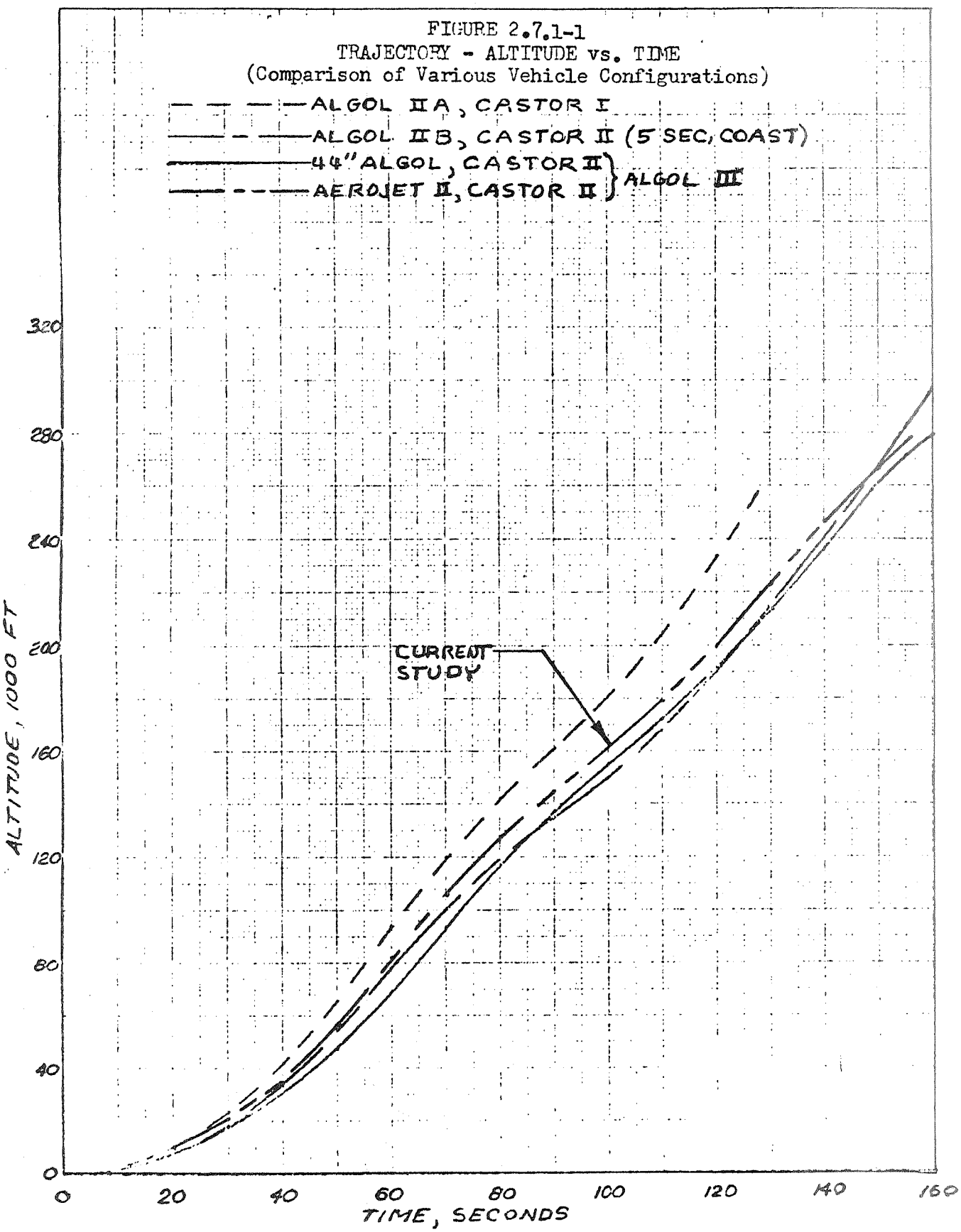

FIGURE 2.7.1-2
TRAJECTORY - MACH NUMBER vs. TIME
(Comparison of Various Vehicle Configurations)

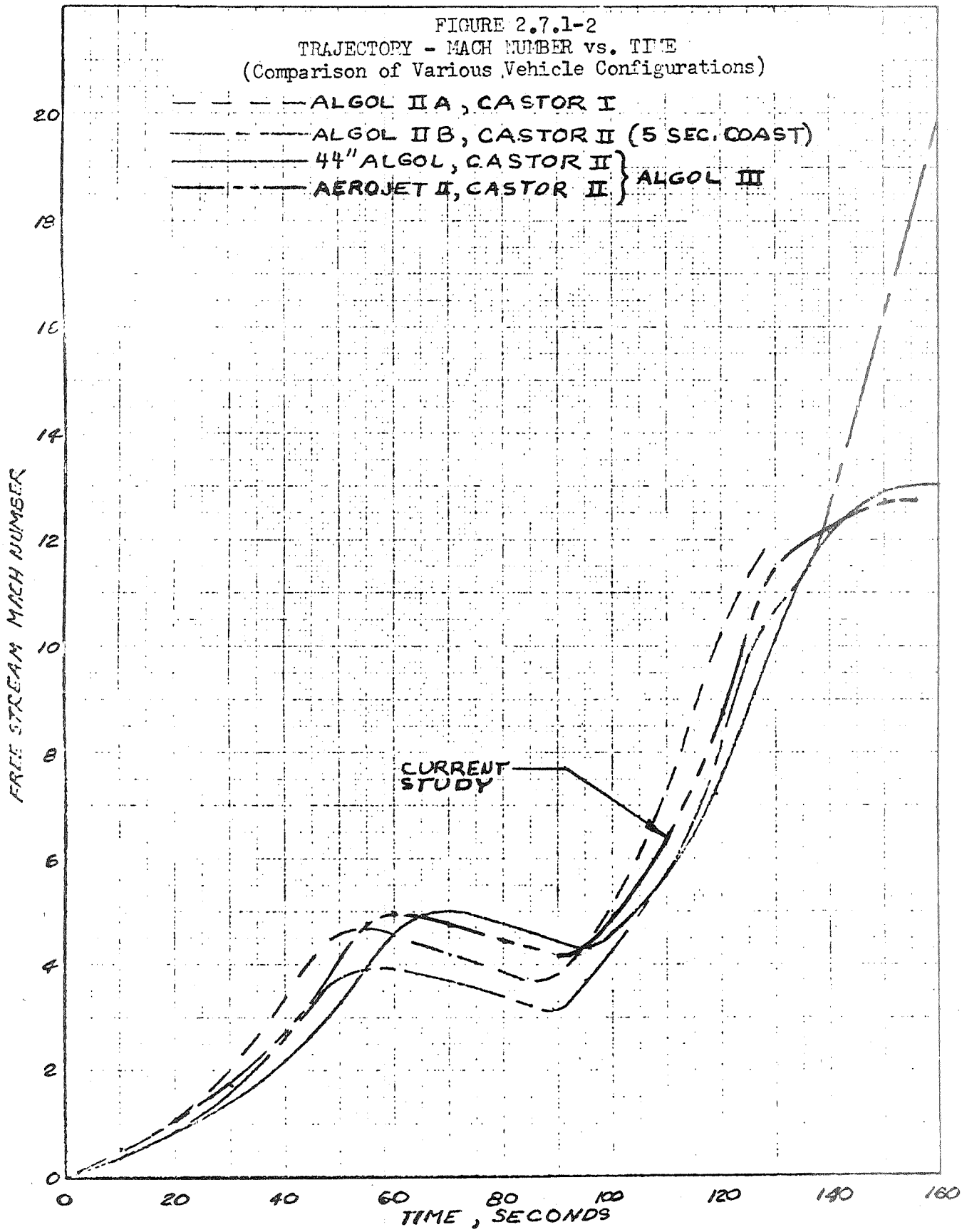

FIGURE 2.7.2-1
MAXIMUM HEATSHIELD TEMPERATURES
vs. HEATSHIELD DIAMETER

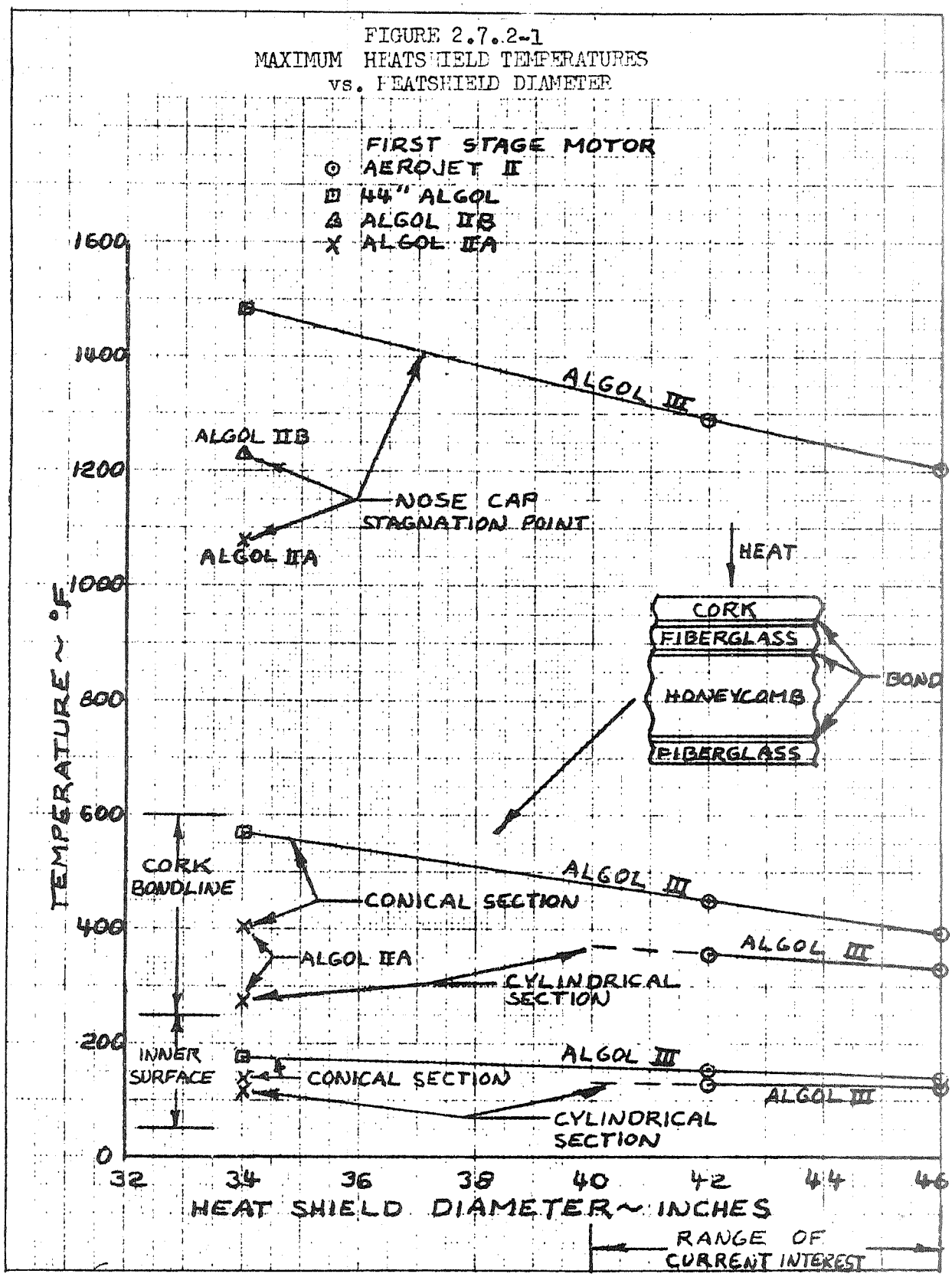

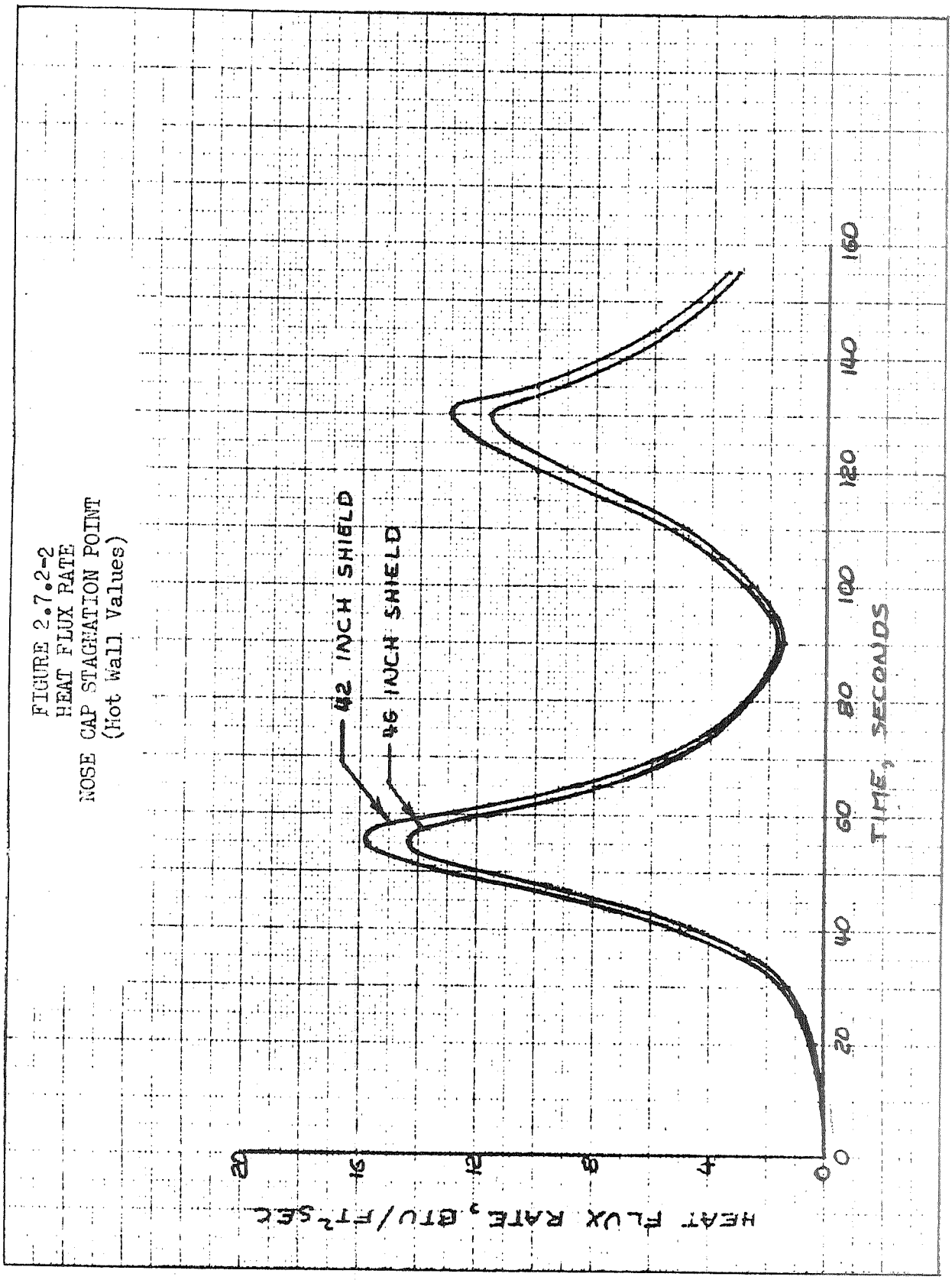

FIGURE 2.7.2-2
HEAT FLUX RATE
NOSE CAP STAGNATION POINT
(Hot Wall Values)

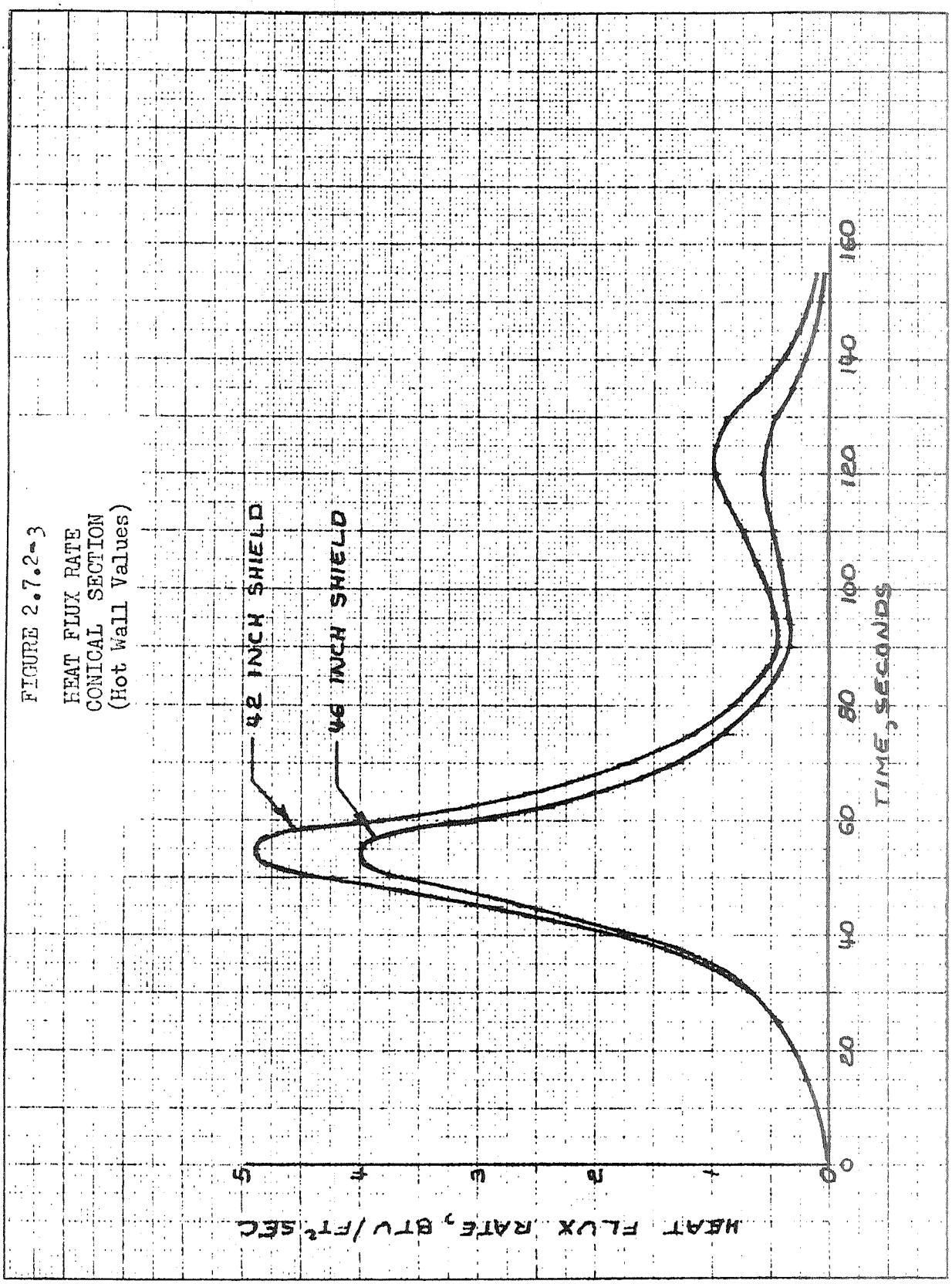

FIGURE 2.7.2-3

HEAT FLUX RATE
CONICAL SECTION
(Hot Wall Values)

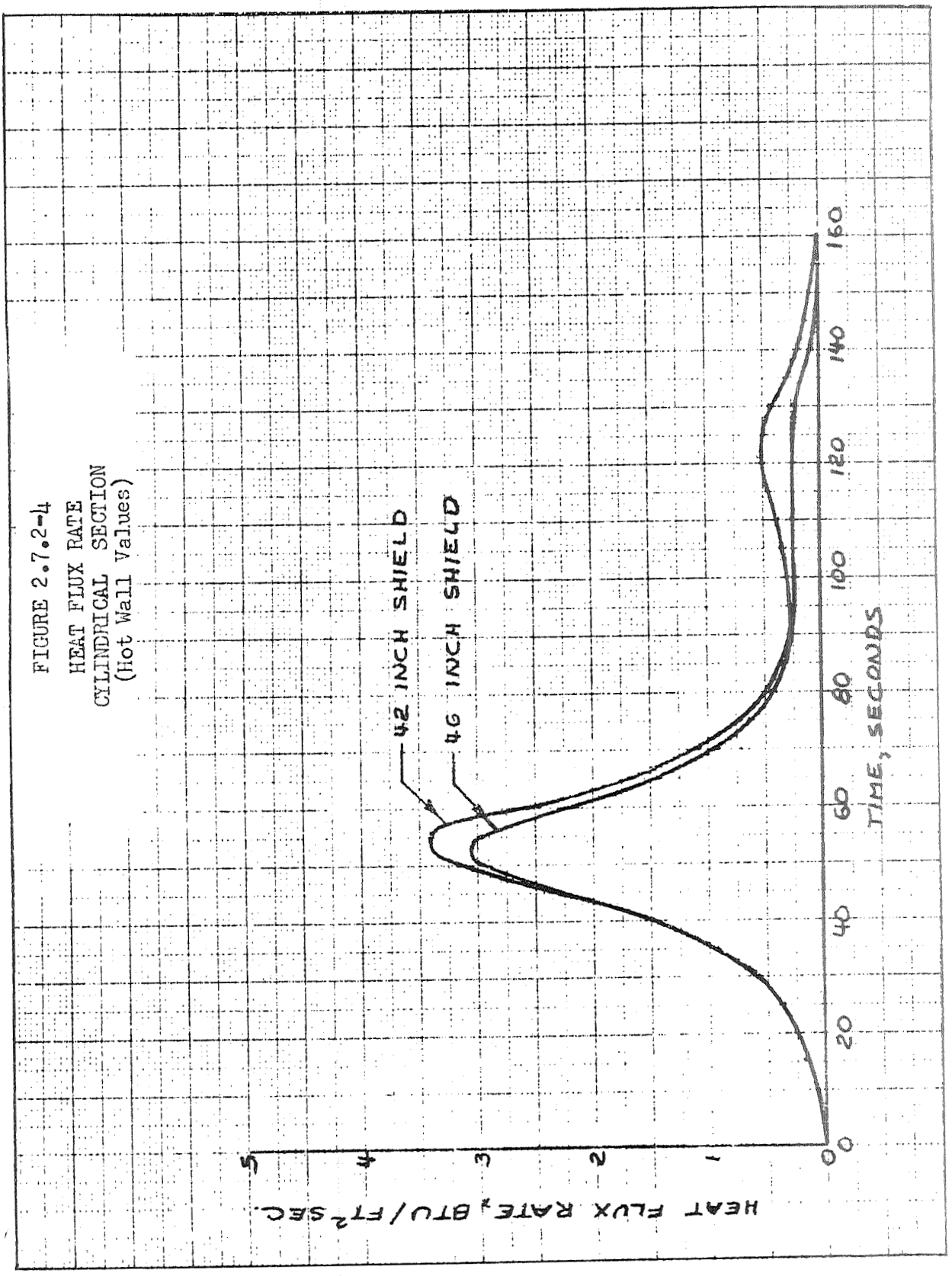

FIGURE 2.7.2-4
HEAT FLUX RATE
CYLINDRICAL SECTION
(Hot Wall Values)

3.0 VEHICLE CONFIGURATIONS

3.1 40 INCH DIAMETER HEATSHIELD INSTALLATION

3.1.1 Summary

The results of the evaluation of the impact of the 40 inch diameter heatshield installation on the Scout D configuration are summarized as follows:

- No vehicle structural changes required except the control surfaces.
- Fin control tip area shall be increased from 45 sq. in. to 78 sq. in. This increases the fin area from 4.5 to 4.735 sq. ft.
- Jet vane control surface area shall be increased from 35 sq. in. to 41 sq. in.
- Guidance system first stage nominal displacement gain shall be increased from 5.0 to 6.75 deg/deg and the rate to displacement ratio shall be 0.4, the same as for the basic Scout.
- The following ground support equipment requires redesign: payload umbilical retract arm, heatshield cradle, dummy heatshield, payload and heatshield hoist, heatshield storage bracket, and the upper cradle assembly.

Detailed discussion of the evaluation is presented in the following paragraphs.

3.1.2 Aerodynamic Characteristics

3.1.2.1 Rigid Vehicle

Normal load distributions aft to station 131.1 are presented in Figures 3.1.2-1 through -4. These data were evaluated using the technique described in Section 3.2.2.1. For load distributions aft of station 131.1, use Figures 3.2.2-11 through -14.

Heatshield drag buildup is presented in Figure 3.1.2-5, and was obtained using the technique described in Section 3.2.2.1 for determining the estimated zero lift drag.

FIGURE 3.1.2-1
NORMAL LOAD DISTRIBUTION
40 MV. C.G. MEATSHIELD
$\Phi_c = 15°$ $r/R = .56$

$M_\infty = 0.8$

$C_{N_\alpha} S = \int C_{N_\alpha} b \, dx = .1263 \text{ FT}^2 \text{ DEG}^{-1}$

c.p. @ STA - 51.4

$C_{N_\alpha} b \sim$ FT DEG^{-1}

.10
.08
.06
.04
.02
0
-.02
-.04
-.06
-.08

-50 0 50 100 150

STATION

x

FIGURE 3.1.2-2
NORMAL LOAD DISTRIBUTION
40. IN. DIA. HEATSHIELD
$\theta_c = 15°$ $r/R = .55$
$M_\infty = 4.0$

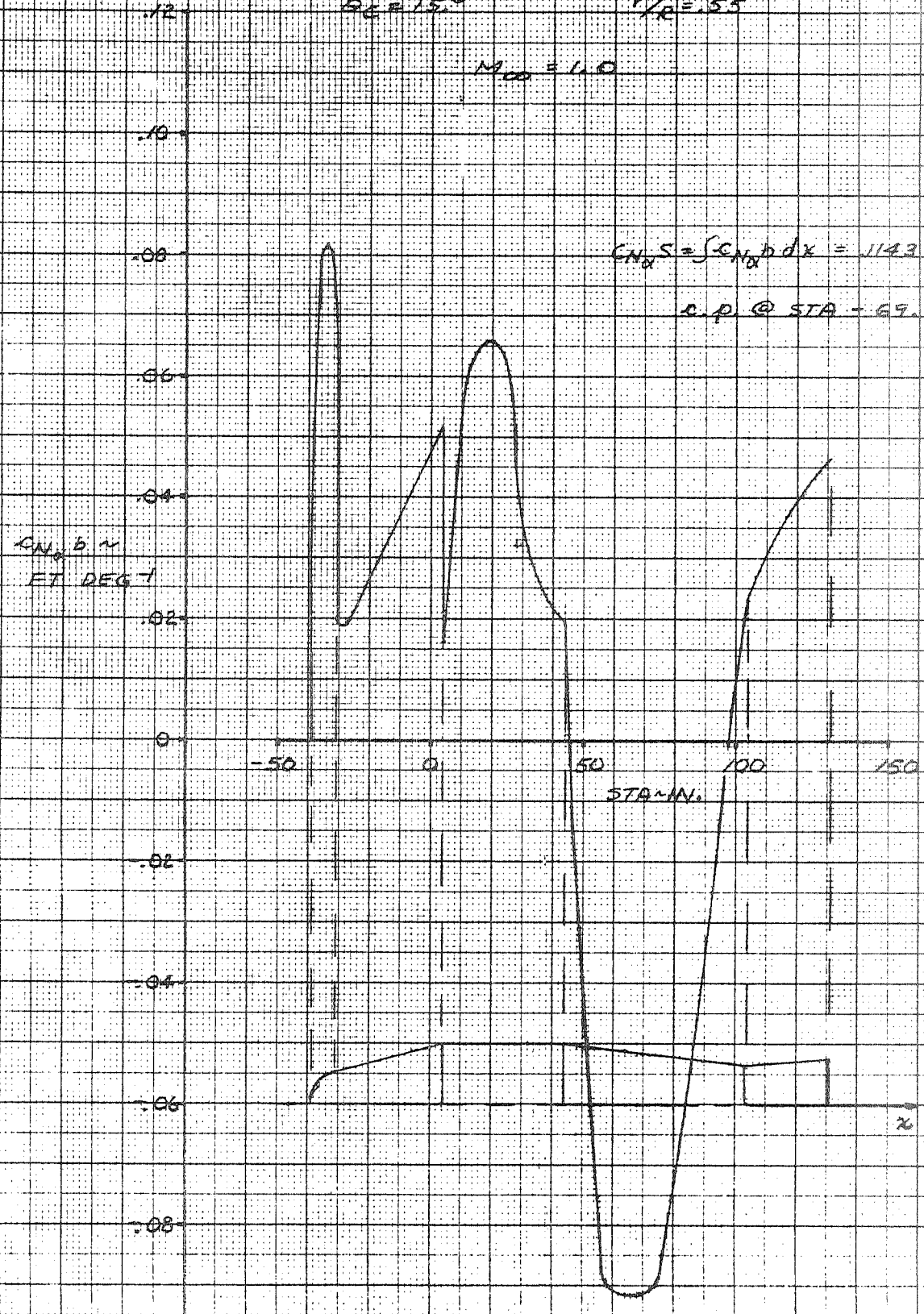

$C_{N_\alpha} S = \int C_{N_\alpha} b \, dx = .1143$ FT² DEG⁻¹

c.p. @ STA - 69.

FIGURE 3.1.2-3
NORMAL LOAD DISTRIBUTION
40 in. dia. HEATSHIELD
$\Phi_{LE} = 45°$ $r/R = .55$
$M_\infty = 4.5$

$C_{N_\alpha} S = \int C_{N_\alpha} b\, dx = .2164$ FT^2/DEG

$C.P. @ STA = 2.6$

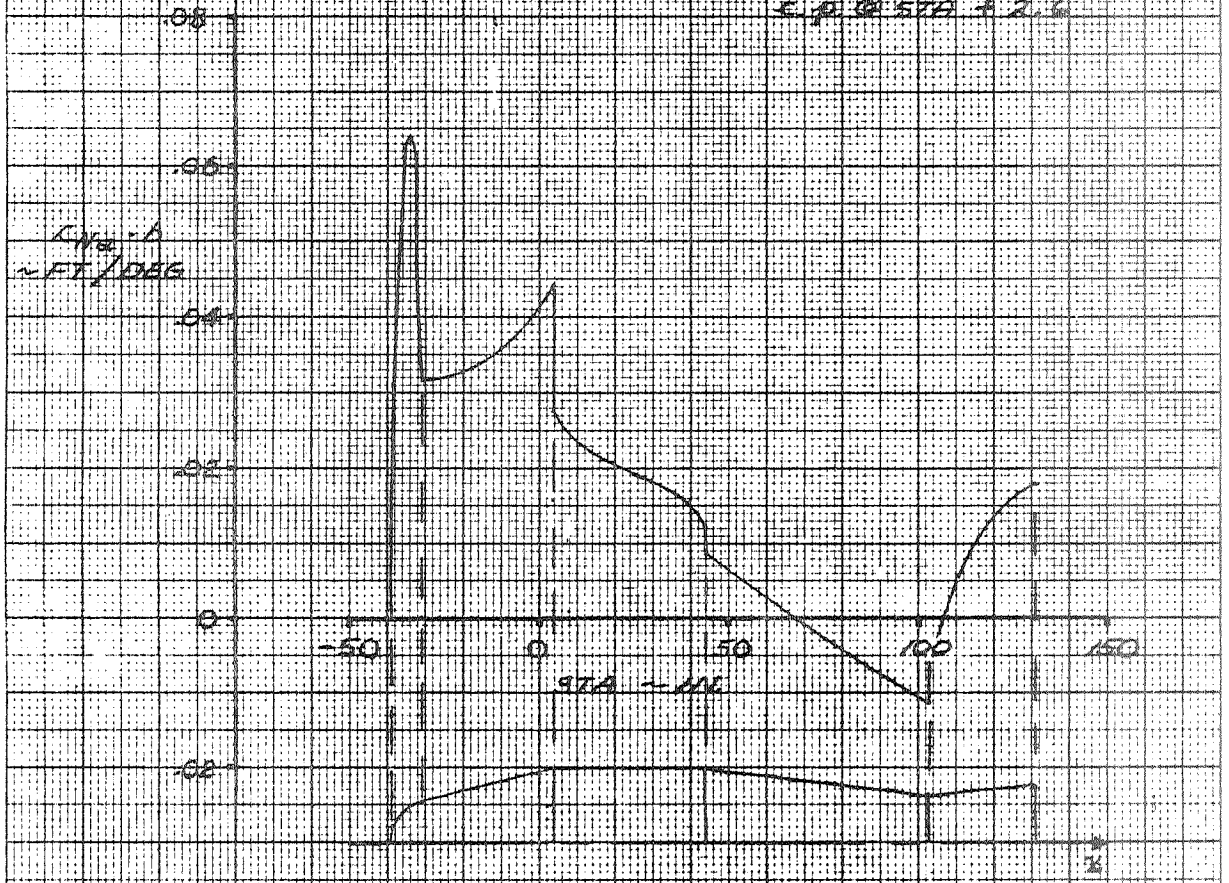

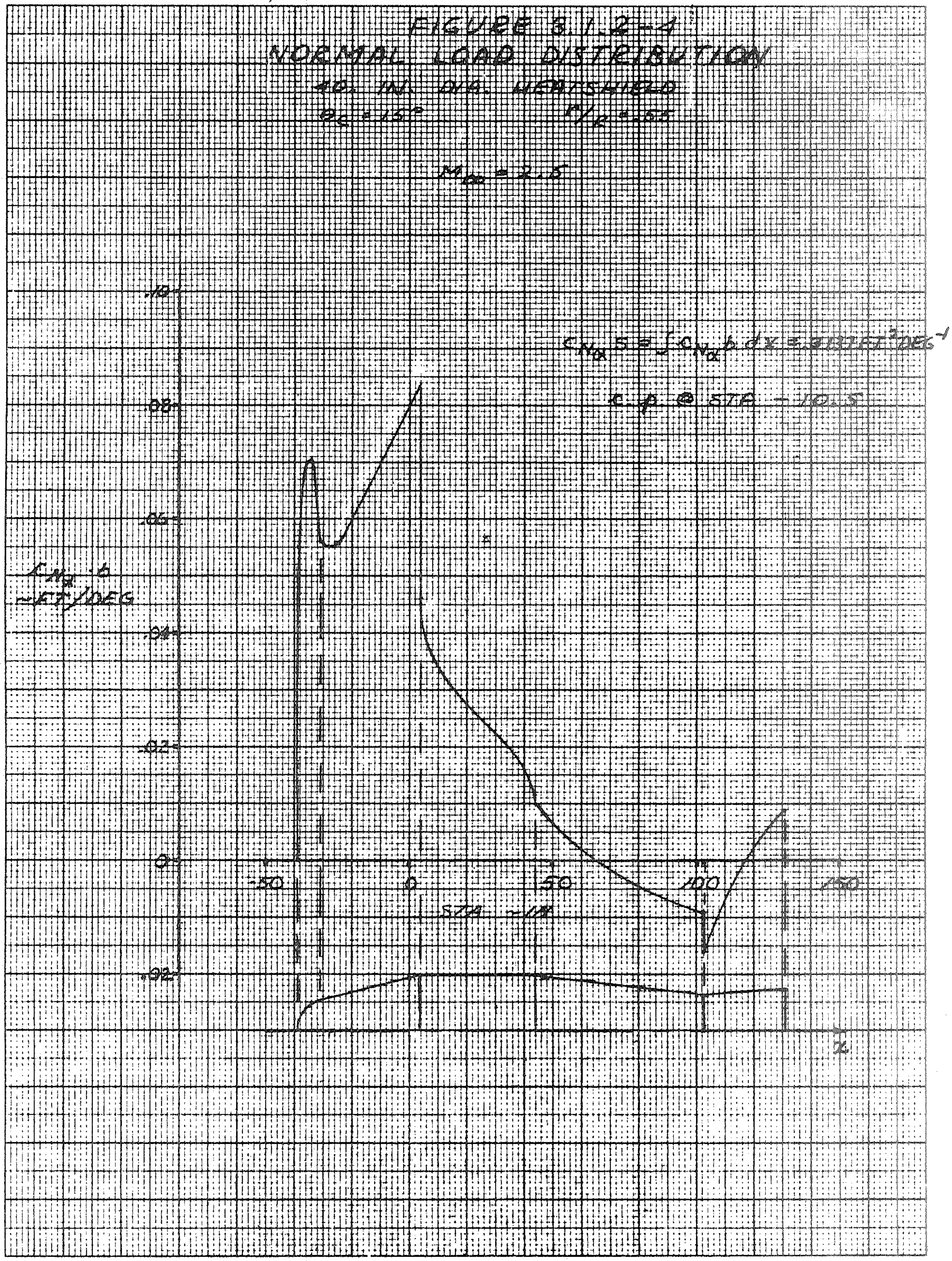
FIGURE 3.1.2-4
NORMAL LOAD DISTRIBUTION
40. IN. DIA. HEATSHIELD
$\theta_c = 15°$
$M_\infty = 2.5$
$C_{N_\alpha} S = \int c_{N_\alpha} b\, dx$
c.p. @ STA - 10.5
$c_{N_\alpha} \cdot b$
~FT/DEG
.10
.08
.06
.04
.02
0
-.02
-50
0
50
100
150
STA ~ IN
x

-15-69

FIGURE - 3.1.2-5
HEATSHIELD DRAG BUILDUP
(PRESSURE AND FRICTION)
40. IN. DIA. HEATSHIELD
$\theta_c = 15°$ $r/2 = .55$

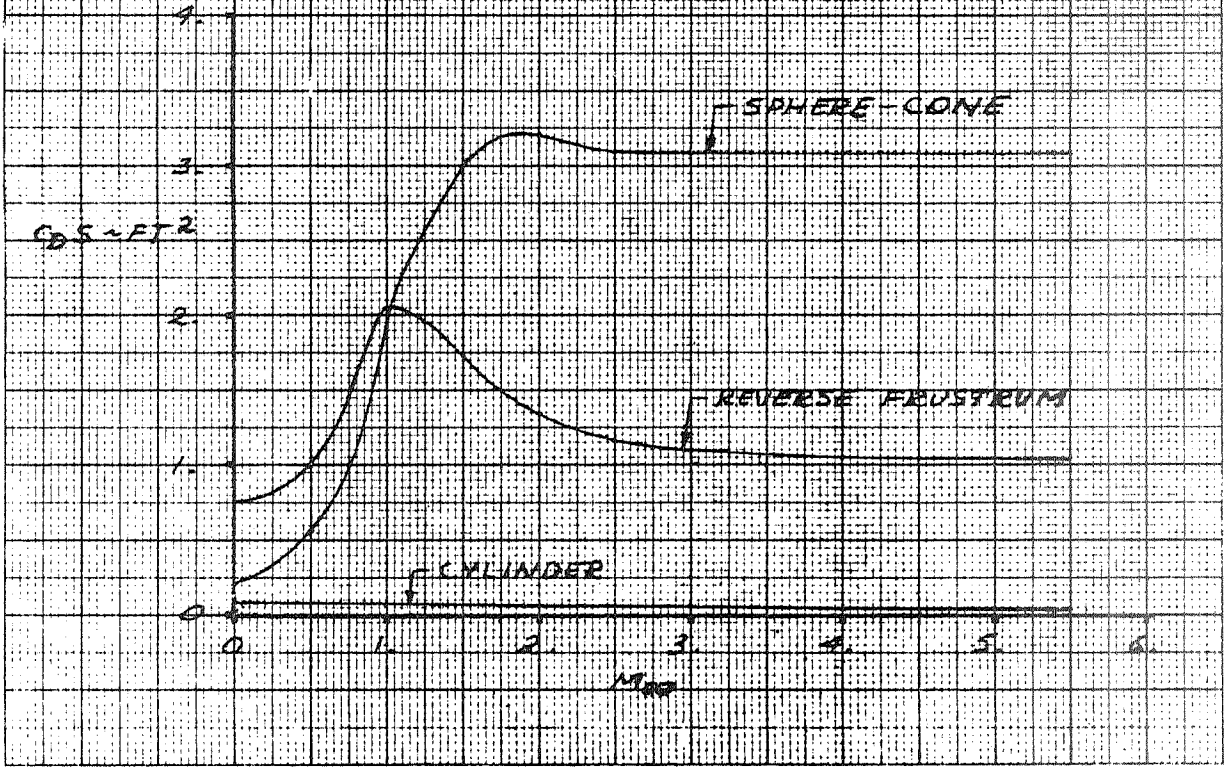

3.1.2.2 Flexible Body Aerodynamics

Discussion on the flexible body aerodynamics for the 40 inch diameter heat shield configuration may be found in Section 3.2.2.2.

3.1.3 Weight and Balance Data

This section presents the weights, longitudinal center of gravity and moments of inertia for a Scout vehicle (S-178 & Sub. configuration) utilizing a 40 inch diameter heatshield and an Algol III (Aerojet Proposal No. 2) first stage motor replacing the standard Algol II first stage motor. The standard Base A and 4.5 sq. ft. fins are included in this data.

The vehicle mass properties data is shown in Table 3.1.3-1 with a 50 pound payload and in Table 3.1.3-2 a 400 pound payload. A 40 inch diameter heatshield of similar construction to the present 34 inch diameter was estimated to weigh 325.45 pounds with the heatshield c.g. at Station 34.0.

TABLE 3.1.3-1
MASS PROPERTIES

40 INCH DIAMETER, -38.93 LARGE VOLUME HEATSHIELD, (50 POUND PAYLOAD)

VEHICLE S- WEIGHT, X(CG), AND MOMENTS OF INERTIA

VERSUS PERCENT OF FUEL CONSUMED

	TOTAL WEIGHT, POUNDS	C.G. SCOUT STA.-IN.	IXX SLUG-FT^2	IYY OR IZZ SLUG-FT^2
	*******	*******	**********	**********
FOURTH STAGE - BURNOUT	118.96	53.35	2.38	23.82
75 0/0	271.79	60.33	5.00	30.66
50 0/0	424.63	62.28	6.87	35.52
25 0/0	577.46	63.20	8.00	39.68
FOURTH STAGE - IGNITION	730.30	63.74	8.38	43.34
SPIN-UP ITEMS	774.68	65.92	9.37	56.93
THIRD STAGE - BURNOUT	1483.95	116.61	29.45	1287.32
75 0/0	2135.08	130.01	56.88	1545.14
50 0/0	2786.22	137.15	76.77	1710.98
25 0/0	3437.35	141.58	89.11	1834.97
THIRD STAGE - IGNITION	4088.49	144.61	93.90	1935.30
LESS N/C - H/S	6159.25	229.28	181.48	23526.18
SECOND STAGE - BURNOUT	6484.78	219.48	201.76	26199.80
75 0/0	8561.02	250.07	294.90	33009.43
50 0/0	10637.27	268.72	362.89	37698.07
25 0/0	12713.51	281.28	405.76	41298.74
SECOND STAGE - IGNITION	14789.76	290.31	423.52	44264.33
FIRST STAGE - BURNOUT	19074.06	379.79	797.87	172808.41
75 0/0	26057.06	451.92	1458.98	266093.12
50 0/0	33040.06	493.56	1949.75	325505.83
25 0/0	40023.06	520.67	2270.45	368731.49
FIRST STAGE - IGNITION	47006.06	539.73	2420.87	402946.11

TABLE 3.1.3-2
MASS PROPERTIES

40 INCH DIAMETER, -38.93 LARGE VOLUME HEATSHIELD, (400 POUND PAYLOAD)

VEHICLE S- WEIGHT, X(CG), AND MOMENTS OF INERTIA

VERSUS PERCENT OF FUEL CONSUMED

	TOTAL WEIGHT, POUNDS	C.G. SCOUT STA.-IN.	IXX SLUG-FT^2	IYY OR IZZ SLUG-FT^2
	*******	*******	**********	**********
FOURTH STAGE - BURNOUT	468.96	31.44	10.88	51.43
75 0/0	621.79	39.88	13.50	85.34
50 0/0	774.63	44.99	15.37	107.31
25 0/0	927.46	48.41	16.50	123.07
FOURTH STAGE - IGNITION	1080.30	50.86	16.88	135.09
SPIN-UP ITEMS	1124.68	52.87	17.87	159.46
THIRD STAGE - BURNOUT	1833.95	98.93	37.95	1822.64
75 0/0	2485.08	115.08	65.38	2285.66
50 0/0	3136.22	124.52	85.26	2581.34
25 0/0	3787.35	130.72	97.60	2794.04
THIRD STAGE - IGNITION	4438.49	135.10	102.40	2958.63
LESS N/C - H/S	6509.25	218.25	189.98	26549.66
SECOND STAGE - BURNOUT	6834.78	209.47	210.26	28949.80
75 0/0	8911.02	241.19	303.40	36729.81
50 0/0	10987.27	260.92	371.39	42089.26
25 0/0	13063.51	274.38	414.26	46176.31
SECOND STAGE - IGNITION	15139.76	284.15	432.02	49509.28
FIRST STAGE - BURNOUT	19424.06	373.38	806.37	182210.21
75 0/0	26407.06	446.25	1467.47	279754.49
50 0/0	33390.06	488.64	1958.25	341999.28
25 0/0	40373.06	516.37	2278.95	387216.93
FIRST STAGE - IGNITION	47356.06	535.92	2429.37	422902.04

3.1.4 Stability and Control

The stability and control of the first and second stages with a proposed Algol III first stage motor and a 40 inch diameter heatshield was analyzed. The first stage pitch axis stability was investigated near the maximum dynamic pressure by the root locus technique. Control gains, fin sizes and control surface effectiveness were determined for the Algol III configuration. The configuration was then analyzed in pitch for the response to the pitch program changes, winds and thrust misalignment. Hinge moments were estimated for the larger sized jet vanes and fin tips. The second stage ignition dynamic pressure limitations were estimated for the Algol III design trajectory. An estimate of the second stage fuel consumption as affected by the larger heatshield was made.

3.1.4.1 First Stage Stability Near Maximum Dynamic Pressure

The first stage pitch axis stability was investigated near the region of maximum dynamic pressure for each of the heatshield configurations. This analysis was done by the root locus technique and included one translational mode, one rotational mode (pitch), the first four bending modes of vibration, and the pitch axis filter-servo-actuator response characteristics. The analysis utilized the Algol III design trajectory for the 50 pound payload described in Section 2.6. The Mach number and dynamic pressure time history was adjusted between 20,000 and 45,000 feet altitude to include a 90 knot headwind. The time histories of Mach number, dynamic pressure, center of mass location, and moment of inertia used in the root locus analysis are shown in Figure 3.1.4-1. The thrust data are presented in Section 2.3, aerodynamic data are presented in Sections 3.1.2 and 3.2.2 and the jet vane data are presented in Section 2.4. Other significant constants used in the analysis are presented in Table 3.1.4-1.

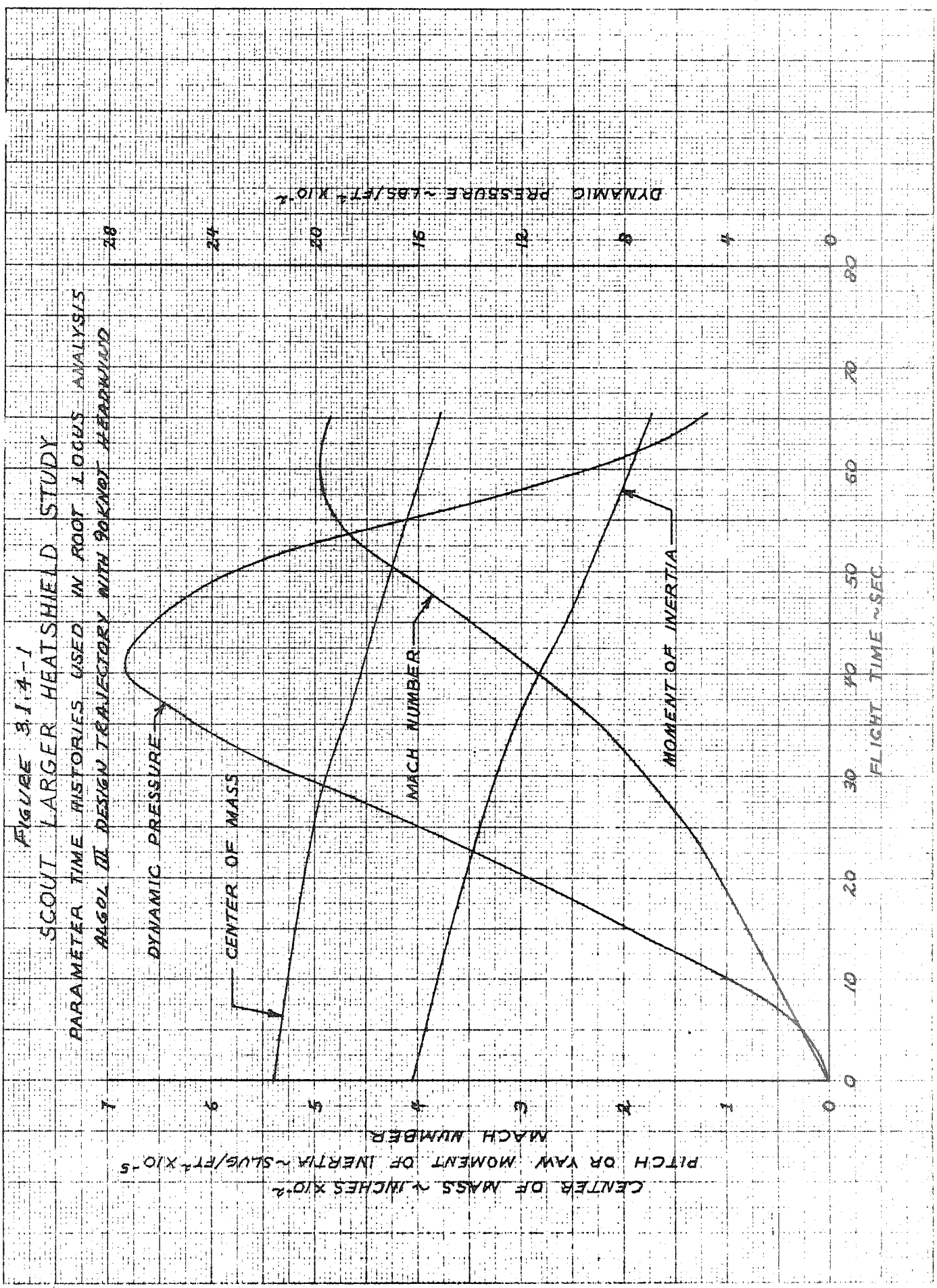
FIGURE 3.1.4-1
SCOUT LARGER HEATSHIELD STUDY
PARAMETER TIME HISTORIES USED IN ROOT LOCUS ANALYSIS
ALGOL III DESIGN TRAJECTORY WITH 90 KNOT HEADWIND
DYNAMIC PRESSURE
CENTER OF MASS
MACH NUMBER
MOMENT OF INERTIA
FLIGHT TIME ~ SEC
MACH NUMBER
PITCH OR YAW MOMENT OF INERTIA ~ SLUG/FT² X10⁻⁵
CENTER OF MASS ~ INCHES X10⁻²
DYNAMIC PRESSURE ~ LBS/FT² X10⁻²

TABLE 3.1.4-1

CONSTANTS USED IN ROOT LOCUS ANALYSIS

Algol III, Castor II, X-259, FW-4S, 50 lb. Payload
(45 seconds flight time)

141000.	Thrust, lbs.
25200.	Weight, lbs.
253500.	Pitch or Yaw Moment of Inertia, slug/ft^2
445.	Center of Mass, in.
3360.	Velocity, ft/sec.
2640.	Dynamic Pressure, lbs/ft^2
0.40	Gain Ratio (seconds)
	Base A Freq. Response Poles:
29.	ω_{1F} filter (rad/sec)
33.	ω_{2F} filter (rad/sec)
13.31	ω_{1S} servo-actuator (rad/sec)
167.54	ω_{2S} servo-actuator (rad/sec)
0.01	Structural Damping Factor
853.45	Control Location (Station)
824.	Thrust Vector Point of Application (Station)

The critical time period for vehicle stability occurs near maximum dynamic pressure where the vehicle aerodynamic center of pressure is forward of the center of mass. Root loci analysis of the vehicle stability indicated that the most critical area occurred at 45 seconds flight time at which time the Mach number is 3.5 and the dynamic pressure is 2640 pounds per square foot. The root loci for this flight time is shown in Figure 3.1.4-2 for the 40 inch diameter heatshield configuration with a fin area including tip of 4.73 square feet, a tip area of 0.542 square feet (78 square inches) and a jet vane area of 41 square inches.

The first bending mode is stabilized by the control system for all gains investigated. The pitching mode is unstable at low gains due to the aerodynamic instability of this configuration. As gain is increased the roots become stable and then unstable. The instability at high gain is the result of increasing control system lag as the pitching frequency increases. If the Base "A" frequency response were adjusted to provide less phase lag at high frequency, the pitching mode could be stabilized at high gain but the first bending mode would be driven unstable by the control system. This problem was encountered in the early Scout vehicle stability studies (Reference 3-1) and was solved by selecting the current Base A frequency response requirements and location of the rate gyros.

The design criteria of providing a gain margin of ± 6 decibels from instability was chosen for this study. That is, the gain selected must be at least 6 decibels (factor of 2) greater than the minimum gain boundary and -6 decibels (one half the value) from the upper gain boundary. This margin of safety in selecting gains is assumed to be adequate to account for possible errors in vehicle aerodynamic data, control surface effectiveness, bending mode data, tolerances in gains, gain ratios, frequency response tolerances,

FIGURE 3.1.4-2
SCOUT LARGER HEATSHIELD STUDY
ROOT LOCI AT 45 SECONDS - 40 INCH HEATSHIELD
ALGOL III CONFIGURATION
41 IN² JET VANE
78 IN² FIN TIP
4.73 FT² FIN

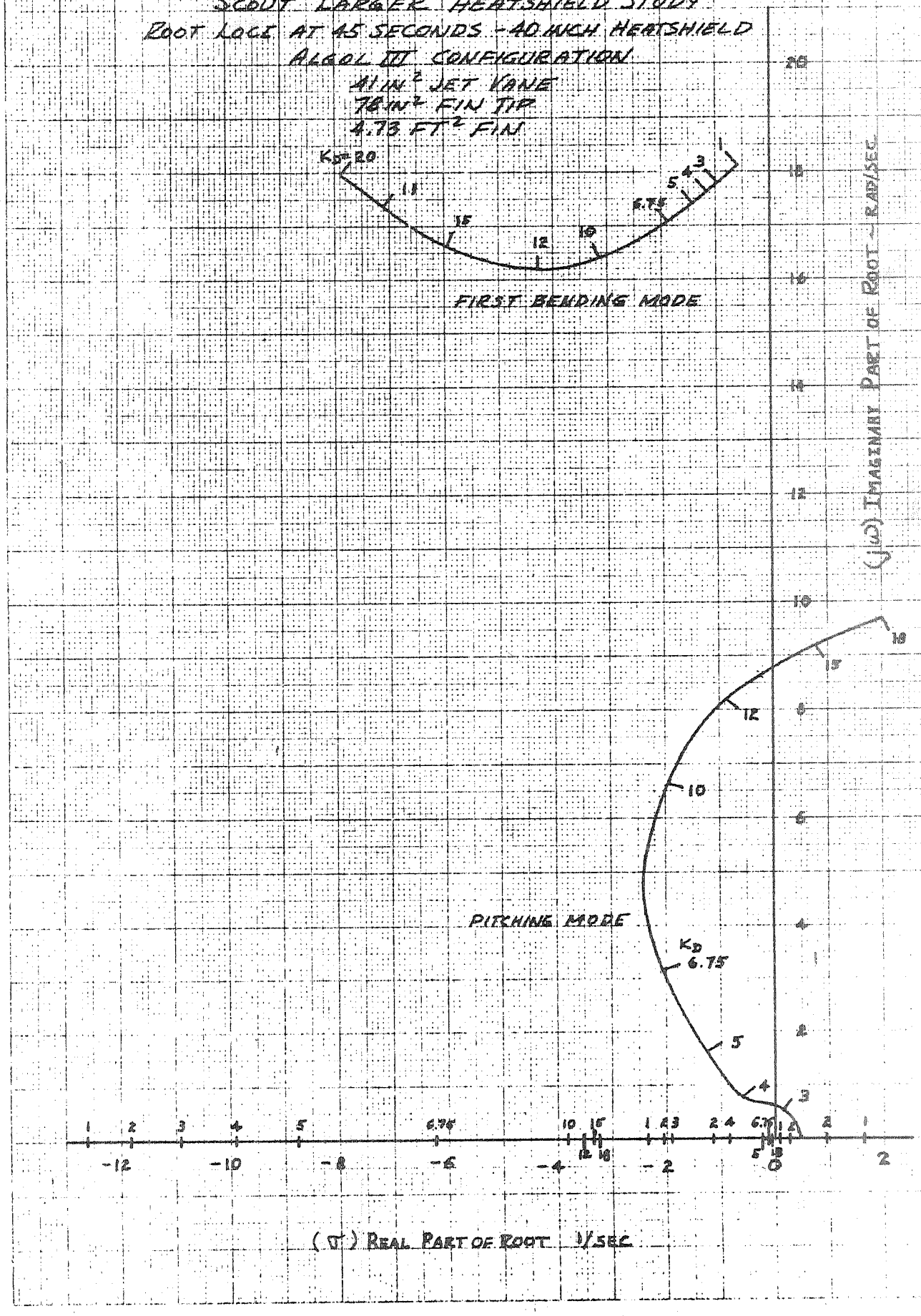

nonlinearities and any small effects which may not be included in the stability model.

The root loci of the 40 inch heatshield configuration was computed for several fin sizes and control fin tip sizes at 45 seconds flight time. The minimum and maximum gain boundaries are presented in Figure 3.1.4-3. The allowable gain boundaries including the ±6 decibel margin of safety are also shown. The increase in fin size has essentially no effect on the maximum gain boundary, but, due to the increase in aerodynamic stability, increased fin size reduces the minimum gain boundary. Increase in fin tip area decreases the maximum gain boundary significantly and also reduces the minimum gain boundary. The root loci trajectories shown in Figure 3.1.4-2 are similar for any change in jet vane or control tip effectiveness. The only difference is the change in the value of gain. This change in gain is governed by the total control effectiveness. The cross-over point in gain for other combinations of jet vane and fin tip sizes can be readily calculated by the following relationship,

$$K_D' = \frac{(L_\delta + C_{N_\delta} S_\beta)}{(L_\delta' + C_{N_\delta} S_\beta')} K_D$$

where K_D' is the cross over gain for the new set of jet vanes and control tips

K_D is the determined cross over gain for given set of jet vanes and fin tips

L_δ is jet vane lift per unit deflection for given jet vanes

L_δ' is jet vane lift per unit deflection for new jet vanes

$C_{N_\delta} S_\beta$ is fin tip normal force per unit deflection for given fin tips

$C_{N_\delta} S_\beta'$ is fin tip normal force per unit deflection for new fin tips

During the course of the parametric analysis it was shown that the minimum fin size was dictated by heatshield size when the criteria for a 6 decibel gain margin of safety is specified. With the 6 decibel gain margin

FIGURE 3.1.4-3
GAIN BOUNDARIES VERSUS FIN SIZE
40 IN HEATSHIELD - ALGOL III

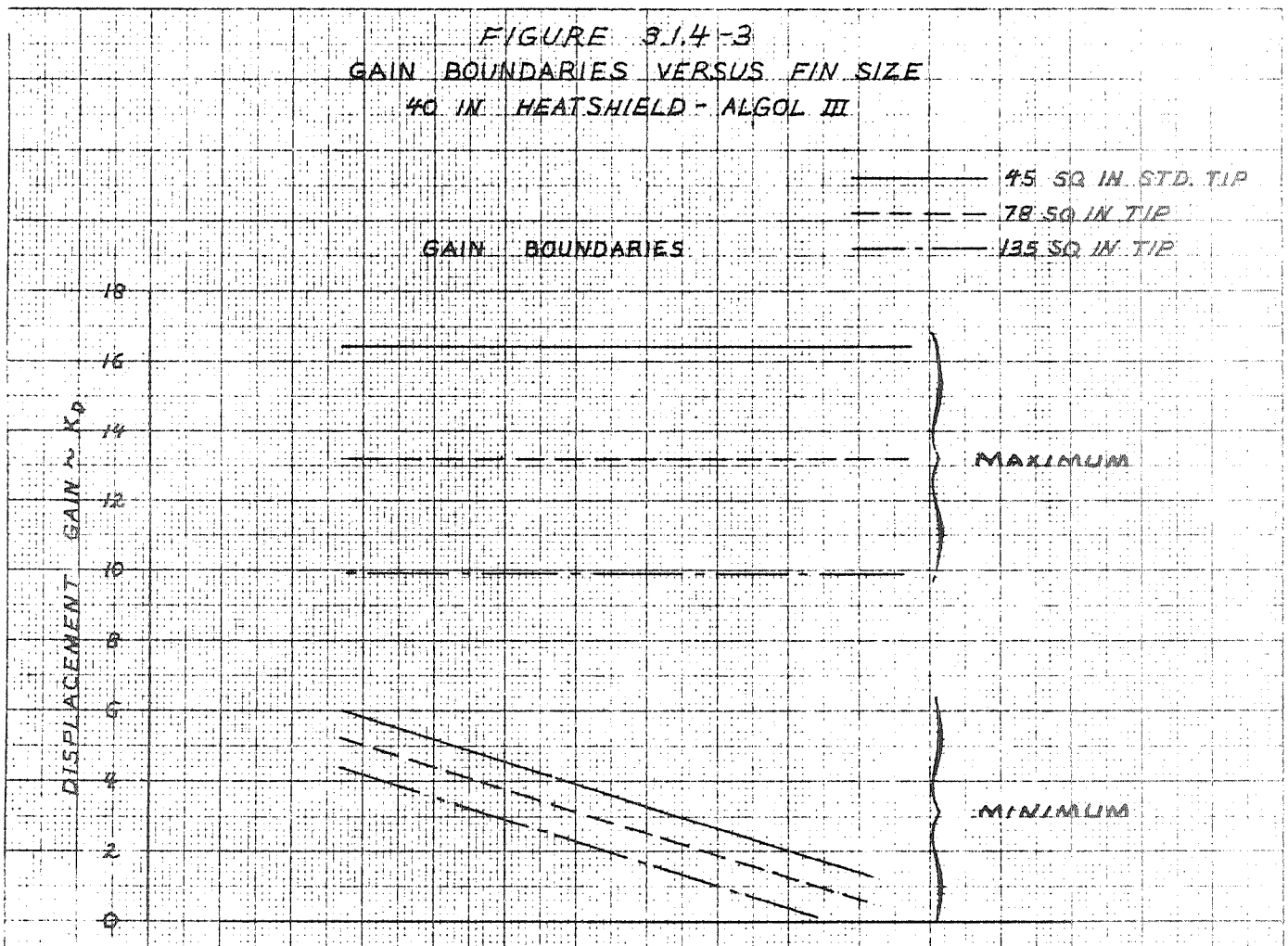

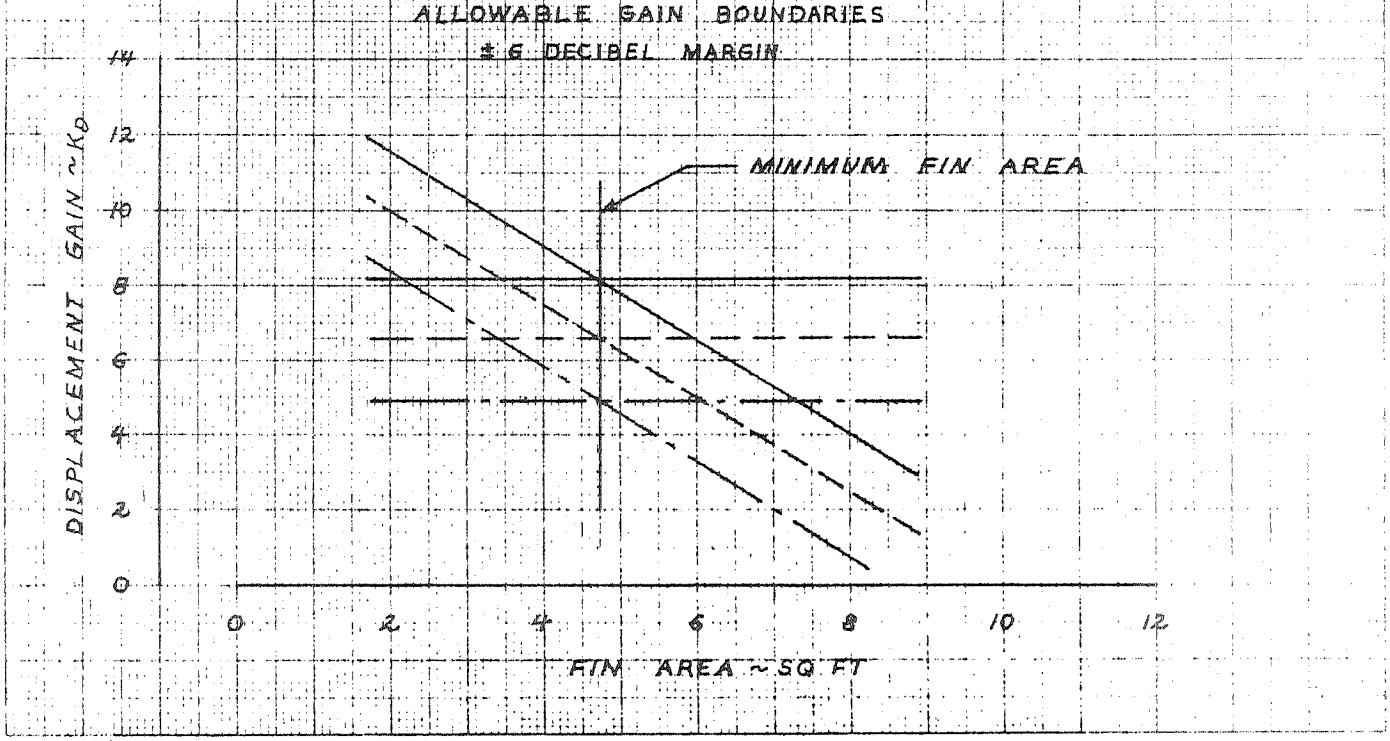

design criteria, minimum fin size is independent of gain, jet vane or fin tip effectiveness. However, the combination of jet vane and fin tip effectiveness at 45 seconds flight time did specify the attitude displacement gain. This gain is 6.75 degrees of control surface per degree of attitude error for the 41 square inch jet vane and the .78 square inches fin tip. The rate to displacement gain ratio K_R/K_D was held at 0.4 seconds to provide sufficient vehicle damping and gain margin. As gain ratio is increased gain margin decreases and damping in pitch increases. The increase in jet vane area was selected to increase the efficiency of control during the first pitch program when the jet vanes provide almost all of the control force. Fin tip size was also increased to provide better control capability during first stage coast when the fin tips provide all of the control force.

For the 40 inch diameter heatshield configuration the fin area increase from 4.5 square feet to 4.73 square feet was accomplished by changing the movable fin tip size only. This allows the use of the current Scout fixed fin with little or no modification. The fin, fin tip and jet vane configuration for the 40 inch diameter heatshield and other heatshields are shown in Figure 2.2.3-1.

The effect of control system gain ratio variations and Base "A" frequency response tolerances were not calculated for the 40 inch diameter heatshield configuration. The effects were assumed to be similar to those for the 42 inch heatshield configuration discussed in Section 3.2.4.

3.1.4.2 First Stage Response

The analysis of the 40 inch diameter heatshield - Algol III configuration response to the pitch program, winds, and thrust misalignment was not performed. It was assumed that this configuration would have response characteristics similar to the 42 inch heatshield configuration discussed in Section 3.2.4.

3.1.4.3 First Stage Hinge Moments

The maximum required hinge moments were estimated for the Algol III configuration with a 41 square inch jet vane and a 78 square inch fin tip control surface. The fin tip used for the large heatshield configuration has the same planform shape as the current Scout fin tip and the hinge line was chosen to be located at the same percentage of the tip root chord. With this similarity it was assumed that the fin tip hinge moment coefficients are the same as the current Scout data presented in Reference 3-2 . The reference area and the length were adjusted for the increase in size. The same adjustment was made in jet vane hinge moment coefficients. The hinge moments for the Algol IIB jet vane presented in Reference 3.1.4-2 were adjusted by the ratio of reference area and length change, and the ratio of vacuum thrust. The hinge moments were calculated as a function of flight time for the design trajectory assuming the maximum deflection angle of 21 degrees and zero angle of attack. To allow for any uncertainties in fin tip hinge moments due to angle of attack and uncertainties in jet vane hinge moments the combination of fin tip and jet vane hinge moment was increased by 50 percent. This approach is quite conservative since the hinge line location of the redesigned jet vane can be relocated after test to reduce hinge moments to a much lower level. The hinge moments determined as stated above are presented in Figure 3.1.4.4. These values are valid for all the Algol III heatshield configurations presented in this study with the 41 square inch jet vane and 78 square inch fin tip. The maximum hinge moments determined by this method is 1680 inch pounds. The current Base A servo-

FIGURE 3.1.4-4
SCOUT LARGER VOLUME HEATSHIED STUDY
HINGE MOMENT REQUIREMENTS
ALGOL III, 41 IN² JET VANE, 78 IN² FIN TIP

NOTE: BASED ON 21° DEFLECTION ANGLE PLUS 50 PERCENT SAFETY FACTOR

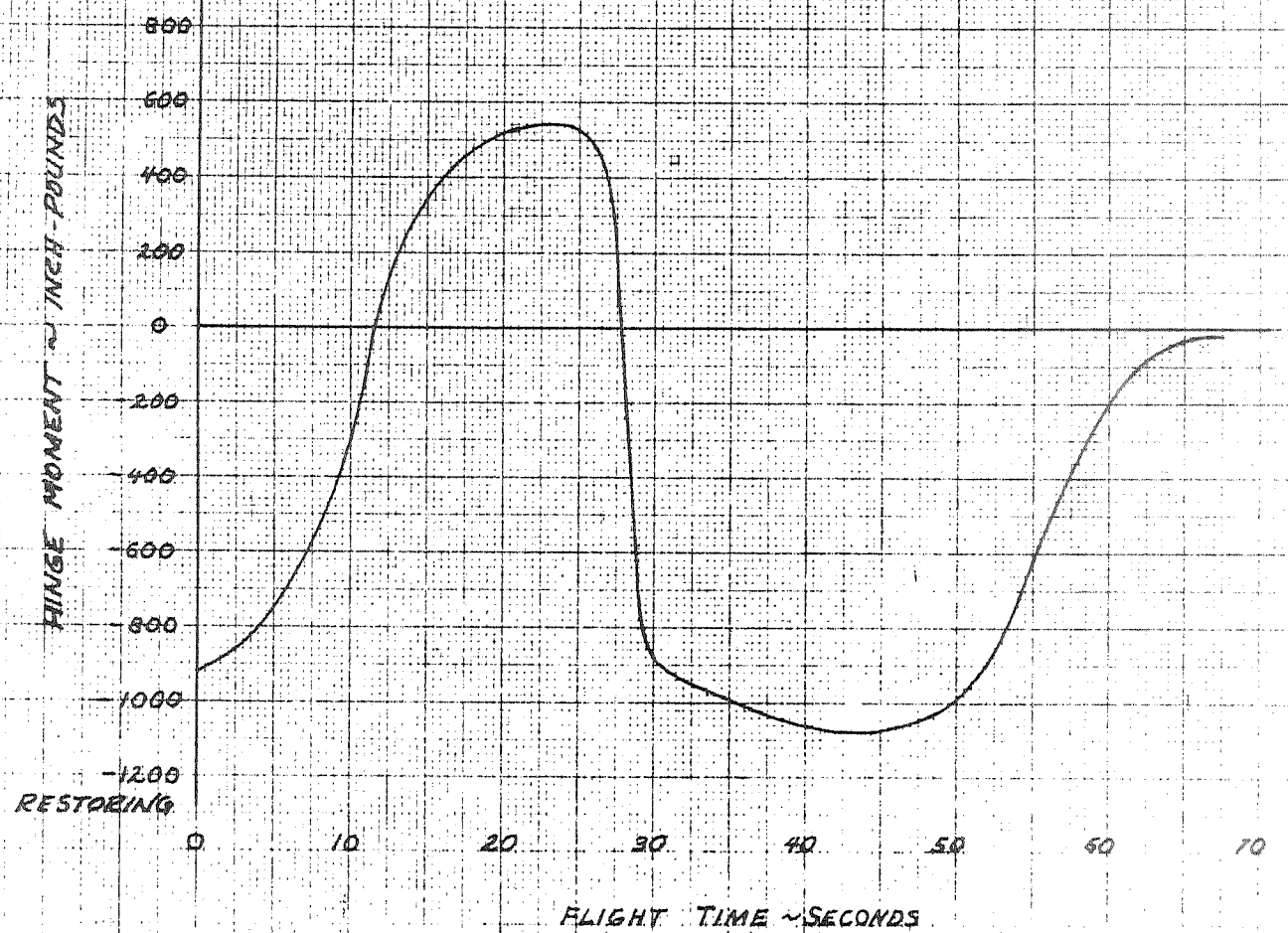

actuator provides at least 1400 inch-pounds of hinge moment according to Reference 3-3. For detail design the hinge moments must be determined for realistic flight conditions. The fin tip hinge moment coefficients should be determined from wind tunnel tests and the jet vane hinge moments should be measured in a static firing of an Algol III motor.

3.1.4.4 Second Stage Ignition Dynamic Pressure Restrictions

The use of a larger heatshield on the Scout vehicle increases the aerodynamic instability of the second stage. The use of the Algol III motor changes the altitude-dynamic pressure relationship at second stage ignition. This change affects the ability of the vehicle to capture since wind speed increases rapidly at these altitudes.

An estimation of the allowable dynamic pressure at second stage ignition was made for the 42 inch diameter heatshield configuration by a Monte Carlo analysis of the second stage capture maneuver. The results of a similar analysis of the current Scout vehicle are presented in Reference 3-4. The dynamic pressure for the 40 inch heatshield configuration was determined by ratioing the aerodynamic pitching moment per degree angle of attack about the center of mass to that of the 42 inch heatshield configuration. This keeps the aerodynamic disturbing moment equal to that determined in the 42 inch heatshield analysis. The resulting nominal dynamic pressure allowable at second stage ignition is 79 psf for orbital missions and 69 psf for reentry missions.

3.1.4.5 Second Stage Fuel Consumption

A preliminary estimate of the second stage control fuel consumption and coast time changes resulting from the change in heatshield lift was made based on the dynamic pressure limitation at ignition of 40 psf on orbital missions and 35 psf on reentry missions. The boost fuel consumption

increases to 80.9 pounds for an orbital mission and to 82.2 pounds for a re-entry mission. This change will reduce coast time. The estimated coast time versus control fuel on-board at liftoff is presented in Figure 3.1.4-5. If the dynamic pressure at second stage ignition is at the maximum allowed boost fuel consumption will increase by about 18 pounds at the 99.5 percent probability level. Coast time for this case is presented in Figure 3.2.4-15.

FIGURE 3.1.4-5

SCOUT LARGER HEATSHIELD STUDY

SECOND STAGE COAST TIME VERSUS USABLE CONTROL FUEL

40 INCH HEATSHIELD - ALGOL III

99.5 PERCENT PROBABILITY, 95 PERCENT COMFIDENCE

50 LB PAYLOAD

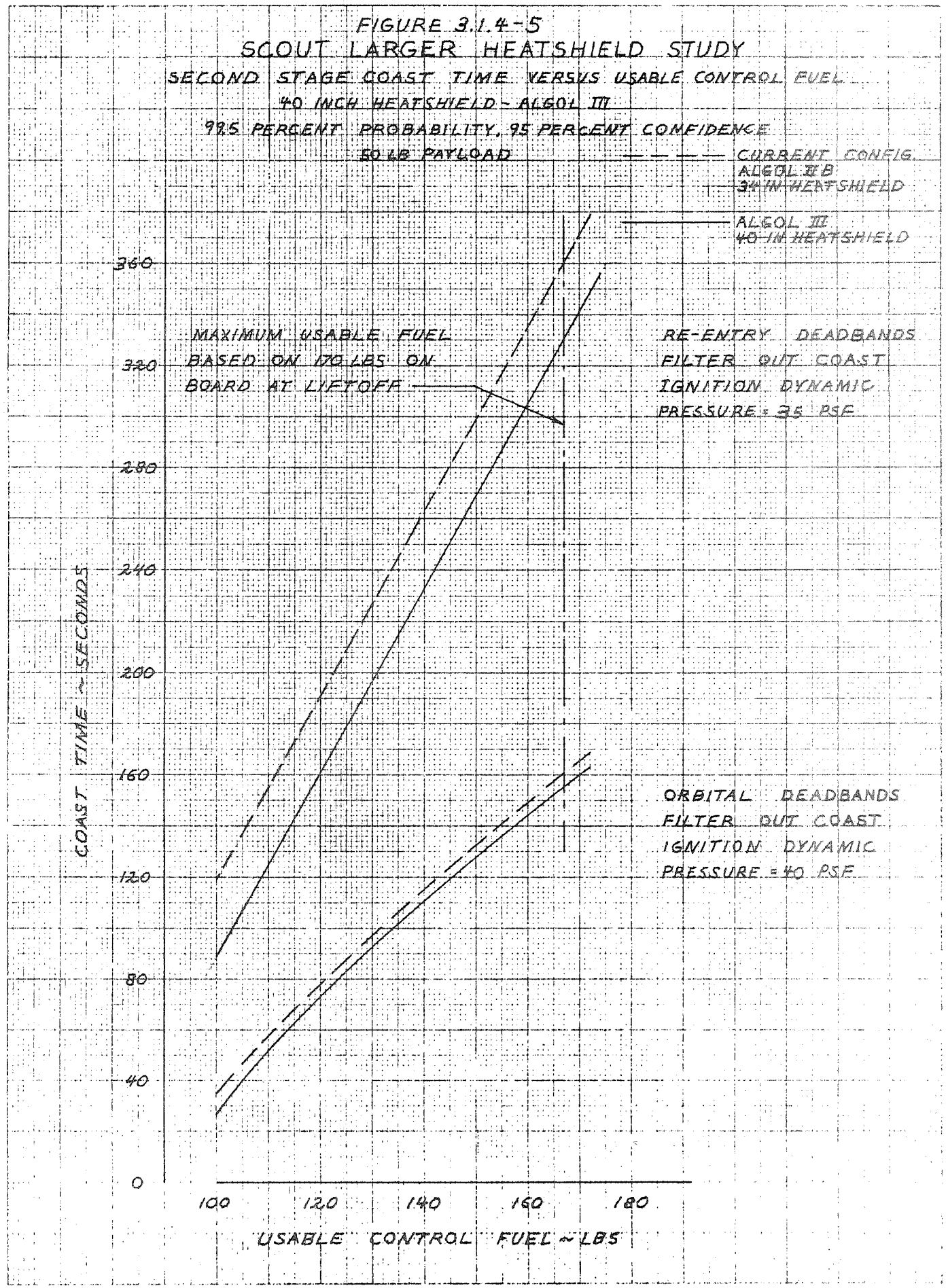

3.1.5 Flight Loads

3.1.5.1 Vehicle Loads

The flexible body loads resulting from a 90 knot headwind that occurs during first stage boost were calculated using a digital computer routine called Mizar (Reference 3-5). Also the maximum bending moments due to 24 fps gust, which has a 0.001 probability (Reference 3-6) of occurrance were determined. The maximum bending moments due to winds and gusts were summed and are presented in Figure 3.1.5-1. The resulting axial loads at the time of maximum bending moments are presented in Figure 3.1.5-2.

The flexible body loads resulting from the 90 knot headwind, which has a profile as shown in Reference 3-6, are calculated by solving the equations of motion for the complete aero-servo-elastic system. The vehicle is subjected to forces from wind shear, aerodynamic lift and drag, gravitational attraction, maneuver and motor thrust. The loads due to the gusts were determined by solving the response of the vehicle when encountering a sharp edge gust.

3.1.5.2 Fin Loads

The fin attachment loads for the 4.735 ft^2 area fin selected for the 40 inch diameter heat shield configuration were determined for the time at which the vehicle experienced the ultimate design bending moment at the critical station. At this time, the controls were also assumed to be at a maximum deflection of ± 18.5 degrees in order to give a more direct comparison with the basic 4.5 ft^2 area fin loads reported in Reference 3-6.

Since the multiple fin attachments result in redundant structural load paths, the loads experienced by the attachments were determined from the influence coefficient data for the 4.5 ft^2 area fin by assuming that all structural members were increased by a constant geometric scale factor determined, by the ratio of the square root of the fin areas. Again, this allowed direct comparison with the basic fin.

FIGURE 3.1.5-1

SCOUT VEHICLE + ALGOL III FIRST STAGE
BENDING MOMENT DISTRIBUTION DUE TO
90 KNOT WIND AND 24 FPS GUST

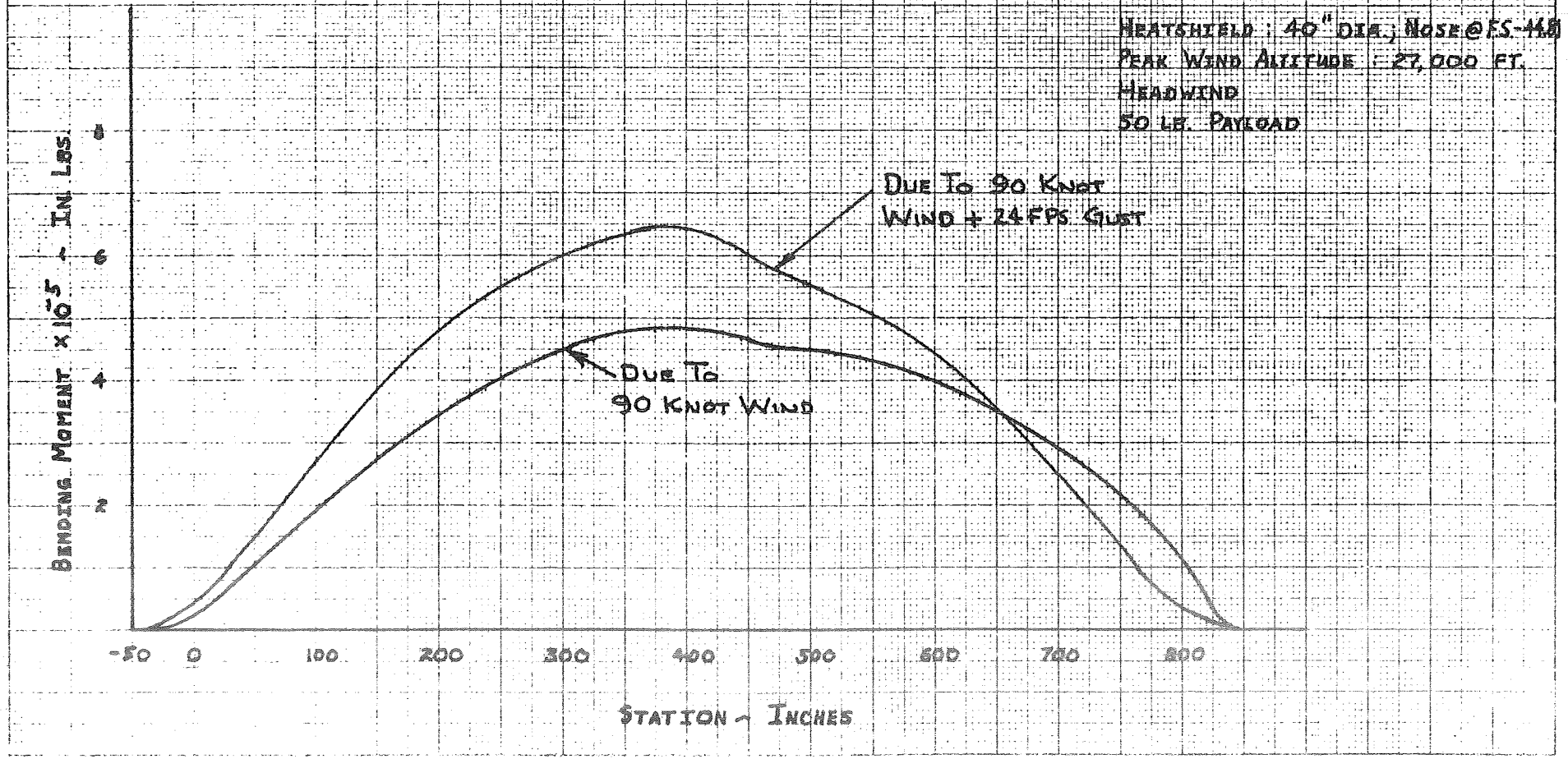

FIGURE 3.1.5-2
SCOUT VEHICLE - ALGOL III FIRST STAGE
AXIAL LOAD DISTRIBUTION DUE TO
90 KNOT HEADWIND

HEATSHIELD: 40° DIA. NOSE @ -38.91
50 LB. PAYLOAD
MACH 2.16
q_o = 2354 PSF
N_x = 3.352

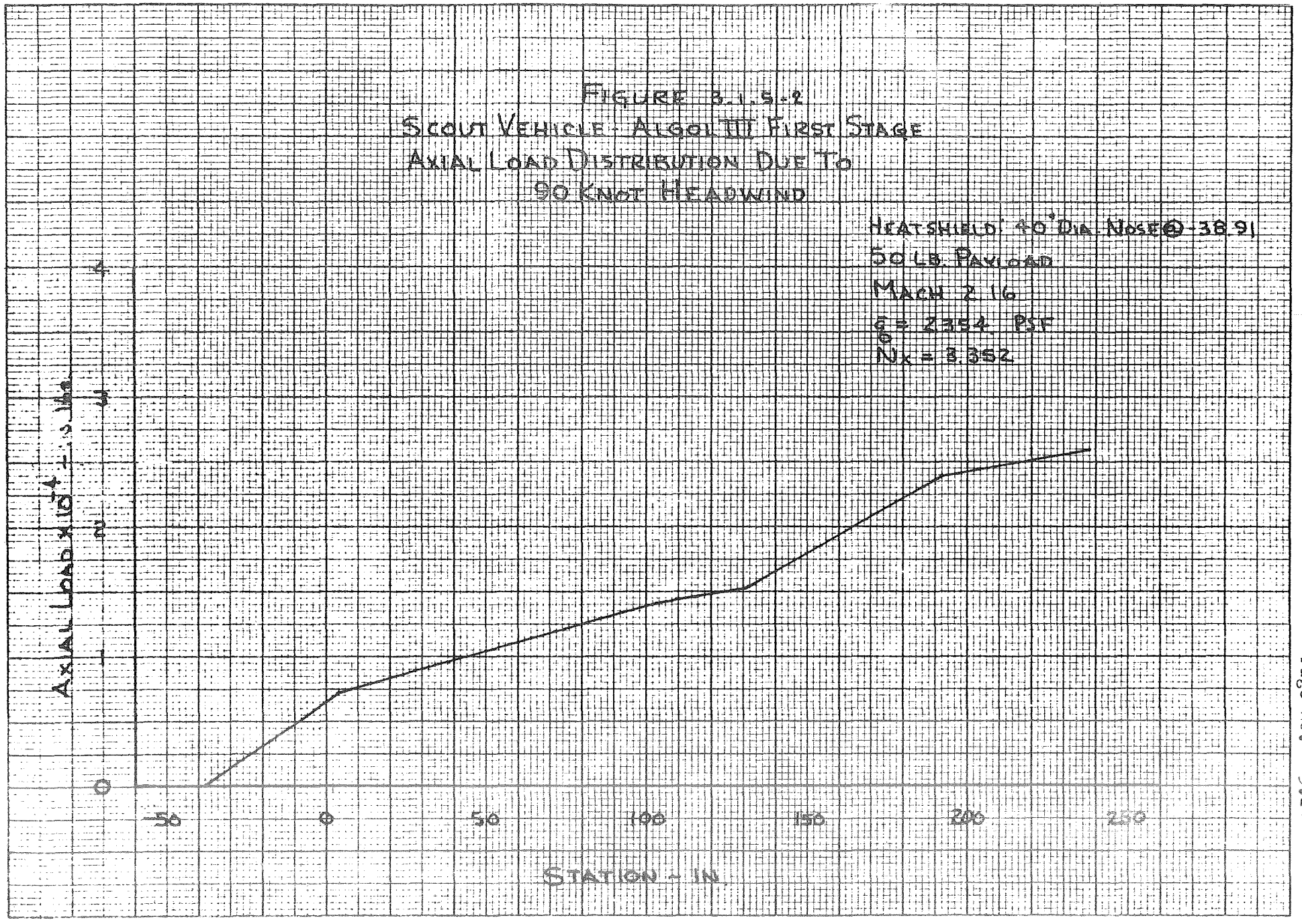

The basic trajectory parameters for the 40 inch diameter heat shield vehicle at the time of maximum loads are as follows:

Dynamic pressure, $q = 2354$ psf

Angle-of-attack, $\alpha = 2.02°$ (effective rigid body)

Mach number, $M = 2.16$

Control deflection, $\delta = \pm 18.5°$

Time, $t = 34.0$ sec

Lateral load factor, $N_Z = -.208$

Axial load factor, $N_X = 3.352$

Pitching acceleration, $\ddot{\theta} = 0.022$ deg/sec^2

Lift coefficient: Tip $C_{N_\alpha} S = 0.0229$ ft^2/deg.

Fin $C_{N_\alpha} S = 0.260$ ft^2/deg

Vane $L_\delta = 42.3$ lbs/deg

Drag coefficient at $\delta = \pm 18.5°$

Tip $C_D S = 0.167$ ft^2

Fin $C_D S = 0.310$ ft^2

Vane $D = 663\#$

The resultant fin attachment loads at this flight time are shown in Figure 3.1.5.2-1 the two cases of $+18.5°$ and $-18.5°$ control deflections, respectively. The letter symbols defineing the loads are as follows:

R_A^X, R_A^Y, R_A^Z: Components of resultant shear reaction at A

R_B : Lateral shear reaction at B

M_A^X, M_A^Y, M_A^Z: Components of resultant moment reaction at A

FIGURE 3.1.5.2-1

SCOUT FIN LOADS VERSUS

HEAT SHIELD DIAMETER AND FIN AREA

Reaction	Heat Shield Diameter									
	34"		40"		42"		44"		46"	
R_{AX}	-1790		-2138		-2420		-3083		-5200	
R_{AY}	-240		-154		-116		-720		-2900	
R_{AZ}	-1590	-4970	-512	-3329	-174	-3633	-303	-4126	-1600	-5400
R_B	-80	210	-117	173	-108	177	-100	188	-80	217
M_{AX}	27,000	-53,000	8,900	-44,000	5,500	-52,900	- 1,375	-73,050	-38,000	-122,700
M_{AY}	-13,500	7,000	-10,000	-13,200	-10,500	14,770	-12,300	18,900	-14,000	-28,300
M_{AZ}	14,500		17,570		23,100		36,000		79,800	
Fin Area (ft^2)	4.5		4.735		5.75		8.6		16.0	

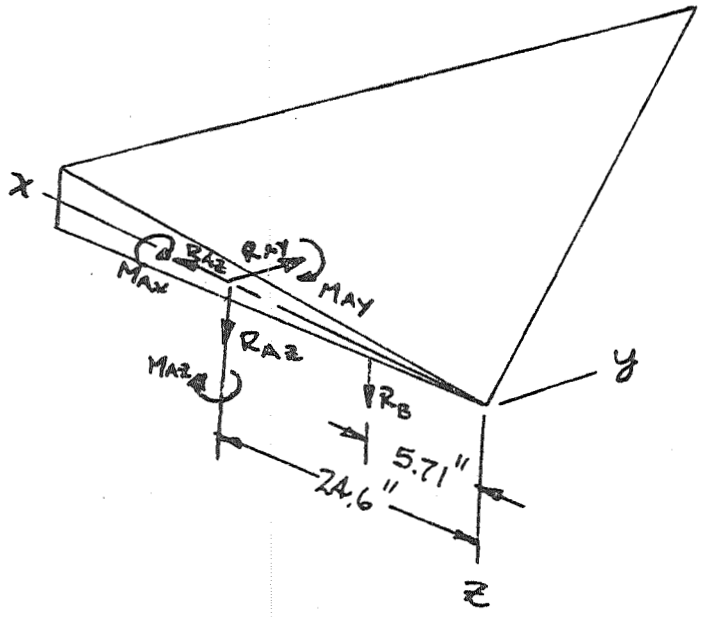

3.1.6 Vehicle Structure

3.1.6.1 Design Criteria

The structural criteria used in evaluating the effects of the larger diameter heat shields is the same as that used for the design of the basic 34 inch diameter heat shield vehicle and designated in Reference 3-3. This criteria requires a positive margin of safety for design yield loads and design ultimate loads. The following applies:

(1) Limit Load = Anticipated load on structure

(2) Design Yield Load = 1.15 x limit load

(3) Design Ultimate Load = 1.5 x limit load

3.1.6.2 Loads

Plots of vehicle ultimate flight loads are shown for each of the four heat shield configurations considered. Plots of vehicle flight ultimate loads for the basic vehicle with the 34 inch diameter heat shield are shown for comparison to the loads with the larger diameter heat shields. The minimum axial loads shown are vehicle limit longitudinal flight loads and are used in combination with bending loads to analyze structure critical for tension loading. The maximum axial loads are ultimate loads and are combined with bending loads to analyze structure critical for compression loading.

Fin reaction loads for the fin to Base "A" attachment points are shown. For comparison, the fin reaction loads for the basic Scout with the 34 inch diameter heat shield are also presented.

Vehicle flight loads with the 40 inch diameter heat shield are shown on Figure 3.1.6-1. Fin reaction loads with the 40 inch diameter heat shield are shown on Figure 3.1.6-3. Fin reaction loads for the basic Scout vehicle with the 34 inch diameter heat shield are shown on Figure 3.1.6-2.

3.1.6.3 Analyses

The methods of analyses used for investigating the vehicle structure for use of the larger heat shield are basically the same as used for the structural analysis of the basic Scout vehicle. The structural analysis of the basic vehicle is presented in Reference 3-7 .

3.1.6.4 Heat Shield Attachment Clamp

The basic Scout 34 inch diameter heat shield attachment clamp is designed for an ultimate tension load in the clamp of 7,600 pounds, Reference 3-7. Vehicle loads of 425,000 inch pounds bending moment and 14,000 pound axial load at station 103.69 for the 40 inch diameter heat shield, Reference Figure 3.1.6-1, result in an ultimate tension load in the attachment clamp of 6,576 pounds. Therefore, the 23-002204-1 clamp is structurally adequate for use on the 40 inch diameter heat shield with Algol III first stage.

3.1.6.5 Lower "D" Transition Section

The lower "D" transition extends from station 103.81 to station 131.1 and joins the heat shield to the third stage motor. The aerodynamic heating of the section during boost results in thermal loads induced in this section. For this investigation, thermal loads in the section were considered to be the same as for the section with the basic Scout 34 inch diameter heat shield.

A review of the lower "D" transition section structure for loading as shown in Figure 3.1.6-1 plus thermal loading from Reference 3-7 , shows positive margins of safety for the section. A comparison of flight ultimate loads plus thermal loads to structural static test loads for the section is shown in Table 3.1.6-1 The static test loads shown did not produce structural failure of lower "D".

Structural analysis of the section and the structural testing results show lower "D" transition section, 23-000067, structurally adequate for use on the Scout vehicle with the 40 inch diameter heat shield and Algol III first stage.

3.1.6.6 X-259 Motor

The X-259 motor extends from station 131.1 to station 191.95 and connects lower "D" transition section to upper "C" transition section. A comparison of flight ultimate loads to structural static test loads for the X-259 motor is shown in Table 3.1.6-2. The static test loads shown did not produce structural failure of the X-259 motor.

Structural analysis of the motor case and the structural testing results show the X-259 motor case structurally adequate for use on the Scout vehicle with the 40 inch diameter heat shield and Algol III first stage.

3.1.6.7 Upper and Lower "C" Transition Sections

Transition section "C" extends from station 191.95 to station 253.06 and joins the X-259 motor to the second stage Castor motor. Upper "C" is the portion between station 191.95 and station 238.18. A separation diaphragm connects the two sections at station 238.18. A comparison of flight ultimate loads to structural static test loads for "C" section is shown in Tables 3.1.6-3 and 3.1.6-4. The static loads shown for load point 55 resulted in structural failure in the forward region of upper "C" section. The mode of failure was shell buckling due to compression loading.

Structural analysis of "C" section and the structural testing results show both upper and lower "C" transition section, 23-002031 and 23-001031 respectively, structurally adequate for use on the Scout vehicle with the 40 inch diameter heat shield and Algol III first stage.

3.1.6.8 Base "A" and Fins

For use with the 40 inch diameter heat shield and Algol III first stage the basic Scout fin tip and the jet vane have been changed as shown on Figure 2.2.3-1. Fin ultimate reaction loads for the fin to base "A" attachment points are shown on Figure 3.1.6-3. For comparison, ultimate reaction loads for the fin on the basic Scout 34 inch diameter heat shield vehicle are shown on Figure 3.1.6-2.

Structural analysis of the Base "A" fin support structure shows the support frame and fitting, 23-001079 and 23-001148 at station 848.075, the support frame and fitting, 23-000093 and 23-001151 at station 840.20, and the forward shear attachment at station 825.71 to be structurally adequate for fin loads resulting from the 40 inch diameter heat shield and the Algol III first stage.

A review of the loads and analysis of the basic fin structure shows the 23-000021 fin to be structurally adequate for use with the 40 inch diameter heat shield although changes to the fin tip and the jet vane will be required as shown on Figure 2.2.3-1.

3.1.6.9 Structure Summary

The only structural changes required in the basic vehicle for using the 40 inch diameter heat shield and the Algol III first stage and vehicle flight ultimate loads as shown on Figure 3.1.6-1 will be in the fin tip and jet vane. The increased size of fin tip and jet vane is shown on Figure 2.2.3-1.

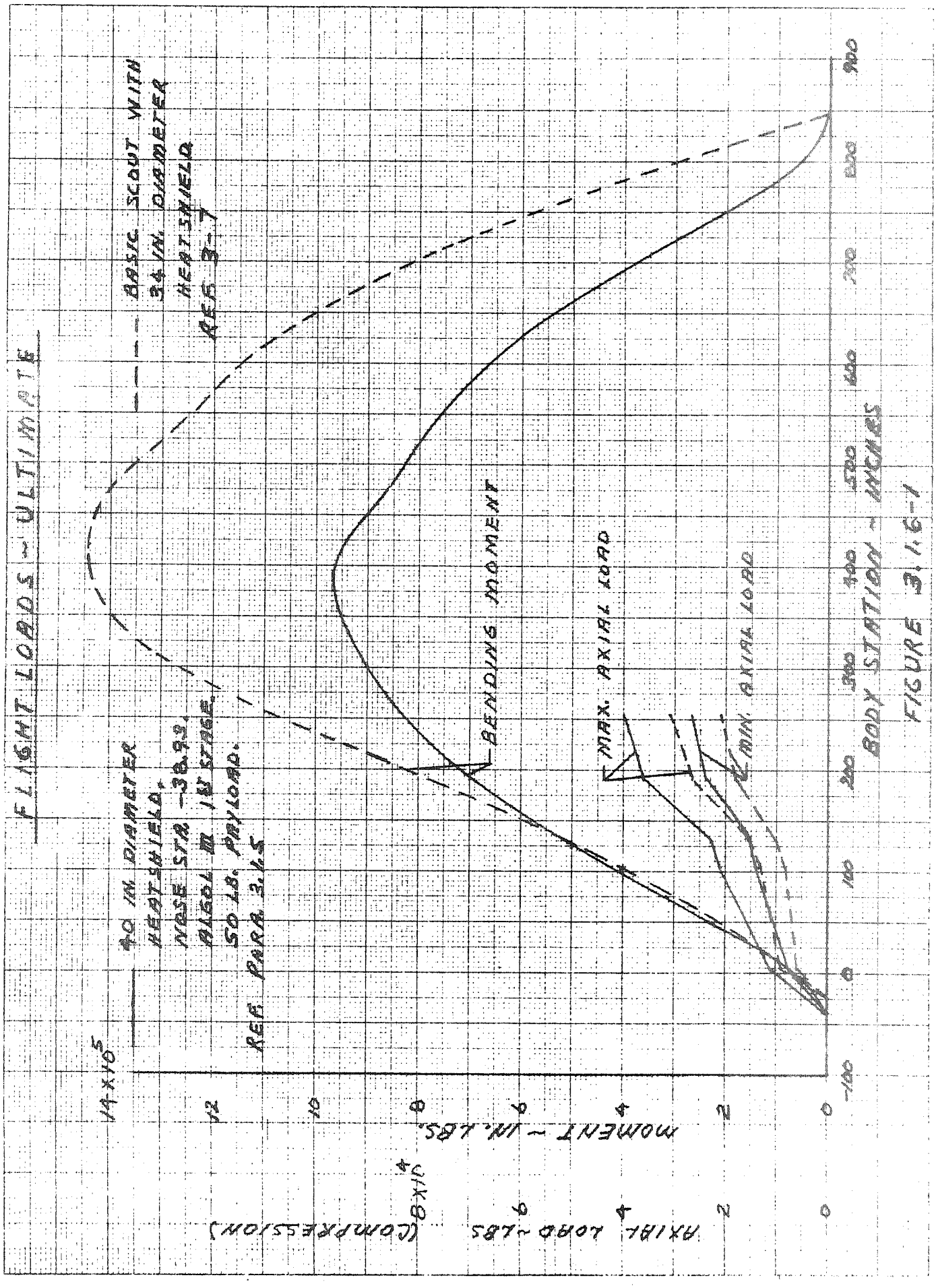
FLIGHT LOADS - ULTIMATE
40 IN DIAMETER HEATSHIELD, NOSE STA -38.93, AFT OF 1ST STAGE, 50 LB. PAYLOAD. REF. PARA. 3.4.5
BASIC SCOUT WITH 34 IN. DIAMETER HEATSHIELD REF 3-7
BENDING MOMENT
MAX. AXIAL LOAD
MIN AXIAL LOAD
AXIAL LOAD - LBS (COMPRESSION)
MOMENT - IN. LBS.
BODY STATION - INCHES
FIGURE 3.1.6-1

TABLE 3.1.6-1

LOWER "D" TRANSITION SECTION

COMPARISON OF FLIGHT ULTIMATE AND TEST LOADS

		40 Inch Diameter Heat Shield Ultimate Loads	(1) Test Loads Ld. Point (47)	Ld. Point (52)
Station 104.5				
(2)	MOM in. lbs.	425,000	500,680	487,659
(2)	P_{max} lbs.	21,000	40,588	375
(2)	P_{min} lbs.	14,000	- - - -	- - - -
(3)	$P_{Thermal}$ lbs.	13,884	- - - -	- - - -
	f_b psi	± 15,725	± 18,482	± 18,002
	$f_{P\ max}$ psi	- 4,605	- 8,879	- 82
	$f_{P\ min}$ psi	- 2,974	- - - -	- - - -
(3)	f_{TH} psi	- 3,038	- - - -	- - - -
	$f_{c\ max}$ psi	- 23,368	- 27,361	- 18,084
	$f_{t\ max}$ psi	+ 12,751	+ 9,603	+ 17,920
Station 131.1				
(2)	MOM in. lbs.	515,000	584,500	565,000
(2)	P_{max} lbs.	22,875	40,588	375
(2)	P_{min} lbs.	15,250	- - - -	- - - -
(3)	$P_{Thermal}$ lbs.	17,080	- - - -	- - - -
	f_b psi	± 13,019	± 15,853	± 15,324
	$f_{P\ max}$ psi	- 4,221	- 7,872	- 73
	$f_{P\ min}$ psi	- 2,816	- - - -	- - - -
(3)	f_{TH} psi	- 3,154	- - - -	- - - -
	$f_{c\ max}$ psi	- 20,394	- 23,725	- 15,397
	$f_{t\ max}$ psi	+ 10,203	+ 7,981	+ 15,251

(1) Reference 3-8
(2) Reference Figure 3.1.6-1
(3) Reference 3-7

$$f_b = \frac{Mc}{I} \qquad f_c = \frac{P}{A}$$

$$f_{c\ max} = f_b + f_{P\ max} + f_{TH}$$

$$f_{t\ max} = f_b + f_{P\ min}$$

TABLE 3.1.6-2

X-259 MOTOR

COMPARISON OF FLIGHT ULTIMATE AND TEST LOADS

		40 Inch Diameter Heat Shield Ultimate Loads	(1) Test Loads Ld. Point (47)	Ld. Point (52)
Station 131.1				
(2)	MOM in. lbs.	515,000	638,983	617,591
(2)	P_{max} lbs.	22,875	40,588	375
(2)	P_{min} lbs.	15,250	- - - -	- - - -
	W_M lbs./in.	± 730	± 906	± 876
	$W_{P\ min}$ lbs./in.	- 162	- - - -	- - - -
	$W_{P\ max}$ lbs./in.	- 243	- 431	- 4
	$W_{c\ max}$ lbs./in.	- 973	- 1,337	- 880
	$W_{t\ max}$ lbs./in.	+ 568	+ 475	+ 872
Station 191.95				
(2)	MOM in. lbs.	695,000	955,343	914,843
(2)	P_{max} lbs.	36,000	40,588	375
(2)	P_{min} lbs.	24,000	- - - -	- - - -
	W_M lbs./in.	± 985	± 1,355	± 1,297
	$W_{P\ max}$ lbs./in.	- 382	- 431	- 4
	$W_{P\ min}$ lbs./in.	- 255	- - - -	- - - -
	$W_{c\ max}$ lbs./in.	- 1,367	- 1,786	- 1,301
	$W_{t\ max}$ lbs./in.	+ 730	+ 924	+ 1,293

(1) Reference 3-8
(2) Reference Figure 3.1.6-1

$W_M = \frac{M}{\pi R^2}$ Where R is radius of shell

$W_P = \frac{P}{\pi D}$ Where D is diameter of shell

$W_{c\ max}$ = Maximum compressive load

$W_{t\ max}$ = Maximum tensile load

TABLE 3.1.6-3

UPPER "C" TRANSITION SECTION

COMPARISON OF FLIGHT ULTIMATE AND TEST LOADS

	40 Inch Diameter Heat Shield Ultimate Loads	(1) Test Loads	
		Ld. Point (52)	Ld. Point (55)
Station 191.95			
(2) MOM. in. lbs.	695,000	914,843	995,845
(2) P_{max} lbs.	36,000	375	35,821
(2) P_{min} lbs.	24,000	- - - -	- - - -
W_M lbs/in	± 945	± 1,244	± 1,354
$W_{P\ max}$ lbs/in	- 374	- 4	- 372
$W_{P\ min}$ lbs/in	- 250	- - - -	- - - -
$W_{c\ max}$ lbs/in	- 1,319	- 1,248	- 1,726
$W_{t\ max}$ lbs/in	+ 695	+ 1,240	+ 982
Station 238.18			
(2) MOM in. lbs.	805,000	1,140,676	1,250,156
(2) P_{max} lbs.	39,000	375	35,821
(2) P_{min} lbs.	26,000	- - - -	- - - -
W_M lbs/in	± 1,000	± 1,416	± 1,552
$W_{P\ max}$ lbs/in	- 388	- 4	- 356
$W_{P\ min}$ lbs/in	- 258	- - - -	- - - -
$W_{c\ max}$ lbs/in	- 1,388	- 1,420	- 1,908
$W_{t\ max}$ lbs/in	+ 742	+ 1,412	+ 1,196

(1) Reference 3-8

(2) Reference Figure 3.1.6-1

$W_M = \frac{M}{\pi R^2}$ Where R is radius of shell

$W_P = \frac{P}{\pi D}$ Where D is diameter of shell

$W_{c\ max}$ = Maximum compressive load

$W_{t\ max}$ = Maximum tensile load

TABLE 3.1.6-4

LOWER "C" TRANSITION SECTION

COMPARISON OF FLIGHT ULTIMATE AND TEST LOADS

	40 Inch Diameter Heat Shield Ultimate Loads	(1) Test Loads Ld. Point (52)	Ld. Point (55)
Station 238.18			
(2) MOM in. lbs.	805,000	1,140,676	1,250,156
(2) P_{max} lbs.	39,000	375	35,821
(2) P_{min} lbs.	26,000	- - - -	- - - -
W_M lbs/in	± 997	± 1,413	± 1,549
$W_{P\ max}$ lbs/in	- 387	- 4	- 356
$W_{P\ min}$ lbs/in	- 264	- - - -	- - - -
$W_{c\ max}$ lbs/in	- 1,384	- 1,417	- 1,905
$W_{t\ max}$ lbs/in	+ 733	+ 1,409	+ 1,193
Station 253.06			
(2) MOM in. lbs.	830,000	1,213,365	1,332,011
(2) P_{max} lbs.	39,900	375	35,821
(2) P_{min} lbs.	26,600	- - - -	- - - -
W_M lbs/in	± 1,081	± 1,581	± 1,736
$W_{P\ max}$ lbs/in	- 405	- 4	- 364
$W_{P\ min}$ lbs/in	- 270	- - - -	- - - -
$W_{c\ max}$ lbs/in	- 1,486	- 1,585	- 2,100
$W_{t\ max}$ lbs/in	+ 811	+ 1,577	+ 1,372

(1) Reference 3-8

(2) Reference Figure 3.1.6-1

$W_M = \frac{M}{\pi R^2}$ Where R is radius of shell

$W_P = \frac{P}{\pi D}$ Where D is diameter of shell

$W_{c\ max}$ = Maximum compressive load

$W_{t\ max}$ = Maximum tensile load

FIGURE 3.1.6-2

FIN REACTION LOADS - ULTIMATE

BASIC SCOUT WITH 34 INCH DIAMETER HEAT SHIELD

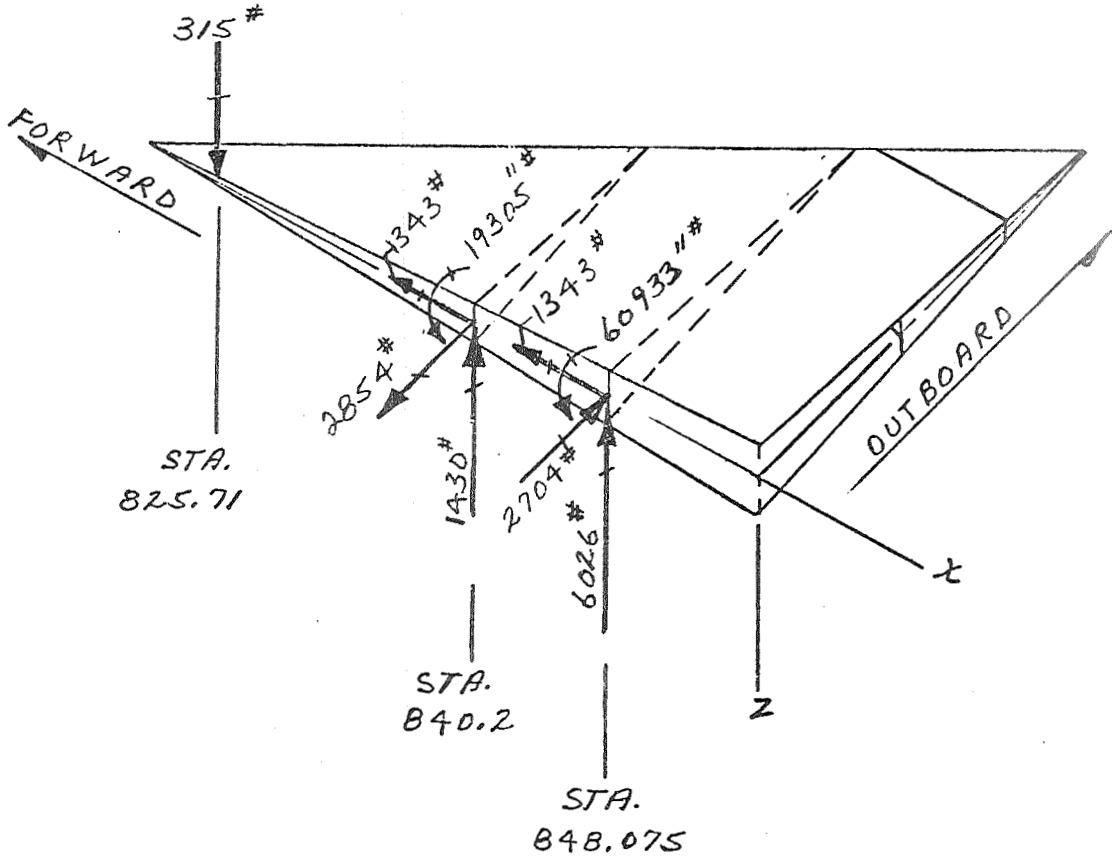

LOADS FROM REFERENCE 3-7

FIGURE 3.1.6-3

FIN REACTION LOADS - ULTIMATE

SCOUT WITH 40 INCH DIAMETER HEAT SHIELD AND ALGOL III FIRST STAGE

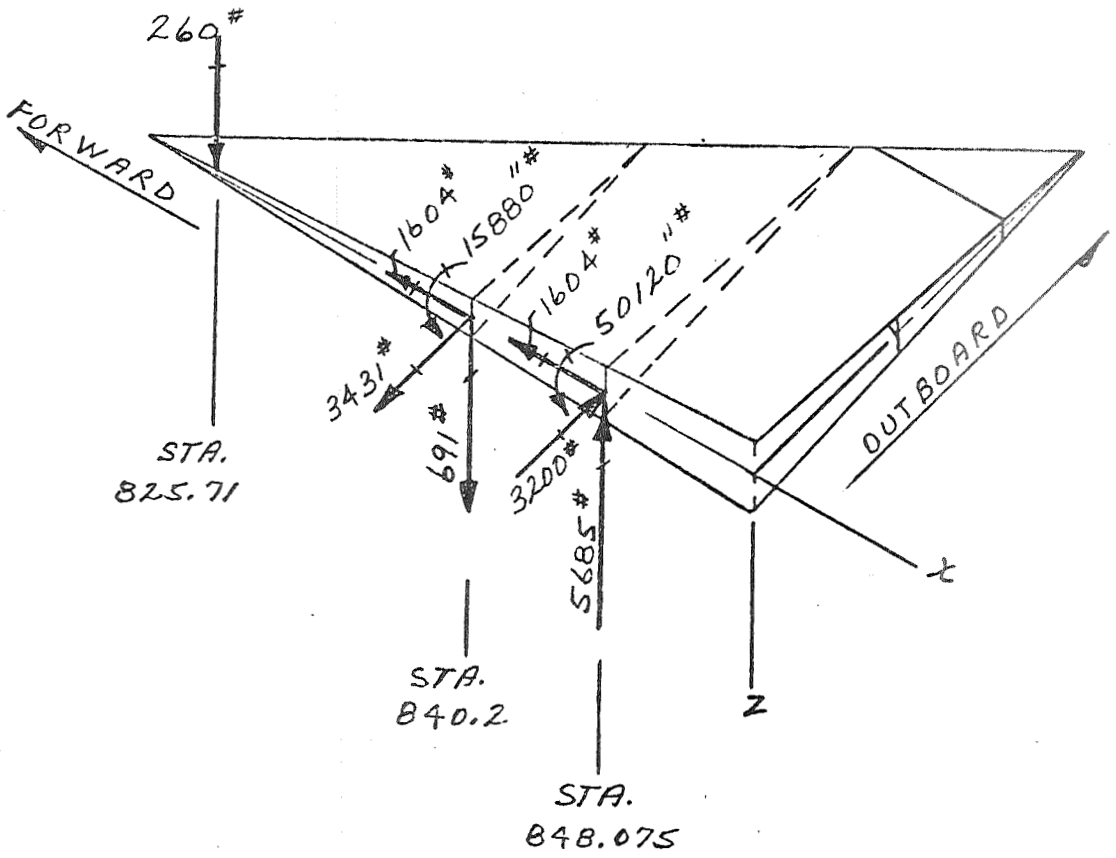

LOADS FROM PARAGRAPH 3.1.5

3.1.7 Ground Support Equipment

A review of the effect of the 40 inch diameter heatshield with 4.73 sq. ft. fins was made on the following ground support equipment: (1) 321-60061 Launcher Payload Umbilical Retract Arm; (2) 321-60619 Heatshield Support Dollies; (3) 331-63098 Dummy Heatshield; (4) 331-63108 Handles, Payload Heatshield; (5) Strap Wrench used for clamping Heatshield Halves; (6) 331-63040 Hoist Assembly, Fourth Step Positioning Fixture; (7) 331-50080 Support Brackets, Heatshield; (8) 331-63208 Cradle Assembly - Fourth Stage, Scout; (9) 331-63205 Vehicle Restraint Assembly - Rocket Vehicle Transporter, Scout; (10) 331-63200 Transporter Assembly, Rocket Vehicle, Scout; (11) 331-63201 Transporter Modification - Letourneau Rocket Vehicle, Scout; (12) 331-61620 Section Assembly - Launch Facility Launch Beam, Lower, (13) 331-63094 Fin Protractor kit; 331-50117 Fixture Assemblies, MGSE Proof Loading, Scout; (14) 23-000716 Beam Assembly, Support Equipment, Base "A" Vertical Hoist; (15) 23-001513 Sling Assembly, Support Equipment, Base Section; and (16) 23-001514 Stand Assembly, Support Equipment, Base Section Support. The results of this review are presented below.

3.1.7.1 Payload Umbilical Retract Arm

The 321-60061-26 payload umbilical retract arm will have to be shortened. This in turn will require the shortening of the 331-63099-2 sway-brace in order to maintain the range of stations from which the payload umbilical plugs may be pulled. Additional lanyard lengths will also be required for the 331-63112-1 lanyard kit.

3.1.7.2 Cradle Assembly

The 321-60619-1 cradle assembly will have to be redesigned so that the height of the heatshield in the cradle is such that it may be checked out and inspected.

3.1.7.3 Dummy Heatshield Assembly

The 331-63098-1 dummy heatshield assembly will have to be redesigned to increase the diameter so that the dummy heatshield will accommodate the same size payload as the flight heatshield. This redesign will require

the design of: 331-50088 Dummy Heatshield Assembly, Upper; 331-50089 Dummy Heatshield Assembly, Lower; and 331-50090 Dummy Heatshield Assembly End Cap.

3.1.7.4 Hoist Assembly

A hoist assembly similar to 331-63040 will need to be designed for handling and positioning the larger diameter payloads and payload with heatshield combinations.

3.1.7.5 Bracket - Heatshield Storage in Shelter

The 331-50080-3 bracket, heatshield storage in shelter, will have to be redesigned to be longer to accommodate the larger diameter heatshield.

3.1.7.6 Upper Cradle Assembly

A new upper cradle assembly similar to 331-63208-3 but with larger diameter to accommodate the larger heatshield, and two new pads similar to 331-63208-17, but made to diameter of the larger heatshield will need to be designed.

3.1.7.7 The 331-50117-1 Proof Loading Fixture Assembly will have to be redesigned to add a spacer to one drum to accommodate the larger diameter strap on the redesigned 331-63040.

3.1.7.8 The 331-63094-1 Fin Protractor Kit will have to be redesigned to place the vernier at the proper distance from the hinge point and to widen the slot of the pointer assembly to fit over the thicker fin tip.

A

3.2 42 INCH DIAMETER HEATSHIELD INSTALLATION

3.2.1 Summary

The results of the evaluation of the impact of the 42 inch diameter heatshield installation on the Scout D configuration are summarized as follows:

- The following vehicle structural changes are required: redesign the base A fins to increase the area from 4.5 to 5.75 sq. ft. per fin; redesign several components of the heatshield attachment clamp; add cork insulation to the lower D section skins.
- Fin control tip areas shall be increased from 45 sq. in. to 78 sq. in. (Same as 40 inch heatshield requirement).
- Jet vane control surface area shall be increased from 35 sq. in. to 41 sq. in. (Same as 40 inch heatshield requirement).
- Guidance system first stage nominal displacement gain shall be increased from 5.0 to 6.75 deg/deg and the rate to displacement gain ratio shall be 0.4, the same as for the basic Scout.
- The following ground support equipment requires redesign: payload umbilical retract arm, heatshield cradle, dummy heatshield, payload and heatshield hoist, heatshield storage bracket, and the upper cradle assembly.

Detailed discussion of the evaluation is presented in the following paragraphs.

3.2.2 Aerodynamic Characteristics

3.2.2.1 Rigid Vehicle

The configuration differences between the 42" diameter heatshield wind tunnel model and the selected configuration were assumed to not significantly affect C_{N_α} and the center of pressure. This permitted using body alone wind tunnel data of the 42" diameter heatshield configuration for the body aerodynamic characteristics of the selected configuration. This body alone wind tunnel model configuration was not actually tested, but the data was synthesized by subtracting the incremental effect of the fins, derived from the 34" diameter heatshield configuration, from the complete 42" diameter heatshield configuration. These data were used to define the body alone variations presented in Figures 3.2.2-1 and -2. The fin incremental effect, Figure 3.2.2-4 was obtained by fairing the experimental data presented in Figure 2.2.2.2-5. These fin experimental data were obtained with a 34" diameter heatshield configuration, but the general heatshield similarity and the physical separation of the heatshield and fins should prevent significant aerodynamic interference between the heatshield and the fins. The body + fins data, Figures 3.2.2-1 through -3, were obtained by adding the incremental effect of the fins to the body alone data.

The fin tip control effectiveness data presented in Figure 3.2.2-5 were obtained from Figure 2.2.2.2-6, using the estimated current Scout data to $M_\infty = 2.3$, and the wind tunnel data to define the variation above $M_\infty = 2.3$.

The estimated zero lift drag coefficient data presented in Figure 3.2.2-6 was obtained by adding to the drag for the 34" diameter heatshield, nose at station -25, Reference 3-9 , the estimated drag increments for the sphere-cone pressure drag, cylinder friction drag, and reverse frustrum wave drag of the larger heatshield.

FIGURE 3.2.2-1

NORMAL FORCE COEFFICIENT DERIVATIVE

42. IN. DIA. HEATSHIELD

$\theta_c = 12.5°$ $r_{1/2} = .6$

$S_{ref} = 5.26$ FT^2

RIGID VEHICLE

FIN AREA = 4.5 FT^2

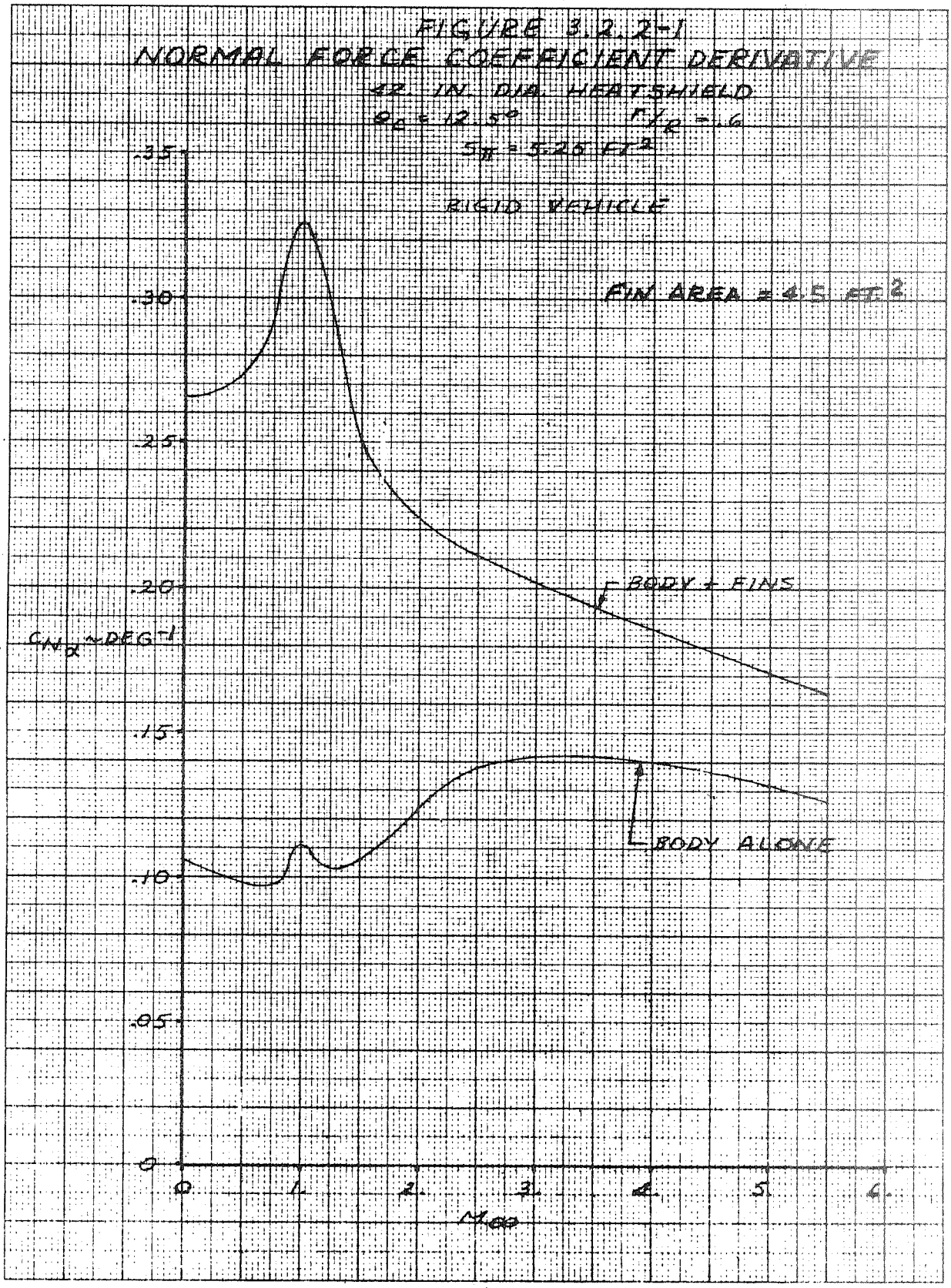

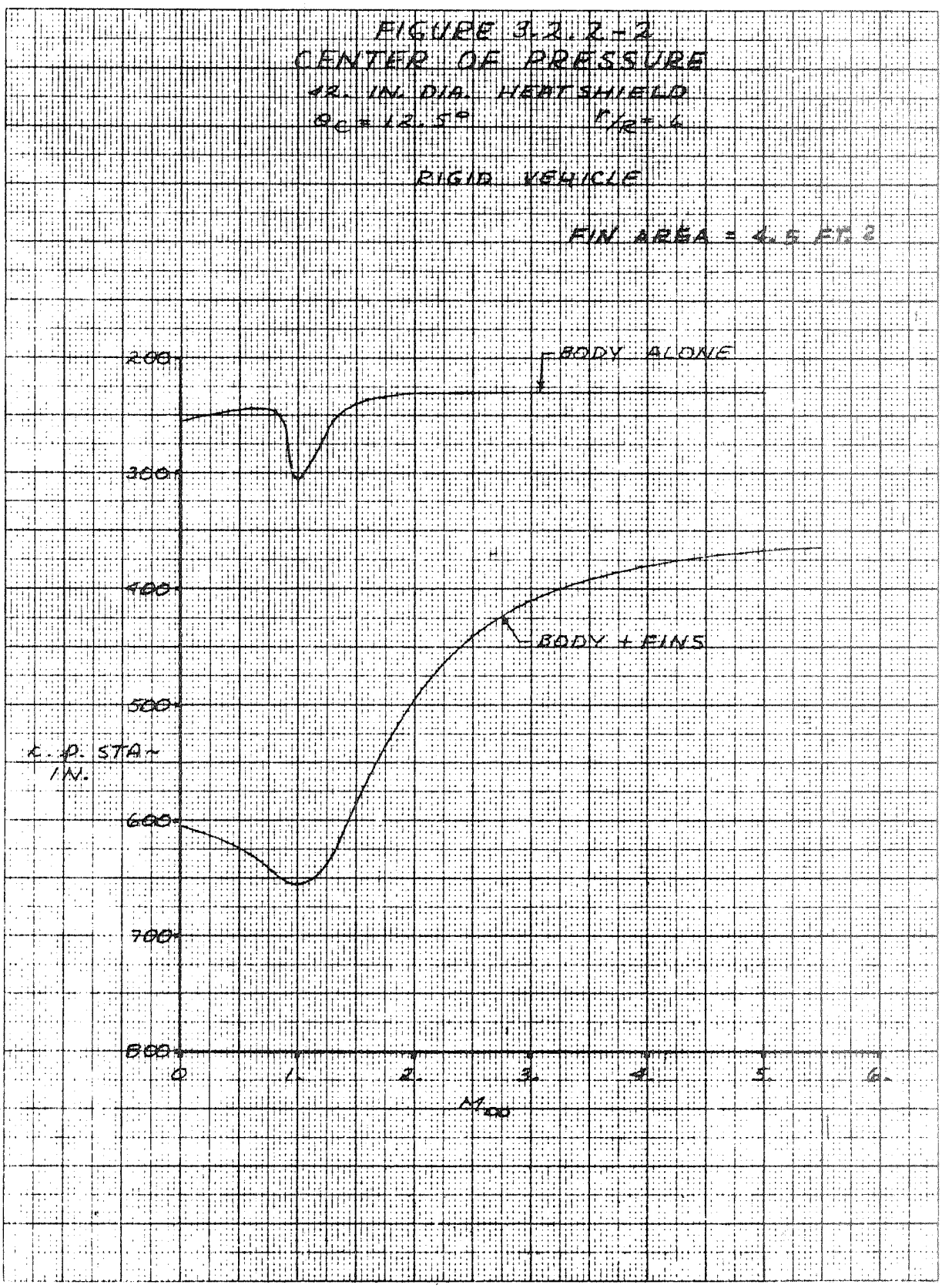
FIGURE 3.2.2-2
CENTER OF PRESSURE
42. IN. DIA. HEAT SHIELD
$\theta_c = 12.5°$
$r_{N_R} = .4$
RIGID VEHICLE
FIN AREA = 4.5 FT.²
BODY ALONE
BODY + FINS
200
300
400
500
600
700
800
C.P. STA ~ IN.
0
1.
2.
3.
4.
5.
6.
M_∞

FIGURE 3.2.2-3
PITCHING MOMENT DERIVATIVE
42. IN. DIA. HEAT SHIELD
$\theta_C = 12.5°$ $r_{/B} = .6$
$S_B = 5.26\ FT^2$ $\ell_B = 2.58\ FT$
CG @ STA 427.8
RIGID VEHICLE
FIN AREA = 4.5 FT^2

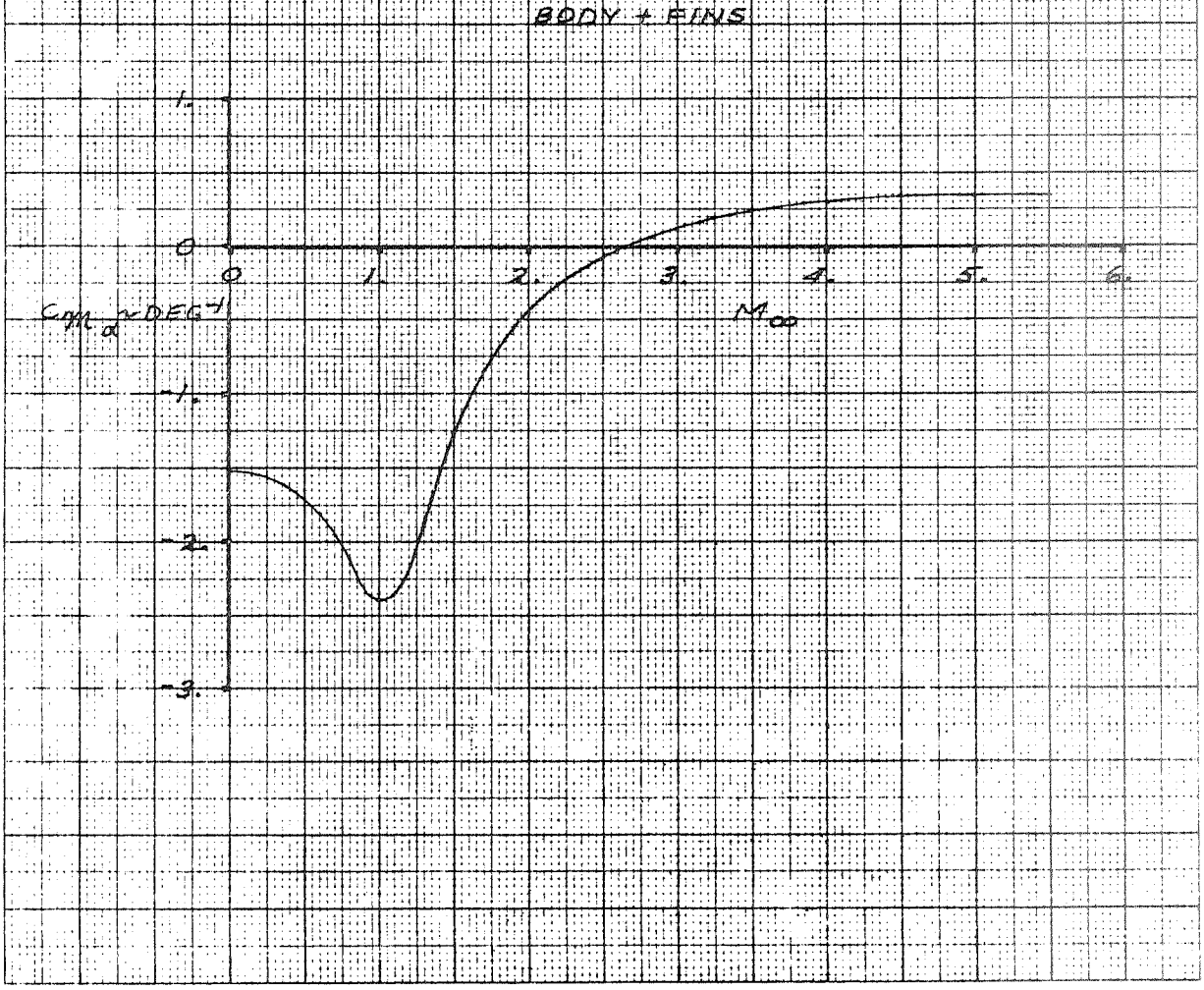

FIGURE 3.2.2.-4
FIN NORMAL FORCE DERIVATIVE
AND CENTER OF PRESSURE

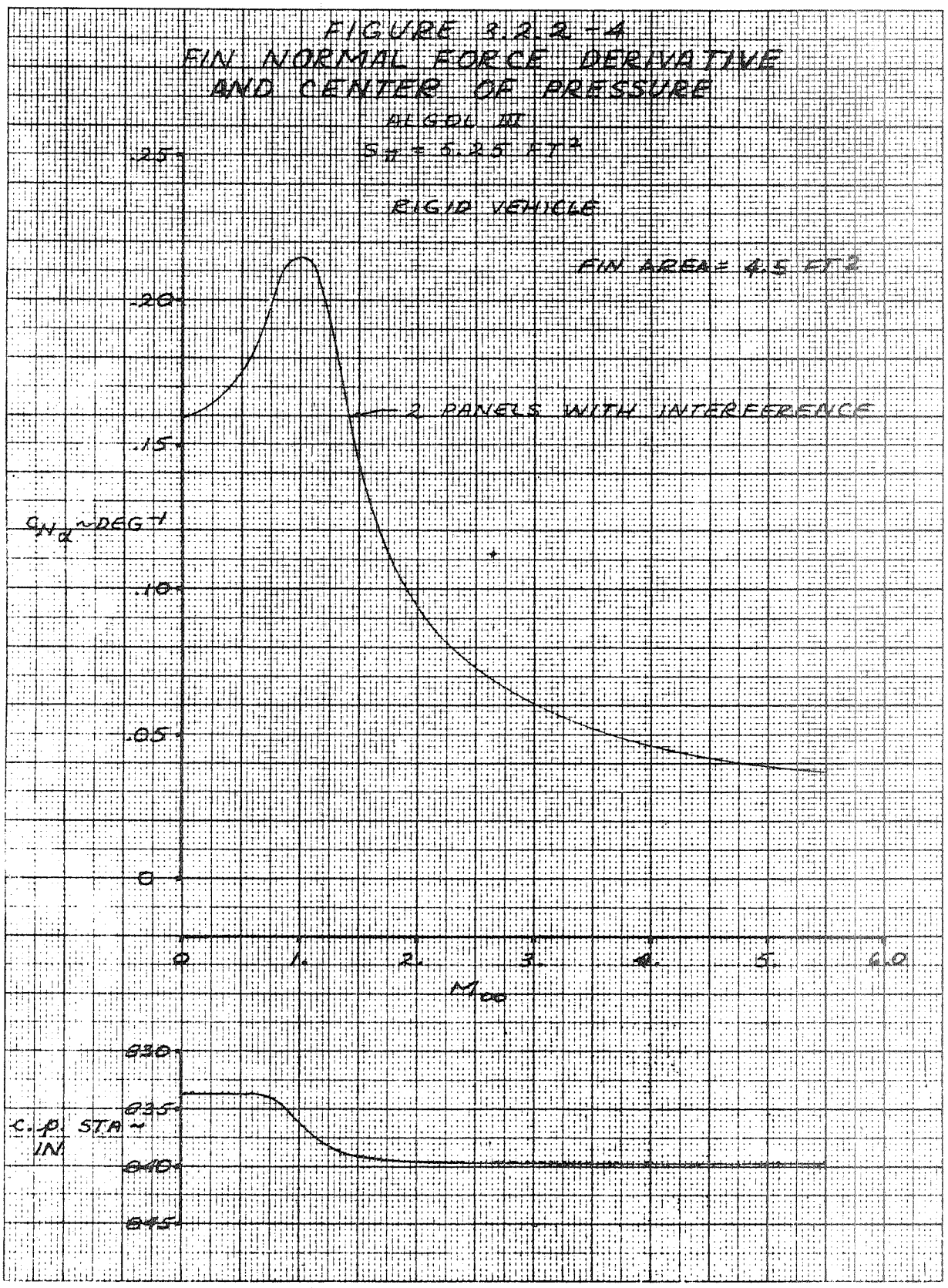

FIGURE 3.2.2-5
FIN TIP CONTROL EFFECTIVENESS
$S_M = 5.25\ FT^2$ $S_{TIP} = .213\ FT^2$
2 PANELS
RIGID VEHICLE

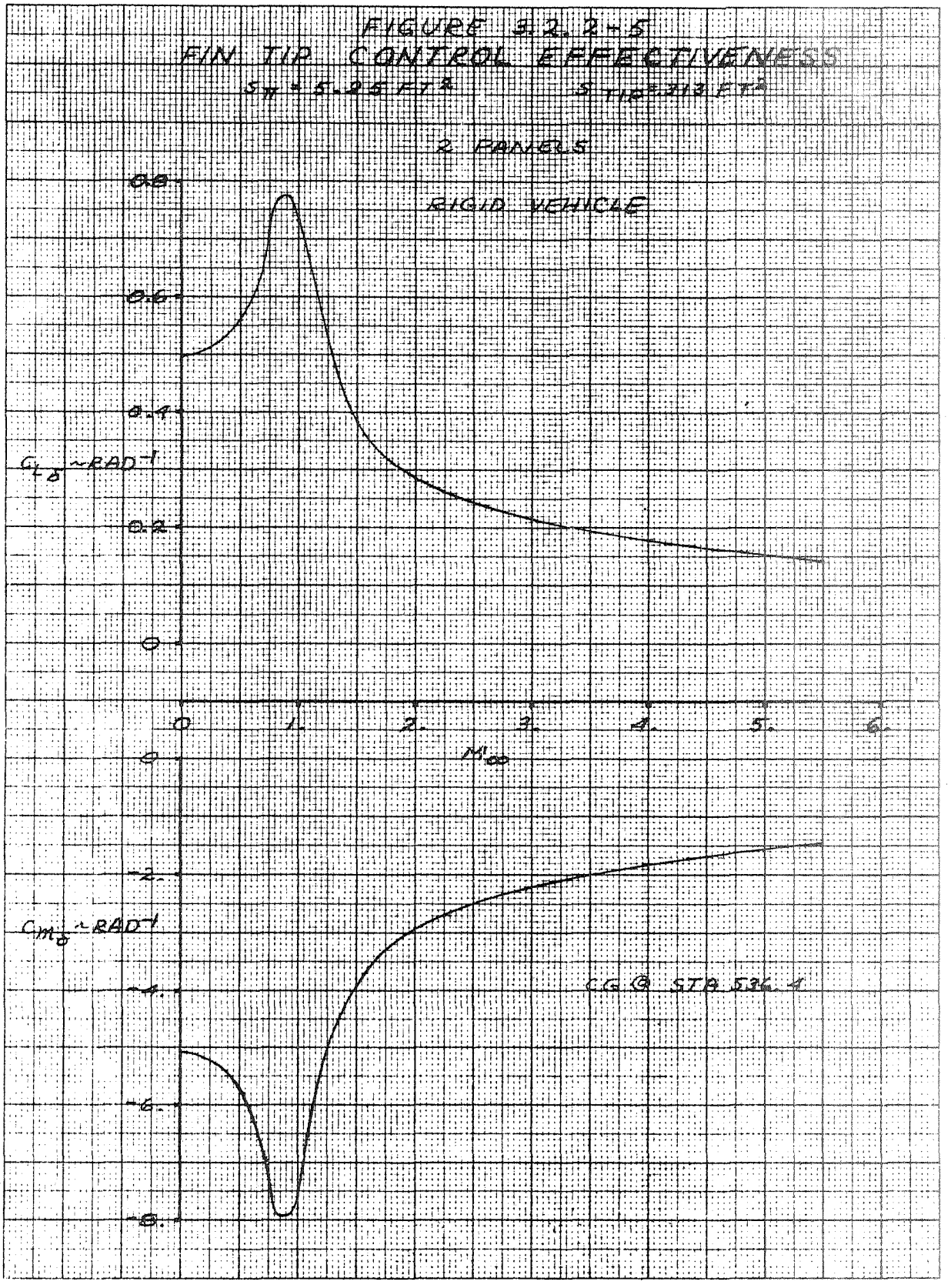

FIGURE 3.2.2-6
ZERO LIFT DRAG COEFFICIENT
12 IN. DIA. HEATSHIELD
$\theta_c = 12.5°$ $r_{/R} = .6$
4.5 SQ. FT. FIN AREA (PER FIN)

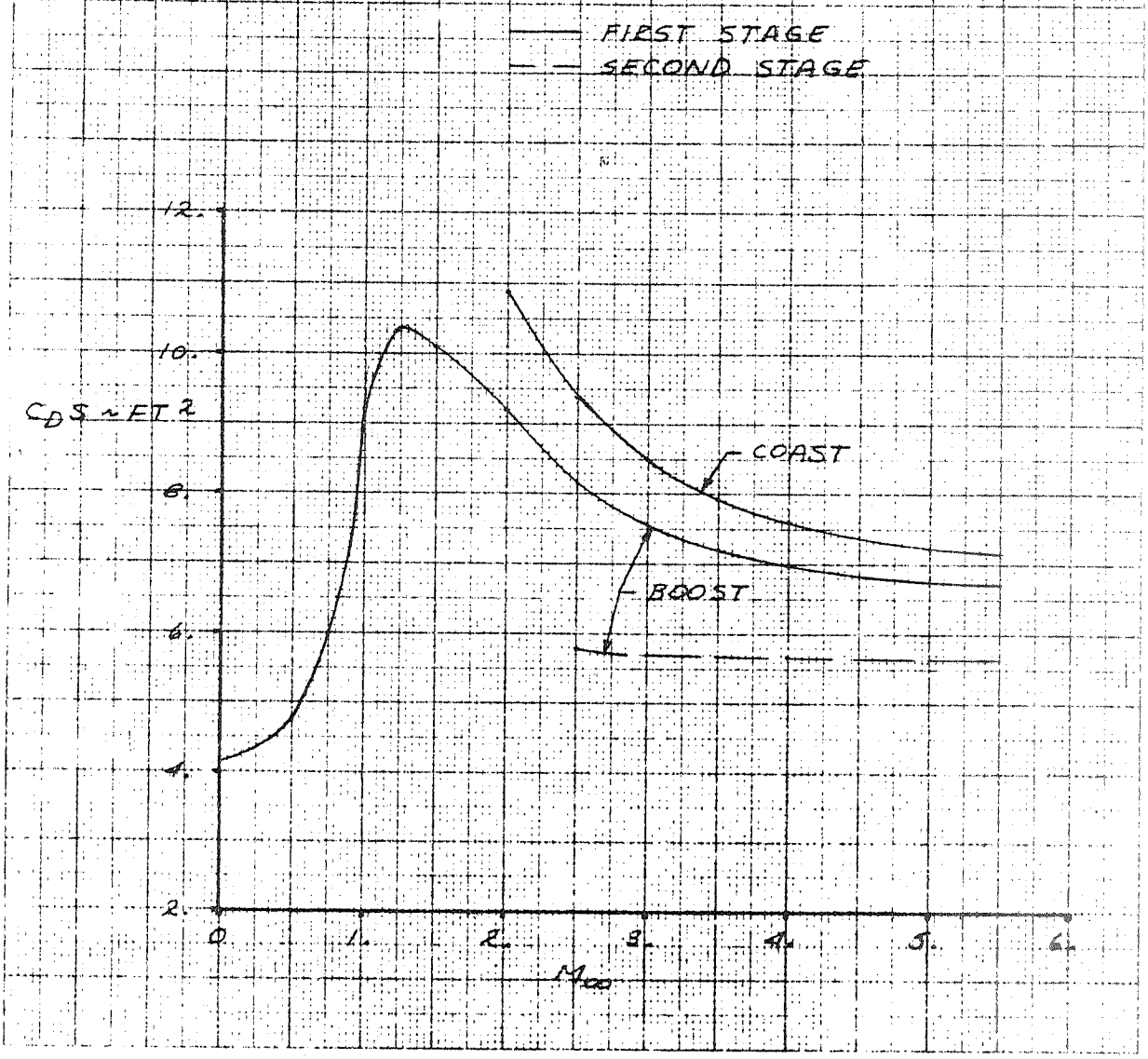

Estimated normal load distributions for the rigid body alone, without protuberances, are presented in Figures 3.2.2-7 through -14. The transonic variations were obtained by using References 3-2 and 3-10, and the supersonic variations using references 2-2, 3-2, 3-11 and 3-12. The C_{N_α} and centers of pressure for load distributions aft to station 131.1 for all selected heatshield configurations were correlated for configuration and Mach number. The body alone C_{N_α} and centers of pressure derived by integrating these data correlate with that presented in Figures 3.2.2-1 and -2.

It was assumed the load distributions aft of station 131.1 were unaffected by the heatshield configuration; thus, the load distributions presented in Figures 3.2.2-11 through -14 are applicable to vehicles utilizing the other heatshield configurations.

Heatshield drag buildup is presented in Figure 3.2.2-15, and is included in the data presented in Figure 3.2.2-6.

The stability and control analysis of the 42" diameter heatshield configuration indicated the need for enlarged fins to satisfy stability criteria. The revised fin has the same planform shape as the current Scout fins, with an area of 5.75 ft^2 per fin, compared to 4.5 ft^2 for the current Scout fin. The fin tip control size was scaled up to utilize the current Scout hinge line location. Estimated aerodynamic characteristics for this enlarged fin configuration are presented in Figures 3.2.2-16 through -20.

FIGURE 3.2.2-7
NORMAL LOAD DISTRIBUTION
42. IN. DIA. HEATSHIELD
$\theta_c = 12.5°$ $r_{/R} = .6$
$M_\infty = 0.8$
$C_{N_\alpha} S = \int c_{N_\alpha} b\,dx = .1152$ FT^2/DEG
C.P. @ STA −43.5
$c_{N_\alpha} b$ ~ FT DEG^{-1}
.10
.08
.06
.04
.02
0
-.02
-.04
-.06
-.08
-.10
-50
0
50
100
150
STA~ IN.
x

FIGURE 3.2.2-8
NORMAL LOAD DISTRIBUTION
-22. IN. DIA. HEATSHIELD
$\theta_c = 12.5°$ $M_{\infty} = 1.6$ $M_{\infty} = 1.0$

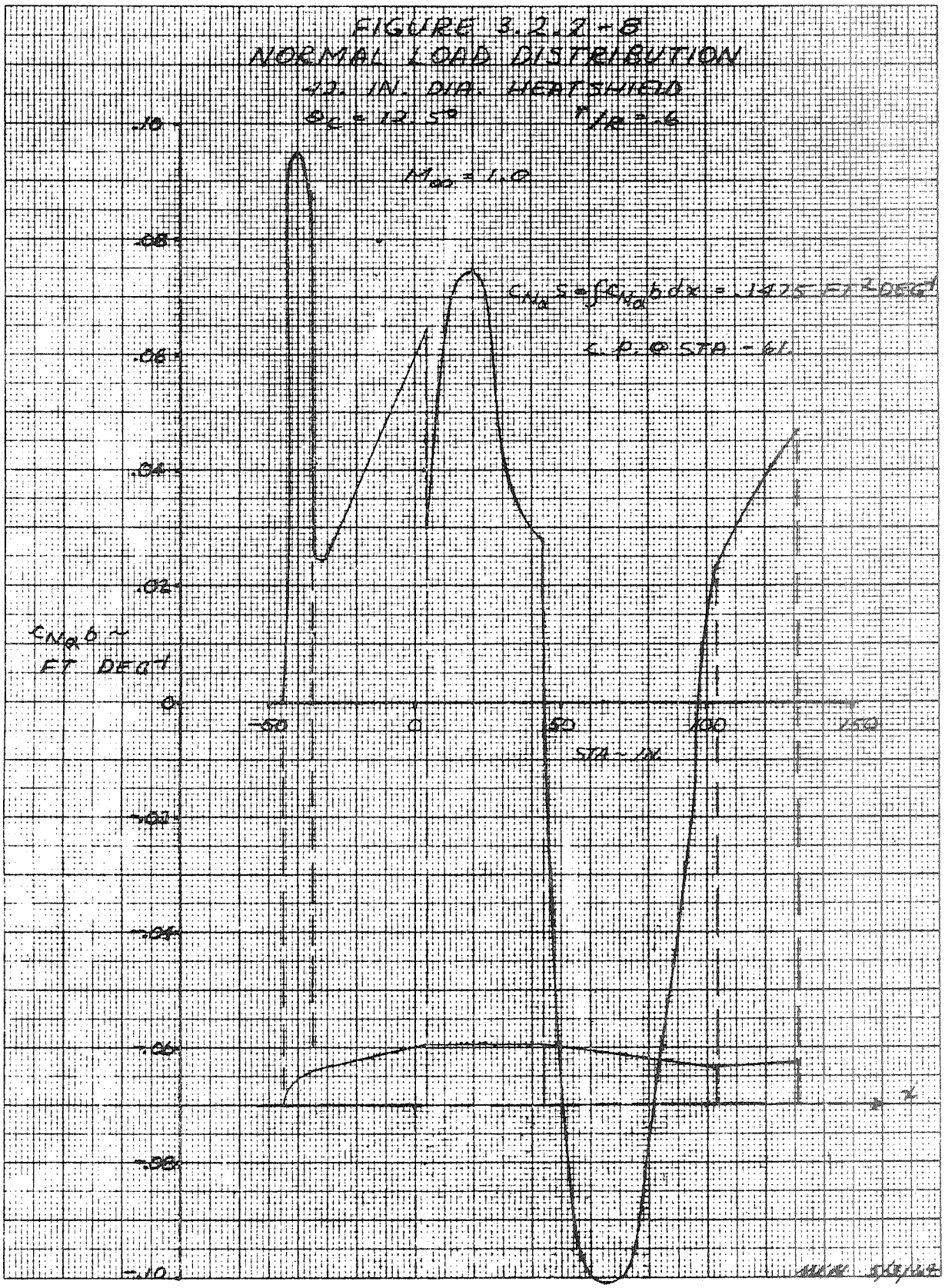

FIGURE 3.2.2-9
NORMAL LOAD DISTRIBUTION
42. IN. DIA. HEATSHIELD
$\theta_c = 12.5°$ $r/R = .6$
$M_\infty = 4.5$

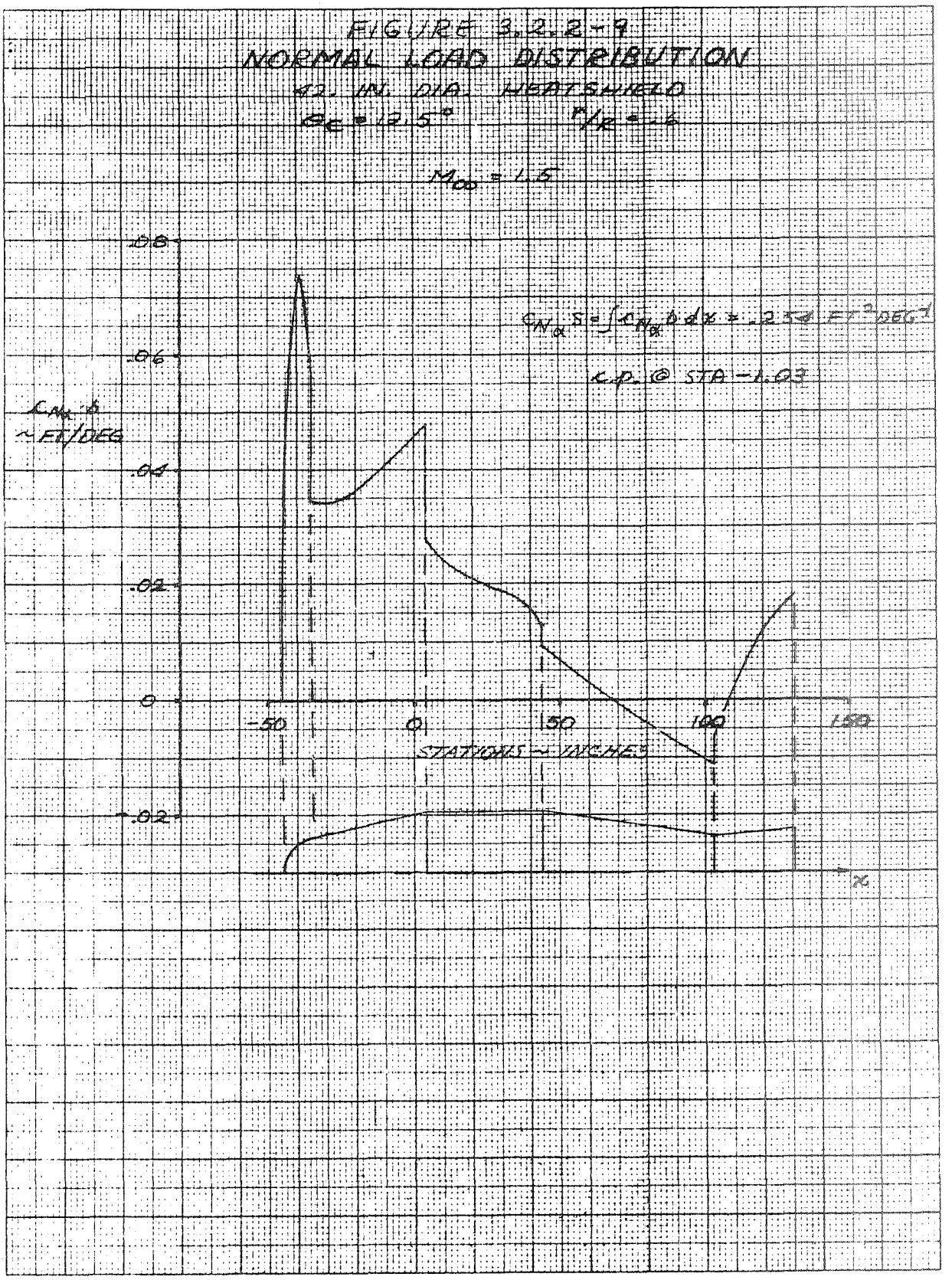

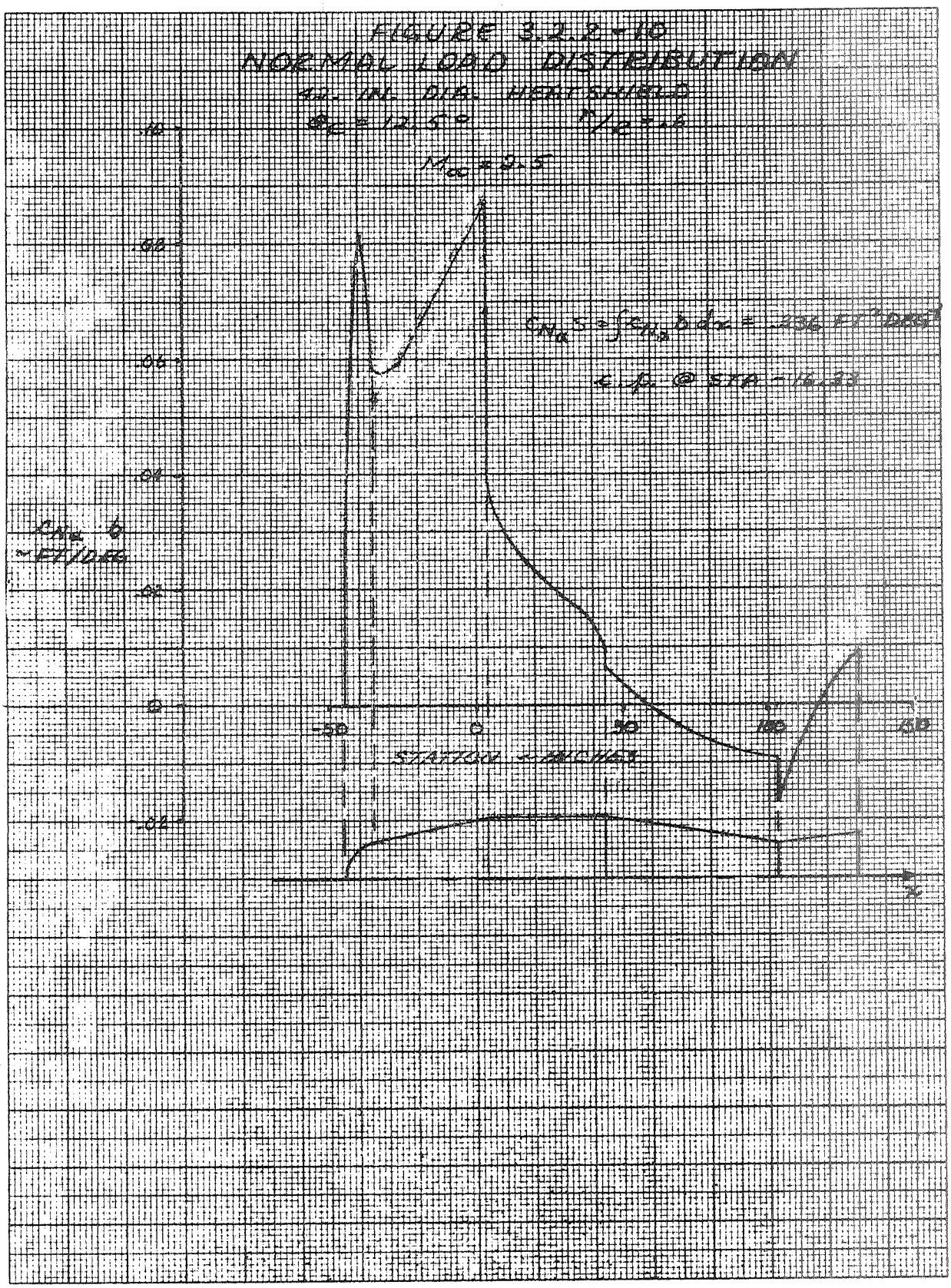
FIGURE 3.2.2-10
NORMAL LOAD DISTRIBUTION
$M_\infty = 0.5$
$C_{N_\alpha} S = \int c_{n_\alpha} b \, d\alpha = .436$ Per Degree
$C_{N_\alpha} b$ Per Degree
.10
.08
.06
.04
.02
0
-.02
-50
0
50
100
150
STATION - INCHES
α

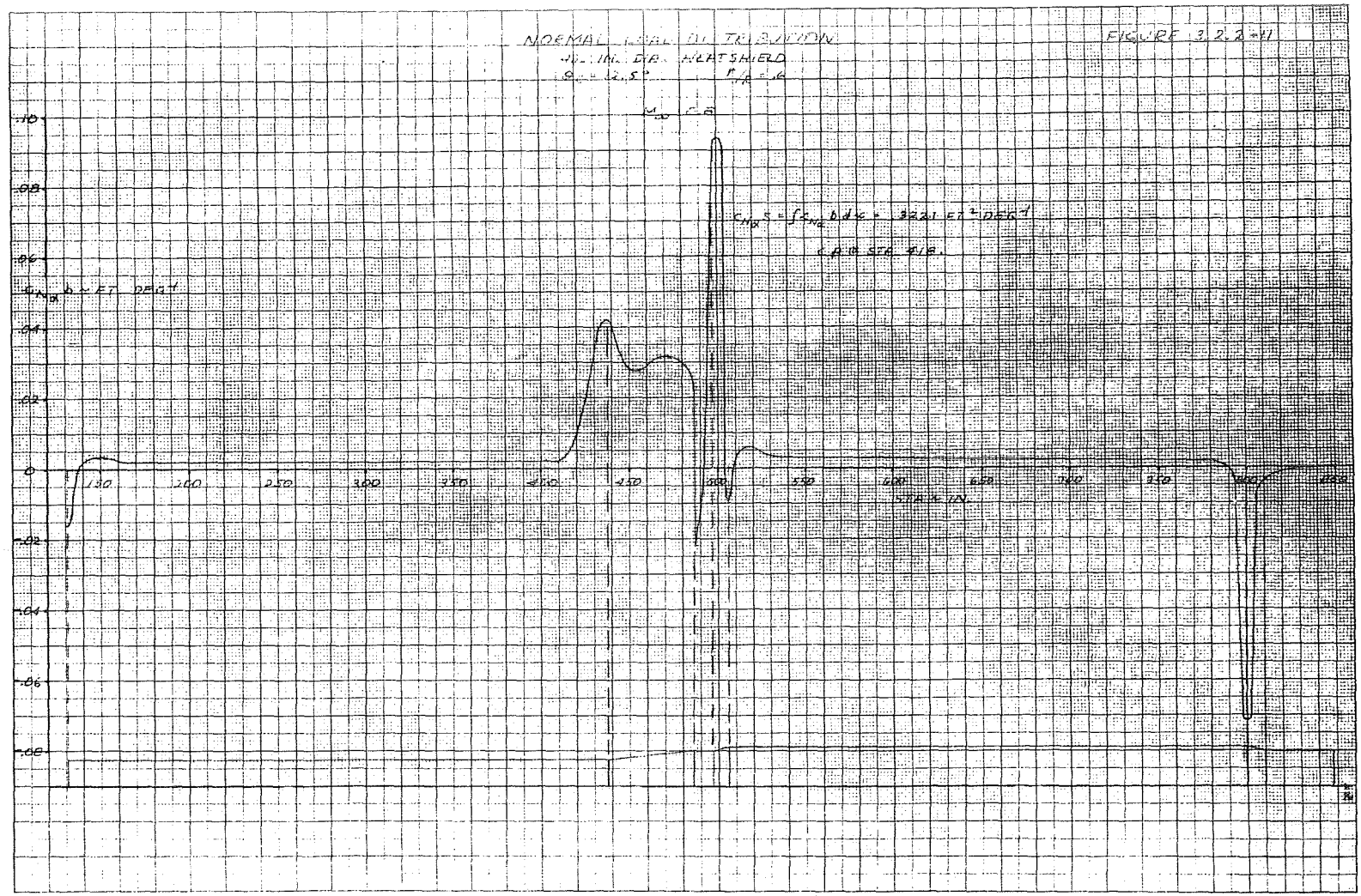

FIGURE 3.2.2-41

10 X 10 TO THE CENTIMETER 47 1513
KEUFFEL & ESSER CO.

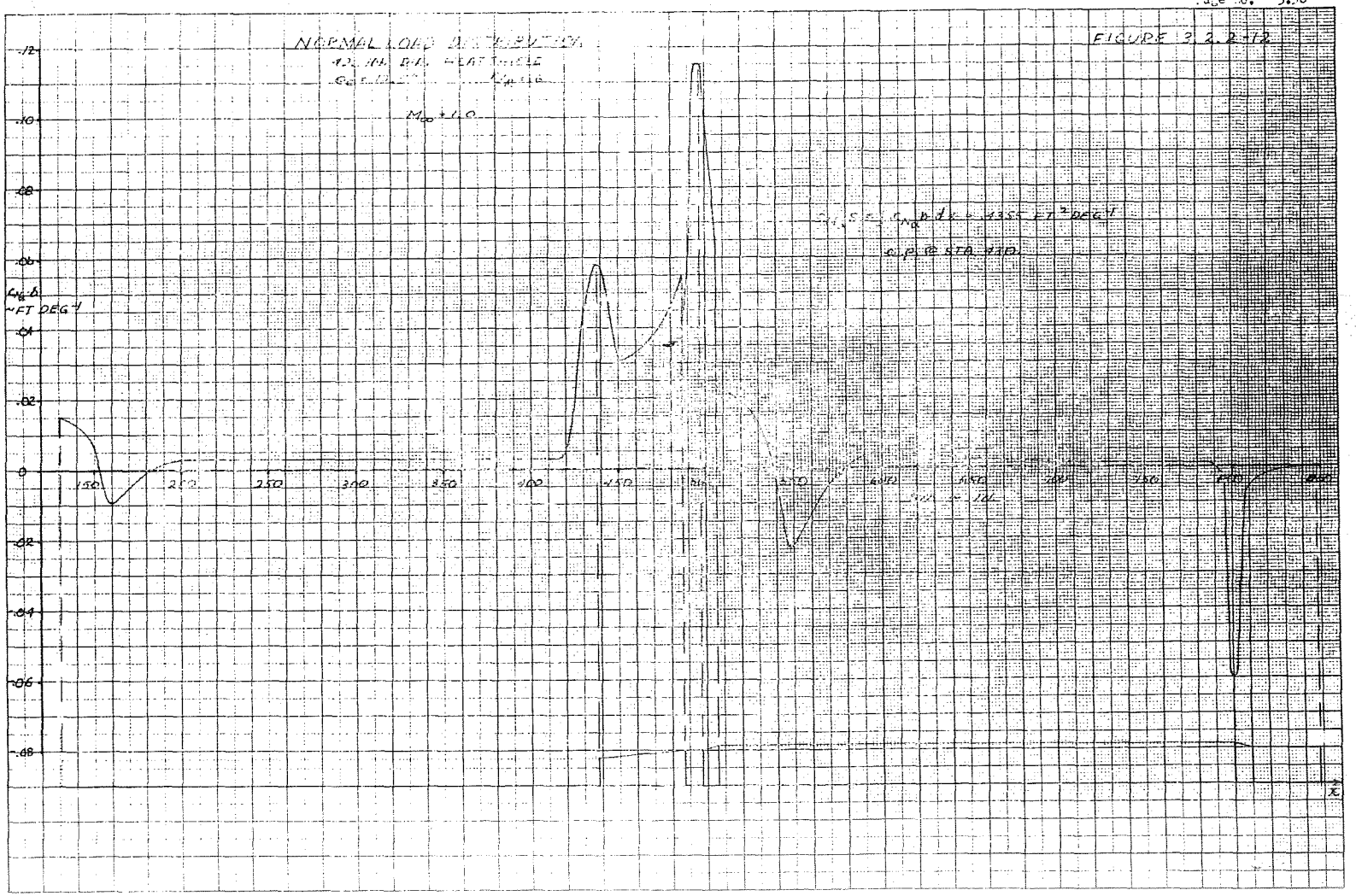

NORMAL LOAD DISTRIBUTION
42. IN. D.A. HEATSHIELD
$\Theta_c = 12.5°$ $r/R = .4$
$M_\infty = 1.5$

FIGURE 3.2.2-13

$C_{N_\alpha} S = \int c_{l_\alpha} b\, dx = .3085$ FT² DEG⁻¹
c.p. @ STA 740

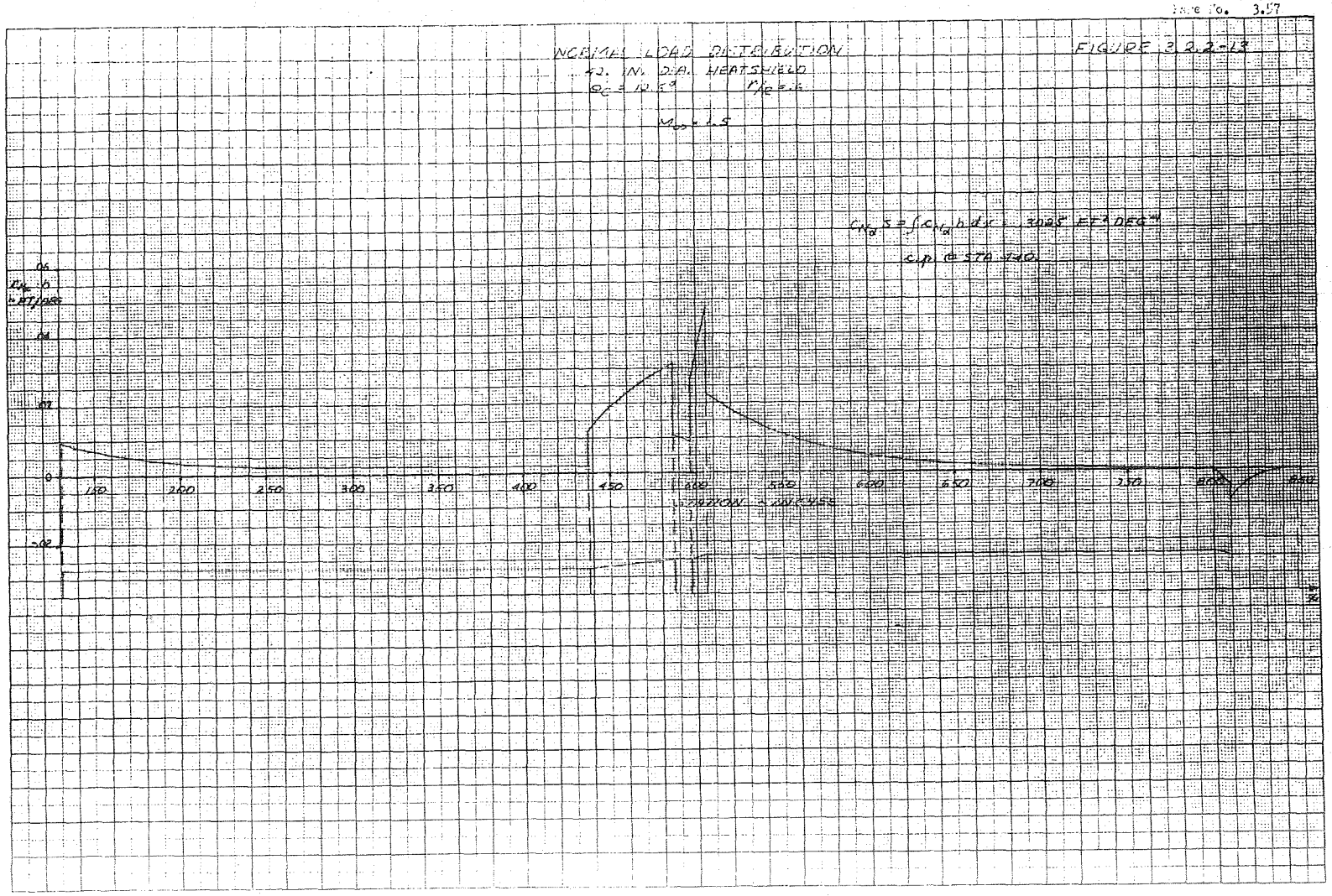

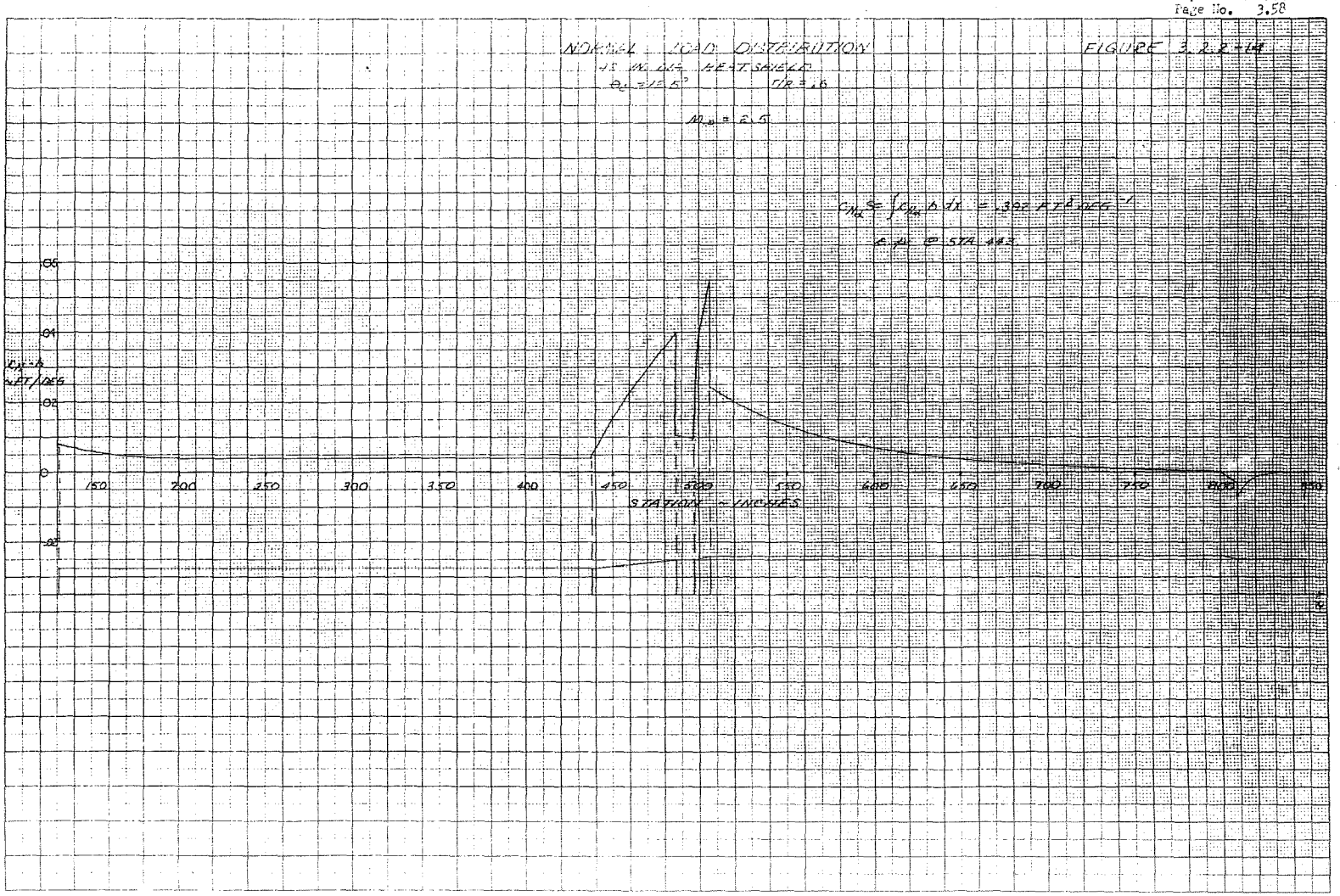

FIGURE 3.2.2-15
HEATSHIELD DRAG BUILDUP
(PRESSURE AND FRICTION)
12 IN. DIA. HEATSHIELD
$\theta_c = 12.5°$ $r_n/R = .6$

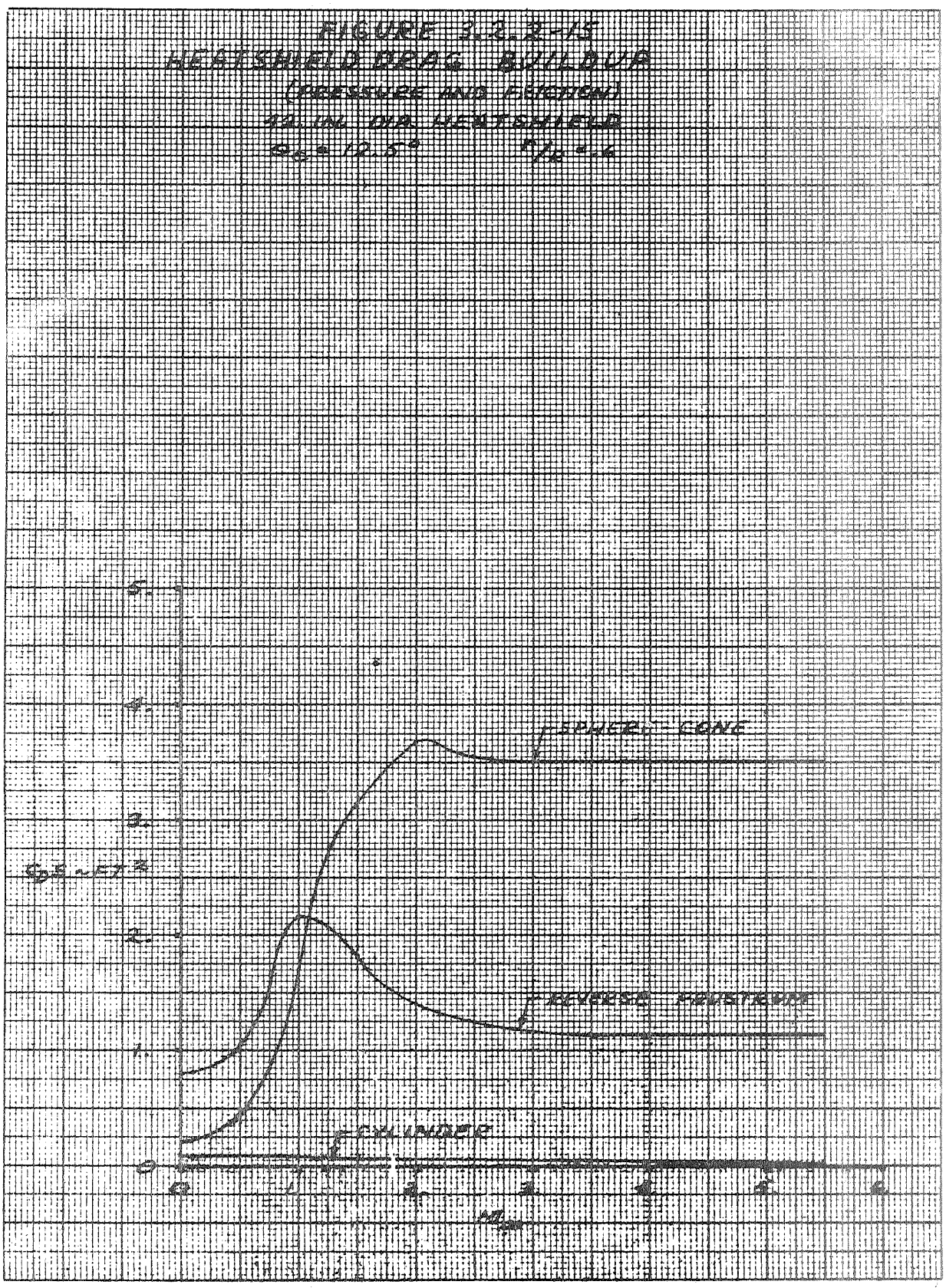

FIGURE 3.2.2-16

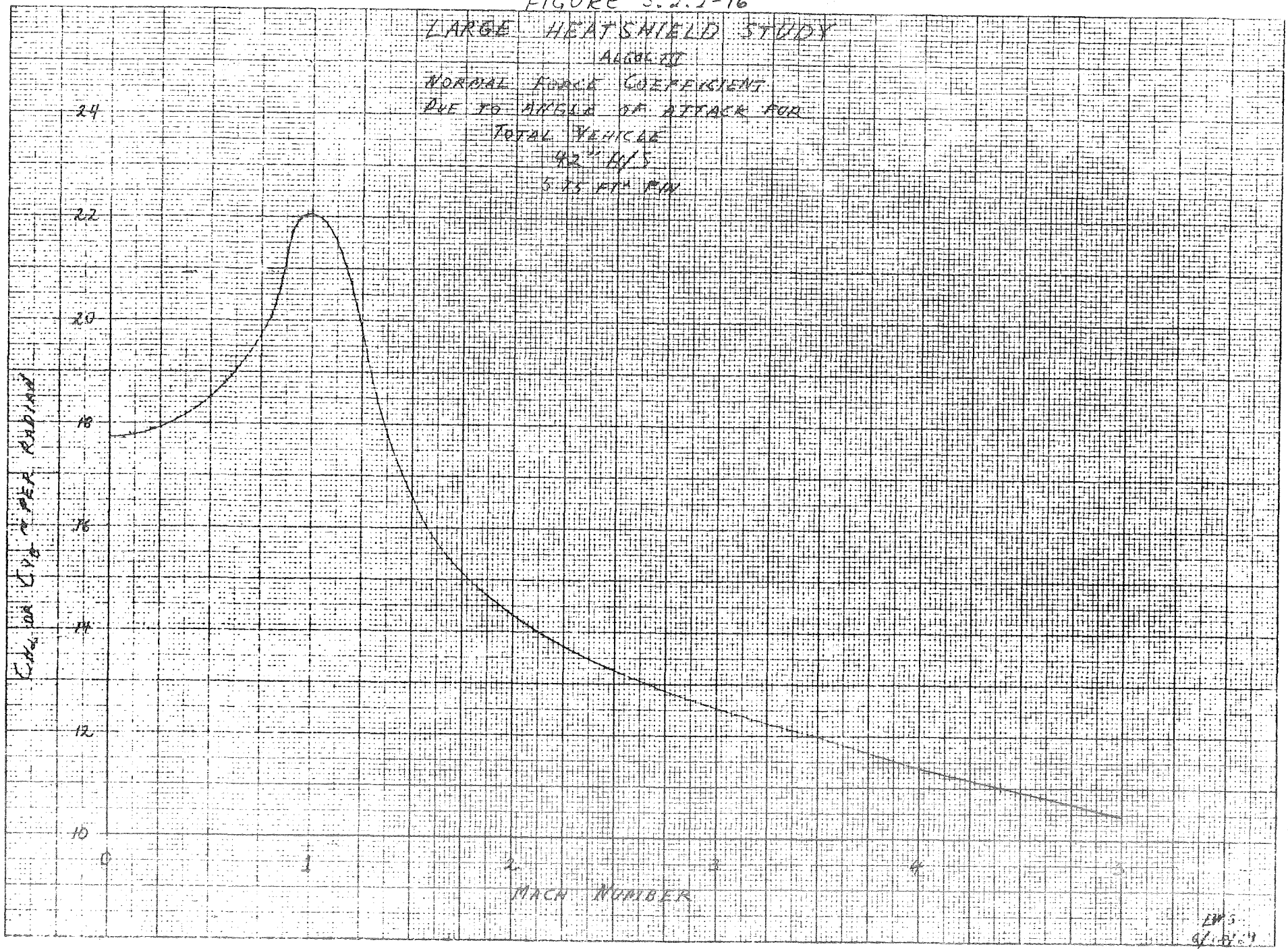

FIGURE 3.2.2-17

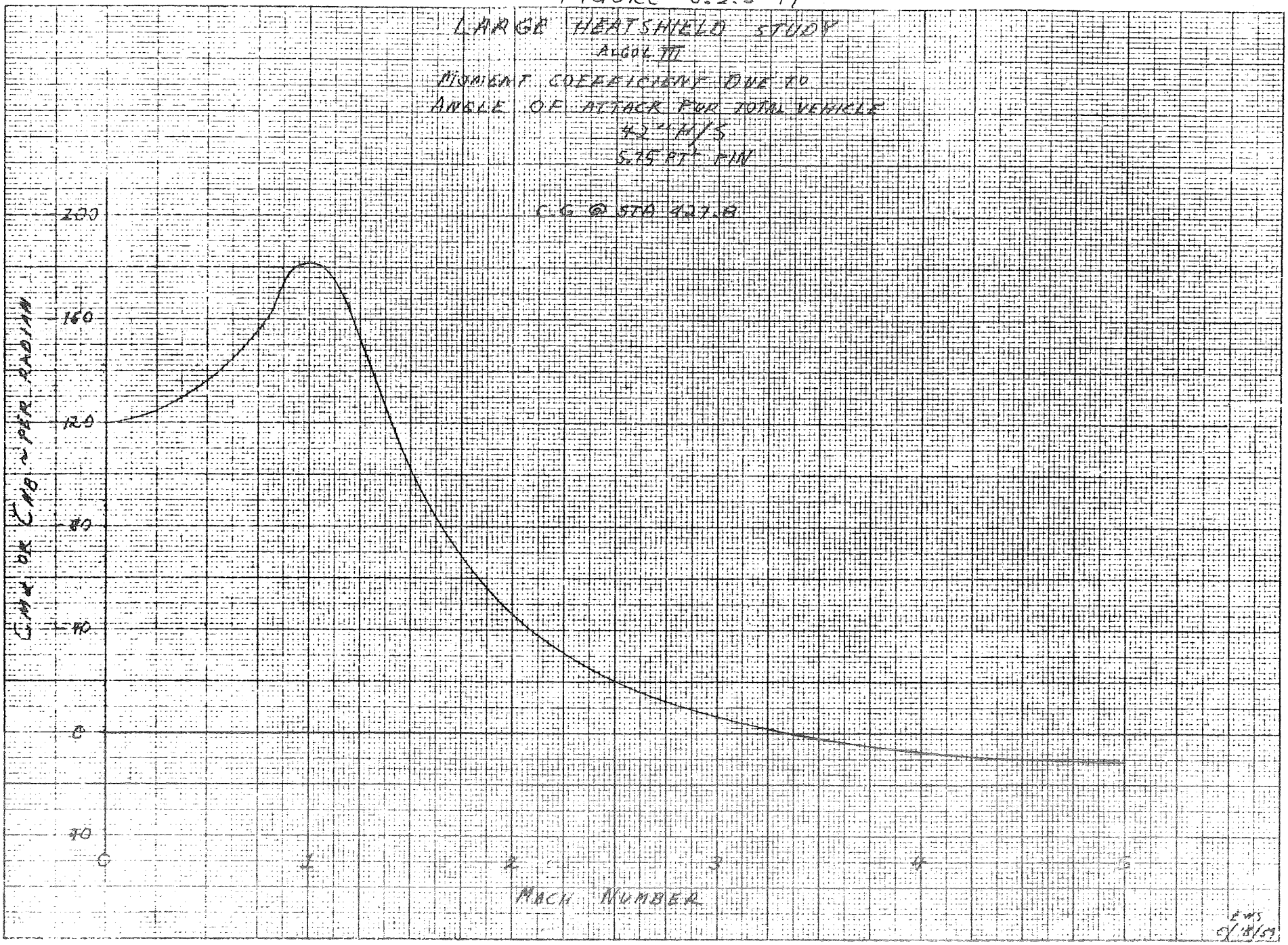

FIGURE 3.2.2-18
LARGE HEATSHIELD STUDY
ALGOL III
NORMAL FORCE COEFFICIENT DUE TO
DEFLECTING TWO FIN CONTROL TIPS
ALL HEATSHIELDS
TIP AREA: 0.542 FT² (PER TIP)
C.P. FIN: STA 853.5

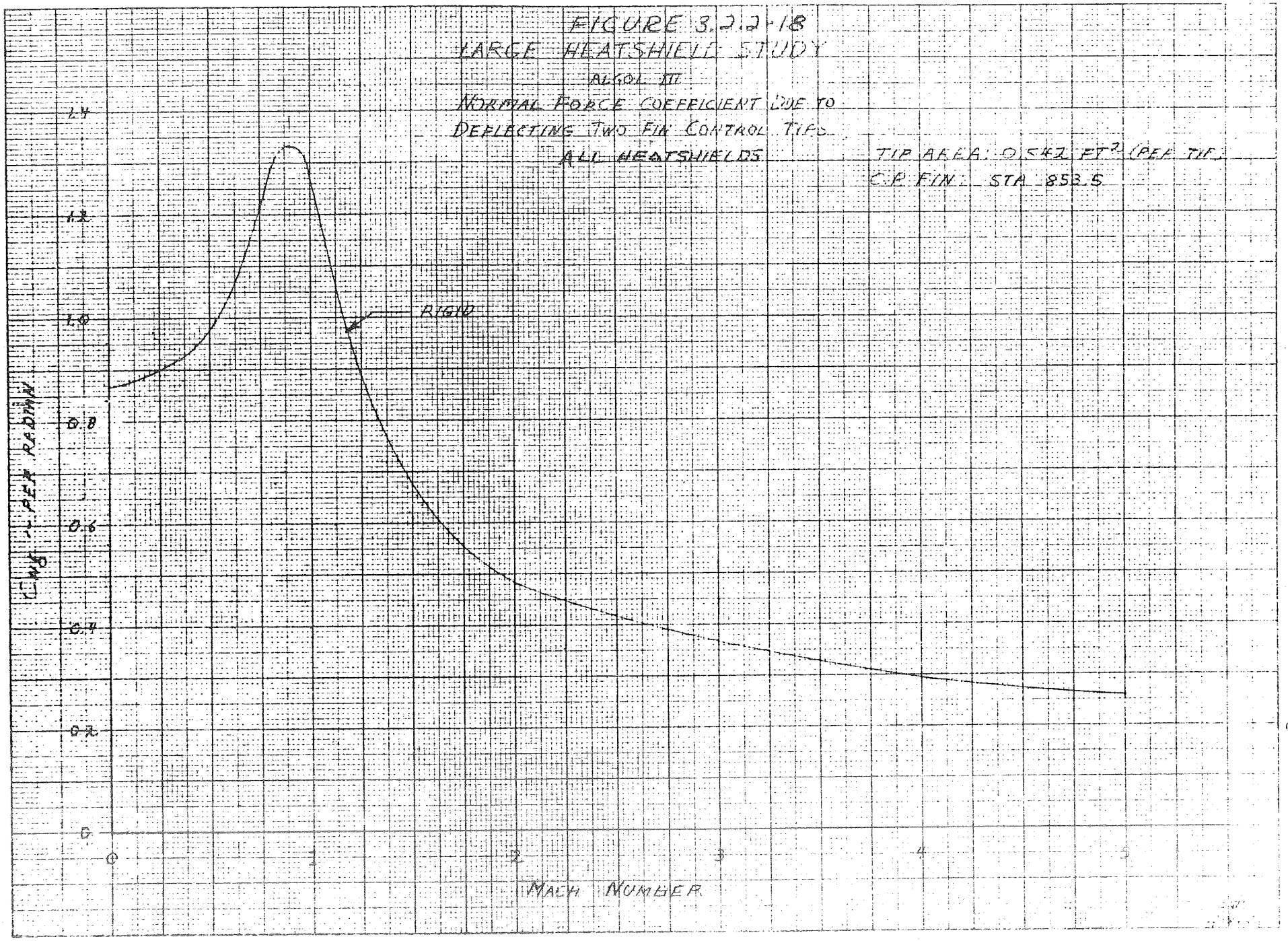

FIGURE 3.2.2-19

LARGE HEATSHIELD STUDY

ALGOL III

MOMENT COEFFICIENT SAVE C_{m_q}

DEFLECTING TWO FIN SCALED TIES

ALL HEATSHIELDS

FIN AREA 0.542 FT^2 (PER FIN)

CG @ STA 427.8 OF F.W.M.^{2} STA 853.5

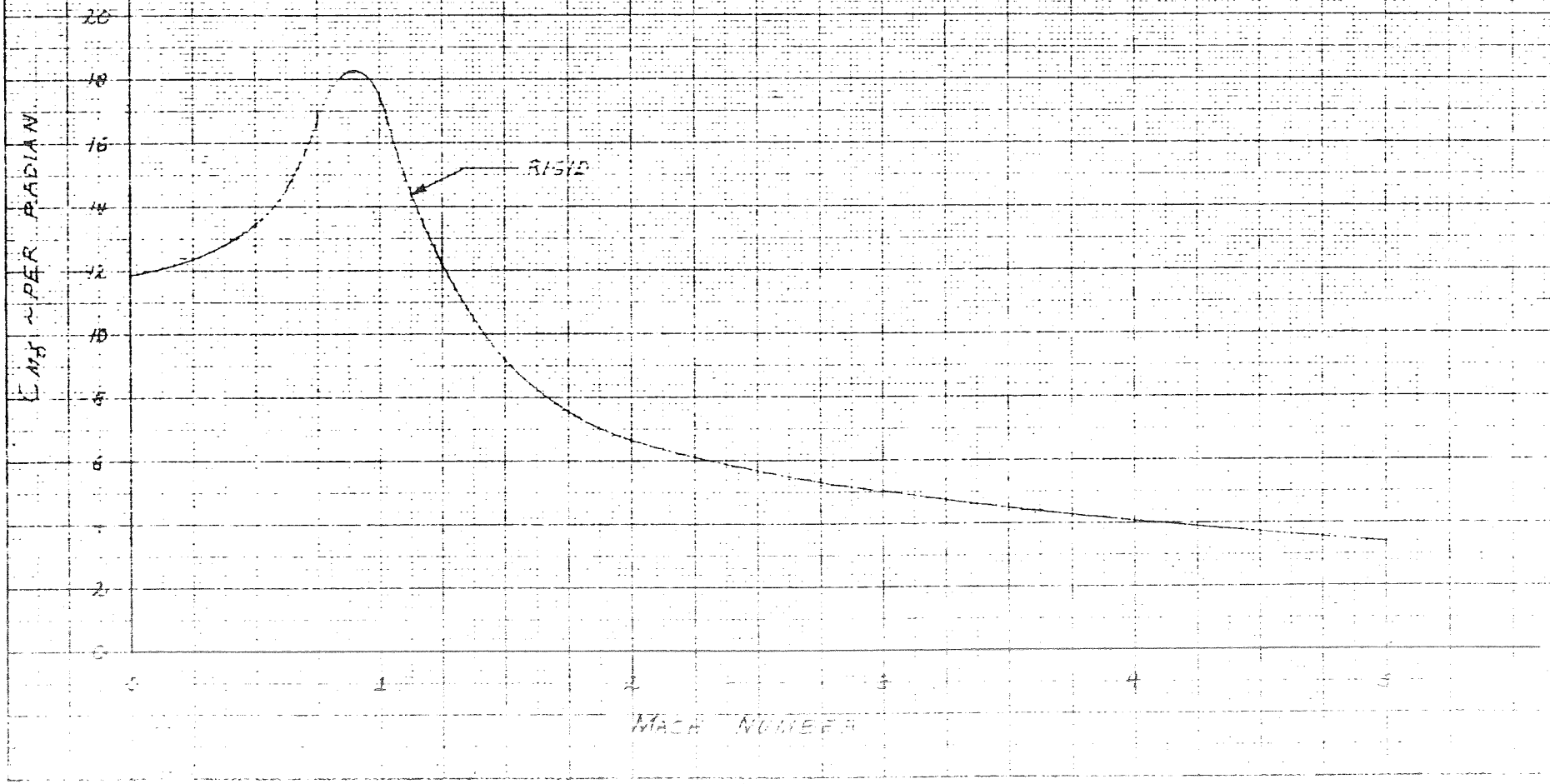

C_{m_q} PER RADIAN

FIGURE 3.2.2-20

ZERO LIFT DRAG COEFFICIENT

2 M DIA. HEATSHIELD
3.75 FT² FIN AREA (REF.)

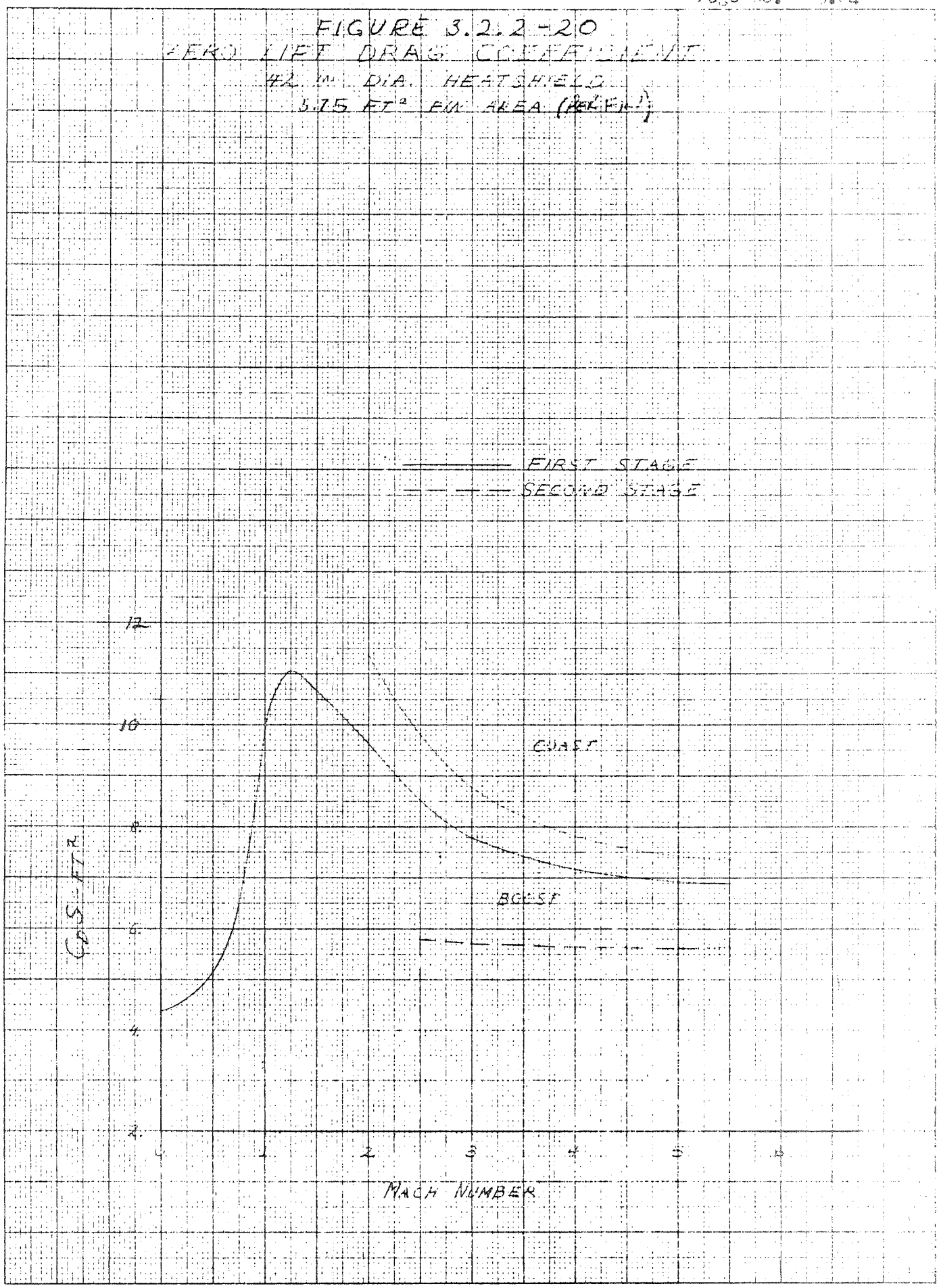

3.2.2.2 Flexible Body Aerodynamics

The flexible aerodynamic coefficients were determined by assuming that the elastic motion is such that the generalized velocity and acceleration are zero. This is known as the "quasi-rigid" assumption and is the basis for the use of flexible corrections to the rigid aerodynamic derivatives. Based on this assumption the local vehicle angle of attack due to elastic deflection may be determined in terms of the dynamic pressure and the overall rigid body angle of attack. Consequently, for Mach numbers at which the rigid body aerodynamic distributions are known, the total force and moments (including the effects of flexibility) may be determined as functions of dynamic pressure and rigid body angle of attack. This yields the flexible body aerodynamic coefficients. No axial loads or thrusting effects were considered in this analysis but past experience has shown them to be negligible. The aeroelastic effects on the aerodynamic coefficients for several dynamic pressures were calculated as a function of Mach number. The results of these calculations for the 42 inch diameter heat shield are presented in Figures 3.2.2.2-1, -2, and -3. Similar data was generated for the 40, 44, and 46 inch heat shield configurations but is not presented in plotted form because the data is not used in this format for the stability or loads analyses. The Scout vehicle configuration assumed for this phase of the study consists of an Algol III first stage motor, Castor II second stage motor, X-259 third stage motor, and an FW-4S fourth stage motor. The standard base "A" and 4.5 ft^2 fins were used for this analysis. A payload of 50 lbs with its center of mass at station 24.0 was used. Figures 3.2.2.2-1 and 3.2.2.2-2 present the normal force coefficient due to angle of attack and Figure 3.2.2.2-3 the center of pressure location.

The above data were used in determining the change in the control parameters and fin size necessary to obtain a controllable vehicle. Once the new fins were sized the body flexibility effects as calculated in the previous

FIGURE 3.2.2.2-1

SCOUT VEHICLE – ALGOL III FIRST STAGE

NORMAL FORCE COEFFICIENT DUE TO ANGLE OF ATTACK FOR TOTAL VEHICLE MACH NUMBER 0 TO 2

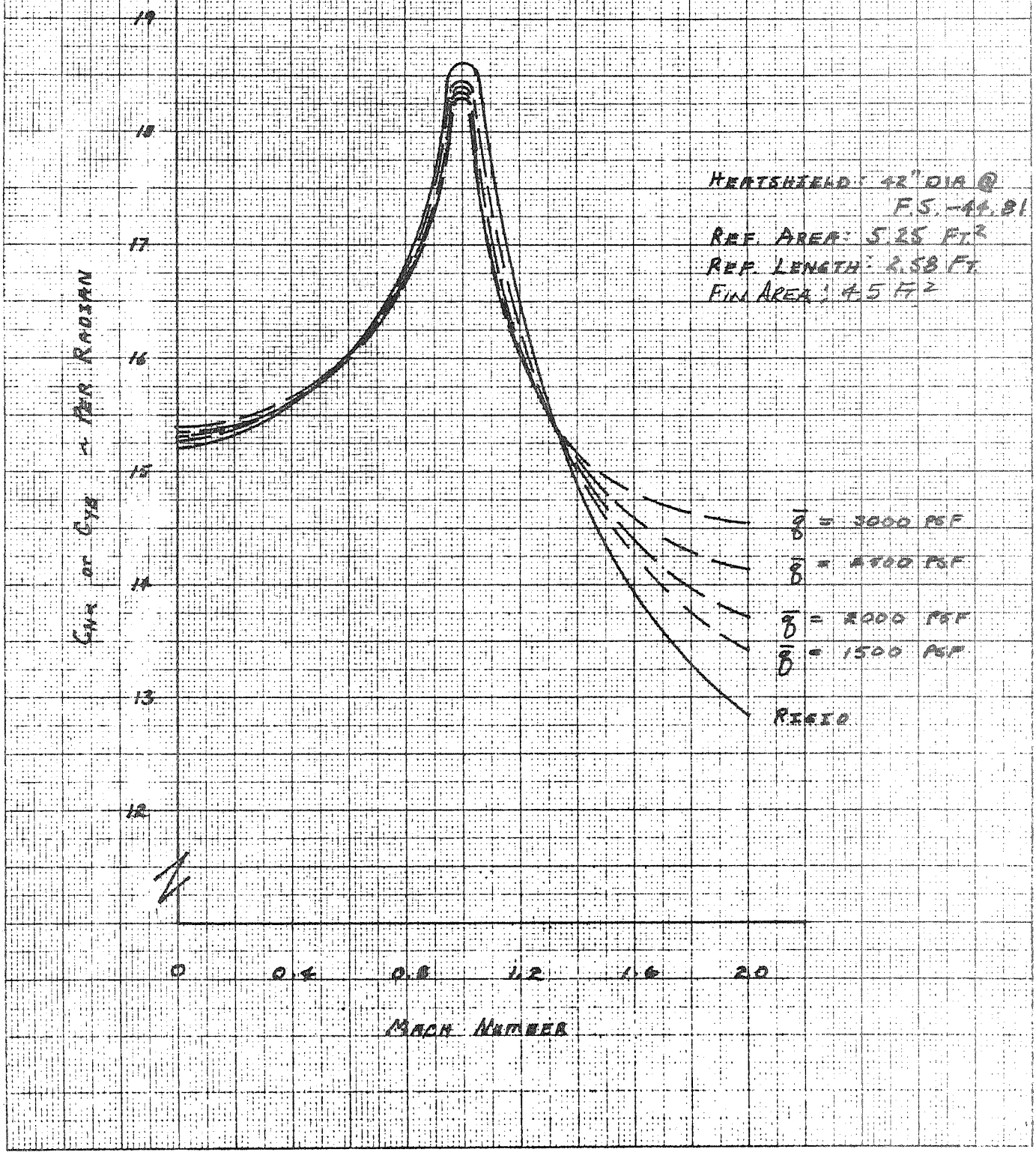

FIGURE 3.2.2.2-2

SCOUT VEHICLE – ALGOL III FIRST STAGE

NORMAL FORCE COEFFICIENT DUE TO ANGLE OF ATTACK FOR TOTAL VEHICLE MACH NUMBER 2 TO 5.5

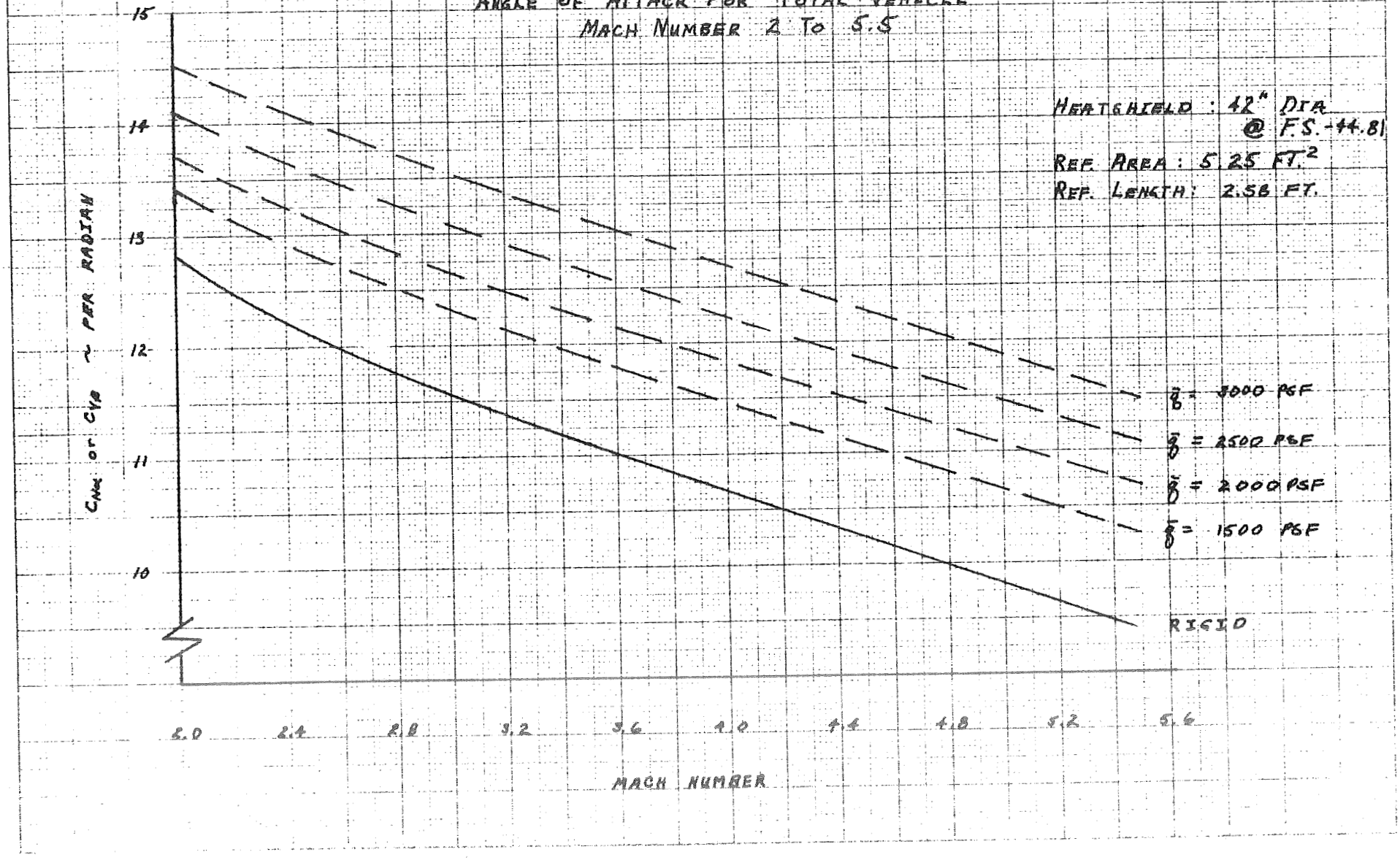

FIGURE 3.2.2.2-3
SCOUT VEHICLE - ALGOL III FIRST STAGE

CENTER OF PRESSURE LOCATION

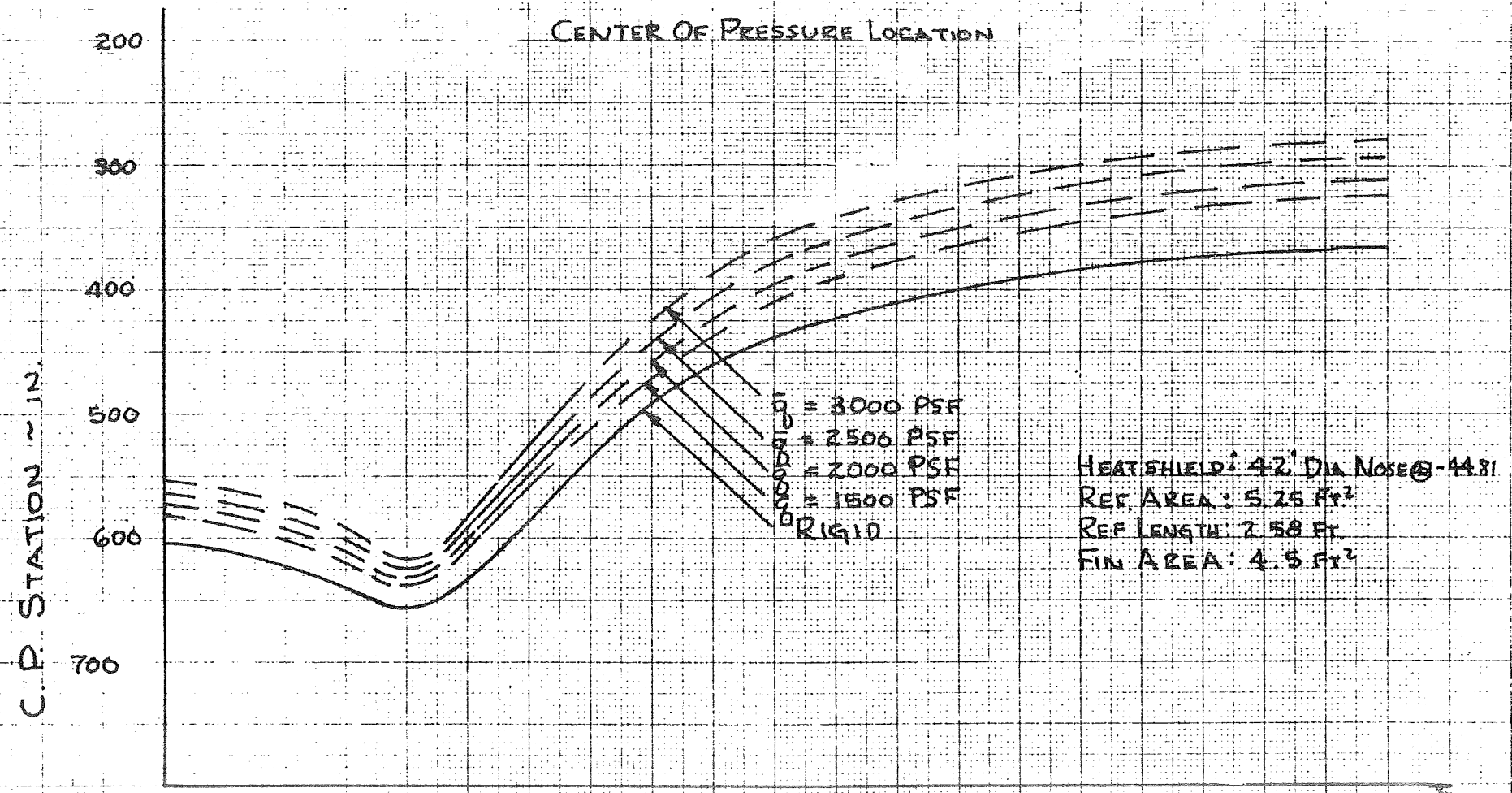

analyses were applied to the new rigid body aerodynamic data. This is an acceptable approach because the change in fin size has a small effect on the flexible body effects due to the fact that the fins are located on the stiffest part of the vehicle.

The flexible aerodynamic coefficients ($C_{N\alpha}$, C.P., $C_{M\alpha}$) for the 42 inch heatshield configuration with 5.75 sq. ft. fins are presented in Figures 3.2.2.2-4, -5 and -6.

Weight and stiffness values for the heatshield portion of the body were changed by taking the ratio of the current Scout values to the larger heatshield diameters. Weight data for the Algol III (Aerojet No. 2 configuration) was used, stiffness data from the 44 inch diameter first stage feasibility study (Reference 3-9) were used. The weight and stiffness distributions used for the 42 inch diameter configuration are presented in Tables 3.2.2.2-1, and -2. The distributed aerodynamic loads for each configuration are presented in Section 3.0 of this report.

FIGURE 3.2.2.2-4
SCOUT VEHICLE - ALGOL III FIRST STAGE
NORMAL FORCE COEFFICIENT DUE TO ANGLE OF ATTACK FOR TOTAL VEHICLE
HEATSHIELD: 42" DIA, NOSE @ FS -44.8
REF. AREA: 5.25 FT²
REF. LENGTH: 2.58 FT.
FIN AREA: 5.75 FT²
q = 3000 PSF
q = 2500 PSF
q = 2000 PSF
q = 1500 PSF
RIGID
C_{N_α} OR C_{N_β} PER RADIAN
MACH NUMBER
22
20
18
16
14
12
10
0
10
30
40

FIGURE 3.2.2.2-5

SCOUT VEHICLE – ALGOL III FIRST STAGE
MOMENT COEFFICIENT DUE TO ANGLE
OF ATTACK FOR TOTAL VEHICLE

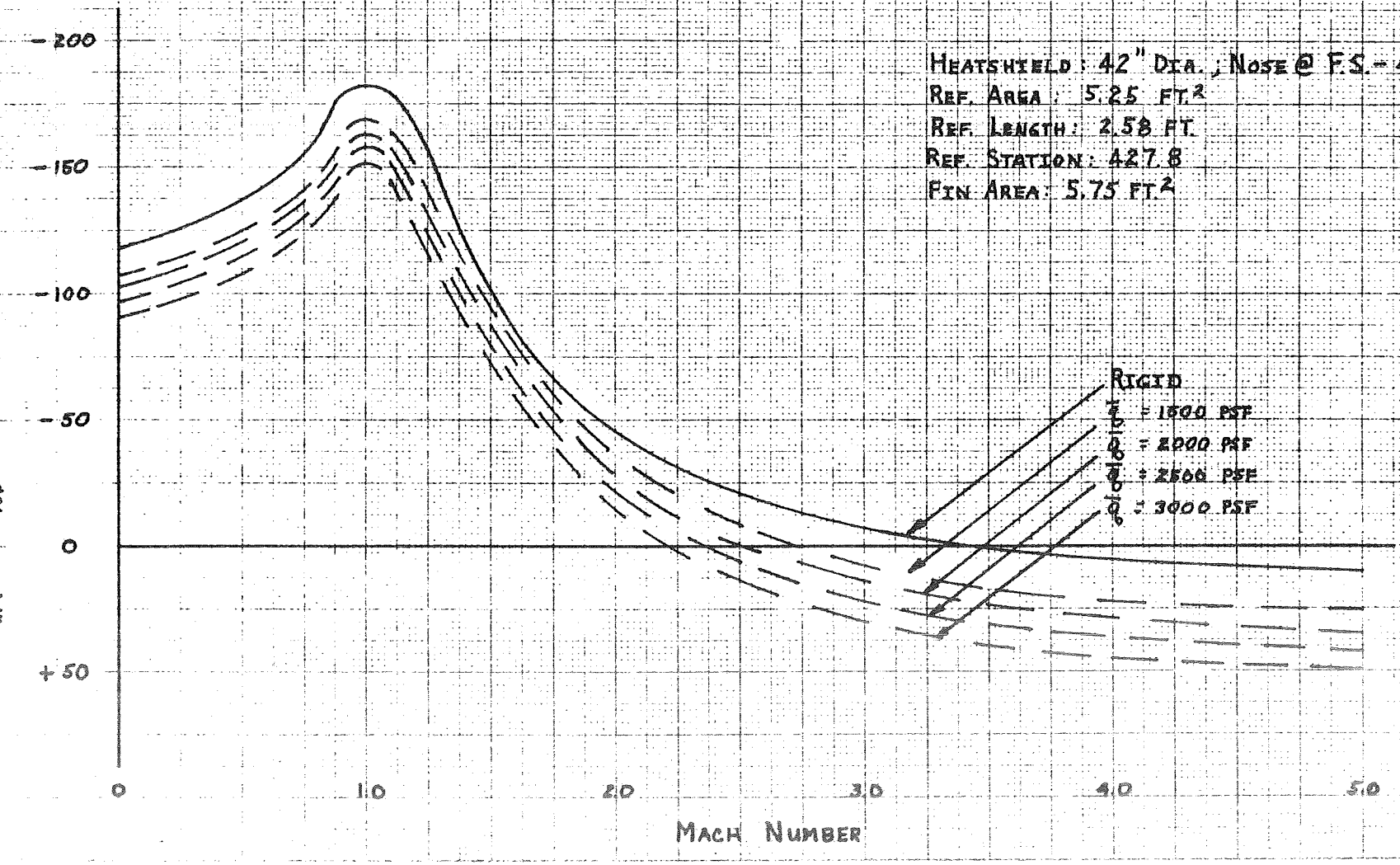

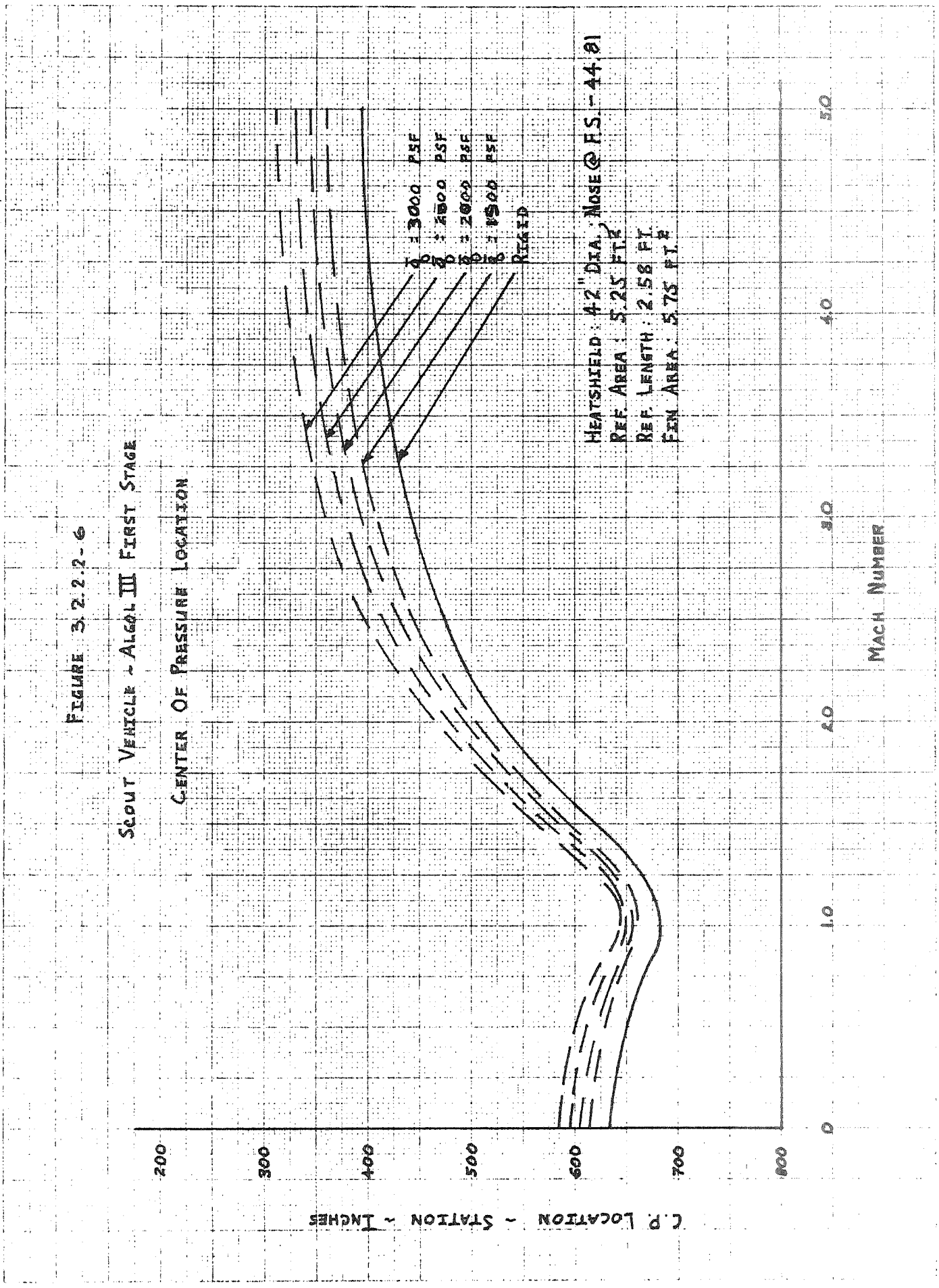

FIGURE 3.2.2.2-6

SCOUT VEHICLE ~ ALGOL III FIRST STAGE

CENTER OF PRESSURE LOCATION

TABLE 3.2.2.2-1

LARGE VOLUME HEAT SHIELD
WEIGHT DISTRIBUTION
42 INCH DIAMETER HEAT SHIELD

STATION From	STATION To	HEAT SHIELD (lbs./in.)	VEHICLE (lbs./in.)	PROPELLANT (lbs./in.)
-44.81	-40.0	0.73	0.73	
-40.0	-38.0	1.40	1.40	
-38.0	-34.0	2.62	2.62	
-34.0	-12.0	1.23	1.23	
-12.0	2.0	2.59	2.59	
2.0	4.0	5.27	5.27	
4.0	6.0	6.22	6.22	
6.0	37.27	2.165	2.165	
37.27	42.0	2.165	4.975	
42.0	46.0	4.32	7.13	
46.0	47.7	2.21	5.02	
47.7	65.87	2.21	20.31	
65.87	68.0	2.21	17.92	
68.0	70.0	1.25	16.96	
70.0	84.27	1.08	6.79	
84.27	85.61	1.08	4.81	
85.61	99.8	1.08	3.07	
99.8	101.5	4.21	14.10	
101.5	102.8	4.21	16.84	
102.8	103.84	9.09	21.32	
103.84	104.8		20.75	
104.8	124.1		9.01	
124.1	131.1		34.07	
131.1	161.5		40.31	
161.5	191.95		40.31	
191.95	200.0		17.69	
200.0	218.5		11.13	
218.5	237.7		4.74	
237.7	238.7		40.0	
238.7	243.9		5.43	
243.9	253.1		52.39	
253.1	345.1		45.26	
345.1	437.6		45.25	
437.6	445.4		66.7	
445.4	465.0		22.97	
465.0	486.0		20.14	
486.0	487.0		80.46	
487.0	491.7		9.87	
491.7	495.9		121.34	76.
495.9	496.9		219.39	84.
496.9	498.9		136.13	86.
498.9	504.8		95.13	86.
504.8	801.8		94.79	86.67
801.8	806.8		95.13	86.
806.8	809.8		125.13	75.
809.8	815.8		66.36	10.
815.8	831.8		22.50	
831.8	849.0		26.21	
849.0	857.5		33.3	

TABLE 3.2.2.2-2

LARGE VOLUME HEAT SHIELD
STIFFNESS DISTRIBUTION

42 INCH DIAMETER HEAT SHIELD

STATION		EI (lb.in.^{2})		GA (lbs.)	
From	To	From	To	From	To
-44.81	-33.26	.122 E+09	.368 E+10	.1195 E+08	.258 E+08
-33.26	4.2	.773 E+09	.902 E+10	.172 E+07	.39 E+07
4.2	44.1	.902 E+10	.92 E+10	.39 E+07	.39 E+07
44.1	103.7	.92 E+10	.639 E+10	.824 E+07	.824 E+07
103.7	125.6	.79 E+10	.128 E+11	.225 E+08	.265 E+08
125.6	131.1	.128 E+11	.143 E+11	.265 E+08	.274 E+08
131.1	191.95	.461 E+10	.461 E+10	.684 E+07	.684 E+07
191.95	238.18	.425 E+10	.486 E+10	.375 E+07	.393 E+07
238.18	253.06	.591 E+10	.548 E+10	.481 E+07	.468 E+07
253.06	254.11	.388 E+12	.102 E+12	.135 E+10	.334 E+09
254.11	255.46	.102 E+12	.433 E+11	.334 E+09	.14 E+09
255.46	430.96	.433 E+11	.382 E+11	.14 E+09	.123 E+09
430.96	431.4	.382 E+11	.382 E+11	.123 E+09	.123 E+09
431.4	432.4	.382 E+11	.398 E+11	.123 E+09	.129 E+09
432.4	433.4	.398 E+11	.392 E+11	.129 E+09	.129 E+09
433.4	434.4	.392 E+11	.500 E+11	.129 E+09	.169 E+09
434.4	435.4	.500 E+11	.57 E+11	.169 E+09	.2 E+09
435.4	436.4	.57 E+11	.652 E+11	.2 E+09	.239 E+09
436.4	437.4	.652 E+11	.74 E+11	.239 E+09	.286 E+09
437.4	438.4	.74 E+11	.83 E+11	.286 E+09	.344 E+09
438.4	439.4	.83 E+11	.914 E+11	.344 E+09	.412 E+09
439.4	440.4	.914 E+11	.98 E+11	.412 E+09	.49 E+09
440.4	441.4	.98 E+11	.102 E+12	.49 E+09	.582 E+09
441.4	442.4	.102 E+12	.102 E+12	.582 E+09	.688 E+09
442.4	443.4	.102 E+12	.16 E+12	.688 E+09	.125 E+09
443.4	445.	.16 E+12	.305 E+11	.125 E+10	.125 E+10
445.0	447.29	.305 E+11	.613 E+11	.355 E+09	.785 E+09
447.25	450.79	.613 E+11	.371 E+11	.785 E+09	.377 E+09
450.79	457.83	.371 E+11	.425 E+11	.377 E+09	.257 E+09
457.83	463.11	.429 E+11	.507 E+11	.257 E+09	.217 E+09
463.11	473.35	.507 E+11	.861 E+11	.217 E+09	.218 E+09
473.35	477.55	.861 E+11	.172 E+12	.218 E+09	.362 E+09
477.55	487.0	.172 E+12	.172 E+12	.362 E+09	.362 E+09
487.0	497.0	.33 E+11	.33 E+11	.306 E+08	.306 E+08
497.0	505.0	.14 E+12	.18 E+12	.125 E+09	.137 E+09
505.0	651.5	.12 E+12	.12 E+12	.825 E+08	.825 E+08
651.5	652.3	.12 E+12	.275 E+12	.825 E+08	.155 E+09
652.3	654.4	.275 E+12	.275 E+12	.155 E+09	.155 E+09
654.4	655.5	.275 E+12	.12 E+12	.155 E+09	.825 E+08
655.5	802.	.12 E+12	.12 E+12	.825 E+08	.825 E+08
802.	810.	.18 E+12	.14 E+12	.137 E+09	.125 E+09
810.	847.95	.264 E+11	.264 E+11	.248 E+08	.246 E+08

3.2.3 Weight and Balance Data

This section presents the weights, longitudinal center of gravity and moments of inertia for a Scout vehicle (S-178 & Sub. configuration) utilizing a 42 inch diameter heatshield and an Algol III (Aerojet Proposal No. 2) first stage motor replacing the standard Algol II first stage motor. The standard Base A and 4.5 sq. ft. fins are included in this data.

The vehicle mass properties data is shown in Table 3.2.3-1 with a 50 pound payload and in Table 3.2.3-2 with a 400 pound payload. Also included is the mass distribution for the 42 inch diameter heatshield, Table 3.2.3-3. A 42 inch diameter heatshield of similar construction to the present 34 inch diameter was estimated to weigh 357.10 pounds with the heatshield c.g. at Station 30.84.

TABLE 3.2.3-1
MASS PROPERTIES

42 INCH DIAMETER, -44.81 LARGE VOLUME HEATSHIELD, (50 POUND PAYLOAD)

VEHICLE S- WEIGHT, X(CG), AND MOMENTS OF INERTIA

VERSUS PERCENT OF FUEL CONSUMED

	TOTAL WEIGHT, POUNDS	C.G. SCOUT STA.-IN.	IXX SLUG-FT^2	IYY OR IZZ SLUG-FT^2
	*******	*******	**********	**********
FOURTH STAGE - BURNOUT	118.96	53.35	2.38	23.82
75 O/O	271.79	60.33	5.00	30.66
50 O/O	424.63	62.28	6.87	35.52
25 O/O	577.46	63.20	8.00	39.68
FOURTH STAGE - IGNITION	730.30	63.74	8.38	43.34
SPIN-UP ITEMS	774.66	65.92	9.37	56.93
THIRD STAGE - BURNOUT	1483.95	116.61	29.45	1287.32
75 O/O	2135.08	130.01	56.88	1545.14
50 O/O	2786.22	137.15	76.77	1710.98
25 O/O	3437.35	141.58	89.11	1834.97
THIRD STAGE - IGNITION	4088.49	144.61	93.90	1935.30
LESS N/C - H/S	6159.25	229.28	181.48	23526.18
SECOND STAGE - BURNOUT	6516.43	218.41	206.03	26548.55
75 O/O	8592.67	249.14	299.18	33456.96
50 O/O	10668.92	267.92	367.16	38212.20
25 O/O	12745.16	280.57	410.04	41860.43
SECOND STAGE - IGNITION	14821.41	289.69	427.79	44861.59
FIRST STAGE - BURNOUT	19105.71	379.16	802.14	173816.74
75 O/O	26088.71	451.37	1463.25	267512.71
50 O/O	33071.71	493.09	1954.02	327195.35
25 O/O	40054.71	520.26	2274.72	370609.54
FIRST STAGE - IGNITION	47037.71	539.37	2425.14	404962.73

TABLE 3.2.3-2
MASS PROPERTIES

42 INCH DIAMETER, -44.81 LARGE VOLUME HEATSHIELD, (400 POUND PAYLOAD)

VEHICLE S- WEIGHT, X(CG), AND MOMENTS OF INERTIA

VERSUS PERCENT OF FUEL CONSUMED

	TOTAL WEIGHT, POUNDS	C.G. SCOUT STA.-IN.	IXX SLUG-FT^2	IYY OR IZZ SLUG-FT^2
	*******	*******	**********	**********
FOURTH STAGE - BURNOUT	468.96	31.44	10.88	51.43
75 0/0	621.79	39.88	13.50	85.34
50 0/0	774.63	44.99	15.37	107.31
25 0/0	927.46	48.41	16.50	123.07
FOURTH STAGE - IGNITION	1080.30	50.86	16.88	135.09
SPIN-UP ITEMS	1124.68	52.87	17.87	159.46
THIRD STAGE - BURNOUT	1833.95	98.93	37.95	1822.64
75 0/0	2485.08	115.08	65.38	2285.66
50 0/0	3136.22	124.52	85.26	2581.34
25 0/0	3787.35	130.72	97.60	2794.04
THIRD STAGE - IGNITION	4438.49	135.10	102.40	2958.63
LESS N/C - H/S	6509.25	218.25	189.98	26549.66
SECOND STAGE - BURNOUT	6866.43	208.50	214.53	29269.22
75 0/0	8942.67	240.33	307.68	37147.53
50 0/0	11018.92	260.17	375.66	42575.15
25 0/0	13095.16	273.72	418.54	46711.80
SECOND STAGE - IGNITION	15171.41	283.56	436.29	50082.34
FIRST STAGE - BURNOUT	19455.71	372.77	810.64	183185.51
75 0/0	26438.71	445.71	1471.75	281139.23
50 0/0	33421.71	488.18	1962.52	343655.72
25 0/0	40404.71	515.96	2283.22	389064.43
FIRST STAGE - IGNITION	47387.71	535.56	2433.64	424890.60

TABLE 3.2.3-3

SCOUT LARGE VOLUME HEATSHIELD 42 INCH DIAMETER, -44.81 MASS DISTRIBUTION

STA. TO STA. INCHES			POUNDS/INCH
-44.81	To	- 44.	.86 POUNDS
-44.		- 40.	.86
-40.		- 38.	1.65
-38.		- 36.	3.12
-36.		- 34.	2.87
-34.		- 12.	1.45
-12.		+ 2.	3.06
+ 2.		4.	5.74
4.		6.	6.63
6.		24.	2.56
24.		42.	2.58
42.		44.	4.47
44.		46.	4.98
46.		68.	2.67
68.		70.	1.51
70.		100.	1.31
100.		102.	4.44
102.		103.84	8.45

3.2.4 Stability and Control

The 42 inch heatshield configuration was analyzed in more detail than the other three diameters. The effects of gain ratio and Base A frequency response tolerances on stability were evaluated. The vehicle movement relative to the launcher was investigated and the response of this vehicle and control deflections to the pitch program steps, winds, and thrust misalignment was also investigated.

3.2.4.1 Root Locus Analysis Near Maximum Dynamic Pressure

The root locus analysis of the first stage configuration was performed using the Algol III design trajectory data with a 90 knot headwind. The input data is the same as that used for the 40 inch heatshield configuration (Section 3.1.4) with the exception of the heatshield aerodynamics presented in Section 3.2.2. The upper and lower pitching mode gain boundaries are presented versus flight time in Figure 3.2.4-1 for the current Scout fin area (4.5 square feet). The critical flight time is 45 seconds. The effect of a fifty percent increase in control effectiveness is also shown in this figure. As discussed in Section 3.1.4 fin size requirements cannot be reduced by increasing control surface effectiveness per se. The gain boundaries are shown as a function of fin area and control tip area in Figure 3.2.4-2. The allowable gains are also shown in this figure based on a ±6 decibel margin of safety. The minimum allowable fin area for the 42 inch heatshield configuration is 5.75 square feet. Jet vane and fin tip area was chosen at 41 sq. inches and 78 sq. inches respectively for the reasons discussed in Section 3.1.4. . The root

FIGURE 3.2.4-1
SCOUT LARGER HEATSHIELD STUDY
PITCH AND YAW GAIN BOUNDARIES
42 INCH DIAMETER HEATSHIELD - ALGOL III

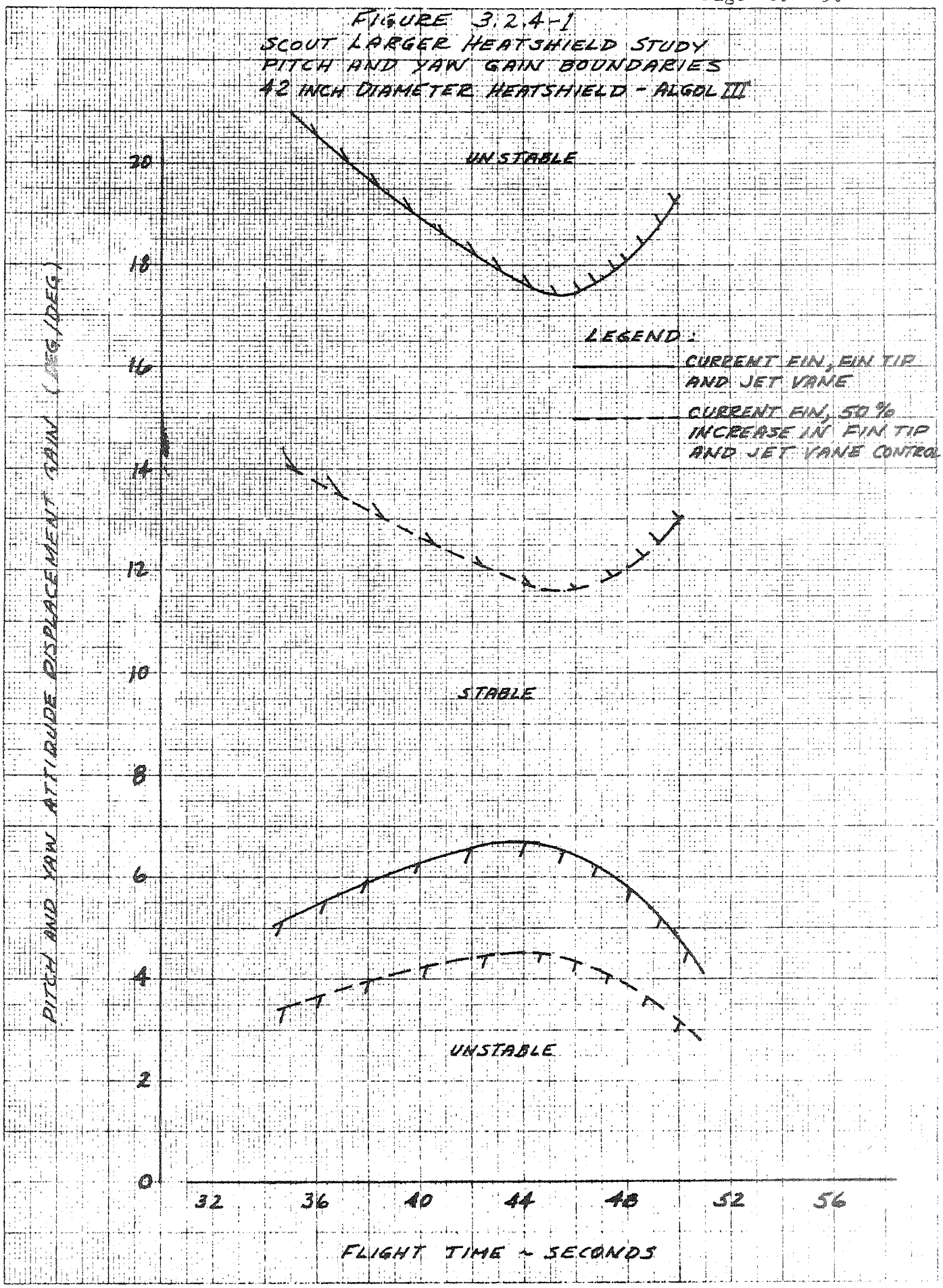

FIGURE 3.2.4-2
GAIN BOUNDARIES VERSUS FIN SIZE
42 IN HEATSHIELD ~ ALGOL III

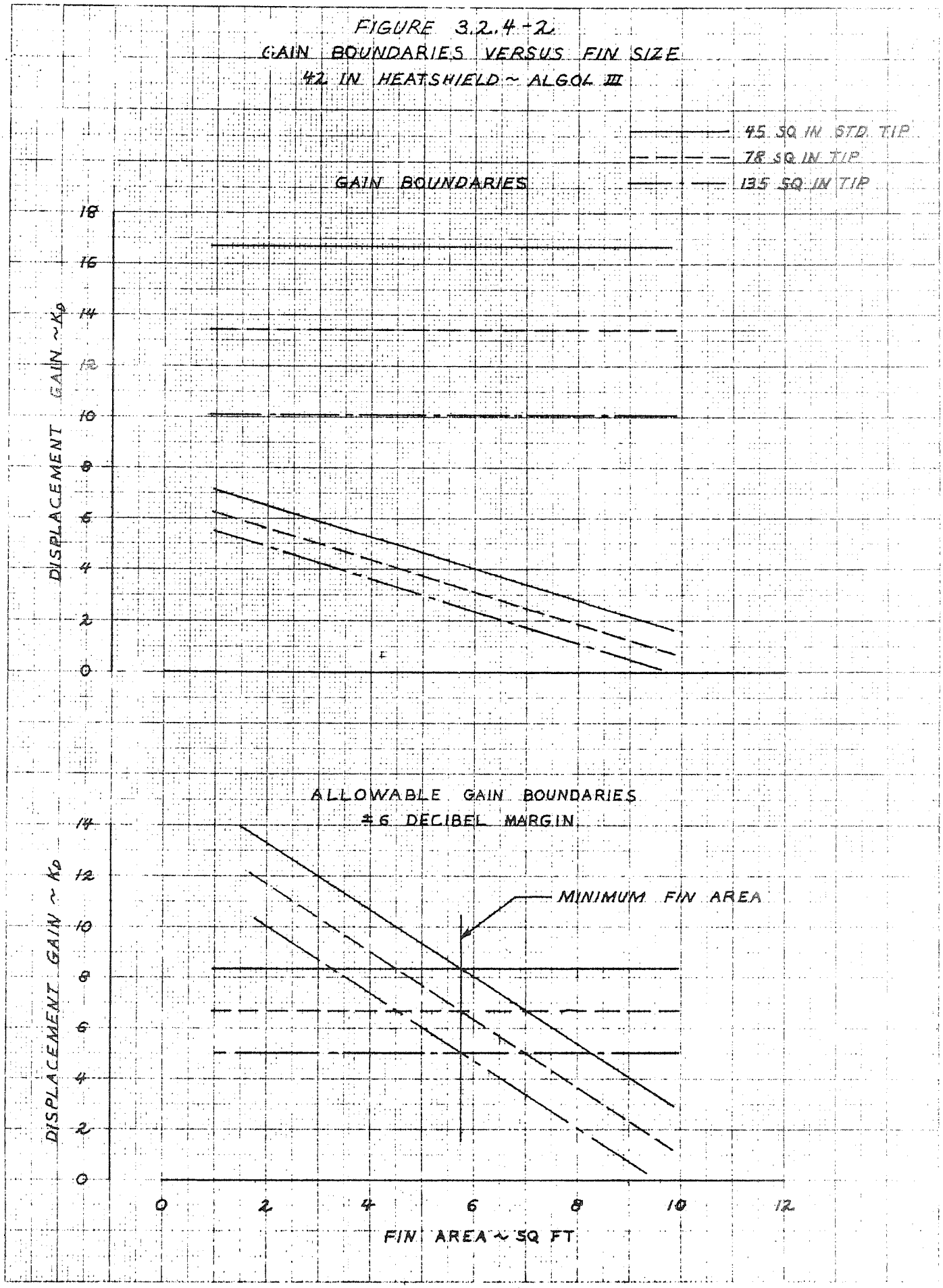

locus of this configuration at 45 seconds flight time is shown in Figure 3.2.4-3. The selected attitude displacement gain (K_D) is 6.75 degrees of surface per degree attitude error and the rate to displacement gain ratio is 0.4 seconds. These values provide a ±6 decibel margin of safety from instability. The root loci of the second, third and fourth bending modes of vibration are shown in Figure 3.2.4-4 for all of the heatshield configurations. The change in gain has very little effect on these modes. The stability of these modes at zero gain is based on the assumption of a 0.01 structural damping factor for each mode of vibration. As indicated in Figures 3.2.4-3 and 3.2.4-4 the first and second bending modes are more stabilized by the control system and the third and fourth bending modes are very slightly destabilized by the control system.

The effect of gain ratio (K_R/K_D) on the root locus of the pitching mode and first bending mode is shown in Figure 3.2.4-5. Increase in gain ratio decreases the value of the upper crossover gain and increases pitching mode damping at low frequencies. The current tolerances on gain ratio are ±10 percent from nominal which is one-half of the variation shown in Figure 3.2.4-5.

The effect of Base A frequency response tolerances on the first stage stability at 45 seconds flight time is shown in Figure 3.2.4-6. The current "Base A" servo, filter, actuator frequency response tolerances shown in Figure 3.2.4-7 were used in this analysis. The high tolerance (less phase lag) reduces the value of the upper cross-over gain and increases the damping at lower gain values. Previous Scout stability studies indicate

FIGURE 3.2.4-3
SCOUT LARGER HEATSHIELD STUDY
ROOT LOCI AT 45 SECONDS - 42 INCH
HEATSHIELD - ALGOL III CONFIGURATION
41 IN² JET VANE
78 IN² FIN TIP
5.75 FT² FIN

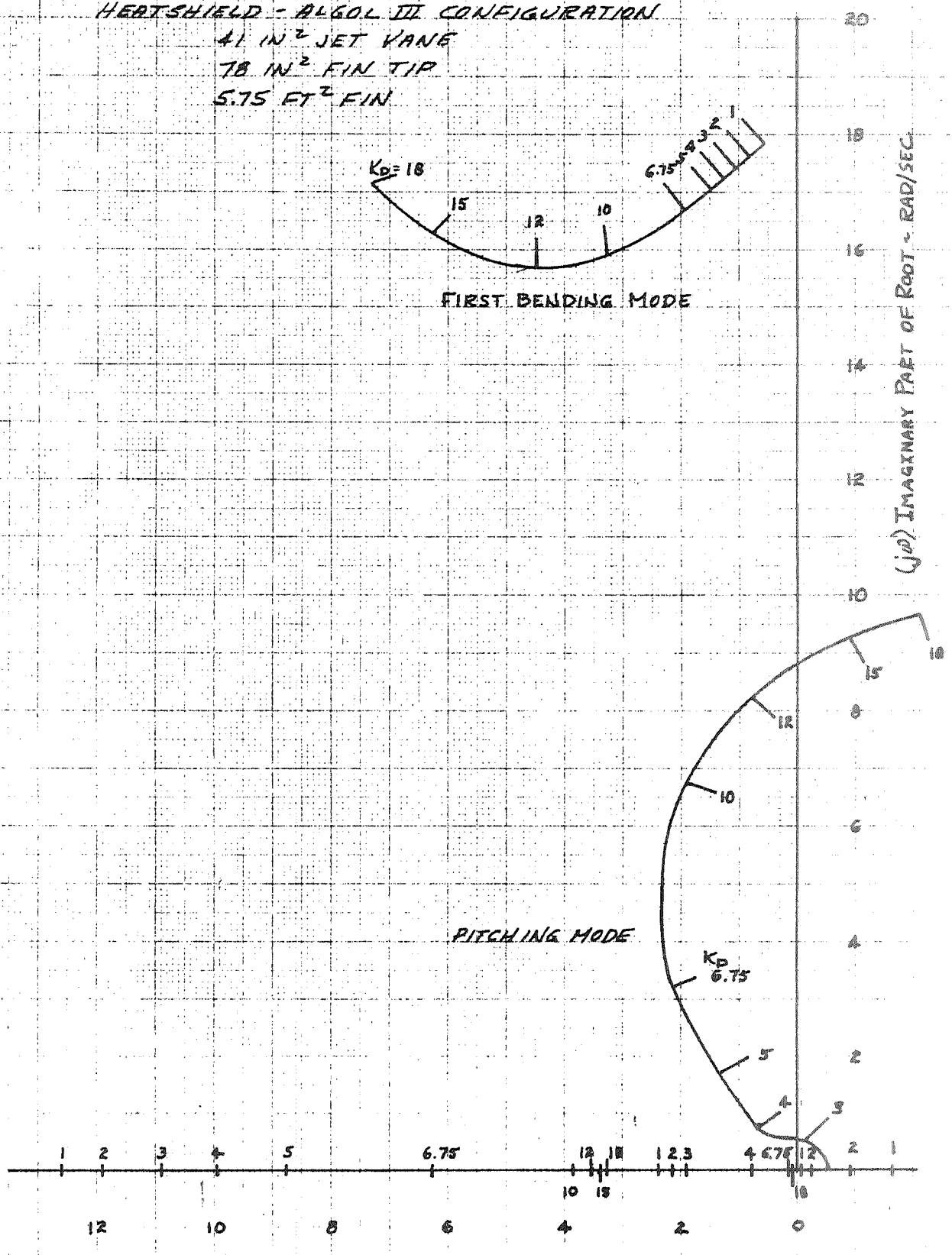

FIGURE 3.2.4-4
SCOUT LARGER HEATSHIELD STUDY
ROOT LOCI AT 45 SECONDS - SECOND, THIRD AND FOURTH BENDING MODES - ALGOL III CONFIGURATIONS

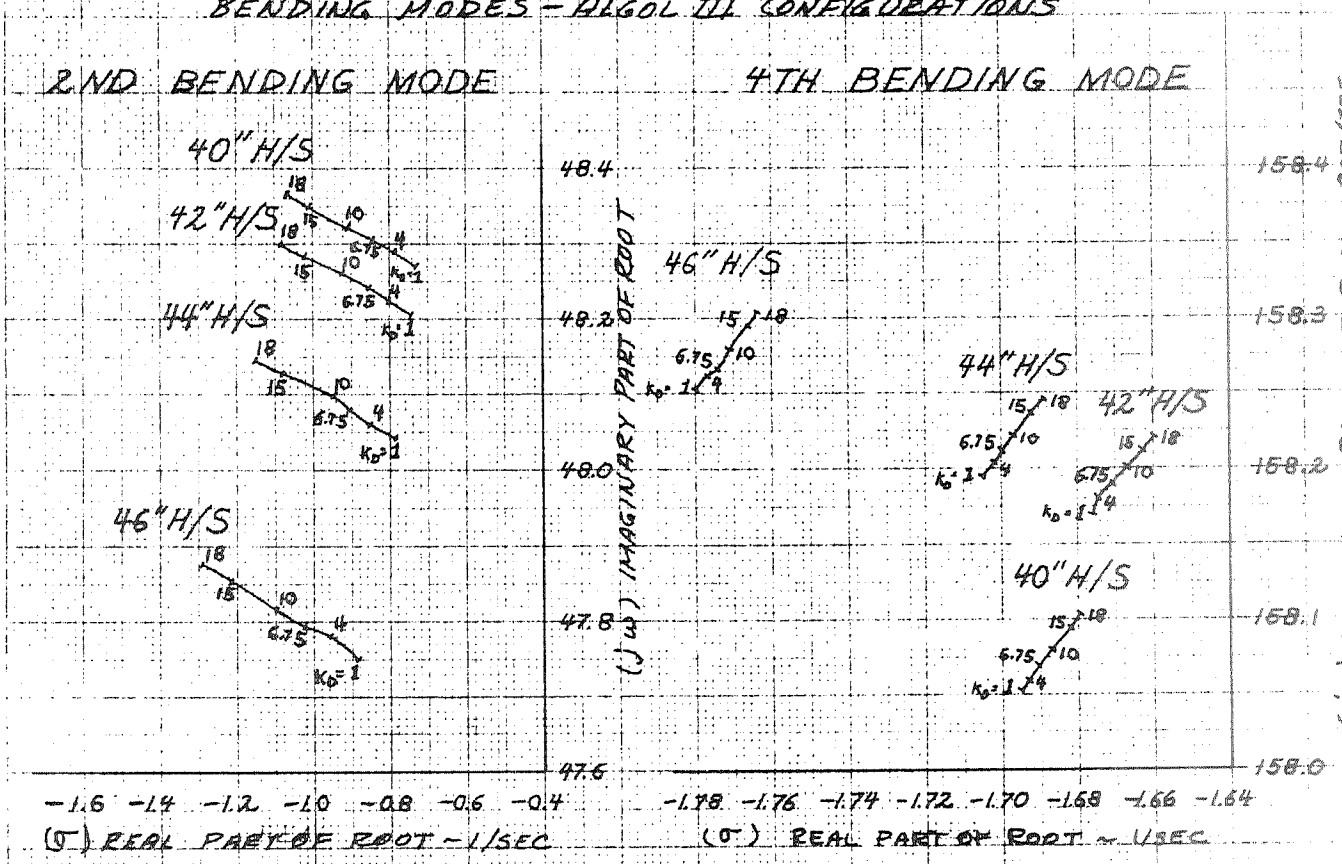

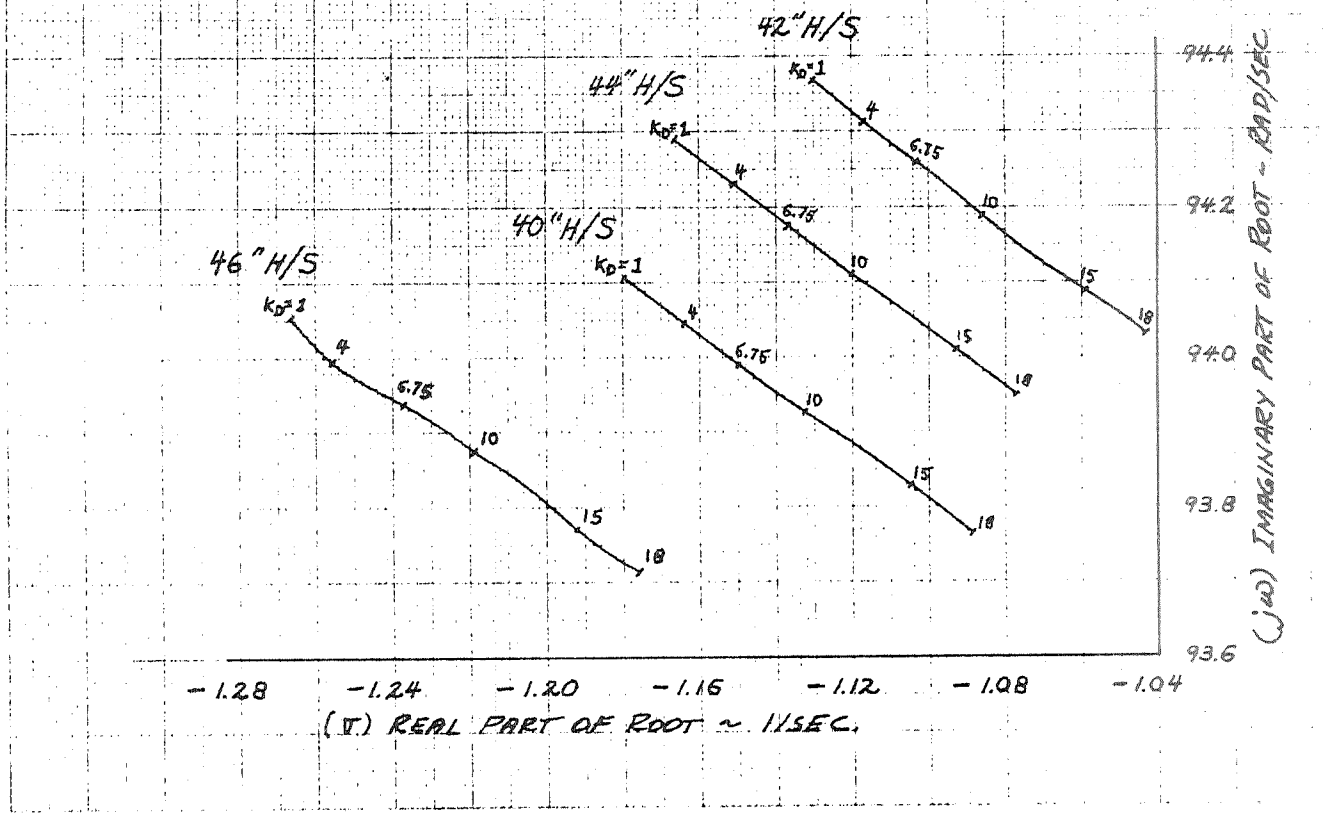

FIGURE 3.2.4-5

SCOUT LARGER HEATSHIELD STUDY

EFFECT OF GAIN RATIO ON ROOT LOCI - 42 INCH HEATSHIELD

ALGOL III CONFIGURATION

41 IN^2 JET VANE

78 IN^2 FIN TIP

5.75 FT^2 FIN

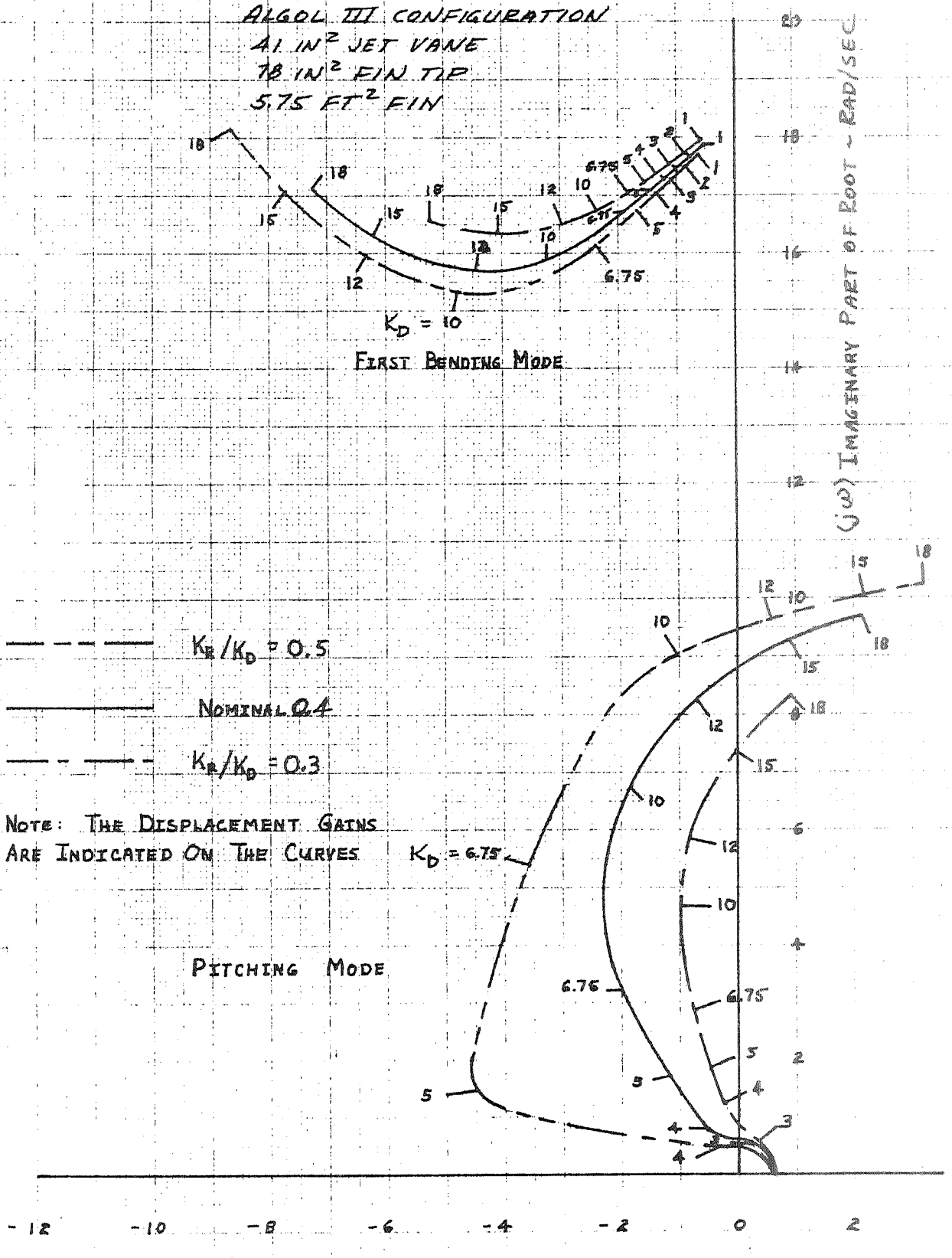

FIGURE 3.2.4-6

SCOUT LARGER HEATSHIELD STUDY

EFFECT OF BASE A FREQUENCY RESPONSE TOLERANCES ON ROOT LOCI - 42 INCH HEATSHIELD-ALGOL III

41 IN^2 JET VANE

78 IN^2 FIN TIP

5.75 FT^2 FIN

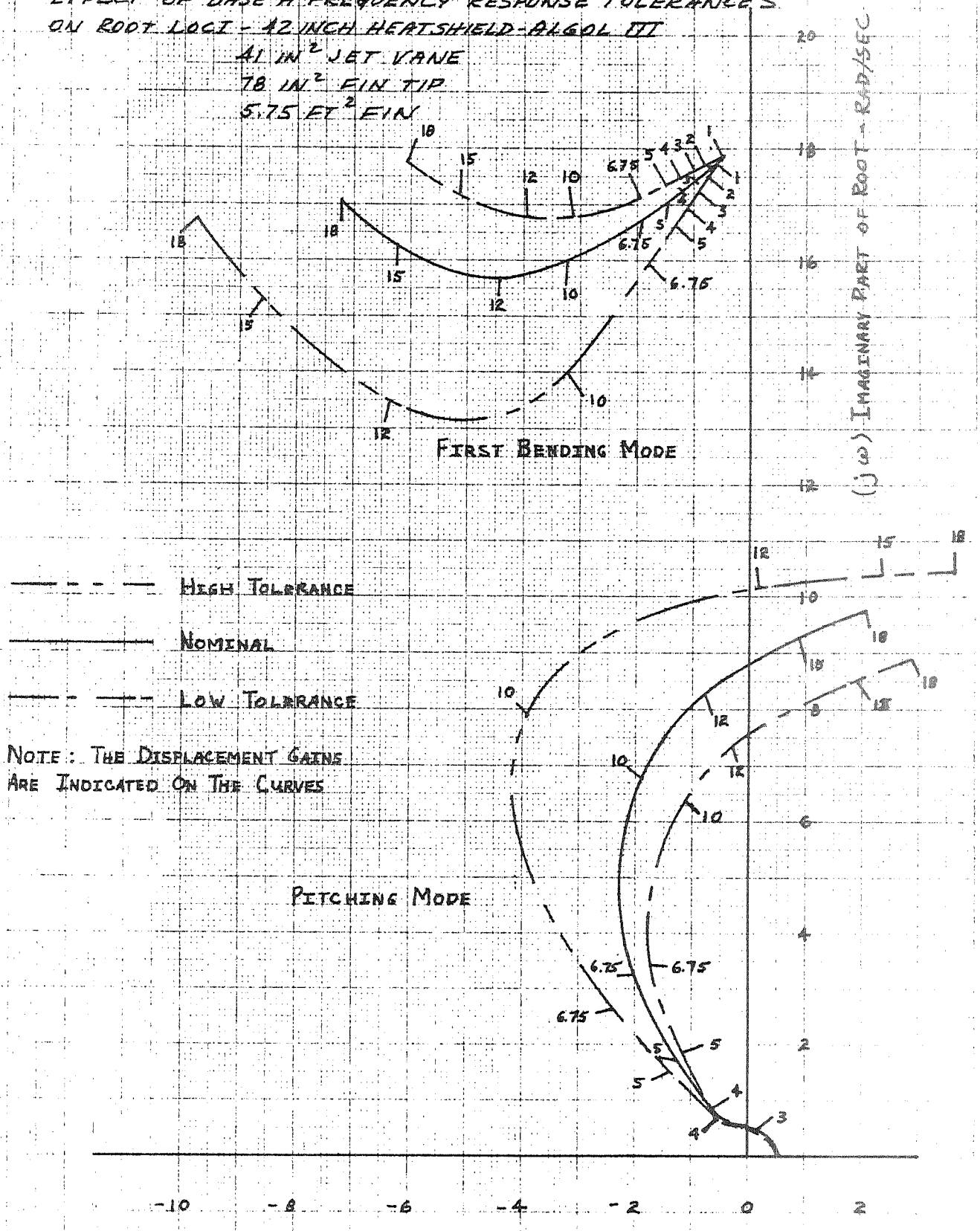

FIGURE 3.2.4-7

FIRST STAGE PITCH AND YAW
BASE A FREQUENCY RESPONSE
TOLERANCES

that even less phase lag than the high tolerance will stabilize the pitching mode but the first bending mode becomes unstable at the higher gains (about 12).

With the 42 inch heatshield-Algol III configuration, a fin area of at least 5.75 square feet is required. This configuration is shown in Figure 2.2.3-1. With a 41 square inch jet vane and a 78 square inch tip control the pitch and yaw gain should be 6.75 degrees of surface deflection per degree attitude error.

The hinge moment requirements are presented in Paragraph 3.1.4.3.

3.2.4.2 Vehicle Movement Relative to Launcher

The higher initial thrust to weight ratio of the Algol III configuration makes it desirable to initiate the pitch program as soon as possible after lift-off. The design trajectory used for this study initiates the pitch program 1 second after lift-off. A launcher-vehicle clearance study was made to verify the acceptibility of this approach as well as the clearance requirements for the larger fin span required for the larger heatshield configurations. The drag coefficients at liftoff at 90 degree angle of attack were assumed to be approximately equal to those generated for the 44 Inch Algol Feasibility Study presented in Reference 3-9. The movement of the fin tip relative to vertical was calculated for the design trajectory with 0.25 degrees thrust misalignment in the pitch plane and a 50 mile per hour wind blowing toward the launcher. The relative movement of the tip toward the launcher due to vehicle translation and rotation is shown as a function of altitude in Figure 3.2.4-8 for the 5.75 square feet fin size. The dashed line in this figure shows the movement with the pitch program initiated 1 second after liftoff. The closest approach to the launcher occurs after a vertical travel of about 7 feet. This data indicates that the first pitch program step

FIGURE 3.2.4-8
SCOUT LARGER HEATSHIELD STUDY
VEHICLE MOVEMENT RELATIVE TO LAUNCHER AT LIFTOFF
42 INCH HEATSHIELD - ALGOL III

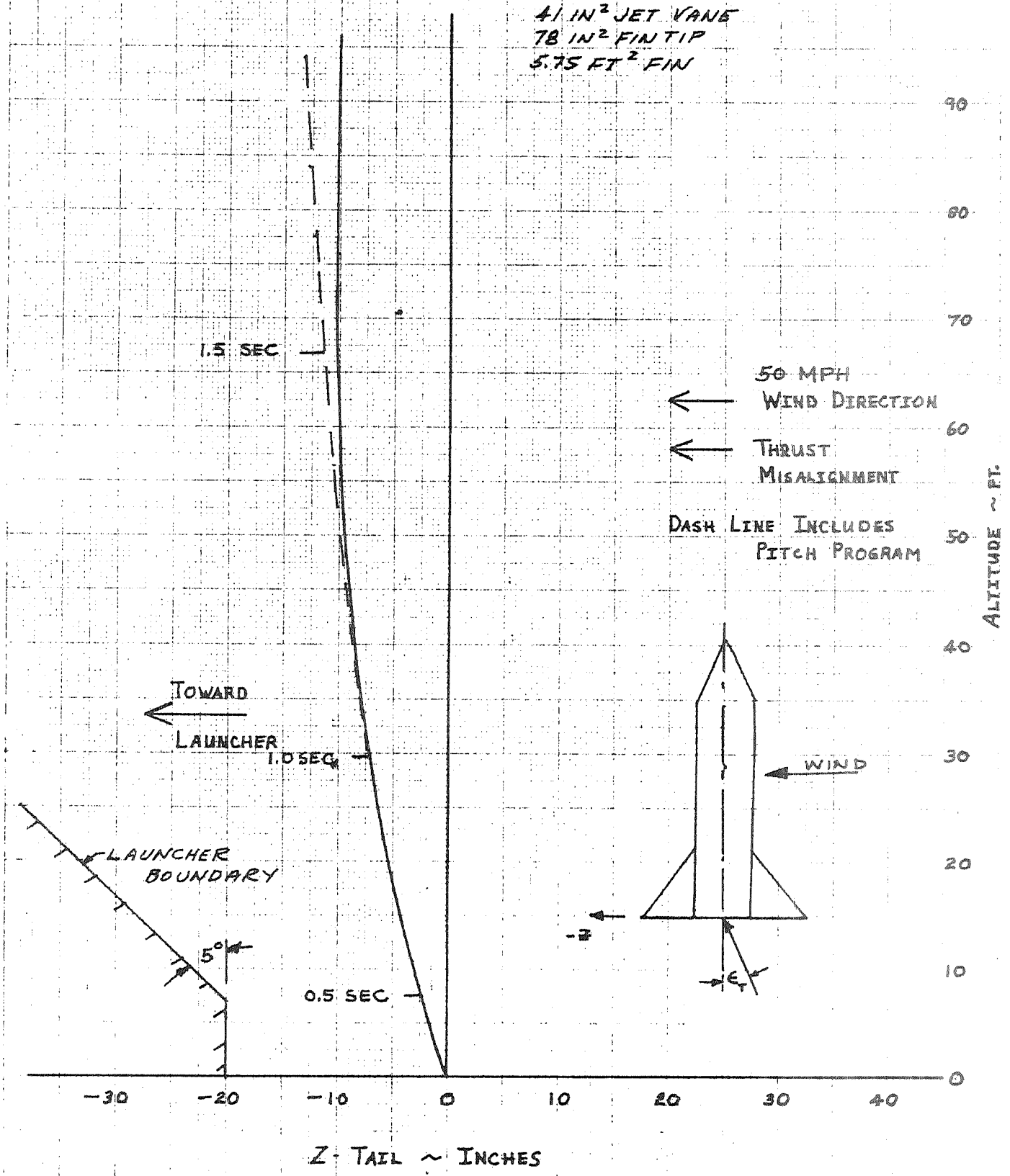

can be initiated earlier than 1 second after liftoff. At one second flight time the vehicle has risen about 29 feet vertically. No GSE changes are required as a result of using the larger fin.

3.2.4.3 Pitch Response to First Pitch Program

The use of the Algol III with a high thrust to weight ratio requires larger pitch program rates initially. The response of the vehicle to these rates was calculated including the effects of control system response, winds and thrust misalignment. A missile trajectory program LVVC-38 described in Reference 3-13 was used for these studies.

The NEMAR trajectory program which was used to calculate the design trajectory assumes a perfect servo. The pitch control surface deflection time history for the undisturbed design trajectory is shown in Figure 3.2.4-9 for the 42 inch heatshield configuration with a 41 square inch jet vane and attitude displacement gain (K_D) of 6.75. The maximum surface deflection occurs at 2 seconds flight time. Assuming a perfect servo the deflections reach 13.6 degrees trailing edge down. The effect of the nominal servo-actuator-filter was calculated by fitting a second order transfer function to the Base A frequency response characteristics presented in Figure 3.2.4-7. The Base 'A' frequency response characteristics inserted in the trajectory program result in an increase in deflection at 2 seconds flight time of 2.4 degrees. The current Scout control authority is ± 18.5 degrees minimum in pitch; however, most vehicles have a control authority of about ± 20.5 degrees.

The effect of 0.25 degrees of pitch-up thrust misalignment on the control surface deflection is shown in Figure 3.2.4-10. During the transient associated with the first pitch program step the control surfaces bottomed at 20.5 degrees for 1.5 seconds. During this time period the

SCOUT LARGER HEATSHIELD STUDY

FIGURE 3.2.4-9

EFFECT OF BASE A FREQUENCY RESPONSE ON CONTROL SURFACE DEFLECTION DURING FIRST PITCH PROGRAM STEPS - 42 INCH HEATSHIELD - ALGOL III

4/IN^2 JET VANE

78 IN^2 FIN TIP

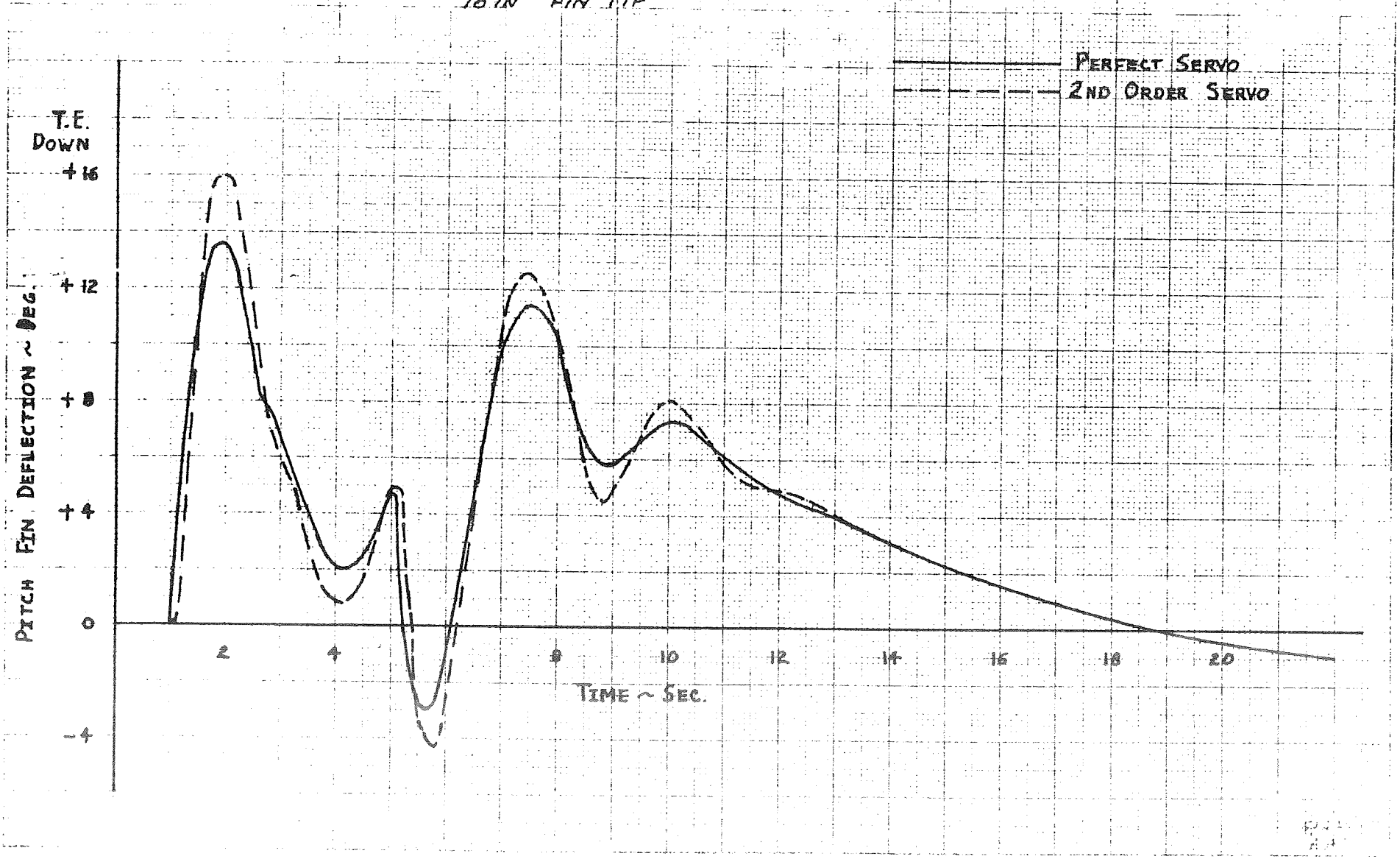

LARGER HEATSHIELD STUDY

FIGURE 3.2.4-10

EFFECT OF THRUST MISALIGNMENT ON PITCH CONTROL SURFACE DEFLECTION

42 INCH HEATSHIELD - ALGOL III CONFIGURATION

41 IN^2 JET VANE, 78 IN^2 EIN TIP, 5.75 FT^2 FIN

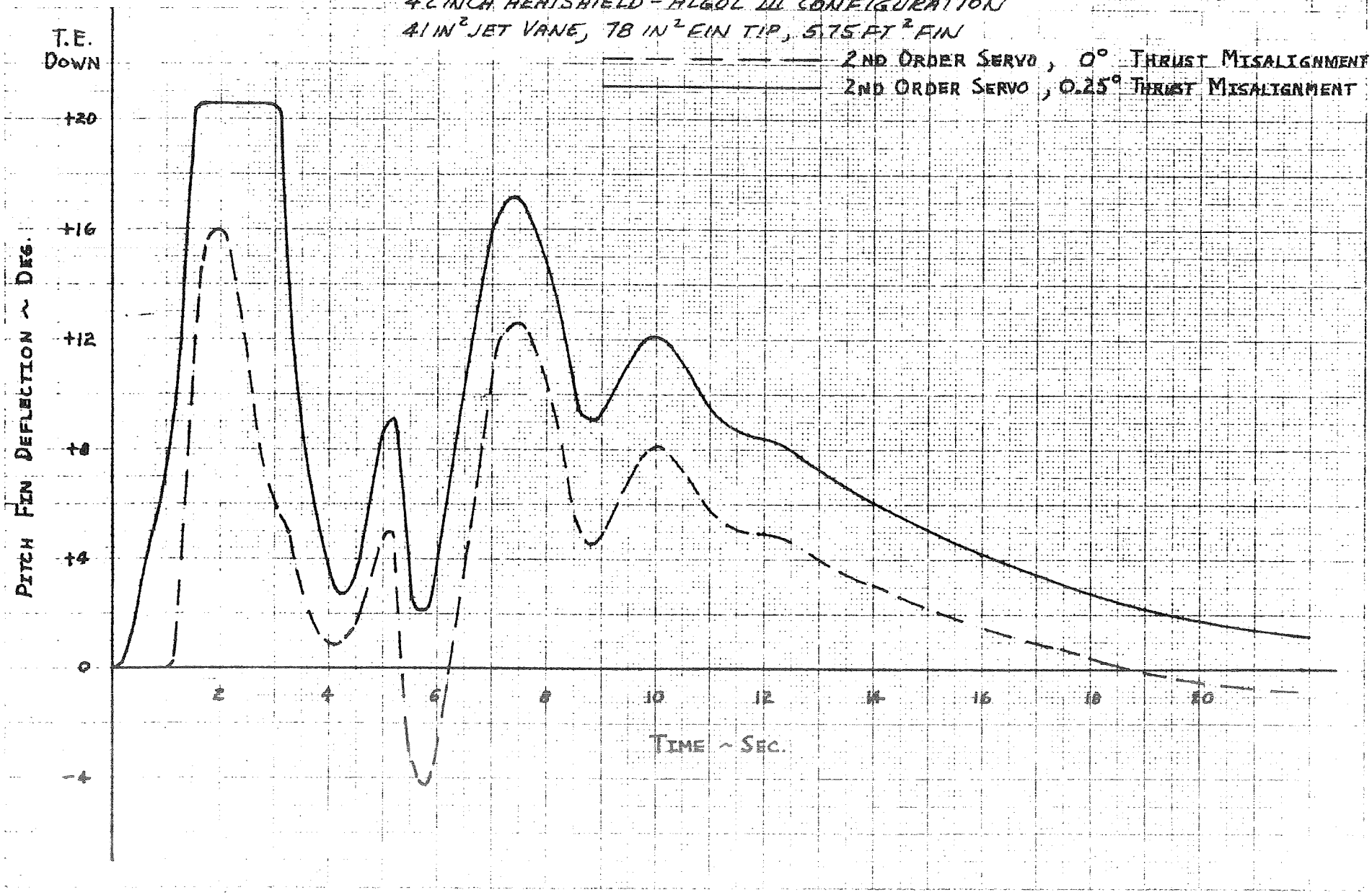

commanded deflections reached 27 degrees trailing edge down. Bottoming of control surfaces at this time does not jeopardize the flight in any way. This phenomenon is peculiar to the Algol III and not the large heatshield configuration. There are several alternatives to prevent the control surfaces from bottoming during this period of time. These alternatives include: (1) increasing the maximum deflection capability to ±30 degrees in pitch by redesign of the bellcrank and shaft assembly, (2) increasing the jet vane lift effectiveness, (3) reducing the need for large initial pitch program steps by angle launching or (4) restrict the pitch program rates during first stage by initiating the pitch program earlier and/or shaping the upper stages to provide lower orbit injection conditions. The shaping approach would result in lower payload performance on low orbit missions.

An estimate was made of the jet vane effectiveness required to limit control deflections in response to the first pitch program. As jet vane effectiveness is increased the displacement gain must be decreased as shown in Figure 3.2.4-11 to provide a ±6 decibel gain margin at 45 seconds flight time. The maximum commanded control surface deflection in response to the first pitch program step is shown in Figure 3.2.4-11 for both the undisturbed design trajectory and the design trajectory with an 0.25 degree pitch-up thrust misalignment. A 60 percent increase in jet vane effectiveness is required to reduce the control surface deflection to 20.5 degrees and an 80 percent increase in effectiveness is required to reduce the deflection to the specified minimum throw of 18.5 degrees.

FIGURE 3.2.4-11
SCOUT LARGER HEATSHIELD STUDY
VARIATION IN CONTROL SURFACE DEFLECTION WITH JET VANE EFFECTIVENESS - 42 INCH HEATSHIELD
ALGOL III

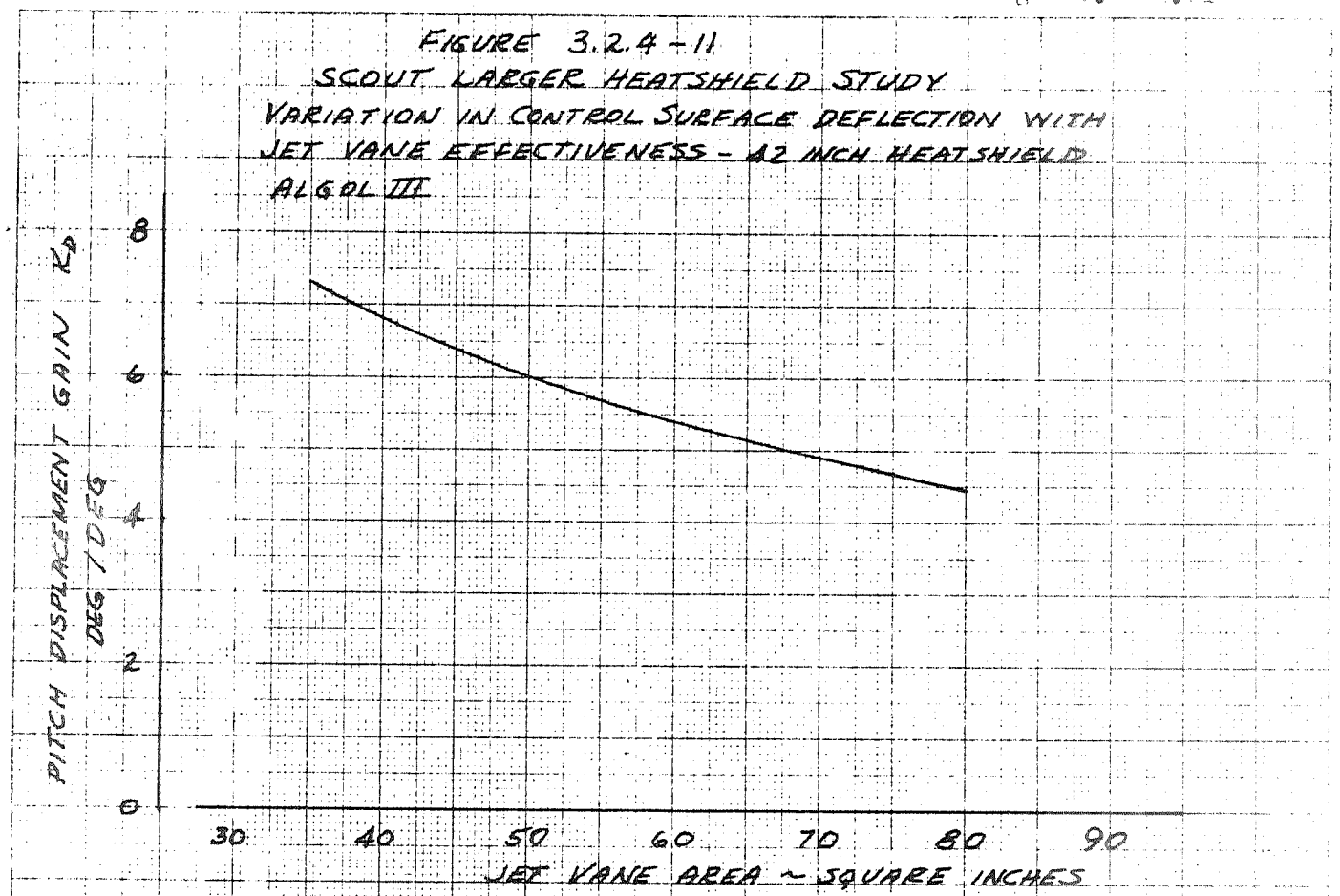

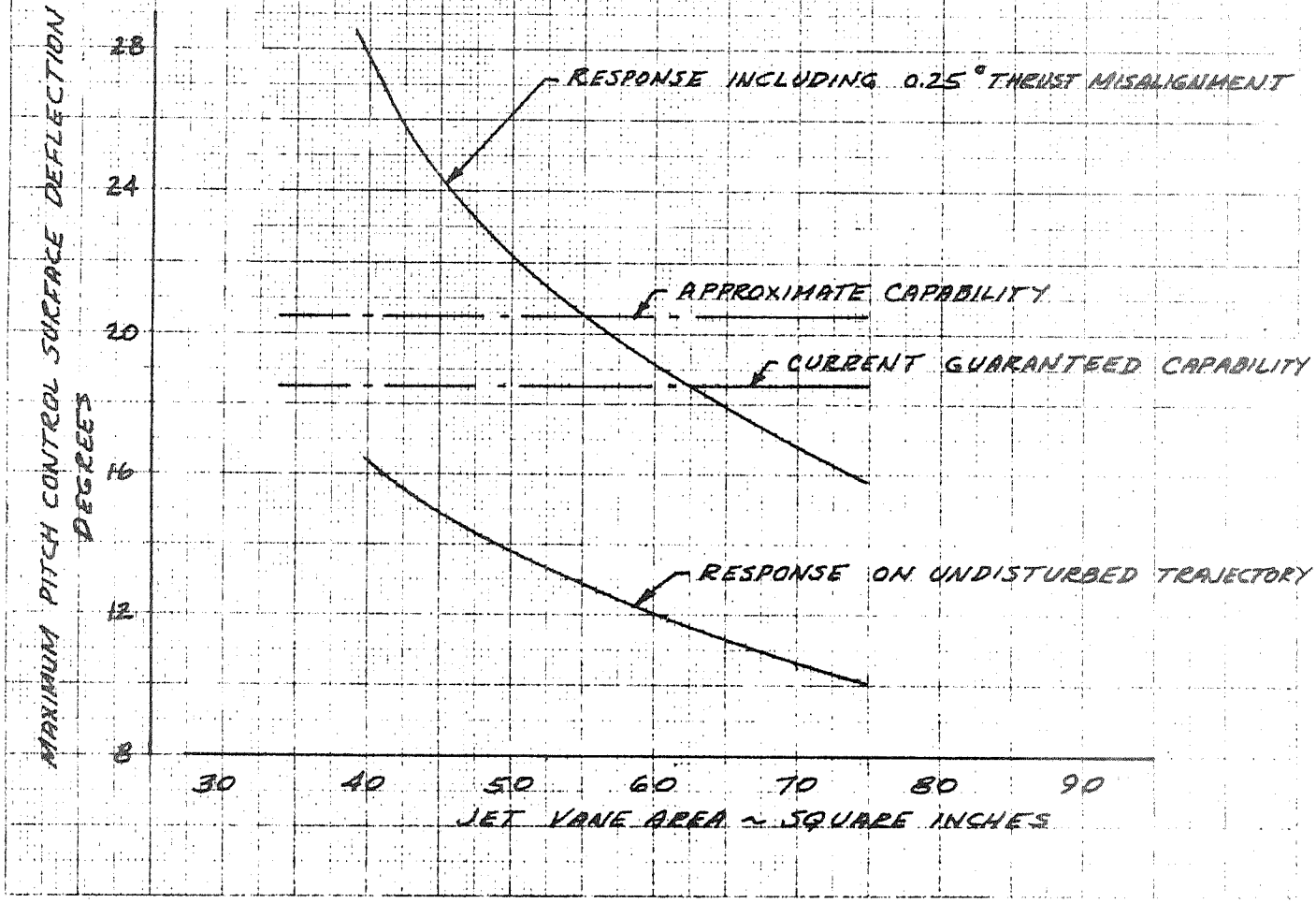

3.2.4.4 Pitch Response to Winds

The missile trajectory routine LVVC-38 described in Reference 3-13 was also used to calculate the pitch control deflections due to winds. This analysis was performed to determine the sensitivity of the vehicle to wind and wind shear near tailoff of the Algol III and during first stage coast.

The pitch control surface deflections were calculated with Scout design wind profiles having peak headwinds of 90 knots at 27000 and 35000 feet altitudes. The wind speed versus altitude is shown in Figure 3.2.4-12. The 99 per cent probability level winds for Wallops Island in December are shown for altitudes of 60000 feet and above. The vehicle response calculations were based on tailwind speed building up from zero to the 99 per cent wind at a shear rate of 40 feet per second per 1000 feet altitude. Calculations included such shears occurring at 60, 80 and 100 thousand feet altitude. The pitch control deflections resulting from these conditions are shown in Figure 3.2.4-13. The deflections are considerably lower than would be expected from the current Scout configuration because this configuration is nearly neutrally stable and control tip effectiveness is significantly greater in this region than is the current Scout configuration. This favorable effect during coast reduces the attitude errors at second stage ignition. In general, the selected combination of fin size, tip size and jet vane size for the larger heatshield with the Algol III first stage provides better controllability than the current Scout configuration with the exception of the first pitch program.

FIGURE 3.2.4-12
SCOUT LARGER HEATSHIELD STUDY
WIND PROFILES USED FOR PITCH CONTROL RESPONSE STUDIES

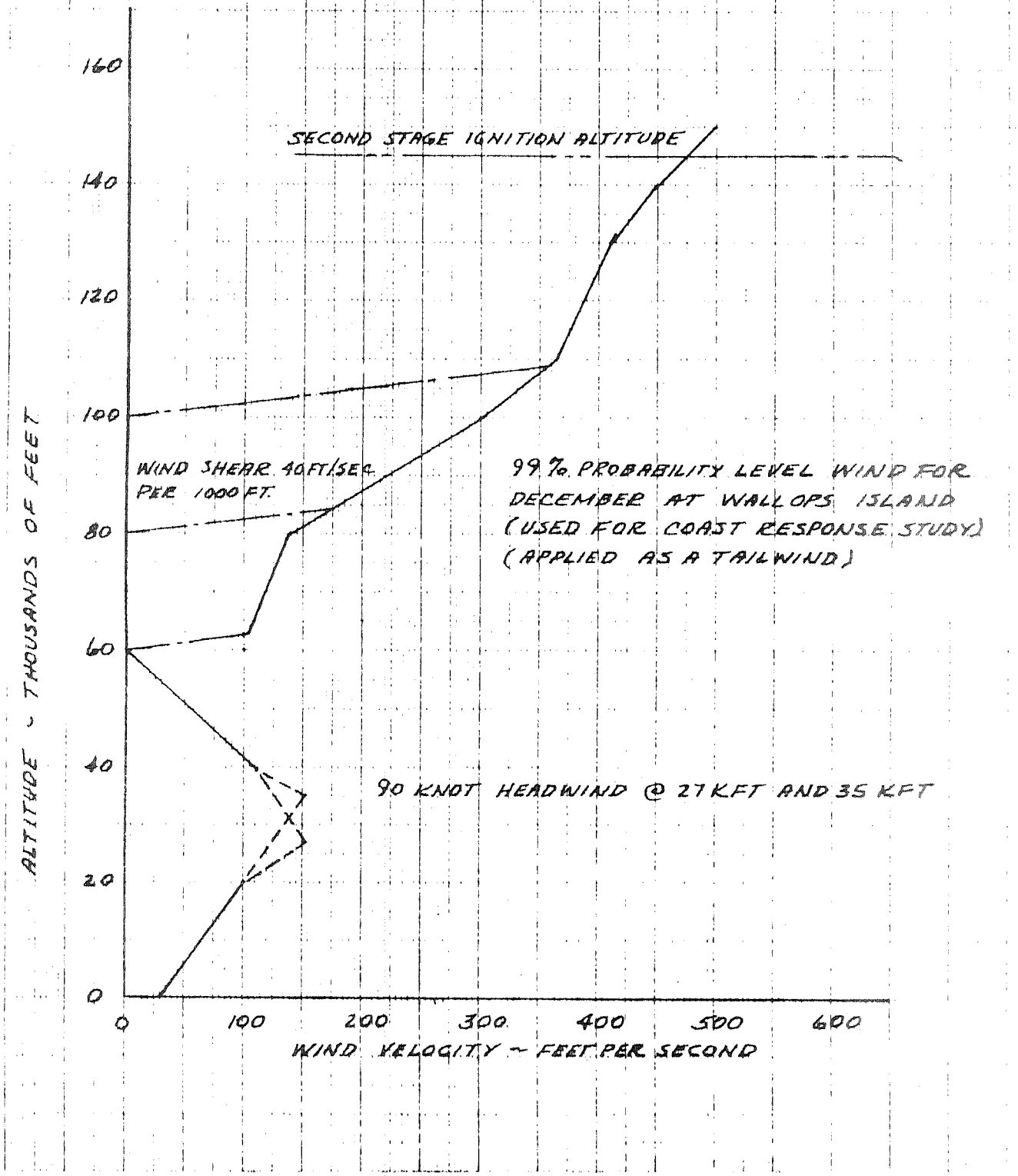

FIGURE 3.2.4-13

SCOUT LARGER HEATSHIELD STUDY

PITCH CONTROL RESPONSE TO WIND - 42 INCH HEATSHIELD

ALGOL III CONFIGURATION

41 IN^2 JET VANE

78 IN^2 FIN TIP

5.75 FT^2 FIN

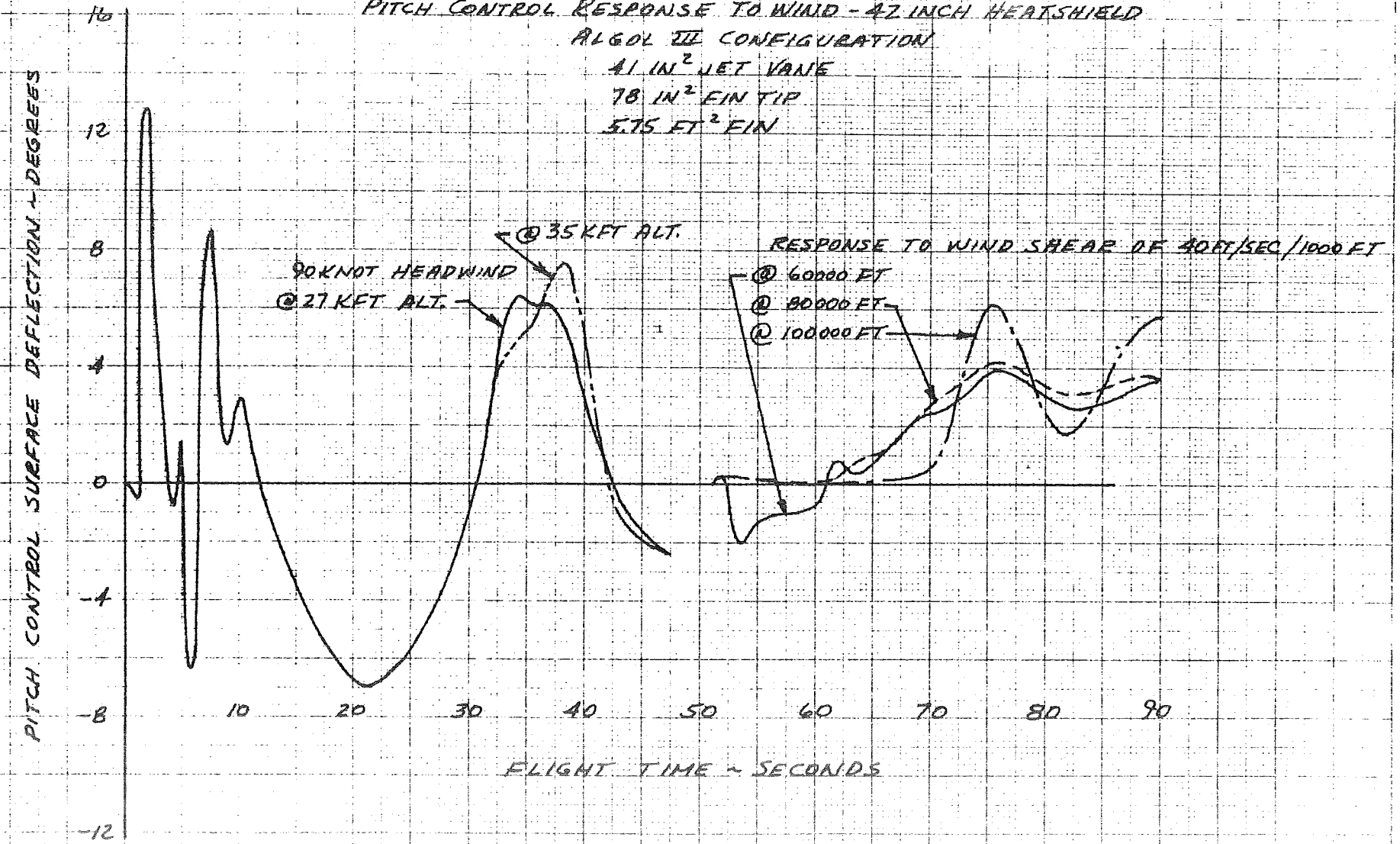

3.2.4.5 Second Stage Ignition Dynamic Pressure Restrictions

The use of a larger heatshield on the Scout vehicle increases the aerodynamic instability of the second stage. This increased instability reduces the probability of capturing the vehicle for a given dynamic pressure at second stage ignition.

The 42-inch heatshield Algol III configuration was analyzed to define the limitations of dynamic pressure at second stage ignition using the same procedure as that used in defining the current Scout vehicle limitations as presented in Reference 3-4. This procedure uses the Monte-Carlo technique using a single-axis mathematical model of the vehicle and control system to define the maximum attitude error. The input data used for this analysis is presented in Table 3.2.4-1. Statistical wind data for December at Wallops Island taken from Reference 3-14 was used in this analysis. Pitch and yaw capture maneuvers with orbital and reentry deadbands were calculated. Successful capture is based on the ability to return the vehicle to the deadbands without exceeding the 10 degree limit of the MIG displacement gyro. Based on 1000 samples of capture maneuvers binomial tables were used to determine the probability of capture with 95 per cent confidence. Crossplots of capture probability versus ignition dynamic pressure were made for orbital and reentry missions. The vehicle with the 42-inch heatshield has a probability of capture of 99.5 per cent with nominal dynamic pressure at ignition of 72 psf on orbital missions and at 63 psf on reentry missions.

TABLE 3.2.4-1

SCOUT SECOND STAGE CAPTURE ANALYSIS
INPUT DATA

Castor II, X-259, FW-4S, 50 Lb Payload

4396.		Velocity @ ignition (ft/sec)
-0.34559		Pitch Program Rate deg/sec
-0.2578		Theta Error/Alpha
0.		Bias in Initial Attitude Error
0.52		$C_{N_\alpha} S$ (40 In. Heatshield) (Ft^2/Deg)
0.54		$C_{N_\alpha} S$ (42 In. Heatshield) (Ft^2/Deg)
0.59		$C_{N_\alpha} S$ (44 In. Heatshield) (Ft^2/Deg)
0.65		$C_{N_\alpha} S$ (46 In. Heatshield) (Ft^2/Deg)
115.32 ◄——►	138.39	Center of Pressure (40 In. Heatshield)
107.24 ◄——►	128.69	Center of Pressure (42 In. Heatshield)
97.32 ◄——►	116.79	Center of Pressure (44 In. Heatshield)
78.48 ◄——►	94.18	Center of Pressure (46 In. Heatshield)
Mean	Standard Deviation	
44861.59	814.	Moment of Inertia (slug-ft^2)
289.69	1.	Center of Mass (station)
270.	90.	Wind Velocity @ Ignition (ft/sec)
22.	0.730	Initial Flight Path Angle (deg)
-1.403	0.4541	Log_e of Amplitude of Attitude Displacement Error Oscillations

Other input data is the same as shown in Reference 3.1.4-1, Addendum H.

3.2.4.6 Second Stage Fuel Consumption and Coast Time

The increase in aerodynamic instability of the second stage results in an increase in boost fuel consumption and an accompanied reduction in coast time capability. The increase in boost fuel consumption and decrease in coast time capability was computed by the same technique as for the current Scout vehicle reported in Reference 3-4. The boost fuel consumption for the 42-inch diameter heatshield configuration is 83 pounds for orbital missions with an ignition dynamic pressure of 40 psf and 84 pounds for reentry missions with an ignition dynamic pressure of 35 psf. These calculations are based on the 99.5 per cent probability level. The resulting decrease in coast time is presented in Figure 3.2.4-14 as a function of usable control fuel. If the ignition dynamic pressure is increased to the maximum allowable, the boost fuel consumption increases by about 16 pounds and there is a further reduction in coast time capability. An estimate of the coast time capability with the maximum allowable dynamic pressure is presented in Figure 3.2.4-15 and is valid for all heatshield configurations analyzed.

FIGURE 3.2.4-14

SCOUT LARGER HEATSHIELD STUDY

SECOND STAGE COAST TIME VERSUS USABLE CONTROL FUEL
42 INCH HEATSHIELD - ALGOL III - 50 LB PAYLOAD
99.5 PERCENT PROBABILITY, 95 PERCENT CONFIDENCE

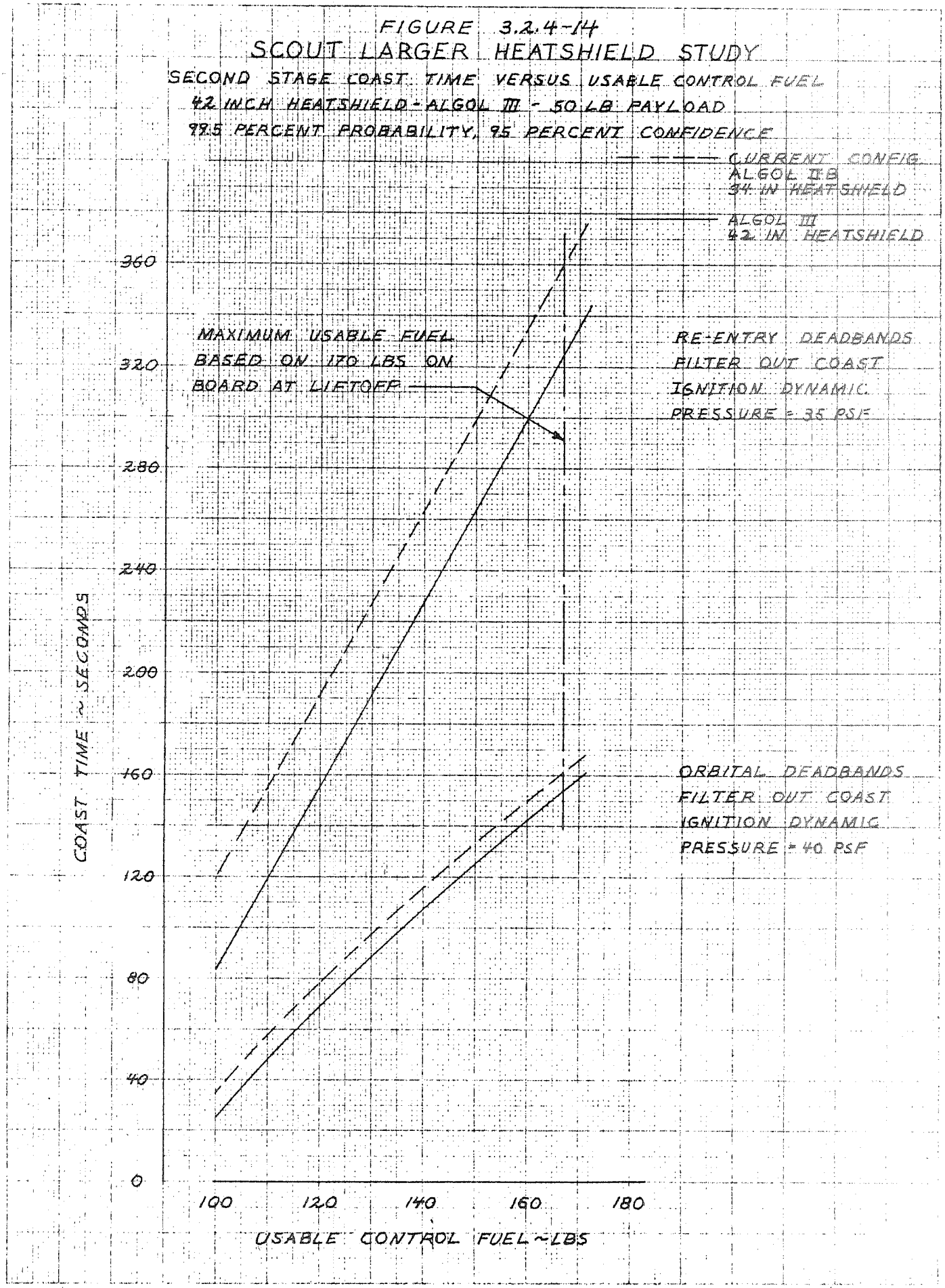

FIGURE 3.2.4-15

SCOUT LARGER HEATSHIELD STUDY

SECOND STAGE COAST TIME AT MAXIMUM IGNITION DYNAMIC PRESSURE

99.5 PERCENT PROBABILITY, 95 PERCENT CONFIDENCE

50 LB PAYLOAD

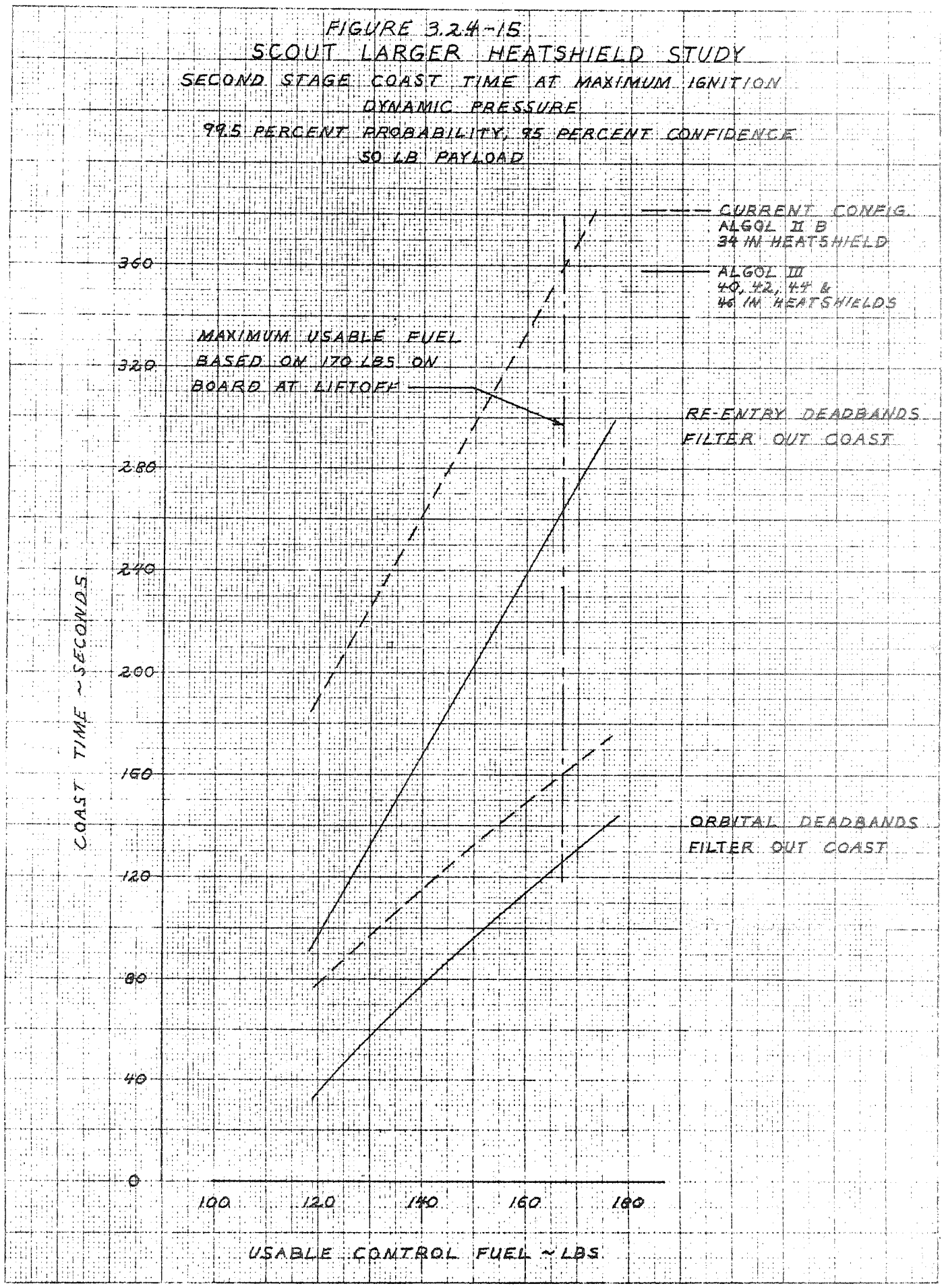

3.2.5 Flight Loads

3.2.5.1 Vehicle Loads

Figures 3.2.5.1-1 and 3.2.5.1-2 present the bending moments due to gust and winds and axial loads for the 42 inch heatshield configurations. The technique used and description of the vehicle is the same as discussed in paragraph 3.1.5.1.

3.2.5.2 Fin Loads

The fin attach loads for the critical flight conditions are presented in Figure 3.1.5.2-1. The assumptions and methods used in determining these loads may be found in paragraph 3.1.5.2.

FIGURE 3.2.5.1-1
SCOUT VEHICLE - ALGOL III FIRST STAGE
BENDING MOMENT DISTRIBUTION DUE
TO 90 KNOT WIND AND 24 FPS GUST

HEAT SHIELD: 42" DIA. NOSE @ 144.81
PEAK WIND ALTITUDE = 27000 FT
HEAD WIND
50 LB. PAYLOAD

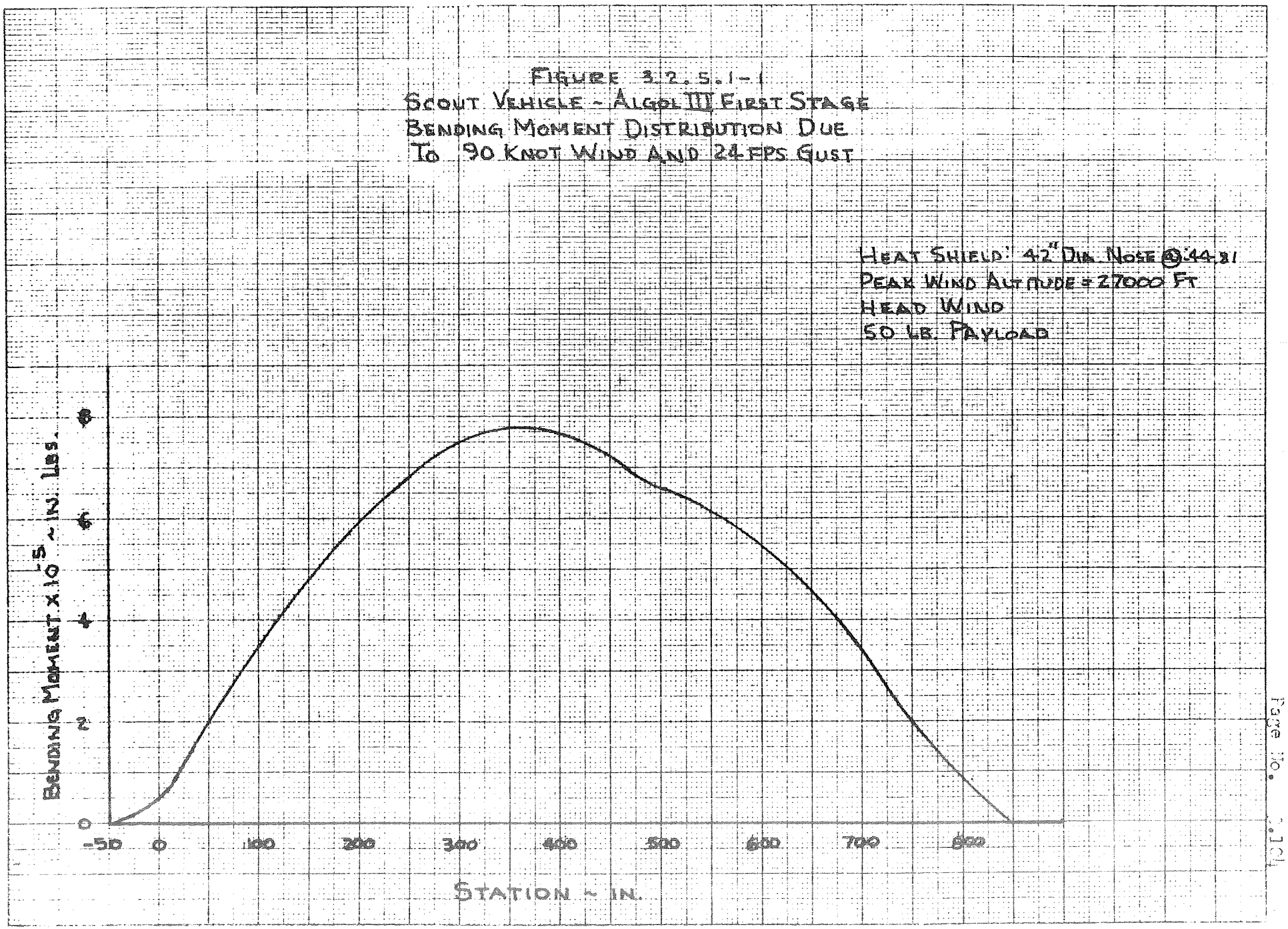

FIGURE 3.2.5.1-2
SCOUT VEHICLE - ALGOL III FIRST STAGE
AXIAL LOAD DISTRIBUTION DUE TO
90 KNOT HEADWIND

HEATSHIELD: 42" DIA. NOSE @ F.S. -448.1
50 LB. PAYLOAD
MACH 2.14
q_∞ = 2348.5 PSF
N_x = 3.345

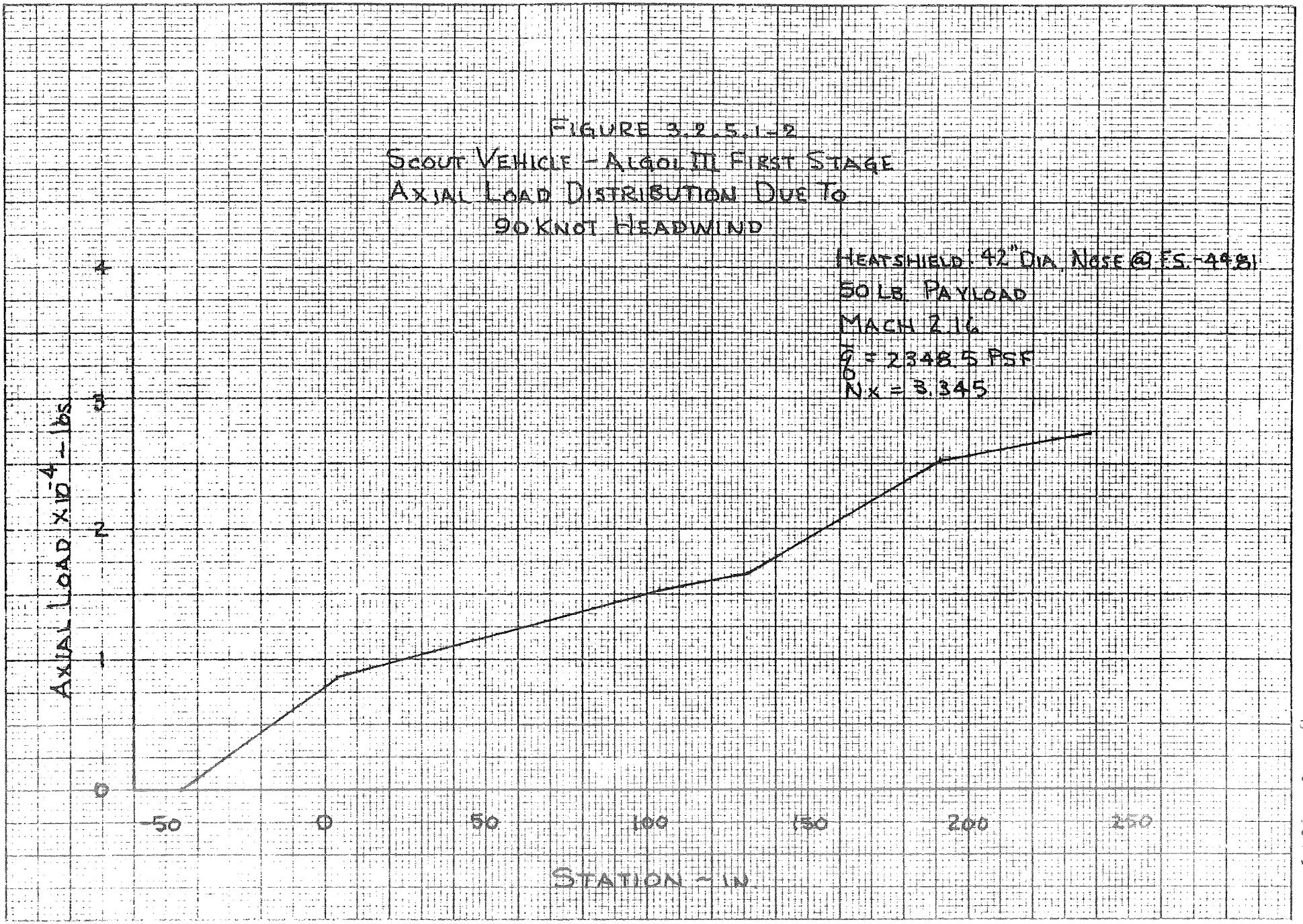

3.2.6 Vehicle Structure

3.2.6.1 Design Criteria

The structural design criteria is as defined in paragraph 3.1.6.1.

3.2.6.2 Loads

Plots of vehicle flight ultimate loads with the 42 inch diameter heat shield with Algol III first stage are shown on Figure 3.2.6-1. For comparison, plots of flight loads for the basic Scout vehicle with the 34 inch diameter heat shield are also shown.

3.2.6.3 Heat Shield Attachment Clamp

The basic Scout 34 inch diameter heat shield attachment clamp is designed for an ultimate tension load in the clamp of 7,600 pounds, Reference 3-7. Vehicle loads of 545,000 inch pounds bending moment and 15,250 pounds axial load at station 103.69 for the 42 inch diameter heat shield, Reference Figure 3.2.6-1, results in an ultimate tension load in the attachment clamp of 8,758 pounds. This is a 15.24% increase over the ultimate design load of the 23-002204 heat shield attachment clamp. Some components of the 23-002204 clamp have a calculated margin of safety less than 15% for the 7,600 pound load, Reference 3-7. These components are the 23-000214-1 pin, 23-000210 link toggle, and the CVC 155-A4 bolt and will require replacement with parts of greater load capability for use with the 42 inch diameter heat shield.

3.2.6.4 Lower "D" Transition Section

The location of the lower "D" transition section in the vehicle and the thermal loads in the section are discussed in paragraph 3.1.6.5.

A review of the lower "D" transition section structure for loading as shown on Figure 3.2.6-1 plus thermal loading from Reference 3-7 gives calculated positive margins of safety for the section. A comparison of flight ultimate loads plus thermal loads to structural static test loads for the section is shown in Table 3.2.6-1. The static test loads shown did not produce structural failure of lower "D".

The section loadings from Table 3.2.6-1 show that the maximum ultimate compression stress in the forward end of lower "D" section is 3% greater than the maximum test load compression stress. If lower "D" section is insulated to eliminate the thermal loading, then the maximum ultimate compression stress will be 93% of the maximum test compression load.

Structural analysis of the section and the structural testing results show lower "D" transition section, 23-000067, structurally adequate for use on the Scout vehicle with the 42 inch diameter heat shield and Algol III first stage.

3.2.6.5 X-259 Motor

A comparison of flight ultimate loads to structural static test loads for the X-259 motor is shown in Table 3.2.6-2. The static test loads shown did not produce structural failure of the X-259 motor.

Structural analysis of the motor case and the structural testing results show the X-259 motor case structurally adequate for use on the Scout vehicle with the 42 inch diameter heat shield and Algol III first stage.

3.2.6.6 Upper and Lower "C" Transition Sections

A comparison of flight ultimate loads to structural static test loads for "C" section is shown in Tables 3.2.6-3 and 3.2.6-4. The static loads shown for load point 55 resulted in structural failure in the forward region of upper "C" section. The mode of failure was shell buckling due to compression loading.

The section loadings from Tables 3.2.6-3 and 3.2.6-4 show that the test compression loads at the forward end of upper "C" section, station 191.95, were 110% of the ultimate compression loads and the test tension loads at this station were 137% of the ultimate tension loads. The ratio of test loads to ultimate loads at other stations of "C" section are greater than the above values.

Structural analysis of "C" section and the structural testing results show both upper and lower "C" transition sections, 23-002031 and 23-001031 respectively, structurally adequate for use on the Scout vehicle with the 42 inch diameter heat shield and Algol III first stage.

3.2.6.7 Base "A" and Fins

For the vehicle with the 42 inch diameter heat shield and Algol III first stage the fin size has been increased from the basic Scout vehicle as shown on Figure 2.2.3-1. Fin ultimate reaction loads for the fin to Base "A" attachments points are shown on Figure 3.2.6-2. For comparison, ultimate reaction loads for the fin on the basic Scout 34 inch diameter heat shield vehicle are shown on Figure 3.1.6-2.

Structural analysis of the Base "A" fin support structure shows the support frame and fitting, 23-001079 and 23-001148 at station 848.075, the support frame and fitting, 23-000093 and 23-001151 at station 840.20, and the forward shear attachment at station 825.71 to be structurally adequate for fin loads resulting from the 42 inch diameter heat shield and the Algol III first stage.

The needed increase in fin area for use with the 42 inch diameter heat shield will require a redesign of the fin.

3.2.6.8 Structure Summary

The basic 34 inch diameter heat shield Scout vehicle will require structural changes in two areas for use with the 42 inch diameter heat shield and Algol III first stage. These areas of required structural change are as follows:

(1) Heat shield attachment clamp 23-002204

(2) Fin, 23-000021, redesigned for required increased area.

Although analysis of the lower "D" transition shows the section to be structurally adequate, recommendation is made to insulate the section to eliminate the thermal loading due to aerodynamic heating. This will increase the small calculated margin of safety for the section.

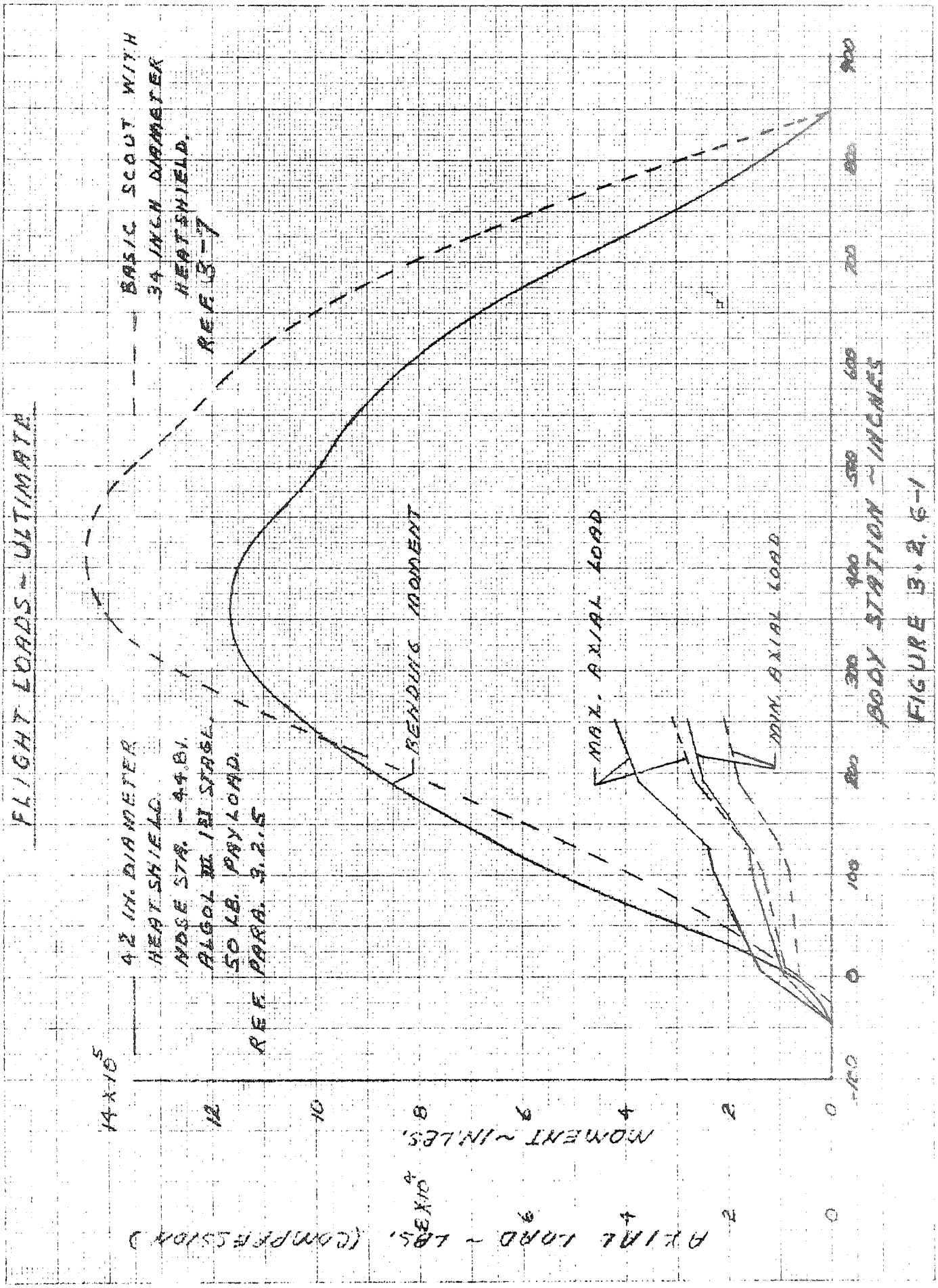
FLIGHT LOADS - ULTIMATE
42 IN. DIAMETER
HEAT SHIELD
NOSE STA. -44.81
ALGOL III 1ST STAGE
50 LB. PAYLOAD
REF PARA. 3.2.2.5
BASIC SCOUT WITH
34 INCH DIAMETER
HEAT SHIELD.
REF 3-7
BENDING MOMENT
MAX. AXIAL LOAD
MIN AXIAL LOAD
14 x 10^5
12
10
8
6
4
2
0
MOMENT - IN.LBS.
0
2
4
6 x 10^4
AXIAL LOAD - LBS. (COMPRESSION)
-100
0
100
200
300
400
500
600
700
800
900
BODY STATION - INCHES

FIGURE 3.2.6-1

TABLE 3.2.6-2

X-259 MOTOR

COMPARISON OF FLIGHT ULTIMATE AND TEST LOADS

		42 Inch Diameter Heat Shield Ultimate Loads	(1) Test Loads Ld. Point (47)	Ld. Point (52)
Station 131.1				
(2)	MOM. in. lbs.	645,000	638,983	617,591
(2)	P_{max} lbs.	25,000	40,588	375
(2)	P_{min} lbs.	16,700	- - - -	- - - -
	W_M lbs/in	± 915	± 906	± 876
	$W_{P\ max}$ lbs/in	- 266	- 431	- 4
	$W_{P\ min}$ lbs/in	- 177	- - - -	- - - -
	$W_{c\ max}$ lbs/in	- 1,181	- 1,337	- 880
	$W_{t\ max}$ lbs/in	+ 738	+ 475	+ 872
Station 191.95				
(2)	MOM in. lbs.	860,000	955,343	914,843
(2)	P_{max} lbs.	37,875	40,588	375
(2)	P_{min} lbs.	25,250	- - - -	- - - -
	W_M lbs/in	± 1,219	± 1,355	± 1,297
	$W_{P\ max}$ lbs/in	- 402	- 431	- 4
	$W_{P\ min}$ lbs/in	- 268	- - - -	- - - -
	$W_{c\ max}$ lbs/in	- 1,621	- 1,786	- 1,301
	$W_{t\ max}$ lbs/in	+ 951	+ 924	+ 1,293

(1) Reference 3-8

(2) Reference Figure 3.2.6-1

$W_M = \frac{M}{\pi R^2}$ Where R is radius of shell

$W_P = \frac{P}{\pi D}$ Where D is diameter of shell

$W_{c\ max}$ = Maximum compressive load

$W_{t\ max}$ = Maximum tensile load

TABLE 3.2.6-3

UPPER "C" TRANSITION SECTION

COMPARISON OF FLIGHT ULTIMATE AND TEST LOADS

		42 Inch Diameter Heat Shield Ultimate Loads	(1) Test Loads Ld. Point (52)	Ld. Point (55)
Station 191.95				
(2)	MOM in lbs.	860,000	914,843	995,845
(2)	P_{max} lbs.	37,875	375	35,821
(2)	P_{min} lbs.	25,250	- - - -	- - - -
	W_M lbs/in	± 1,169	± 1,244	± 1,354
	$W_{P\ max}$ lbs/in	- 394	- 4	- 372
	$W_{P\ min}$ lbs/in	- 262	- - - -	- - - -
	$W_{c\ max}$ lbs/in	- 1,563	- 1,248	- 1,726
	$W_{t\ max}$ lbs/in	+ 907	+ 1,240	+ 982
Station 238.18				
(2)	MOM in lbs.	990,000	1,140,676	1,250,156
(2)	P_{max} lbs	41,100	375	35,821
(2)	P_{min} lbs	27,400	- - - -	- - - -
	W_M lbs/in	± 1,229	± 1,416	± 1,552
	$W_{P\ max}$ lbs/in	- 409	- 4	- 356
	$W_{P\ min}$ lbs/in	- 272	- - - -	- - - -
	$W_{c\ max}$ lbs/in	- 1,638	- 1,420	- 1,908
	$W_{t\ max}$ lbs/in	+ 957	+ 1,412	+ 1,196

(1) Reference 3-8

(2) Reference Figure 3.2.6-1

$W_M = \frac{M}{\pi R^2}$ Where R is radius of shell

$W_P = \frac{P}{\pi D}$ Where D is diameter of shell

$W_{c\ max}$ = Maximum compressive load

$W_{t\ max}$ = Maximum tensile load

TABLE 3.2.6-4

LOWER "C" TRANSITION SECTION

COMPARISON OF FLIGHT ULTIMATE AND TEST LOADS

		42 Inch Diameter Heat Shield Ultimate Loads	(1) Test Loads Ld. Point (52)	Ld. Point (55)
Station 238.18				
(2)	MOM in. lbs.	990,000	1,140,676	1,250,156
(2)	P_{max} lbs.	41,100	375	35,821
(2)	P_{min} lbs.	27,400	- - - -	- - - -
	W_M lbs/in	± 1,226	± 1,413	± 1,549
	$W_{P\ max}$ lbs/in	- 408	- 4	- 356
	$W_{P\ min}$ lbs/in	- 272	- - - -	- - - -
	$W_{c\ max}$ lbs/in	- 1,634	- 1,417	- 1,905
	$W_{t\ max}$ lbs/in	+ 954	+ 1,409	+ 1,193
Station 253.06				
(2)	MOM in. lbs.	1,030,000	1,213,365	1,322,011
(2)	P_{max} lbs.	42,000	375	35,821
(2)	P_{min} lbs.	28,000	- - - -	- - - -
	W_M lbs/in	± 1,342	± 1,581	± 1,736
	$W_{P\ max}$ lbs/in	- 426	- 4	- 364
	$W_{P\ min}$ lbs/in	- 284	- - - -	- - - -
	$W_{c\ max}$ lbs/in	- 1,768	- 1,585	- 2,100
	$W_{t\ max}$ lbs/in	+ 1,058	+ 1,577	+ 1,372

(1) Reference 3-8

(2) Reference Figure 3.2.6-1

$W_M = \frac{M}{\pi R^2}$ Where R is radius of shell

$W_P = \frac{P}{\pi D}$ Where D is diameter of shell

$W_{c\ max}$ = Maximum compressive load

$W_{t\ max}$ = Maximum tensile load

FIGURE 3.2.6-2

FIN REACTION LOADS - ULTIMATE

SCOUT WITH 42 INCH DIAMETER HEAT SHIELD AND ALGOL III FIRST STAGE

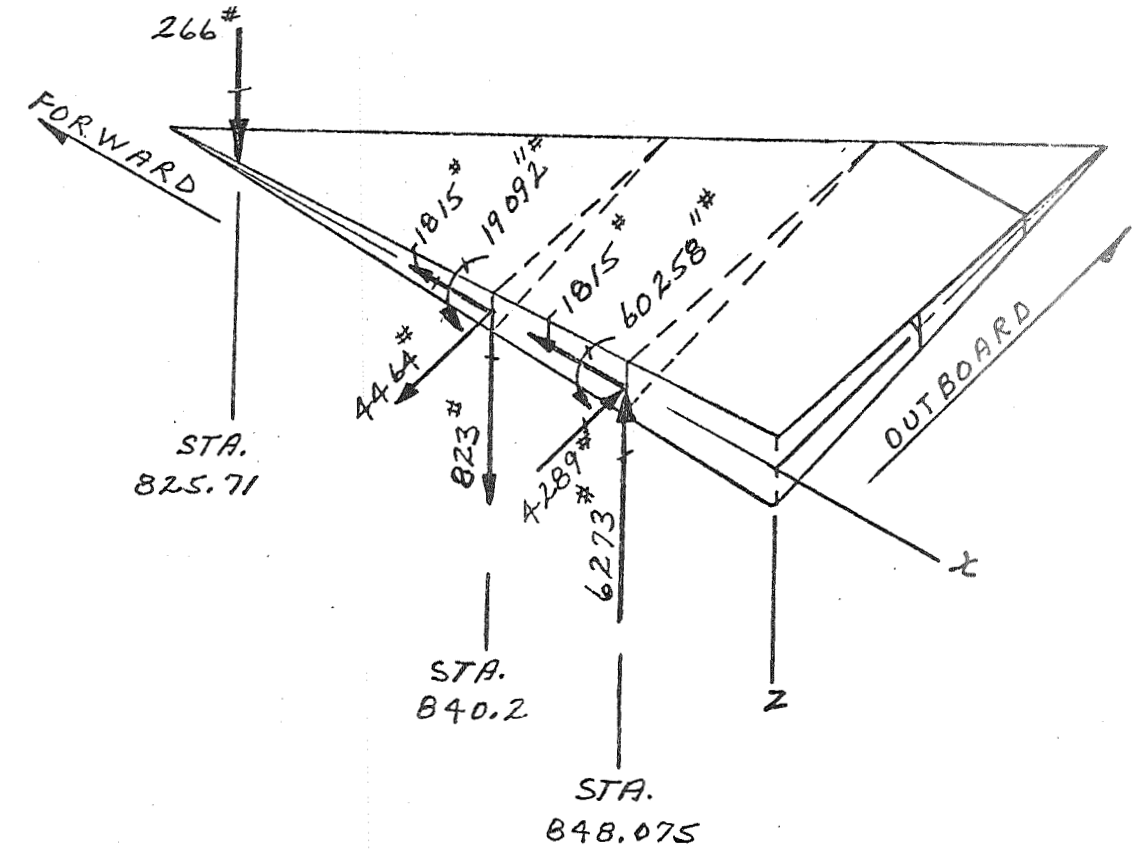

LOADS FROM PARAGRAPH 3.2.5

3.2.7 Ground Support Equipment

The ground support equipment noted in Section 3.1.7 was also reviewed to determine the effects of the 42 inch diameter heatshield with the 5.75 sq. ft. fins. The parts requiring redesign are the same as those noted in paragraphs 3.1.7.1 through 3.1.7.8.

3.3 44 INCH DIAMETER HEATSHIELD INSTALLATION

3.3.1 Summary

The results of the evaluation of the impact of the 44 inch diameter heatshield installation on the Scout D configuration are summarized as follows:

- The following vehicle structural changes are required: redesign the base A fins to increase the area from 4.5 to 8.6 sq. ft. per fin; redesign base A for fin loads; test lower C transition section for increased loads; redesign upper C transition section; test X-259 motor case for increased loads; add insulation to lower D transition section and test the section for increased loads; redesign heatshield attachment clamp.
- Fin tip control area shall be increased from 45 sq. in. to 78 sq. in. (Same as 40 and 42 inch heatshield requirements).
- Jet vane control surface area shall be increased from 35 sq. in. to 41 sq. in. (Same as 40 and 42 Inch heatshield requirements).
- Guidance system first stage nominal displacement gain shall be increased from 5.0 to 6.75 deg/deg and the rate to displacement gain ratio shall be 0.4, the same as for the basic Scout.
- The following ground support equipment requires redesign: payload umbilical retract arm, heatshield cradle, dummy heatshield, payload and heatshield hoist, heatshield storage bracket, the upper cradle assembly, strap wrench, transporter aft restraint assembly.

Detailed discussion of the evaluation is presented in the following paragraphs.

3.3.2 Aerodynamic Characteristics

3.3.2.1 Rigid Vehicle

Normal load distributions aft to station 131.1 are presented in Figures 3.3.2-1 through -4. These data were evaluated using the technique described in Section 3.2.2.1. For load distributions aft of station 131.1, use Figures 3.2.2-11 through -14.

Heatshield drag buildup is presented in Figure 3.3.2-5, and was obtained using the technique described in Section 3.2.2.1 for determining the estimated zero lift drag.

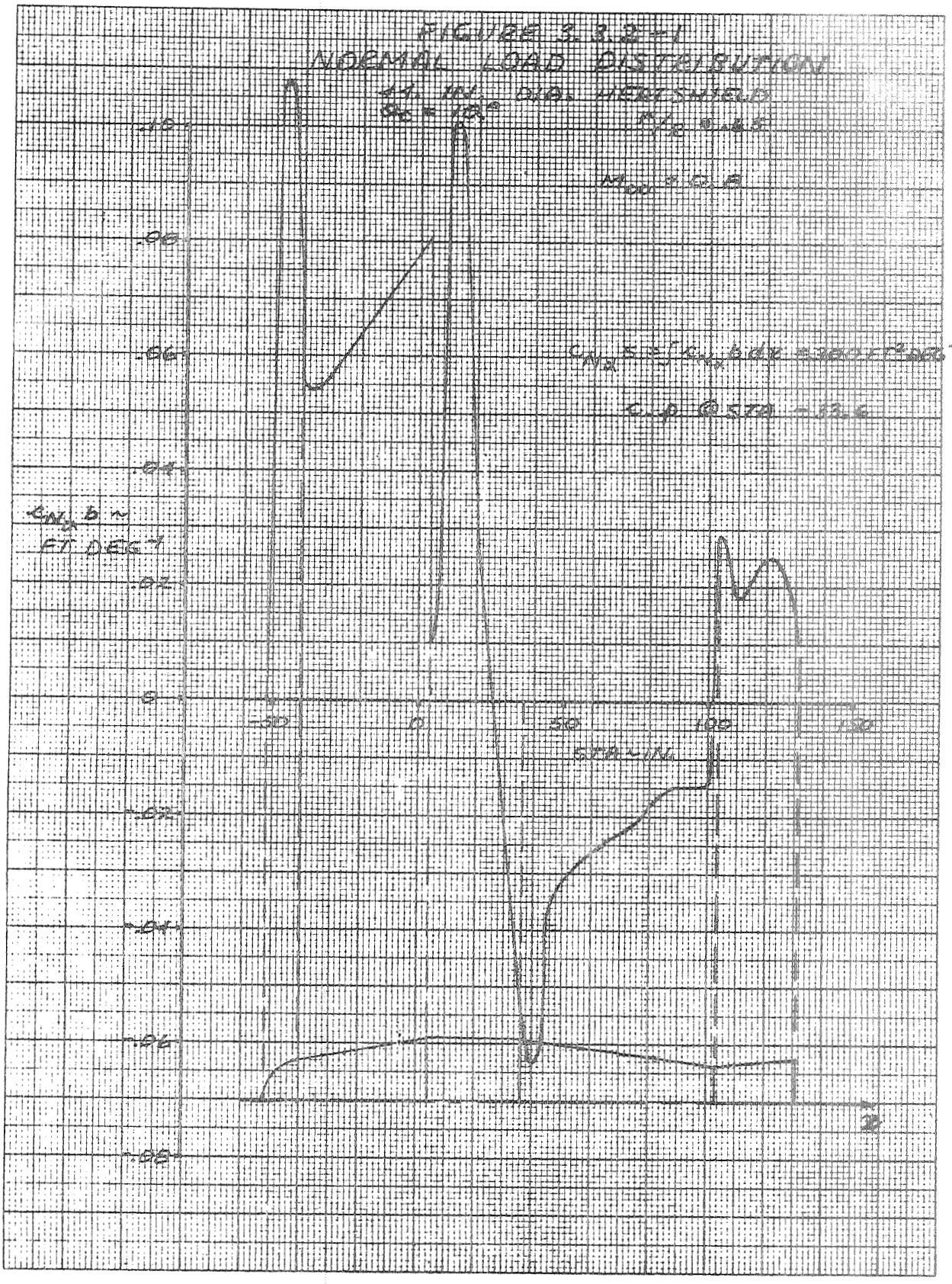
FIGURE 3.3.2-1
NORMAL LOAD DISTRIBUTION
-.10
-.08
-.06
-.04
-.02
0
-50
0
50
100
150
-.02
-.04
-.06
-.08
2

FIGURE 3.3.2-2
NORMAL LOAD DISTRIBUTION
44 IN. DIA. HEATSHIELD
$\theta_c = 10.^\circ$ $r/R = .65$

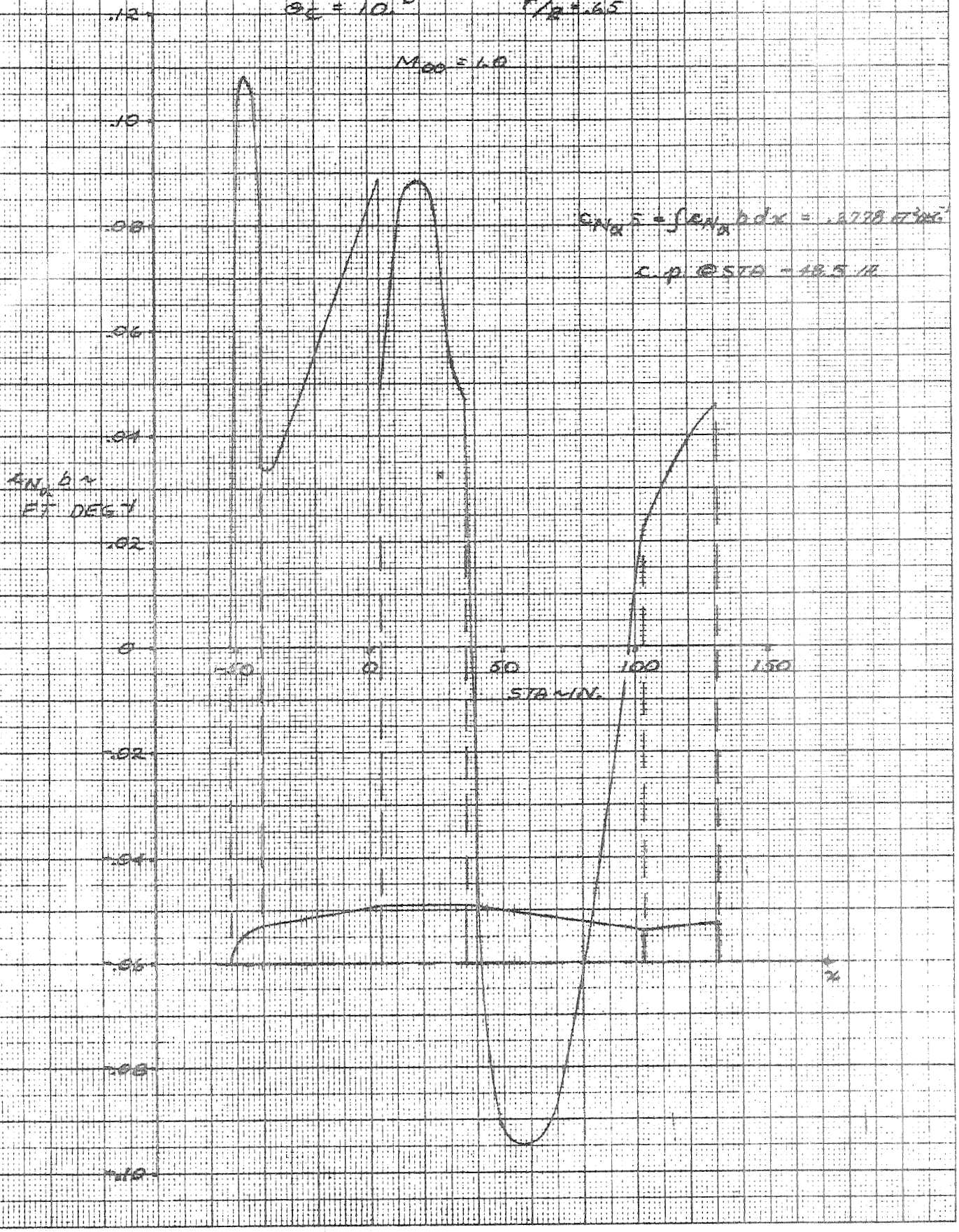

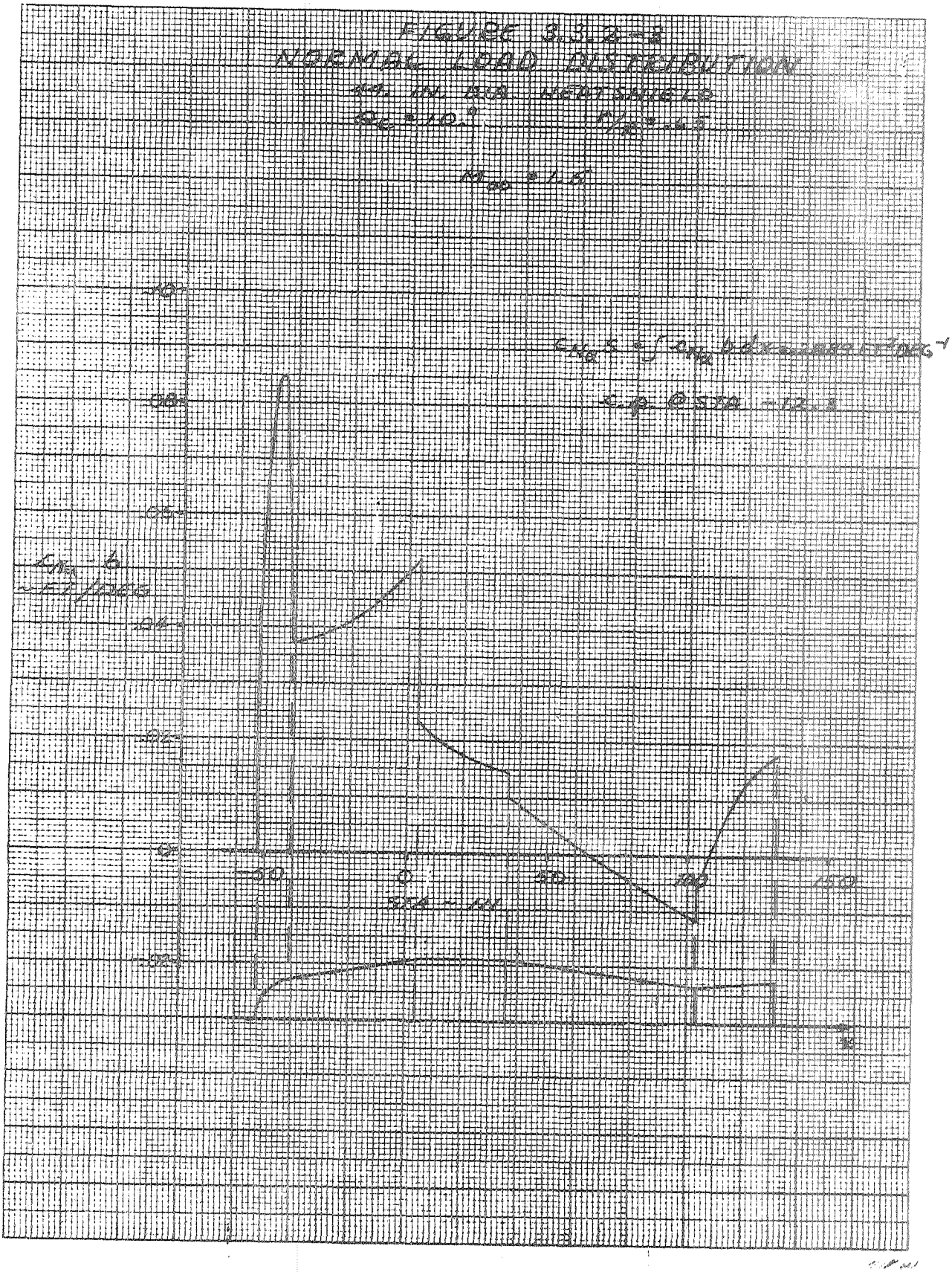
FIGURE 3.3.2-3
NORMAL LOAD DISTRIBUTION
$M_\infty = 1.6$
$\alpha_c = 10.1°$
$C_{N_\alpha} = 4.3$
$C_{N_\alpha} = \int c_{N_\alpha} b\, dx$
C_p @ STA -12.1
STA - INCHES

FIGURE 3.3.2-4
NORMAL LOAD DISTRIBUTION
44 IN. DIA HEAT SHIELD
$\theta_c = 10°$ $\bar{C}_A = 0.65$
$M_{\infty} = 2.5$

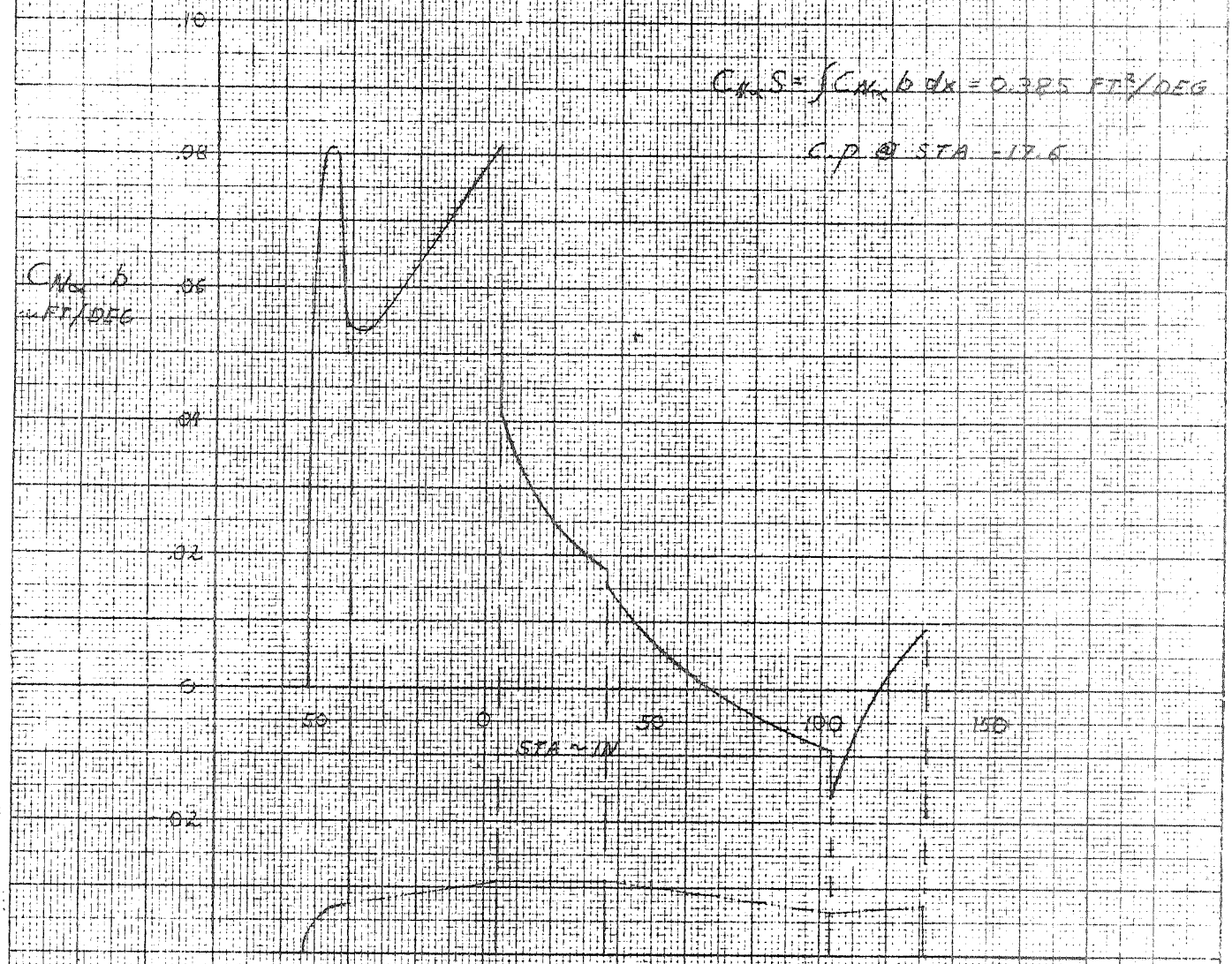

FIGURE 3.3.2-5
HEATSHIELD DRAG BUILDUP
(PRESSURE AND FRICTION)
AR. IN. DIA. HEATSHIELD
$\theta_c = 10.2°$ $r_n/R = .26$

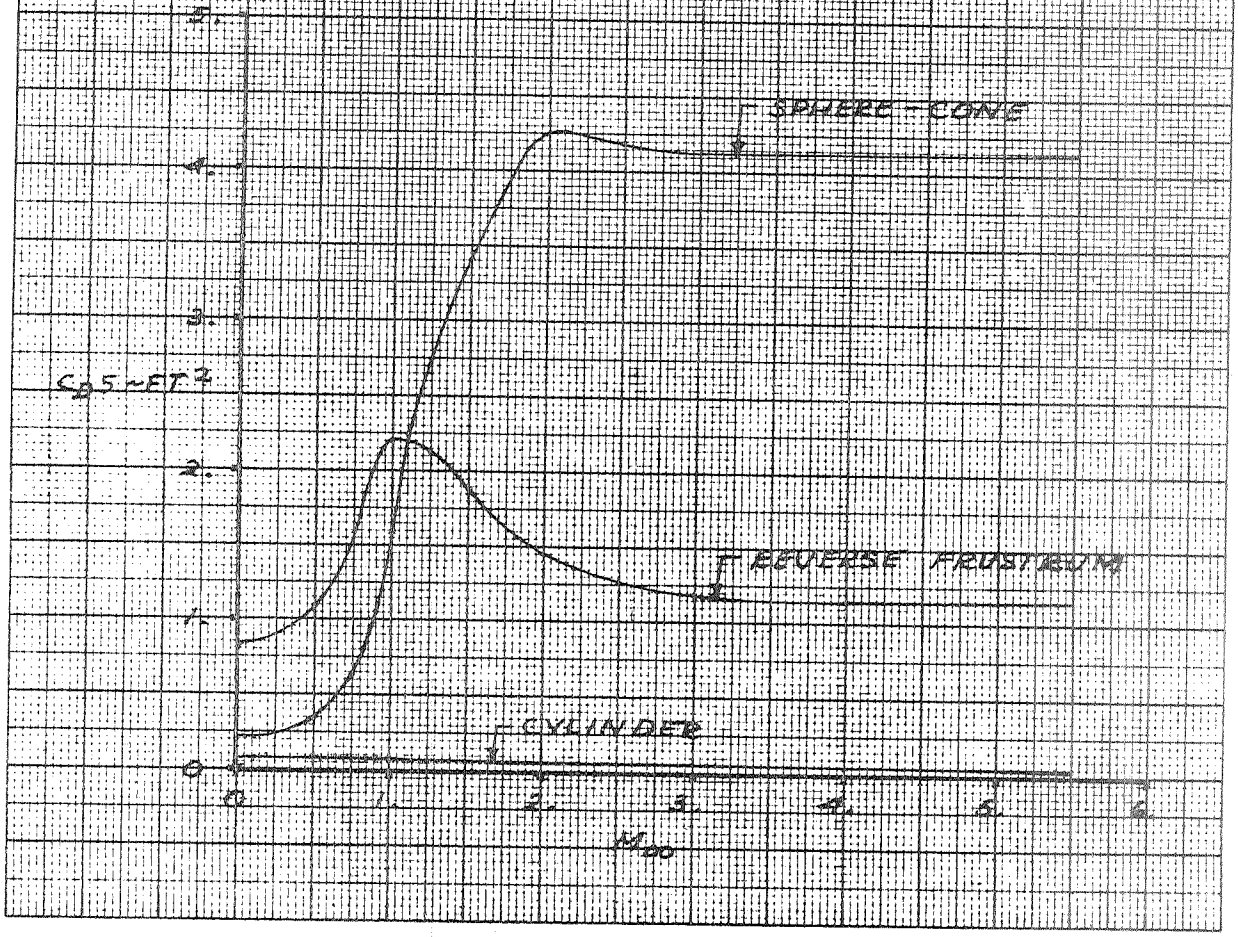

3.3.2.2 Flexible Body Aerodynamics

Discussion on the flexible body aerodynamics for the 44 inch diameter heat shield configuration may be found in Section 3.2.2.2..

3.3.3 Weight and Balance Data

This section presents the weights, longitudinal center of gravity and moments of inertia for a Scout vehicle (S178 & Sub. configuration) utilizing a 44 inch diameter heatshield and an Algol III (Aerojet Proposal No. 2) first stage motor. The standard Base A and 4.5 sq. ft. fins are included in this data.

The vehicle mass properties data is shown in Table 3.3.3-1 with a 50 pound payload and in Table 3.3.3-2 with a 400 pound payload. A 44 inch diameter heatshield of similar construction to the present 34 inch diameter was estimated to weigh 389.29 pounds with the heatshield c.g. at Station 27.3.

TABLE 3.3.3-1
MASS PROPERTIES

44 INCH DIAMETER, -52.51 LARGE VOLUME HEATSHIELD, (50 POUND PAYLOAD)

VEHICLE S- WEIGHT, X(CG), AND MOMENTS OF INERTIA

VERSUS PERCENT OF FUEL CONSUMED

	TOTAL WEIGHT, POUNDS	C.G. SCOUT STA.-IN.	IXX SLUG-FT^2	IYY OR IZZ SLUG-FT^2
	*******	*******	**********	**********
FOURTH STAGE - BURNOUT	118.96	53.35	2.38	23.82
75 0/0	271.79	60.33	5.00	30.66
50 0/0	424.63	62.28	6.87	35.52
25 0/0	577.46	63.20	8.00	39.68
FOURTH STAGE - IGNITION	730.30	63.74	8.38	43.34
SPIN-UP ITEMS	774.68	65.92	9.37	56.93
THIRD STAGE - BURNOUT	1483.95	116.61	29.45	1287.32
75 0/0	2135.08	130.01	56.88	1545.14
50 0/0	2786.22	137.15	76.77	1710.98
25 0/0	3437.35	141.58	89.11	1834.97
THIRD STAGE - IGNITION	4088.49	144.61	93.90	1935.30
LESS N/C - H/S	6159.25	229.28	181.48	23526.18
SECOND STAGE - BURNOUT	6548.62	217.27	210.88	26934.74
75 0/0	8624.86	248.17	304.02	33948.10
50 0/0	10701.11	267.08	372.01	38774.00
25 0/0	12777.35	279.84	414.88	42472.69
SECOND STAGE - IGNITION	14853.60	289.03	432.63	45511.58
FIRST STAGE - BURNOUT	19137.90	378.50	806.99	174896.79
75 0/0	26120.90	450.80	1468.09	269021.29
50 0/0	33103.90	492.60	1958.86	328984.66
25 0/0	40086.90	519.84	2279.56	372594.77
FIRST STAGE - IGNITION	47069.90	538.99	2429.98	407091.88

TABLE 3.3.3-2
MASS PROPERTIES

44 INCH DIAMETER, -52.51 LARGE VOLUME HEATSHIELD, (400 POUND PAYLOAD)

VEHICLE S- WEIGHT, X(CG), AND MOMENTS OF INERTIA

VERSUS PERCENT OF FUEL CONSUMED

	TOTAL WEIGHT, POUNDS	C.G. SCOUT STA.-IN.	IXX SLUG-FT^2	IYY OR IZZ SLUG-FT^2
	*******	*******	**********	**********
FOURTH STAGE - BURNOUT	468.96	31.44	10.88	51.43
75 0/0	621.79	39.88	13.50	85.34
50 0/0	774.63	44.99	15.37	107.31
25 0/0	927.46	48.41	16.50	123.07
FOURTH STAGE - IGNITION	1080.30	50.86	16.88	135.09
SPIN-UP ITEMS	1124.68	52.87	17.87	159.46
THIRD STAGE - BURNOUT	1833.95	98.93	37.95	1822.64
75 0/0	2485.08	115.08	65.38	2285.66
50 0/0	3136.22	124.52	85.26	2581.34
25 0/0	3787.35	130.72	97.60	2794.04
THIRD STAGE - IGNITION	4438.49	135.10	102.40	2958.63
LESS N/C - H/S	6509.25	218.25	189.98	26549.66
SECOND STAGE - BURNOUT	6898.62	207.47	219.37	29624.63
75 0/0	8974.86	239.43	312.52	37607.43
50 0/0	11051.11	259.38	380.50	43107.39
25 0/0	13127.35	273.02	423.38	47296.63
SECOND STAGE - IGNITION	15203.60	282.93	441.13	50706.98
FIRST STAGE - BURNOUT	19487.90	372.13	815.49	184231.22
75 0/0	26470.90	445.16	1476.59	282611.68
50 0/0	33453.90	487.70	1967.36	345410.78
25 0/0	40436.90	515.54	2288.06	391018.04
FIRST STAGE - IGNITION	47419.90	535.19	2438.48	426990.73

3.3.4 Stability and Control

The stability analysis of the first and second stages with the 44-inch diameter heatshield was performed in the same way as the 40-inch and 42-inch configurations discussed in Sections 3.1.4 and 3.2.4. The first stage jet vane and fin tip size as well as control system gains are the same as those selected for the 40 and 42-inch heatshield configurations. The basic differences occur in the fin size required to stabilize the vehicle at 45 seconds flight time and the second stage ignition dynamic pressure constraints and fuel consumption.

3.3.4.1 First Stage Stability Near Maximum Dynamic Pressure

The stability of the 44-inch diameter heatshield Algol III configuration was analyzed at the critical flight time of 45 seconds by a parametric procedure involving fin size and control tip size variations. The gain boundaries are presented as a function of fin area and tip size in Figure 3.3.4-1. The allowable gain is also shown including the ±6 decibel margin of safety. The minimum fin size required to stabilize this configuration is 8.6 square feet. Based on a 41 square inch jet vane area and a 78 square inch control tip the attitude displacement gain in pitch and yaw should be about 6.75 degrees of surface deflection per degree attitude error. The root loci for this configuration is shown in Figure 3.3.4-2. The root loci of the second, third and fourth bending modes of vibration for this configuration are shown in Figure 3.2.4-4.

3.3.4.2 Vehicle-Launcher Clearance

The 8.6 square feet fin area required on the 44-inch heatshield configuration results in an increase in semi-span of 9 inches more than the 42-inch heatshield configuration. The launcher-clearance shown in Figure 3.2.4-8 would therefore be reduced by 9 inches for the 44-inch heatshield configuration. This configuration would still have adequate margin.

FIGURE 3.3.4-1
GAIN BOUNDARIES VERSUS FIN SIZE
4Y IN HEATSHIELD – ALGOL III

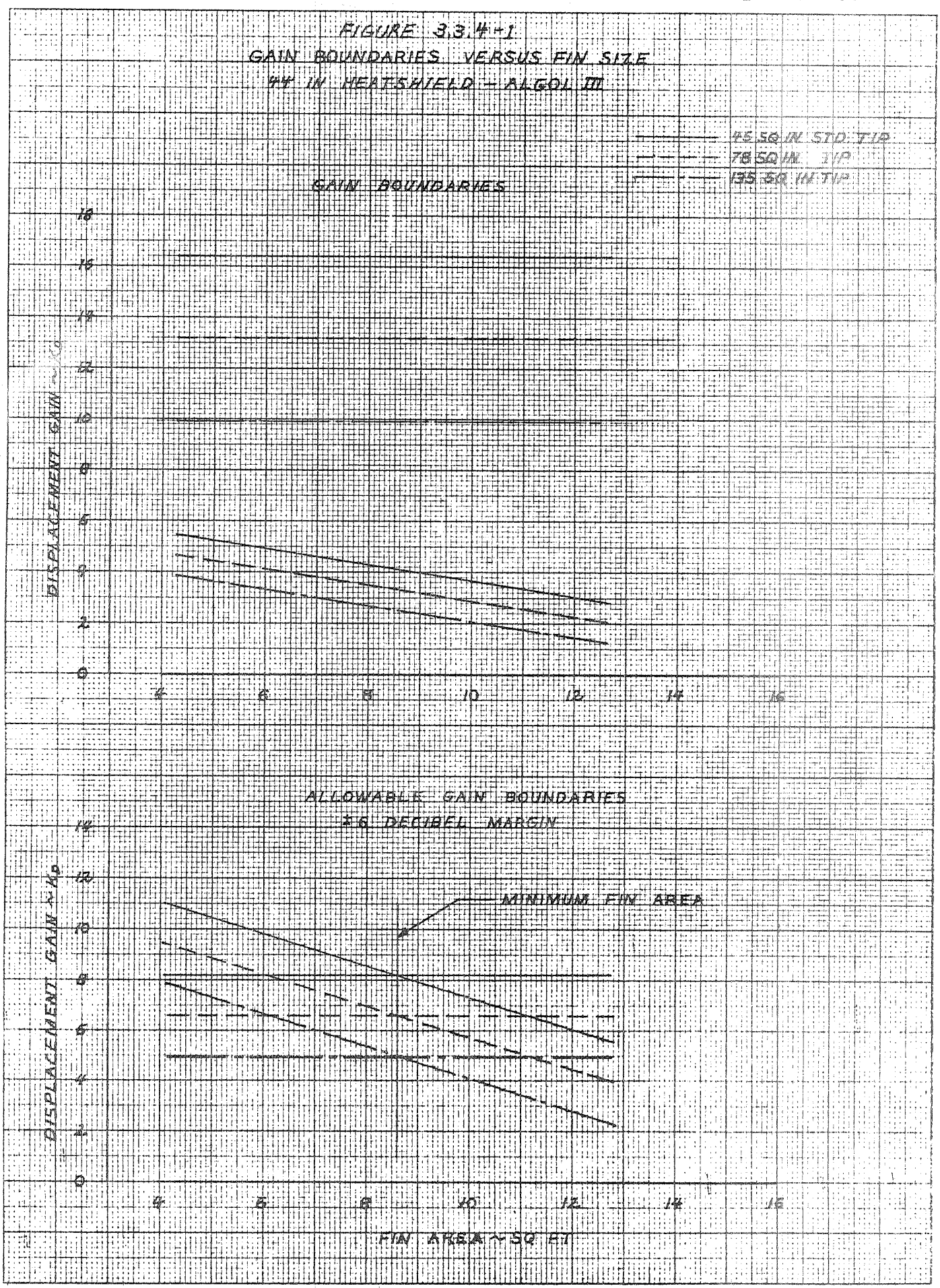

FIGURE 3.3.4-2
ROOT LOCI AT 45 SECONDS - 44 INCH HEATSHIELD
ALGOL III CONFIGURATION
41 IN² JET VANE
78 IN² FIN TIP
8.6 FT² FIN

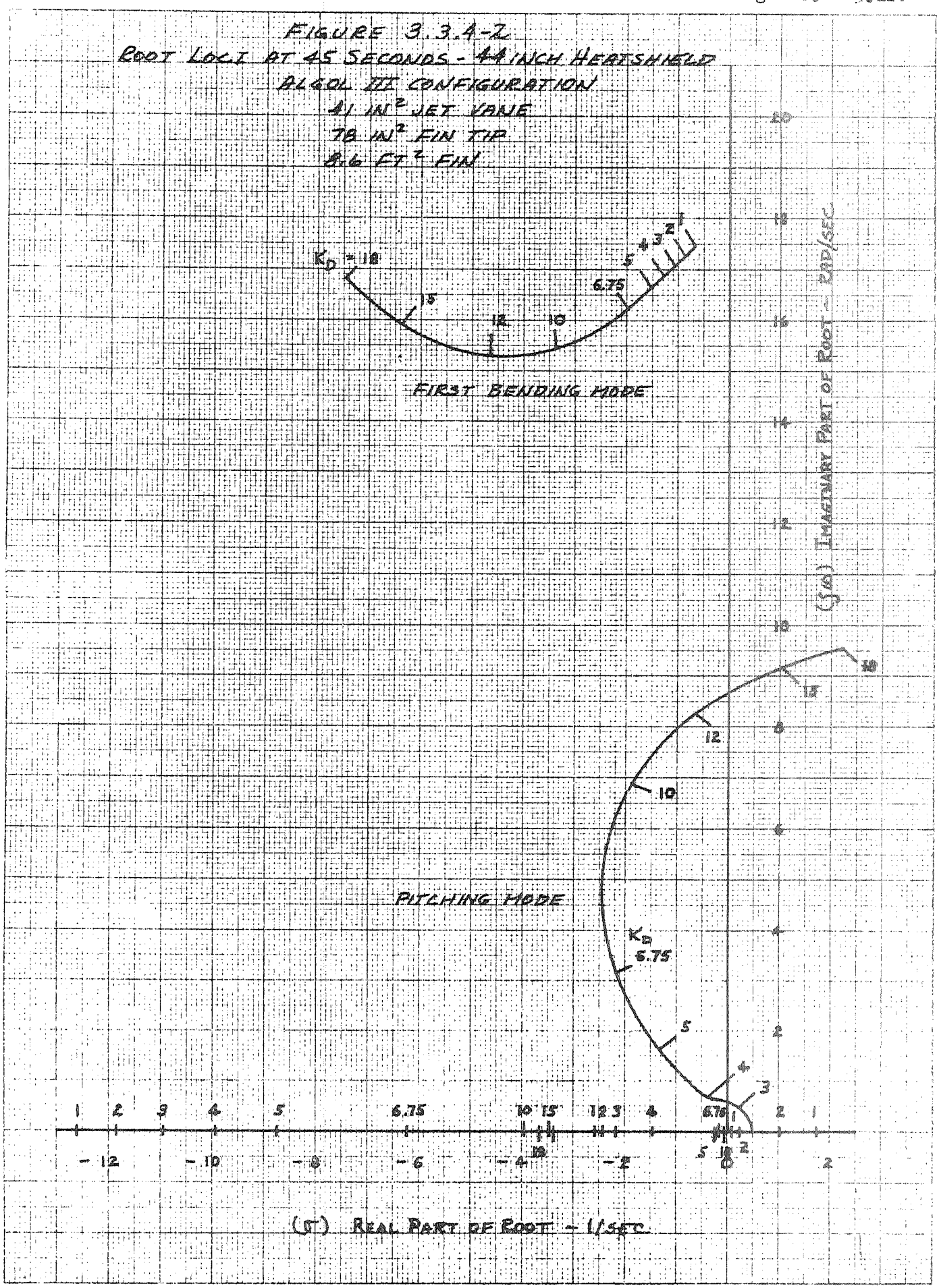

3.3.4.3 Second Stage Ignition Dynamic Pressure

The dynamic pressure allowable at second stage ignition was determined by ratioing the aerodynamic moment coefficient slope of the 44 inch heatshield configuration to that for the 42 inch configuration and reducing the ignition dynamic pressure accordingly. This keeps this aerodynamic disturbing moment equal to that determined in the 42 inch heatshield analysis. The resulting dynamic pressure allowable at second stage ignition for the 44 inch diameter heatshield Algol III configuration is 62 psf for orbital missions and 54 psf for reentry missions.

3.3.4.4 Second Stage Fuel Consumption and Coast Time

The second stage boost fuel consumption and coast times were calculated by the same procedure as the 42 inch heatshield configuration discussed in Section 3.1.4. Based on an ignition dynamic pressure of 40 psf the boost fuel consumption at the 99.5 percent probability level is 85.6 pounds. For reentry missions with an ignition dynamic pressure of 35 psf the boost fuel consumption will be 87 pounds. The second stage coast time capability with this heatshield is presented in Figure 3.3.4-3. If ignition dynamic pressure is increased to the maximum allowable, boost fuel consumption will increase by about 13 pounds and coast time capability will be reduced to that presented in Figure 3.2.4-15.

FIGURE 3.3.4-3

SCOUT LARGER HEATSHIELD STUDY

SECOND STAGE COAST TIME VERSUS USABLE CONTROL FUEL
44 IN HEATSHIELD - ALGOL III - 50 LB PAYLOAD
99.5 PERCENT PROBABILITY, 95 PERCENT CONFIDENCE

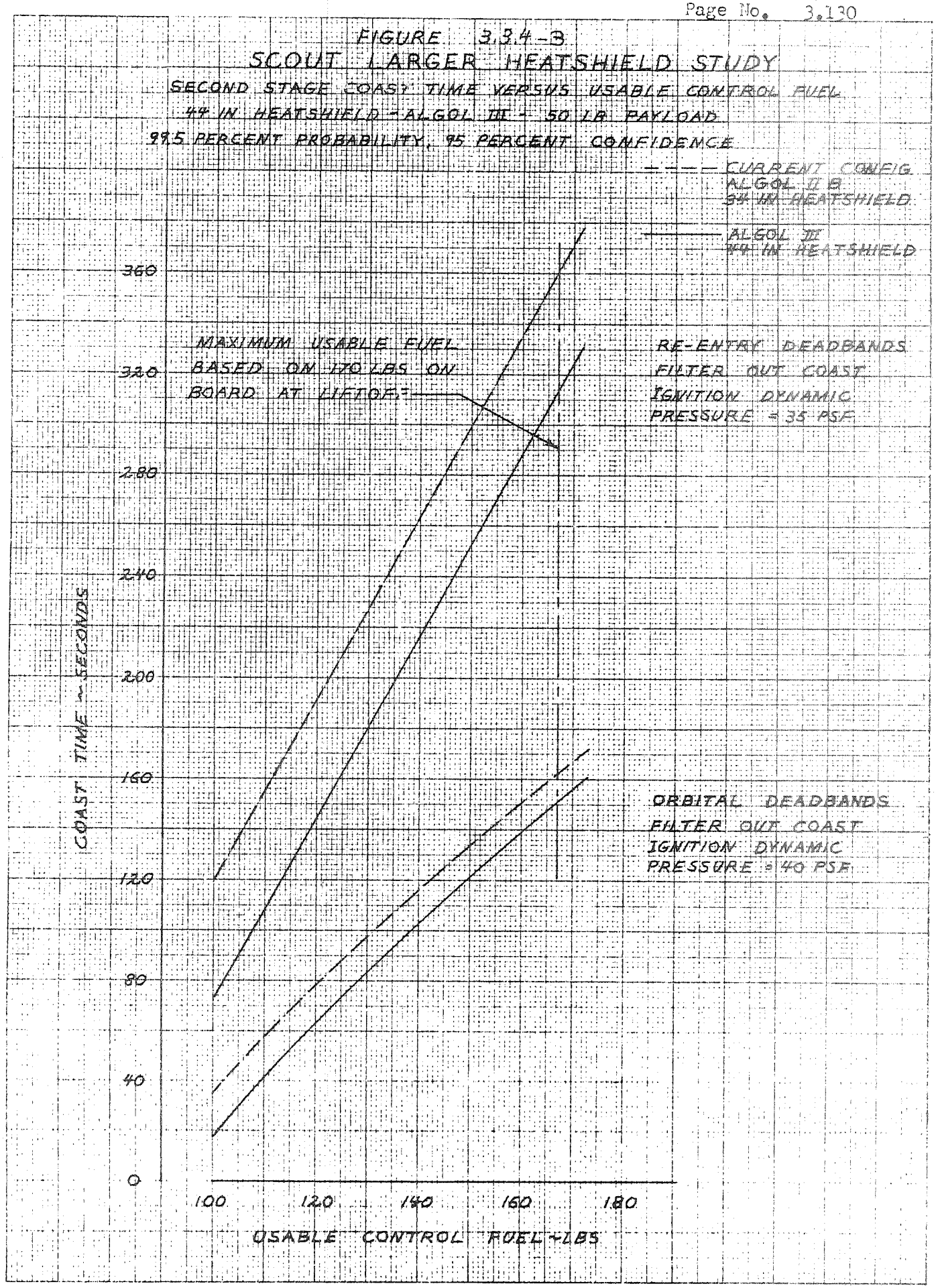

3.3.5 Flight Loads

3.3.5.1 Vehicle Loads

Figures 3.3.5.1-1 and 3.3.5.1-2 present the bending moments due to gust and winds and axial loads for the 44 inch heatshield configurations. The technique used and description of the vehicle is the same as discussed in paragraph 3.1.5.1.

3.3.5.2 Fin Loads

The fin attach loads for the critical flight conditions are presented in Figure 3.1.5.2-1. The assumptions and methods used in determining these loads may be found in paragraph 3.1.5.2.

Figure 3.2.5.1-1
Scout Vehicle - Algol III First Stage
Bending Moment Distribution Due
90 Knot Wind And 24 FPS Gust

Heatshield 44" Dia Nose @ Fs 525
Peak Wind Altitude 35,000 Ft
Headwind
50 Lb. Payload

Figure 3.3.5.1-2
Scout Vehicle - Algol III First Stage
Axial Load Distribution For
90 Knot Headwind

3.3.6 Vehicle Structure

3.3.6.1 Design Criteria

The structural design criteria is as defined in paragraph 3.1.6.1.

3.3.6.2 Loads

Plots of vehicle flight ultimate loads with the 44 inch diameter heat shield and Algol III first stage are shown on Figure 3.3.6-1. For comparison, plots of flight loads for the basic Scout vehicle with the 34 inch diameter heat shield are also shown.

3.3.6.3 Heat Shield Attachment Clamp

The basic Scout 34 inch diameter heat shield attachment clamp is designed for an ultimate tension load in the clamp of 7,600 pounds, Reference 3-7. Vehicle loads of 650,000 inch pounds bending moment and 18,000 pounds axial load at station 103.69 for the 44 inch diameter heat shield, Reference Figure 3.3.6-1, result in an ultimate tension load in the attachment clamp of 10,660 pounds. This is a 40% increase over the ultimate design load of the 23-002204 heat shield attachment clamp. Several components of the 23-002204 clamp have a calculated margin of safety less than 40% for the 7,600 pound load, Reference 3-7. Therefore for use with the 44 inch diameter heat shield the 23-002204 attachment clamp will require a redesign to increase the load capability of the clamp.

3.3.6.4 Lower "D" Transition Section

The location of the lower "D" transition section in the vehicle and the thermal loads in the section are discussed in paragraph 3.1.6.5.

A review of the lower "D" transition structure was made using the analyses and thermal loads from Reference 3-7 and flight loads from Figure 3.3.6-1. The combined thermal and flight loads result in calculated negative margins of safety for lower "D" section. If the thermal loads are eliminated by insulation of the section the analysis results in calculated positive margins of safety for lower "D".

A comparison of flight ultimate loads plus thermal loads to structural static test loads for the section is shown in Table 3.3.6-1. As shown by these values,

if the thermal stresses are eliminated by using a thin layer of cork insulation, the maximum compression ultimate stress in the forward end of lower "D" section will be 110% of the test maximum compression stress. The test loads as shown did not produce structural failure in lower "D".

Therefore use of the lower "D" transition section, 23-000067, with the 44 inch diameter heat shield and the Algol III first stage vehicle will require insulation of the section and testing for the vehicle increased loads.

3.3.6.5 X-259 Motor

Shell stability analysis of the X-259 motor case using methods of References3-15 and 3-16 shows the motor case to be marginal for ultimate loads as shown on Figure 3.3.6-1. A comparison of flight ultimate loads to structural static test loads is shown in Table 3.3.6-2. As shown by these values, at station 131.1, the maximum compression ultimate load is 106% of test loads and the maximum tension ultimate load is 103% of test loads. At station 191.95 the maximum compression ultimate load is 108% of test loads. The test loads shown did not produce structural failure in the X-259 motor case.

Use of the X-259 motor with the 44 inch diameter heat shield and Algol III first stage vehicle will require testing of the motor case for the vehicle increased loads.

3.3.6.6 Upper and Lower "C" Transition Sections

The "C" transition section is described in paragraph 3.1.6.7. The structural analysis of "C" section for loads shown on Figure 3.3.6-1 results in negative calculated margins of safety for upper "C" and positive margins of safety for lower "C" section.

A comparison of flight ultimate loads to structural static test loads for "C" section is shown in Tables 3.3.6-3 and 3.3.6-4. The static test loads shown for load point 55 resulted in structural failure in the forward region of upper "C" section. The mode of failure was shell buckling. As shown by these values, at station 191.95, the maximum compression ultimate loads are 108% of the test failing loads.

The 44 inch diameter heat shield and Algol III first stage vehicle will require rework of upper "C", 23-002031, for increased load capability and testing of lower "C", 23-001031, for vehicle increased loads.

3.3.6.7. Base "A" and Fins

For the vehicle with the 44 inch diameter heat shield and Algol III first stage the fin size has been increased from the basic Scout vehicle as shown on Figure 2.2.3-1. Fin ultimate reaction loads for the fin to Base "A" attachment points are shown on Figure 3.3.6-2. For comparison, ultimate reaction loads for the fin on the basic Scout 34 inch diameter heat shield vehicle are shown on Figure 3.1.6-2.

Structural analysis of the Base "A" fin support structure shows that the support frame and fitting, 23-001079 and 23-001148 at station 848.075, and the support frame, 23-000093 at station 840.20, are not structurally adequate for fin loads resulting from the 44 inch diameter heat shield and the Algol III first stage. If the redesigned increased area fin requires forward movement of the fin front beam, more extensive rework of Base "A" will be necessary. This is due to the fin front beam support frame being moved forward into the Base "A" access door.

3.3.6.8 Structure Summary

The basic 34 inch diameter heat shield Scout vehicle will require structural changes and additional structural static load testing for use with the 44 inch diameter heat shield and the Algol III first stage. All redesigned components will require static load tests. In addition, some sections of the vehicle will require additional static load tests in order to be qualified for the vehicle increased loads.

The areas of required structural changes and additional static testing are as follows:

(1) Heat shield attachment clamp - redesign and test.

(2) Lower "D" transition section, 23-000067 - insulate section to eliminate aerodynamic heating and test.

(3) X-259 motor case - test case for increased loads.

(4) Upper "C" transition section - redesign and test.

(5) Lower "C" transition section - test section for increased loads.

(6) Base "A" - redesign and test.

(7) Fin - redesign and test.

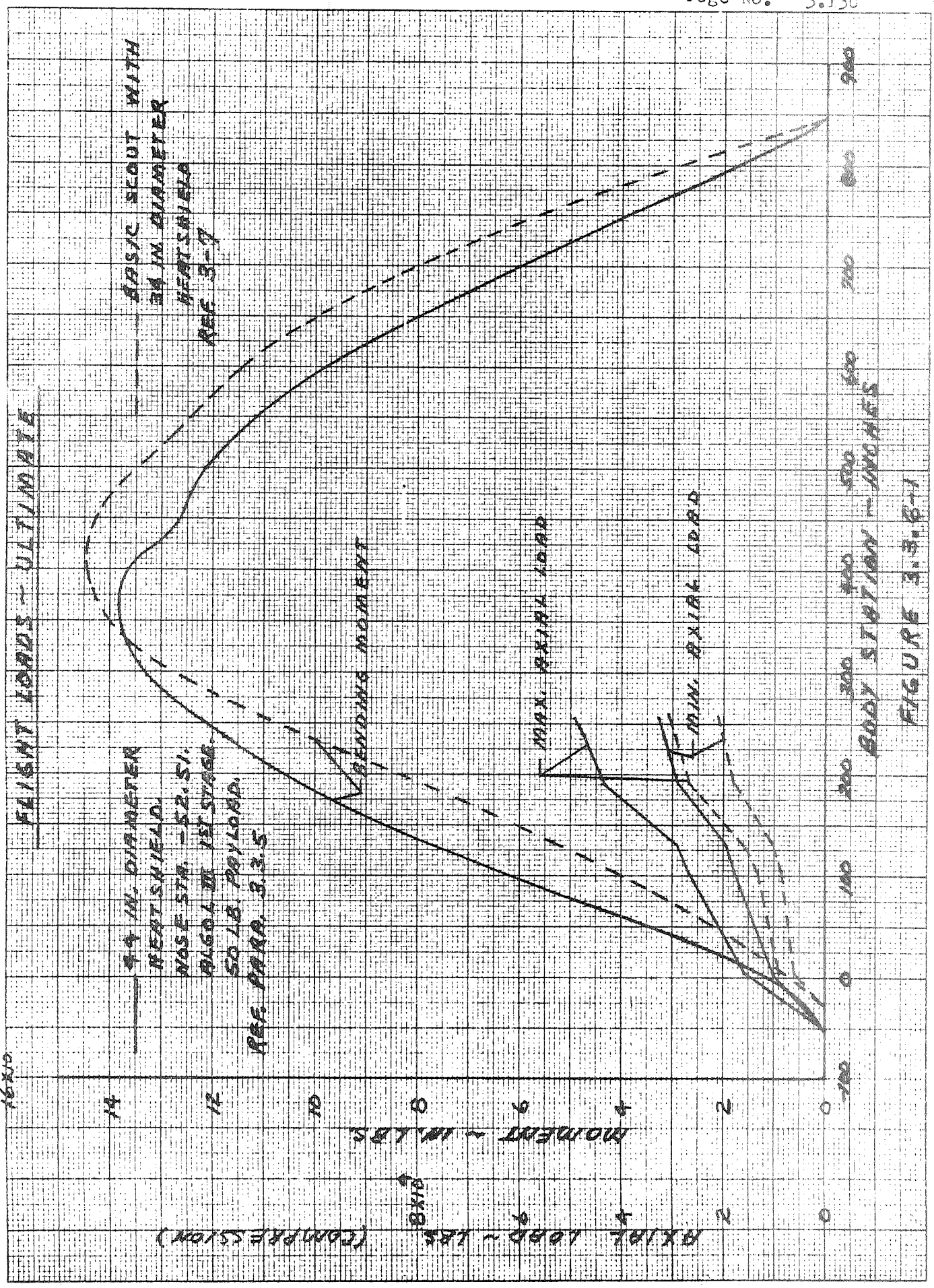

TABLE 3.3.6-1

LOWER "D" TRANSITION SECTION

COMPARISION OF FLIGHT ULTIMATE AND TEST LOADS

		44 Inch Diameter Heat Shield Ultimate Loads	(1) Test Loads	
			Ld. Point (47)	Ld. Point (52)
Station 104.5				
(2)	MOM in. lbs.	650,000	500,680	487,659
(2)	P_{max} lbs.	27,000	40,588	375
(2)	P_{min} lbs.	18,000	- - - -	- - - -
(3)	$P_{Thermal}$ lbs.	13,880	- - - -	- - - -
	f_b psi	± 24,050	± 18,482	± 18,002
	$f_{P\ max}$ psi	- 5,920	- 8,879	- 82
	$f_{P\ min}$ psi	- 3,939	- - - -	- - - -
(3)	f_{TH} psi	- 3,038	- - - -	- - - -
	$f_{c\ max}$ psi	- 33,008	- 27,361	- 18,084
	$f_{t\ max}$ psi	+ 20,111	+ 9,603	+ 17,920
Station 131.1				
(2)	MOM in. lbs.	780,000	584,500	565,000
(2)	P_{max} lbs.	29,250	40,588	375
(2)	P_{min} lbs.	19,500	- - - -	- - - -
(3)	$P_{Thermal}$ lbs.	17,080	- - - -	- - - -
	f_b psi	± 19,725	± 15,853	± 15,324
	$f_{P\ max}$ psi	- 5,397	- 7,872	- 73
	$f_{P\ min}$ psi	- 3,599	- - - -	- - - -
(3)	f_{TH} psi	- 3,154	- - - -	- - - -
	$f_{c\ max}$ psi	- 28,276	- 23,725	- 15,397
	$f_{t\ max}$ psi	+ 16,126	+ 7,981	+ 15,251

(1) Reference 3-8
(2) Reference Figure 3.3.6-1
(3) Reference 3-7

$$f_b = \frac{Mc}{I} \qquad f_c = \frac{P}{A}$$

$$f_{c\ max} = f_b + f_{P\ max} + f_{TH}$$

$$f_{t\ max} = f_b + f_{P\ min}$$

TABLE 3.3.6-2

X-259 MOTOR

COMPARISON OF FLIGHT ULTIMATE AND TEST LOADS

		44 Inch Diameter Heat Shield Ultimate Loads	(1) Test Loads	
			Ld. Point (47)	Ld. Point (52)
Station 131.1				
(2)	MOM in. lbs.	780,000	638,983	617,591
(2)	P_{max} lbs.	29,250	40,588	375
(2)	P_{min} lbs.	19,500	- - - -	- - - -
	W_M lbs/in	± 1,106	± 906	± 876
	$W_{P\ max}$ lbs/in	- 311	- 431	- 4
	$W_{P\ min}$ lbs/in	- 207	- - - -	- - - -
	$W_{c\ max}$ lbs/in	- 1,417	- 1,337	- 880
	$W_{t\ max}$ lbs/in	+ 899	+ 475	+ 872
Station 191.95				
(2)	MOM in. lbs.	1,035,000	955,343	914,843
(2)	P_{max} lbs	43,000	40,588	375
(2)	P_{min} lbs.	29,000	- - - -	- - - -
	W_M lbs/in	± 1,468	± 1,355	± 1,297
	$W_{P\ max}$ lbs/in	- 462	- 431	- 4
	$W_{P\ min}$ lbs/in	- 308	- - - -	- - - -
	$W_{c\ max}$ lbs/in	- 1,930	- 1,786	- 1,301
	$W_{t\ max}$ lbs/in	+ 1,160	+ 924	+ 1,293

(1) Reference 3-8

(2) Reference Figure 3.3.6-1

$W_M = \frac{M}{\pi R^2}$ Where R is radius of shell

$W_P = \frac{P}{\pi D}$ Where D is diameter of shall

$W_{c\ max}$ = Maximum compressive load

$W_{t\ max}$ = Maximum tensile load

TABLE 3.3.6-3

UPPER "C" TRANSITION SECTION

COMPARISON OF FLIGHT ULTIMATE AND TEST LOADS

		44 Inch Diameter Heat Shield Ultimate Loads	(1) Test Loads	
			Ld. Point (52)	Ld. Point (55)
Station 191.95				
(2)	MOM in. lbs.	1,035,000	914,843	995,845
(2)	P_{max} lbs.	43,500	375	35,821
(2)	P_{min} lbs.	29,000	- - - -	- - - -
	W_M lbs/in	± 1,407	± 1,244	± 1,354
	$W_{P\ max}$ lbs/in	- 452	- 4	- 372
	$W_{P\ min}$ lbs/in	- 330	- - - -	- - - -
	$W_{c\ max}$ lbs/in	- 1,859	- 1,248	- 1,726
	$W_{t\ max}$ lbs/in	+ 1,077	+ 1,240	+ 982
Station 238.18				
(2)	MOM in. lbs.	1,180,000	1,140,676	1,250,156
(2)	P_{max} lbs.	47,625	375	35,821
(2)	P_{min} lbs.	31,750	- - - -	- - - -
	W_M lbs/in	± 1,465	± 1,416	± 1,552
	$W_{P\ max}$ lbs/in	- 473	- 4	- 356
	$W_{P\ min}$ lbs/in	- 316	- - - -	- - - -
	$W_{c\ max}$ lbs/in	- 1,938	- 1,420	- 1,908
	$W_{t\ max}$ lbs/in	+ 1,149	+ 1,412	+ 1,196

(1) Reference 3-8

(2) Reference Figure 3.3.6-1

$W_M = \frac{M}{\pi R^2}$ Where R is radius of shell

$W_P = \frac{P}{\pi D}$ Where D is diameter of shell

$W_{c\ max}$ = Maximum compressive load

$W_{t\ max}$ = Maximum tensile load

TABLE 3.3.6-4

LOWER "C" TRANSITION SECTION

COMPARISON OF FLIGHT ULTIMATE AND TEST LOADS

		44 Inch Diameter Heat Shield Ultimate Loads	(1) Test Loads Ld. Point (52)	Ld. Point (55)
Station 238.18				
(2)	MOM in. lbs.	1,180,000	1,140,676	1,250,156
(2)	P_{max} lbs.	47,625	375	35,821
(2)	P_{min} lbs.	31,750	- - - -	- - - -
	W_M lbs/in	± 1,462	± 1,413	± 1,549
	$W_{P\ max}$ lbs/in	- 473	- 4	- 356
	$W_{P\ min}$ lbs/in	- 315	- - - -	- - - -
	$W_{c\ max}$ lbs/in	- 1,935	- 1,417	- 1,905
	$W_{t\ max}$ lbs/in	+ 1,147	+ 1,409	+ 1,193
Station 253.06				
(2)	MOM in. lbs.	1,225,000	1,213,365	1,332,011
(2)	P_{max} lbs.	49,500	375	35,821
(2)	P_{min} lbs.	33,000	- - - -	- - - -
	W_M lbs/in	± 1,596	± 1,581	± 1,736
	$W_{P\ max}$ lbs/in	- 502	- 4	- 364
	$W_{P\ min}$ lbs/in	- 335	- - - -	- - - -
	$W_{c\ max}$ lbs/in	- 2,098	- 1,585	- 2,100
	$W_{t\ max}$ lbs/in	+ 1,261	+ 1,577	+ 1,372

(1) Reference 3-8

(2) Reference Figure 3.3.6-1

$W_M = \frac{M}{\pi R^2}$ Where R is radius of shell

$W_P = \frac{P}{\pi D}$ Where D is diameter of shell

$W_{c\ max}$ = Maximum compressive load

$W_{t\ max}$ = Maximum tensile load

FIGURE 3.3.6-2

FIN REACTION LOADS - ULTIMATE

SCOUT WITH 44 INCH DIAMETER HEAT SHIELD AND ALGOL III FIRST STAGE

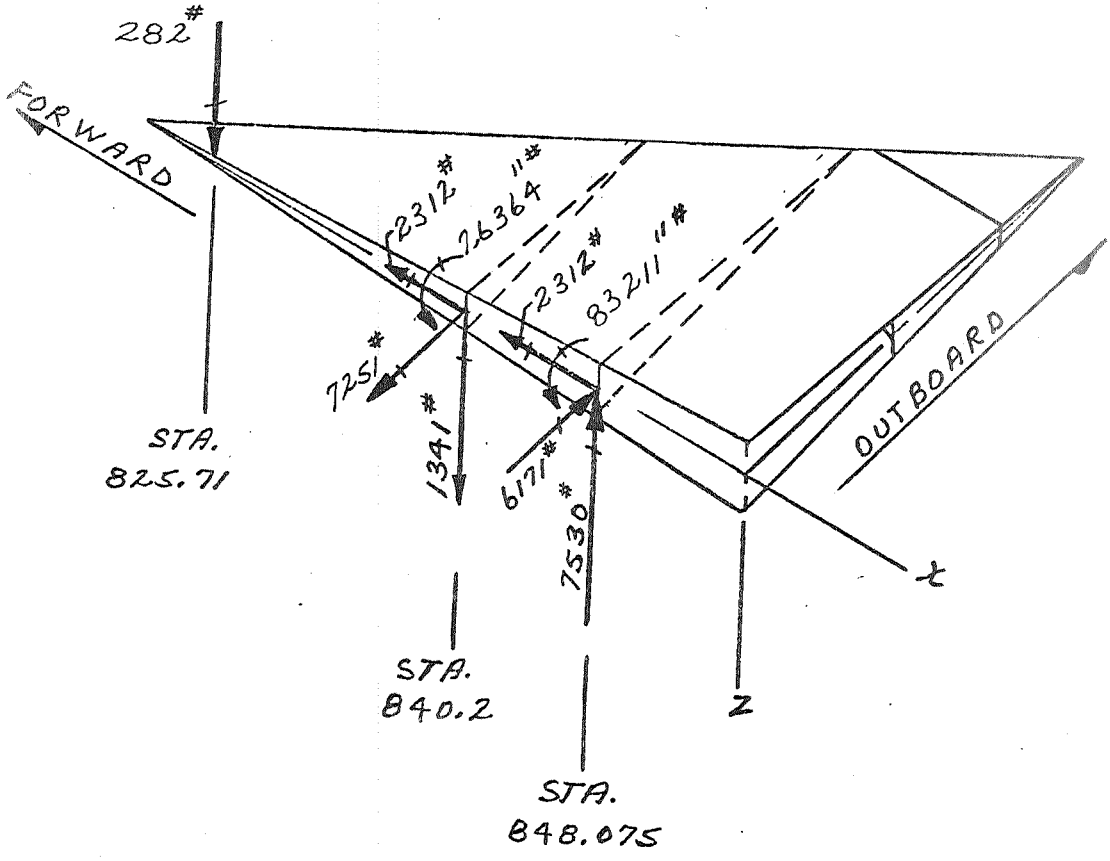

LOADS FROM PARAGRAPH 3.3.5

3.3.7 Ground Support Equipment

The ground support equipment noted in Section 3.1.7 was also reviewed to determine the effects of the 44 inch diameter heatshield with the 8.6 sq. ft. fins. The parts requiring redesign are the same as those noted in paragraphs 3.1.7.1 through 3.1.7.8 plus those noted below.

3.3.7.1 Strap Wrench

The strap wrench used for clamping heatshield halves together will have to have a longer strap installed.

3.3.7.2 Restraint Assembly

The 331-63205-1 restraint assembly will have to be notched on the aft side to clear the fin and redesigned to add the strength back in that was lost due to the notching. This fin will have only 18 inches clearance when on the transporter.

3.3.7.3 The 23-001513-2 Sling Assembly will have to be redesigned to increase cable lengths so that spreader bar will clear fins.

3.3.7.4 The 23-001514-1 Stand Assembly will have to be redesigned to make the base wider to clear the fins when the section is rotated.

3.4 46 INCH DIAMETER HEATSHIELD INSTALLATION

3.4.1 Summary

The results of the impact of 46 inch heatshield installation on the Scout D configuration are summarized as follows:

- The following vehicle structural changes are required: redesign the base A fins to increase the area from 4.5 to 16.0 sq. ft. per fin; redesign base A for increased fin size and loads; redesign lower C transition section; redesign upper C transition section; redesign X-259 motor case; redesign lower D transition section; redesign heatshield attachment clamp.
- Fin control tip area shall be increased from 45 sq. in. to 78 sq. in. (Same as 40, 42 and 44 inch heatshield configurations).
- Jet vane control surface area shall be increased from 35 sq. in. to 41 sq. in. (Same as 40, 42 and 44 inch heatshield configurations).
- Guidance system nominal displacement gain shall be increased from 5.0 to 6.75 deg/deg and the rate to displacement gain ratio shall be 0.4, the same as for the basic Scout.
- The following ground support equipment requires redesign: payload umbilical retract arm, heatshield cradle, dummy heatshield, payload and heatshield hoist, heatshield storage bracket, the upper cradle assembly, strap wrench, vehicle transporter (complete redesign required), and the launcher (significant redesign required).

Detailed discussion of the evaluation is presented in the following paragraphs.

3.4.2 Aerodynamic Characteristics

3.4.2.1 Rigid Vehicle

Normal load distributions aft to station 131.1 are presented in Figures 3.4.2-1 through -4. These data were evaluated using the technique described in Section 3.2.2.1. For load distributions aft of station 131.1, use Figures 3.2.2-11 through -14.

Heatshield drag buildup is presented in Figure 3.4.2-5, and was obtained using the technique described in Section 3.2.2.1 for determining the estimated zero lift drag.

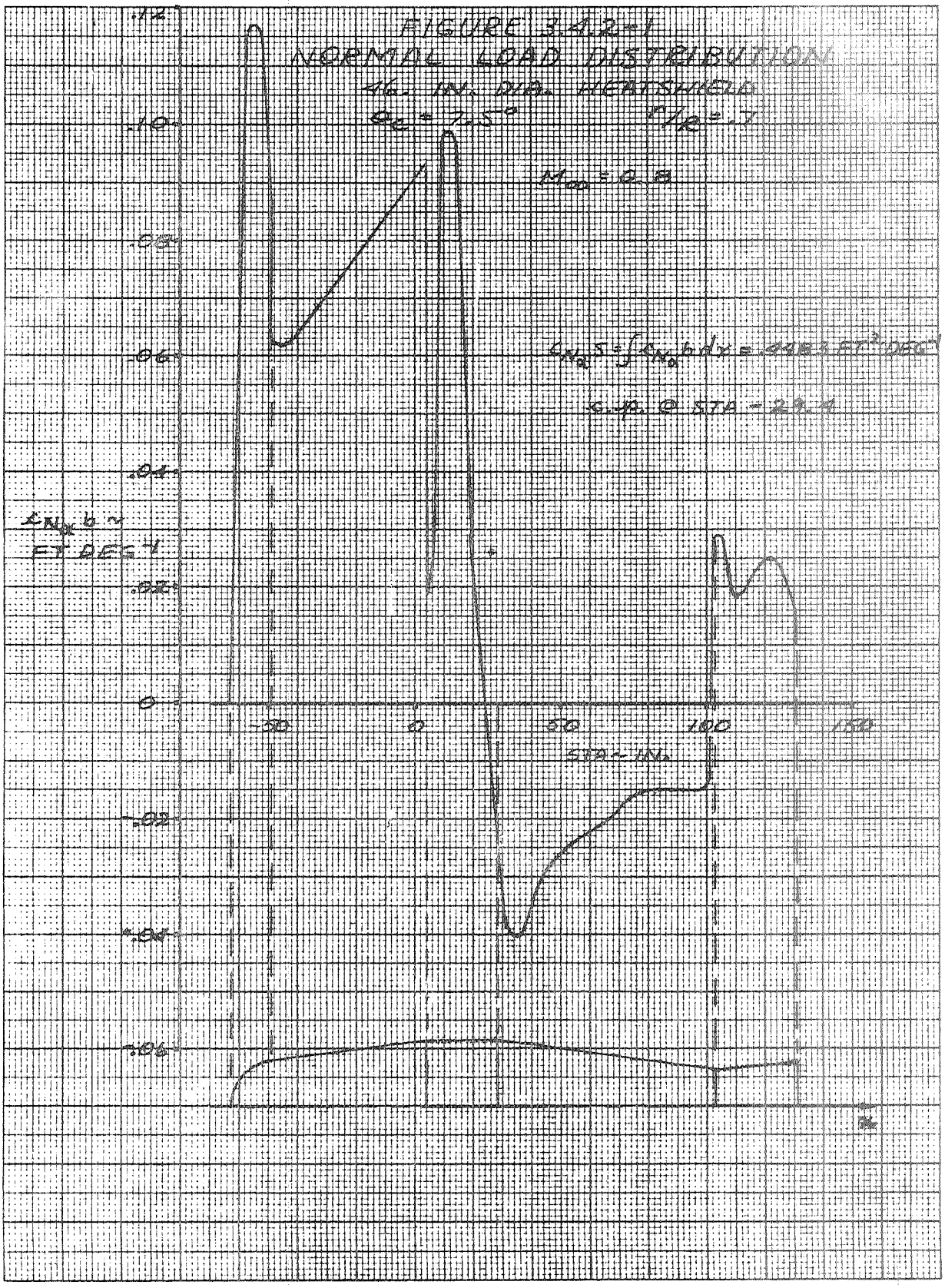
FIGURE 3.4.2-1
NORMAL LOAD DISTRIBUTION
46. IN. DIA. HEATSHIELD
$\theta_c = 7.5°$
$M_\infty = 2.8$
$C_{N_\alpha} S = \int C_{N_\alpha} b\, dx$
C.P. @ STA - 29.4
$C_{N_\alpha} b$
PER DEG
STA - IN.
.12
.10
.08
.06
.04
.02
0
-.02
-.04
-.06
-50
0
50
100
150
R

FIGURE 3.4.2-2
NORMAL LOAD DISTRIBUTION
46. IN. DIA. HEATSHIELD

$\theta_c = 2.5°$ $r/R = .7$

$M_\infty = 1.0$

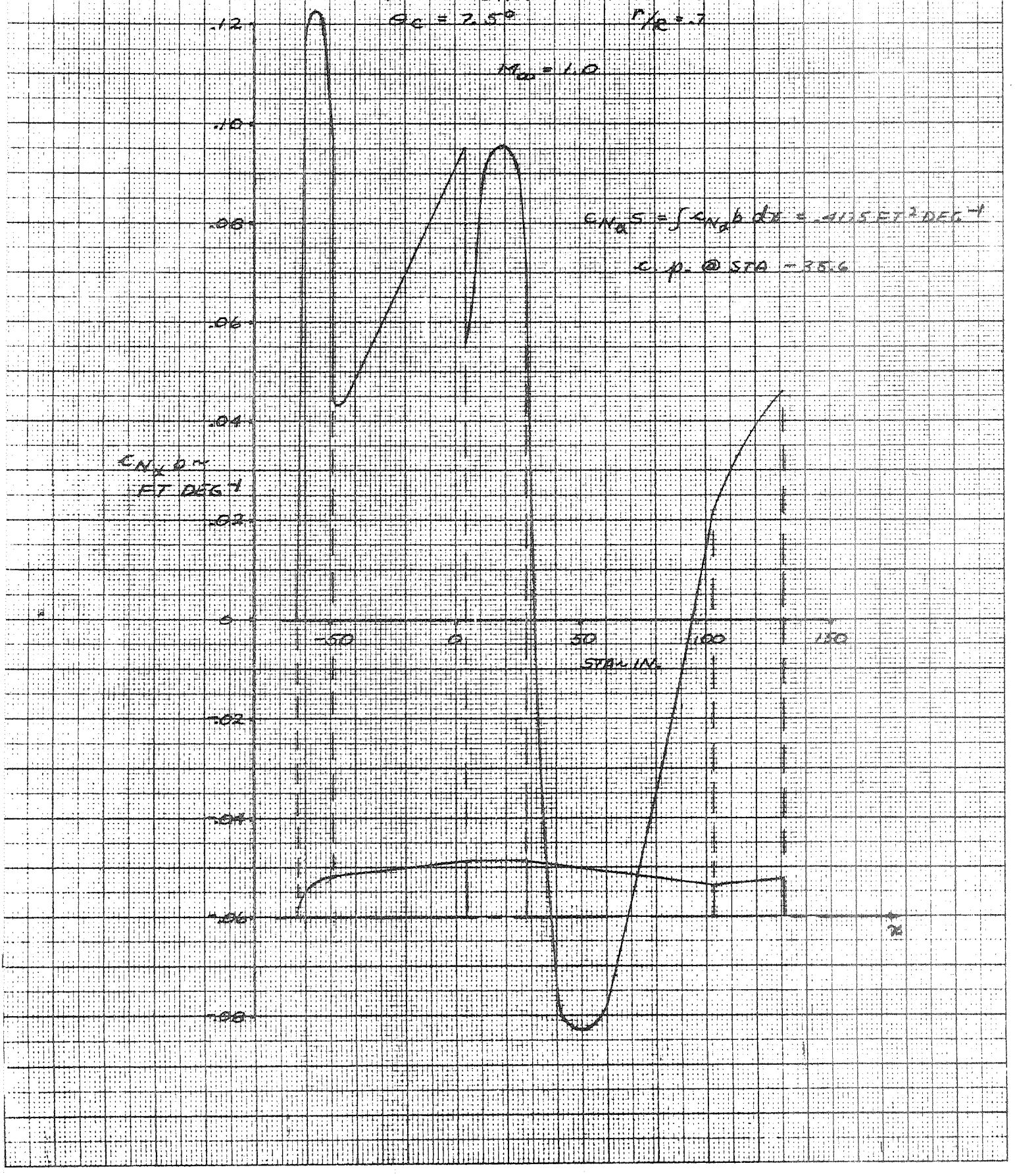

FIGURE 3.4.2-3
NORMAL LOAD DISTRIBUTION
46 IN DIA. HEATSHIELD
$\theta_c = 7.5°$ $r/R = .1$
$M_\infty = 1.5$

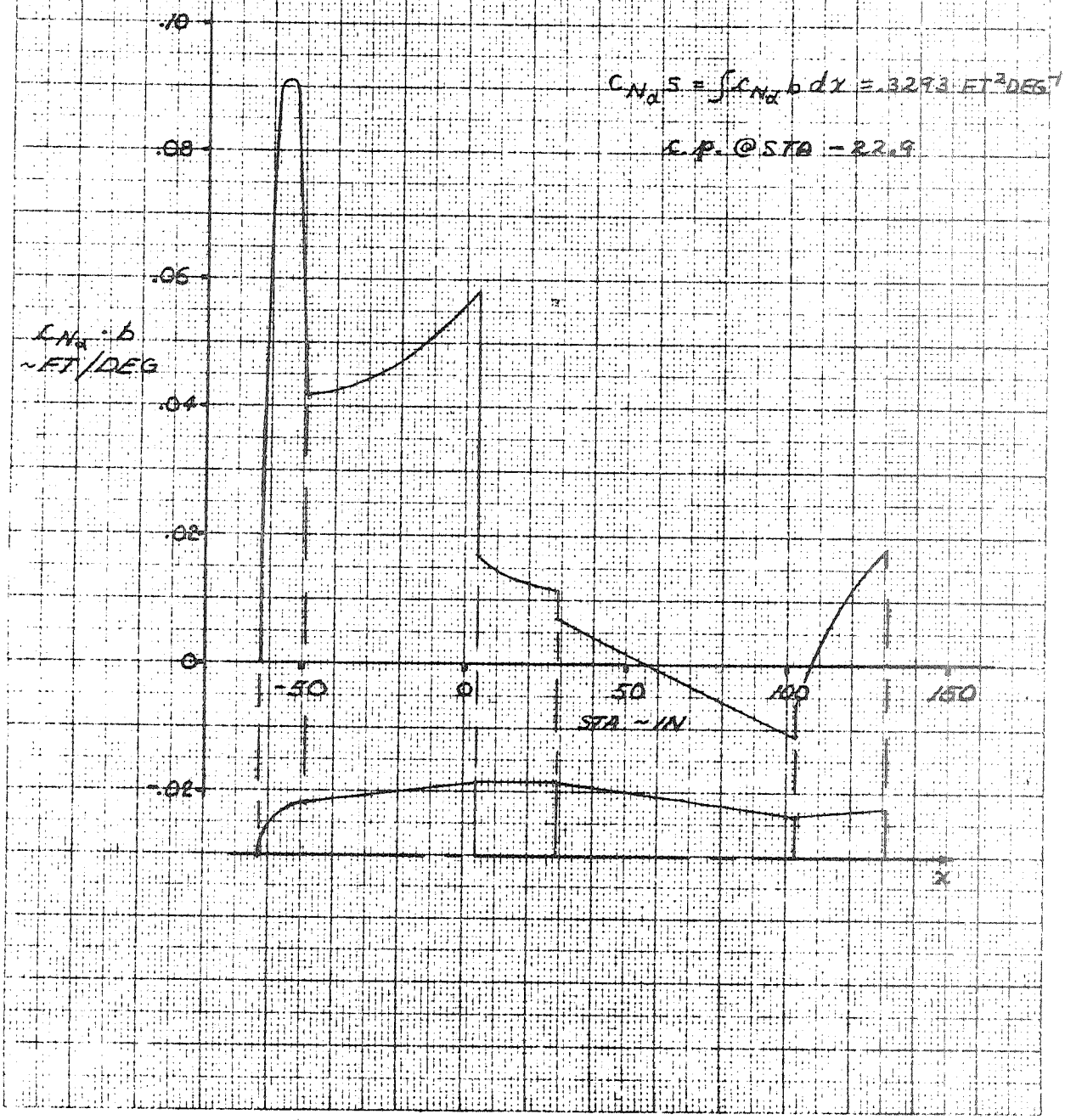

$C_{N_\alpha} S = \int C_{N_\alpha} b\, dx = .3293$ FT²DEG⁻¹

C.P. @ STA = 22.9

MKW
5-16-67

FIGURE 3.4.2-4
NORMAL LOAD DISTRIBUTION
46 IN. DIA. HEAT SHIELD

$\theta_c = 7.5°$ $\quad r/R = .1$

$M_\infty = 2.5$

$C_{N_\alpha S} = .4475$ FT²/DEG

C.P. @ STA -27.16

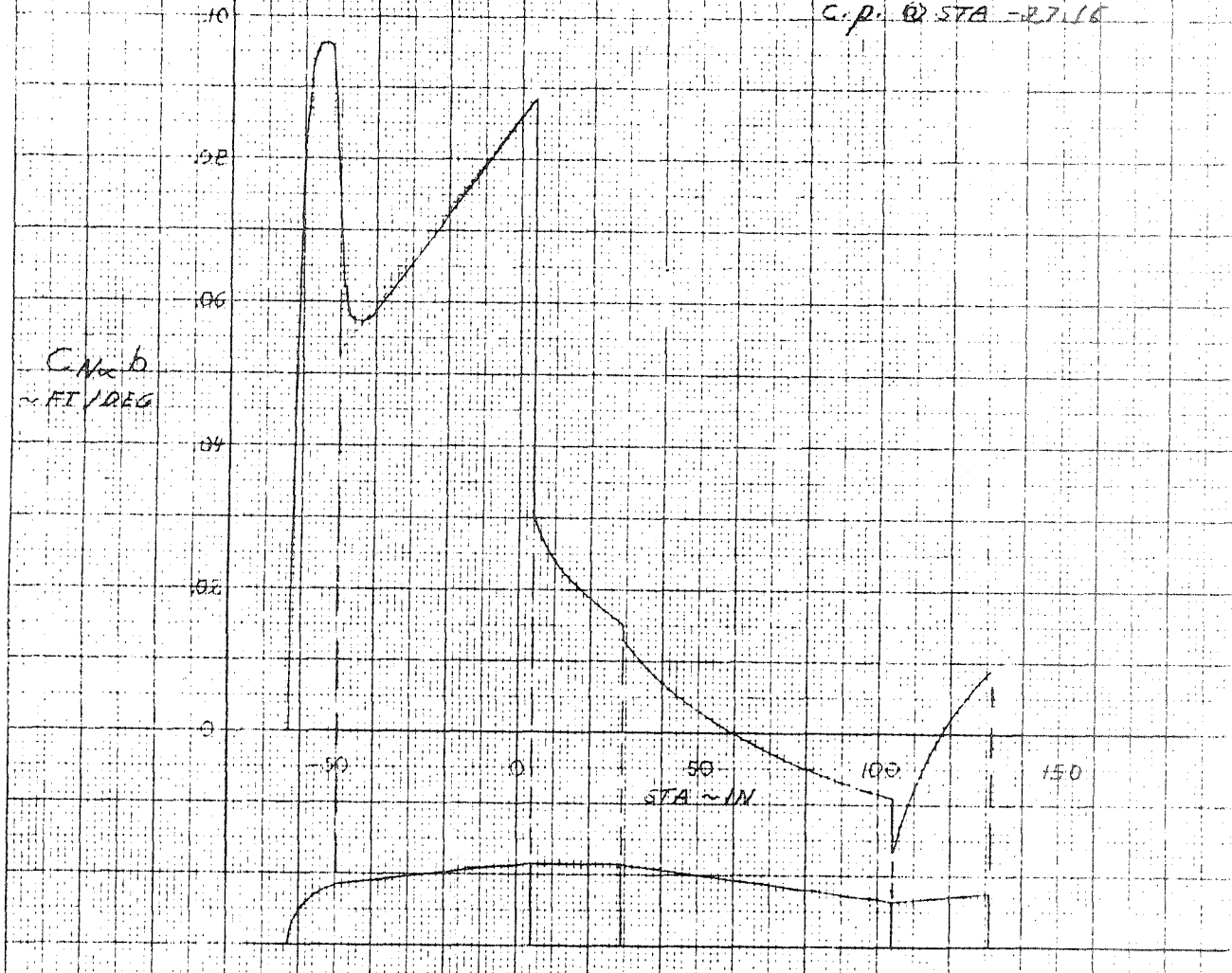

FIGURE 3.4.2-5
HEATSHIELD DRAG BUILDUP
(PRESSURE AND FRICTION)
46. IN. DIA. HEATSHIELD
$\theta_C = 7.5°$ $r/R = .7$

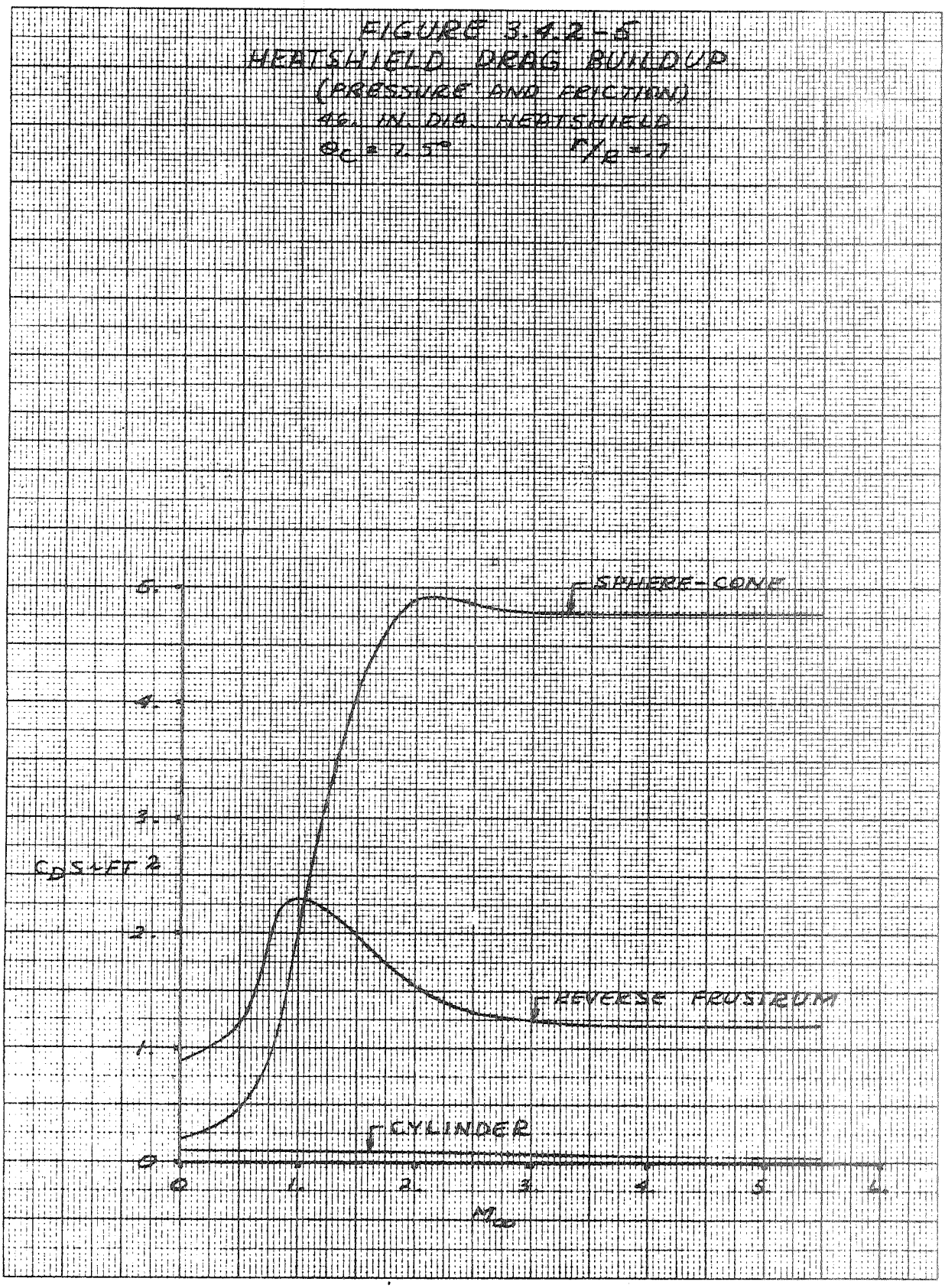

3.4.2.2 Flexible Body Aerodynamics

Discussion on the flexible body aerodynamics for the 46 inch diameter heat shield configuration may be found in Section 3.2.2.2.

3.4.3 Weight and Balance Data

This section presents the weights, longitudinal center of gravity and moments of inertia for a Scout vehicle (S-178 and Sub. configuration) utilizing a 46 inch diameter heatshield and an Algol III (Aerojet Proposal No. 2) first stage motor replacing the standard Algol II first stage motor. The standard Base A and 4.5 sq. ft. fins are included in this data.

The vehicle mass properties data is shown in Table 3.4.3-1 with a 50 pound payload and in Table 3.4.3-2 with a 400 pound payload. A 46 inch diameter heatshield of similar construction to the present 34 inch diameter was estimated to weigh 431.05 pounds with the heatshield c.g. at Station 23.0.

TABLE 3.4.3-1
MASS PROPERTIES

46 INCH DIAMETER, -63.14 LARGE VOLUME HEATSHIELD, (50 POUND PAYLOAD)

VEHICLE S- WEIGHT, X(CG), AND MOMENTS OF INERTIA

VERSUS PERCENT OF FUEL CONSUMED

	TOTAL WEIGHT, POUNDS	C.G. SCOUT STA.-IN.	IXX SLUG-FT^2	IYY OR IZZ SLUG-FT^2
	*******	*******	**********	**********
FOURTH STAGE - BURNOUT	118.96	53.35	2.38	23.82
75 0/0	271.79	60.33	5.00	30.66
50 0/0	424.63	62.28	6.87	35.52
25 0/0	577.46	63.20	8.00	39.68
FOURTH STAGE - IGNITION	730.30	63.74	8.38	43.34
SPIN-UP ITEMS	774.68	65.92	9.37	56.93
THIRD STAGE - BURNOUT	1483.95	116.61	29.45	1287.32
75 0/0	2135.08	130.01	56.88	1545.14
50 0/0	2786.22	137.15	76.77	1710.98
25 0/0	3437.35	141.58	89.11	1834.97
THIRD STAGE - IGNITION	4088.49	144.61	93.90	1935.30
LESS N/C - H/S	6159.25	229.28	181.48	23526.18
SECOND STAGE - BURNOUT	6590.37	215.79	217.06	27458.28
75 0/0	8666.61	246.89	310.21	34610.83
50 0/0	10742.86	265.97	378.19	39530.57
25 0/0	12819.10	278.87	421.07	43296.33
SECOND STAGE - IGNITION	14895.35	288.17	438.82	46385.41
FIRST STAGE - BURNOUT	19179.65	377.64	813.18	176335.69
75 0/0	26162.65	450.05	1474.28	271022.71
50 0/0	33145.65	491.96	1965.05	331354.50
25 0/0	40128.65	519.28	2285.75	375221.74
FIRST STAGE - IGNITION	47111.65	538.50	2436.17	409907.76

TABLE 3.4.3-2
MASS PROPERTIES

46 INCH DIAMETER, -63.14 LARGE VOLUME HEATSHIELD, (400 POUND PAYLOAD)

VEHICLE S- WEIGHT, X(CG), AND MOMENTS OF INERTIA

VERSUS PERCENT OF FUEL CONSUMED

	TOTAL WEIGHT, POUNDS	C.G. SCOUT STA.-IN.	IXX SLUG-FT^2	IYY OR IZZ SLUG-FT^2
	*******	*******	**********	**********
FOURTH STAGE - BURNOUT	468.96	31.44	10.88	51.43
75 0/0	621.79	39.88	13.50	85.34
50 0/0	774.63	44.99	15.37	107.31
25 0/0	927.46	48.41	16.50	123.07
FOURTH STAGE - IGNITION	1080.30	50.86	16.88	135.09
SPIN-UP ITEMS	1124.68	52.87	17.87	159.46
THIRD STAGE - BURNOUT	1833.95	98.93	37.95	1822.64
75 0/0	2485.08	115.08	65.38	2285.66
50 0/0	3136.22	124.52	85.26	2581.34
25 0/0	3787.35	130.72	97.60	2794.04
THIRD STAGE - IGNITION	4438.49	135.10	102.40	2958.63
LESS N/C - H/S	6509.25	218.25	189.98	26549.66
SECOND STAGE - BURNOUT	6940.37	206.12	225.56	30108.02
75 0/0	9016.61	238.24	318.71	38229.37
50 0/0	11092.86	258.34	386.69	43825.30
25 0/0	13169.10	272.10	429.57	48084.37
SECOND STAGE - IGNITION	15245.35	282.11	447.32	51547.64
FIRST STAGE - BURNOUT	19529.65	371.30	821.67	185625.25
75 0/0	26512.65	444.43	1482.78	284565.92
50 0/0	33495.65	487.07	1973.55	347735.90
25 0/0	40478.65	514.99	2294.25	393603.71
FIRST STAGE - IGNITION	47461.65	534.70	2444.67	429768.69

3.4.4 Stability and Control

The stability analysis of the first and second stages with the 46-inch diameter heathsield was performed in the same way as the 40 and 42-inch heatshield configurations discussed in Sections 3.1.4 and 3.2.4. The first stage jet vane and fin tip size as well as control system gains were selected to be the same as for the 40 and 42-inch heatshield configurations. The basic differences of the 46-inch heatshield configuration lies in the fin size required for stability and the second stage control limitations.

3.4.4.1 First Stage Stability Near Maximum Dynamic Pressure

The stability of the 46-inch diameter heatshield Algol III configuration was analyzed at the critical flight time of 45 seconds by a parametric procedure involving fin size and control tip size variations. The gain boundaries are presented as a function of fin area and tip size in Figure 3.4.4-1. The allowable gain boundaries based on a ±6 decibel gain margin are also shown in this figure. The minimum fin size required to stabilize this configuration is 16 square feet. Based on jet vane area of 41 square inches and a 78 square inch fin tip area, the attitude displacement gain (K_D) should be about 6.75 degrees of control surface deflection per degree of attitude error in pitch and yaw. The root loci for this configuration is presented in Figure 3.4.4-2. The root loci of the second, third and fourth bending modes of vibration for this configuration are shown in Figure 3.2.4-4.

3.4.4.2 Vehicle-Launcher Clearance

The fin area required for this configuration is 16 square feet for a 45 degree sweep angle with a straight trailing edge. The configuration is shown in Figure 2.2.3-1. The semi-span of this fin configuration is 27 inches greater than the 42-inch heatshield configuration and would interfere with the launcher. The launcher-vehicle relationship is presented for the 42-inch

FIGURE 3.4.4-1
GAIN BOUNDARIES VERSUS FIN SIZE
46 INCH HEATSHIELD - ALGOL III

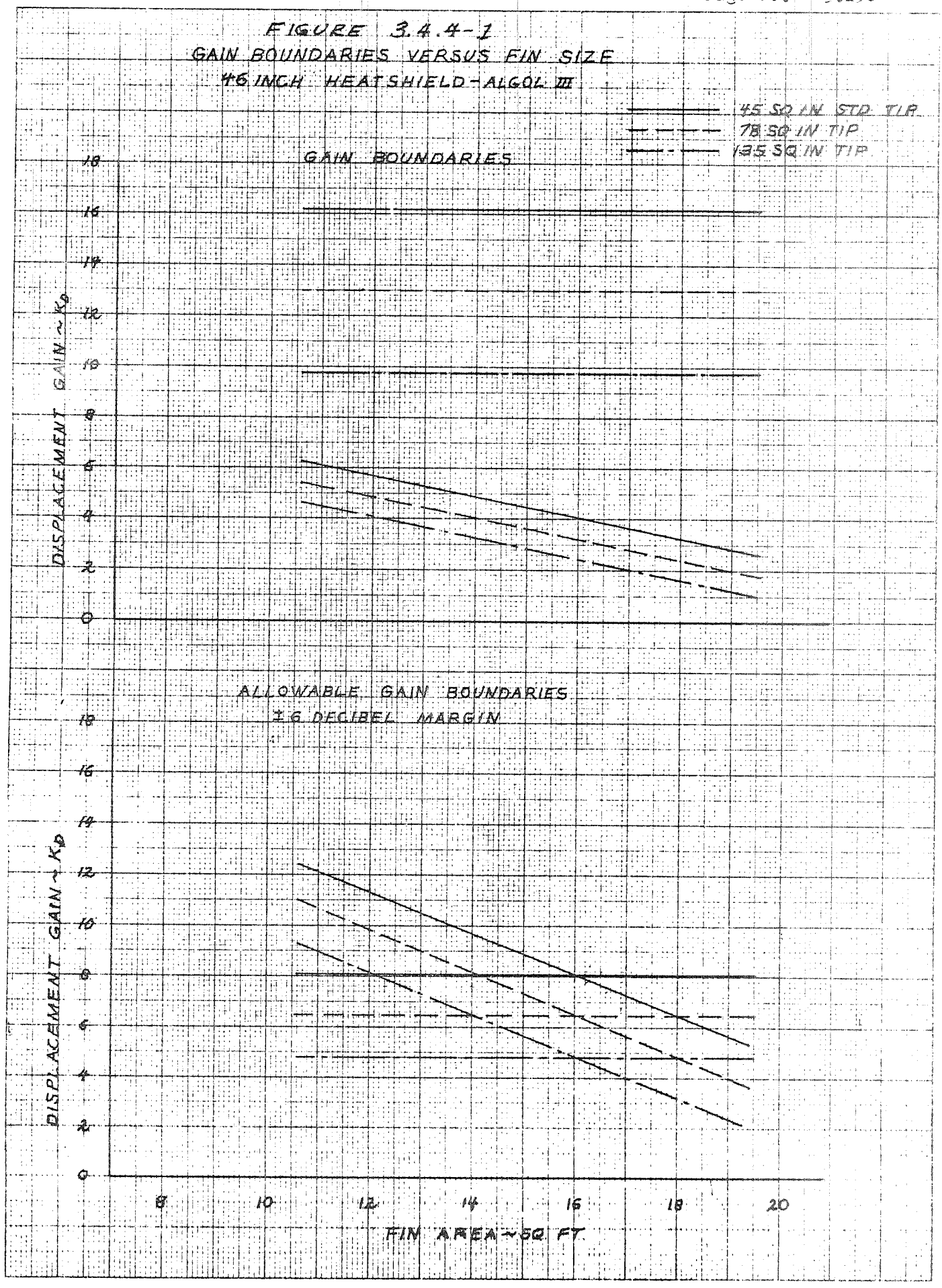

FIGURE 3.4.4-2
SCOUT LARGER HEATSHIELD STUDY
ROOT LOCI AT 45 SECONDS - 46 INCH HEATSHIELD
ALGOL III CONFIGURATION
41 IN² JET VANE
78 IN² FIN TIP
16 FT² FIN

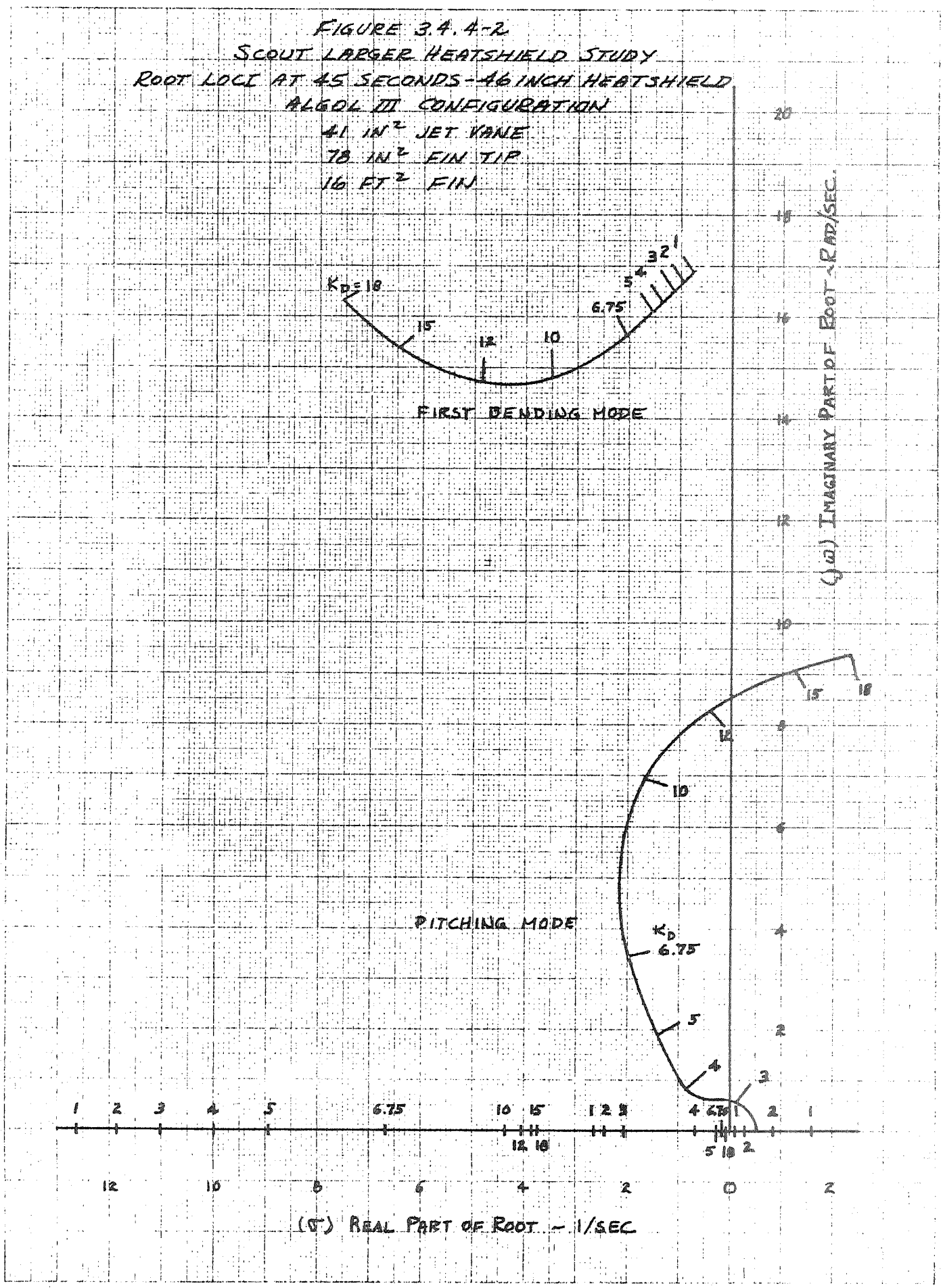

heatshield configuration in Figure 3.2.4-8. In order to accomodate this fin configuration modifications to the launcher and associated GSE would be required. These changes are discussed in Section 3.4.7.

3.4.4.3 Second Stage Ignition Dynamic Pressure

The dynamic pressure allowable at second stage ignition was determined by raticing the aerodynamic moment coefficient slope of the 46 inch heatshield configuration to that of the 42 inch heatshield configuration and reducing the dynamic pressure accordingly. This keeps the aerodynamic disturbing moment equal to that determined in the 42 inch heatshield analysis. The resulting dynamic pressure allowable at second stage ignition for the 46 inch diameter heatshield Algol III configuration is 50 psf for orbital missions and 44 psf for reentry missions.

3.4.4.4 The second stage boost fuel consumption and coast times were calculated by the same procedure used for the 42 inch heatshield configuration discussed in Section 3.1.4. Based on an ignition dynamic pressure of 40 psf the boost fuel consumption at the 99.5 percent probability level is 90.7 pounds. For reentry missions with an ignition dynamic pressure of 35 psf the boost fuel consumption will be 92.4 pounds. The second stage coast time capability with this heatshield is presented in Figure 3.4.4-3. If ignition dynamic pressure is increased to the maximum allowable, boost fuel consumption will increase by about 7.6 pounds and coast time will be reduced to that presented in Figure 3.2.4-15.

FIGURE 3.4.4-3

SCOUT LARGER HEATSHIELD STUDY

SECOND STAGE COAST TIME VERSUS USABLE CONTROL FUEL
46 IN HEATSHIELD - ALGOL III - 50 LB PAYLOAD
99.5 PERCENT PROBABILITY, 95 PERCENT CONFIDENCE

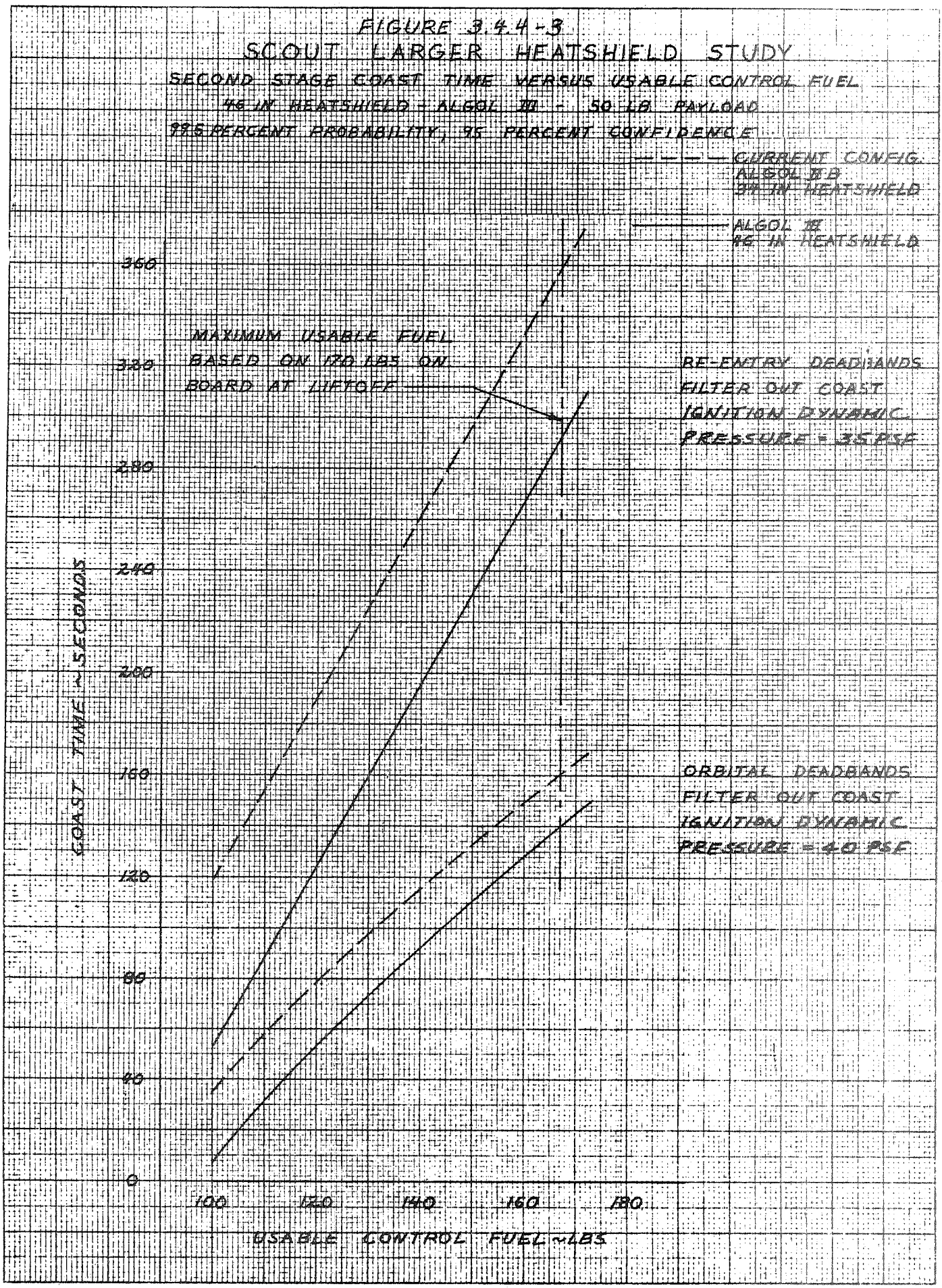

3.4.5 Flight Loads

3.4.5.1 Vehicle Loads

Figures 3.4.5.1-1 and 3.4.5.1-2 present the bending moments due to gust and winds and axial loads for the 46 inch heatshield configuration. The technique used and description of the vehicle is the same as discussed in paragraph 3.1.5.1.

3.4.5.2 Fin Loads

The fin attach loads for the critical flight condition are presented in Figure 3.1.5.2-1. The assumptions and methods used in determining these loads may be found in paragraph 3.1.5.2.

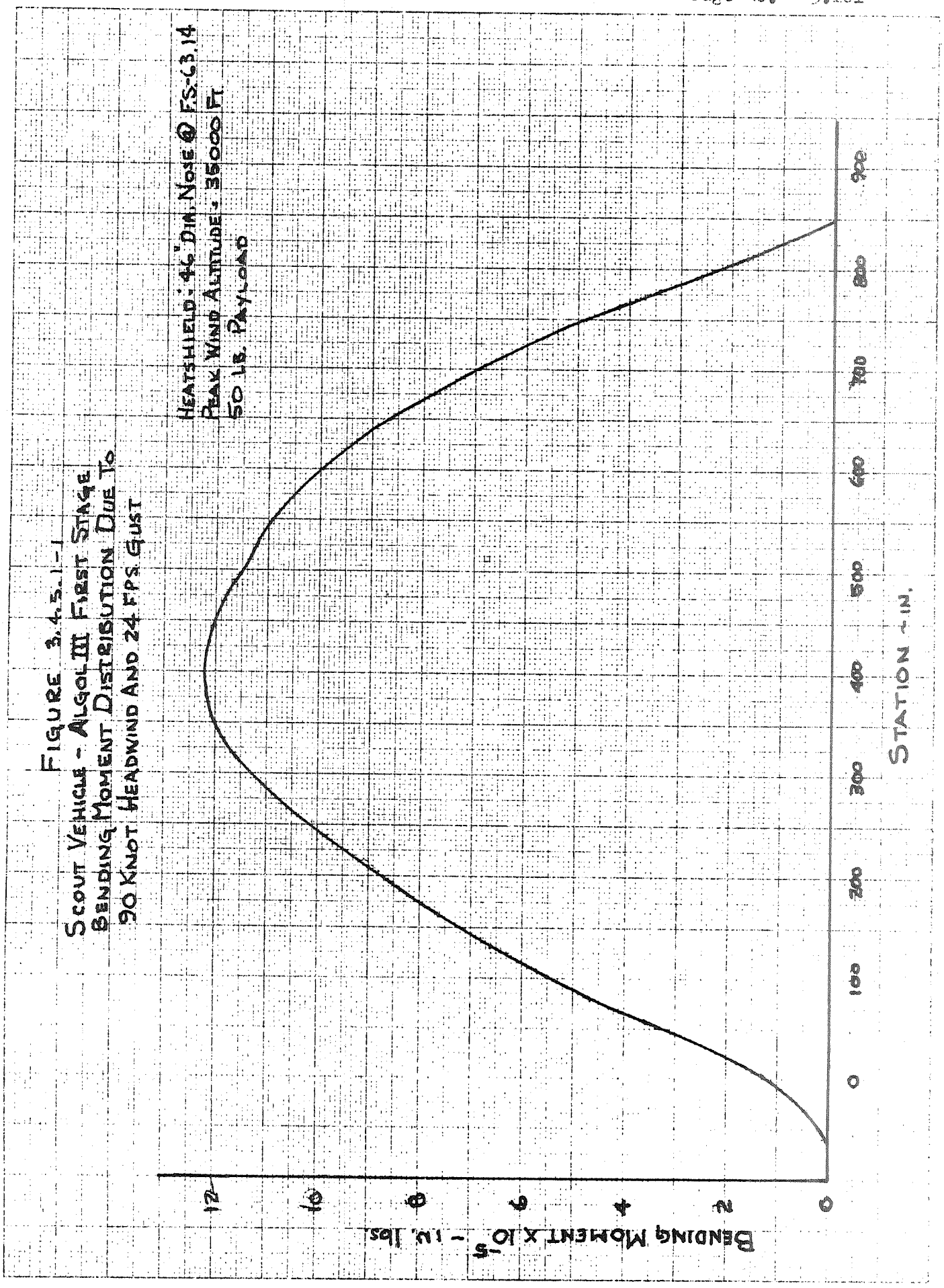

FIGURE 3.4.5.1-1
SCOUT VEHICLE - ALGOL III FIRST STAGE
BENDING MOMENT DISTRIBUTION DUE TO
90 KNOT HEADWIND AND 24 FPS GUST

FIGURE 3.4.5.1-2
SCOUT VEHICLE - ALGOL III FIRST STAGE
AXIAL LOAD DISTRIBUTION FOR
90 KNOT HEADWIND

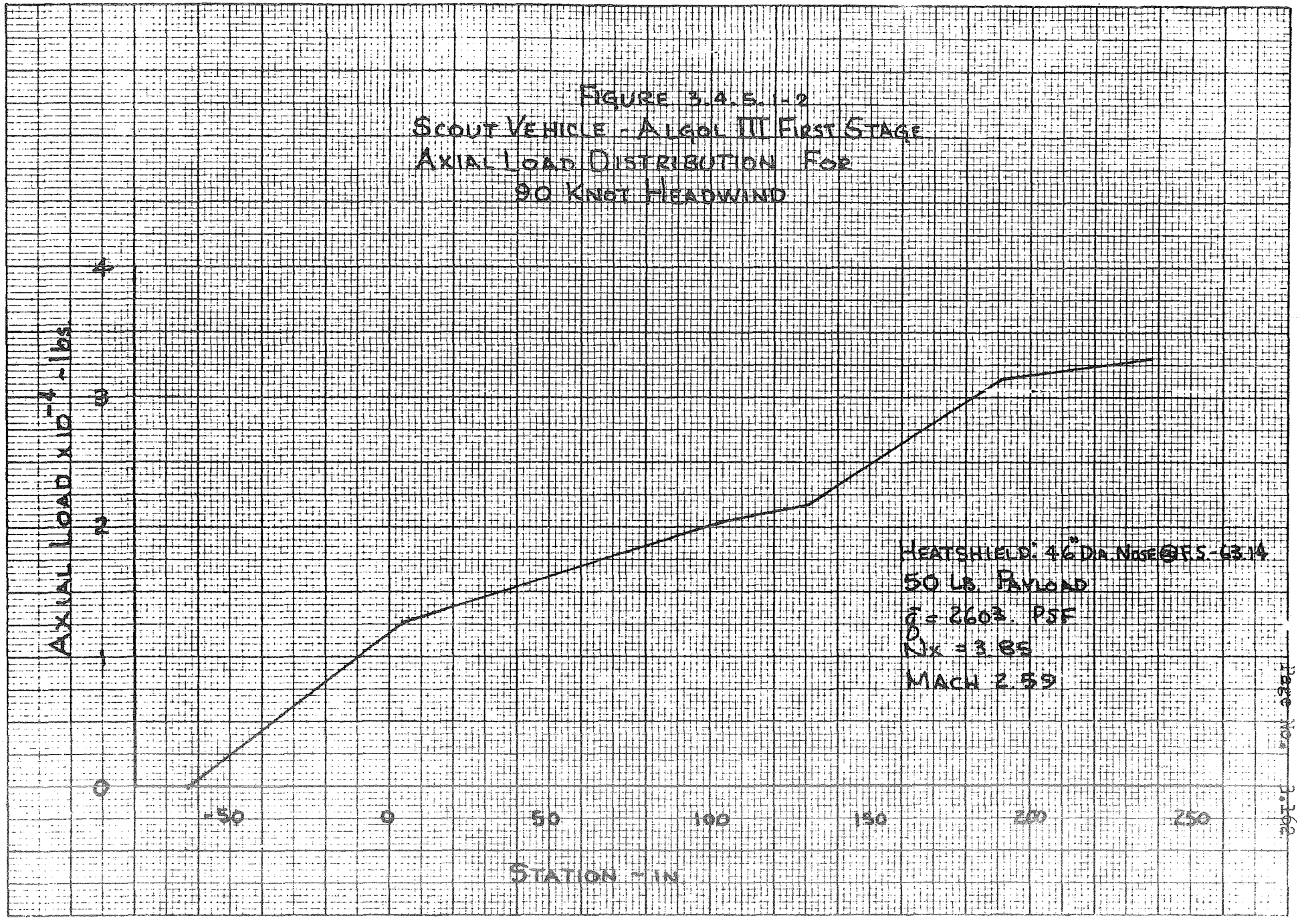

3.4.6 Vehicle Structure

3.4.6.1 Design Criteria

The structural design criteria is as defined in paragraph 3.1.6.1.

3.4.6.2 Loads

Plots of vehicle flight ultimate loads with the 46 inch diameter heat shield and Algol III first stage are shown on Figure 3.4.6-1. For comparison, of flight loads for the basic Scout vehicle with the 34 inch diameter heat shield are also shown.

3.4.6.3 Heat Shield Attachment Clamp

The basic Scout 34 inch diameter heat shield attachment clamp is designed for an ultimate tension load in the clamp of 7,600 pounds, Reference 3-7. Vehicles loads of 820,000 inch pounds bending moment and 20,500 pounds axial load at station 103.69 for the 46 inch diameter heat shield, Reference Figure 3.4.6-1, result in an ultimate tension load in the attachment clamp of 13,459 pounds. This is a 77% increase over the ultimate design load of the 23-002204 heat shield attachment clamp. All components of the 23-002204 clamp have a calculated margin of safety less than 77% for the 7,600 pound load, Reference 3-7. Therefore for use with the 46 inch diameter heat shield the 23-002204 attachment clamp will require a redesign to increase the load capability of the clamp.

3.4.6.4 Lower "D" Transition Section

The location of the lower "D" transition section in the vehicle and the thermal loads in the section are discussed in paragraph 3.1.6.5.

A review of the lower "D" transition section structure was made using the analyses and thermal loads from Reference 3-7 and flight loads from Figure 3.4.6-1. The combined thermal and flight loads result in calculated negative margins of safety for the section. Elimination of the thermal loads in the section by insulation still gives calculated negative margins of safety for lower "D" section.

A comparison of flight ultimate loads plus thermal loads to structural static test loads for the section is shown in Table 3.4.6-1. As shown by these values, even if the thermal loads are eliminated the ultimate loads will be much higher than test loads. At station 104.5 assuming no thermal loads, maximum compression ultimate loads are 136% of test loads and maximum tension ultimate loads are 144% of test loads. At station 131.1, assuming no thermal loads, maximum compression ultimate loads are 129% of test loads and maximum tension ultimate loads are 135% of test loads. Although the lower "D" transition section test loads did not produce failure, analysis of the section indicates that the section is not structurally adequate for use with the 46 inch diameter heat shield and Algol III first stage with loads as shown on Figure 3.4.6-1.

3.4.6.5 X-259 Motor

The shell stability of the X-259 motor was analyzed by two different methods, References 3-15 and 3-16. Both methods resulted in calculated negative margins of safety for loads from Figure 3.4.6-1.

A comparison of flight ultimate loads to structural static test loads is shown in Table 3.4.6-2. As shown by these values, at station 131.1 the maximum compression ultimate loads are 129% of test loads and the maximum tension ultimate loads are 131% of test loads. At station 191.95 the maximum compression ultimate loads are 130% of test loads and the maximum tension ultimate loads are 115% of test loads. Although the test loads shown in Table 3.4.6-2 did not produce failure of the X-259 motor case, analysis indicates that the motor case is not structurally adequate for use with the 46 inch diameter heat shield and the Algol III first stage with loads shown on Figure 3.4.6-1.

3.4.6.6 Upper and Lower "C" Transition Sections

A review of the "C" transition sections using analyses from Reference 3-7 and loads from Figure 3.4.6-1 resulted in calculated negative margins of safety for both upper and lower "C" sections.

A comparison of ultimate loads and structural static test loads for the section is shown in Tables 3.4.6-3 and 3.4.6-4. As shown by these values, at station 191.95, the maximum compression ultimate loads are 129% of test loads and maximum tension ultimate loads are 115% of test loads. Test loads shown for load point 55 produced failure in the forward end of upper "C" section. The mode of failure was shell buckling due to compression loads. For lower "C" section the maximum compression ultimate load are 122% of test loads. Therefore both analysis and static tests show that upper and lower "C" transition sections, 23-002031 and 23-001031, are not structurally adequate for use with the 46 inch diameter heat shield and Algol III first stage with loads shown on Figure 3.4.6-1.

3.4.6.7 Base "A" and Fins

For the vehicle with the 46 inch diameter heat shield and Algol III first stage the fin size has been increased from the basic Scout vehicle as shown on Figure 2.2.3-1. Fin ultimate reaction loads for the fin to Base "A" attachment points are shown on Figure 3.4.6-2. For comparison, ultimate reaction loads for the fin on the basic Scout 34 inch diameter heat shield vehicle are shown on Figure 3.1.6-2.

Structural analysis of the Base "A" fin support structure shows that the support frame and fittings 23-001079 and 23-001148 at station 848.075 and the support frame and fitting 23-000093 and 23-001151, at station 840.20 are not structurally adequate for fin loads resulting from the 46 inch diameter heat shield and the Algol III first stage. If the redesigned increased area fin requires forward movement of the fin front beam, more extensive rework of Base "A" will be necessary. This is due to the fin front beam support frame being moved forward into the Base "A" access doors.

3.4.6.8 Structure Summary

The basic 34 inch diameter heat shield Scout vehicle will require structural changes in many sections for use with the 46 inch diameter heat shield and Algol III first stage. All redesigned components will require static load tests.

The areas of required structural redesign are as follows:

(1) Heat shield attachment clamp.

(2) Lower "D" transition section.

(3) X-259 motor case.

(4) Upper "C" transition section.

(5) Lower "C" transition section.

(6) Base "A".

(7) Fin

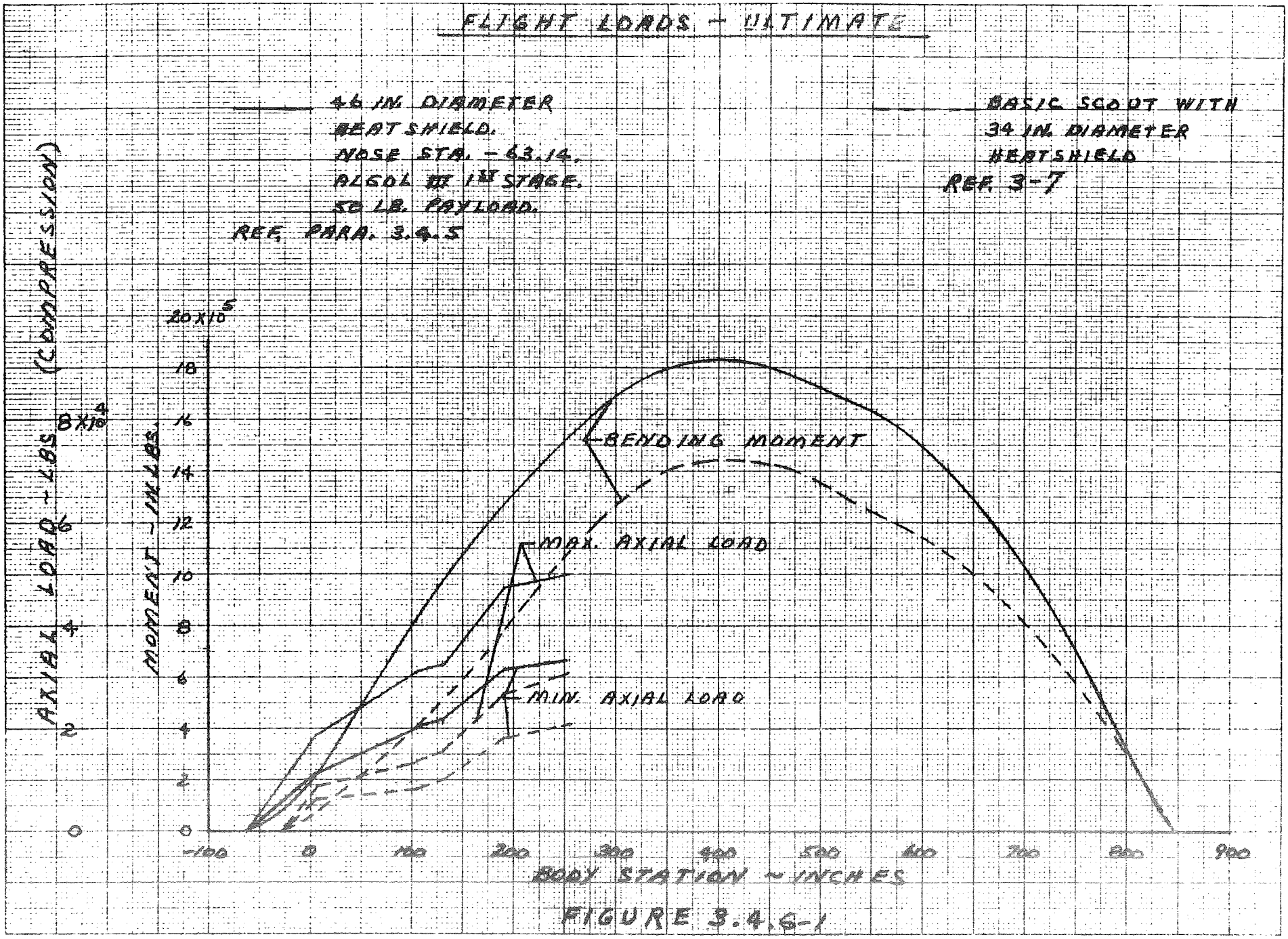
FLIGHT LOADS - ULTIMATE
46 IN. DIAMETER
HEAT SHIELD.
NOSE STA. - 63.14.
ALCOL III 1ST STAGE.
50 LB. PAYLOAD.
REF. PARA. 3.4.5
BASIC SCOUT WITH
34 IN. DIAMETER
HEATSHIELD
REF. 3-7
AXIAL LOAD - LBS. (COMPRESSION)
MOMENT - IN. LBS.
BENDING MOMENT
MAX. AXIAL LOAD
MIN. AXIAL LOAD
BODY STATION - INCHES
-100
0
100
200
300
400
500
600
700
800
900

FIGURE 3.4.6-1

TABLE 3.4.6-1

LOWER "D" TRANSITION SECTION

COMPARISON OF FLIGHT ULTIMATE AND TEST LOADS

		46 Inch Diameter Heat Shield Ultimate Loads	(1) Test Loads Ld. Point (47)	Ld. Point (52)
Station 104.5				
(2)	MOM in lbs.	820,000	500,680	487,659
(2)	P_{max} lbs	30,750	40,588	375
(2)	P_{min} lbs	20,500	- - - -	- - - -
(3)	$P_{Thermal}$ lbs.	13,880	- - - -	- - - -
	f_b psi	± 30,340	± 18,482	± 18,002
	$f_{P\ max}$ psi	- 6,740	- 8,879	- 82
	$f_{P\ min}$ psi	- 4,486	- - - -	- - - -
(3)	f_{TH} psi	- 3,038	- - - -	- - - -
	$f_{c\ max}$ psi	- 40,118	- 27,361	- 18,084
	$f_{t\ max}$ psi	+ 25,854	+ 9,603	+ 17,920
Station 131.1				
(2)	MOM in lbs.	970,000	584,500	565,000
(2)	P_{max} lbs.	32,550	40,588	375
(2)	P_{min} lbs.	21,700	- - - -	- - - -
(3)	$P_{Thermal}$ lbs.	17,080	- - - -	- - - -
	f_b psi	± 24,529	± 15,853	± 15,324
	$f_{P\ max}$ psi	- 6,006	- 7,872	- 73
	$f_{P\ min}$ psi	- 4,007	- - - -	- - - -
(3)	f_{TH} psi	- 3,154	- - - -	- - - -
	$f_{c\ max}$ psi	- 33,689	- 23,725	- 15,397
	$f_{t\ max}$ psi	+ 20,522	+ 7,981	+ 15,251

(1) Reference 3-8
(2) Reference Figure 3.4.6-1
(3) Reference 3-7

$$f_b = \frac{Mc}{I} \qquad f_c = \frac{P}{A}$$

$$f_{c\ max} = f_b + f_{P\ max} + f_{TH}$$

$$f_{t\ max} = f_b + f_{P\ min}$$

TABLE 3.4.6-2

X-259 MOTOR

COMPARISON OF FLIGHT ULTIMATE AND TEST LOADS

		46 Inch Diameter Heat Shield Ultimate Loads	(1) Test Loads Ld. Point (47)	Ld. Point (52)
Station 131.1				
(2)	MOM in lbs.	970,000	638,983	617,571
(2)	P_{max} lbs.	32,550	40,588	375
(2)	P_{min} lbs.	21,700	- - - -	- - - -
	W_M lbs/in	± 1,375	± 906	± 876
	$W_{P\ max}$ lbs/in	- 346	- 431	- 4
	$W_{P\ min}$ lbs/in	- 231	- - - -	- - - -
	$W_{c\ max}$ lbs/in	- 1,721	- 1,337	- 880
	$W_{t\ max}$ lbs/in	+ 1,144	+ 475	+ 872
Station 191.95				
(2)	MOM in lbs.	1,280,000	955,343	914,843
(2)	P_{max} lbs.	47,100	40,588	375
(2)	P_{min} lbs.	31,400	- - - -	- - - -
	W_M lbs/in	± 1,815	± 1,355	± 1,297
	$W_{P\ max}$ lbs/in	- 500	- 431	- 4
	$W_{P\ min}$ lbs/in	- 334	- - - -	- - - -
	$W_{c\ max}$ lbs/in	- 2,315	- 1,786	- 1,301
	$W_{t\ max}$ lbs/in	+ 1,481	+ 924	+ 1,293

(1) Reference 3-8

(2) Reference Figure 3.4.6-1

$W_M = \frac{M}{\pi R^2}$ Where R is radius of shell

$W_P = \frac{P}{\pi D}$ Where D is diameter of shell

$W_{c\ max}$ = Maximum compressive load

$W_{t\ max}$ = Maximum tensile load

TABLE 3.4.6-3

UPPER "C" TRANSITION SECTION

COMPARISON OF FLIGHT ULTIMATE AND TEST LOADS

		46 Inch Diameter Heat Shield Ultimate Loads	(1) Test Loads Ld. Point (52)	Ld. Point (55)
Station 191.95				
(2)	MOM in lbs.	1,280,000	914,843	995,845
(2)	P_{max} lbs.	47,100	375	35,821
(2)	P_{min} lbs.	31,400	- - - -	- - - -
	W_M lbs/in	± 1,741	± 1,244	± 1,354
	$W_{P\ max}$ lbs/in	- 490	- 4	- 372
	$W_{P\ min}$ lbs/in	- 327	- - - -	- - - -
	$W_{c\ max}$ lbs/in	- 2,231	- 1,248	- 1,726
	$W_{t\ max}$ lbs/in	+ 1,414	+ 1,240	+ 982
Station 238.18				
(2)	MOM in lbs.	1,475,000	1,140,676	1,250,156
(2)	P_{max} lbs.	49,500	375	35,821
(2)	P_{min} lbs.	33,000	- - - -	- - - -
	W_M lbs/in	± 1,832	± 1,416	± 1,552
	$W_{P\ max}$ lbs/in	- 492	- 4	- 356
	$W_{P\ min}$ lbs/in	- 328	- - - -	- - - -
	$W_{c\ max}$ lbs/in	- 2,324	- 1,420	- 1,908
	$W_{t\ max}$ lbs/in	+ 1,504	+ 1,412	+ 1,196

(1) Reference 3-8

(2) Reference Figure 3.4.6-1

$W_M = \frac{M}{\pi R^2}$ Where R is radius of shell

$W_P = \frac{P}{\pi D}$ Where D is diameter of shell

$W_{c\ max}$ = Maximum compressive load

$W_{t\ max}$ = Maximum tensile load

TABLE 3.4.6-4

LOWER "C" TRANSITION SECTION

COMPARISON OF FLIGHT ULTIMATE AND TEST LOADS

		46 Inch Diameter Heat Shield Ultimate Loads	(1) Test Loads Ld. Point (52)	(1) Test Loads Ld. Point (55)
Station 238.18				
(2)	MOM in lbs.	1,475,000	1,140,676	1,250,156
(2)	P_{max} lbs.	49,500	375	35,821
(2)	P_{min} lbs.	33,000	- - - -	- - - -
	W_M lbs/in	± 1,827	± 1,413	± 1,549
	$W_{P\ max}$ lbs/in	- 491	- 4	- 356
	$W_{P\ min}$ lbs/in	- 328	- - - -	- - - -
	$W_{c\ max}$ lbs/in	- 2,318	- 1,417	- 1,905
	$W_{t\ max}$ lbs/in	+ 1,499	+ 1,409	+ 1,193
Station 253.06				
(2)	MOM in lbs.	1,525,000	1,213,365	1,332,011
(2)	P_{max} lbs.	50,250	375	35,821
(2)	P_{min} lbs.	33,500	- - - -	- - - -
	W_M lbs/in	± 1,987	± 1,581	± 1,736
	$W_{P\ max}$ lbs/in	- 511	- 4	- 364
	$W_{P\ min}$ lbs/in	- 340	- - - -	- - - -
	$W_{c\ max}$ lbs/in	- 2,498	- 1,585	- 2,100
	$W_{t\ max}$ lbs/in	+ 1,647	+ 1,577	+ 1,372

(1) Reference 3-8

(2) Reference Figure 3.4.6-1

$W_M = \frac{M}{\pi R^2}$ Where R is radius of shell

$W_P = \frac{P}{\pi D}$ Where D is diameter of shell

$W_{c\ max}$ = Maximum compressive load

$W_{t\ max}$ = Maximum tensile load

FIGURE 3.4.6-2

FIN REACTION LOADS - ULTIMATE
SCOUT WITH 46 INCH DIAMETER HEAT SHIELD AND ALGOL III FIRST STAGE

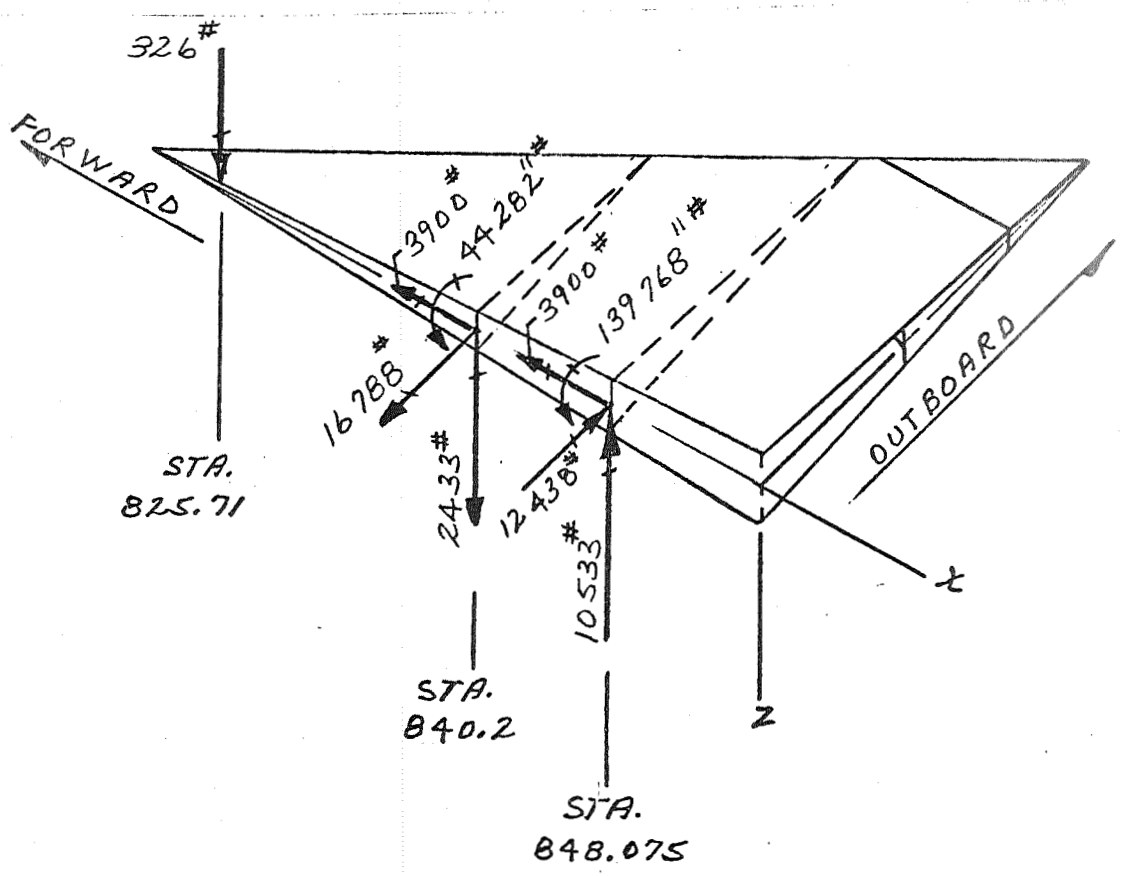

LOADS FROM PARAGRAPH 3.4.5

3.4.7 Ground Support Equipment

The ground support equipment noted in Section 3.1.7 was also reviewed to determine the effedts of the 46 inch diameter heatshield with the 16 sq. ft. fins. The parts requiring redesign are the same as those noted in paragraphs 3.1.7.1 through 3.1.7.8, 3.3.7.1 through 3.3.7.4 plus those noted below. A

3.4.7.1 Transporter

The transporter will have to be redesigned to raise the missile, to move the aft restraint forward to clear the fins, and to increase the cut-out for fin clearance. This is not feasible without a complete redesign of the transporter.

3.4.7.2 Launcher

The launcher will have to be redesigned to relocate five main structural members so as to clear fin travel. Reference 331-61620-61, 62, -41, -47 (2), -49 (2). This is not feasible without a significant redesign of the launcher.

4.0 DISCUSSION OF RESULTS AND RECOMMENDATIONS

The purpose of this phase of the study was to define the impact of installing a range of larger heatshields on the Scout vehicle such that the NASA could identify a larger heatshield compatible with future Scout requirements. The detailed results are presented in the previous sections and reflect a wide range of impact on the basic Scout vehicle and GSE. The 40 inch diameter heatshield configuration has almost no impact on the vehicle structure, and minimum impact on the GSE, but the 46 inch heatshield configuration requires redesign of most vehicle structure plus the transporter and launcher.

The estimated aerodynamic data as presented in this report are adequate for preliminary design analyses, but final design will require more precise definition of the aerodynamic characteristics. It is recommended that the following wind tunnel testing be performed to verify the estimated vehicle loads, stability and control characteristics of the selected configuration:

- Force and pressure model testing of the first stage configuration over the entire Mach number range.
- Fin and fin tip control effectiveness over the entire Mach number range.
- Force model testing of the second stage configuration at high supersonic Mach numbers.

It is also recommended that preparation for these tests be started immediately after selection of the Scout D configuration, at the completion of Phase I of the study.

5.0 Scout B Vehicle Configuration

5.1 Summary

The effects of putting larger heatshields on the Scout vehicle were determined for the Scout D configuration (Algol III motor installed), as presented in the preceding sections, because that configuration is most critical from the stability and control standpoint. Based on those results the 42-inch diameter heatshield was selected by the NASA for the second phase of the study, to determine the effects of putting the larger heatshield on the Scout B configuration (Algol IIB motor installed).

The results of this phase of the study show the need for increased fin tip control area and control gains and redesign of some ground support equipment. The specific changes required are summarized below:

- The following structural changes are required: redesign several components of the heatshield attachment clamp: add cork insulation to the lower D section skins.
- Fin tip control area shall be increased from 45 sq. in. to 78 sq. in. This increases the fin area from 4.5 to 4.735 sq. ft.
- Guidance system first stage nominal displacement gain shall be increased from 5.0 to 6.75 deg/deg and the rate to displacement ratio shall be 0.4, the same as for the basic Scout.
- The following ground support equipment requires redesign; payload umbilical retract arm, heatshield cradle, dummy heatshield, payload and heatshield hoist, heatshield storage bracket, upper cradle assembly, proof loading fixture assembly, and the fin protractor kit.

Detailed discussion of the evaluation is presented in the following paragraphs.

5.2 ALGOL II PERFORMANCE

The Algol IIB Motor's nominal performance and plus 3 sigma range safety limits, used in the larger heatshield study, are given in Tables 5.2-1 and 5.2-2, respectively. A plot of these data is presented in Figure 5.2-1.

TABLE 5.2-1

ALGOL IIB

Total Weight = 23799.20 lb
Cons Weight = 21391.70 lb
Burn Out Wt. = 2407.50 lb
Exit Area = 5.666 Sq. ft.

NOMINAL

Prop Weight = 21175.70 lb
Spec Impulse = 258.875 Sec.
Web (or Action) Time = 47.111 Sec.
Total Impulse = 5481859.3 lb-Sec.

STEP	TIME-SEC	THRUST VACUUM-lb	TOTAL IMPULSE (ACCUMULATING) lb-Sec.	WEIGHT REMAINING-lb
1	0.00	0.0	0.0	21391.70
2	0.13	87324.3	5894.4	21366.90
3	0.21	98866.4	12503.0	21353.63
4	0.51	93882.8	42271.7	21240.44
5	0.72	91404.4	61440.8	21167.32
6	1.34	89627.1	117355.8	20954.95
7	2.78	89712.6	246694.6	20471.12
8	5.15	89378.2	458916.8	19670.75
9	9.28	92095.7	832957.4	18232.28
10	13.81	96493.4	1260496.1	16572.43
11	19.59	98312.5	1822564.9	14382.68
12	26.29	98715.0	2482327.3	11796.24
13	35.05	101841.9	3360094.8	8333.30
14	43.91	106573.0	4284102.3	4667.01
15	47.11	106312.4	4624149.1	3315.69
16	47.83	103787.4	4699963.0	3015.17
17	48.97	97986.8	4814320.5	2560.39
18	49.89	91163.3	4901954.4	2213.80
19	52.99	60760.9	5136805.6	1298.23
20	56.49	32108.7	5299490.7	664.14
21	58.55	23045.1	5356330.2	441.76
22	61.03	16818.6	5405620.6	263.45
23	68.04	3266.9	5475990.2	24.04
24	69.17	1069.5	5478447.9	10.02
25	69.27	972.3	5478553.0	0.02
26	76.08	0.0	5481859.3	0.00

TABLE 5.2-2

ALGOL IIB

Total Weight = 23920.58 lb.
Cons Weight = 21518.75 lb.
Burn Out Wt. = 2401.83 lb.
Exit Area = 5.666 Sq. ft.

3 SIGMA-RANGE SAFETY

Prop Weight = 21302.75 lb.
Spec Impulse = 260.61 Sec.
Web (or Action) Time = 44.058 Sec.
Total Impulse =5551812.0 lb-Sec.

STEP	TIME-SEC	THRUST VACUUM-lb	TOTAL IMPULSE (ACCUMULATING) lb-Sec.	WEIGHT REMAINING-lb
1	0.00	0.0	0.0	21518.73
2	0.13	94567.12	5969.6	21493.79
3	0.19	107021.19	12662.2	21480.44
4	0.48	101626.50	42809.3	21366.58
5	0.68	98943.69	62223.0	21293.02
6	1.25	97019.81	118851.6	21079.39
7	2.60	97112.44	249841.1	20592.70
8	4.82	96750.31	464771.7	19787.56
9	8.68	99692.06	843586.1	18340.55
10	12.92	104452.37	1276581.0	16670.84
11	18.32	106421.62	1845822.0	14468.09
12	24.58	106857.31	2514004.0	11866.30
13	32.78	110242.12	3403582.0	8382.79
14	41.07	115363.44	4338775.0	4694.72
15	44.06	115081.37	4683161.0	3335.38
16	44.73	112348.12	4759942.0	3033.08
17	45.79	106069.00	4875759.0	2575.60
18	46.66	98682.69	4964511.0	2226.95
19	49.55	65772.69	5202359.0	1305.94
20	52.83	34757.14	5367119.0	668.08
21	54.76	24945.91	5424683.0	444.38
22	57.07	18205.82	5474602.0	265.01
23	63.63	3536.34	5545869.0	24.18
24	64.69	1157.74	5548358.0	10.08
25	64.79	1052.49	5548464.0	9.07
26	71.15	0.00	5551812.0	0.00

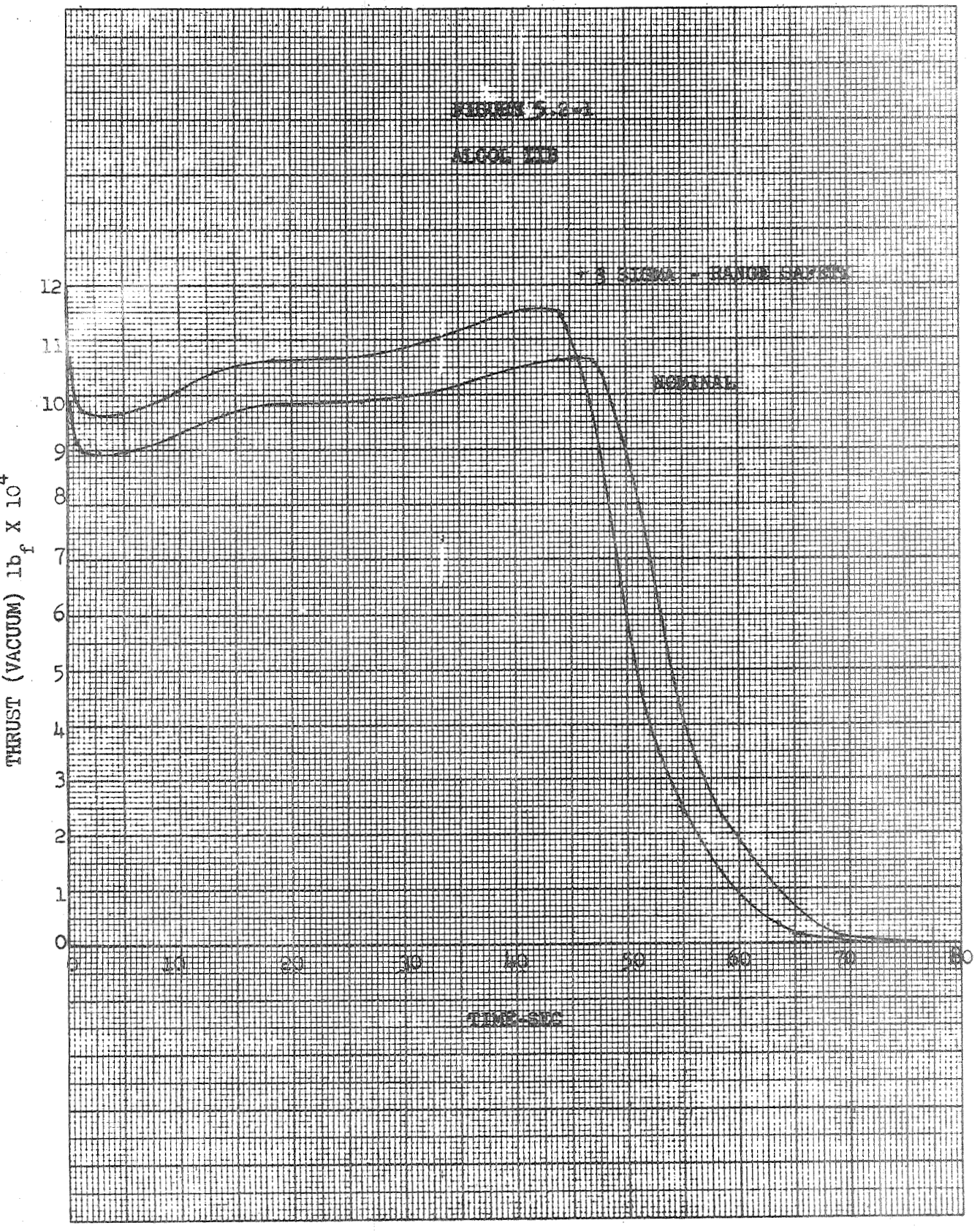
FIGURE 5.2-1
ALCOL ETS
+3 SIGMA - HANDS SAFETY
NOMINAL
THRUST (VACUUM) lb_f X 10^4
TIME-SEC
0
1
2
3
4
5
6
7
8
9
10
11
12
10
20
30
40
50
60
70
80

5.3 Vibrational Bending Modes

The first four vibrational bending modes for this vehicle configuration were calculated and are presented in Figures 5.3-1 and 5.3-2. Figures 5.3-3 and 5.3-4 present the first four modal slopes. The method used to determine these mode shapes and slopes is presented in Section 2.5 of this report.

The stiffness and mass data used in these calculations are a combination of those given in Section 3.2.2.2 for the forward part of the vehicle, to station 131.1, and Reference 3.6 for the aft part.

Figure 5.3-1

Scout Vehicle Algol II First Stage
42" Dia. Heat Shield 50 Lb. Payload
75% Fuel Burned

First And Second Bending Modes

Figure 5.3-2
Scout Vehicle Algol II First Stage
42" Dia Heat Shield 50 lb Payload
75% Fuel Burned
Third And Fourth Bending Modes

FIGURE 5.3-3

SCOUT VEHICLE ALGOL II FIRST STAGE
42" DIA. HEAT SHIELD 50 LB. PAYLOAD
75% FUEL BURNED

FIRST AND SECOND BENDING MODAL SLOPES

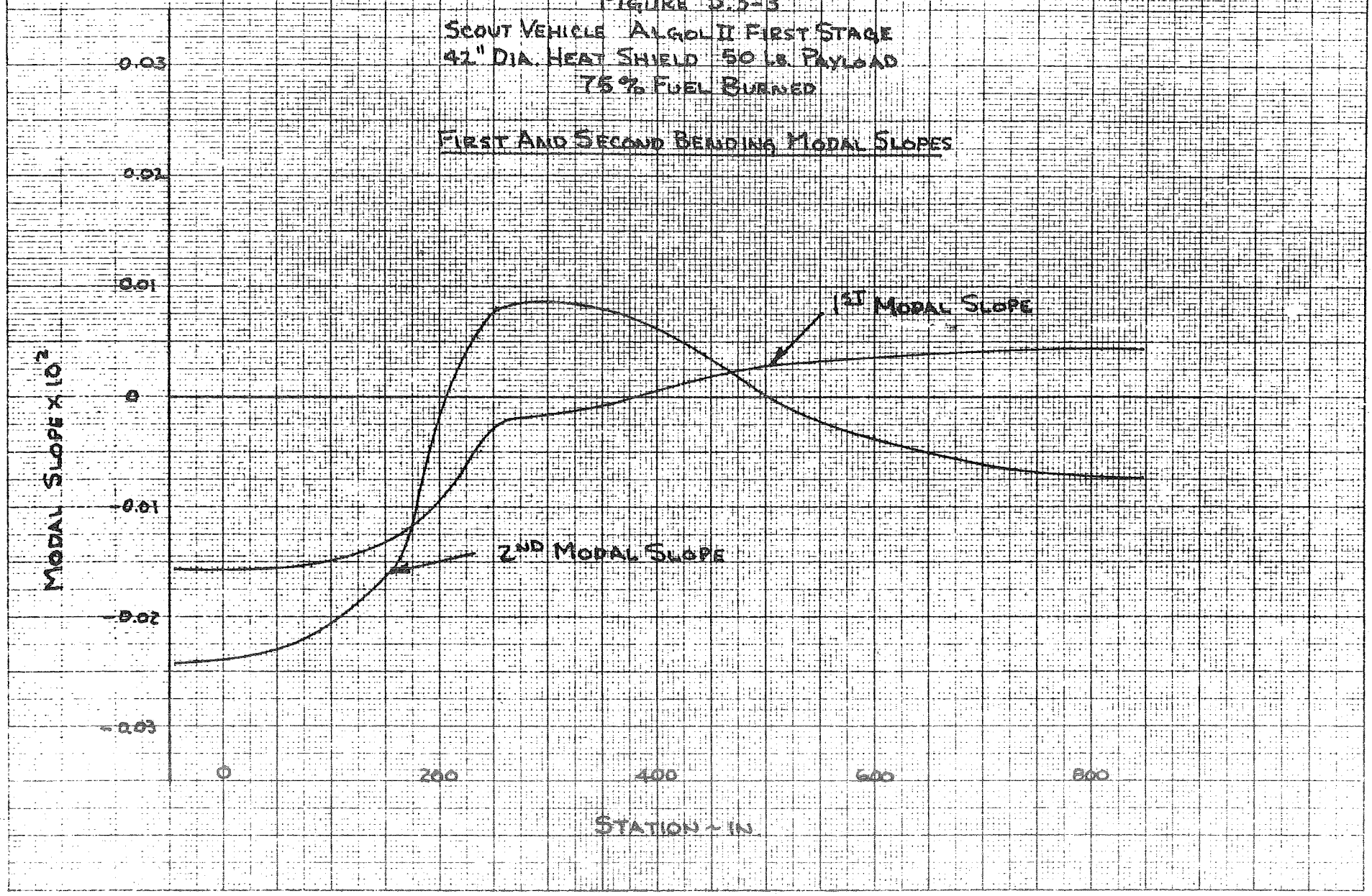

FIGURE 5.3-4
SCOUT VEHICLE ALGOL II FIRST STAGE
42" DIA. HEAT SHIELD 50 LB. PAYLOAD
75% FUEL BURNED

THIRD AND FOURTH BENDING MODAL SLOPES

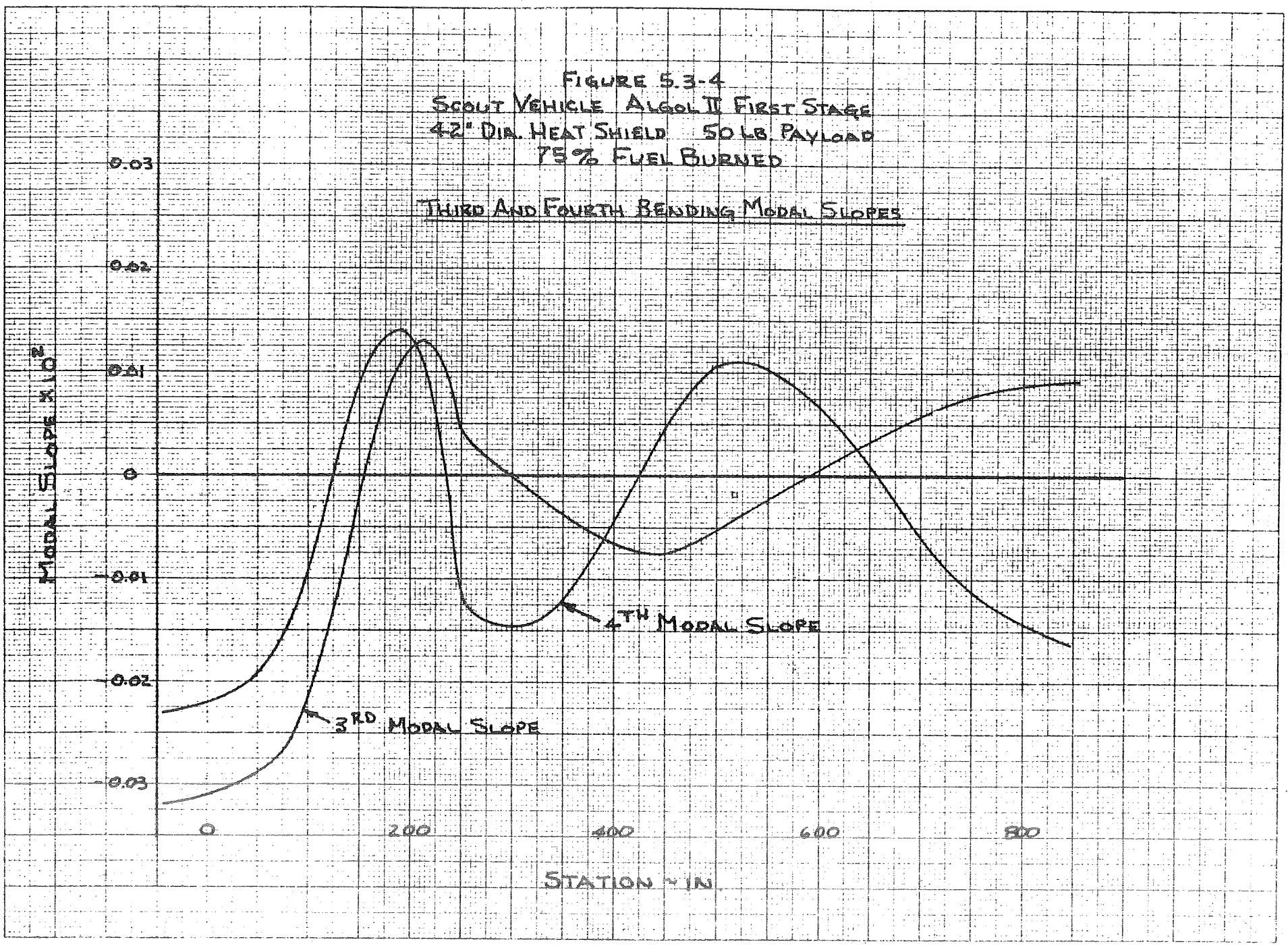

5.4 Aerodynamic Characteristics

The aerodynamic characteristics for the Scout configuration having a 42 inch diameter heatshield with the Algol II first stage are based on heatshield data presented in Section 3.2.2 and vehicle data presented in Reference 3-2. The zero lift drag coefficient for the subject configuration is presented in Figure 5.4-1, and is based on drag data presented in Reference 3-2. The distributed normal force coefficient for the 42 inch heatshield configuration is the same as that presented in Section 3.2.2 forward of Scout station 131. Aft of station 131, the distributed normal force coefficient was assumed to be the same as that for the 34 inch diameter heatshield Algol II configuration presented in Reference 3-2. The fin normal force coefficient derivative and center of pressure were derived from data presented in Reference 3-2.

5.4.1 Rigid Vehicle Aerodynamics

The body alone $C_{N_\alpha} S$, x_{cp} and C_{m_α} were derived by integration of the distributed aerodynamic normal force coefficient derivatives at Mach 0.8, 1.0, 1.5 and 2.5. The variations with Mach number are based on wind tunnel data and Scout data for other heatshield configurations. Normal force coefficient derivatives and centers of pressure are presented in Figures 5.4-2 and 5.4-3. These are compared with similar data for the configuration having a 34 inch diameter heatshield with nose at station -40. The 42 inch heatshield configuration is more stable subsonically and transonically due to the large predicted negative lift on the heatshield reverse frustrum.

The normal force coefficient derivative for the proposed 4.73 square feet area fin is presented in Figure 5.4.4 with data for the current 4.5 ft^2 fin obtained from Reference 3-2.

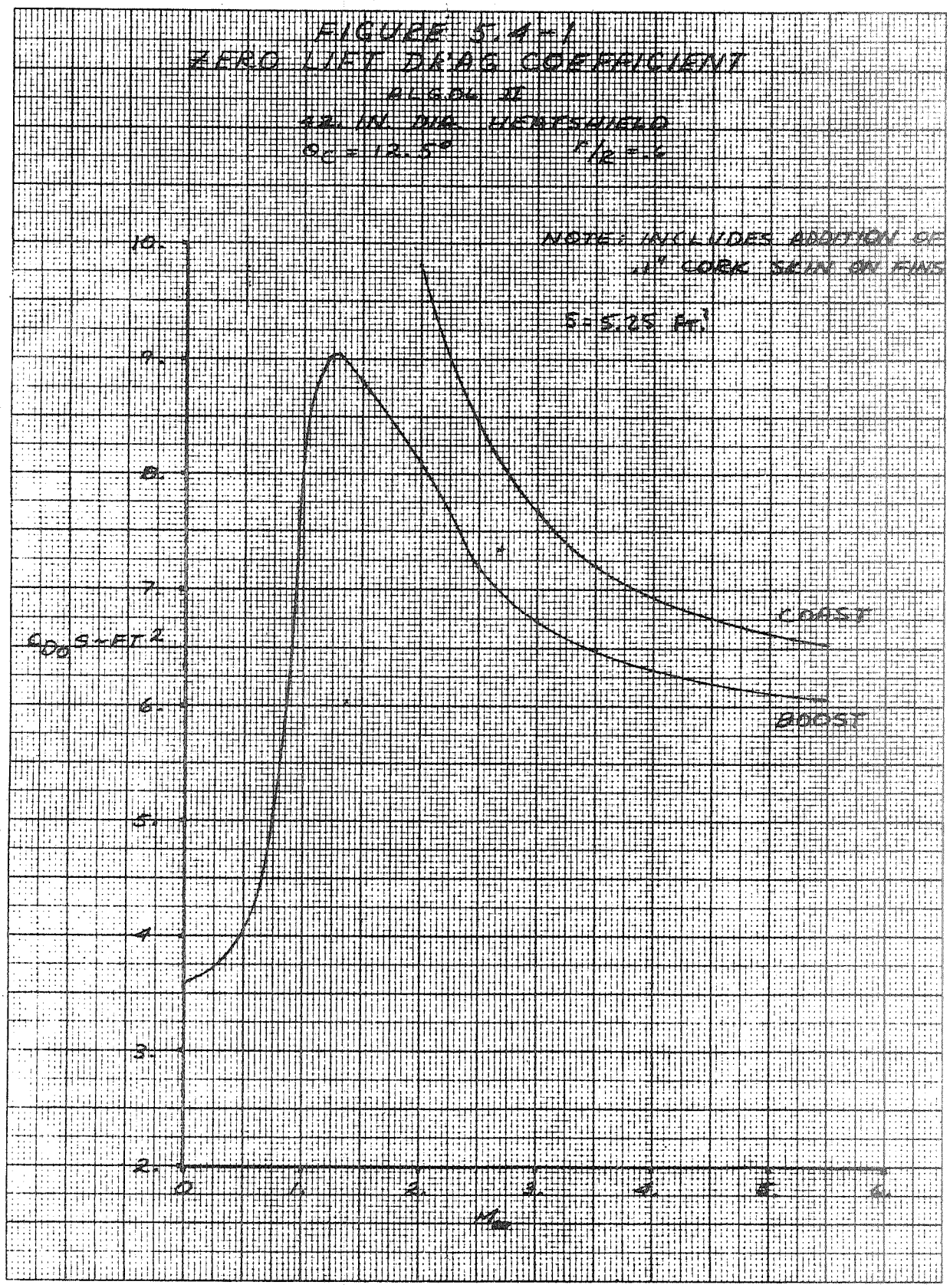
FIGURE 5.4-1
ZERO LIFT DRAG COEFFICIENT
AERO. INC.
22. IN. DIA. HEMISPHERE
$\theta_C = 12.5°$
$r/R = .6$
NOTE: INCLUDES ADDITION OF
.1" CORK SKIN ON FINS
S = 5.25 Ft.²
$C_{D_0} S - Ft^2$
10.
9.
8.
7.
6.
5.
4.
3.
2.
0
1.
2.
3.
4.
5.
6.
M_∞
COAST
BOOST

FIGURE 5.4-2

NORMAL FORCE COEFFICIENT DERIVATIVE
ALGOL II FIRST STAGE

———— 42 INCH DIA. H/S NOSE AT STA. -44.81
4.73 FT² FIN
— — — — 34 INCH DIA. H/S NOSE AT STA. -40
4.5 FT² FIN

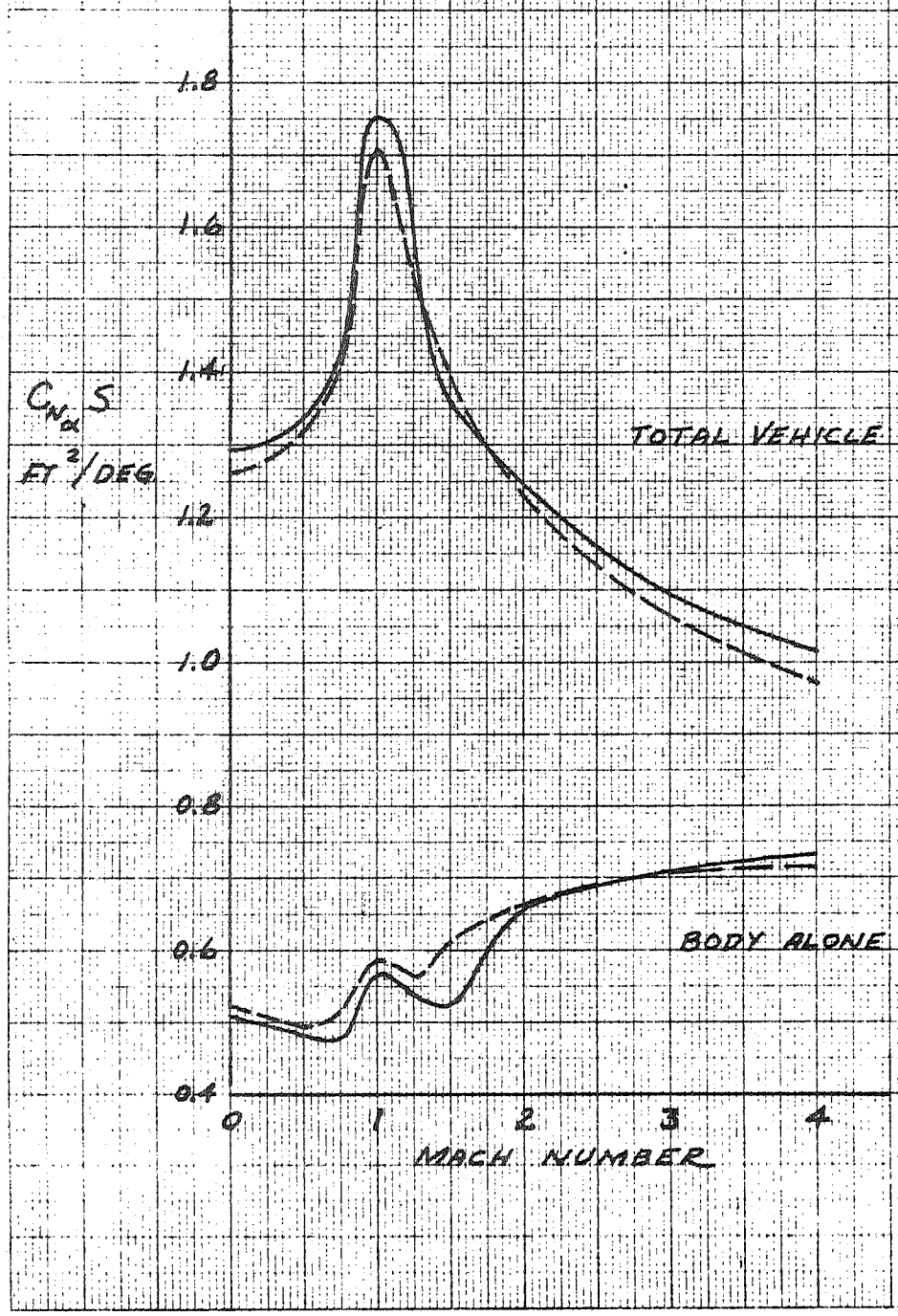

FIGURE 5.4-3

CENTER OF PRESSURE LOCATION
ALGOL I FIRST STAGE

——— 42 INCH DIA. H/S NOSE AT STA -44.81
4.73 FT² FIN

— — — — 34 INCH DIA H/S NOSE AT STA -40
4.5 FT² FIN

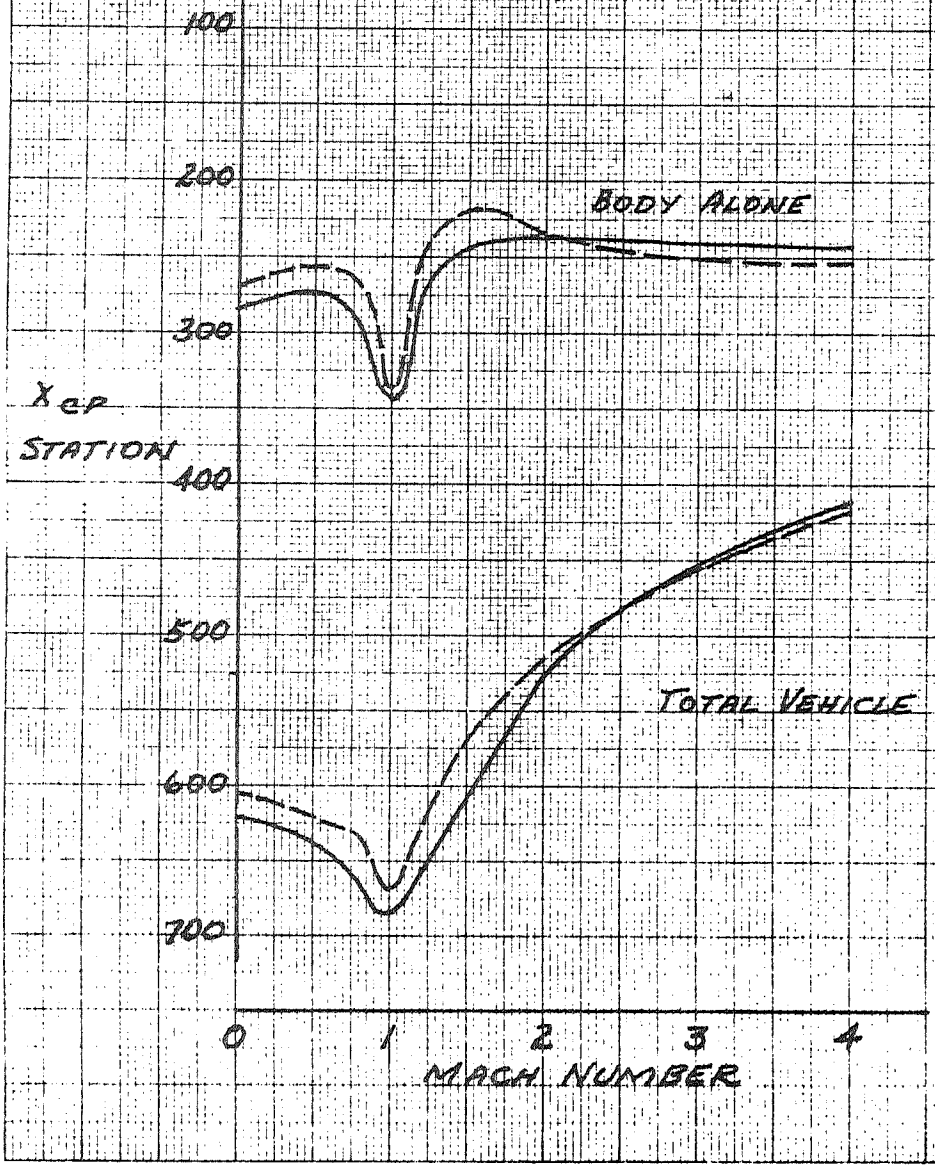

FIGURE 5.4-4
FIN NORMAL FORCE COEFFICIENT DERIVATIVE
TWO FINS - ALGOL II FIRST STAGE

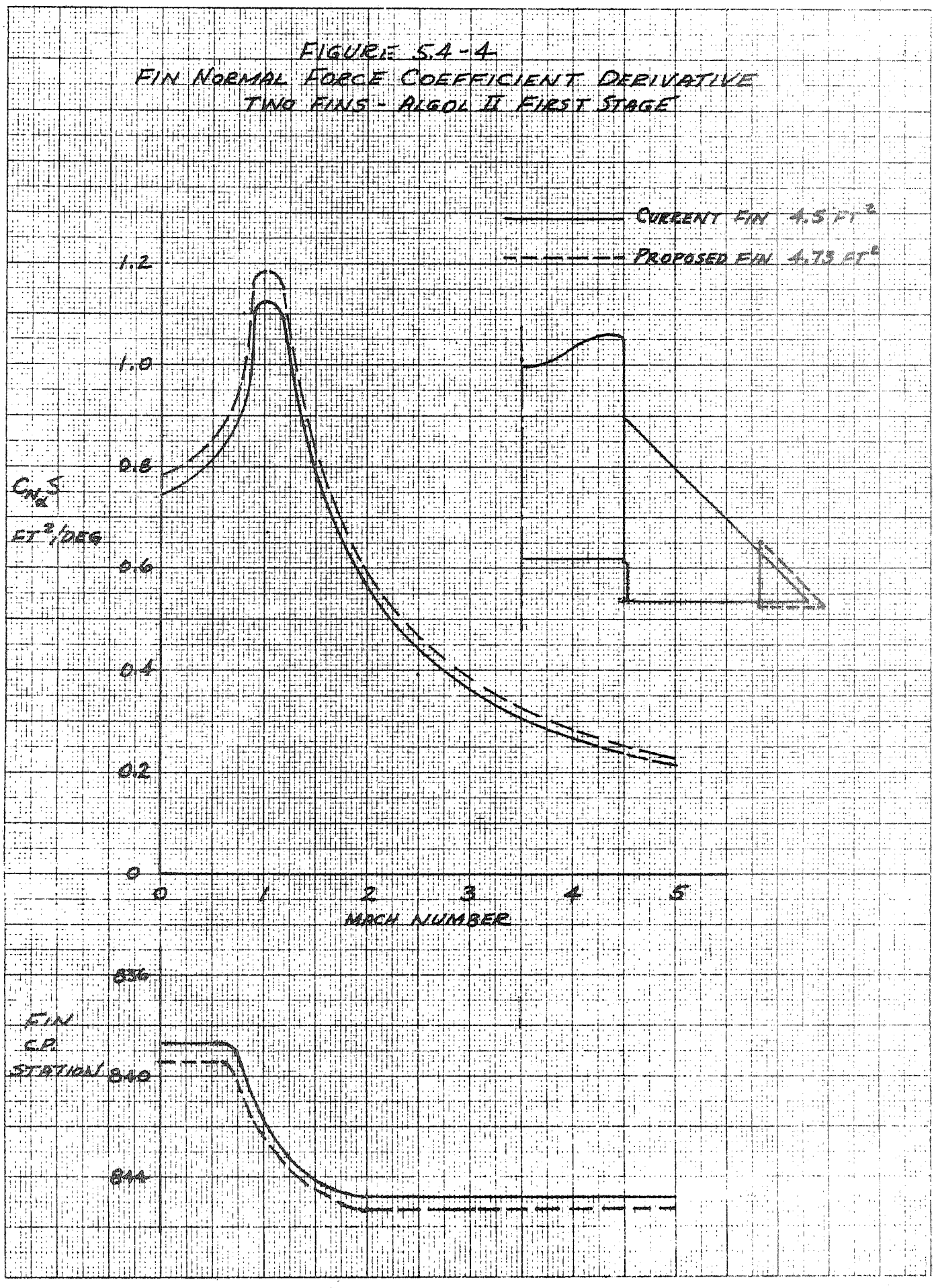

The normal force coefficient derivative for the 4.73 ft^2 fin was derived by proportionally adjusting that for the 4.5 ft^2 fin as a function of the planform areas. The fixed portion of the fin has the same geometry as the current fin. The increase in fin area is achieved by increasing the fin tip control area from 0.313 ft^2 to 0.542 ft^2. The added lift at the tip results in a slight rearward shift in total fin center of pressure as shown in Figure 5.4-4.

The total vehicle normal force coefficient slope, center of pressure and pitching moment coefficient derivatives are presented in Figures 5.4-2, 5.4-3 and 5.4-5 respectively. This information is compared with the 34 inch diameter heatshield configuration having nose at station -40. The predicted aerodynamic stability of the 42 inch heatshield configuration with an Algol II first stage and 4.73 ft^2 Base A fins is approximately the same as the 34 inch diameter heatshield nose at station -40 with 4.5 ft^2 Base A fins.

The fin tip normal force coefficient and pitching moment derivatives due to deflecting two 0.542 square foot fin tips are presented in Figures 3.2.2-18 and 3.2.2-19 in Section 3.2.2. Fin tip and fin interference effects are assumed to be the same as the current Scout fins and fin tip geometry.

It is recommended that thorough wind tunnel testing of the 42 inch heatshield configuration be performed to verify the predicted stability, and fin and fin tip effectiveness. The fin tip hinge moment coefficients for this configuration should be determined from wind tunnel measurement to guarantee adequate balance with the current Base A hydraulic system.

FIGURE 5.4-5

PITCHING MOMENT COEFFICIENT DERIVATIVE
ALGOL II FIRST STAGE

———— 47 INCH DIA. H/S NOSE AT STA. -44.21
4.73 FT² FIN

— — — — 34 INCH DIA. H/S NOSE AT STA. -40
4.5 FT² FIN

$X_{REF} = 427.6$

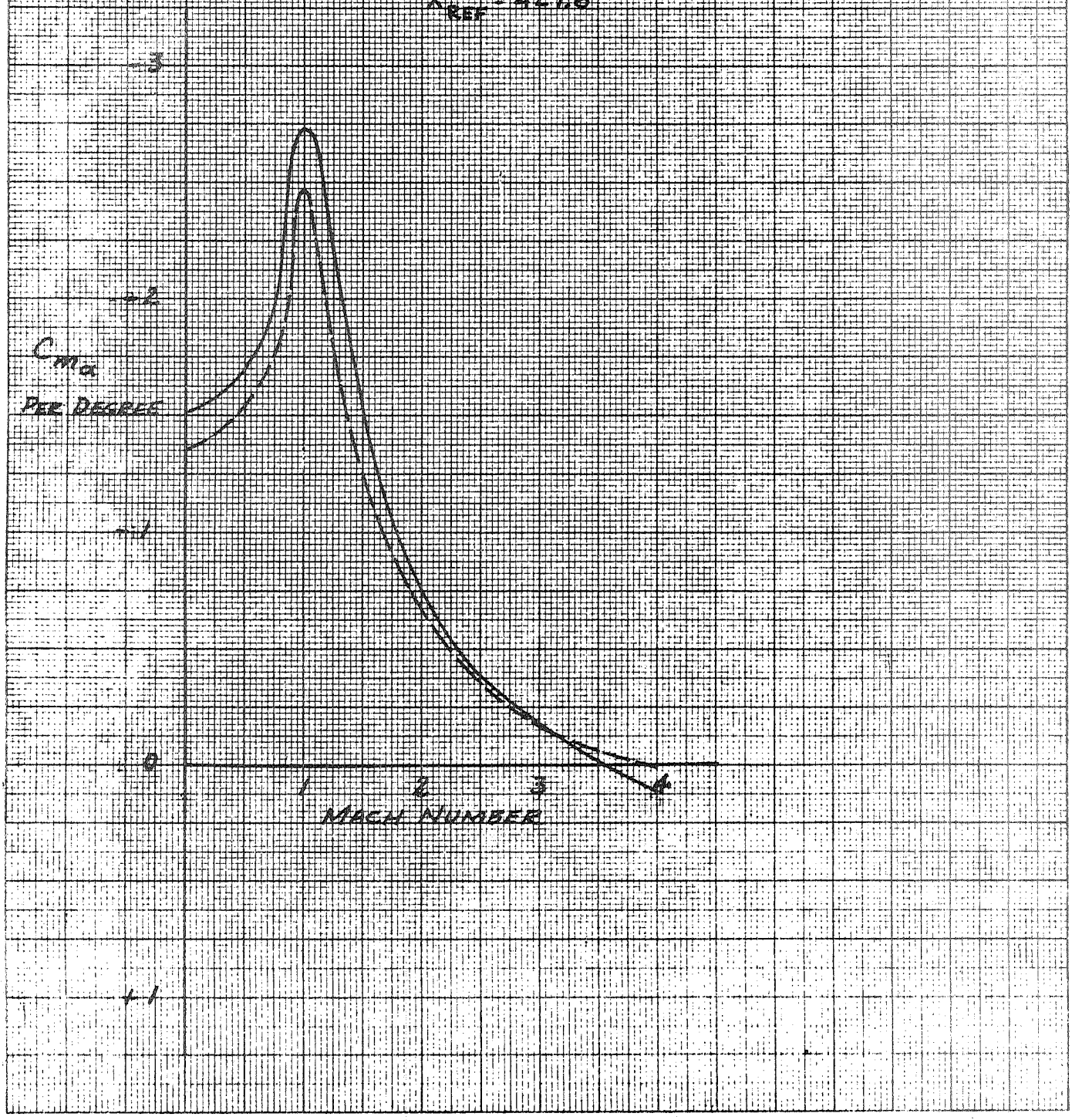

5.4.2 Flexible Aerodynamic Coefficients

The flexible aerodynamic coefficients (Cn_α, Cm_α, Cmq) and the center of pressure for this configuration were determined and are presented in Figures 5.4-6 through 5.4-9.

The techniques used to calculate these coefficients are discussed in Section 3.2.2.2 of this report.

The aerodynamic load distribution used was a combination of those presented in Reference 3-2 for the aft portion of the vehicle, aft of station 131.1, and those given in Section 3.2.2 of this report for the forward portion of the vehicle.

FIGURE 5.4-6
SCOUT VEHICLE - ALGOL IIB FIRST STAGE

NORMAL FORCE COEFFICIENT DUE TO
ANGLE OF ATTACK FOR TOTAL VEHICLE

HEATSHIELD 42" DIA. NOSE @ -44.81
REFERENCE AREA 5.25 FT.²
REFERENCE LENGTH 2.58 FT.

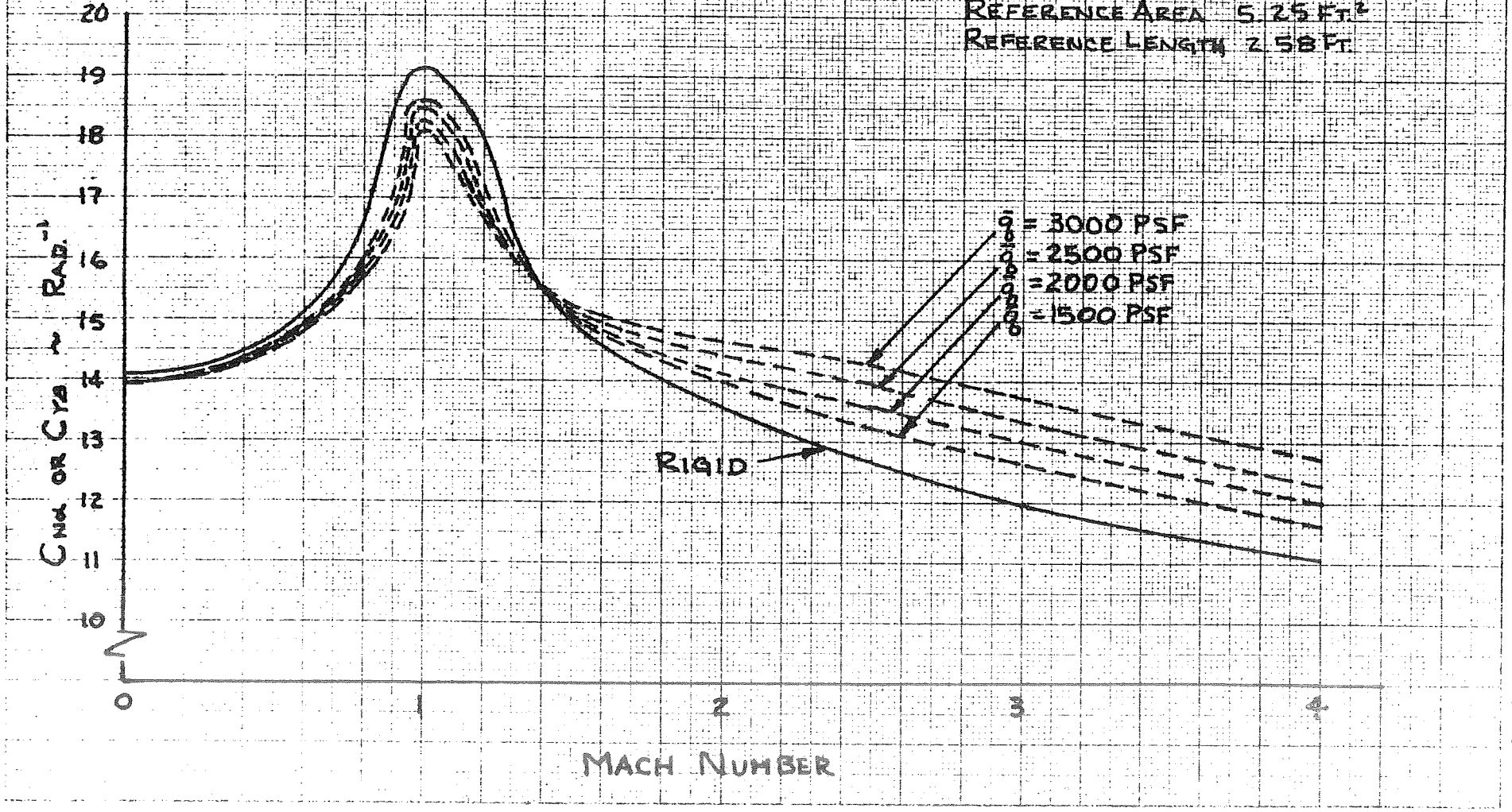

FIGURE 5.4-7
SCOUT VEHICLE - ALGOL IIB FIRST STAGE

MOMENT COEFFICIENT DUE TO ANGLE OF ATTACK FOR TOTAL VEHICLE

HEATSHIELD: 42" DIA. NOSE @ -44.81
REFERENCE AREA: 5.25 FT.²
REFERENCE LENGTH: 2.58 FT.
REFERENCE STATION: 427.8

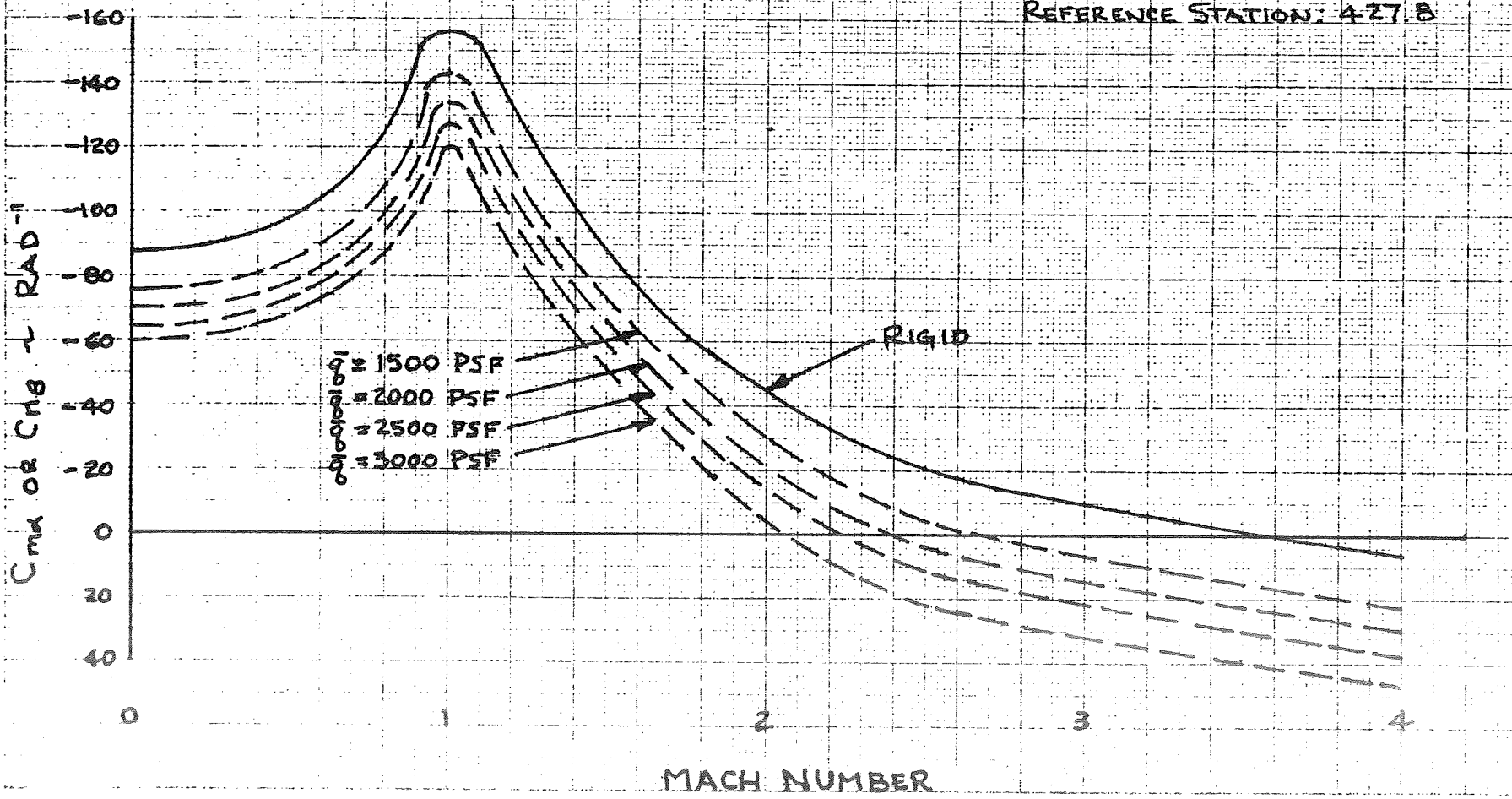

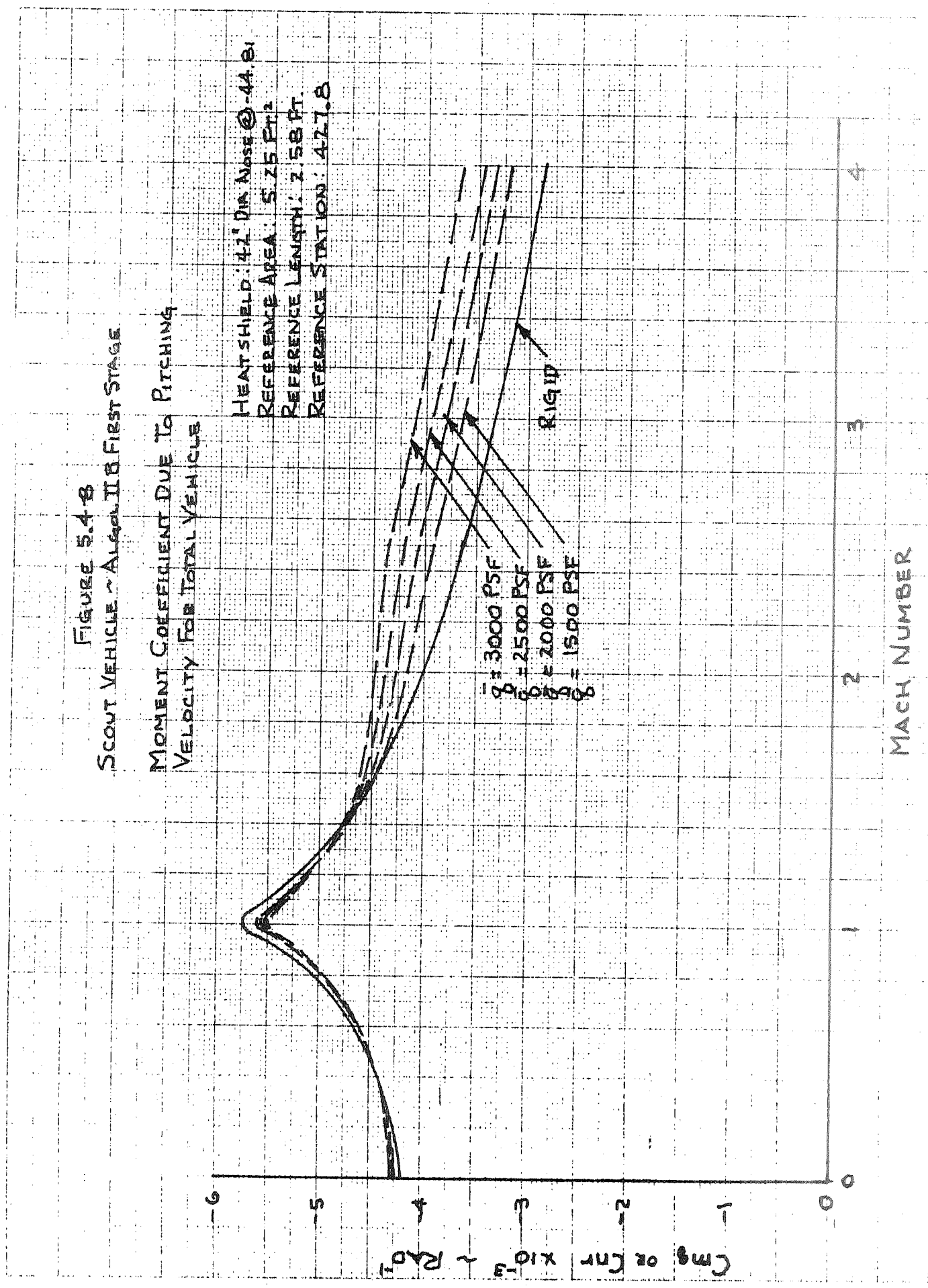

FIGURE 5.48
SCOUT VEHICLE ~ ALGOL IIB FIRST STAGE
MOMENT COEFFICIENT DUE TO PITCHING
VELOCITY FOR TOTAL VEHICLE

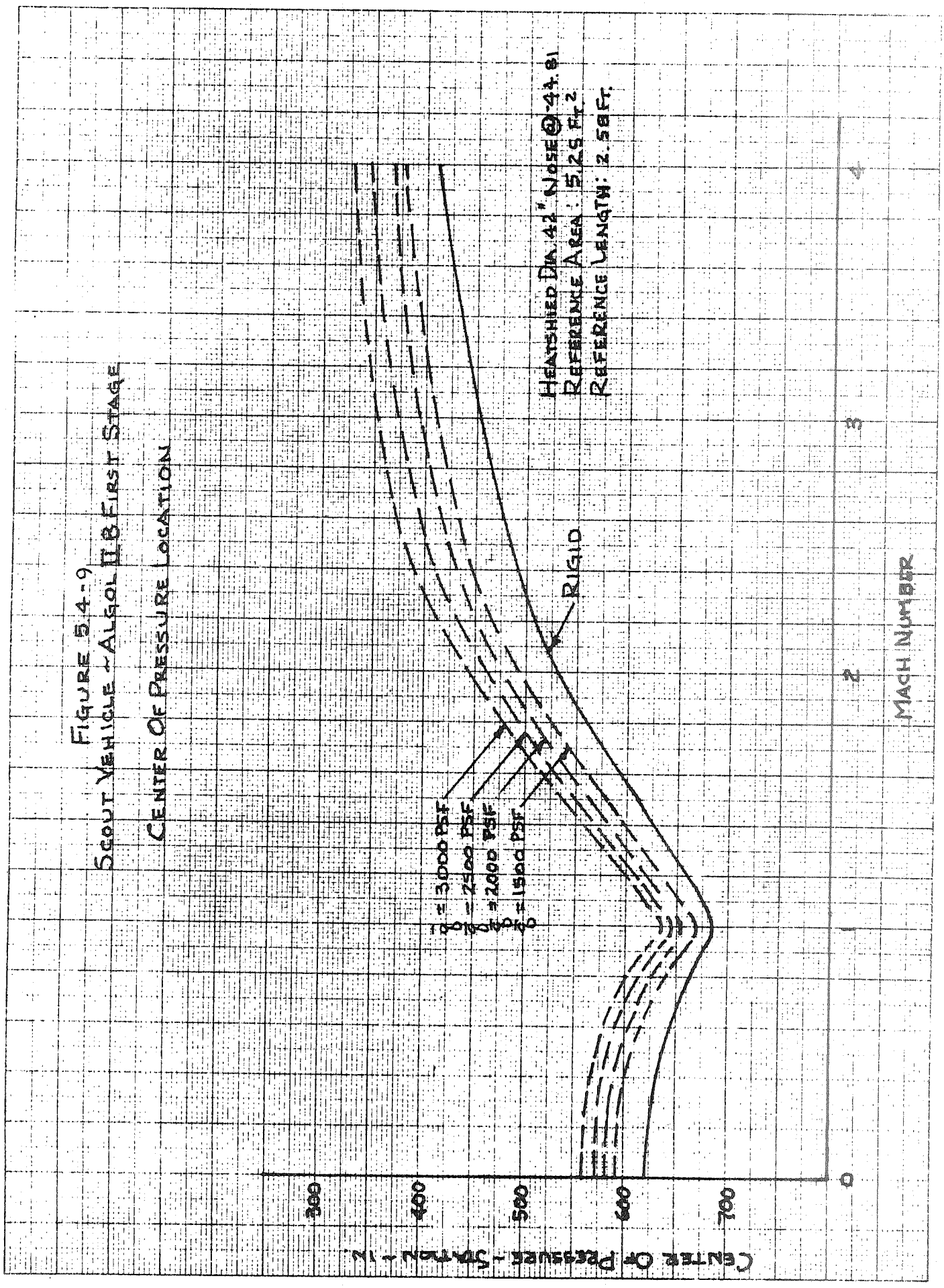

FIGURE 5.4-9
SCOUT VEHICLE - ALGOL IIB FIRST STAGE
CENTER OF PRESSURE LOCATION

5.5 Weight and Balance Data

This section presents the weights, longitudinal center of gravity and moments of inertia for a nominal Scout vehicle (S-178 and Subs. configuration) with a 50 pound payload and 42 inch diameter heatshield.

A similar vehicle was shown in section 3.2.3, Table 3.2.3-1. The vehicle reported in this section uses a nominal Algol II first stage motor, the earlier configuration, an Algol III (Aerojet Proposal #2) first stage motor. This motor substitution is the only change.

TABLE 5.5-1
MASS PROPERTIES

42 INCH DIAMETER, -44.81 LARGE VOLUME HEATSHIELD, (50 POUND PAYLOAD)

VEHICLE S- WEIGHT, X(CG), AND MOMENTS OF INERTIA

VERSUS PERCENT OF FUEL CONSUMED

	TOTAL WEIGHT, POUNDS	C.G. SCOUT STA.-IN.	IXX SLUG-FT^2	IYY OR IZZ SLUG-FT^2
	*******	*******	**********	**********
H STAGE - BURNOUT	118.96	53.35	2.38	23.82
75 0/0	271.79	60.33	5.00	30.66
50 0/0	424.63	62.28	6.87	35.52
25 0/0	577.46	63.20	8.00	39.68
H STAGE - IGNITION	730.30	63.74	8.38	43.34
PIN-UP ITEMS	774.68	65.92	9.37	56.93
STAGE - BURNOUT	1483.95	116.61	29.45	1287.32
75 0/0	2135.08	130.01	56.88	1545.14
50 0/0	2786.22	137.15	76.77	1710.98
25 0/0	3437.35	141.58	89.11	1834.97
STAGE - IGNITION	4088.49	144.61	93.90	1935.30
FSS N/C - H/S	6159.25	229.28	181.48	23526.18
D STAGE - BURNOUT	6516.43	218.41	206.03	26548.55
75 0/0	8592.67	249.14	299.18	33456.96
50 0/0	10668.92	267.92	367.16	38212.20
25 0/0	12745.16	280.57	410.04	41860.43
D STAGE - IGNITION	14821.41	289.69	427.79	44861.59
STAGE - BURNOUT	18323.54	369.48	708.56	164237.18
75 0/0	23703.23	433.24	1108.69	244949.12
50 0/0	29082.91	473.40	1407.60	299408.41
25 0/0	34462.60	501.03	1605.41	339885.67
STAGE - IGNITION	39842.29	521.20	1702.08	372024.18

5.6 DESIGN TRAJECTORIES

Two design trajectories were developed with the Algol IIB as the first stage motor in place of the Algol III. These trajectories are based on a 50 pound payload weight and injection at 100 n. mi. The +3 sigma high range safety deviation from nominal motor performance of the Algol IIB first stage motor was used. The motor characteristics are presented in Section 5.2. The weight data are presented in Section 5.5. Rigid body aerodynamic coefficients that were used in this design trajectory are presented in Section 5.4.

The first design trajectory simulated a controls locked "gravity turn" mode of flight which is angle launched to achieve the desired injection altitude. This trajectory was used for the stability and control and the thermal analyses.

A series of pitch rate commands was developed to control the vehicle along the gravity turn trajectory. The pitch program design trajectory was used for the structural loads analysis. The computer listings of both design trajectories are presented in Appendix A.

5.6.1 Pitch Program

In developing the pitch program for the Algol IIB configuration design trajectory, the current Scout flight restrictions were adhered to. In particular the first pitch rate was not commanded until 2.5 seconds flight time, the magnitude of that rate did not exceed approximately 3.6 degrees per second, and the maximum product of dynamic pressure and angle of attack did not exceed 1000 degrees-psf.

TABLE 5.6-1

DESIGN TRAJECTORY PITCH PROGRAM
100 N. MI. INJECTION ALTITUDE
50 LB. PAYLOAD

TIME AFTER LIFTOFF, SEC.	PITCH RATE, DEG/SEC	PITCH RATE NO.
0	0	
2.50	-3.60752	1
8.00	-0.84000	2
26.99	-0.72000	3
31.00	-0.58600	4
38.00	-0.47500	5
46.00	-0.37300	6
61.00	-0.44000	7
112.00	-0.15400	8
210.00	-1.00000	9
226.53	0.00000	10

Table 5.6-1 presents the pitch program developed for the Algol IIB configuration design trajectory. Even though the pitch program started at 2.5 seconds, the magnitude of the first rate had to be 3.6 degrees per second to obtain the desired injection altitude. The magnitude of that first rate could have been reduced considerably if the pitch program could start earlier than 2.5 seconds. A smaller first pitch rate magnitude would in turn result in smaller fin deflections.

5.6.2 Results

The results of the two design trajectories are presented graphically in Figures 5.6.2-1 through 5.6.2-8. These figures present time histories of vehicle and trajectory parameters important for design purposes. Because the flight profiles of the two trajectories are nearly identical, only time histories of the pitch program design trajectory are shown.

As a result of the stability and control analysis, the first stage fin tip area was increased and the guidance system gains were increased. A discussion of these changes are in Section 5.7.

It was possible to stay within the current Scout flight restrictions in the design trajectories. The maximum product of dynamic pressure and angle of attack was 973 degrees-psf (negative) at 9.25 seconds.

FIGURE 5.6 -1
ALTITUDE TIME HISTORY
100 NM INJECTION ALTITUDE DESIGN TRAJECTORY
FIRST STAGE BOOST AND COAST

- 50 LB PAYLOAD
- ALGOL IIB FIRST STAGE MOTOR (+3 SIGMA)
- 42 IN. DIAMETER HEATSHIELD
- INCREASED SIZE FIRST STAGE FIN-TIPS AND HIGHER GUIDANCE SYSTEM GAINS

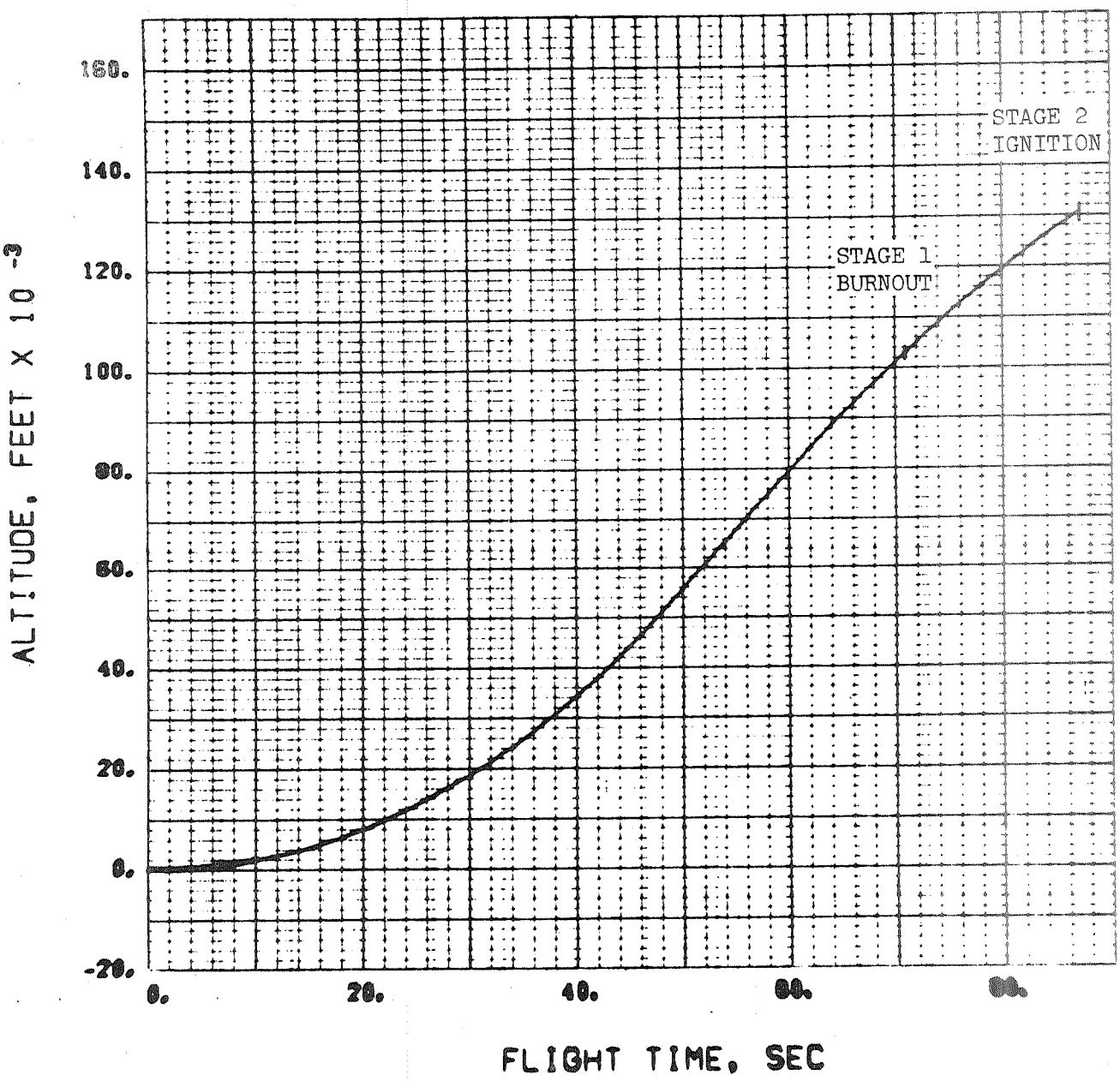

FIGURE 5.6 -2
RELATIVE VELOCITY TIME HISTORY
100 NM INJECTION ALTITUDE DESIGN TRAJECTORY
FIRST STAGE BOOST AND COAST

- 50 LB PAYLOAD
- ALGOL IIB FIRST STAGE MOTOR (+3 SIGMA)
- 42 IN. DIAMETER HEATSHIELD
- INCREASED SIZE FIRST STAGE FIN-TIPS AND HIGHER GUIDANCE SYSTEM GAINS

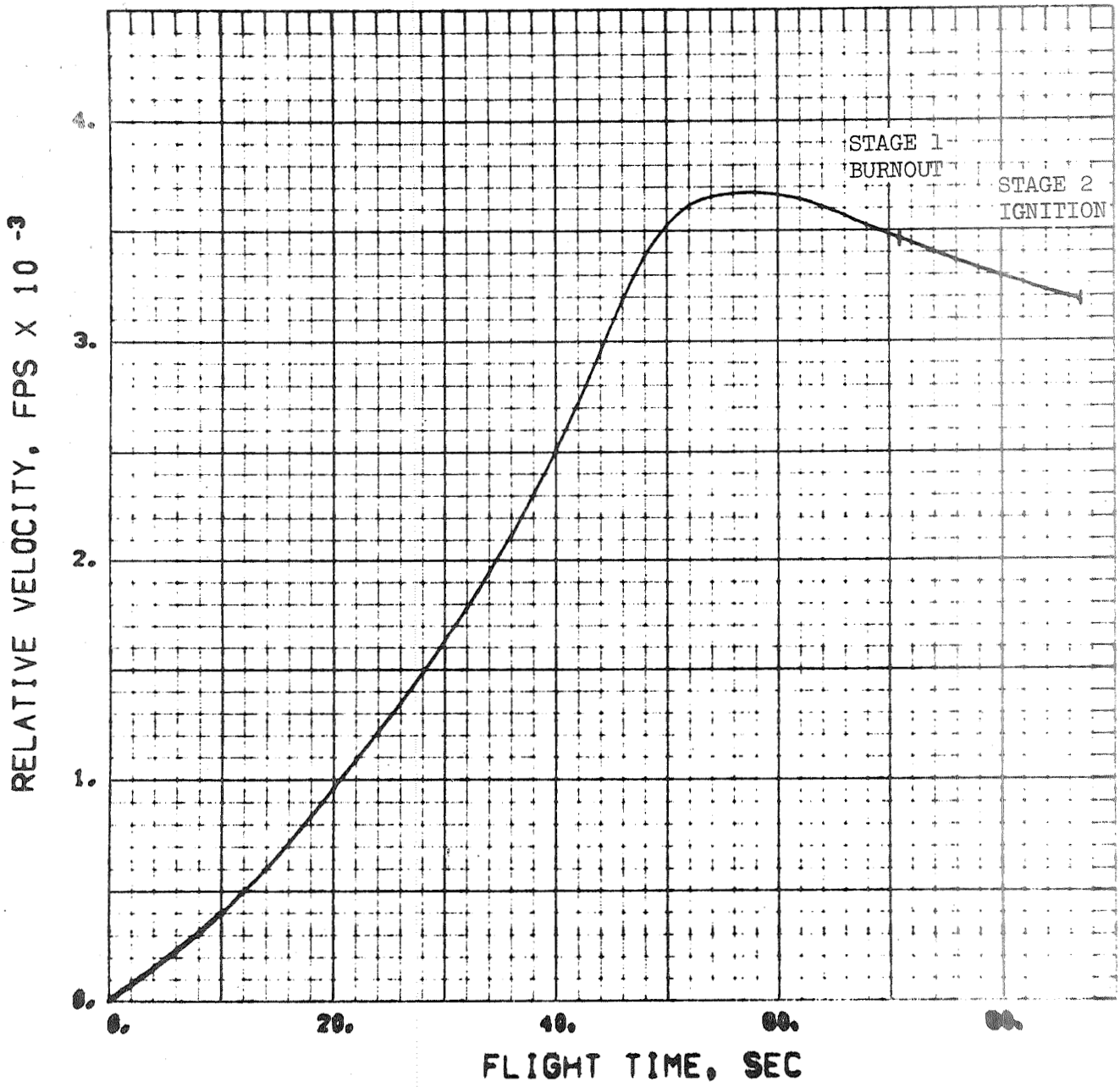

FIGURE 5.6 -3
MACH NUMBER TIME HISTORY
100 NM INJECTION ALTITUDE DESIGN TRAJECTORY
FIRST STAGE BOOST AND COAST

- 50 LB PAYLOAD
- ALGOL IIB FIRST STAGE MOTOR (+3 SIGMA)
- 42 IN. DIAMETER HEATSHIELD
- INCREASED SIZE FIRST STAGE FIN-TIPS AND HIGHER GUIDANCE SYSTEM GAINS

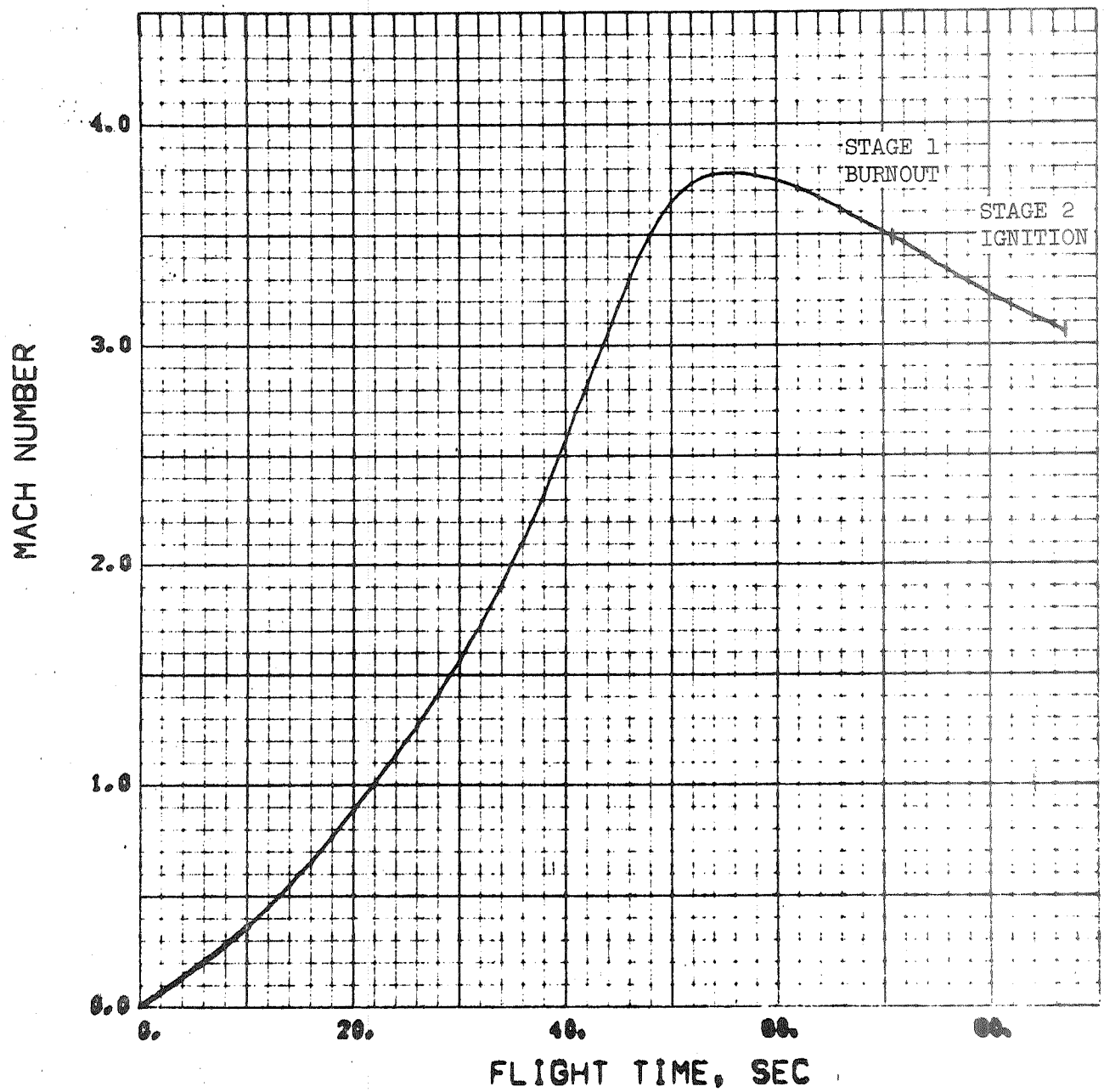

FIGURE 5.6 -4
DYNAMIC PRESSURE TIME HISTORY
100 NM INJECTION ALTITUDE DESIGN TRAJECTORY
FIRST STAGE BOOST AND COAST

- 50 LB PAYLOAD
- ALGOL IIB FIRST STAGE MOTOR (+3 SIGMA)
- 42 IN. DIAMETER HEATSHIELD
- INCREASED SIZE FIRST STAGE FIN-TIPS AND HIGHER GUIDANCE SYSTEM GAINS

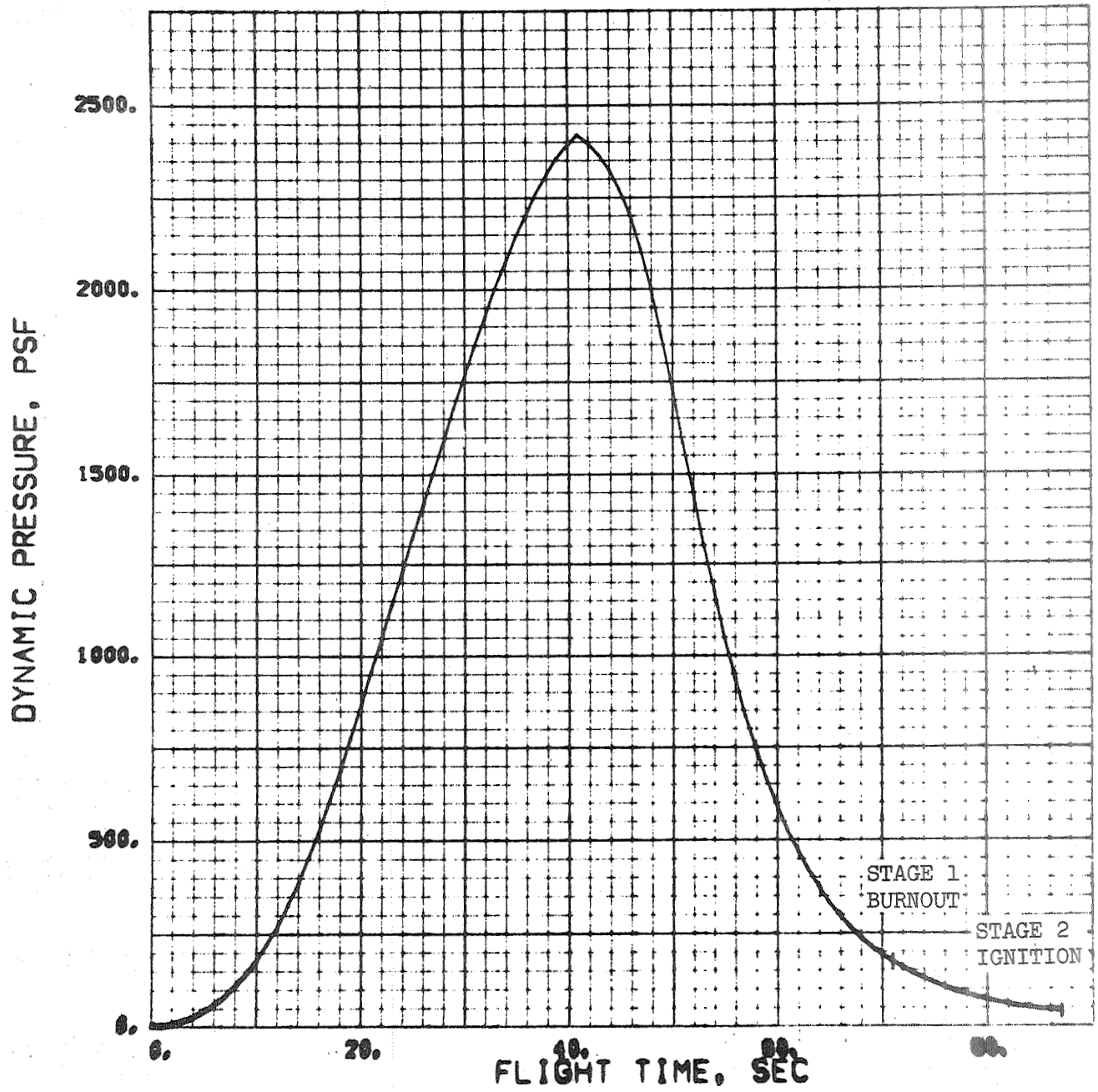

FIGURE 5.6 -5
PRODUCT OF DYNAMIC PRESSURE AND
ANGLE OF ATTACK TIME HISTORY
100 NM INJECTION ALTITUDE DESIGN TRAJECTORY
FIRST STAGE BOOST AND COAST

- 50 LB PAYLOAD
- ALGOL IIB FIRST STAGE MOTOR (+3 SIGMA)
- 42 IN. DIAMETER HEATSHIELD
- INCREASED SIZE FIRST STAGE FIN-TIPS AND HIGHER GUIDANCE SYSTEM GAINS

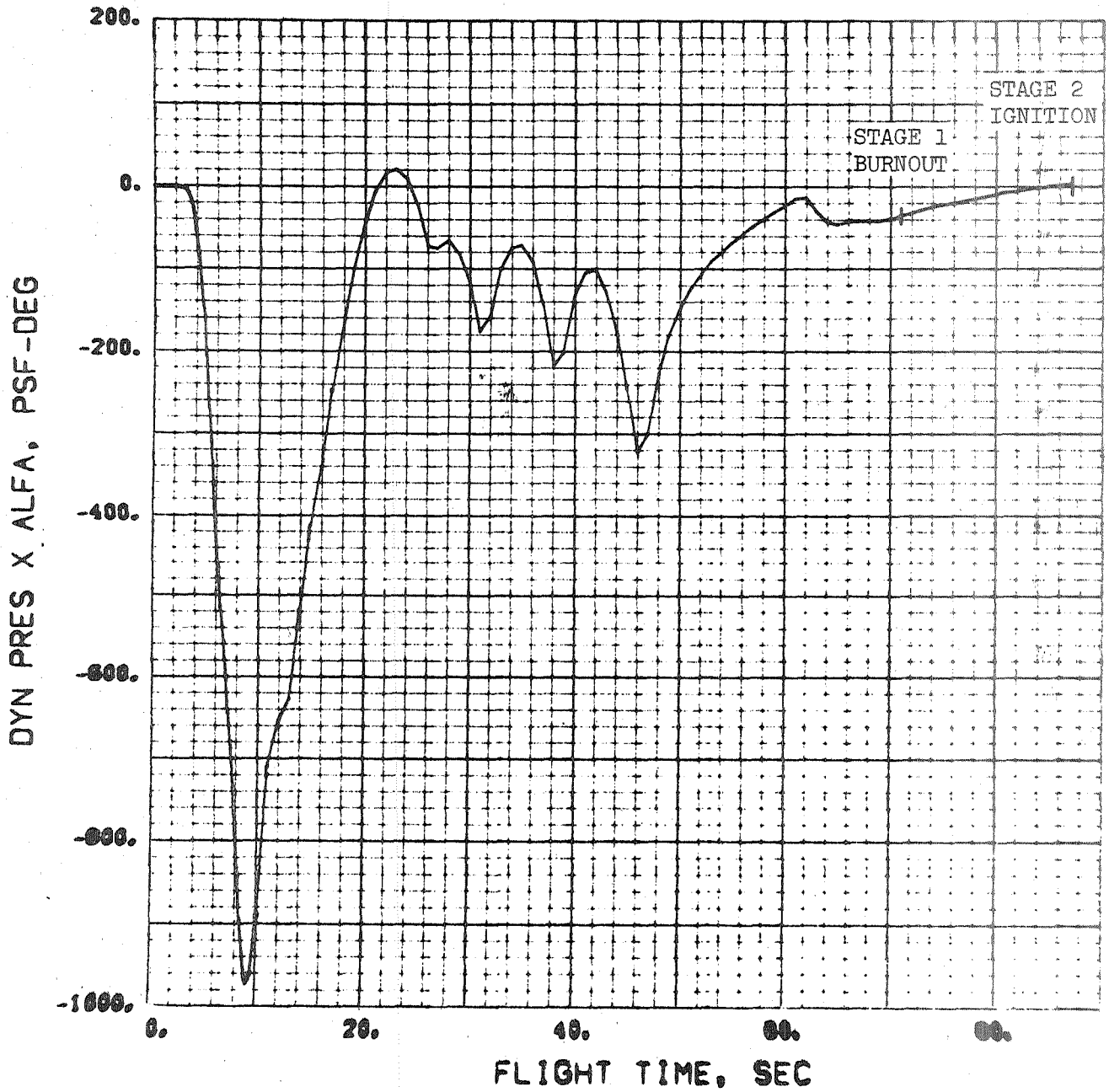

FIGURE 5.6 -6
PITCH FIN DEFLECTION TIME HISTORY
100 NM INJECTION ALTITUDE DESIGN TRAJECTORY
FIRST STAGE BOOST AND COAST

- 50 LB PAYLOAD
- ALGOL IIB FIRST STAGE MOTOR (+3 SIGMA)
- 42 IN. DIAMETER HEATSHIELD
- INCREASED SIZE FIRST STAGE FIN-TIPS AND HIGHER GUIDANCE SYSTEM GAINS

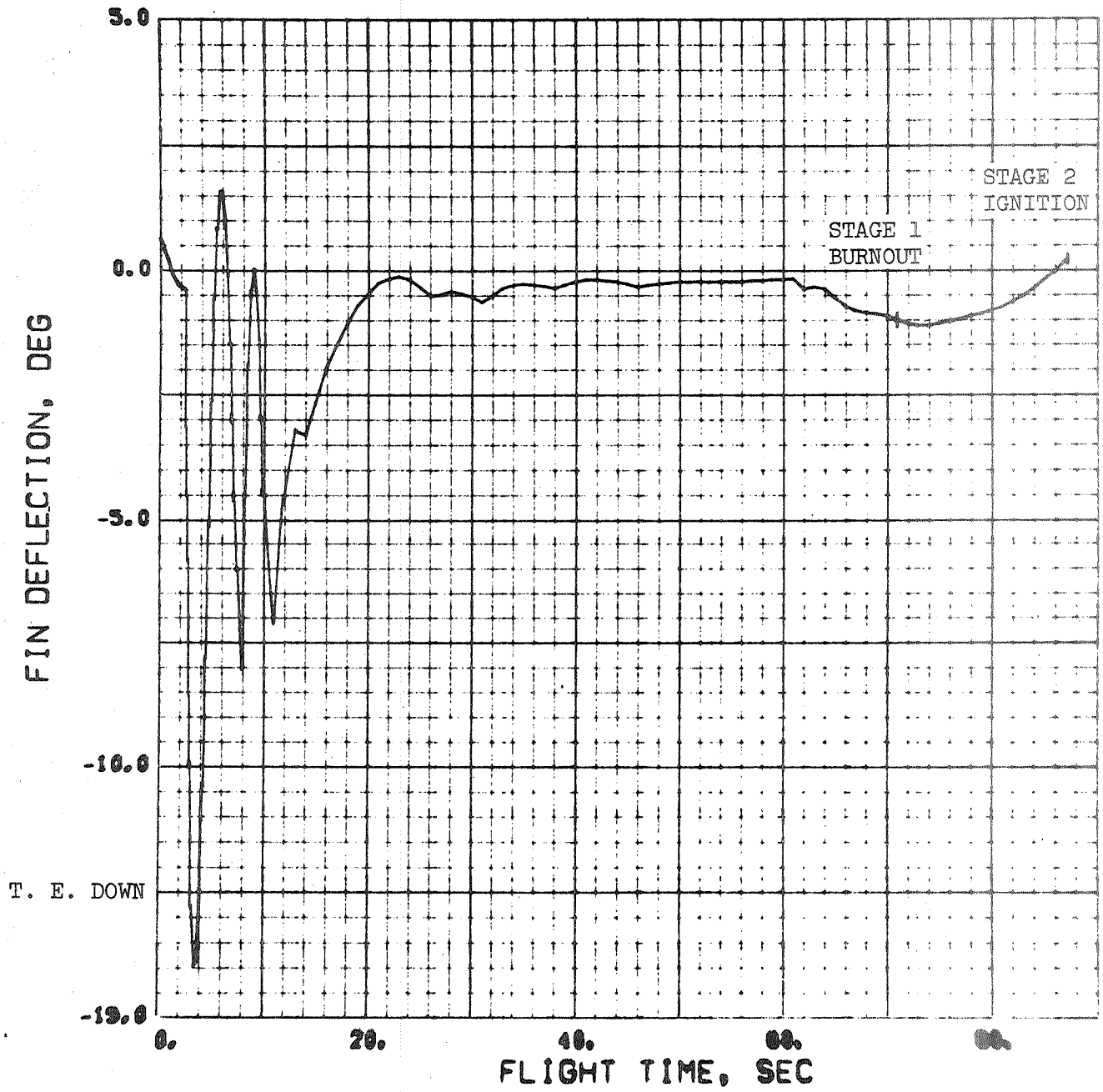

FIGURE 5.6 -7
VEHICLE WEIGHT TIME HISTORY
100 NM INJECTION ALTITUDE DESIGN TRAJECTORY
FIRST STAGE BOOST AND COAST

- 50 LB. PAYLOAD
- ALGOL IIB FIRST STAGE MOTOR (+3 SIGMA)
- 42 IN. DIAMETER HEATSHIELD
- INCREASED SIZE FIRST STAGE FIN-TIPS AND HIGHER GUIDANCE SYSTEM GAINS

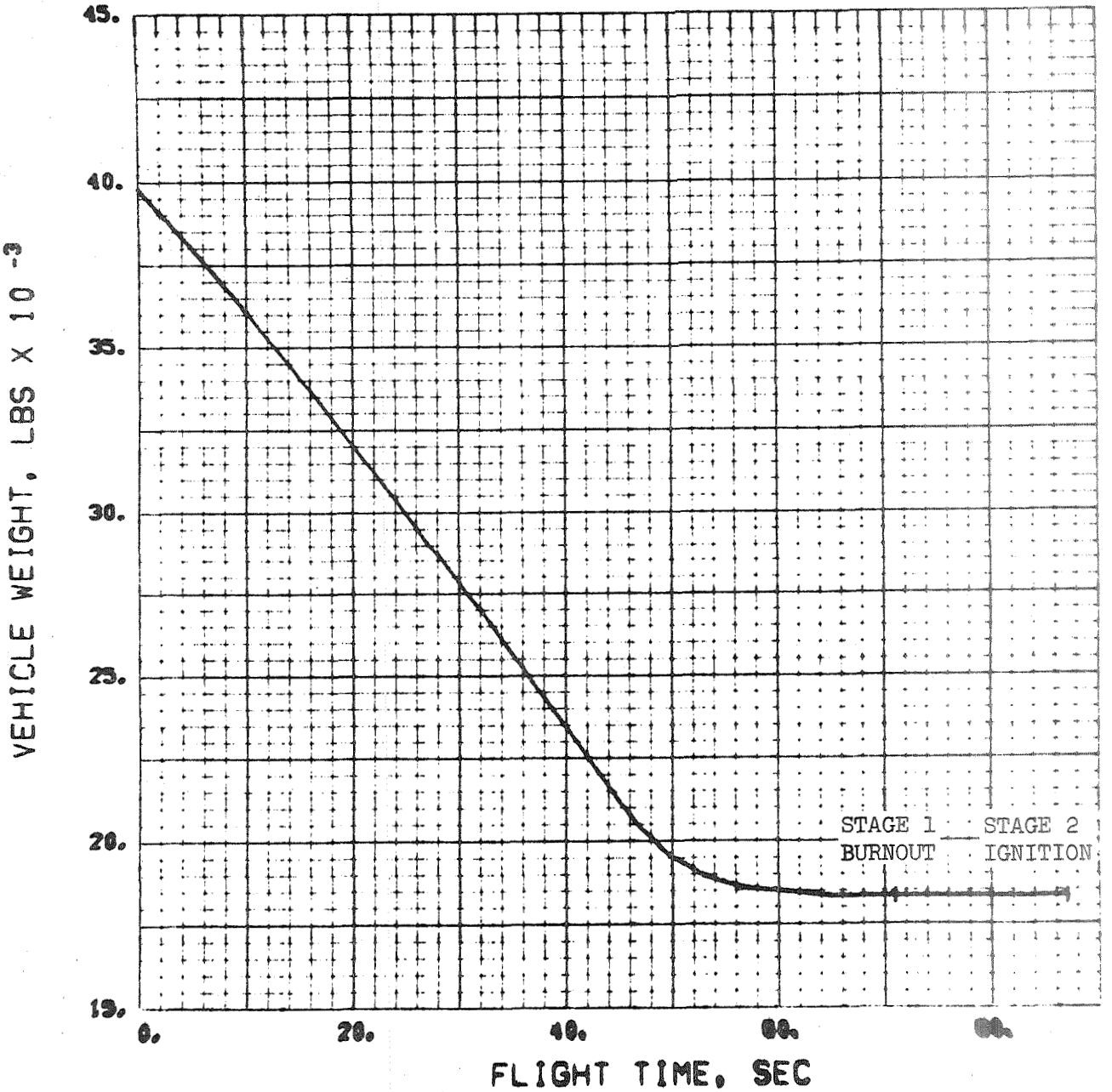

FIGURE 5.6 -8
ACTUAL THRUST TIME HISTORY
100 NM INJECTION ALTITUDE DESIGN TRAJECTORY
FIRST STAGE BOOST AND COAST

- 50 LB PAYLOAD
- ALGOL IIB FIRST STAGE MOTOR (+3 SIGMA)
- 42 IN. DIAMETER HEATSHIELD
- INCREASED SIZE FIRST STAGE FIN-TIPS AND HIGHER GUIDANCE SYSTEM GAINS

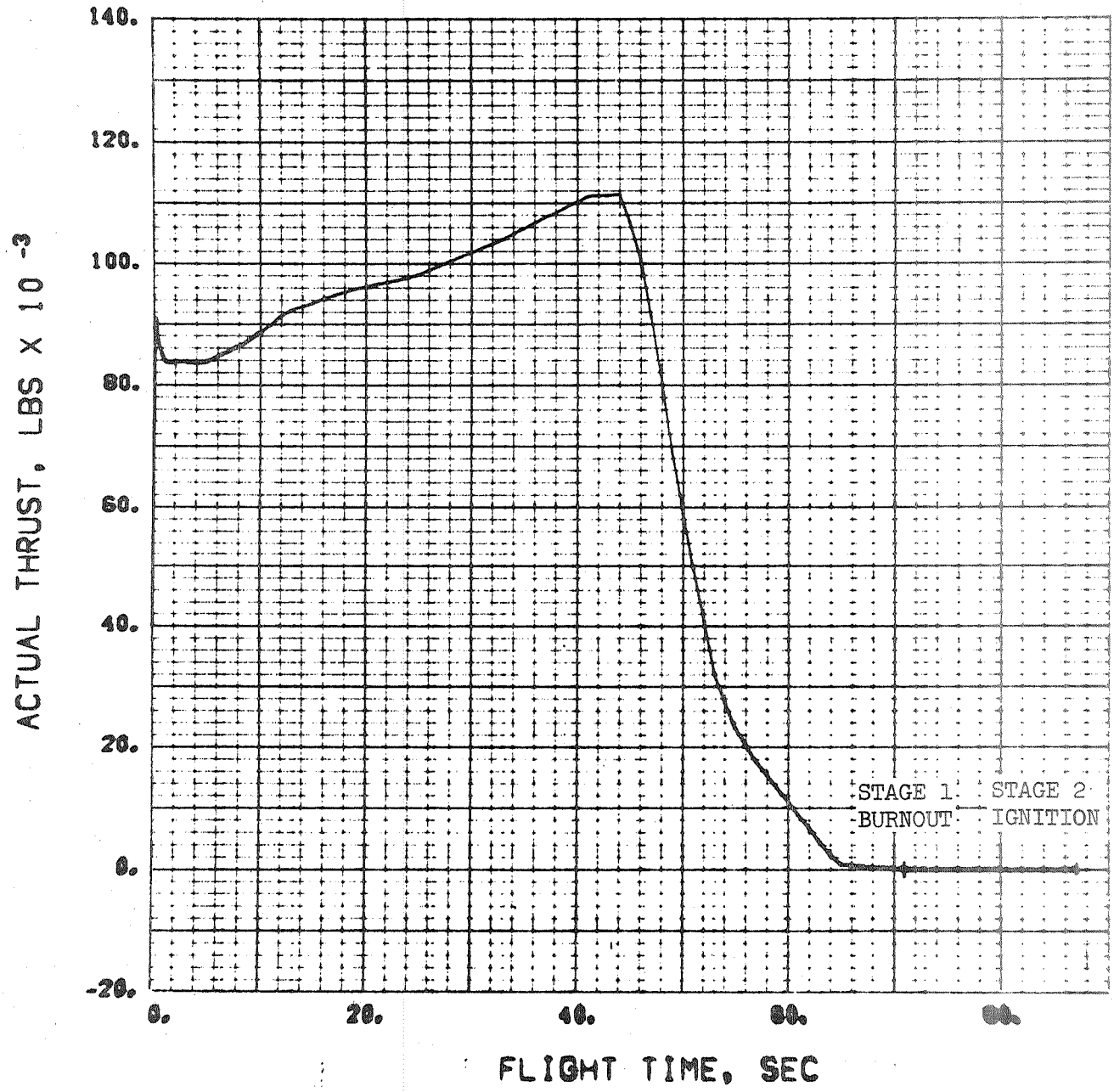

5.7 Stability and Control

The stability and control of the Scout vehicle with an Algol IIB first stage and a 42 inch diameter heatshield was analyzed. The dynamic stability of first stage pitch was analyzed during the critical period near maximum dynamic pressure. The proper control gains, fin size and control effectiveness were determined. The maximum allowable dynamic pressure at second stage ignition was also determined for orbital and re-entry missions.

5.7.1 First Stage Stability near Maximum Dynamic Pressure

Dynamic stability of first stage pitch was analyzed in the area of maximum dynamic pressure by the root locus technique described in Section 3.1.4.1. The analysis utilized the Algol IIB design trajectory for the 50 pound payload described in Section 5.6. The Mach number and dynamic pressure were adjusted to include a 90 knot headwind between 20,000 and 45,000 feet altitude. Mach number, dynamic pressure, center of mass location, and moment of inertia time histories used in the root locus analysis are shown in Figure 5.7-1. Thrust data, aerodynamic data and jet vane data are presented in Sections 5.2, 5.4 and 2.4 respectively. Other significant constants used in the root locus analysis are presented in Table 5.7-1.

The first bending mode is stabilized by the control system for all gains considered. The pitching mode is unstable at low gains due to the vehicle's aerodynamic instability. As gain is increased the roots become stable and then unstable. Instability at high gains is due to the increasing control system lag as the pitching frequency increases. Stabilization of the pitching mode at high gains could be accomplished by adjusting the frequency response of the Base "A" but would result in instability of the first bending mode (Reference 3-1). Root loci analysis reveals that the critical time for vehicle stability occurs at 42 seconds flight time which is near maximum dynamic

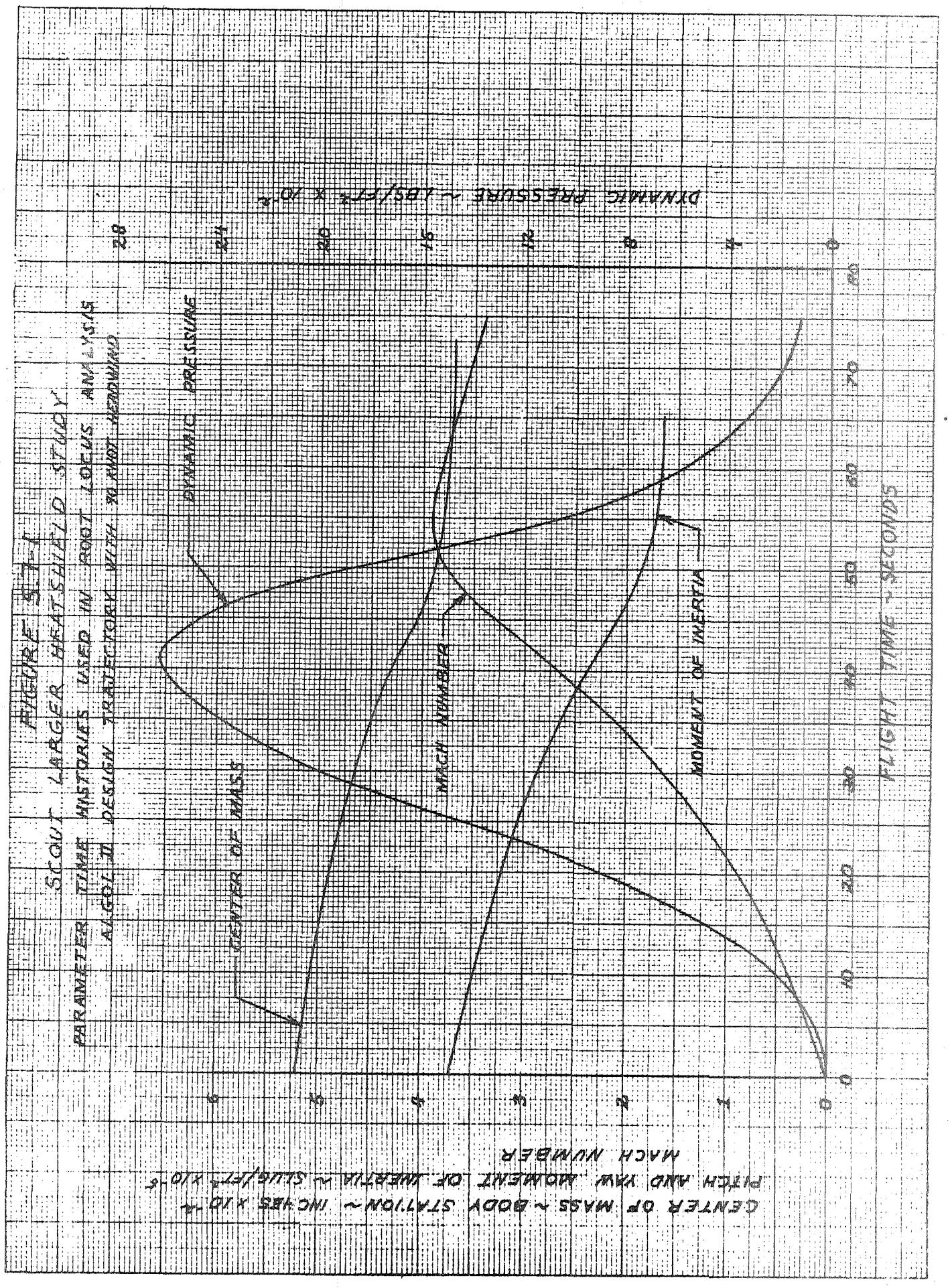
FIGURE S-7-1
SCOUT LARGER HEATSHIELD STUDY
PARAMETER HISTORIES USED IN ROOT LOCUS ANALYSIS
ALGOL II DESIGN TRAJECTORY WITH 30 KNOT HEADWIND
DYNAMIC PRESSURE
CENTER OF MASS
MACH NUMBER
MOMENT OF INERTIA
FLIGHT TIME - SECONDS
DYNAMIC PRESSURE ~ LBS/FT² x 10⁻²
CENTER OF MASS ~ BODY STATION ~ INCHES x 10⁻²
PITCH AND YAW MOMENT OF INERTIA ~ SLUG/FT² x 10⁻⁵
MACH NUMBER

TABLE 5.7-1

CONSTANTS USED IN ROOT LOCUS ANALYSIS

Algol IIB, Castor II, X-259, FW-4S, 50 Lb. Payload, 42 Inch Dia. Heatshield
(42 seconds flight time)

115000.	Thrust, lbs.
22500.	Weight, lbs.
229000.	Pitch or Yaw Moment of Inertia, slug/ft^2
422.	Center of Mass, in. (Body Station)
2842.	Velocity, ft/sec.
2610.	Dynamic Pressure, lbs/ft^2
0.40	Gain Ratio (seconds) K_R/K_D
	Base A Freq. Response Poles:
29.	ω_{1F} filter (rad/sec)
33.	ω_{2F} filter (rad/sec)
13.31	ω_{1S} servo-actuator (rad/sec)
167.54	ω_{2S} servo-actuator (rad/sec)
0.01	Structural Damping Factor
853.45	Control Location (Station)
824.	Thrust Vector Point of Application (Station)

pressure, Figure 5.7-2. The Mach number at this time is 2.93 and the dynamic pressure is 2610 pounds per square foot.

The design criteria of providing a gain margin of ± 6 decibels from instability was chosen for the reasons given in Section 3.1.4.1. At least ± 6 decibels gain margin at the critical time period (42 seconds) can be achieved with the current Scout fin, fin tip and jet vane. However, an attitude control gain of 8 degrees of surface per degree of attitude error is required. A high attitude control gain is desirable for tighter control during first stage but it can cause bottoming out of the control surfaces during the transient motion following the first pitch program step. Tighter control can be achieved at lower gains by increasing the control surface effectiveness. By implementing a fin tip size of 0.542 square feet (78 square inches) the control gains can be reduced to 6.75 degrees of surface deflection per degree of attitude error. This is the same tip size and control gain selected for the Algol III configuration with a 42 inch heatshield. The standard gain and tip size for Algol II and Algol III configurations with a 42 inch heatshield would simplify considerably the tooling and checkout procedures for each vehicle. The increased tip area will also provide better control during first stage coast when the jet vanes are ineffective. This configuration will meet the design criteria of ± 6 decibels from instability. The root loci for the Algol II first stage with 4.73 square feet fin area (includes the larger 0.542 ft^2 tip) and current Algol II jet vane is shown in Figure 5.7-3. The increase in fin area from 4.5 square feet to 4.73 square feet is accomplished by the increased moveable control tip area change only. The external lines of the fixed fin will be the same as the current Scout configuration.

FIGURE 5.7-2
SCOUT LARGER HEATSHIELD STUDY
PITCH AND YAW GAIN BOUNDARIES TIME HISTORY 92 INCH HEATSHIELD, ALGOL II

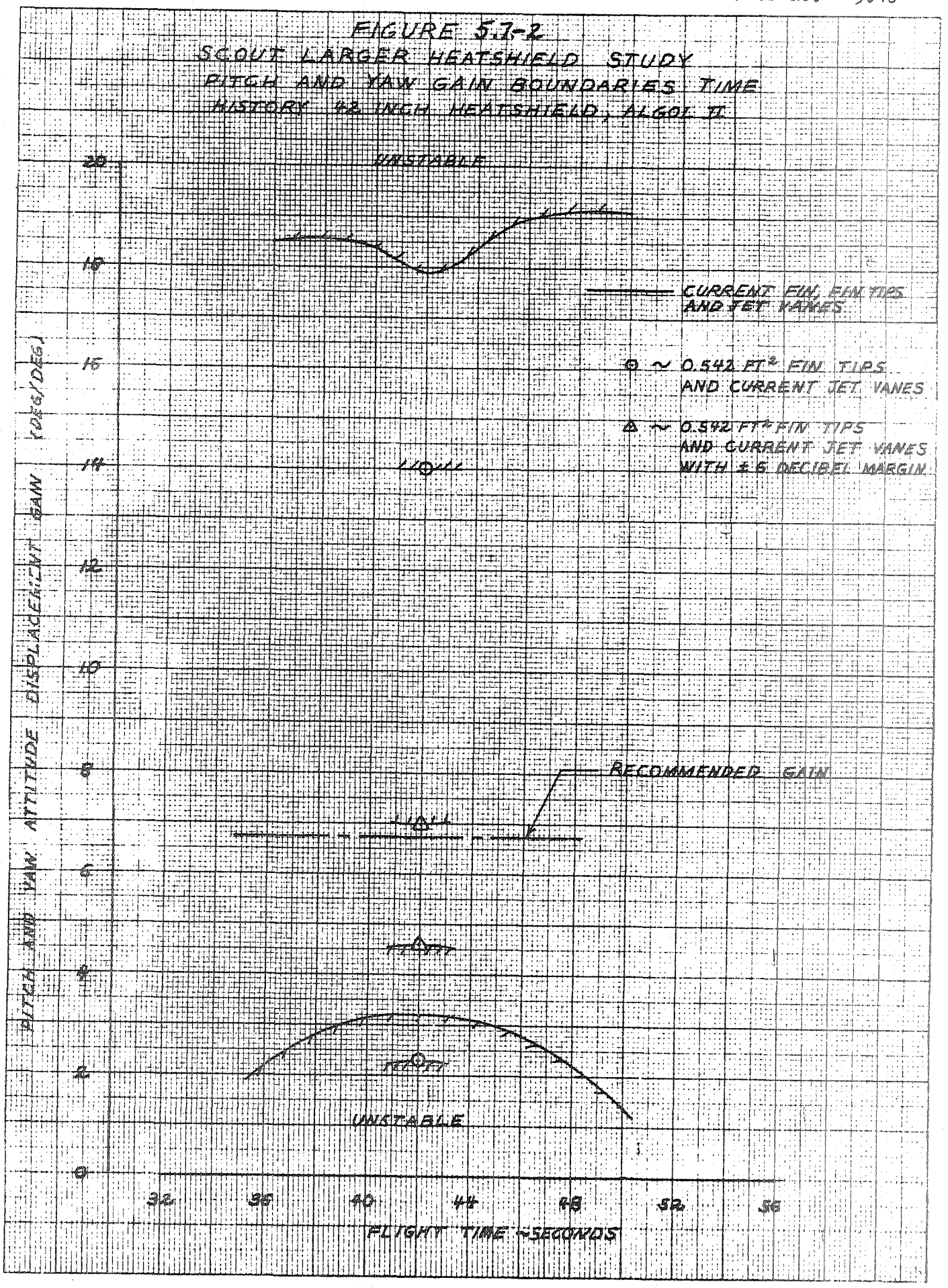

FIGURE 5.7-3
SCOUT LARGER HEATSHIELD STUDY
ROOT LOCI AT 42 SECONDS ~ 42 INCH
HEATSHIELD ALGOL II
CURRENT JET VANE
78 IN² FIN TIP
4.75 FT² FIN
GAIN RATIO $K_\theta/K_{\dot\theta} = 0.4$ SEC.

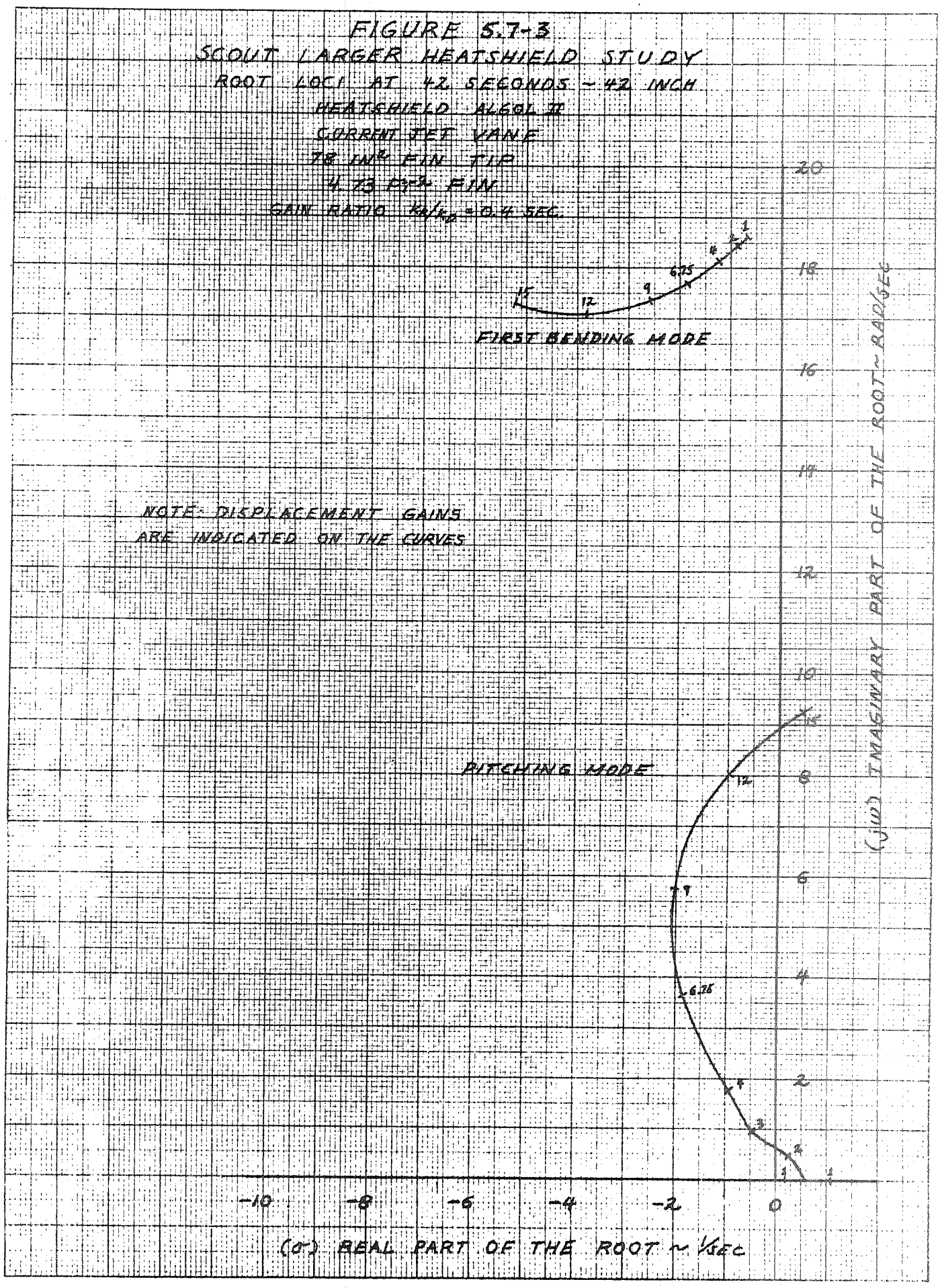

The effect of gain ratio tolerances (K_R/K_D) on the root loci of the pitching mode & first bending mode is shown in Figure 5.7-4.

The effect of Base A frequency response tolerances of the first stage stability at 42 seconds flight time is shown in Figure 5.7-5.

5.7.2 First Stage Hinge Moments

The fin tip configuration (78 square inches) is the same as that used for the Algol III analysis described in Section 3.2.4. However, the Algol II jet vanes are smaller than those selected for the Algol III configuration. Therefore, the Algol II configuration has lower predicted total hinge moments than those presented in Figure 3.1.4-4. The current Base A hydraulic system can provide that hinge moment. However, aerodynamic interference effects with the changed fin-fin tip geometry may increase fin tip hinge moments. It is recommended that wind tunnel testing of this planform be conducted over the transonic and supersonic range to define the fin tip lift and hinge moment coefficients.

5.7.3 Second Stage Ignition Dynamic Pressure Restrictions

The integration of the 42 inch heatshield into the Scout vehicle increases the aerodynamic instability of the second stage. The probability of capturing the vehicle for a given dynamic pressure at second stage ignition is decreased.

The maximum allowable dynamic pressure at second stage ignition was defined by the same method described in Section 3.2.4.5. The input data used in the analysis is presented in Table 5.7-2. The allowable nominal dynamic pressure at second stage ignition is 60 psf and 55 psf for orbital and re-entry missions respectively. This is based on a 99.5 percent probability (95 percent confidence level) of successfully capturing at second stage ignition with less than 10 degrees of attitude error excursion.

FIGURE 5.7-4.
SCOUT LARGER HEATSHIELD STUDY
EFFECT OF GAIN RATIO ON ROOT LOCI
42 INCH HEATSHIELD, ALGOL II
CURRENT JET VANE
78 IN² FIN TIP
4.73 FT² TIP

FIRST BENDING MODE

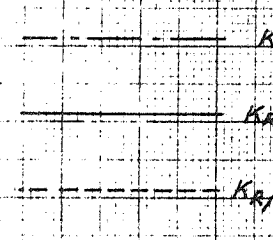

NOTE: THE DISPLACEMENT GAINS ARE INDICATED ON THE CURVES

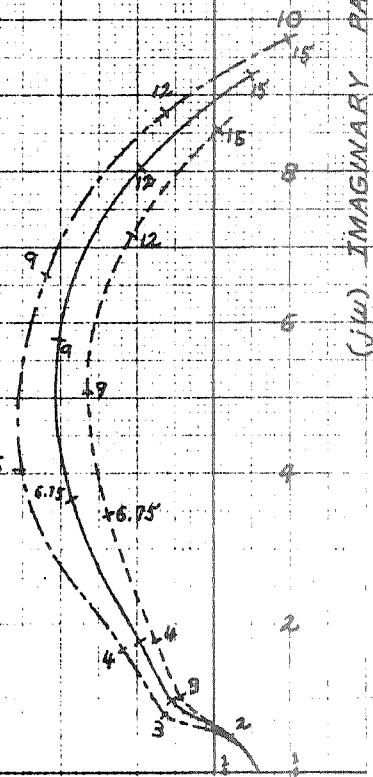

PITCHING MODE

FIGURE 5.7-5
SCOUT LARGER HEATSHIELD STUDY
EFFECT OF BASE "A" FREQUENCY
RESPONSE TOLERANCES ON ROOT LOCI ~42 INCH
HEATSHIELD. ALGOL II
CURRENT JET VANE
.78 IN² FIN TIP
4.73 FT² TIP

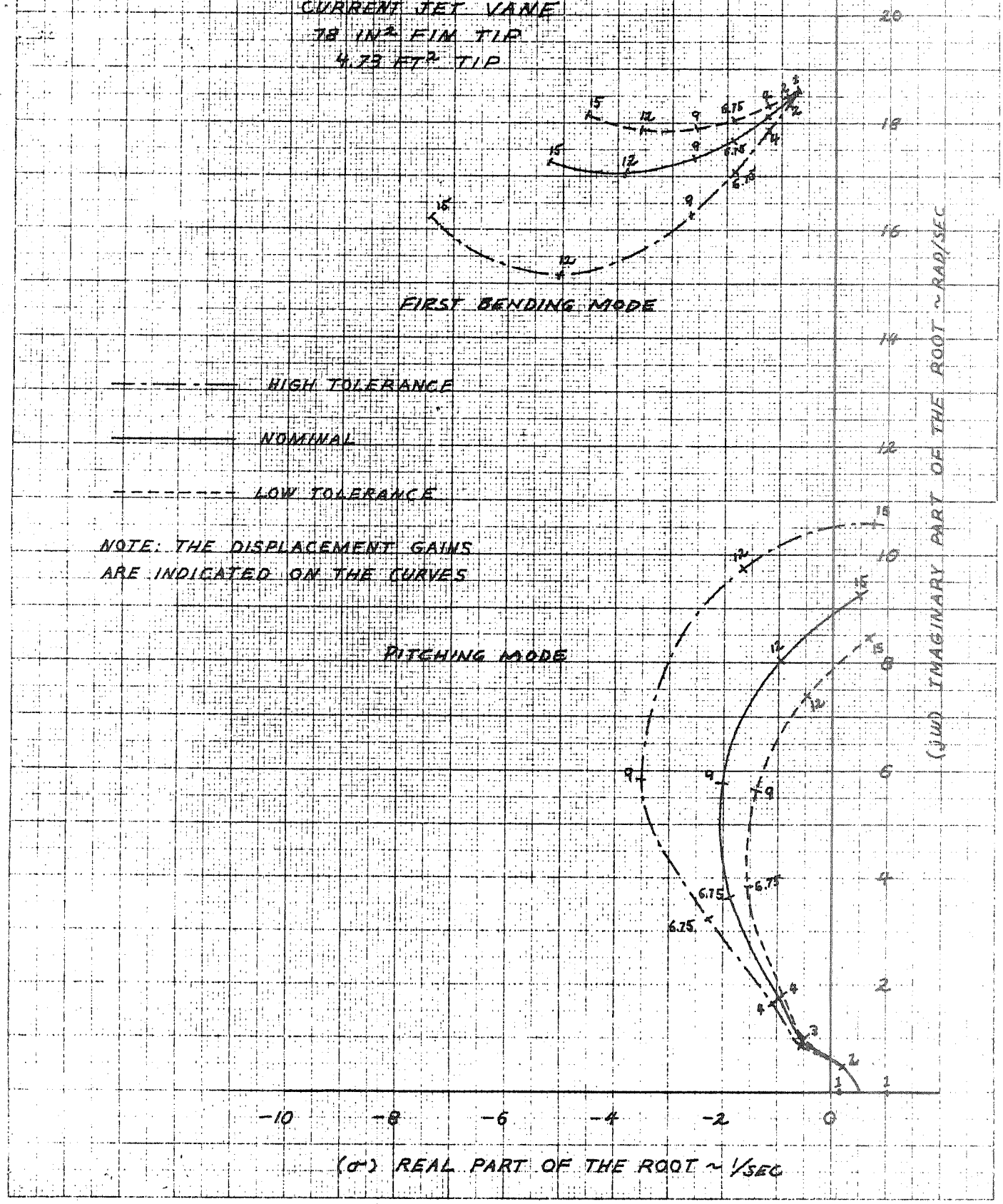

TABLE 5.7-2

SCOUT SECOND STAGE CAPTURE ANALYSIS
INPUT DATA

Algol II, Castor II, X-259, FW-4S, 50 Lb. Payload, 42 Inch Dia. Heatshield

3200.		Velocity @ ignition (ft/sec)
-0.445		Pitch Program Rate deg/sec
-0.4440		Theta Error/Alpha of First Stage
0.4362		Bias in Initial Attitude Error (degrees)
0.54		C_{N_α} S (42 In. Heatshield) (Ft^2/Deg)
107.24	128.69	Center of Pressure (42 In. Heatshield) Body Station
Mean	Standard Deviation	
44861.59	814.	Moment of Inertia (slug-ft^2)
289.69	1.	Center of Mass (station)
178.	90.	Wind Velocity @ Ignition (ft/sec)
27.0	0.894	Initial Flight Path Angle (deg)
-1.403	0.4541	Log_e of Amplitude of Attitude Displacement Error Oscillations

Other input data is the same as shown in Reference 3-1 , Addendum H.

5.7.4 Recommendations

Before the 42 inch heatshield is integrated into the Scout Algol II configuration the following tests and analyses should be completed:

(1) A wind tunnel test of the Algol II configuration with the 42 inch heatshield and larger fin tips to verify the vehicle's stability derivatives, fin tip effectiveness and fin tip hinge moments used in this analysis. If wind tunnel force model data with the larger heatshield is significantly different than predicted data, a pressure model should be tested to define the distributed aerodynamic loads. Fin, fin tip and control gains requirements should then be re-evaluated.

(2) A roll stability analysis using the larger fin tips.

(3) Define first pitch program step limitations with higher attitude control gain.

(4) Re-evaluation of the Base "A" hydraulic system requirements based on wind tunnel hinge moment data and Algol II jet vane hinge moments.

5.8 Flight Loads

5.8.1 Vehicle Loads

The flexible body loads resulting from a 90 knot headwind that occurs during first stage boost were calculated. These loads were combined with the loads due to a 24 fps gust as calculated in Section 3.2.5.1 and are presented in Figure 5.8-1. Although the gust loads were calculated for a vehicle with an Algol III first stage, they are considered sufficiently accurate for this configuration.

The axial loads at the time of maximum bending moments are presented in Figure 5.8-2.

Section 3.1.5.1 discusses the methods used to determine these loads.

5.8.2 Fin Loads

The fins and fin tips used with this configuration are the same as those used with the 40 inch diameter heatshield in the Phase I study. Consequently, the fin loads are the same and may be found in Section 3.1.5.2 of this report.

FIGURE 5.8-1
SCOUT VEHICLE - ALPHA TUB FIRST STAGE
BENDING MOMENT DISTRIBUTION DUE TO
90 KNOT WIND AND 24 FPS GUST

AXIAL LOAD x 10⁻⁴ ~ LBS
4
3
2
1
0
-50
0
50
100
150
200
250
STATION ~ IN.
SCOUT VEHICLE - ALGOL B FIRST STAGE
AXIAL LOAD DISTRIBUTION DUE TO
90 KNOT HEADWIND
HEATSHIELD 42" DIA NOSE E.S. - 44.81
50 LB PAYLOAD
MACH 2.14
$q = 2522.8$
$N_x = 3.51$

FIGURE 5.8-7

5.9 Vehicle Structure

5.9.1 Design Criteria

The structural design criteria is as defined in paragraph 3.1.6.1.

5.9.2 Loads

Plots of vehicle flight ultimate loads with the 42 inch diameter heat shield with Algol II B first stage are shown on Figure 5.9-1. For comparison, plots of flight loads for the basic Scout vehicle with the 34 inch diameter heat shield are also shown.

5.9.3 Heat Shield Attachment Clamp

The basic Scout 34 inch diameter heat shield attachment clamp is designed for an ultimate tension load in the clamp of 7,600 pounds, Reference 3-7. Vehicle loads of 560,000 inch pounds bending moment and 16,000 pounds axial load at station 103.69 for the 42 inch diameter heat shield, Reference Figure 5.9.1, result in an ultimate tension load in the attachment clamp of 8,965 pounds. This is a 17.96% increase over the ultimate design load of the 23-002204 heat shield attachment clamp. Some components of the 23-002204 clamp have a calculated margin of safety less than 18% for the 7,600 pound load, Reference 3-7. These components are the 23-000214-1 pin, 23-000210 link toggle, and the CVC 155-A4 bolt and will require replacement with parts of greater load capability for use with the 42 inch diameter heat shield.

5.9.4 Lower "D" Transition Section

The location of the lower "D" transition section in the vehicle and the thermal loads in the section are discussed in paragraph 3.1.6.5.

A review of the lower "D" transition section structure for loading as shown on Figure 5.9.1 plus thermal loading from Reference 3-7 gives calculated positive margins of safety for the section. A comparison of flight ultimate loads plus thermal loads to structural static test loads for the section is shown in Table 5.9-1. The static test loads shown did not produce structural failure of lower "D".

The section loadings from Table 5.9-1 show that the maximum ultimate compression stress in the aft end of lower "D" section is 10% greater than the maximum test load compression stress. If lower "D" section is insulated to eliminate the thermal loading, then the maximum ultimate compression stress will be 96% of the maximum test compression load.

Structural analysis of the section and the structural testing results show lower "D" transition section, 23-000067, structurally adequate for use on the Scout vehicle with the 42 inch diameter heat shield and Algol II B first stage.

5.9.5 X-259 Motor

A comparison of flight ultimate loads to structural static test loads for the X-259 motor is shown in Table 5.9-2. The static test loads shown did not produce structural failure of the X-259 motor.

Structural analysis of the motor case and the structural testing results show the X-259 motor case structurally adequate for use on the Scout vehicle with the 42 inch diameter heat shield and Algol II B first stage.

5.9.6 Upper and Lower "C" Transition Section

A comparison of flight ultimate loads to structural static test loads for "C" section is shown in Tables 5.9-3 and 5.9-4. The static loads shown for load point 55 resulted in structural failure in the forward region of upper "C" section. The mode of failure was shell buckling due to compression loading.

The section loadings from Table 5.9-3 show that the test compression loads at the forward and aft end of upper "C" section, stations 191.95 and 238.18, were 105% of the ultimate compression loads. The test tension loads at station 238.18 were 130% of the ultimate tension loads. The ratio of test loads to ultimate loads at other stations of "C" section are greater than the above values.

Structural analysis of "C" section and the structural testing results show both upper and lower "C" transition sections, 23-002031 and 23-001031 respectively, structurally adequate for use on the Scout vehicle with the 42 inch diameter heat shield and Algol II B first stage.

5.9.7 Base "A" and Fins

For use with the 42 inch diameter heat shield and Algol II B first stage the basic Scout fin tip has been changed. This change is as shown on Figure 2.2.3-1 for the 40 inch diameter heat shield and Algol III first stage. Fin ultimate reaction loads for the fin to base "A" attachment points are shown on Figure 5.9-2. For comparison, ultimate reaction loads for the fin on the basic Scout 34 inch diameter heat shield vehicle are shown on Figure 3.1.6-2.

Structural analysis of the Base "A" fin support structure shows the support frame and fitting, 23-001079 and 23-001148 at station 848.075, the support frame and fitting, 23-000093 and 23-001151 at station 840.20, and the forward shear attachment at station 825.71 to be structurally adequate for fin loads resulting from the 42 inch diameter heat shield and the Algol II B first stage.

A review of the loads and analysis of the basic fin structure shows the 23-000021 fin to be structurally adequate for use with the 42 inch diameter heat shield although changes to the fin tip will be required as shown on Figure 2.2.3-1.

5.9.8 Structure Summary

The basic 34 inch diameter heat shield Scout vehicle will require structural changes in two areas for use with the 42 inch diameter heat shield and Algol II B first stage. These areas of required structural change are as follows:

(1) Heat shield attachment clamp 23-002204

(2) Fin, 23-000021, redesigned tip for required increased area.

Although analysis of the lower "D" transition shows the section to be structurally adequate, recommendation is made to insulate the section to eliminate the thermal loading due to aerodynamic heating. This will increase the small calculated margin of safety for the section.

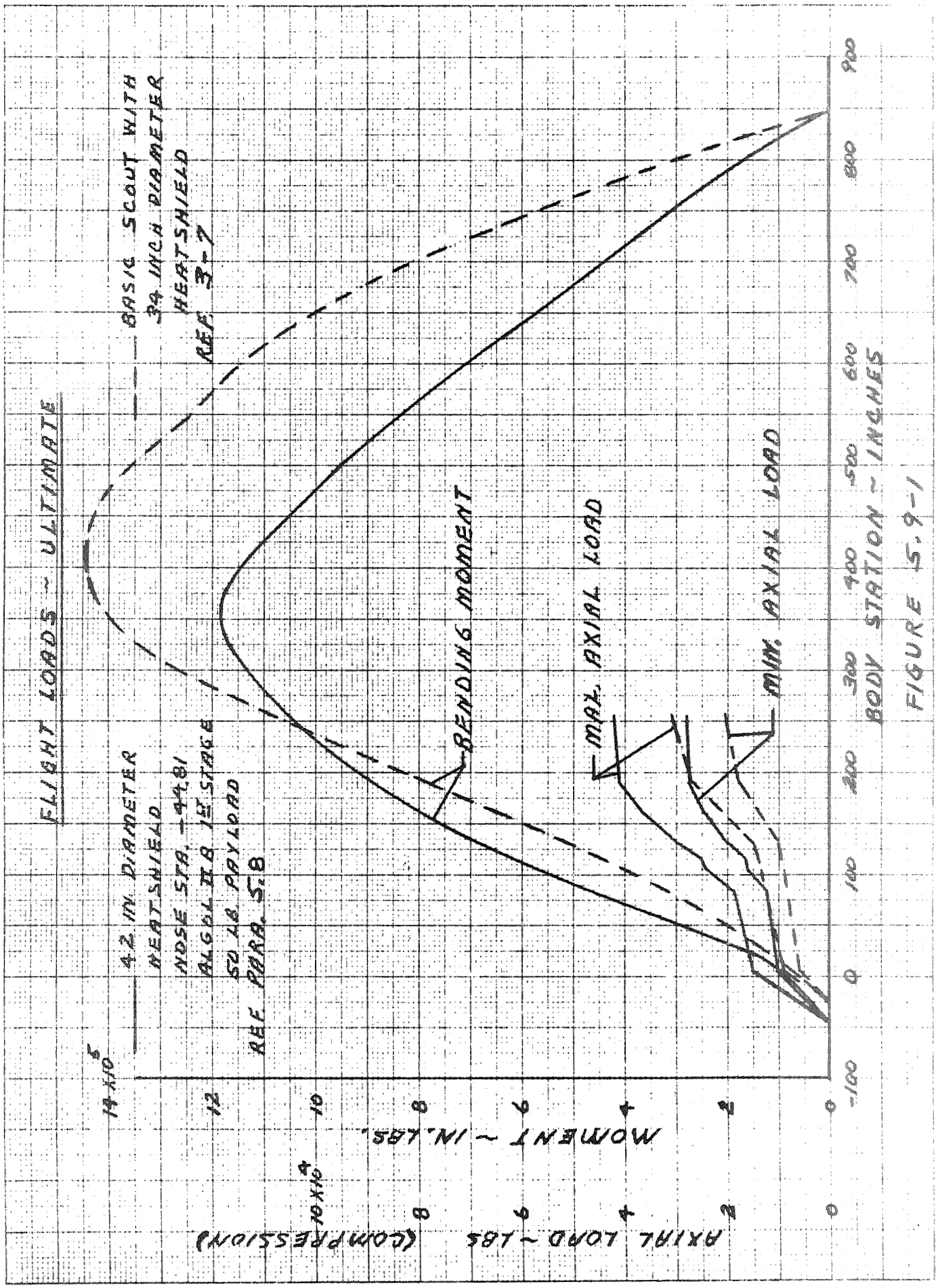
FLIGHT LOADS - ULTIMATE
42 IN. DIAMETER
HEATSHIELD
NOSE STA. +44.81
ALGOL IIB 1ST STAGE
50 LB PAYLOAD
REF PARA 5.8
BASIC SCOUT WITH
34 INCH DIAMETER
HEATSHIELD
REF 3-7
BENDING MOMENT
MAX. AXIAL LOAD
MIN. AXIAL LOAD
14 x 10^5
12
10
8
6
4
2
0
AXIAL LOAD - LBS (COMPRESSION)
8 x 10^4
8
6
4
2
0
MOMENT - IN. LBS.
-100
0
100
200
300
400
500
600
700
800
900
BODY STATION - INCHES

FIGURE 5.9-1

TABLE 5.9-1

LOWER "D" TRANSITION SECTION

COMPARISON OF FLIGHT ULTIMATE AND TEST LOADS

		42 Inch Diameter Heat Shield Ultimate Loads	(1) Test Loads Ld. Point (47)	(1) Test Loads Ld. Point (52)
Station 104.5				
(2)	MOM in. lbs.	560,000	500,680	487,659
(2)	P_{max} lbs.	24,000	40,588	375
(2)	P_{min} lbs.	16,000	- - - -	- - - -
(3)	$P_{Thermal}$ lbs.	13,884	- - - -	- - - -
	f_b psi	± 20,720	± 18,482	± 18,002
	$f_{P\ max}$ psi	- 5,262	- 8,879	- 82
	$f_{P\ min}$ psi	- 3,501	- - - -	- - - -
(3)	f_{TH} psi	- 3,038	- - - -	- - - -
	$f_{c\ max}$ psi	- 29,020	- 27,361	- 18,084
	$f_{t\ max}$ psi	+ 17,219	+ 9,603	+ 17,920
Station 131.1				
(2)	MOM in. lbs.	685,000	584,500	565,000
(2)	P_{max} lbs.	30,000	40,588	375
(2)	P_{min} lbs.	20,000	- - - -	- - - -
(3)	$P_{Thermal}$ lbs.	17,080	- - - -	- - - -
	f_b psi	± 17,322	± 15,853	± 15,324
	$f_{P\ max}$ psi	- 5,536	- 7,872	- 73
	$f_{P\ min}$ psi	- 3,693	- - - -	- - - -
(3)	f_{TH} psi	- 3,154	- - - -	- - - -
	$f_{c\ max}$ psi	- 26,012	- 23,725	- 15,397
	$f_{t\ max}$ psi	+ 13,629	+ 7,981	+ 15,251

(1) Reference 3-8
(2) Reference Figure 5.9-1
(3) Reference 3-7

$$f_b = \frac{Mc}{I} \qquad f_c = \frac{P}{A}$$

$$f_{c\ max} = f_b + f_{P\ max} + f_{TH}$$

$$f_{t\ max} = f_b + f_{P\ min}$$

TABLE 5.9-2

X-259 MOTOR

COMPARISON OF FLIGHT ULTIMATE AND TEST LOADS

		42 Inch Diameter Heat Shield Ultimate Loads	(1) Test Loads	
			Ld. Point (47)	Ld. Point (52)
Station 131.1				
(2)	MOM. in. lbs.	685,000	638,983	617,591
(2)	P_{max} lbs.	30,000	40,588	375
(2)	P_{min} lbs.	20,000	- - - -	- - - -
	W_M lbs/in	± 971	± 906	± 876
	$W_{P\ max}$ lbs/in	- 319	- 431	- 4
	$W_{P\ min}$ lbs/in	- 212	- - - -	- - - -
	$W_{c\ max}$ lbs/in	- 1,290	- 1,337	- 880
	$W_{t\ max}$ lbs/in	+ 759	+ 475	+ 872
Station 191.95				
(2)	MOM in. lbs.	895,000	955,343	914,843
(2)	P_{max} lbs	41,000	40,588	375
(2)	P_{min} lbs	27,333	- - - -	- - - -
	W_M lbs/in	± 1,269	± 1,355	± 1,297
	$W_{P\ max}$ lbs/in	- 436	- 431	- 4
	$W_{P\ min}$ lbs/in	- 290	- - - -	- - - -
	$W_{c\ max}$ lbs/in	- 1,705	- 1,786	- 1,301
	$W_{t\ max}$ lbs/in	+ 979	+ 924	+ 1,293

(1) Reference 3-8
(2) Reference Figure 5.9-1

$W_M = \frac{M}{\pi R^2}$ Where R is radius of shell

$W_P = \frac{P}{\pi D}$ Where D is diameter of shell

$W_{c\ max}$ = Maximum compressive load

$W_{t\ max}$ = Maximum tensile load

TABLE 5.9-3

UPPER "C" TRANSITION SECTION

COMPARISON OF FLIGHT ULTIMATE AND TEST LOADS

		42 Inch Diameter Heat Shield Ultimate Loads	(1) Test Loads	
			Ld. Point (52)	Ld. Point (55)
Station 191.95				
(2)	MOM in. lbs.	895,000	914,943	995,845
(2)	P_{max} lbs	41,000	375	35,821
(2)	P_{min} lbs	27,333	- - - -	- - - -
	W_M lbs/in	± 1,217	± 1,244	± 1,354
	$W_{P\ max}$ lbs/in	- 426	- 4	- 372
	$W_{P\ min}$ lbs/in	- 284	- - - -	- - - -
	$W_{c\ max}$ lbs/in	- 1,643	- 1,248	- 1,726
	$W_{t\ max}$ lbs/in	+ 933	+ 1,240	+ 982
Station 238.18				
(2)	MOM in. lbs.	1,015,000	1,140,676	1,250,156
(2)	P_{max} lbs	42,000	375	35,821
(2)	P_{min} lbs	28,000	- - - -	- - - -
	W_M lbs/in	± 1,380	± 1,416	± 1,552
	$W_{P\ max}$ lbs/in	- 437	- 4	- 356
	$W_{P\ min}$ lbs/in	- 291	- - - -	- - - -
	$W_{c\ max}$ lbs/in	- 1,817	- 1,420	- 1,908
	$W_{t\ max}$ lbs/in	+ 1,089	+ 1,412	+ 1,196

(1) Reference 3-8
(2) Reference Figure 5.9-1

$W_M = \frac{M}{\pi R^2}$ Where R is radius of shell

$W_P = \frac{P}{\pi D}$ Where D is diameter of shell

$W_{c\ max}$ = Maximum compressive load

$W_{t\ max}$ = Maximum tensile load

TABLE 5.9-4

LOWER "C" TRANSITION SECTION

COMPARISON OF FLIGHT ULTIMATE AND TEST LOADS

		42 Inch Diameter Heat Shield Ultimate Loads	(1) Test Loads	
			Ld. Point (52)	Ld. Point (55)
Station 238.18				
(2)	MOM in. lbs.	1,015,000	1,140,676	1,250,156
(2)	P_{max} lbs	42,000	375	35,821
(2)	P_{min} lbs	28,000	- - - -	- - - -
	W_M lbs/in	± 1,257	± 1,413	± 1,549
	$W_{P\ max}$ lbs/in	- 417	- 4	- 356
	$W_{P\ min}$ lbs/in	- 278	- - - -	- - - -
	$W_{c\ max}$ lbs/in	- 1,674	- 1,417	- 1,905
	$W_{t\ max}$ lbs/in	+ 979	+ 1,409	+ 1,193
Station 253.06				
(2)	MOM in. lbs.	1,045,000	1,213,365	1,332,011
(2)	P_{max} lbs	42,200	375	35,821
(2)	P_{min} lbs	28,133	- - - -	- - - -
	W_M lbs/in	± 1,362	± 1,581	± 1,736
	$W_{P\ max}$ lbs/in	- 428	- 4	- 364
	$W_{P\ min}$ lbs/in	- 286	- - - -	- - - -
	$W_{c\ max}$ lbs/in	- 1,790	- 1,585	- 2,100
	$W_{t\ max}$ lbs/in	+ 1,076	+ 1,577	+ 1,372

(1) Reference 3-8
(2) Reference Figure 5.9-1

$W_M = \frac{M}{\pi R^2}$ Where R is radius of shell

$W_P = \frac{P}{\pi D}$ Where D is diameter of shell

$W_{c\ max}$ = Maximum compressive load

$W_{t\ max}$ = Maximum tensile load

FIGURE 5.9-2

FIN REACTION LOADS - ULTIMATE

SCOUT WITH 42 INCH DIAMETER HEAT SHIELD AND ALGOL II B FIRST STAGE

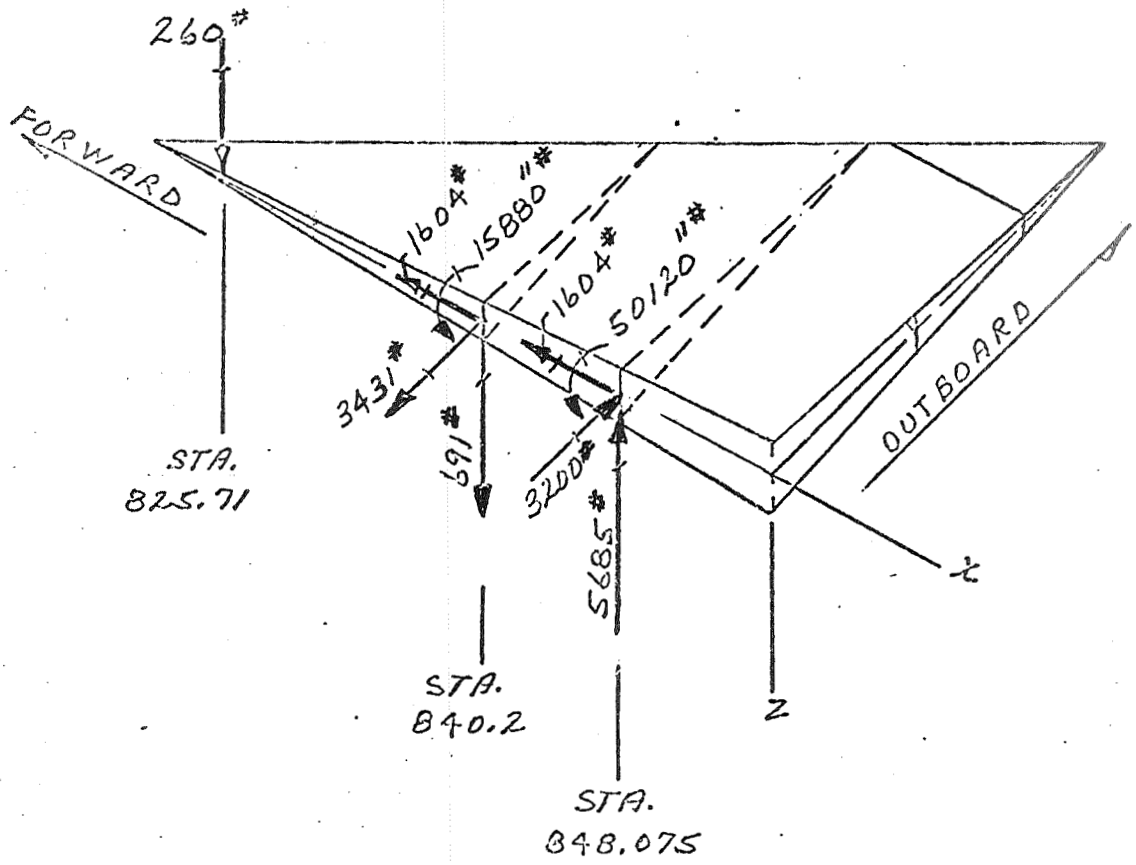

LOADS FROM PARAGRAPH 5.8

5.10 Thermal Analysis

The thermal design trajectory for the 42 inch diameter heatshield on Scout with an Algol IIB booster was compared with previous design trajectories used in thermal analysis of the heatshield. This comparison showed that heating with the Algol IIB booster will be less severe than with the Algol III booster assumed in previous thermal analysis of the 42 inch heatshield. The Algol IIB trajectory is equal in severity from a thermal standpoint to the Algol IIA trajectory used in previous analyses of the 34 inch heatshield. Previous analyses, presented in Section 2.7, showed that for a given trajectory, heating on the 42 inch heatshield is less severe than that on the 34 inch shield. It was concluded, therefore, that no additional thermal protection is required for the 42 inch heatshield with the Algol IIB booster.

5.11 Ground Support Equipment

The ground support equipment noted in Section 3.1.7 was also reviewed to determine the effects of the 42 inch diameter heatshield with the 4.73 sq. ft. fins and Algol II first stage motor. The parts requiring redesign are the same as those noted in paragraphs 3.1.7.1 through 3.1.7.8 and are summarized as follows: payload umbilical retract arm, heatshield cradle, dummy heatshield, payload and heatshield hoist, heatshield storage bracket, the upper cradle assembly, proof loading fixture assembly, and the fin protractor kit.

5.12 Discussion of Results and Recommendations

The purpose of this phase of the study was to define the impact of installing a 42 inch diameter heatshield on the Scout B configuration (Algol IIB motor installed). This configuration is less critical from the stability and control standpoint than the Scout D configuration previously evaluated and as a result has a lesser impact on the vehicle configuration. The analysis has shown that adequate stability and control is provided if the fin tip control surfaces are increased in size from 45 to 78 sq. in. and the guidance system displacement gain is increased from 5.0 to 6.75. The changes to these systems are the same as those required for the Scout D configuration except that the basic vehicle fins and jet vanes are not changed. This approach standardizes the guidance system checkouts for all vehicle with 42 in. diameter heatshields.

The vehicle structural changes required are to the heatshield attachment clamp and the fin tip plus the addition of cork thermal protection to lower "D" section. The G.S.E. changes are the same as required for the 42 inch heatshield installation on the Scout D configuration.

It was recommended in Section 4.0 that the aerodynamic characteristics of the Scout D configuration with the large heatshield be determined by wind tunnel testing to support final design effort. It is likewise recommended that the Scout B configuration with the large heatshield and larger fin tips be tested to define: (1) vehicle stability characteristics, (2) fin tip effectiveness, (3) fin tip hinge moments.

REFERENCES

2-1 NASA SP8001 "Buffeting During Launch and Exit", dated 4 May 1964.

2-2 USAF Stability and Control Datcom, Douglas Aircraft Co., dated October 1960.

2-3 Dye, Jr., F. E. Irwin, H.M., "Development of Empirical Aerodynamic Data - Nose Drag and Base Pressure Drag, 3-50000 /2M-787", dated 11 June 1962.

2-4 LTV MSD-T 23-DIR-463 "Preliminary Estimation of Aerodynamics with the 34" Diameter Payload and 44.3" Diameter Algol Motor", dated 7 February 1967.

2-5 LTV MSD-T Report No. 23-361 "Semi-Annual Review of Scout Orbital Performance Capability", Revision C, dated 11 June 1969.

2-6 LTV MSD-T Report No. 00.302, "Recommended Procedures for Analysis of Aerodynamic Heating of Booster Components", dated 2 October 1963.

3-1 LTV MSD-T Report No. AST/EIR-13381 "Stability and Control Report", dated 2 March 1961.

3-2 LTV MSD-T Report No. 23.390 "Scout Aerodynamic Design Data Report", dated 31 January 1969.

3-3 NASA Langley Research Center "Detail Specification for FY '63 Scout ", Specification No. L-2880, dated 7 January 1963.

3-4 LTV MSD-T 23-DIR-872 "Scout Second and Third Stage Ignition Dynamic Pressure Restrictions", dated 28 March 1969.

3-5 LTV MSD-T Report No. 00.651 "Mizor Flexible Body Trajectory and Loads Routine", dated 10 June 1965.

3-6 LTV MSD-T Report No. 23.392 "Scout Structural Dynamics Report", dated 31 January 1969.

3-7 LTV MSD-T Report No. 23.385 "Scout Vehicles 163 and Subsequent Stress Analysis", dated 30 January 1969.

3-8 LTV MSD-T Report No. 23.276 "Structural Load Test Results Evaluation ABL X-259 Motor Loaded and Unloaded Case", dated 29 April 1966.

3-9 LTV MSD-T Report No. 23.324 "Final Report Feasibility Study for a 44" First Stage Rocket Motor", dated 31 August 1967.

3-10 Muraca, R. J., "An Empirical Method for Determining Static Distribution Aerodynamic Loads on Axisymmetric Multi-stage Launch Vehicles", NASA TN-D 3283, dated March 1966.

REFERENCES (Concluded)

3-11 Gray, J. Don, "Drag and Stability Derivatives of Missile Components According to the Modified Newtonian Theory", AEDC-TN-60-191, dated November 1960.

3-12 LTV MSD-T Report No. 00.83, Damstrom, E. K., Dye, Jr. F.E., "Computation of Local Flow Conditions and Aerodynamic Parameters by a Second-Order Shock Expansion Method Applicable to Bodies of Revolution Near Zero Lift and at Supersonic Speeds", dated September 1962.

3-13 LTV MSD-T Report No. 00.457 "Description of a Guided Missile Trajectory Routine, LVVC-38", dated 29 September 1964.

3-14 LTV MSD-T 23-DIR-814 "Upper Atmospheric Wind Data 65K to 210K Feet Altitude", dated 16 August 1968.

3-15 LTV MSD-T Report No. 00.190 "The Buckling of Cylindrical Shells Under Compressive or Bending Loads", dated 29 March 1963.

3-16 NASA Report No. CR-912 "Shell Analysis Manual", dated April 1968.

APPENDIX A

COMPUTER LISTING OF DESIGN TRAJECTORIES

DEFINITION OF TERMS FOR DIGITAL COMPUTER

TRAJECTORY PROGRAM NEMAR

ROUTINE NO. LV-VC-27

The terms which appear as tabular functions of time on the output pages of routine NEMAR are defined below.

WEIGHT	total vehicle weight (lbs.)
THRUST	total thrust force (lbs.)
ALT	altitude (ft.)
REL VEL	earth relative velocity or velocity with respect to the frame of reference that rotates with the earth (ft/sec.)
MACH	airspeed divided by local sound speed
DYN. P	dynamic pressure; one-half density times airspeed squared (lbs./ft.^{2})
ALPHA	angle of attack; angle between the body x (longitudinal) axis and the airspeed vector projection on the body x, z (pitch) plane
Q-ALPHA	product of dynamic pressure and angle of attack (lbs./ft.^{2})
Q-COMM	the command pitch rate (deg./sec.)
Q	body axis angular velocity about the lateral axis (deg./sec.)
PITCH ERR	the guidance system pitch attitude error (deg.)
Q-CONT	control surface deflection (deg.)
THETA	angle between the body x (longitudinal) axis and the geocentric horizontal plane (deg.)
R-GAM	geocentric path angle of the earth-relative velocity vector (deg.)

LARGER VOLUME HEATSHIELD STUDY, 100 NM DESIGN TRAJECTORY MAY 59
AEROJET II, +3 SIGMA (RANGE SAFETY) 50 LB PAYLOAD

LTV AEROSPACE [illegible]
ROUTINE NO. [illegible]

TIME SEC	WEIGHT LBS	THRUST LBS	FT	REL VEL FT/SEC	MACH	DYN. LBS/FT2	ALPHA DEG	Q-ALPHA LB/SQ FT	Q-COMM DEG/SEC	Q DEG/SEC	PITCH ERR DEG	Q-CONT DEG	THETA DEG	R-GAM DEG
0.0	47130.	35515.	-0.	0.0	0.0	0.0	0.0	0.	0.0	0.0	0.0	0.00	89.814	0.0
0.50	46851.	135415.	7.	28.2	0.03	0.9454	-0.00	-0.	0.0	0.00	-0.000	-0.00	89.814	89.313
1.00	46573.	134794.	28.	58.7	0.05	4.0856	-0.00	-0.	-2.75007	-0.00	-0.014	-0.07	89.814	89.814
1.50	46294.	134180.	65.	89.1	0.08	9.4260	-0.24	-2.	-5.50000	-0.89	-2.596	-11.20	89.761	89.792
2.00	46016.	133572.	117.	119.6	0.11	16.9453	-1.13	-19.	-5.76591	-2.97	-4.465	-16.38	88.901	89.808
2.50	45738.	132971.	185.	150.1	0.13	26.6297	-2.73	-73.	-5.76591	-5.33	-5.264	-15.66	86.830	89.529
3.00	45459.	132377.	267.	180.6	0.16	38.4634	-4.84	-186.	-5.76591	-7.13	-4.995	-10.71	83.682	88.515
3.50	45181.	131738.	365.	211.1	0.19	52.3863	-7.06	-370.	-5.76591	-7.92	-4.070	-4.52	79.877	86.938
4.00	44903.	131206.	478.	241.4	0.22	68.2995	-8.99	-614.	-5.76591	-7.67	-3.019	0.24	75.945	84.937
4.50	44624.	130630.	606.	271.6	0.24	86.1297	-10.35	-892.	-5.76591	-6.72	-2.287	2.00	72.332	82.684
5.00	44357.	129576.	747.	301.7	0.27	105.8219	-11.08	-1172.	-3.68444	-5.56	-2.091	0.67	69.266	80.344
5.50	44094.	128326.	903.	331.6	0.30	127.2397	-11.16	-1420.	-1.60000	-3.92	-0.492	5.39	66.857	78.019
6.00	43832.	127082.	1072.	361.4	0.32	150.4080	-10.40	-1565.	-1.60000	-1.87	0.154	4.51	65.414	75.816
6.50	43565.	125843.	1253.	391.3	0.35	175.4314	-8.95	-1569.	-1.60000	-0.30	-0.138	-0.09	64.907	73.853
7.00	43306.	124608.	1447.	421.5	0.38	202.3157	-7.22	-1461.	-1.60000	0.32	-0.987	-5.58	64.958	72.179
7.50	43044.	123379.	1654.	451.7	0.41	230.9473	-5.70	-1316.	-1.19604	0.02	-1.902	-9.54	65.077	70.774
8.00	42781.	122154.	1874.	481.9	0.43	261.1719	-4.65	-1214.	-0.79111	-0.68	-2.134	-9.31	64.913	69.562
8.50	42518.	120933.	2106.	512.0	0.46	292.8525	-4.04	-1183.	-0.79111	-1.23	-2.041	-7.75	64.427	68.467
9.00	42256.	119717.	2350.	542.1	0.49	325.8621	-3.69	-1203.	-0.79111	-1.44	-1.755	-5.90	63.747	67.438
9.50	42001.	118513.	2606.	572.0	0.52	360.0791	-3.41	-1228.	-0.79111	-1.33	-1.448	-4.59	63.047	66.457
10.00	41759.	117327.	2874.	601.8	0.54	395.3804	-3.07	-1214.	-0.79111	-1.05	-1.247	-4.13	62.452	65.523
10.50	41518.	116145.	3154.	631.4	0.57	431.6528	-2.65	-1144.	-0.79111	-0.81	-1.183	-4.30	61.994	64.643
11.00	41277.	114967.	3445.	660.9	0.60	468.7820	-2.20	-1030.	-0.79111	-0.71	-1.207	-4.62	61.625	63.822
11.50	41036.	113792.	3747.	690.2	0.63	506.6331	-1.79	-905.	-0.79111	-0.74	-1.244	-4.74	61.268	63.055
12.00	40794.	112620.	4060.	719.3	0.65	545.0730	-1.46	-794.	-0.79111	-0.83	-1.247	-4.57	60.878	62.334
12.50	40553.	111451.	4384.	748.1	0.68	583.9670	-1.21	-705.	-0.79111	-0.92	-1.204	-4.19	60.441	61.649
13.00	40312.	110285.	4719.	776.8	0.71	623.1919	-1.02	-635.	-0.79111	-0.96	-1.129	-3.73	59.973	60.993
13.50	40071.	109121.	5063.	805.1	0.73	662.6135	-0.86	-572.	-0.79111	-0.96	-1.045	-3.31	59.496	60.360
14.00	39829.	107961.	5418.	833.3	0.76	702.1011	-0.72	-508.	-0.79111	-0.94	-0.967	-2.96	59.024	59.747
14.50	39608.	107214.	5783.	861.2	0.79	741.6663	-0.59	-438.	-0.79111	-0.92	-0.899	-2.66	58.563	59.154
15.00	39387.	106465.	6158.	889.0	0.81	781.3179	-0.47	-368.	-0.79111	-0.91	-0.837	-2.35	58.107	58.579
15.50	39166.	105725.	6542.	916.6	0.84	820.9258	-0.37	-302.	-0.79111	-0.92	-0.774	-2.04	57.652	58.020
16.00	38945.	104983.	6935.	944.0	0.87	860.3892	-0.28	-241.	-0.79111	-0.92	-0.711	-1.71	57.195	57.476
16.50	38724.	104242.	7338.	971.?	0.89	899.6028	-0.21	-186.	-0.79111	-0.92	-0.647	-1.40	56.738	56.944
17.00	38503.	103503.	7749.	998.3	0.92	938.4082	-0.14	-133.	-0.79111	-0.91	-0.585	-1.10	56.283	56.425
17.50	38281.	102765.	8169.	1025.1	0.95	976.5691	-0.09	-83.	-0.79111	-0.91	-0.526	-0.82	55.831	55.915
18.00	38060.	102026.	8597.	1051.5	0.97	1013.9546	-0.04	-36.	-0.79111	-0.90	-0.470	-0.55	55.381	55.417
18.50	37839.	101292.	9035.	1077.5	1.00	1050.4521	0.01	8.	-0.79111	-0.89	-0.416	-0.29	54.935	54.923
19.00	37622.	101196.	9480.	1103.4	1.02	1086.2349	0.05	50.	-0.79111	-0.89	-0.367	-0.06	54.493	54.446
19.50	37405.	101444.	9937.	1129.4	1.05	1121.5773	0.08	90.	-0.79111	-0.88	-0.320	0.16	54.053	53.973
20.00	37193.	101693.	10393.	1155.5	[illegible]	1157.66[illegible]	0.11	127.	-0.79111	-0.67	-0.277	0.36	53.617	53.507
20.00	37193.	101663.	10393.	1155.5	[illegible]	1157.67[illegible]	0.11	127.	-0.79111	-0.87	-0.277	0.36	53.617	53.507
20.00	37173.	[illegible]	10393.	1155.5	[illegible]	1157.[illegible]	0.11	127.	-0.79111	-0.87	-0.277	0.35	53.617	53.507
21.00	36754.	[illegible]	[illegible]	1206.3	[illegible]	1229.7140	0.16	195.	-0.79111	-0.86	-0.201	0.72	52.755	[illegible]
22.00	[illegible]	[illegible]	[illegible]	[illegible]	[illegible]	[illegible]	[illegible]	[illegible]	-0.79111	-0.84	-0.141	[illegible]	51.907	51.712

LARGER VOLUME HEATSHIELD STUDY, [illegible]
AEROJET II, +3 SIGMA (RANGE SAFETY) 50 LB PAYLOAD

LTV AEROSPACE CORP.-MSD
[illegible] NO. LVVC27

TIME SEC	WEIGHT LBS	THRUST LBS	ALT FT	REL VEL FT/SEC	MACH [illegible]	DYN. P LBS/FT2	ALPHA DEG	Q-ALPHA LB/SQ FT	Q-COMM DEG/SEC	Q DEG/SEC	PITCH ERR DEG	Q-CONT DEG	THETA DEG	R-DAY DEG
23.00	35906.	103187.	13316.	1316.3	1.24	1358.7717	0.23	309.	-0.79111	-0.83	-0.096	1.17	51.079	50.853
24.00	35468.	104442.	14355.	1372.0	1.29	1438.1401	0.25	362.	-0.79111	-0.81	-0.072	1.25	50.269	50.018
25.00	35025.	106104.	15421.	1429.9	1.35	1508.6169	0.27	407.	-0.79111	-0.79	-0.064	1.27	49.476	49.206
26.00	34581.	107764.	16520.	1489.9	1.42	1580.0186	0.28	443.	-0.79111	-0.78	-0.071	1.20	48.698	48.417
27.00	34138.	109422.	17651.	1552.3	1.48	1652.1665	0.29	473.	-0.79111	-0.76	-0.095	1.04	47.937	47.651
28.00	33695.	111077.	18815.	1617.2	1.55	1724.7634	0.28	491.	-0.79111	-0.75	-0.134	0.82	47.191	46.907
29.00	33226.	113196.	20013.	1684.9	1.62	1797.9634	0.27	492.	-0.79111	-0.74	-0.185	0.55	46.458	46.184
30.00	32756.	115326.	21247.	1755.6	1.70	1871.9438	0.24	452.	-0.73551	-0.75	-0.234	0.32	45.722	45.481
31.00	32286.	117451.	22517.	1829.7	1.78	1946.3403	0.23	441.	-0.68000	-0.66	-0.207	0.28	45.021	44.795
32.00	31816.	119572.	23825.	1907.2	1.87	2020.7368	0.26	517.	-0.68000	-0.64	-0.247	0.05	44.388	44.133
33.00	31336.	121628.	25173.	1988.2	1.96	2094.6113	0.25	519.	-0.68000	-0.66	-0.273	-0.05	43.742	43.494
34.00	30832.	123534.	26563.	2072.9	2.05	2167.2539	0.22	472.	-0.68000	-0.66	-0.296	-0.17	43.092	42.874
35.00	30327.	125435.	27995.	2161.4	2.15	2238.1074	0.17	373.	-0.61138	-0.67	-0.313	-0.23	42.437	42.271
36.00	29823.	127330.	29471.	2253.9	2.26	2306.5801	0.14	334.	-0.54286	-0.55	-0.237	-0.09	41.826	41.681
37.00	29318.	129220.	30993.	2350.5	2.37	2371.9824	0.21	491.	-0.54286	-0.50	-0.269	-0.35	41.323	41.116
38.00	28797.	130918.	32563.	2451.5	2.49	2433.3398	0.25	601.	-0.54286	-0.52	-0.306	-0.49	40.825	40.578
39.00	28265.	132498.	34183.	2556.9	2.62	2489.5781	0.25	616.	-0.54286	-0.53	-0.325	-0.57	40.309	40.062
40.00	27733.	134069.	35855.	2666.6	2.75	2539.5488	0.22	555.	-0.54286	-0.55	-0.332	-0.57	39.782	39.564
41.00	27201.	135633.	37580.	2781.1	2.87	2549.9648	0.16	403.	-0.54286	-0.56	-0.320	-0.47	39.236	39.079
42.00	26670.	137185.	39362.	2900.6	3.00	2547.0391	0.07	180.	-0.48805	-0.58	-0.289	-0.28	38.673	38.602
43.00	26126.	137928.	41200.	3025.0	3.12	2536.8164	0.01	30.	-0.43333	-0.47	-0.185	0.02	38.145	38.133
44.00	25583.	138613.	43098.	3154.1	3.26	2516.4121	0.05	120.	-0.43333	-0.40	-0.192	-0.16	37.728	37.680
45.00	25035.	138926.	45057.	3287.8	3.40	2491.5371	0.09	213.	-0.43333	-0.41	-0.222	-0.28	37.335	37.250
46.00	24484.	138995.	47079.	3425.8	3.54	2455.6328	0.08	199.	-0.43333	-0.44	-0.228	-0.26	36.918	36.837
47.00	23940.	138784.	49165.	3568.3	3.69	2411.0020	0.04	106.	-0.43333	-0.45	-0.213	-0.16	36.481	36.437
48.00	23414.	137826.	51313.	3714.4	3.84	2356.8848	-0.01	-23.	-0.38943	-0.46	-0.191	-0.04	36.038	36.048
49.00	22888.	136858.	53537.	3863.3	3.99	2293.5859	-0.03	-71.	-0.34559	-0.36	-0.124	0.09	35.637	35.668
50.00	22363.	132818.	55824.	4014.9	4.15	2219.9004	0.02	41.	-0.34559	-0.32	-0.142	-0.08	35.321	35.303
51.00	21837.	128538.	58177.	4164.8	4.30	2134.6616	0.05	111.	-0.34559	-0.34	-0.162	-0.14	35.008	34.956
52.00	21400.	118266.	60595.	4310.9	4.45	2037.3916	0.05	112.	-0.34559	-0.35	-0.163	-0.12	34.676	34.522
53.00	21025.	103861.	63077.	4440.9	4.58	1920.2065	0.04	83.	-0.34559	-0.35	-0.160	-0.10	34.340	34.297
54.00	20650.	89447.	65598.	4552.6	4.73	1789.3345	0.03	45.	-0.34559	-0.35	-0.156	-0.08	34.004	33.979
55.00	20276.	75024.	68157.	4645.7	4.79	1653.7544	0.00	2.	-0.34559	-0.35	-0.151	-0.05	33.668	33.666
56.00	19901.	60593.	70747.	4719.7	4.86	1494.9570	-0.03	-39.	-0.34559	-0.35	-0.146	-0.03	33.331	33.357
57.00	19732.	50301.	73344.	4776.3	4.91	1348.9047	-0.06	-79.	-0.34559	-0.35	-0.138	0.02	32.992	33.051
58.00	19532.	40383.	75905.	4819.0	4.94	1210.0144	-0.09	-112.	-0.34559	-0.35	-0.131	0.05	32.653	32.745
59.00	19432.	30459.	78354.	4847.5	4.95	1079.5422	-0.12	-135.	-0.34559	-0.35	-0.125	0.08	32.316	32.441
60.00	19283.	20529.	80674.	4861.4	4.97	956.2561	-0.15	-150.	-0.34559	-0.35	-0.120	0.10	31.980	32.137
61.00	19184.	19303.	82873.	4860.7	4.96	846.7402	-0.19	-161.	-0.34559	-0.35	-0.113	0.14	31.643	31.833
62.00	19137.	749[illegible]	[illegible]	4853.2	4.96	747.1748	-0.23	-170.	-0.34559	-0.36	-0.101	0.22	31.299	31.527
63.00	19111.	[illegible]	[illegible]	4842.3	4.95	657.5977	-0.27	-176.	-0.34559	-0.36	-0.086	0.29	30.953	31.220
64.00	19085.	377[illegible]	[illegible]	4827.7	4.93	577.8135	-0.30	-177.	-0.34559	-0.36	-0.071	0.36	30.607	30.911
65.00	19059.	1[illegible]	[illegible]	4809.1	4.91	507.8335	-0.34	-174.	-0.34559	-0.36	-0.055	0.44	30.261	30.[illegible]
65.44	19047.	-1[illegible]	[illegible]	4800.1	4.90	477.2397	-0.35	-171.	-0.34559	-0.36	-0.049	0.48	30.109	30.[illegible]
65.44	19047.	[illegible]	[illegible]	4800.1	4.90	477.2397	-0.35	-171.	-0.34559	-0.36	-0.049	0.48	30.109	30.[illegible]

LARGER VOLUME HEATSHIELD STUDY, 100 NM DESIGN TRAJECTORY MAY 64
AEROJET TI, +3 SIGMA (RANGE SAFETY) 50 LB PAYLOAD

LTV AEROSPACE [illegible]-MSD
ROUTINE NO. LVVC27

PAGE 3

TIME SEC	WEIGHT LBS	THRUST LBS	ALT FT	REL VEL FT/SEC	MACH	DYN. P LBS/FT2	ALPHA DEG	Q-ALPHA LB/SQ FT	Q-COMM DEG/SEC	Q DEG/SEC	PITCH ERR DEG	Q-CONT DEG	THETA DEG	R-DAM DEG
65.44	19048.	0.	94824.	4800.0	4.86	487.3176	-0.35	-173.	-0.34559	-0.36	-0.049	0.48	30.109	30.464
66.00	19048.	0.	96189.	4787.7	4.84	454.6414	-0.38	-171.	-0.34559	-0.37	-0.037	0.55	29.912	30.287
67.00	19048.	0.	98587.	4766.3	4.81	402.6233	-0.41	-167.	-0.34559	-0.37	-0.014	0.67	29.557	29.972
68.00	19048.	0.	100951.	4745.7	4.79	357.3516	-0.45	-161.	-0.34559	-0.37	0.010	0.79	29.202	29.654
69.00	19048.	0.	103282.	4725.8	4.76	317.8538	-0.48	-154.	-0.34559	-0.36	0.030	0.88	28.851	29.334
70.00	19048.	0.	105581.	4706.5	4.73	283.2747	-0.51	-143.	-0.34559	-0.36	0.045	0.94	28.505	29.012
71.00	19048.	0.	107848.	4687.8	4.69	251.7386	-0.52	-131.	-0.34559	-0.35	0.053	0.97	28.166	28.687
72.00	19048.	0.	110082.	4669.6	4.66	224.3114	-0.53	-118.	-0.34559	-0.34	0.055	0.96	27.833	28.361
73.00	19048.	0.	112284.	4651.9	4.62	200.3922	-0.53	-105.	-0.34559	-0.34	0.051	0.93	27.506	28.032
74.00	19048.	0.	114454.	4634.6	4.59	179.4738	-0.52	-93.	-0.34559	-0.34	0.043	0.88	27.183	27.701
75.00	19048.	0.	116592.	4617.7	4.55	161.1338	-0.50	-81.	-0.34559	-0.33	0.031	0.82	26.864	27.368
76.00	19048.	0.	118699.	4601.3	4.52	145.0128	-0.49	-71.	-0.34559	-0.33	0.017	0.75	26.546	27.033
77.00	19048.	0.	120775.	4585.2	4.49	130.8097	-0.47	-61.	-0.34559	-0.33	0.002	0.67	26.230	26.696
78.00	19048.	0.	122819.	4569.4	4.45	118.2654	-0.44	-52.	-0.34559	-0.33	-0.013	0.60	25.914	26.357
79.00	19048.	0.	124832.	4553.9	4.42	107.1616	-0.42	-45.	-0.34559	-0.33	-0.027	0.53	25.597	26.016
80.00	19048.	0.	126814.	4538.8	4.39	97.3107	-0.39	-38.	-0.34559	-0.33	-0.041	0.46	25.280	25.673
81.00	19048.	0.	128764.	4523.9	4.37	88.5540	-0.37	-32.	-0.34559	-0.33	-0.054	0.40	24.962	25.327
82.00	19048.	0.	130684.	4509.3	4.34	80.7522	-0.34	-27.	-0.34559	-0.33	-0.066	0.34	24.642	24.980
83.00	19048.	0.	132573.	4495.0	4.31	73.7884	-0.31	-23.	-0.34559	-0.33	-0.077	0.29	24.322	24.630
84.00	19048.	0.	134430.	4480.9	4.28	67.5600	-0.28	-19.	-0.34559	-0.34	-0.087	0.23	24.002	24.279
85.00	19048.	0.	136257.	4467.1	4.26	61.9790	-0.24	-15.	-0.34559	-0.34	-0.098	0.18	23.681	23.925
86.00	19048.	0.	138053.	4453.6	4.23	56.9692	-0.21	-12.	-0.34559	-0.34	-0.108	0.13	23.360	23.570
87.00	19048.	0.	139819.	4440.3	4.21	52.4627	-0.17	-9.	-0.34559	-0.34	-0.118	0.08	23.039	23.212
88.00	19048.	0.	141553.	4427.2	4.18	48.4033	-0.13	-7.	-0.34559	-0.34	-0.127	0.04	22.717	22.852
89.00	19048.	0.	143257.	4414.4	4.16	44.7393	-0.09	-4.	-0.34559	-0.34	-0.137	-0.01	22.396	22.491
90.00	19048.	0.	144930.	4401.8	4.14	41.4274	-0.05	-2.	-0.34559	-0.34	-0.146	-0.06	22.074	22.127
90.46	19048.	0.	145696.	4396.0	4.13	39.9990	-0.03	-1.	-0.34559	-0.34	-0.151	-0.08	21.924	21.957

LARGER VOLUME HEATSHIELD STUDY, 100 NM DESIGN TRAJECTORY, MAY 69
AEROJET II, +3 SIGMA (RANGE SAFETY) 400 LB PAYLOAD

PAGE 1

TIME SEC	WEIGHT LBS	THRUST LBS	ALT FT	REL VEL	MACH	DYN PRES LBS/FT2	ALPHA DEG	Q-ALPHA LB/SQ FT	Q-COMP DEG/SEC	Q DEG/SEC	PITCH ERR DEG	Q-CONT DEG	THETA DEG	R-GAM DEG
0.0	47480.	35515.	-0.	0.0	0.0	0.0	0.0	0.	0.0	0.0	0.0	0.00	89.814	0.0
0.50	47201.	135415.	6.	27.9	0.02	0.9237	-0.00	-0.	0.0	0.00	-0.000	-0.00	89.814	89.813
1.00	46923.	134794.	28.	58.0	0.05	3.9927	-0.00	-0.	-3.75007	-0.00	-0.014	-0.07	89.814	89.814
1.50	46644.	134180.	64.	88.1	0.08	9.2117	-0.24	-2.	-5.50000	-0.86	-2.601	-11.28	89.764	89.791
2.00	46366.	133572.	116.	118.2	0.11	16.5562	-1.11	-18.	-5.46053	-2.89	-4.434	-16.39	88.932	89.806
2.50	46088.	132970.	183.	148.4	0.13	26.0293	-2.66	-69.	-5.46053	-5.15	-5.147	-15.44	86.927	89.550
3.00	45809.	132375.	264.	178.5	0.16	37.6313	-4.68	-176.	-5.46053	-6.86	-4.841	-10.49	83.896	88.568
3.50	45531.	131787.	361.	208.7	0.19	51.2064	-6.80	-348.	-5.46053	-7.60	-3.914	-4.37	80.241	87.041
4.00	45253.	131204.	473.	238.7	0.21	66.7774	-8.64	-577.	-5.46053	-7.36	-2.869	0.36	76.468	85.106
4.50	44974.	130628.	599.	268.6	0.24	84.2366	-9.93	-836.	-5.46053	-6.44	-2.132	2.22	73.003	82.931
5.00	44707.	129572.	739.	298.4	0.27	103.5302	-10.61	-1098.	-3.53165	-5.31	-1.916	1.04	70.068	80.673
5.50	44444.	128322.	893.	328.0	0.29	124.5221	-10.66	-1328.	-1.60000	-3.74	-0.428	5.35	67.772	78.434
6.00	44182.	127077.	1060.	357.6	0.32	147.2284	-9.93	-1462.	-1.60000	-1.82	0.159	4.44	66.387	76.314
6.50	43919.	125837.	1240.	387.1	0.35	171.7316	-8.54	-1467.	-1.60000	-0.34	-0.132	0.01	65.880	74.423
7.00	43656.	124602.	1433.	416.5	0.38	198.0273	-6.91	-1368.	-1.60000	0.26	-0.954	-5.30	65.903	72.809
7.50	43394.	123372.	1639.	445.8	0.40	226.0056	-5.45	-1232.	-1.19604	-0.01	-1.847	-9.22	66.000	71.452
8.00	43131.	122147.	1857.	475.1	0.43	255.6200	-4.44	-1135.	-0.79111	-0.66	-2.080	-9.08	65.837	70.279
8.50	42868.	120925.	2087.	504.3	0.46	286.4399	-3.85	-1103.	-0.79111	-1.19	-2.004	-7.65	65.368	69.219
9.00	42606.	119709.	2330.	533.3	0.48	318.6421	-3.52	-1121.	-0.79111	-1.41	-1.736	-5.86	64.707	68.224
9.50	42351.	118504.	2585.	562.2	0.51	352.0066	-3.26	-1148.	-0.79111	-1.33	-1.436	-4.53	64.013	67.274
10.00	42109.	117318.	2851.	590.9	0.54	386.4355	-2.95	-1142.	-0.79111	-1.07	-1.228	-4.00	63.412	66.366
10.50	41868.	116136.	3129.	619.6	0.56	421.7573	-2.57	-1082.	-0.79111	-0.83	-1.153	-4.11	62.942	65.508
11.00	41627.	114957.	3419.	648.2	0.59	457.9150	-2.14	-979.	-0.79111	-0.71	-1.171	-4.44	62.567	64.705
11.50	41386.	113781.	3720.	676.7	0.62	494.7662	-1.74	-862.	-0.79111	-0.73	-1.210	-4.58	62.213	63.954
12.00	41144.	112609.	4032.	705.1	0.65	532.1907	-1.42	-756.	-0.79111	-0.82	-1.219	-4.46	61.828	63.248
12.50	40903.	111440.	4354.	733.4	0.67	570.1447	-1.18	-672.	-0.79111	-0.91	-1.182	-4.10	61.398	62.577
13.00	40662.	110273.	4687.	761.6	0.70	608.2078	-1.00	-608.	-0.79111	-0.95	-1.111	-3.66	60.934	61.933
13.50	40421.	109109.	5031.	789.7	0.73	646.5576	-0.85	-550.	-0.79111	-0.95	-1.031	-3.25	60.460	61.311
14.00	40179.	107949.	5385.	817.6	0.75	684.9819	-0.72	-491.	-0.79111	-0.93	-0.956	-2.92	59.992	60.709
14.50	39958.	107201.	5749.	850.1	0.78	723.4.32	-0.59	-427.	-0.79111	-0.91	-0.892	-2.64	59.534	60.125
15.00	39737.	106455.	6122.	877.4	0.80	76...1	-0.48	-362.	-0.79111	-0.91	-0.834	-2.36	59.083	59.556
15.50	39516.	105712.	6505.	904.6	0.83	800.5	-0.38	-301.	-0.79111	-0.91	-0.776	-2.06	58.632	59.007
16.00	39295.	104970.	6897.	931.6	0.86	839.0	-0.29	-245.	-0.79111	-0.91	-0.716	-1.76	58.179	58.470
16.50	39074.	104229.	7299.	958.5	0.88	877.5	-0.22	-193.	-0.79111	-0.91	-0.656	-1.46	57.725	57.946
17.00	38853.	103490.	7709.	985.1	0.91	916.0	-0.16	-145.	-0.79111	-0.90	-0.598	-1.18	57.274	57.432
17.50	38631.	102752.	8129.	1011.5	0.93	954.4	-0.10	-99.	-0.79111	-0.90	-0.542	-0.91	56.826	56.929
18.00	38410.	102015.	8557.	1037.7	0.96	992.8	-0.06	-55.	-0.79111	-0.89	-0.490	-0.66	56.380	56.436
18.50	38189.	101278.	8993.	1063.8	0.98	1031.2	-0.01	-15.	-0.79111	-0.89	-0.440	-0.42	55.937	55.951
19.00	37972.	101182.	9438.	1089.8	1.01	1069.5	0.02	24.	-0.79111	-0.88	-0.393	-0.20	55.497	55.474
19.50	37758.	101431.	9892.	1115.6	1.03	1107.8	0.05	60.	-0.79111	-0.88	-0.349	0.01	55.060	55.005
20.00	37543.	101679.	10356.	1141.2	1.06	1146.0	0.08	94.	-0.79111	-0.87	-0.308	0.20	54.626	54.543
20.00	37543.	101679.	1	1	1.	1	0.08	94.	-0.79111	-0.87	-0.308	0.20	54.626	54.543
20.00	37543.	101679.	1	1.			0.08	94.	-0.79111	-0.87	-0.308	0.20	54.626	54.543
21.00	37114.	102174.	11	1.			0.13	154.	-0.79111	-0.86	-0.247	-0.53	53.760	53.642
22.00	36695.	102677.	1	1.			0.16	203.	-0.79111	-0.84	-0.195	-0.79	52.925	52.761

LARGER VOLUME HEATSHIELD STUDY, [illegible] DESIGN TRAJECTORY, MAY 69
AEROJET II, +3 SIGMA (RANGE SAFETY) 400 LB PAYLOAD

CTV AEROSPACE CORP.-MSD
ROUTINE NO. LVVC27

TIME SEC	WEIGHT LBS	THRUST LBS	ALT FT	REL VEL FT/SEC	MACH	DYN. P LB/FT2	ALPHA DEG	Q-ALPHA LB/SQ FT	Q-COMM DEG/SEC	Q DEG/SEC	PITCH ER. DEG	G-CONT DEG	THETA DEG	R-GAM DEG
23.00	36256.	103176.	13278.	1298.7	1.22	1334.1313	0.19	254.	-0.79111	-0.83	-0.136	0.97	52.097	51.907
24.00	35818.	104431.	14315.	1353.6	1.28	1401.4044	0.21	297.	-0.79111	-0.81	-0.112	1.05	51.186	51.075
25.00	35375.	106094.	15384.	1410.6	1.34	1469.9238	0.23	334.	-0.79111	-0.79	-0.103	1.07	50.492	50.265
26.00	34931.	107755.	16496.	1469.7	1.40	1539.2664	0.23	360.	-0.79111	-0.78	-0.107	1.02	49.712	49.477
27.00	34488.	109414.	17619.	1531.2	1.46	1609.3490	0.24	379.	-0.79111	-0.76	-0.127	0.89	48.946	48.711
28.00	34045.	111070.	18786.	1595.2	1.53	1679.6589	0.23	385.	-0.79111	-0.75	-0.160	0.70	48.195	47.965
29.00	33576.	113191.	19989.	1661.9	1.60	1750.6270	0.21	374.	-0.79111	-0.74	-0.204	0.47	47.454	47.240
30.00	33106.	115321.	21227.	1731.6	1.68	1822.3308	0.18	332.	-0.73551	-0.75	-0.250	0.25	46.715	46.533
31.00	32636.	117448.	22503.	1804.7	1.76	1894.3545	0.17	313.	-0.68000	-0.67	-0.216	0.25	46.008	45.843
32.00	32166.	119576.	23817.	1881.1	1.84	1966.3206	0.19	376.	-0.68000	-0.65	-0.248	0.06	45.366	45.175
33.00	31686.	121628.	25172.	1961.0	1.93	2037.6992	0.18	372.	-0.68000	-0.67	-0.268	-0.01	44.713	44.531
34.00	31182.	123535.	26568.	2044.5	2.03	2107.8086	0.15	322.	-0.68000	-0.66	-0.284	-0.10	44.057	43.904
35.00	30677.	125437.	28006.	2131.7	2.12	2176.0703	0.11	232.	-0.61138	-0.67	-0.301	-0.17	43.401	43.294
36.00	30173.	127334.	29492.	2222.9	2.23	2241.9023	0.09	200.	-0.54286	-0.55	-0.223	-0.01	42.788	42.699
37.00	29668.	129225.	31023.	2318.2	2.34	2304.6309	0.15	348.	-0.54286	-0.50	-0.248	-0.23	42.278	42.127
38.00	29147.	130924.	32603.	2417.8	2.46	2363.3320	0.19	446.	-0.54286	-0.53	-0.276	-0.33	41.771	41.582
39.00	28615.	132504.	34233.	2521.7	2.58	2416.9219	0.19	456.	-0.54286	-0.53	-0.287	-0.37	41.248	41.059
40.00	28083.	134077.	35916.	2630.0	2.71	2464.3545	0.17	411.	-0.54286	-0.54	-0.294	-0.38	40.720	40.554
41.00	27551.	135642.	37654.	2742.9	2.83	2471.7988	0.12	291.	-0.54286	-0.56	-0.287	-0.32	40.180	40.062
42.00	27020.	137195.	39448.	2860.8	2.96	2467.5176	0.04	110.	-0.48805	-0.57	-0.267	-0.20	39.626	39.582
43.00	26476.	137938.	41300.	2983.5	3.08	2456.0234	0.00	1.	-0.43333	-0.46	-0.175	0.05	39.110	39.110
44.00	25933.	138623.	43212.	3110.8	3.21	2436.4824	0.04	105.	-0.43333	-0.40	-0.187	-0.14	38.699	38.655
45.00	25385.	139937.	45187.	3242.7	3.35	2408.6699	0.08	189.	-0.43333	-0.42	-0.214	-0.23	38.303	38.224
46.00	24834.	139006.	47226.	3378.8	3.49	2372.0020	0.07	172.	-0.43333	-0.44	-0.217	-0.20	37.882	37.810
47.00	24290.	138795.	49330.	3519.2	3.64	2326.8047	0.04	92.	-0.43333	-0.45	-0.205	-0.13	37.448	37.409
48.00	23764.	137837.	51502.	3663.2	3.78	2272.3594	-0.01	-17.	-0.38943	-0.45	-0.189	-0.05	37.010	37.019
49.00	23238.	136869.	53741.	3810.5	3.94	2209.0449	-0.02	-52.	-0.34559	-0.35	-0.128	0.07	36.614	36.638
50.00	22713.	132829.	56050.	3959.3	4.09	2136.6914	0.02	53.	-0.34559	-0.32	-0.145	-0.08	36.298	36.273
51.00	22187.	128549.	58426.	4107.0	4.24	2051.2617	0.05	112.	-0.34559	-0.34	-0.160	-0.12	35.980	35.925
52.00	21750.	118277.	60869.	4250.8	4.39	1955.3208	0.06	115.	-0.34559	-0.35	-0.160	-0.10	35.646	35.590
53.00	21375.	103871.	63378.	4379.6	4.52	1840.9197	0.05	85.	-0.34559	-0.35	-0.157	-0.09	35.311	35.264
54.00	21000.	89457.	65952.	4488.6	4.64	1712.4534	0.03	52.	-0.34559	-0.35	-0.154	-0.07	34.976	34.946
55.00	20626.	75034.	68590.	4580.3	4.72	1570.4854	0.01	13.	-0.34559	-0.35	-0.151	-0.06	34.640	34.632
56.00	20251.	60602.	71293.	4652.6	4.79	1424.3318	-0.02	-24.	-0.34559	-0.35	-0.148	-0.04	34.305	34.322
57.00	20082.	50309.	73752.	4708.6	4.84	1285.1626	-0.05	-59.	-0.34559	-0.35	-0.143	-0.01	33.969	34.015
58.00	19932.	40391.	76344.	4755.5	4.87	1161.1646	-0.08	-98.	-0.34559	-0.35	-0.138	0.01	33.632	33.709
59.00	19782.	30466.	79025.	4778.3	4.89	1025.5405	-0.11	-108.	-0.34559	-0.35	-0.136	0.01	33.299	33.404
60.00	19633.	20536.	81797.	4791.4	4.93	908.9788	-0.13	-121.	-0.34559	-0.35	-0.135	0.02	32.967	33.097
61.00	19513.	12310.	84293.	4798.4	4.96	801.9156	-0.16	-129.	-0.34559	-0.35	-0.134	0.02	32.634	32.794
62.00	19487.	9505.	86839.	4793.3	4.97	706.6338	-0.19	-134.	-0.34559	-0.35	-0.129	0.06	32.298	32.499
63.00	19461.	6696.	89380.	4772.1	4.95	622.8418	-0.22	-137.	-0.34559	-0.35	-0.122	0.09	31.960	32.190
64.00	19435.	3884.	91917.	4747.4	4.93	549.1172	-0.25	-136.	-0.34559	-0.35	-0.116	0.12	31.623	31.879
65.00	19409.	1069.	94413.	4714.3	4.90	484.2266	-0.27	-131.	-0.34559	-0.35	-0.112	0.14	31.287	31.558
65.44	19398.	-161.	[illegible]	[illegible]	[illegible]	[illegible]	-0.28	-129.	-0.34559	-0.35	-0.110	0.15	31.140	31.421
65.44	19398.	0.	[illegible]	[illegible]	[illegible]	[illegible]	-0.28	-129.	-0.34559	-0.35	-0.110	0.15	31.140	31.421

LARGER VOLUME HEATSFIELD STUDY; 107 NM DESIGN TRAJECTORY MAY 64
AEROJET II, +3 SIGMA (RANGE SAFETY) 50 LB PAYLOAD

LTV AEROSPACE CORP.-MSD
ROUTINE NO. LVVC27

TIME SEC	WEIGHT LBS	THRUST LBS	ALT FT	REL VEL FT/SEC	MACH	DYN. P LBS/FT2	ALPHA DEG	Q-ALPHA LB/SQ FT	Q-COMM DEG/SEC	Q DEG/SEC	PITCH ERR DEG	Q-CONT DEG	THETA DEG	R-DAM DEG
65.44	19048.	0.	94824.	4800.0	4.86	487.3176	-0.35	-173.	-0.34559	-0.36	-0.049	0.48	30.109	30.464
66.00	19048.	0.	96189.	4787.7	4.84	454.6414	-0.38	-171.	-0.34559	-0.37	-0.037	0.55	29.912	30.287
67.00	19048.	0.	98587.	4766.3	4.81	402.6233	-0.41	-167.	-0.34559	-0.37	-0.014	0.67	29.557	29.972
68.00	19048.	0.	100951.	4745.7	4.79	357.3516	-0.45	-161.	-0.34559	-0.37	0.010	0.79	29.202	29.654
69.00	19048.	0.	103282.	4725.8	4.76	317.8538	-0.48	-154.	-0.34559	-0.36	0.030	0.88	28.851	29.334
70.00	19048.	0.	105581.	4706.5	4.73	283.2747	-0.51	-143.	-0.34559	-0.36	0.045	0.94	28.505	29.012
71.00	19048.	0.	107848.	4687.8	4.69	251.7386	-0.52	-131.	-0.34559	-0.35	0.053	0.97	28.166	28.687
72.00	19048.	0.	110082.	4669.6	4.66	224.3114	-0.53	-118.	-0.34559	-0.34	0.055	0.96	27.833	28.361
73.00	19048.	0.	112284.	4651.9	4.62	200.3922	-0.53	-105.	-0.34559	-0.34	0.051	0.93	27.506	28.032
74.00	19048.	0.	114454.	4634.6	4.59	179.4738	-0.52	-93.	-0.34559	-0.34	0.043	0.88	27.183	27.701
75.00	19048.	0.	116592.	4617.7	4.55	161.1338	-0.50	-81.	-0.34559	-0.33	0.031	0.82	26.864	27.368
76.00	19048.	0.	118699.	4601.3	4.52	145.0128	-0.49	-71.	-0.34559	-0.33	0.017	0.75	26.546	27.033
77.00	19048.	0.	120775.	4585.2	4.49	130.8097	-0.47	-61.	-0.34559	-0.33	0.002	0.67	26.230	26.696
78.00	19048.	0.	122819.	4569.4	4.45	118.2654	-0.44	-52.	-0.34559	-0.33	-0.013	0.60	25.914	26.357
79.00	19048.	0.	124832.	4553.9	4.42	107.1616	-0.42	-45.	-0.34559	-0.33	-0.027	0.53	25.597	26.016
80.00	19048.	0.	126814.	4538.8	4.39	97.3107	-0.39	-38.	-0.34559	-0.33	-0.041	0.46	25.280	25.673
81.00	19048.	0.	128764.	4523.9	4.37	88.5540	-0.37	-32.	-0.34559	-0.33	-0.054	0.40	24.962	25.327
82.00	19048.	0.	130684.	4509.3	4.34	80.7522	-0.34	-27.	-0.34559	-0.33	-0.066	0.34	24.642	24.980
83.00	19048.	0.	132573.	4495.0	4.31	73.7884	-0.31	-23.	-0.34559	-0.33	-0.077	0.29	24.322	24.630
84.00	19048.	0.	134430.	4480.9	4.28	67.5600	-0.28	-19.	-0.34559	-0.34	-0.087	0.23	24.002	24.279
85.00	19048.	0.	136257.	4467.1	4.26	61.9790	-0.24	-15.	-0.34559	-0.34	-0.098	0.18	23.681	23.925
86.00	19048.	0.	138053.	4453.6	4.23	56.9692	-0.21	-12.	-0.34559	-0.34	-0.108	0.13	23.360	23.570
87.00	19048.	0.	139819.	4440.3	4.21	52.4627	-0.17	-9.	-0.34559	-0.34	-0.118	0.08	23.039	23.212
88.00	19048.	0.	141553.	4427.2	4.18	48.4033	-0.13	-7.	-0.34559	-0.34	-0.127	0.04	22.717	22.852
89.00	19048.	0.	143257.	4414.4	4.16	44.7393	-0.09	-4.	-0.34559	-0.34	-0.137	-0.01	22.396	22.491
90.00	19048.	0.	144930.	4401.8	4.14	41.4274	-0.05	-2.	-0.34559	-0.34	-0.146	-0.06	22.074	22.127
90.46	19048.	0.	145696.	4396.0	4.13	39.9990	-0.03	-1.	-0.34559	-0.34	-0.151	-0.08	21.924	21.957

LARGER VOLUME HEATSHIELD STUDY, 100 NM DESIGN TRAJECTORY MAY 69
AEROJET II, +3 SIGMA (RANGE SAFETY) 50 LB PAYLOAD

LTV AEROSPACE CORP.-MSD
ROUTINE NO. LVVC27

TIME SEC	WEIGHT LBS	THRUST LBS	ALT FT	REL VEL FT/SEC	RANGE	DYN. P LBS/FT2	ALPHA DEG	Q-ALPHA LB/SQ FT	Q-COMM DEG/SEC	Q DEG/SEC	PITCH ERR DEG	Q-CONT DEG	THETA DEG	R-GAM DEG
0.0	47130.	35464.	-0.	0.0	0.0	0.0	0.0	0.	0.0	0.0	0.0	0.0	89.814	89.813
0.20	47018.	135632.	1.	9.9	0.01	0.1176	-0.00	-0.	0.0	-0.00	0.000	0.00	89.814	89.814
0.40	46907.	135382.	4.	22.1	0.02	0.5795	-0.00	-0.	0.0	0.00	-0.000	-0.00	89.814	89.814
0.60	46795.	135132.	10.	34.2	0.03	1.3921	-0.00	-0.	0.0	0.00	-0.000	-0.00	89.814	89.813
0.80	46684.	134884.	18.	46.4	0.04	2.5558	-0.00	-0.	0.0	0.00	-0.000	-0.00	89.814	89.814
1.00	46573.	134637.	28.	58.5	0.05	4.0709	-0.00	-0.	-2.23787	-0.00	-0.011	-0.08	89.814	89.814
1.20	46461.	134391.	41.	70.7	0.06	5.9372	-0.04	-0.	-4.47560	-0.19	-0.883	-5.46	89.813	89.811
1.40	46350.	134146.	56.	82.9	0.07	8.1529	-0.17	-1.	-4.47560	-0.68	-1.695	-9.60	89.793	89.796
1.60	46239.	133902.	74.	95.1	0.09	10.7165	-0.41	-4.	-4.47560	-1.40	-2.385	-12.30	89.650	89.780
1.80	46127.	133658.	- 95.	107.2	0.10	13.6272	-0.77	-10.	-4.47560	-2.25	-2.915	-13.60	89.315	89.786
2.00	46016.	133416.	117.	119.4	0.11	16.8852	-1.23	-21.	-4.47560	-3.13	-3.272	-13.63	88.788	89.811
2.20	45905.	133176.	142.	131.6	0.12	20.4911	-1.78	-37.	-4.47560	-3.97	-3.456	-12.61	88.083	89.775
2.40	45793.	132936.	170.	143.8	0.13	24.4448	-2.41	-59.	-4.47560	-4.70	-3.482	-10.81	87.217	89.589
2.60	45682.	132697.	200.	156.0	0.14	28.7446	-3.08	-89.	-5.30434	-5.28	-3.381	-8.57	86.219	89.282
2.80	45571.	132459.	232.	168.2	0.15	33.3871	-3.78	-126.	-6.13324	-5.74	-3.500	-8.12	85.118	88.887
3.00	45459.	132222.	267.	180.4	0.16	38.3678	-4.50	-172.	-6.13324	-6.15	-3.536	-7.27	83.929	88.417
3.20	45348.	131986.	304.	192.6	0.17	43.6830	-5.22	-228.	-6.13324	-6.46	-3.501	-6.19	82.668	87.879
3.40	45237.	131751.	344.	204.8	0.18	49.3285	-5.93	-292.	-6.13324	-6.66	-3.413	-5.04	81.355	87.280
3.60	45125.	131518.	386.	216.9	0.19	55.2995	-6.62	-366.	-6.13324	-6.76	-3.295	-3.99	80.011	86.625
3.80	45014.	131285.	431.	229.1	0.21	61.5913	-7.27	-448.	-6.13324	-6.76	-3.169	-3.14	78.659	85.922
4.00	44903.	131053.	478.	241.2	0.22	68.2005	-7.87	-536.	-6.13324	-6.66	-3.052	-2.61	77.316	85.179
4.20	44791.	130822.	527.	253.4	0.23	75.1225	-8.41	-631.	-6.13324	-6.50	-2.961	-2.42	75.999	84.403
4.40	44680.	130592.	578.	265.5	0.24	82.3554	-8.89	-732.	-6.13324	-6.30	-2.907	-2.61	74.719	83.603
4.60	44569.	130364.	632.	277.6	0.25	89.8971	-9.30	-836.	-6.13324	-6.07	-2.896	-3.15	73.482	82.784
4.80	44462.	129925.	689.	289.7	0.26	97.7374	-9.66	-945.	-6.13324	-5.85	-2.930	-3.98	72.291	81.953
5.00	44357.	129424.	747.	301.7	0.27	105.8555	-9.98	-1056.	-3.90070	-5.65	-2.996	-4.98	71.143	81.117
5.20	44252.	128925.	809.	313.7	0.28	114.2434	-10.23	-1168.	-1.66667	-5.27	-2.244	-0.92	70.046	80.270
5.40	44147.	128426.	871.	325.7	0.29	122.8965	-10.36	-1273.	-1.66667	-4.59	-1.587	1.70	69.056	79.416
5.60	44042.	127928.	936.	337.6	0.30	131.8165	-10.34	-1364.	-1.66667	-3.74	-1.084	2.79	68.221	78.565
5.80	43937.	127430.	1003.	349.6	0.31	141.0096	-10.17	-1434.	-1.66667	-2.83	-0.760	2.50	67.565	77.731
6.00	43832.	126934.	1072.	361.5	0.32	150.4861	-9.84	-1480.	-1.66667	-1.96	-0.617	1.12	67.089	76.924
6.20	43727.	126439.	1144.	373.4	0.34	160.2510	-9.38	-1503.	-1.66667	-1.21	-0.636	-1.03	66.775	76.153
6.40	43622.	125944.	1217.	385.4	0.35	170.3059	-8.83	-1504.	-1.66667	-0.64	-0.788	-3.58	66.594	75.424
6.60	43517.	125450.	1293.	397.3	0.36	180.6487	-8.23	-1487.	-1.66667	-0.28	-1.032	-6.20	66.506	74.739
6.80	43411.	124957.	1371.	409.3	0.37	191.2706	-7.63	-1459.	-1.66667	-0.13	-1.327	-8.60	66.469	74.099
7.00	43306.	124464.	1451.	421.3	0.38	202.1630	-7.06	-1427.	-1.66667	-0.17	-1.633	-10.56	66.442	73.499
7.20	43201.	123973.	1532.	433.3	0.39	213.3171	-6.54	-1396.	-1.66667	-0.36	-1.916	-11.97	66.392	72.937
7.40	43096.	123482.	1616.	445.3	0.40	224.7236	-6.11	-1373.	-1.66667	-0.64	-2.150	-12.78	66.294	72.405
7.60	42991.	122992.	1702.	457.3	0.41	236.3729	-5.77	-1363.	-1.66667	-0.98	-2.322	-13.03	66.133	71.898
7.80	42886.	122502.	1790.	469.2	0.42	248.2577	-5.51	-1367.	-1.66667	-1.31	-2.426	-12.83	65.904	71.410
8.00	42781.	122013.	1880.	481.2	0.43	260.3721	-5.32	-1386.	-1.23360	-1.61	-2.464	-12.30	65.613	70.936
8.00	42781.	122013.	1880.	481.2	0.43	260.3721	-5.32	-1386.	-1.23360	-1.61	-2.464	-12.30	65.613	70.936
8.20	42676.	121525.	1971.	493.1	0.44	272.7107	-5.20	-1418.	-0.80000	-1.79	-2.285	-10.60	65.271	70.471
8.40	42571.	121039.	2064.	505.1	0.45	285.2656	-5.10	-1456.	-0.80000	-1.82	-2.082	-9.15	64.909	70.012
8.60	42466.	120552.	2159.	517.0	0.46	297.9997	-5.00	-1491.	-0.80000	-1.72	-1.887	-8.10	64.555	69.559

LARGER VOLUME HEATSHIELD STUDY, 100 NM DESIGN TRAJECTORY MAY 69
AEROJET II, 4 SIGMA (RANGE SAFETY) 50 LB PAYLOAD

LTV AEROSPACE CORP.-MSD
ROUTINE NO. LVVC27

TIME SEC	WEIGHT LBS	THRUST LBS	ALT FT	REL VEL FT/SEC	MACH	DYN. P LBS/FT2	ALPHA DEG	Q-ALPHA LB/SQ FT	Q-COMM DEG/SEC	Q DEG/SEC	PITCH ERR DEG	Q-CONT DEG	THETA DEG	R-GAM DEG
8.80	42361.	120066.	2260.	528.9	0.48	310.9971	-4.88	-1519.	-0.80000	-1.53	-1.721	-7.47	64.230	69.113
9.00	42256.	119581.	2360.	540.7	0.49	324.1577	-4.73	-1533.	-0.80000	-1.30	-1.597	-7.26	63.946	68.675
9.20	42151.	119096.	2461.	552.6	0.50	337.5076	-4.54	-1532.	-0.80000	-1.07	-1.519	-7.37	63.710	68.248
9.40	42049.	118616.	2565.	564.4	0.51	351.0420	-4.32	-1515.	-0.80000	-0.87	-1.486	-7.69	63.518	67.833
9.60	41952.	118141.	2670.	576.3	0.52	364.7480	-4.07	-1485.	-0.80000	-0.71	-1.489	-8.12	63.361	67.432
9.80	41856.	117668.	2778.	588.1	0.53	378.6199	-3.82	-1444.	-0.80000	-0.63	-1.516	-8.54	63.229	67.044
10.00	41759.	117195.	2887.	599.8	0.54	392.6521	-3.56	-1399.	-0.80000	-0.60	-1.554	-8.87	63.108	66.670
10.20	41663.	116723.	2998.	611.6	0.55	406.8325	-3.32	-1352.	-0.80000	-0.63	-1.592	-9.05	62.986	66.309
10.40	41566.	116251.	3111.	623.3	0.56	421.1584	-3.10	-1307.	-0.80000	-0.70	-1.620	-9.06	62.855	65.959
10.60	41470.	115780.	3226.	635.0	0.58	435.6184	-2.91	-1268.	-0.80000	-0.78	-1.632	-8.91	62.708	65.620
10.80	41373.	115309.	3342.	646.7	0.59	450.2090	-2.75	-1236.	-0.80000	-0.87	-1.627	-8.64	62.544	65.289
11.00	41277.	114839.	3461.	658.3	0.60	464.9180	-2.60	-1210.	-0.80000	-0.95	-1.605	-8.28	62.363	64.966
11.20	41180.	114369.	3581.	669.9	0.61	479.7410	-2.48	-1190.	-0.80000	-1.00	-1.570	-7.90	62.169	64.650
11.40	41084.	113900.	3703.	681.5	0.62	494.6619	-2.37	-1174.	-0.80000	-1.03	-1.527	-7.53	61.966	64.339
11.60	40987.	113431.	3827.	693.1	0.63	509.6807	-2.27	-1159.	-0.80000	-1.04	-1.480	-7.19	61.760	64.034
11.80	40891.	112963.	3952.	704.6	0.64	524.7856	-2.18	-1143.	-0.80000	-1.02	-1.434	-6.92	61.555	63.733
12.00	40794.	112496.	4079.	716.1	0.65	539.9612	-2.08	-1126.	-0.80000	-1.00	-1.392	-6.70	61.353	63.438
12.20	40698.	112029.	4208.	727.5	0.66	555.2100	-1.99	-1105.	-0.80000	-0.97	-1.358	-6.53	61.157	63.148
12.40	40601.	111562.	4339.	739.0	0.67	570.5208	-1.90	-1081.	-0.80000	-0.94	-1.324	-6.39	60.967	62.862
12.60	40505.	111096.	4471.	750.3	0.68	585.8845	-1.80	-1055.	-0.80000	-0.92	-1.297	-6.26	60.782	62.582
12.80	40408.	110630.	4605.	761.7	0.69	601.2915	-1.71	-1026.	-0.80000	-0.91	-1.274	-6.14	60.599	62.306
13.00	40312.	110165.	4741.	773.0	0.70	616.7375	-1.62	-997.	-0.80000	-0.91	-1.252	-6.06	60.418	62.035
13.20	40215.	109700.	4878.	784.2	0.71	632.2065	-1.53	-968.	-0.80000	-0.91	-1.230	-5.84	60.237	61.768
13.40	40119.	109235.	5017.	795.5	0.73	647.6931	-1.45	-940.	-0.80000	-0.92	-1.207	-5.66	60.055	61.506
13.60	40022.	108771.	5158.	806.6	0.74	663.1858	-1.38	-913.	-0.80000	-0.93	-1.182	-5.46	59.870	61.247
13.80	39926.	108307.	5300.	817.8	0.75	678.6765	-1.31	-888.	-0.80000	-0.94	-1.155	-5.26	59.684	60.992
14.00	39829.	107845.	5444.	828.9	0.76	694.1597	-1.24	-864.	-0.80000	-0.94	-1.126	-5.06	59.497	60.741
14.20	39741.	107546.	5590.	839.9	0.77	709.6401	-1.18	-840.	-0.80000	-0.94	-1.097	-4.86	59.309	60.493
14.40	39652.	107248.	5737.	850.9	0.78	725.1416	-1.13	-817.	-0.80000	-0.94	-1.069	-4.67	59.121	60.247
14.60	39564.	106950.	5885.	861.9	0.79	740.6472	-1.07	-793.	-0.80000	-0.94	-1.041	-4.49	58.934	60.005
14.80	39476.	106652.	6035.	872.9	0.80	756.1565	-1.02	-770.	-0.80000	-0.93	-1.013	-4.32	58.748	59.765
15.00	39387.	106355.	6187.	883.8	0.81	771.6531	-0.97	-746.	-0.80000	-0.93	-0.987	-4.16	58.562	59.529
15.20	39299.	106058.	6340.	894.7	0.82	787.1331	-0.92	-721.	-0.80000	-0.92	-0.963	-4.02	58.379	59.295
15.40	39210.	105761.	6494.	905.6	0.83	802.5911	-0.87	-695.	-0.80000	-0.91	-0.940	-3.89	58.197	59.063
15.60	39122.	105464.	6651.	916.5	0.84	818.0122	-0.82	-669.	-0.80000	-0.90	-0.919	-3.77	58.017	58.834
15.80	39033.	105168.	6808.	927.3	0.85	833.3948	-0.77	-642.	-0.80000	-0.90	-0.899	-3.64	57.838	58.608
16.00	38945.	104872.	6967.	938.1	0.86	848.7295	-0.73	-616.	-0.80000	-0.90	-0.879	-3.51	57.659	58.384
16.20	38856.	104576.	7128.	948.8	0.87	864.0112	-0.68	-590.	-0.80000	-0.90	-0.859	-3.37	57.480	58.162
16.40	38768.	104280.	7290.	959.5	0.88	879.2302	-0.64	-565.	-0.80000	-0.90	-0.839	-3.24	57.301	57.943
16.60	38679.	103985.	7453.	970.2	0.89	894.3865	-0.60	-540.	-0.80000	-0.90	-0.819	-3.10	57.122	57.726
16.80	38591.	103690.	7618.	980.8	0.90	909.4666	-0.57	-517.	-0.80000	-0.90	-0.799	-2.96	56.943	57.511
17.00	38503.	103395.	7784.	991.4	0.91	924.4600	-0.53	-493.	-0.80000	-0.90	-0.779	-2.83	56.764	57.297
17.20	38414.	103100.	7951.	1002.0	0.92	939.3477	-0.50	-471.	-0.80000	-0.90	-0.760	-2.71	56.585	57.086
17.40	38326.	102805.	8120.	1012.5	0.93	954.1304	-0.47	-448.	-0.80000	-0.89	-0.741	-2.59	56.407	56.877
17.60	38237.	102511.	8291.	1022.9	0.94	968.8131	-0.44	-426.	-0.80000	-0.89	-0.723	-2.47	56.230	56.669

LARGER VOLUME HEATSHIELD STUDY, 100 NM DESIGN TRAJECTORY (MAY 70
AEROJET II, +3 SIGMA (RANGE SAFETY) 50 LB PAYLOAD

LTV AEROSPACE CORP.-MSD
ROUTINE NO. LVVC27

TIME SEC	WEIGHT LBS	THRUST LBS	ALT FT	VELOCITY FT/SEC	MACH NO.	DYN. P LBS/SQ FT	ALPHA DEG	Q-ALPHA LB/SQ FT	Q-COMM DEG/SEC	Q DEG/SEC	PITCH ERR DEG	Q-CONT DEG	THETA DEG	R-GAM DEG
17.80	38149.	102216.	8462.	1033.3	[illegible]	[illegible]	-0.41	-403.	-0.80000	-0.89	-0.705	2.36	56.053	56.463
18.00	38060.	101922.	8635.	1043.7	0.96	997.7985	-0.38	-382.	-0.80000	-0.89	-0.687	-2.24	55.876	56.259
18.20	37972.	101628.	8809.	1054.0	0.97	1012.0923	-0.36	-361.	-0.80000	-0.89	-0.670	-2.13	55.700	56.056
18.40	37883.	101334.	8985.	1064.2	0.98	1026.2522	-0.33	-340.	-0.80000	-0.89	-0.653	-2.01	55.524	55.855
18.60	37795.	101040.	9162.	1074.4	0.99	1040.2690	-0.31	-321.	-0.80000	-0.88	-0.635	-1.90	55.348	55.656
18.80	37708.	100992.	9340.	1084.6	1.00	1054.1572	-0.29	-301.	-0.80000	-0.88	-0.619	-1.79	55.172	55.458
19.00	37622.	101091.	9519.	1094.8	1.01	1068.0325	-0.26	-283.	-0.80000	-0.88	-0.602	-1.69	54.997	55.261
19.20	37537.	101191.	9700.	1105.0	1.02	1081.9084	-0.24	-264.	-0.80000	-0.88	-0.587	-1.59	54.822	55.066
19.40	37451.	101290.	9881.	1115.2	1.03	1095.7681	-0.22	-246.	-0.80000	-0.87	-0.572	-1.50	54.648	54.872
19.60	37365.	101389.	10064.	1125.5	1.04	1109.6243	-0.20	-227.	-0.80000	-0.87	-0.557	-1.41	54.474	54.679
19.80	37279.	101489.	10249.	1135.7	1.06	1123.4592	-0.19	-210.	-0.80000	-0.87	-0.543	-1.32	54.301	54.488
20.00	37193.	101588.	10434.	1146.0	1.07	1137.2742	-0.17	-193.	-0.80000	-0.87	-0.529	-1.22	54.128	54.298
20.00	37193.	101588.	10434.	1146.0	1.07	1137.2773	-0.17	-193.	-0.80000	-0.87	-0.529	-1.22	54.128	54.298
20.00	37193.	101588.	10434.	1146.0	1.07	1137.2773	-0.17	-193.	-0.80000	-0.87	-0.529	-1.22	54.128	54.298
21.00	36764.	102086.	11380.	1197.9	1.12	1205.9758	-0.10	-118.	-0.80000	-0.86	-0.462	-0.80	53.267	53.365
22.00	36335.	102584.	12357.	1250.6	1.17	1274.1028	-0.04	-54.	-0.80000	-0.85	-0.408	-0.46	52.417	52.460
23.00	35906.	103082.	13363.	1304.1	1.23	1341.4438	-0.00	-2.	-0.90000	-0.84	-0.364	-0.19	51.579	51.581
24.00	35468.	104335.	14400.	1358.8	1.28	1408.5178	0.03	38.	-0.80000	-0.83	-0.331	-0.01	50.752	50.725
25.00	35025.	105995.	15467.	1415.7	1.34	1476.6892	0.05	67.	-0.80000	-0.81	-0.311	0.10	49.938	49.892
25.00	35025.	105995.	15467.	1415.7	1.34	1476.6892	0.05	67.	-0.80000	-0.81	-0.311	0.10	49.938	49.892
26.00	34581.	107654.	16566.	1474.8	1.40	1545.7954	0.05	84.	-0.80000	-0.80	-0.302	0.13	49.135	49.081
27.00	34138.	109310.	17697.	1536.3	1.47	1615.6663	0.05	85.	-0.80000	-0.79	-0.304	0.09	48.343	48.290
28.00	33695.	110963.	18860.	1600.2	1.54	1686.0969	0.04	68.	-0.80000	-0.79	-0.315	-0.00	47.560	47.519
29.00	33226.	113080.	20057.	1666.9	1.61	1757.2756	0.02	27.	-0.80000	-0.78	-0.332	-0.13	46.783	46.767
30.00	32756.	115206.	21289.	1736.9	1.68	1829.3992	-0.02	-44.	-0.73995	-0.78	-0.351	-0.26	46.008	46.032
31.00	32286.	117329.	22558.	1810.0	1.76	1902.0632	-0.03	-58.	-0.68000	-0.68	-0.299	-0.17	45.283	45.314
32.00	31816.	119447.	23864.	1886.7	1.85	1974.8269	-0.01	-15.	-0.68000	-0.68	-0.299	-0.18	44.611	44.618
33.00	31336.	121500.	25209.	1966.8	1.94	2047.1660	-0.01	-22.	-0.68000	-0.68	-0.296	-0.16	43.935	43.945
34.00	30832.	123403.	26594.	2050.5	2.03	2118.4238	-0.03	-65.	-0.68000	-0.68	-0.295	-0.15	43.261	43.291
35.00	30327.	125301.	28021.	2138.1	2.13	2188.1094	-0.07	-151.	-0.61138	-0.69	-0.291	-0.12	42.585	42.654
36.00	29823.	127194.	29492.	2229.7	2.24	2255.6758	-0.06	-133.	-0.54286	-0.55	-0.215	0.02	41.973	42.033
37.00	29318.	129080.	31008.	2325.5	2.35	2320.4746	0.01	34.	-0.54286	-0.53	-0.231	-0.14	41.454	41.439
38.00	28797.	130776.	32571.	2425.6	2.47	2381.5215	0.06	135.	-0.54286	-0.53	-0.242	-0.19	40.931	40.874
39.00	28265.	132353.	34181.	2530.1	2.59	2437.7187	0.07	172.	-0.54286	-0.54	-0.249	-0.22	40.403	40.332
40.00	27733.	133922.	35846.	2639.1	2.72	2488.0996	0.06	151.	-0.54286	-0.55	-0.250	-0.22	39.870	39.810
41.00	27201.	135483.	37563.	2752.7	2.84	2530.3418	0.03	68.	-0.54286	-0.55	-0.244	-0.16	39.330	39.303
42.00	26670.	137033.	39334.	2871.5	2.97	2499.4844	-0.03	-63.	-0.48805	-0.56	-0.231	-0.05	38.784	38.809
43.00	26126.	137774.	41163.	2995.2	3.09	2491.6055	-0.03	-85.	-0.43333	-0.43	-0.164	0.06	38.293	38.327
44.00	25583.	138458.	43050.	3123.7	3.23	2475.7832	0.02	48.	-0.43333	-0.41	-0.182	-0.11	37.887	37.868
45.00	25035.	138771.	44998.	3256.8	3.36	2451.6230	0.05	114.	-0.43333	-0.43	-0.194	-0.16	37.476	37.430
46.00	24484.	138839.	47010.	3394.1	3.51	2419.4482	0.04	109.	-0.43333	-0.44	-0.196	-0.14	37.055	37.010
47.00	23940.	139628.	49095.	3535.9	3.65	2378.6133	0.02	56.	-0.43333	-0.44	-0.191	-0.10	36.628	36.605
48.00	23414.	137671.	51227.	3681.3	3.80	2325.2578	-0.01	-31.	-0.38943	-0.44	-0.182	-0.04	36.199	36.211
49.00	22888.	136705.	53435.	3830.1	3.94	2264.7559	-0.01	-28.	-0.34559	-0.34	-0.135	0.01	35.816	35.820
50.00	22363.	137669.	55711.	3980.[illegible]	4.11	2194.8047	0.03	69.	-0.34559	-0.33	-0.147	-0.09	35.495	35.483

LARGER VOLUME HEATSHIELD STUDY, 100 NM DESIGN TRAJECTORY MAY 69
AEROJET II, +3 SIGMA (RANGE SAFETY) 50 LB PAYLOAD

LTV AEROSPACE CORP./MSD
ROUTINE NO. LVVC27

TIME SEC	WEIGHT LBS	THRUST LBS	ALT FT				ALPHA DEG	Q-ALPHA LB/SQ FT	Q (DMA DEG/SEC	Q DEG/SEC	PITCH ERR DEG	Q-CONT DEG	THETA	R-GAM DEG
51.00	21837.	128394.	59053.		4.42	2016.5091	0.05	113.	-0.34559	-0.34	-0.154	-0.11	35.168	35.114
52.00	21400.	118134.	60461.		4.58	1902.4009	0.06	116.	-0.34559	-0.35	-0.154	-0.11	34.836	34.778
53.00	21025.	103744.	62927.		4.55	1773.4084	0.05	97.	-0.34559	-0.35	-0.153	-0.10	34.502	34.451
54.00	20650.	89346.	65440.		4.75	1630.4319	0.04	64.	-0.34559	-0.35	-0.151	-0.08	34.168	34.132
55.00	20276.	74939.	67990.		4.92	1483.6165	0.02	25.	-0.34559	-0.35	-0.148	-0.06	33.833	33.818
56.00	19901.	60523.	70565.		4.87	1339.3201	-0.01	-13.	-0.34559	-0.35	-0.146	-0.04	33.498	33.507
57.00	19732.	50242.	73155.		4.90	1201.9575	-0.04	-50.	-0.34559	-0.35	-0.141	-0.00	33.162	33.199
58.00	19582.	40335.	75751.		4.92	1072.8069	-0.07	-79.	-0.34559	-0.35	-0.137	0.01	32.827	32.893
59.00	19432.	30422.	78344.		4.93	952.6467	-0.09	-100.	-0.34559	-0.35	-0.135	0.03	32.494	32.587
60.00	19283.	20503.	80927.		4.92	841.9900	-0.12	-116.	-0.34559	-0.35	-0.132	0.05	32.160	32.281
61.00	19163.	12287.	83491.		4.90	743.3220	-0.15	-126.	-0.34559	-0.35	-0.129	0.07	31.826	31.975
62.00	19137.	9485.	86031.		4.88	656.3950	-0.18	-133.	-0.34559	-0.35	-0.123	0.12	31.489	31.668
63.00	19111.	6680.	88544.		4.86	579.7993	-0.21	-136.	-0.34559	-0.35	-0.118	0.15	31.152	31.359
64.00	19085.	3872.	91028.		4.83	512.2939	-0.23	-134.	-0.34559	-0.35	-0.114	0.17	30.817	31.048
65.00	19059.	1060.	93480.		4.82	485.3829	-0.25	-129.	-0.34559	-0.35	-0.111	0.20	30.483	30.735
65.44	19048.	-168.	94541.		4.82	485.3645	-0.26	-127.	-0.34559	-0.35	-0.109	0.21	30.336	30.598
65.44	19048.	0.	94542.		4.82	485.3645	-0.26	-127.	-0.34559	-0.35	-0.109	0.21	30.336	30.598
65.44	19048.	0.	94542.		4.82	485.3645	-0.26	-127.	-0.34559	-0.35	-0.109	0.21	30.336	30.598
66.00	19048.	0.	95900.		4.80	452.9089	-0.27	-124.	-0.34559	-0.35	-0.106	0.24	30.146	30.420
67.00	19048.	0.	98287.		4.77	401.2368	-0.29	-118.	-0.34559	-0.35	-0.099	0.28	29.809	30.103
68.00	19048.	0.	100640.		4.75	356.2512	-0.31	-111.	-0.34559	-0.35	-0.094	0.31	29.472	29.783
69.00	19048.	0.	102960.		4.72	316.9922	-0.32	-102.	-0.34559	-0.35	-0.092	0.32	29.139	29.461
70.00	19048.	0.	105247.		4.69	282.6533	-0.33	-93.	-0.34559	-0.34	-0.092	0.31	28.808	29.137
71.00	19048.	0.	107502.		4.65	251.4255	-0.33	-83.	-0.34559	-0.34	-0.093	0.30	28.47	28.810
72.00	19048.	0.	109725.		4.62	224.0990	-0.33	-74.	-0.34559	-0.34	-0.095	0.29	28.149	28.482
73.00	19048.	0.	111916.		4.58	200.2609	-0.33	-66.	-0.34559	-0.34	-0.097	0.28	27.819	28.151
74.00	19048.	0.	114075.		4.55	179.4104	-0.33	-59.	-0.34559	-0.34	-0.098	0.27	27.489	27.817
75.00	19048.	0.	116202.		4.51	161.1240	-0.32	-52.	-0.34559	-0.34	-0.099	0.27	27.159	27.482
76.00	19048.	0.	118297.		4.48	145.0470	-0.32	-46.	-0.34559	-0.34	-0.099	0.26	26.828	27.144
77.00	19048.	0.	120361.		4.45	130.8774	-0.31	-40.	-0.34559	-0.34	-0.100	0.25	26.498	26.804
78.00	19048.	0.	122394.		4.42	118.3610	-0.29	-35.	-0.34559	-0.34	-0.102	0.24	26.168	26.463
79.00	19048.	0.	124396.		4.39	107.2791	-0.28	-30.	-0.34559	-0.34	-0.104	0.23	25.839	26.118
80.00	19048.	0.	126366.		4.36	97.4456	-0.26	-25.	-0.34559	-0.34	-0.106	0.21	25.511	25.772
81.00	19048.	0.	128305.		4.33	88.7014	-0.24	-21.	-0.34559	-0.34	-0.110	0.18	25.183	25.424
82.00	19048.	0.	130214.		4.30	80.9102	-0.22	-18.	-0.34559	-0.34	-0.115	0.15	24.856	25.073
83.00	19048.	0.	132091.		4.27	73.9543	-0.19	-14.	-0.34559	-0.34	-0.120	0.11	24.530	24.720
84.00	19048.	0.	133937.		4.25	67.7310	-0.16	-11.	-0.34559	-0.34	-0.125	0.07	24.205	24.366
85.00	19048.	0.	135753.		4.22	62.1535	-0.13	-8.	-0.34559	-0.34	-0.131	0.03	23.879	24.009
86.00	19048.	0.	137537.		4.19	57.1453	-0.10	-5.	-0.34559	-0.34	-0.137	-0.01	23.553	23.650
87.00	19048.	0.	139291.		4.17	52.6404	-0.06	-3.	-0.34559	-0.34	-0.142	-0.04	23.228	23.288
88.00	19048.	0.	141014.		4.14	48.5808	-0.02	-1.	-0.34559	-0.34	-0.147	-0.07	22.901	22.925
89.00	19048.	0.	142706.		4.12	44.9166	0.01	1.	-0.34559	-0.34	-0.152	-0.10	22.574	22.560
90.00	19048.	0.	144369.		4.10	41.6039	0.05	2.	-0.34559	-0.34	-0.155	-0.13	22.247	22.193
90.52	19048.	0.	145224.		4.09	39.9993	0.08	3.	-0.34559	-0.34	-0.157	-0.14	22.076	22.000

LTV AEROSPACE CORP.-MSD
ROUTINE NO. LAOC76

GRAVITY TURN

TIME SEC	WEIGHT LBS	THRUST LBS	ALT FT	RELVEL FT/SEC	MACH	DYN. P LBS/FT2	ALPHA DEG	N-ALPHA LB/SQ FT	Q-COMM DEG/SEC	Q DEG/SEC	PITCH ERR DEG	THETA DEG	K-GAM DEG
0.0	339260.	471460.	-0.	0.0	0.0	0.0	0.	0.	0.0	0.0	0.0	83.746	0.0
1.000	339467.	391225.	19.	38.2	0.03	1.7353	0.	0.	0.0	-0.01	0.0	83.746	78.502
2.000	339652.	391237.	74.	75.1	0.07	6.6851	0.	0.	0.0	-0.10	0.0	83.700	78.413
3.000	339833.	391337.	165.	112.5	0.10	14.9903	0.	77.	0.0	-0.34	0.0	83.497	78.369
4.000	340013.	391437.	295.	150.7	0.14	26.7464	0.	127.	0.0	-0.77	0.0	82.962	78.228
5.000	340194.	391537.	461.	189.4	0.17	42.0582	0.	169.	0.0	-1.46	0.0	81.894	77.888
6.000	340374.	391637.	665.	229.4	0.21	61.3272	0.	177.	0.0	-2.46	0.0	80.148	77.261
7.000	340555.	391737.	909.	270.9	0.24	84.9481	0.	165.	0.0	-3.75	0.0	77.747	76.275
8.000	340735.	391837.	1192.	314.1	0.28	113.2233	0.	9.	0.0	-5.28	0.0	74.995	74.927
9.000	340916.	391937.	1516.	358.4	0.32	146.4545	-0.09	-123.	0.0	-7.18	0.0	72.478	73.319
10.000	341096.	392037.	1880.	405.8	0.37	185.1650	-0.05	-106.	0.0	-9.19	0.0	70.786	71.645
11.000	341276.	392137.	2285.	454.8	0.41	229.7617	-0.03	-30.	0.0	-10.52	0.0	70.000	70.130
12.000	341457.	392237.	2736.	505.8	0.46	280.5076	0.07	101.	0.0	-10.82	0.0	69.421	69.847
13.000	341637.	392337.	3230.	559.0	0.51	337.5828	0.05	101.	0.0	-11.66	0.0	68.173	67.696
14.000	341818.	392437.	3771.	614.0	0.56	400.6199	-0.13	-96.	0.0	-11.69	0.0	66.389	66.514
15.000	341998.	392537.	4357.	670.4	0.61	469.2910	-0.17	-87.	0.0	-10.64	0.0	65.115	65.304
16.000	342178.	392637.	4989.	728.3	0.66	543.3904	0.03	123.	0.0	-10.56	0.0	64.418	64.192
17.000	342359.	392737.	5668.	787.6	0.72	622.5774	0.12	74.	0.0	-11.46	0.0	63.283	63.164
18.000	342539.	392837.	6395.	848.3	0.78	706.3455	-0.09	-83.	0.0	-10.94	0.0	62.042	62.131
19.000	342719.	392937.	7168.	910.1	0.84	793.9543	0.15	101.	0.0	-10.84	0.0	61.274	61.147
20.000	342900.	393037.	7984.	972.7	0.90	884.2449	0.00	4.	0.0	-11.13	0.0	60.219	60.214
21.000	343080.	393137.	8856.	1035.8	0.96	976.0742	0.08	34.	0.0	-10.73	0.0	59.330	59.295
22.000	343260.	393237.	9770.	1099.1	1.02	1068.1082	0.03	38.	0.0	-11.00	0.0	58.457	58.424
23.000	343441.	393337.	10729.	1162.9	1.08	1160.1729	0.02	27.	0.0	-10.74	0.0	57.593	57.570
24.000	343621.	393437.	11733.	1227.3	1.15	1261.8577	0.03	32.	0.0	-10.69	0.0	56.777	56.751
25.000	343801.	393537.	12782.	1292.7	1.21	1342.9116	0.03	35.	0.0	-10.73	0.0	55.977	55.952
26.000	343982.	393637.	13875.	1359.3	1.28	1433.6436	0.02	27.	0.0	-10.81	0.0	55.200	55.181
27.000	344162.	393737.	15014.	1427.5	1.35	1523.7449	0.03	41.	0.0	-10.71	0.0	54.458	54.431
28.000	344342.	393837.	16197.	1497.3	1.42	1612.6096	0.02	27.	0.0	-10.74	0.0	53.723	53.706
29.000	344523.	393937.	17427.	1568.8	1.50	1699.8892	0.03	44.	0.0	-10.69	0.0	53.028	53.002
30.000	344703.	394037.	18704.	1642.2	1.58	1785.0566	0.02	34.	0.0	-10.65	0.0	52.339	52.320
31.000	344883.	394137.	20027.	1717.6	1.66	1867.5425	0.02	45.	0.0	-10.64	0.0	51.683	51.658
32.000	345064.	394237.	21398.	1795.0	1.74	1946.7517	0.02	44.	0.0	-10.61	0.0	51.040	51.017
33.000	345244.	394337.	22818.	1874.7	1.83	2022.1328	0.03	51.	0.0	-10.61	0.0	50.421	50.396
34.000	345424.	394437.	24287.	1957.0	1.92	2093.5547	0.02	57.	0.0	-10.58	0.0	49.822	49.794
35.000	345605.	394537.	25807.	2042.1	2.02	2160.5996	0.03	64.	0.0	-10.56	0.0	49.236	49.211
36.000	345785.	394637.	27380.	2130.2	2.12	2222.7402	0.03	72.	0.0	-10.55	0.0	48.675	48.646
37.000	345965.	394737.	29006.	2221.6	2.22	2279.4156	0.03	80.	0.0	-10.52	0.0	48.125	48.100
38.000	346146.	394837.	30683.	2316.5	2.34	2332.9648	0.03	88.	0.0	-10.51	0.0	47.597	47.570
39.000	346326.	394937.	32415.	2415.1	2.45	2373.6347	0.03	94.	0.0	-10.50	0.0	47.085	47.059
40.000	346506.	395037.	34224.	2517.5	2.58	2409.7256	0.04	96.	0.0	-10.50	0.0	46.587	46.563
41.000	346687.	395137.	36093.	2624.0	2.71	2437.3231	0.04	99.	0.0	-10.49	0.0	46.108	46.085
42.000	346867.	395237.	37905.	2734.2	2.82	2415.1504	0.04	94.	0.0	-10.47	0.0	45.644	45.622
43.000	347047.	395337.	39726.	2845.1	2.94	2342.7305	0.04	87.	0.0	-10.45	0.0	45.194	45.175
44.000	347228.	395437.	41545.	2955.7	3.04	2241.7358	0.04	78.	0.0	-10.43	0.0	44.762	44.742

SCOUT R/J STUDY, PHASE III, 43 SIGMA R/S SECT IIIB MOTOR
100 N. MI. INJ., DESIGN TRAJECTORY, 50 LB. PAYLOAD WEIGHT

GRAVITY TURN

LTV AEROSPACE CORP.-MSD
ROUTINE NO. LAC076

TIME SEC	WEIGHT LBS	THRUST LBS	ALT FT	REL VEL FT/SEC	MACH	DYN. P LBS/FT2	ALPHA DEG	Q-ALPHA LB/SQ FT	Q-COMM DEG/SEC	Q DEG/SEC	PITCH ERR DEG	THETA DEG	R-GAM DEG
45.00	21207.	107014.	44168.	3084.6	3.19	2288.4551	0.02	42.	0.0	-0.42	0.0	44.343	44.325
46.00	20734.	100619.	46355.	3199.0	3.30	2216.7422	0.02	37.	0.0	-0.41	0.0	43.937	43.920
47.00	20417.	92196.	48603.	3305.1	3.41	2124.8184	0.02	34.	0.0	-0.40	0.0	43.543	43.527
48.00	20099.	80123.	50904.	3397.8	3.51	2011.6438	0.01	29.	0.0	-0.39	0.0	43.159	43.144
49.00	19780.	69036.	53247.	3476.0	3.59	1882.1594	0.02	29.	0.0	-0.38	0.0	42.784	42.769
50.00	19527.	58931.	55621.	3539.7	3.66	1742.2913	0.01	26.	0.0	-0.39	0.0	42.414	42.399
51.00	19332.	49703.	58017.	3590.4	3.71	1598.5903	0.01	19.	0.0	-0.38	0.0	42.045	42.033
52.00	19139.	40473.	60426.	3628.2	3.75	1454.8928	0.01	21.	0.0	-0.37	0.0	41.684	41.670
53.00	18963.	32301.	62839.	3652.9	3.77	1314.2139	0.02	21.	0.0	-0.38	0.0	41.324	41.308
54.00	18847.	27362.	65247.	3669.2	3.79	1181.8308	0.01	13.	0.0	-0.38	0.0	40.957	40.946
55.00	18743.	23101.	67646.	3678.9	3.80	1056.9226	0.01	13.	0.0	-0.37	0.0	40.595	40.583
56.00	18666.	20290.	70033.	3684.6	3.80	943.3281	0.01	14.	0.0	-0.37	0.0	40.234	40.220
57.00	18588.	17476.	72404.	3686.9	3.79	841.3538	0.02	12.	0.0	-0.38	0.0	39.868	39.854
58.00	18552.	15318.	74757.	3686.2	3.78	750.1279	0.01	8.	0.0	-0.38	0.0	39.498	39.487
59.00	18512.	13154.	77091.	3682.9	3.77	668.7444	0.01	7.	0.0	-0.38	0.0	39.129	39.118
60.00	18475.	10985.	79404.	3676.8	3.76	596.1545	0.01	5.	0.0	-0.38	0.0	38.760	38.740
61.00	18441.	8812.	81693.	3667.9	3.75	531.4150	0.02	9.	0.0	-0.39	0.0	38.388	38.371
62.00	18405.	6634.	83957.	3656.1	3.73	473.6875	0.02	7.	0.0	-0.39	0.0	38.009	37.994
63.00	18388.	4453.	86193.	3641.3	3.71	422.2202	0.01	6.	0.0	-0.39	0.0	37.627	37.613
64.00	18342.	2267.	88401.	3623.3	3.69	376.3478	0.01	5.	0.0	-0.40	0.0	37.242	37.228
65.00	18332.	788.	90577.	3602.4	3.66	335.4929	0.02	5.	0.0	-0.40	0.0	36.855	36.839
66.00	18331.	643.	92720.	3581.0	3.63	299.5408	0.02	5.	0.0	-0.41	0.0	36.463	36.446
67.00	18329.	497.	94831.	3560.0	3.61	267.9624	0.02	4.	0.0	-0.41	0.0	36.065	36.048
68.00	18328.	349.	96910.	3539.2	3.58	240.1686	0.02	4.	0.0	-0.42	0.0	35.662	35.646
69.00	18327.	199.	98956.	3518.6	3.55	215.6581	0.02	4.	0.0	-0.42	0.0	35.255	35.239
70.00	18325.	48.	100970.	3498.3	3.53	194.0028	0.02	3.	0.0	-0.42	0.0	34.845	34.828
71.00	18324.	-104.	102952.	3478.0	3.50	174.8353	0.02	3.	0.0	-0.43	0.0	34.431	34.412
71.07	18324.	-115.	103087.	3476.6	3.50	173.6016	0.02	3.	0.0	-0.43	0.0	34.402	34.383
71.07	18324.	0.	103087.	3476.6	3.50	173.6016	0.02	3.	0.0	-0.43	0.0	34.402	34.383
72.00	18324.	0.	104901.	3458.0	3.48	157.8497	0.02	3.	0.0	-0.43	0.0	34.012	33.992
73.00	18324.	0.	106818.	3438.4	3.45	142.3595	0.02	3.	0.0	-0.44	0.0	33.589	33.566
74.00	18324.	0.	108703.	3419.2	3.42	128.5045	0.02	3.	0.0	-0.44	0.0	33.160	33.137
75.00	18324.	0.	110556.	3400.3	3.39	116.2679	0.02	3.	0.0	-0.45	0.0	32.726	32.703
76.00	18324.	0.	112377.	3381.8	3.36	105.4361	0.02	2.	0.0	-0.45	0.0	32.287	32.264
77.00	18324.	0.	114167.	3363.6	3.33	95.8265	0.02	2.	0.0	-0.46	0.0	31.844	31.820
78.00	18324.	0.	115924.	3345.8	3.30	87.2826	0.02	2.	0.0	-0.46	0.0	31.397	31.372
79.00	18324.	0.	117650.	3323.3	3.27	79.6713	0.03	2.	0.0	-0.46	0.0	30.946	30.919
80.00	18324.	0.	119344.	3311.1	3.25	72.8765	0.03	2.	0.0	-0.47	0.0	30.490	30.462
81.00	18324.	0.	121007.	3294.2	3.22	66.7989	0.03	2.	0.0	-0.47	0.0	30.030	30.000
82.00	18324.	0.	122639.	3277.5	3.20	61.3524	0.03	2.	0.0	-0.48	0.0	29.566	29.533
83.00	18324.	0.	124239.	3261.2	3.17	56.4627	0.03	2.	0.0	-0.48	0.0	29.097	29.062
84.00	18324.	0.	125807.	3245.2	3.15	52.0648	0.04	2.	0.0	-0.49	0.0	28.623	28.586
85.00	18324.	0.	127344.	3229.4	3.12	48.1024	0.04	2.	0.0	-0.49	0.0	28.144	28.106
86.00	18324.	0.	128849.	3214.0	3.10	44.5266	0.04	2.	0.0	-0.50	0.0	27.661	27.621
87.00	18324.	0.	130323.	3198.9	3.08	41.2941	0.04	2.	0.0	-0.50	0.0	27.173	27.132
87.[illegible]	18324.	0.	130943.	3192.4	3.07	39.9992	[illegible]	2.	0.0	-0.50	0.0	26.961	26.920

LARGE A/S STUDY, PHASE II, +3 SIGMA A/S ALTOL IIB MOTOR
100 N. MI. INJ., DESIGN TRAJECTORY, 50 LB. PAYLOAD WEIGHT

PITCH PROGRAM

LTV AEROSPACE CORP.-MSD
ROUTINE NO. LA0076

TIME SEC	WEIGHT LBS	THRUST LBS	ALT FT	REL VEL FT/SEC	MACH	DYN. P LBS/FT2	ALPHA DEG	Q-ALPHA LB/SQ FT	Q-GAM DEG/SEC	THETA DEG	PITCH RTE DEG	Q-CONT DEG	Q DEG/SEC	Q-GAM DEG
0.0	39823.	39750.	-0.	0.0	0.0	0.0	0.0	0.	0.0	89.814	0.099	0.67	0.0	0.0
0.25	39754.	91272.	1.	8.9	0.01	0.0948	0.04	0.	0.0	89.814	0.095	0.55	0.03	89.810
0.50	39657.	87088.	4.	18.9	0.02	0.4259	0.04	0.	0.0	89.813	0.083	0.40	0.06	89.812
0.75	39563.	85176.	10.	28.3	0.03	0.9529	0.04	0.	0.0	89.810	0.066	0.23	0.08	89.814
1.00	39471.	84358.	19.	37.5	0.03	1.6736	0.04	0.	0.0	89.805	0.045	0.07	0.09	89.813
1.25	39379.	83760.	29.	46.6	0.04	2.5820	0.04	0.	0.0	89.797	0.024	-0.07	0.08	89.809
1.50	39289.	83788.	42.	55.7	0.05	3.6856	0.03	0.	0.0	89.788	0.003	-0.19	0.08	89.802
1.75	39199.	83812.	57.	64.9	0.06	4.9909	0.03	0.	0.0	89.779	-0.014	-0.27	0.06	89.793
2.00	39108.	83836.	74.	74.0	0.07	6.5002	0.02	0.	0.0	89.771	-0.028	-0.32	0.05	89.783
2.25	39018.	83862.	94.	83.3	0.07	8.2156	0.01	0.	0.0	89.764	-0.038	-0.33	0.03	89.771
2.50	38928.	83888.	116.	92.5	0.08	10.1396	-0.00	-0.	-1.89281	89.761	-0.051	-0.37	0.01	89.760
2.75	38837.	83866.	140.	101.8	0.09	12.2725	-0.05	-1.	-3.60752	89.769	-0.930	-5.82	-0.17	89.739
3.00	38747.	83837.	167.	111.2	0.10	14.6121	-0.19	-3.	-3.60752	89.809	-1.737	-10.02	-0.63	89.705
3.25	38656.	83809.	196.	120.5	0.11	17.1583	-0.46	-8.	-3.60752	89.731	-2.402	-12.74	-1.29	89.678
3.50	38565.	83782.	227.	129.9	0.12	19.9124	-0.86	-17.	-3.60752	89.364	-2.888	-13.96	-2.05	89.684
3.75	38474.	83756.	261.	139.3	0.12	22.8766	-1.41	-32.	-3.60752	88.767	-3.179	-13.79	-2.84	89.736
4.00	38383.	83732.	297.	148.7	0.13	26.0532	-2.06	-54.	-3.60752	87.970	-3.278	-12.49	-3.57	89.810
4.25	38293.	83708.	335.	158.2	0.14	29.4435	-2.79	-82.	-3.60752	87.003	-3.208	-10.37	-4.18	89.725
4.50	38202.	83685.	376.	167.7	0.15	33.0471	-3.56	-118.	-3.60752	85.900	-3.005	-7.79	-4.63	89.432
4.75	38111.	83663.	419.	177.2	0.16	36.8623	-4.33	-159.	-3.60752	84.707	-2.713	-5.09	-4.90	89.019
5.00	38017.	83871.	464.	186.8	0.17	40.8975	-5.05	-207.	-3.60752	83.471	-2.374	-2.60	-4.98	88.513
5.25	37924.	84079.	512.	196.4	0.18	45.1634	-5.70	-257.	-3.60752	82.234	-2.040	-0.55	-4.90	87.929
5.50	37830.	84289.	563.	206.1	0.18	49.6627	-6.25	-310.	-3.60752	81.036	-1.743	0.87	-4.68	87.287
5.75	37736.	84499.	615.	215.9	0.19	54.3992	-6.69	-364.	-3.60752	79.904	-1.512	1.60	-4.37	86.587
6.00	37642.	84711.	670.	225.7	0.20	59.3779	-7.01	-416.	-3.60752	78.856	-1.365	1.67	-4.01	85.859
6.25	37548.	84924.	728.	235.7	0.21	64.6060	-7.21	-466.	-3.60752	77.899	-1.309	1.02	-3.65	85.110
6.50	37455.	85137.	788.	245.7	0.22	70.0909	-7.33	-513.	-3.60752	77.029	-1.340	-0.07	-3.32	84.353
6.75	37361.	85352.	850.	255.8	0.23	75.8387	-7.36	-558.	-3.60752	76.234	-1.445	-1.49	-3.06	83.594
7.00	37267.	85567.	915.	266.0	0.24	81.8564	-7.35	-602.	-3.60752	75.493	-1.606	-3.06	-2.88	82.841
7.25	37173.	85784.	982.	276.3	0.25	88.1494	-7.31	-644.	-3.60752	74.787	-1.801	-4.62	-2.79	82.095
7.50	37077.	86001.	1052.	286.7	0.26	94.7217	-7.27	-688.	-3.61752	74.093	-2.007	-6.03	-2.78	81.358
7.75	36986.	86220.	1124.	297.2	0.27	101.5787	-7.24	-735.	-3.60752	73.391	-2.206	-7.20	-2.85	80.628
8.00	36892.	86439.	1198.	307.8	0.28	108.7235	-7.24	-787.	-2.22739	72.666	-2.376	-8.04	-2.96	79.904
8.25	36798.	86659.	1275.	318.5	0.29	116.1629	-7.26	-843.	-0.84000	71.923	-1.848	-4.52	-2.95	79.177
8.50	36704.	86881.	1355.	329.4	0.30	123.9029	-7.23	-896.	-0.84000	71.216	-1.351	-1.90	-2.67	78.445
8.75	36608.	87154.	1437.	340.3	0.31	131.9514	-7.11	-938.	-0.84000	70.602	-0.946	-0.38	-2.22	77.713
9.00	36509.	87466.	1521.	351.4	0.32	140.3312	-6.88	-965.	-0.84000	70.113	-0.666	0.06	-1.69	76.991
9.25	36411.	87778.	1608.	362.6	0.33	149.0566	-6.53	-973.	-0.84000	69.760	-0.522	-0.41	-1.15	76.289
9.50	36313.	88092.	1697.	374.0	0.34	158.1496	-6.08	-962.	-0.84000	69.532	-0.503	-1.53	-0.69	75.615
9.75	36216.	88407.	1789.	385.5	0.35	167.5896	-5.57	-933.	-0.84000	69.405	-0.585	-2.99	-0.35	74.974
10.00	36116.	88722.	1883.	397.2	0.36	177.4130	-5.03	-892.	-0.84000	69.344	-0.733	-4.50	-0.17	74.370
10.00	36116.	88722.	1883.	397.2	0.36	177.4143	-5.03	-892.	-0.84000	69.344	-0.733	-4.50	-0.17	74.370
10.00	36116.	88722.	1883.	397.2	0.36	177.4143	-5.03	-892.	-0.84000	69.344	-0.733	-4.50	-0.17	74.370
11.00	35222.	89994.	2287.	445.5	0.40	220.5103	-3.21	-708.	-0.84000	69.071	-1.297	-7.09	-0.62	72.284
12.00	35323.	91281.	2713.	496.1	0.45	269.8350	-2.42	-654.	-0.84000	68.996	-1.156	-4.56	-1.20	70.517

LARGER W/S STUDY, PHASE II, +3 SIGMA W/S ALGOL IIB MOTOR — PITCH PROGRAM — LTV AEROSPACE CORP.-MSD
100 N. MI. INJ., DESIGN TRAJECTORY, 5J LB. PAYLOAD WEIGHT — ROUTINE NO. LA0076

TIME SEC	WEIGHT LBS	THRUST LBS	ALT FT	REL VEL FT/SEC	MACH	DYN. P LBS/FT2	ALPHA DEG	W-ALPHA LB/SQ FT	Q-COMM DEG/SEC	Q DEG/SEC	PITCH ERR DEG	Q-CONT DEG	THETA DEG	R-GAM DEG
13.00	34933.	92469.	3229.	548.9	0.50	325.5813	-1.93	-627.	-0.84000	-0.98	-0.858	-3.20	66.970	68.895
14.00	34525.	93038.	3757.	603.6	0.55	387.3992	-1.33	-517.	-0.84000	-0.85	-0.826	-3.29	66.092	67.427
15.00	34117.	93621.	4337.	659.9	0.60	454.9424	-0.91	-412.	-0.84000	-0.95	-0.768	-2.63	65.198	66.104
16.00	33709.	94217.	4964.	717.6	0.65	528.0066	-0.63	-332.	-0.84000	-0.93	-0.659	-1.93	64.253	64.882
17.00	33301.	94826.	5637.	776.9	0.71	606.2781	-0.40	-244.	-0.84000	-0.91	-0.583	-1.48	63.341	63.744
18.00	32893.	95447.	6358.	837.5	0.77	689.2705	-0.24	-165.	-0.84000	-0.90	-0.516	-1.04	62.439	62.678
19.00	32479.	95859.	7125.	899.3	0.83	776.2424	-0.13	-98.	-0.84000	-0.89	-0.458	-0.69	61.545	61.672
20.00	32064.	96210.	7941.	961.9	0.89	866.0530	-0.05	-41.	-0.84000	-0.88	-0.415	-0.44	60.668	60.716
21.00	31649.	96568.	8803.	1025.1	0.95	957.6270	-0.00	-4.	-0.84000	-0.87	-0.382	-0.24	59.799	59.803
22.00	31234.	96935.	9713.	1088.5	1.01	1049.5469	0.02	18.	-0.84000	-0.85	-0.361	-0.13	58.943	58.926
23.00	30818.	97307.	10668.	1152.4	1.07	1141.4822	0.02	22.	-0.84000	-0.84	-0.353	-0.11	58.099	58.080
24.00	30403.	97684.	11669.	1216.9	1.14	1233.0779	0.01	10.	-0.84000	-0.83	-0.357	-0.17	57.268	57.260
25.00	29983.	98229.	12715.	1282.2	1.20	1324.0806	-0.02	-20.	-0.84000	-0.82	-0.373	-0.31	56.449	56.465
26.00	29558.	98952.	13806.	1348.8	1.27	1414.7419	-0.05	-71.	-0.77995	-0.81	-0.398	-0.50	55.640	55.690
27.00	29133.	99675.	14943.	1417.0	1.34	1504.8367	-0.05	-75.	-0.72000	-0.72	-0.358	-0.47	54.885	54.935
28.00	28708.	100399.	16126.	1486.7	1.41	1593.7371	-0.04	-65.	-0.72000	-0.73	-0.351	-0.41	54.164	54.205
29.00	28283.	101123.	17355.	1558.2	1.49	1681.0515	-0.05	-81.	-0.72000	-0.72	-0.351	-0.44	53.449	53.497
30.00	27858.	101845.	18631.	1631.6	1.56	1766.2959	-0.07	-116.	-0.72000	-0.71	-0.359	-0.51	52.743	52.809
31.00	27433.	102566.	19955.	1706.9	1.65	1848.8892	-0.09	-175.	-0.65295	-0.70	-0.372	-0.61	52.043	52.138
32.00	27008.	103283.	21327.	1784.3	1.73	1928.2495	-0.08	-155.	-0.58600	-0.60	-0.313	-0.49	51.404	51.484
33.00	26577.	104055.	22747.	1863.9	1.82	2003.8030	-0.05	-99.	-0.58600	-0.61	-0.294	-0.35	50.805	50.855
34.00	26132.	104965.	24218.	1946.1	1.91	2075.4199	-0.04	-74.	-0.58600	-0.60	-0.279	-0.28	50.211	50.247
35.00	25687.	105870.	25740.	2031.2	2.01	2142.6680	-0.03	-70.	-0.58600	-0.59	-0.273	-0.25	49.626	49.658
36.00	25242.	106769.	27315.	2119.2	2.11	2204.9941	-0.04	-92.	-0.54600	-0.58	-0.272	-0.26	49.046	49.088
37.00	24797.	107661.	28944.	2210.5	2.21	2261.8555	-0.06	-140.	-0.59600	-0.58	-0.276	-0.30	48.471	48.533
38.00	24352.	108545.	30628.	2305.3	2.32	2312.6055	-0.09	-217.	-0.53046	-0.58	-0.282	-0.34	47.899	47.993
39.00	23908.	109422.	32370.	2403.8	2.44	2356.4941	-0.09	-201.	-0.47500	-0.48	-0.232	-0.26	47.381	47.466
40.00	23463.	110290.	34172.	2506.1	2.57	2392.8223	-0.05	-131.	-0.47500	-0.49	-0.224	-0.20	46.906	46.961
41.00	23018.	111147.	36034.	2612.6	2.70	2420.7051	-0.04	-104.	-0.47500	-0.48	-0.216	-0.17	46.431	46.474
42.00	22563.	111292.	37961.	2722.7	2.81	2399.9980	-0.04	-101.	-0.47500	-0.48	-0.214	-0.16	45.963	46.005
43.00	22108.	111422.	39952.	2836.6	2.93	2367.9375	-0.05	-127.	-0.47500	-0.47	-0.215	-0.17	45.497	45.551
44.00	21654.	111491.	42011.	2954.3	3.05	2327.4824	-0.08	-176.	-0.47500	-0.47	-0.218	-0.20	45.034	45.110
45.00	21211.	107070.	44138.	3073.0	3.17	2274.4258	-0.11	-243.	-0.47500	-0.47	-0.224	-0.25	44.574	44.681
46.00	20788.	100701.	46331.	3187.4	3.29	2203.2246	-0.15	-322.	-0.42396	-0.47	-0.232	-0.31	44.116	44.263
47.00	20420.	91307.	48585.	3293.6	3.40	2111.9141	-0.14	-301.	-0.37300	-0.37	-0.190	-0.27	43.712	43.854
48.00	20102.	80234.	50892.	3386.4	3.50	1999.4207	-0.11	-227.	-0.37300	-0.38	-0.188	-0.25	43.346	43.459
49.00	19783.	69147.	53241.	3464.8	3.58	1870.6311	-0.10	-180.	-0.37300	-0.38	-0.183	-0.22	42.979	43.075
50.00	19529.	59024.	55621.	3528.6	3.65	1731.4565	-0.09	-147.	-0.37300	-0.38	-0.181	-0.20	42.613	42.698
51.00	19334.	49801.	58023.	3579.5	3.70	1598.4233	-0.08	-124.	-0.37300	-0.37	-0.179	-0.20	42.249	42.327
52.00	19140.	40567.	60438.	3617.4	3.74	1445.3870	-0.07	-106.	-0.37300	-0.37	-0.179	-0.20	41.886	41.960
53.00	18946.	32352.	62857.	3642.2	3.76	1305.3499	-0.07	-91.	-0.37300	-0.37	-0.179	-0.20	41.525	41.594
54.00	18844.	27413.	65279.	3658.5	3.78	1173.5496	-0.07	-79.	-0.37300	-0.37	-0.179	-0.20	41.162	41.229
55.00	18744.	23131.	67674.	3668.3	3.78	1049.1692	-0.05	-67.	-0.37300	-0.37	-0.179	-0.20	40.800	40.865
56.00	18644.	20320.	70071.	3674.0	3.78	936.1211	-0.05	-57.	-0.37300	-0.37	-0.179	-0.20	40.438	40.493
57.00	18545.	17502.	72447.	3676.3	3.78	834.6592	-0.05	-47.	-0.37300	-0.37	-0.178	-0.19	40.075	40.132

LARGER H/S STUDY, PHASE II, +3 SIGMA 3/S ALGOL IIB MOTOR — PITCH PROGRAM — LTV AEROSPACE CORP.-MSD
100 N. MI. INJ., DESIGN TRAJECTORY, 50 LB. PAYLOAD WEIGHT — ROUTINE NO. LA0076

TIME SEC	WEIGHT LBS	THRUST LBS	ALT FT	REL VEL FT/SEC	MACH	DYN. P LBS/FT2	ALPHA DEG	Q-ALPHA LB/SQ FT	Q-CONV DEG/SEC	Q DEG/SEC	PITCH ERR DEG	Q-CONT DEG	THETA DEG	R-GAM DEG
58.00	18532.	15341.	74810.	3675.6	3.77	743.9084	-0.05	-38.	-0.37300	-0.37	-0.177	-0.18	39.712	39.763
59.00	18515.	13177.	77151.	3672.2	3.76	662.9712	-0.05	-30.	-0.37300	-0.37	-0.175	-0.17	39.348	39.393
60.00	18478.	11608.	79470.	3666.1	3.75	590.8022	-0.04	-21.	-0.37300	-0.37	-0.173	-0.16	38.984	39.021
61.00	18442.	8835.	81766.	3657.2	3.74	526.4573	-0.03	-13.	-0.40653	-0.38	-0.171	-0.14	38.620	38.646
62.00	18405.	6657.	84037.	3645.4	3.72	469.0991	-0.03	-13.	-0.44000	-0.42	-0.219	-0.36	38.240	38.268
63.00	18368.	4476.	86281.	3630.5	3.70	417.9758	-0.07	-29.	-0.44000	-0.44	-0.226	-0.32	37.817	37.886
64.00	18342.	2290.	88495.	3612.5	3.67	372.4189	-0.11	-42.	-0.44000	-0.43	-0.225	-0.36	37.388	37.501
65.00	18332.	790.	90679.	3591.5	3.65	331.8655	-0.13	-44.	-0.44000	-0.41	-0.243	-0.52	36.977	37.111
66.00	18331.	646.	92829.	3570.1	3.62	296.1848	-0.14	-42.	-0.44000	-0.41	-0.270	-0.71	36.575	36.716
67.00	18329.	500.	94947.	3549.0	3.59	264.8542	-0.15	-40.	-0.44000	-0.43	-0.290	-0.80	36.166	36.318
68.00	18328.	352.	97033.	3528.1	3.57	237.2848	-0.17	-40.	-0.44000	-0.44	-0.297	-0.83	35.744	35.915
69.00	18327.	202.	99086.	3507.5	3.54	212.9877	-0.19	-40.	-0.44000	-0.44	-0.301	-0.85	35.319	35.507
70.00	18325.	51.	101107.	3487.0	3.52	191.5259	-0.20	-38.	-0.44000	-0.43	-0.306	-0.90	34.896	35.095
71.00	18324.	-102.	103096.	3466.7	3.49	172.5353	-0.20	-35.	-0.44000	-0.43	-0.316	-0.98	34.477	34.678
71.08	18324.	-114.	103251.	3465.1	3.49	171.1362	-0.20	-34.	-0.44000	-0.43	-0.317	-0.98	34.444	34.645
71.08	18324.	0.	103251.	3465.1	3.49	171.1362	-0.20	-34.	-0.44000	-0.43	-0.317	-0.99	34.444	34.645
72.00	18324.	0.	105052.	3446.6	3.47	155.7122	-0.20	-31.	-0.44000	-0.43	-0.327	-1.05	34.059	34.256
73.00	18324.	0.	106976.	3426.8	3.44	140.3282	-0.19	-27.	-0.44000	-0.43	-0.335	-1.09	33.638	33.830
74.00	18324.	0.	108867.	3407.5	3.41	126.6247	-0.19	-24.	-0.44000	-0.44	-0.338	-1.09	33.211	33.400
75.00	18324.	0.	110727.	3389.6	3.37	114.5257	-0.19	-21.	-0.44000	-0.44	-0.335	-1.06	32.779	32.965
76.00	18324.	0.	112555.	3370.0	3.35	103.8189	-0.18	-19.	-0.44000	-0.45	-0.328	-1.01	32.344	32.525
77.00	18324.	0.	114351.	3351.7	3.32	94.3228	-0.17	-16.	-0.44000	-0.45	-0.321	-0.96	31.908	32.081
78.00	18324.	0.	116115.	3333.7	3.29	85.8829	-0.16	-14.	-0.44000	-0.45	-0.314	-0.91	31.471	31.632
79.00	18324.	0.	117847.	3316.1	3.26	78.3655	-0.14	-11.	-0.44000	-0.45	-0.306	-0.86	31.035	31.178
80.00	18324.	0.	119549.	3298.8	3.23	71.6565	-0.12	-9.	-0.44000	-0.45	-0.298	-0.80	30.598	30.720
81.00	18324.	0.	121217.	3281.8	3.21	65.6579	-0.10	-6.	-0.44000	-0.45	-0.287	-0.72	30.158	30.257
82.00	18324.	0.	122855.	3265.0	3.18	60.2832	-0.07	-4.	-0.44000	-0.45	-0.274	-0.62	29.716	29.790
83.00	18324.	0.	124462.	3248.6	3.16	55.4594	-0.05	-3.	-0.44000	-0.46	-0.258	-0.50	29.271	29.318
84.00	18324.	0.	126036.	3232.5	3.13	51.1219	-0.02	-1.	-0.44000	-0.46	-0.238	-0.36	28.822	28.841
85.00	18324.	0.	127580.	3216.6	3.11	47.2151	0.01	0.	-0.44000	-0.46	-0.214	-0.19	28.370	28.360
86.00	18324.	0.	129092.	3201.0	3.09	43.6901	0.04	2.	-0.44000	-0.47	-0.188	-0.01	27.914	27.874
87.00	18324.	0.	130573.	3185.7	3.06	40.5043	0.07	3.	-0.44000	-0.47	-0.160	0.19	27.457	27.384
87.17	18324.	0.	130819.	3183.2	3.06	39.9998	0.08	3.	-0.44000	-0.47	-0.155	0.22	27.380	27.301